

**A novel photocatalytic strategy for complex aliphatic amine synthesis and
the total synthesis of alkaloids (–)-FR901483 and (+)-TAN1251C**

Dominik Reich

Hughes Hall

University of Cambridge



This dissertation is submitted for the Degree of Doctor of Philosophy

December 2019

Department of Chemistry
University of Cambridge
Lensfield Road,
Cambridge
CB2 1EW
United Kingdom

Declaration and Statement of Length

This dissertation is the result of my own work and includes nothing which is the outcome of work done in collaboration except as declared in the Preface or specified in the text.

It is not substantially the same as any that I have submitted, or, is being concurrently submitted for a degree or diploma or other qualification at the University of Cambridge or any other University or similar institution except as declared in the Preface and specified in the text. I further state that no substantial part of my dissertation has already been submitted, or, is being concurrently submitted for any such degree, diploma or other qualification at the University of Cambridge or any other University or similar institution except as declared in the Preface and specified in the text.

This thesis does not exceed the prescribed word limit of 60,000 as set by the Degree Committee for the faculty of Physics and Chemistry.

Dominik Reich

“The impediment to action advances action. What stands in the way becomes the way.”

– Marcus Aurelius

Acknowledgements

First and foremost, I would like to express my sincere gratitude to Prof. Matthew Gaunt for giving me the opportunity to carry out my PhD research in his group. Thank you, Matt, for placing the trust in me and offering me a position, and for your continuous guidance, inspiration and support during my four years in your group. I am deeply grateful to have learned so much through your mentorship.

The completion of my studies would not have been possible without the generous financial support offered by the AstraZeneca Studentship during the four years of my PhD.

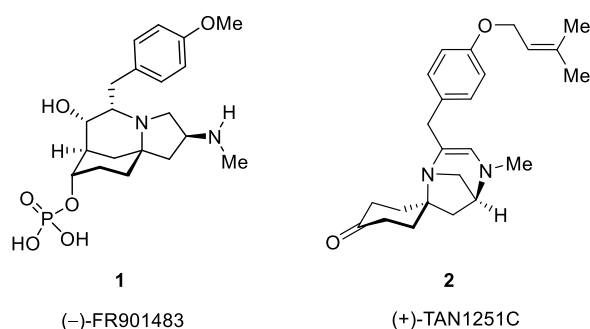
I would like to thank the members of the Gaunt group - past and present - for their help and support, friendship, and for making labs 180 and 177 such great places to work at. I am very grateful to have worked alongside all of you. Manuel, I want to thank you for all your unwavering support, both in and out of labs. It was great to be fumehood neighbors for the past 4 years. Jaime, Daniel and Rudy, thank you for being there for me when I first arrived in Cambridge, I will never forget my tenure track on Catherine Street. John, thank you for devoting your time for our endless discussions and for running all those SciFinder searches with me. Dave, thank you for always being upbeat and for providing Cholula and even mug repairs. Patrick and Keishi, thank you for all the great music. Aaron, it was a pleasure working so closely with you for the last two years. I am thankful for your trust and dedication, and I will miss our trips to Costa. Special thanks go to Scarlett, Manuel, John, Connie, Henry and Nils for their help editing this work.

I would like to thank Duncan, Andrew and Peter for assistance with NMR facilities. Furthermore, thanks to Nic and Naomi and all the technical staff for their continued hard work, help and support.

Finally, I would like to thank my family and my wife for their love and support, without which none of this would have been possible.

Abstract

Owing to their unique properties, the synthesis and functionalization of aliphatic amines plays a central role in the field of visible light photoredox chemistry. In this thesis, the development of a novel, visible light mediated process for the synthesis of complex aliphatic amines is described. The novel multicomponent reaction between secondary amines, aldehydes and electron-deficient olefins efficiently furnishes complex aliphatic tertiary amine products. Selective generation of an α -amino radical species is achieved via photocatalytic single electron reduction of *in situ* generated all-alkyl iminium ions. Under optimized reaction conditions, the photocatalytic olefin-hydroaminoalkylation procedure was shown to be compatible with a broad range of benzyl amine, aldehyde, and olefin substrates. A detailed study of the mechanism of the transformation is described, revealing an unusual 1,5-hydrogen atom transfer step and an unprecedented redox-relay of iminium ions. In further studies, the reaction scope was expanded to include non-benzylic amines and enamines, enabling the generation of synthetically valuable α -tertiary amines.



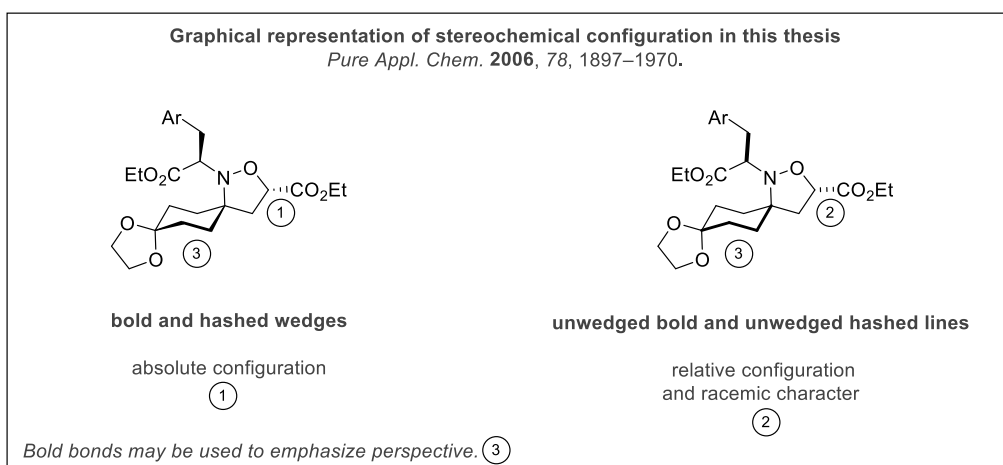
α -Tertiary amines are a common feature in a number of bioactive natural products. Immunosuppressant (-)-FR901483 (**1**) and muscarinic antagonist (+)-TAN1251C (**2**) are biosynthetically related di-tyrosine-derived alkaloids, which have attracted significant attention from the synthetic community by virtue of their biological activity and the challenges posed by their architecturally complex structures. The development of a variant of the multicomponent photocatalytic olefin-hydroaminoalkylation approach to couple primary amines, ketones and olefins, and its use in total synthesis, is described. The novel transformation enabled the rapid, divergent total synthesis of both (-)-FR901483 and (+)-TAN1251C via a common spiro lactam precursor. Finally, the reaction proved amenable to a number of primary amines and ketones, giving direct, modular access to a series of useful chiral spiro lactam scaffolds.

Overview

This thesis is comprised of an introduction followed by two main chapters of results and discussion. In the first chapter, an introduction of the chemical tools used in the main body of the work is given. The introduction is divided into two parts. In the first part, an overview of the field of photochemistry is given. The second part is a brief review of amine synthesis via visible light photoredox approaches, followed by a review of the development of visible light mediated α -amino radical generation as an attempt to provide a context for the work of this thesis to be viewed in.

This is followed by the second chapter, which describes the work on and development of a novel photocatalytic amine synthesis via multicomponent olefin-hydroaminoalkylation, and discusses the results obtained over the course of the project. Chapter three describes in detail the use of a variant of this chemistry to access α -tertiary secondary amines, spirolactams, and a key precursor enabling the rapid total synthesis of the two alkaloids (–)-FR901483 and (+)-TAN1251C.

The main body of work in this thesis is followed by concluding remarks and a future outline of the discussed chemistry. In further sections, experimental procedures and data, and the references cited in the text are provided. This thesis includes four appendices, containing further experimental procedures, supplementary data, published articles from the work of this thesis, and ^1H -NMR and ^{13}C -NMR spectral data of what are considered to be key compounds mentioned in the text.



Abbreviations

18-crown-6	1,4,7,10,13,16-hexaoxacyclooctadecane
4,4'-dOMe-bpy	4,4'-dimethoxy-2,2'-bipyridine
4,7-dOMe-phen	4,7-dimethoxy-1,10-phenanthroline
4Cz-IPN	1,2,3,5-tetrakis(carbazol9-yl)-4,6-dicyanobenzene
Å	ångström
ABNO	9-azabicyclo[3.3.1]nonane N-oxyl
Ac	acetyl
AIBN	azobisisobutyronitrile
Am	amyl
aq.	aqueous
Ar	aryl
atm	atmosphere
ATR	attenuated total reflection
AZADO	2-azaadamantane N-oxyl
b.p.	boiling point
BArF	tetrakis[3,5-bis(trifluoromethyl)phenyl]borate
BDE	bond dissociation energy
Bn	benzyl
BNAH	1-benzyl-1,4-dihydronicotinamide
BnNADH	N-benzyl-1,4-dihydronicotinamide
Boc	<i>tert</i> -butyloxycarbonyl
bpy	2,2'-bipyridine
bpz	2,2'-bipyrazinato
br	broad
Bu	butyl
Bz	benzoyl
c	concentration
cal	calories
cat.	catalytic
Cbz	carboxylbenzyl
CFL	compact fluorescence light
cod	1,5-cyclooctadiene
COSY	correlated spectroscopy
CSA	camphor sulfonic acid
Cy	cyclohexyl
d	doublet
d.r.	diastereomeric ratio
DABCO	1,4-diazabicyclo[2.2.2]octane
DBU	1,8-diazabicyclo[5.4.0]undec-7-ene
DCC	<i>N,N'</i> -dicyclohexylcarbodiimide
DDQ	2,3-dichloro-5,6-dicyano-1,4-benzoquinone
DEAD	diethyl azodicarboxylate
DEPT	distortionless enhancement by polarization transfer
dF(CF ₃)ppy	3,5-difluoro-2-[5-(trifluoromethyl)-2-phenylpyridinato
DFT	density functional theory
DIAD	diisopropyl azodicarboxylate
DIBALH	diisobutylaluminium hydride
DIPEA	<i>N,N</i> -diisopropylethylamine

DMA	dimethylacetamide
DMAP	4-dimethylaminopyridine
DMF	dimethylformamide
DMP	Dess-Martin periodinane
DMSO	dimethylsulfoxide
DPPA	diphenylphosphoryl azide
dppf	1,1'-bis(diphenylphosphino)ferrocene
dppp	1,3-bis(diphenylphosphino)-propane
dtbbpy	4,4'-di-tert-butyl-2,2'-bipyridine
DTBMP	2,6-di-tert-butyl-4-methylpyridine
$E_{1/2}$	half-wave potential
ED ₅₀	median effective dose
EDC	1-ethyl-3-(3-dimethylaminopropyl)carbodiimide
ee	enantiomeric excess
eq.	equivalents
equiv	equivalents
ESI	electrospray ionization
ESR	electron spin resonance
Et	ethyl
FAB-MS	fast atom bombardment–mass spectrometry
<i>fac</i>	facial
FT-IR	fourier-transform infrared spectroscopy
GC-MS	gas chromatography–mass spectrometry
glyme	ethylene glycol dimethyl ether
Grubbs I	Benzylidene-bis(tricyclohexylphosphino)-dichlororuthenium
h	hour(s)
HAT	hydrogen atom transfer
HFIP	hexafluoroisopropanol
HMBC	heteronuclear multiple bond correlation
HMPA	hexamethylphosphoramide
HOBt	hydroxybenzotriazole
HOMO	highest occupied molecular orbital
HRMS	high resolution mass spectrometry
HSQC	heteronuclear single quantum coherence
Hz	Hertz
<i>i</i>	iso
IC	internal conversion
IR	infrared (spectroscopy)
ISC	inter system crossing
<i>J</i>	coupling constant
k	kilo
KHMDS	potassium bis(trimethylsilyl)amide
k_q	quenching rate constant
L	neutral ligand <i>or</i> liter
LA	Lewis acid
LC-MS	liquid chromatography–mass spectrometry
LDA	lithium diisopropylamide
LED	light emitting diode
L-Na-Pro	sodium proline

L-selectride	lithium tri-sec-butyl(hydrido)borate
LUMO	lowest unoccupied molecular orbital
M	molar <i>or</i> metal
m	multiplet
<i>m</i>	meta
m.p.	melting point
<i>m</i> -CBPA	meta-chloroperoxybenzoic acid
<i>m</i> -DNB	<i>m</i> -dinitrobenzene
Me	methyl
Me ₂ phen	2,9-dimethyl-1,10-phenanthroline
Mes	mesityl
MIDA	<i>N</i> -methyliminodiacetic acid
MLCT	metal to ligand charge transfer
mol. sieves	molecular sieves
Ms	mesyl
MTBE	methyl tert-butyl ether
MW	microwave
<i>n</i>	normal
NADH	1,4-dihydronicotinamide
NaHMDS	sodium bis(trimethylsilyl)amide
NBS	<i>N</i> -bromosuccinimide
NCS	<i>N</i> -chlorosuccinimide
NHC	<i>N</i> -heterocyclic carbene
NMM	<i>N</i> -methylmorpholine
NMO	<i>N</i> -methylmorpholine <i>N</i> -oxide
NMP	<i>N</i> -methyl-2-pyrrolidone
NMR	nuclear magnetic resonance
NOE	nuclear Overhauser effect
NOESY	nuclear Overhauser effect spectroscopy
Ns	nosyl
Nu	nucleophile
<i>o</i>	ortho
ox	oxidation
<i>p</i>	para
P.E.	petroleum ether
PCET	proton coupled electron transfer
PG	protecting group
Ph	phenyl
Phth	phthalimide
pin	pinacolato
Piv	pivaloyl
p <i>K</i> _a	logarithmic acid dissociation constant
PLC	preparative thin-layer chromatography
PMB	<i>p</i> -methoxybenzyl
ppm	parts per million
PPTS	pyridinium <i>p</i> -toluenesulfonate
ppy	2-phenylpyridinato
Pr	propyl
psi	pound per square inch

PTFE	polytetrafluoroethylene
PTSA	<i>p</i> -toluenesulfonic acid
py	pyridine
Pybox	2,6-bis(oxazolin-2-yl)pyridine
q	quartet
quant	quantitative
quint	quintet
R	undefined group
r.t.	room temperature
rac	racemic
Red-Al	sodium bis(2-methoxyethoxy)aluminium hydride
R _f	retention factor
ROESY	rotating frame nuclear Overhauser effect spectroscopy
s	singlet
sat	saturated
SCE	saturated calomel electrode
scint.	scintillation
SCX	strong cation exchange
SET	single electron transfer
sext	sextet
spt	septet
t	triplet
TBAF	tetra- <i>n</i> -butylammonium fluoride
TBDPS	<i>tert</i> -butyldiphenylsilyl
TBS	<i>tert</i> -butyldimethylsilyl
TEMPO	(2,2,6,6-tetramethylpiperidin-1-yl)oxyl
TES	triethylsilyl
Tf	trifluoromethanesulfonyl
TFA	trifluoroacetic acid
TFAA	trifluoroacetic anhydride
THF	tetrahydrofuran
TIPS	triisopropylsilyl
TLC	thin-layer chromatography
TMEDA	tetramethylethylenediamine
TMS	trimethylsilyl
TOCSY	total correlated spectroscopy
TPAP	tetrapropylammonium perruthenate
TRIP	3,3'-bis(2,4,6-triisopropylphenyl)-1,1'-binaphthyl-2,2'-diyl hydrogenphosphate
trisyl	2,4,6-triisopropylbenzenesulfonyl
Troc	2,2,2-trichloro-ethoxycarbonyl
Ts	tosyl
UV	ultraviolet
UV-Vis	ultraviolet–visible spectrophotometry
VR	vibrational relaxation
vs	versus
X	halogen <i>or</i> anionic ligand
λ	wavelength
τ	excited state lifetime
Φ	quantum yield

Contents

<i>Declaration and Statement of Length</i>	i
<i>Acknowledgements</i>	v
<i>Abstract</i>	vii
<i>Overview</i>	ix
<i>Abbreviations</i>	xi
1. Introduction	1
1.1 Photochemistry	1
1.1.1 Early photochemistry	1
1.1.2 Overview and background	3
1.1.3 Photoredox catalysis.....	7
1.1.4 Photoredox catalysis – From early work to recent developments.....	9
1.1.5 Photoredox catalysis in natural product synthesis	18
1.2 Amine synthesis and functionalization via photoredox catalysis	22
1.2.1 Background	22
1.2.2 Amine reactivity	22
1.2.3 Functionalization of iminium ions	24
1.2.4 α -Amino radicals	29
1.2.5 α -Aminoalkyl radicals in transition metal – photoredox dual catalysis.....	38
1.2.6 Summary and outlook	45
2. Photocatalytic multicomponent olefin-hydroaminoalkylation.....	46
2.1 Introduction.....	46
2.1.1 α -Aminoalkyl radicals via reductive pathways	46
2.1.2 Previous work.....	49
2.2 Project Aims	54

2.3	Results and Discussion.....	57
2.3.1	Discovery and early studies	57
2.3.2	Reaction optimization.....	59
2.3.3	Scope of the reaction	64
2.3.4	Mechanistic studies.....	75
2.3.5	Extended scope and functionalization of enamines.....	81
2.3.6	Functionalization of pharmaceutical agents	85
2.4	Summary	86
3.	Total synthesis of alkaloids FR901483 and TAN1251C.....	87
3.1	Introduction	87
3.1.1	FR901483 – Structure, isolation, bioactivity and proposed biosynthesis....	87
3.1.2	FR901483 – Previous syntheses	89
3.1.2.1	Overview.....	89
3.1.2.2	Snider’s desmethylamino-FR901483 study	90
3.1.2.3	First total synthesis of (–)-FR901483 by Snider.....	91
3.1.2.4	Sorensen’s synthesis	93
3.1.2.5	Ciufolini’s synthesis.....	94
3.1.2.6	Funk’s synthesis of (±)-FR901483.....	96
3.1.2.7	Fukuyama’s first generation synthesis of FR901483.....	97
3.1.2.8	Fukuyama’s second generation enantiocontrolled synthesis	98
3.1.2.9	Brummond’s formal synthesis of FR901483	100
3.1.2.10	Kerr’s formal synthesis of FR901483	101
3.1.2.11	Tu’s total synthesis of FR901483	103
3.1.2.12	Huang’s Synthesis of FR901483.....	104
3.1.2.13	Other approaches towards the FR901483 core structure	106
3.1.3	TAN1251C – Structure, isolation, bioactivity and proposed biosynthesis	107
3.1.4	TAN1251 series – Previous syntheses.....	109

3.1.4.1	Overview	109
3.1.4.2	Kawahara and Nagumo's first generation synthesis of TAN1251A ..	110
3.1.4.3	Snider's synthesis of TAN1251A, B, C and D	112
3.1.4.4	Wardrop's synthesis of TAN1251A	116
3.1.4.5	Kawahara and Nagumo's 2 nd generation synthesis of TAN1251A	118
3.1.4.6	Ciufolini's synthesis of TAN1251C	119
3.1.4.7	Honda's formal synthesis of TAN1251A	120
3.1.4.8	Hayes' formal synthesis of TAN1251A	122
3.1.4.9	Honda's synthesis of TAN1251C and TAN1251D	123
3.1.4.10	Kan's total synthesis of TAN1251C	125
3.2	Summary and Project aims	127
3.3	Results and Discussion	130
3.3.1	Strategy for the total synthesis of (–)-FR901483 and (+)-TAN1251C	130
3.3.2	Development of the primary amine multicomponent reaction	134
3.3.3	Completion of the total synthesis of (+)-TAN1251C	142
3.3.4	Synthesis of the keto-aldehyde towards FR901483	147
3.3.5	Biomimetic aldol-reaction	151
3.3.6	Completion of the total synthesis of FR901483	158
3.3.7	Additional studies	161
3.4	Summary	162
4.	Conclusions and Future Outlook	165
5.	Experimental Section	169
5.1	Materials and Methods	169
5.2	Experimental procedures	171
5.2.1	Photocatalytic olefin-hydroaminoalkylation	171
5.2.2	Total synthesis of (–) FR901483 and (+)-TAN1251C	196

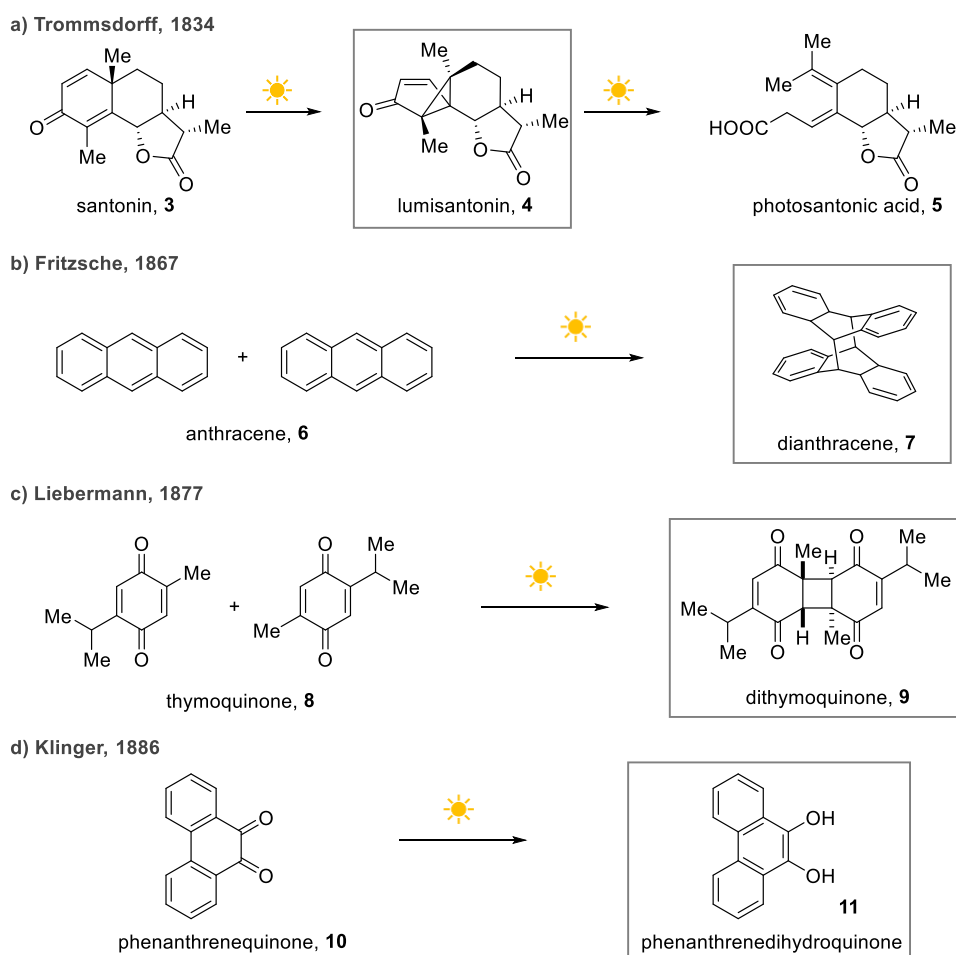
5.2.2.1	Development of the multicomponent reaction.....	196
5.2.2.2	Synthesis of TAN1251C	200
5.2.2.3	Synthesis of FR901483	203
6.	References	214
	Appendix I: Miscellaneous experimental procedures	231
	Appendix II: Supplementary data	244
	Appendix III: Published work.....	253
	Appendix IV: ^1H and ^{13}C NMR spectral data	265

1. Introduction

1.1 Photochemistry

1.1.1 Early photochemistry

The scientific investigation of light mediated photochemical reactions can be traced back to as early as the late eighteenth century.^[1] Perhaps the first genuine photoreactions were observed 1790 by English theologian, natural philosopher, reformer, and chemist Joseph Priestley,^[2-3] who identified that colorless “spirit of nitre” (nitric acid) could be darkened under the action of a focused beam of sunlight.^[4] More than 40 years later, in 1831, Döbereiner discovered the first photoreduction of a metal salt. He observed the light-induced liberation of CO₂ and precipitation of basic Iron-(II)-oxide from a solution of oxalic acid and iron-(III)-oxide.^[5]



Scheme 1. Examples of early photochemical reactions.

Only a few years later, the earliest purely organic photoreaction was discovered, the photorearrangement of santonin (**3**) (Scheme 1a),^[6-7] a sesquiterpene lactone first isolated in

1830 by Kahler^[8] and Alms^[9]. In 1834, Trommsdorff found santonin to turn yellow upon irradiation with sunlight, and its crystals to burst.^[10] Remarkably, Trommsdorff established that only blue and violet light induces color change in santonin.^[10] Santonin's interesting photochemistry was investigated further by Sestini and Cannizarro,^[11] but it was not until 1963, that the reaction and its intermediates were fully understood.^[12-14] In 1867, Fritzsche serendipitously discovered the photodimerization of anthracene **6** (Scheme 1b). He observed the precipitation microscopic crystals from a saturated solution of anthracene when it was exposed to sunlight.^[15-16] Liebermann, who was familiar with Fritzsche's work,^[1] observed in 1877 that when irradiated with sunlight, crystals of thymoquinone **8** would be converted into a white mass (Scheme 1c). Later elucidation would show that he had indeed discovered the first known organic [2+2] cycloaddition. In 1881, Perkin discovered the first example of another important photoreaction, olefin isomerization. He observed isomerization in his studies of 2-alkoxycinnamic acids upon exposure to sunlight. The reaction required either violet or ultraviolet light.^[17] The rate of these conversions could be increased by the addition of iodine, as reported in 1895 by Liebermann.^[18-19] A major contribution to light-induced quinone reactivity was made by Klinger when he was faced with reproducibility issues in his experiments with benzil.^[20] Only vials in a part of his laboratory which was exposed to "direct sunlight in the early morning hours" showed a partial reduction of the dissolved benzil. His serendipitous discovery was the first report of a photochemical carbonyl reduction (Scheme 1d). Giacomo Ciamician and Paul Silber reported photochemical carbonyl reductions of benzoquinone almost simultaneously with Klinger.^[21]

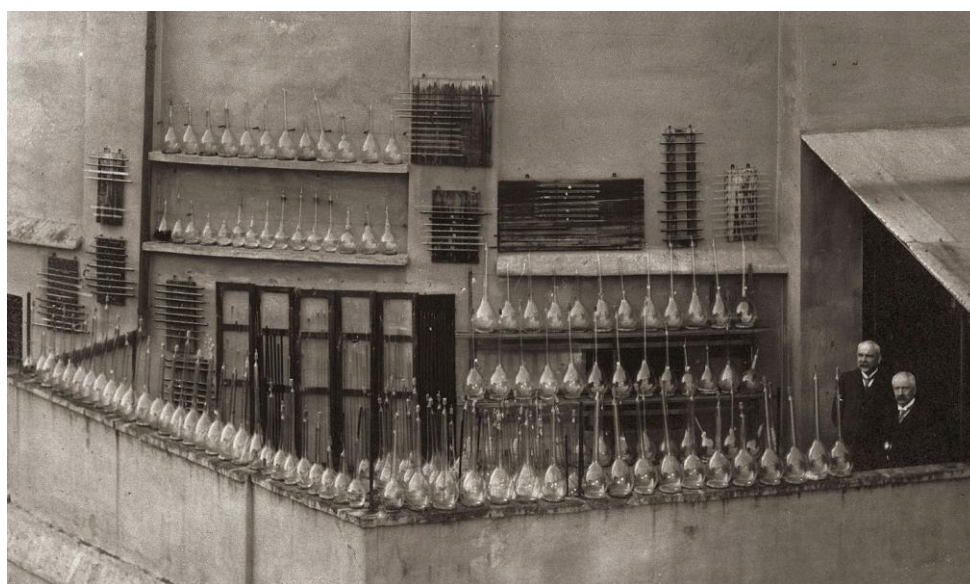


Figure 1. "Portraits of Giacomo Ciamician and Paolo Silber on the rooftop of the laboratory at the University of Bologna", 1915-1920.^[22]

At the dawn of the 20th century, Ciamician and Silber formed a very successful collaboration to systematically investigate photochemical reactivity (Figure 1). Their achievements surpassed all previous efforts, and virtually established the field of organic photochemistry as an independent field of research.^[1, 23] Over the next 15 years, they published 85 notes, papers and memoirs on the subject of photochemistry, in what was the first comprehensive study of light-mediated chemical reactivity.^[23-24]

1.1.2 Overview and background

Photochemistry can be defined as the branch of chemistry concerned with the physical and chemical change initiated by the absorption of light quanta (photons) by atoms and molecules.^[25] Two fundamental laws have been formulated for photochemistry; according to the Grotthus-Draper law, *only light that has been absorbed by the molecule can be effective in inducing chemical change in the system*. The Stark-Einstein law states that *every one photon that is absorbed will cause one chemical or physical reaction*.^[25] Accordingly, the absorption of a photon of light by a molecule leads to its transition from the electronic ground state to the excited electronic state. From the excited state, a number of processes can occur, most of which are photophysical processes, in which the chemical structure of the molecule remains unchanged, and some are photochemical processes,^[26] which lead to an array of chemical structural changes.

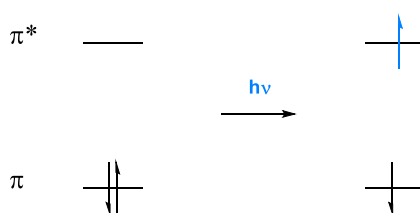


Figure 2. Schematic of molecular electronic excitation.^[27]

In a unimolecular process, chemical change can only occur from an excited state when the energy absorbed by the system exceeds the bond dissociation energy of the weakest bond in the molecule. Bond dissociation energies typically range from ca. 100 kJ/mol to 1072 kJ/mol,^[28] which can be translated into the correlating range of wavelengths 1200 – 110 nm in the electromagnetic spectrum. With these energies in mind, the determination can be made that UV light (10 – 400 nm), visible light (400 – 700 nm) and parts of infrared light (700 nm to 1 mm) will be suitable energy sources for photochemical transformations. In contrast to thermal reactions, which sometimes have to overcome large energy barriers, photochemical

reactions start from a high energy level, and can take an intrinsically complex reaction path.^[29]

While some substances, such as O₃ or NO₂ absorb visible light, most organic molecules only absorb in the ultraviolet region.^[25] As an example, absorption of UV light of the wavelength 254 nm can result in the $\pi \rightarrow \pi^*$ transition in buta-1,3-diene (corresponding to 471 kJ/mol) in a typical molecular excitation process (Figure 2).^[27] In this excitation of a multi-electron system, the total spin angular momentum of is conserved, which leads to a transition from a singlet ground state (S_0) to a singlet excited state (S_1). Transitions from S_0 to triplet states T_1 are “spin-forbidden”, which results in lower population of these events than singlet-singlet transitions. The excited state cannot persist indefinitely, and due to being unstable in respect to the ground state the lifetime of the excited state is short (typically between 10^{-9} and 10^{-6} s).^[29] In an unimolecular example in which no chemical reaction occurs, the electronically excited molecule can either undergo radiative transitions or non-radiative transitions. Radiative transitions result in the emission of radiation that is typically lower in energy than the one absorbed to reach the excited state (“vertical transitions”). As every closed shell molecule possesses a S_0 ground state, the most commonly observed emission results from the transition of the singlet excited state to the singlet ground state (i.e. $S_1 \rightarrow S_0$), called fluorescence. If the emission occurs from the triplet excited state to the singlet ground state, the process is termed phosphorescence (i.e. $T_1 \rightarrow S_0$). Non-radiative transitions involve conversions from one state to another state at constant energy (“horizontal transitions”). If the spin multiplicity of both states is identical, they are called internal conversion (IC). For conversions of different spin multiplicity, for example $S_1 \rightarrow T_1$, the term inter system crossing (ISC) is used (see Jablonski diagram, Figure 3).

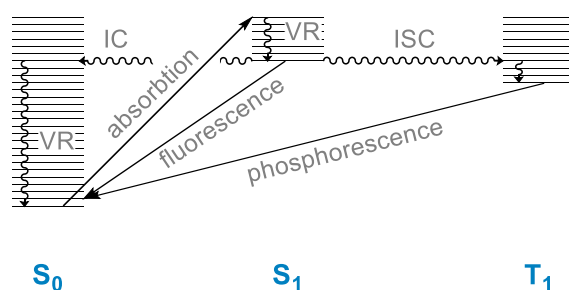


Figure 3. Jablonski Diagram. Radiative transitions are depicted as straight arrows, non-radiative transitions as wiggly arrows.^[27]

If the ISC is to a vibrationally excited electronic state, with some excess vibrational energy over the (vibrationless) T_1 level, a small amount of energy will be released via collisions with other molecules or solvent (vibrational relaxation, VR). Importantly, an excited molecule will

simply undergo de-excitation via radiation and return to its ground state, if no unimolecular chemical reaction can occur from the excited state.^[27] In contrast, in a bimolecular process, where a species interacts with the excited state molecule (typically called a quencher), a new pathway will now compete with radiative transitions back to the ground state. The photoexcited state can engage in bimolecular electron transfer and energy transfer reactions which are disfavored from the singlet ground state S_0 . This becomes most apparent in the ability of the species to act as a single electron donor or acceptor, and hence a reductant or oxidant. These processes result in emission quenching and are particularly important in the field of transition metal catalyzed, visible light mediated photochemistry. The bimolecular processes also enable facile detection of an excited state interacting with a potential quencher by simply observing if the amount of emission is diminished in the presence of the quencher.

An important practical aspect of photochemistry is the light source. In fact, the necessity of a devoted reactor and suitable light source still is the prime factor that photochemical reactions are oftentimes not considered for transformations on an industrial scale, if a thermal alternative is at all available.^[29] One of the oldest artificial light sources, incandescent lamps, emit light by heating a tungsten wire by conduction which is protected from oxidation by a gas filled or evacuated bulb. These lamps emit a continuous spectrum between 400 and 600 nm, in which most organic molecules do not absorb, and have no UV contribution. Thus, as UV-light is often required for classical photochemical applications, the most commonly used lamps are low-pressure mercury arc lamps. Arc lamps are ampoules containing a filling gas and electrodes at both ends. Light is produced by sending electrical discharge through the ionized gas or plasma, achieved by modulation of frequency or current. In the case of mercury, emission of light is caused by transition of the singlet (185 nm) and triplet (254 nm) state.

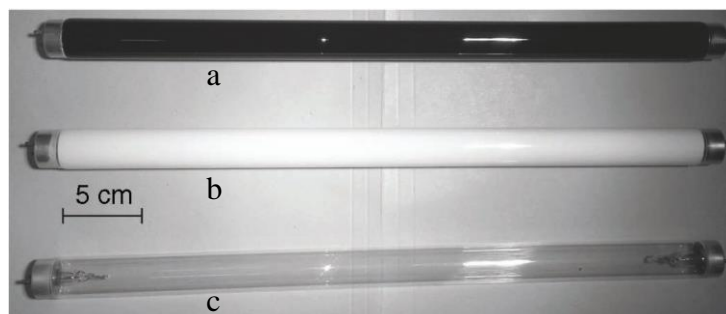


Figure 4. Low pressure mercury arc lamps. **a.** ‘black light’ (360 nm) **b.** phosphor-coated (305-310 nm) **c.** “germicidal lamp”, quartz, emitting 254 nm. Licensed reprint from Fagnoni *et al.*^[29]

As the 185 nm light is in almost all cases absorbed by mercury vapor itself, the architecture of the lamp, or the photochemical setup, Hg low pressure lamps are essentially monochromatic

sources of 254 nm light.^[29] This light is entirely absorbed by Pyrex and other laboratory glassware and only high purity quartz vessels can conserve the 254 nm emission. Arc lamps with phosphor coating on the inside ampule of the lamp are available to modulate emission (Figure 4). The coating absorbs the monochromatic 254 nm Hg-emission and emits longer wavelength light, in the case of a white phosphor UV-B (305 to 310 nm), or in case of a dark phosphor coating, “black-light” (350-370 nm). Due to self-absorption, mercury emission changes at higher pressures from monochromatic to longer-wave polychromatic. This is used in medium-pressure mercury arc lamps, which emit at 313, 366, 405, and 550 nm, with the 254 nm line diminished. Sodium arc lamps (589 nm) and XeCl excimer arc lamps (308 nm) are also commercially available, but have only niche use in photochemistry due to their wavelength or cost.

There are some obvious disadvantages when considering the use of UV-light, such as the necessary health and safety considerations, but also the prerequisite for dedicated, expensive quartz glassware and incompatibility of a broad range of functional groups and solvents due to their absorption of UV light. Thus, the interest in using visible light sources to drive chemical transformations, either via direct absorption, or via a mediator (sensitizer, *vide infra*) has sharply increased over the past three decades. To this end, visible light emitting household compact fluorescence light (CFL) bulbs have been used extensively in photochemistry (Figure 5, left). CFL bulbs are also mercury-containing arc-lamps, with a phosphor coating emitting in the visible spectrum, and have mostly replaced incandescent lamps for general illumination.

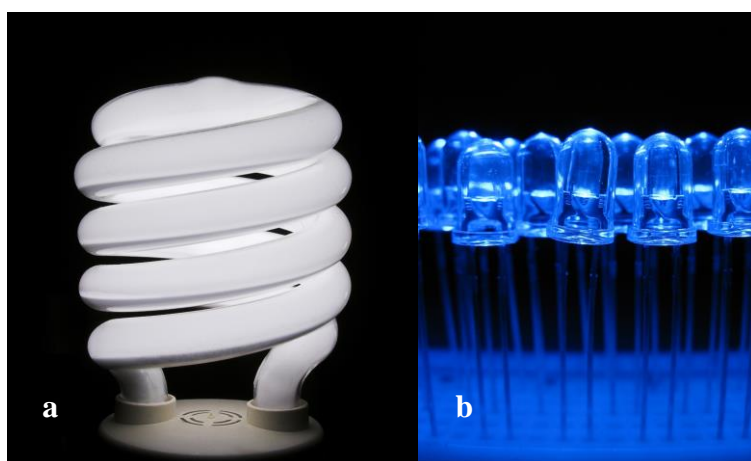


Figure 5. a. “Compact-Fluorescent-Bulb”.^[30] b. “Blue light emitting diodes over a proto-board”.^[31]

Arguably the most important light source for visible light photochemistry today are light emitting diodes (LEDs, Figure 5, right), semiconductors that emit an incoherent

electroluminescence over a short wavelength range.^[29] These relatively novel sources of light have been a transformative influence for the photochemical community, but also for general illumination over the last decade. While LEDs emitting in the UV are available (as low as 310 nm), they are suffering from low efficiency and high cost. LEDs are an excellent light source for the visible light range, with a ten-fold higher efficiency than for UV applications, low cost, and long lifetimes (10^4 h). There is a high availability of LEDs emitting on any wavelength in the visible range. LEDs are also of a large advantage due to their narrow emission window, inherently focused emission, and robustness, and due to their ease of use the number of their photochemical applications has increased sharply over the last decade.

1.1.3 Photoredox catalysis

In the last decades the synthetic community has witnessed the revival of photochemistry due to the novel approach of visible light photoredox catalysis, which has also reignited the interest in radical and single-electron-transfer (SET) processes. This mode of catalysis relies on the capability of light-absorbing catalysts, such as polypyridyl metal complexes and a number of organic dyes,^[32] to undergo photoexcitation with visible light and subsequently engage in SET or energy-transfer processes with organic substrates.^[33]

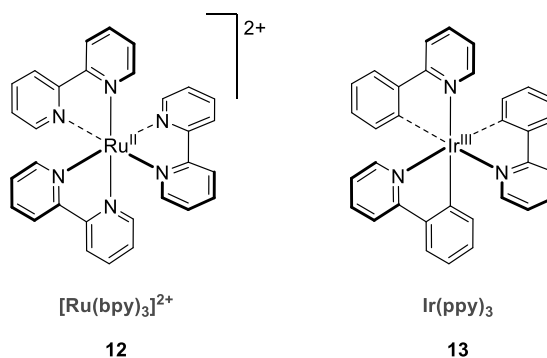
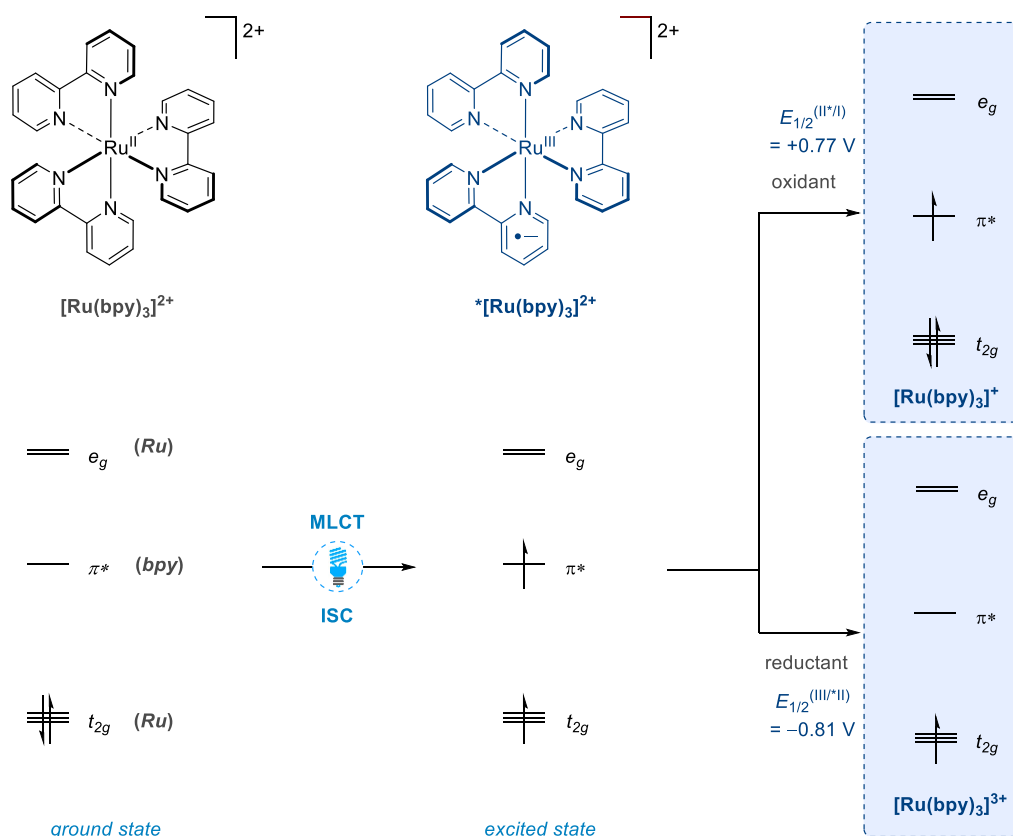


Figure 6. Common photoredox catalysts [Ru(bpy)₃]²⁺ and Ir(ppy)₃.

Commonly employed visible light photocatalysts are iridium and ruthenium polypyridyl complexes, due to their favorable absorption in the visible range, bench stability, and long lived excited state,^[34–35] for example, lifetimes of 1100 ns for [Ru(bpy)]²⁺ (**12**),^[36] and 1900 ns for *fac*-Ir(ppy)₃ (**13**, Figure 6).^[37] Common photoredox catalysts typically rely on the absorption of blue or green ($\lambda = 450 - 550$ nm) light to access high energy states. The relatively stable, long-lived photoexcited states can then evoke bimolecular electron transfer reactions, albeit in competition with other deactivation pathways. While the chemically inert ground state species of these complexes are poor single-electron oxidants and reductants, the

respective excited states can be remarkably potent SET reagents. This dual-character of photoredox catalysts enables powerful oxidative and reductive processes to occur concurrently in the same vessel via a redox-neutral catalytic cycle. This forms the basis of the exciting manifold of novel reactivity that has been achieved through photoredox chemistry, featuring astounding catalytic electron transfer cycles in high chemoselectivity initiated by simple, inexpensive household lights under mild chemical conditions.^[33]

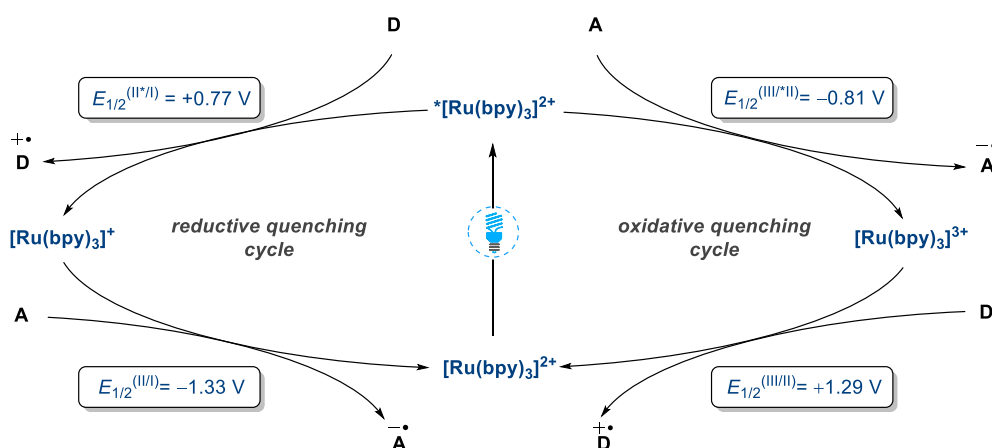
Mechanistically, exemplified by $[\text{Ru}(\text{bpy})_3]^{2+}$, the excitation process constitutes a metal to ligand charge transfer (MLCT) between the central Ru^{II} atom and the 2',2'-bipyridine ligand-sphere (Scheme 2). Thus, upon absorption of a visible light photon, an electron of the catalysts metal-centered t_{2g} orbitals is promoted into a ligand-centered π^* orbital,^[38] resulting in an oxidized Ru^{III} central metal and a ligand sphere that has undergone single electron reduction.^[39] The initially formed singlet MLCT state then undergoes rapid inter system crossing (ISC) to the respective triplet MLCT state. The transition of the triplet MLCT state back to the ground state is spin forbidden, which causes the species to exhibit a sufficiently long lifetime to engage in bimolecular electron transfer.



Scheme 2. Simplified molecular orbital depiction of $[\text{Ru}(\text{bpy})_3]^{2+}$ photochemistry.^[33-34]

Due to the nature of the photocatalyst's photoexcited state, a high energy electron is available in the ligand sphere. This electron is readily available for transfer to substrates, rendering the

photocatalyst a reductant. At the same time, the electron “hole”, which is created in the t_{2g} orbital via excitation (Scheme 2), is low in energy and can be filled by an electron transferred to the system, establishing the oxidizing properties of the excited state. The propensity of a species to undergo oxidation or reduction can be described by their respective half-wave reduction potentials ($E_{1/2}^{\text{red}}$). In the case of the excited state $^*[\text{Ru}(\text{bpy})_3]^{2+}$, the reduction potential for the half reaction $\text{Ru}^{\text{III}} \rightarrow ^*\text{Ru}^{\text{II}}$ is $E_{1/2}^{\text{III/II}^*} = -0.81 \text{ V}$ (vs saturated calomel electrode, SCE),^[40] which shows that the excited state is a much stronger reductant than the ground state, $E_{1/2}^{\text{III/II}} = +1.29 \text{ V}$. Similarly, the reduction potential for the half reaction $^*\text{Ru}^{\text{II}} \rightarrow \text{Ru}^{\text{I}}$ of $E_{1/2}^{\text{II}^*/\text{I}} = +0.77 \text{ V}$ (vs SCE) demonstrates that $^*[\text{Ru}(\text{bpy})_3]^{2+}$ is significantly more oxidizing than the ground state, $E_{1/2}^{\text{III/I}} = -1.33 \text{ V}$ (vs SCE). Depending on whether the excited state photocatalyst first undergoes oxidation or reduction, via interaction with a reaction partner (quencher), the resulting catalytic cycles are termed oxidative quenching cycle, or reductive quenching cycle, respectively (Scheme 3).

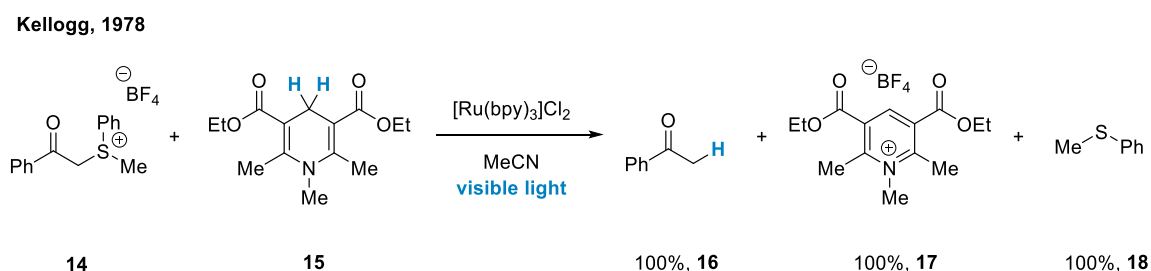


Scheme 3. Oxidative and reductive quenching cycles of $[\text{Ru}(\text{bpy})_3]^{2+}$.

1.1.4 Photoredox catalysis – From early work to recent developments

While the respective iridium and ruthenium polypyridyl complexes were originally used for water-splitting, as early as in the 1970s,^[41] their extended use in organic photochemical transformations has only emerged relatively recently. Photoredox chemistry was pioneered in early (1978 - 1993) examples by Kellogg,^[42-43] Deronzier,^[44-46] and Okada,^[47-49] and was further established in the 2000's most notably by MacMillan, Yoon, and Stephenson, and complemented recently by developments using organic chromophores by Nicewicz.^[32] As a result of this research, a myriad of novel visible light-mediated technologies have emerged.^[50]

In 1978, Kellogg and co-workers investigated the reduction of sulfonium salts and activated halides by 1,4-dihydropyridines (Hantzsch Esters),^[42-43] which led to the serendipitous observation that the reduction of methylphenacylphenylsulfonium tetrafluoroborate **14** with Hantzsch Ester **15** would not proceed if the reaction mixture is placed inside a UV spectrometer. It was suspected that room-lighting would be involved in the reaction. Further studies confirmed that the reaction could be carried out by irradiation with a light bulb much more efficiently compared to the “thermal protocol”, which often was also induced by low-level light. Indeed, the reaction would not take place if set up in a dark room under red light. Remarkably, Kellogg and co-workers reasoned that due to the small absorption band of Hantzsch Ester **15** in the visible region, the reaction could be improved via the addition of sensitizers. Employing catalytic levels of tetraphenylporphyrine and Eosin disodium salt gave significant increase in reaction rate. Most strikingly, upon the addition of $[\text{Ru}(\text{bpy})_3]\text{Cl}_2$, a reduction of the reaction half-time, from $t_{1/2} = 48$ h under normal irradiation, to $t_{1/2} = 18$ min was observed in the presence of photocatalyst.

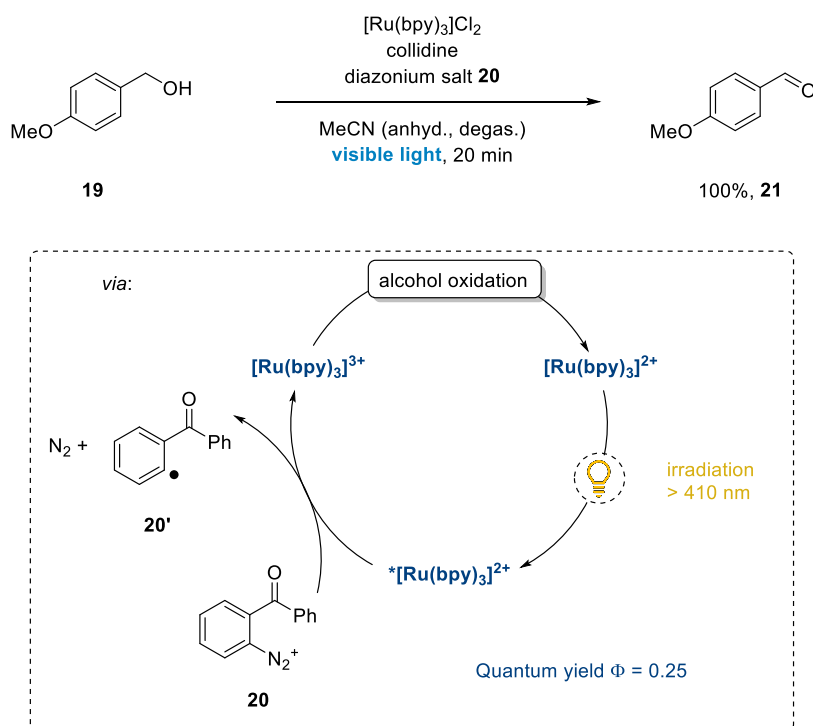


Scheme 4. Kellogg’s photocatalytic reductive desulfuration.

Following Kellogg’s seminal report, Tanaka reported $[\text{Ru}(\text{bpy})_3]\text{Cl}_2$ catalyzed 1-benzyl-1,4-dihydronicotinamide (BNAH) reductions of benzyl bromide^[51] and benzoquinones,^[52] and a $[\text{Ru}(\text{bpy})_3]\text{Cl}_2$ catalyzed 9,10-dihydro-10-methylacridine reduction of phenacyl halides.^[53] In addition, Pac and co-workers also published a series of reports on similar dihydropyridine- $[\text{Ru}(\text{bpy})_3]\text{Cl}_2$ catalyzed reductive systems for a variety of substrates.^[54-58]

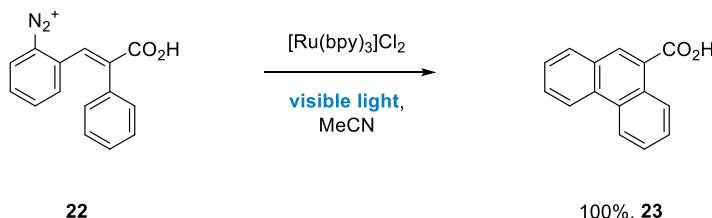
An early example of a transition metal catalyzed reaction featuring an oxidative quenching cycle was reported by Deronzier in 1984 (Scheme 5).^[44] The photocatalyzed redox reaction was able to efficiently oxidize benzylic carbinols **19** to their respective aldehydes **21** using aryl diazonium salts **20** as oxidant. The reaction required collidine (2,4,6-trimethylpyridine) to proceed and gave good aldehyde yields for electron rich benzylic carbinols.

Deronzier, 1984

**Scheme 5.** Deronzier's photo-oxidation of benzylic carbinols.

The Deronzier group later published another example of the use of transition metal photocatalysis^[45-46] with a study of phenanthrene (**23**) generation from aryl diazonium salts (**22**) via a photoinduced Pschorr reaction (Scheme 6).^[59] Deronzier conducted extensive mechanistic studies, including Stern-Volmer quenching studies, in order to determine the mechanism of the reaction. It was concluded that electron transfer from the excited photocatalyst is most likely occurring, while a possible energy transfer pathway was not entirely rejected.

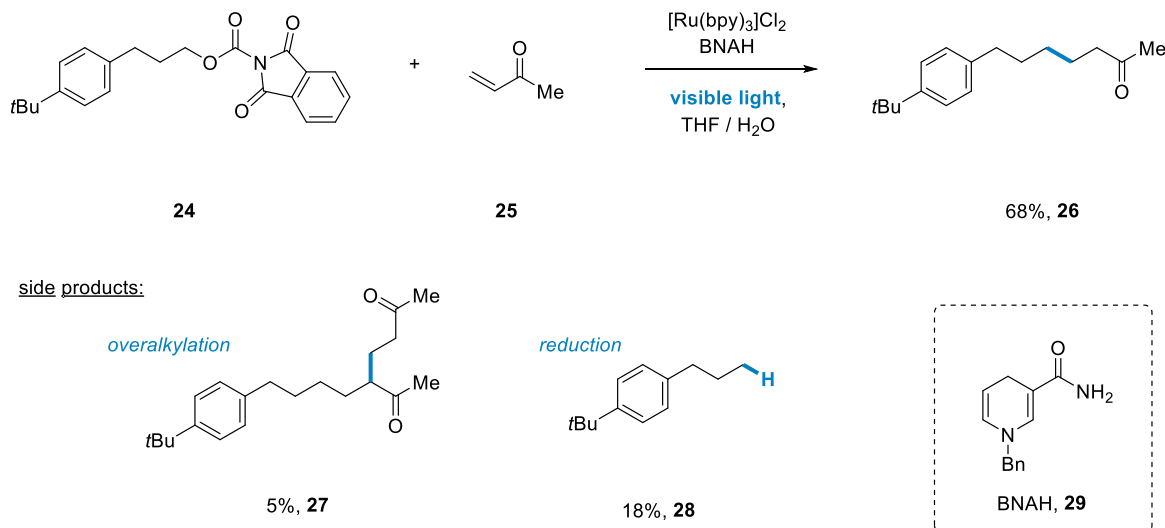
Deronzier, 1984

**Scheme 6.** Deronzier's photocatalytic Pschorr reaction.

Arguably one of the most important, early reports of modern photoredox chemistry, and the first example of an intermolecular photoredox coupling, was disclosed in 1991 by Okada and Oda.^[47] A novel radical addition methodology was developed by using a combination of $[\text{Ru}(\text{bpy})_3]\text{Cl}_2$, a radical precursor bearing a *N*-(acyloxy)phthalimide (**24**), and 1-benzyl-1,4-

dihydronicotinamide **29** as terminal reductant (Scheme 7). Irradiation was achieved by use of a 500 W Xenon lamp ($\lambda > 460$ nm).

Okada and Oda, 1991

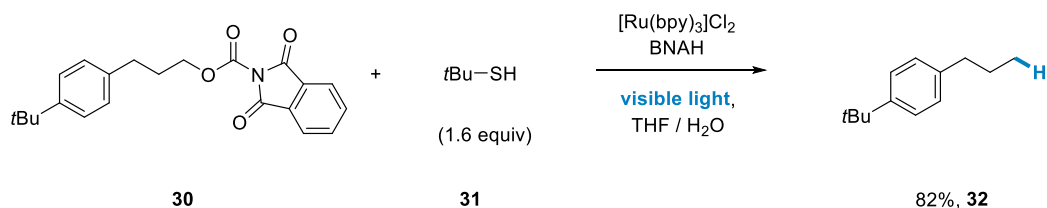


Scheme 7. Okada and Oda's photosensitized decarboxylative radical addition.

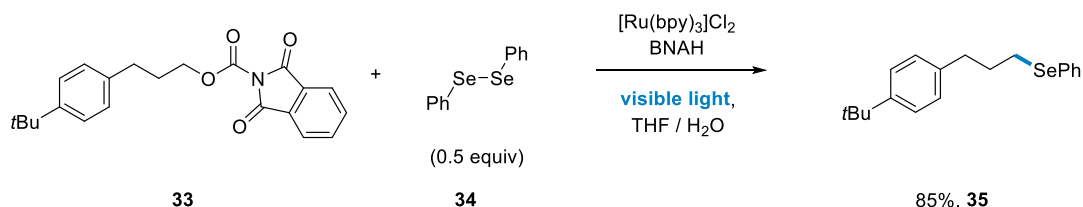
Okada and co-workers found that photocatalytic decarboxylation of **24**, with formation of phthalimide and carbon dioxide, furnished a carbon centered radical, which was available for addition into radical acceptors, such as methyl vinyl ketone (**25**) (Scheme 7), 2-cyclopentanone and methyl acrylate, to form e.g. addition product **26**. Aqueous THF was found to be a suitable solvent for the reactions. Small amounts of side products were formed, such the reduced hydrocarbon **28**, resulting from the reaction of BNAH with the alkyl radical, and low amounts of overalkylation product **27** were observed. Notably, the quantum yield of the experiments was over unity ($\Phi = 1.3$ for the shown transformation), providing evidence for a radical chain process operating. This seminal study showed that *N*-(acyloxy)phthalimides can be used as convenient alkyl radical precursors.

Furthermore, Okada utilized the photocatalytic activation of these redox-active esters for a number of subsequent transformations, including chlorination (under UV light),^[60] reduction,^[48] and phenylselenenylation (Scheme 8).^[49] Okada's reports were the first instance of a general photoredox substrate activation strategy and showed the great potential of the area of visible light mediated catalysis. However, the field remained out of focus of the synthetic community for more than 15 years.

Okada and Oda, 1992

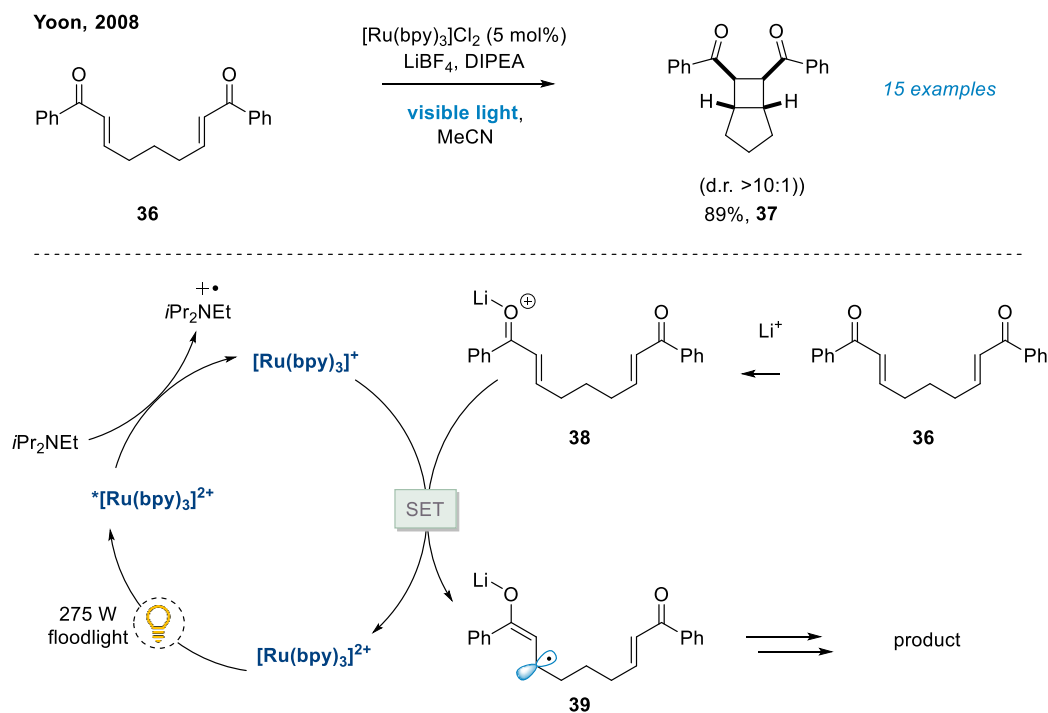


Okada and Oda, 1993



Scheme 8. Okada's photocatalytic reductive decarboxylation and decarboxylative phenylselenenylation of *N*-acyloxyphthalimides.

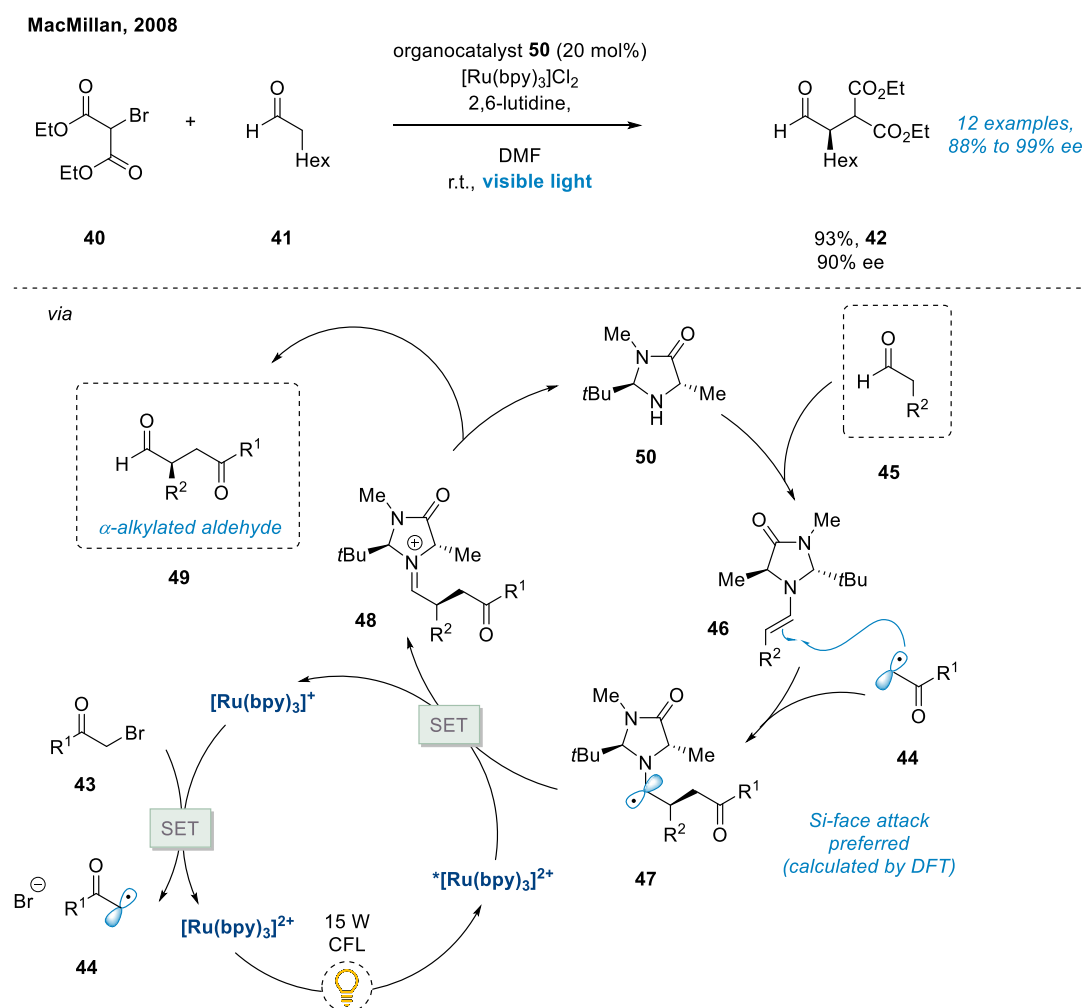
The first of three significant, more recent, reports was Yoon's disclosure of a photoredox catalyzed intramolecular [2+2] cycloaddition of enones in 2008.^[61] On the basis of Krische's report of single-electron induced cobalt and copper catalyzed [2+2] cyclization of bis(enones) **36**,^[62–66] Yoon and co-workers speculated that this cycloaddition might also be initiated by a photocatalytically generated photoexcited reductant, such as $^*[\text{Ru}(\text{bpy})_3]\text{Cl}_2$ (Scheme 9).



Scheme 9. Yoon's visible light photocatalytic [2+2] enone cycloaddition.

Under irradiation with a 275 W floodlight, and Lewis-acid activation, the reaction was achieved with a variety of substrates with excellent stereoselectivity (4:1 to >10:1 d.r.) and in high yields (54% to 98%). Due to the absence of conversion in the absence of DIPEA, even with elevated amounts of $[\text{Ru}(\text{bpy})_3]\text{Cl}_2$, a reductive quenching cycle is proposed (Scheme 9). First, the excited state $[\text{Ru}(\text{bpy})_3]\text{Cl}_2^*$ undergoes reductive quenching with the amine, generating the amine radical cation, and the reducing $[\text{Ru}(\text{bpy})_3]^+$ species ($E_{1/2}^{\text{II/I}} = -1.33 \text{ V}$ vs SCE). Subsequent reduction of the activated aryl enone **38** by $[\text{Ru}(\text{bpy})_3]^+$ generates the alkyl radical **39**, from which cyclization to the products (**37**) occurs. Notably, the reaction could also be conducted using sunlight as the sole light source. Yoon and co-workers later suggested a chain propagation mechanism for the reaction.^[67]

Almost simultaneously, MacMillan and co-workers published their seminal work on the photocatalytic asymmetric α -alkylation of aldehydes.^[68] The work combined, for the first time, the advantages of organocatalysis and photoredox through use of a dual catalytic processes (Scheme 10).

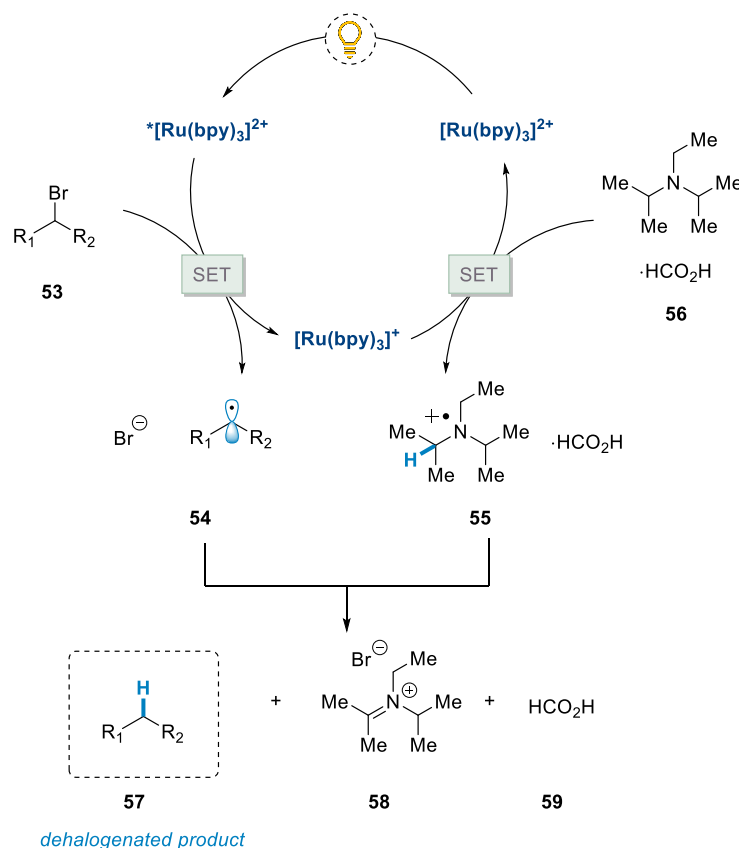
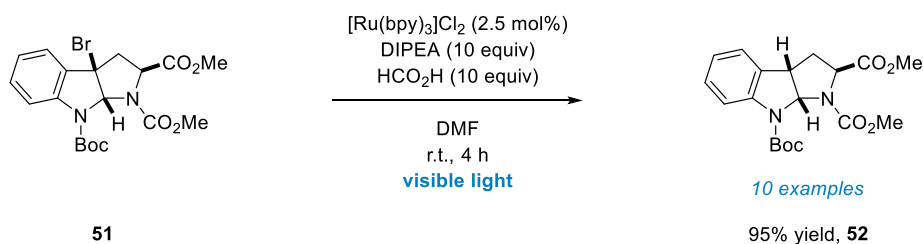


Scheme 10. MacMillan's direct asymmetric alkylation of aldehydes with mechanistic proposal.

MacMillan reported the efficient transformation to this product class using convenient and inexpensive irradiation with a household 15 W fluorescent light bulb (CFL bulb). The organocatalyst **50**, a derivative of which has been used in α -oxidation of aldehydes,^[69] was based on a design from prior work in the MacMillan group.^[70-72] It was selected for its excellent levels of kinetic enantiocontrol while not participating in enamine formation with the 2,2'-disubstituted aldehyde alkylation product. This transformation enabled access to a variety of chiral α -alkylated aldehydes in high yields (63% to 93%) and high enantiomeric excess (88% to 99%). The reaction employs $[\text{Ru}(\text{bpy})_3]\text{Cl}_2$, which leads to generation of alkyl radical **44** from the respective halide **43** and oxidation of α -amino radical **47** to the respective iminium ion **48**. At the same time, an organocatalytic cycle generates a chiral enamine **46**, which can be trapped by the alkyl radical **44**, leading to α -amino radical **47**. Following oxidation, hydrolysis of the iminium ion **48** regenerates the organocatalyst and the product, enantioenriched α -alkylated aldehydes (**49**). A chain propagation mechanism was later proposed for the reaction by Yoon and co-workers.^[67]

Moreover, in 2009, Stephenson and co-workers reported the visible light mediated reductive dehalogenation of an alkyl halide, without the use of toxic tin-reagents.^[73] The reaction uses $[\text{Ru}(\text{bpy})_3]\text{Cl}_2$ as a photocatalyst, an excess of DIPEA and either Hantzsch Ester or formic acid to convert a number of activated alkyl halides via efficient reductive dehalogenation. Mechanistically, it was proposed that reductive quenching of the $\text{Ru}(\text{II})^*$ species by the ammonium formate complex **56** gives the strongly reducing $\text{Ru}(\text{I})$ species and the radical cation of the ammonium formate complex **55**. Subsequent reduction of the alkyl halide **53** by $[\text{Ru}(\text{bpy})_3]^+$ furnishes the alkyl radical **54** which in turn undergoes hydrogen atom transfer (HAT) with the radical cation **55** of the amine base via abstraction of hydrogen atoms from either of the methine positions, forming dehalogenated product **57** (Scheme 11). The reaction is tolerant to a number of functional groups, such as free hydroxyls, olefins, alkynes, aryl bromides and iodides, silyl ethers, and carbamates. In addition to its favorable selectivity the reaction is high yielding (79% to 99% yield) and can be carried out with a simple 14 W CFL bulb. Stephenson and co-workers conducted a series of reactions to probe the mechanism. When deuterated triethylamine ($d_{15}\text{-NEt}_3$) was used instead of DIPEA, the reaction gave low yield with no deuterium incorporation. Studies with deuterated formic acid confirmed DIPEA as the hydrogen atom source in the reaction. Finally, a radical clock experiment gave evidence for the presence of the alkyl radical.

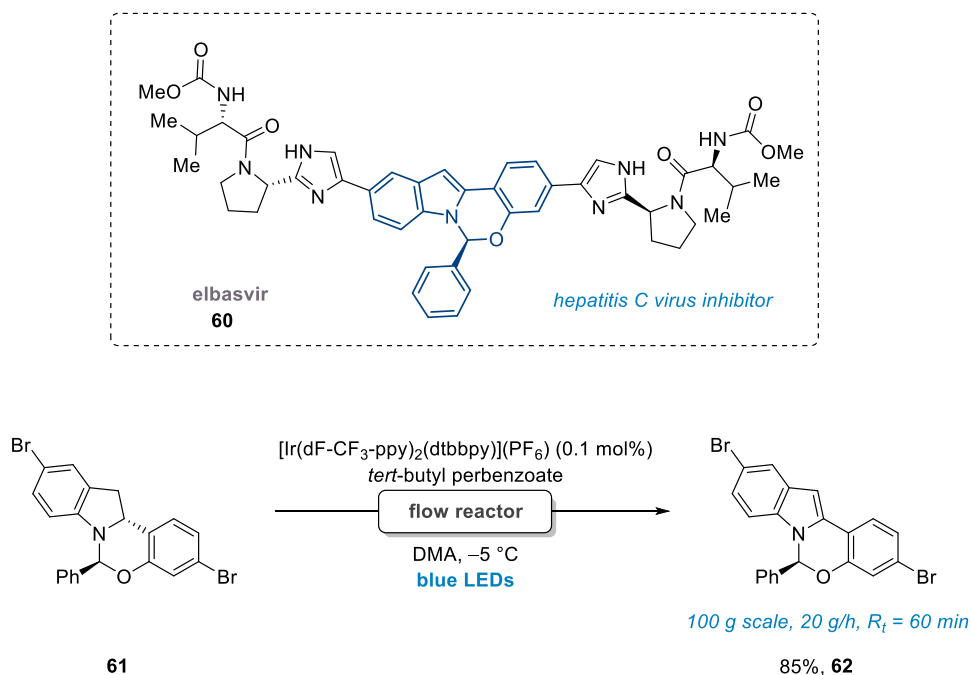
Stephenson, 2009

**Scheme 11.** Stephenson's tin free reductive dehalogenation with proposed mechanism.

The seminal reports of Yoon, MacMillan and Stephenson showcased the synthetic utility, operational convenience and benign conditions of photoredox reactions. Photoredox catalysis has since risen to the forefront of synthetic organic chemistry and has become an indispensable tool for many transformations.^[74] A plethora of novel photoredox catalysts with easily modifiable electronic properties^[75] allowed for new transformations, and enabled the discovery of a myriad of novel methodologies.^[50] A considerable interest in single-electron chemistry has re-emerged in the wake of this development, and led to the development of cooperative catalysis stemming from classic transition-metal catalyzed reactivity coupled with photoredox systems to achieve novel transformations.^[76-78] The unique possibility of employing excited-state photocatalysts simultaneously as reductant and oxidant has largely contributed to this surge of unprecedented reactivity.^[74]

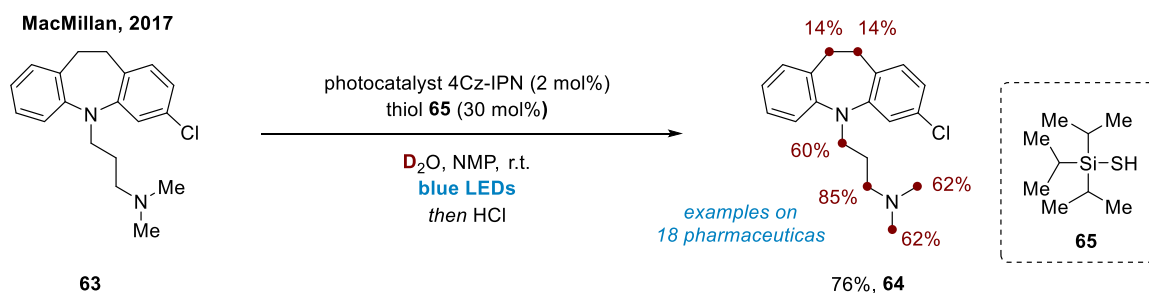
Underpinning the success of this new field, industry has developed several large-scale photochemistry flow platforms,^[79] for the late-stage drug modifications as well as for the generation of key synthetic intermediates.^[74] In particular, Merck have established this approach, demonstrated by DiRocco and co-workers, showing the direct photoredox C–H functionalization of biologically active heterocycles,^[80] many of which are pharmaceutical and agrochemical agents.

DiRocco and Knowles, 2016



Scheme 12. DiRocco and Knowles' photocatalytic indoline dehydrogenation for the synthesis of elbasvir.

In a collaboration with Knowles and co-workers, a photocatalytic indoline dehydrogenation was subsequently reported as key step for the synthesis of elbasvir **60**,^[81] an inhibitor of the hepatitis C virus NS51 protein, which has been clinically studied as highly effective oral regimen for the treatment of hepatitis C virus infection (Scheme 12). The transformation could formerly only be conducted with KMnO_4 as an oxidant without eroding the hemiaminal stereocenter, however this was problematic due to purification issues and detrimental environmental impact due to generated amounts of MnO_2 on large-scale. The photoredox alternative was developed using high-throughput screening, and identified photocatalyst $[\text{Ir}(\text{dF-CF}_3\text{-ppy})_2(\text{dtbbpy})](\text{PF}_6)$ and *tert*-butylperbenzoate as the optimal catalyst/oxidant combination. On a Merck in-house flow reactor, ~100 g of indoline product **62** could be processed over a short period of time (5 hours) in high yield and without the loss of optical purity. The highly efficient process showcases the utility of photoredox chemistry as a novel tool for catalysis on process-relevant scales.



Scheme 13. MacMillan's photoredox-catalyzed deuteration and tritiation (not pictured) of pharmaceutical compounds.

Another recent example of the development of pharmaceutical highly valuable methods through photoredox chemistry is MacMillan's report of the photoredox catalyzed deuteration of pharmaceutical compounds.^[82] Deuterated versions of existing drugs are an important and growing field interest due to their improved pharmacokinetics or toxicological properties, often due to the stronger deuterium-carbon bond altering their metabolism.^[83] A combination of photocatalyst [1,2,3,5-tetrakis(carbazol-9-yl)-4,6-dicyanobenzene] (4Cz-IPN, $E_{1/2}^{red}$ (4Cz-IPN⁻/4Cz-IPN) = +1.21 V vs SCE),^[84] thiol **65**, D_2O and blue light-irradiation allows selective deuteration (and tritiation, with T_2O respectively) of α -amino sp^3 C–H bonds (Scheme 13). With heavy water as convenient deuterium source, this operationally simple single step procedure has been demonstrated on 18 pharmaceutical compounds.

1.1.5 Photoredox catalysis in natural product synthesis

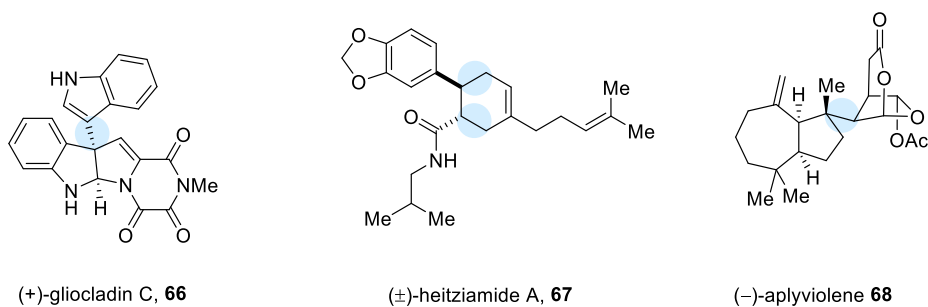
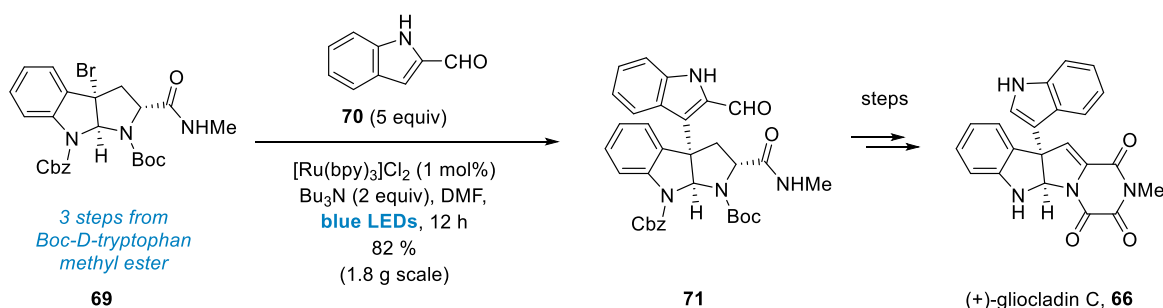


Figure 7. Examples of key bonds formed in natural products via photoredox catalysis.

Given the success of the photoredox catalysis, it is maybe unsurprising that a series of novel photoredox reactions have been exploited in the context of natural product synthesis.^[85] Key bond-forming photoredox transformations have been used for a number of natural product syntheses in the recent years, exemplified by complex scaffolds such as (+)-gliocladin C, (±)-heitziamide A, and (-)-aplyviolene (Figure 7).

In 2011, Stephenson and co-workers disclosed their total synthesis of (+)-gliocladin C (**66**),^[86] a natural product which is part of a class of alkaloids formally derived from two units of tryptophan. In line with the group's prior work on the dehalogenation of bromopyrroloindolines,^[73] the synthesis featured a visible light mediated photoredox coupling of pyrroloindolines with indoles. In the key step of the synthesis, an alkyl radical was generated from bromopyrroloindoline **69** and coupled with indole-2-carboxaldehyde **70** under irradiation of blue LED using photocatalyst $[\text{Ru}(\text{bpy})_3]\text{Cl}_2$. A five-fold excess of the coupling partner was necessary to preclude reductive dehalogenation. The addition of tributylamine as stoichiometric reducing agent proved slightly superior to triethylamine, and yielded the desired product **71** in 82% yield on gram-scale exclusively via desired C3' addition (Scheme 14).

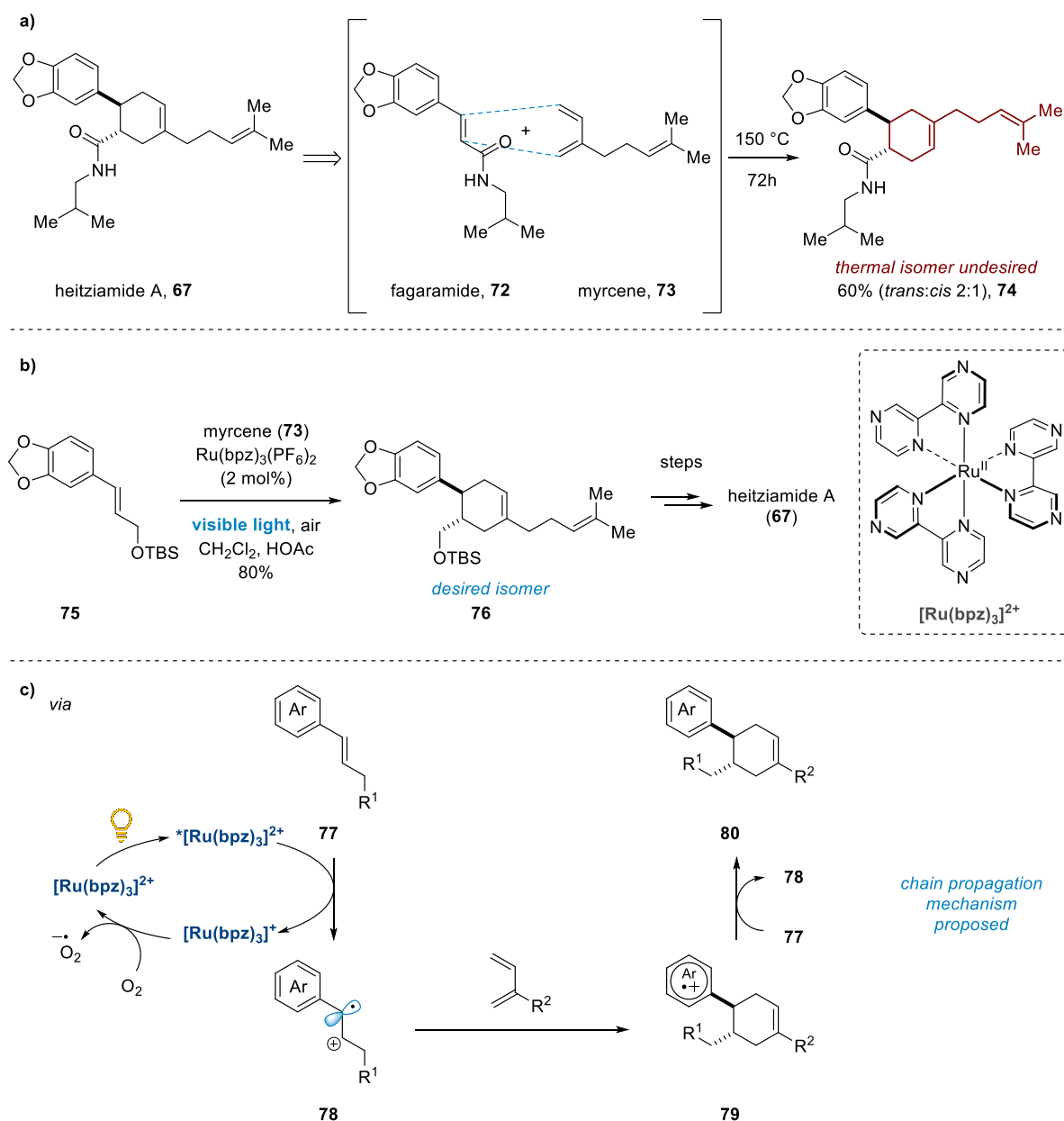


Scheme 14. Photocatalytic key step in Stephenson's total synthesis of (+)-gliocladin C.

In their 2011 synthesis of (\pm)-heitziamide A (**67**),^[87] Yoon and co-workers elegantly demonstrated the utility of a photoredox process to oxidize electron-rich dienophiles via SET to generate cationic radical intermediates, which readily underwent [4+2]-cycloaddition reactions, notably in opposite regioselectivity than the corresponding thermal Diels-Alder reaction. Key to the success was the use of ligand-modified ruthenium complex $[\text{Ru}(\text{bpz})_3]^{2+}$,^[88] which, in contrast to $[\text{Ru}(\text{bpy})_3]^{2+}$, was able to directly oxidize the dienophiles with only air as co-oxidant through a proposed reductive quenching cycle, owing to its slightly greater excited state reduction potential ($E_{1/2}^{\text{red}} = \text{up to } +1.4 \text{ V vs SCE}$) (Scheme 15b).

While the thermal reaction between fagaramide (**72**) and myrcene (**73**) yielded the undesired regioisomer **74** (Scheme 15a), Yoon and co-workers commenced their concise synthesis from electron rich dienophile **75** (Scheme 15b). Under the reaction conditions, desired regioisomer **76** was formed in a facile fashion in good yield, which could be elaborated to the natural product **67** in a series of standard operations (4 steps). In the proposed mechanism the electron-rich dienophile **77** is first oxidized to the its radical cation **78** by the photocatalytic

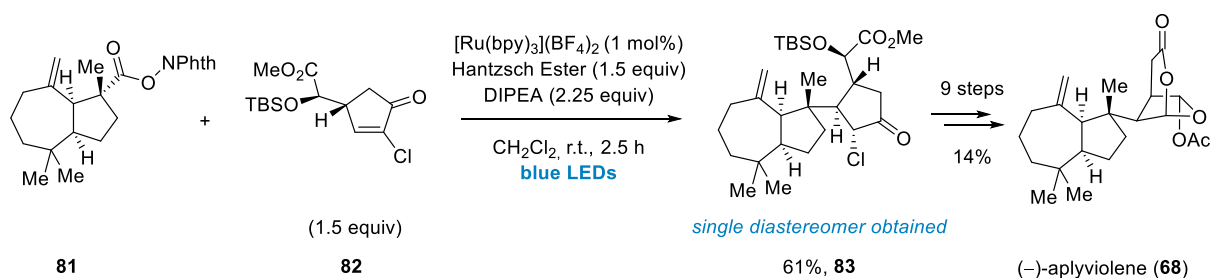
system. Yoon and co-workers hypothesized that a chain-propagation mechanism is operative, in which, after the radical cycloaddition step, the aryl radical cation **79** is quenched by starting dienophile **77** (Scheme 15c). Finally, the role of oxygen in the photocatalytic step has been determined to be the facilitation of catalyst turnover, since reactions conducted in degassed solvents, in the absence of air, give cycloadduct but will not proceed to the product.



Scheme 15. Yoon's total synthesis of (±)-heitziamide A.

In 2012, the Overman group reported their synthesis of the diterpene natural product (–)-aplyviolene (**68**) via a visible light-mediated tertiary radical conjugate addition strategy.^[89] This was the second generation approach by Overman and co-workers after the group had achieved the first total synthesis of (–)-aplyviolene in 2011.^[90] After difficulties in

forming the critical key quaternary carbon stereocenter,^[91] a radical addition strategy was chosen. Inspired by Okada's early work^[47] on fragmentation of *N*-(acyloxy)phthalimides, Overman opted to utilize a visible light mediated radical addition, employing *N*-(acyloxy)phthalimide **81** as radical precursor, and chiral alkene **82** as radical acceptor (Scheme 16). Notably, the *N*-(acyloxy)phthalimide **81** was readily obtained from the corresponding carboxylic acid.



Scheme 16. Photocatalytic key step in Overman's second generation synthesis of (-)-aplyviolene.

The reaction was first attempted under Okada's initial conditions, in THF/H₂O, which resulted in product formation, favorably as a single diastereomer, albeit in low yield due to hydrolysis and dehalogenation byproducts. After optimization, anhydrous conditions yielded the product **83** in an improved yield of 61% with only minor contamination of reductively dechlorinated byproduct. This vastly improved synthesis of key intermediate **83** enabled synthesis of the natural product **68** via Overman's established route. Importantly, other avenues of generation of the tertiary alkyl radical, such as from bromide or iodide precursors, and Barton esters were found to be unsuitable for the transformation, showcasing the benign conditions for radical generation in photoredox catalysis can enable priorly inaccessible radical chemistry to elegantly solve this synthetic challenge.

1.2 Amine synthesis and functionalization via photoredox catalysis

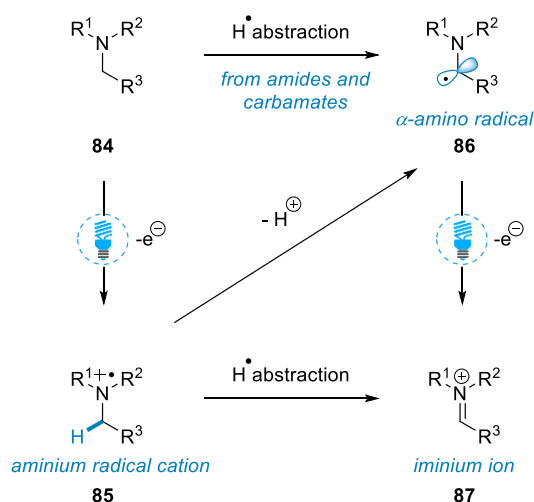
1.2.1 Background

Since the revival of photoredox catalysis by the reports of Yoon, MacMillan and Stephenson in 2008 and 2009, the chemistry of amines has been intimately connected to this re-emerging field.^[61, 68, 73, 92] Starting from early work in the field of photoredox methods, trialkylamines are used as inexpensive reductants, to drive photocatalytic turn-over.^[93] Like most organic compounds, amines do not absorb visible light unless they feature a suitable chromophore, such as highly conjugated π -bond systems. Therefore, the photoredox catalyst has to engage in single electron transfer (SET) events with the amine, so that redox processes can be initiated. Amines are thus classically used as electron donors, quenching the photoexcited state of the catalyst, generating the respective aminium radical cation.

Early use of this concept aimed at accessing a more highly reducing photocatalyst intermediate, enabling more potent reductions to be carried out. However, the use of amines in the last decade has shifted from their employment as mere reductive additives to their use as complex substrates and intermediates in a variety of photoredox transformations, including natural product applications.^[93] Under photoredox conditions, the number of reaction pathways available to amines is vast, and can range from single-electron oxidation, C-H abstraction, deprotonation and β -scission to the formation of highly reactive intermediates such as α -amino radicals and iminium ions. Furthermore, due to the ubiquity of the amine functional group in alkaloids, pharmaceuticals and agrochemicals, the transformations of amines and thus the synthesis of new, complex amine derivatives have become a focal point of interest for the synthetic community.

1.2.2 Amine reactivity

The reactivity of the oxidation product, the aminium radical cation, can be explained by means of a simple trialkylamine example (Scheme 17). Single electron oxidation of triethylamine to the radical cation requires a reduction potential of $E_{1/2}^{\text{red}} = 0.83 \text{ V}$ vs SCE,^[94] and leads to dramatic acidification of the α -amino C-H bond, lowering the bond dissociation energy (BDE) of the α -amino C-H bond from 90.7 kcal/mol to an estimated ~42 kcal/mol.^[93] The oxidation accordingly entails a change of pK_a of the α -amino proton from $pK_a = \geq 40$ to an estimated $pK_a = \sim 14.7$. This remarkable activation can lead a number of subsequent mechanistic pathways.



Scheme 17. Reactivity of amines under photocatalytic conditions.^[93]

Direct oxidation of the starting amine **84** by the photocatalytic system furnishes the aminium radical cation **85**. In contrast, direct abstraction of a hydrogen atom from starting amine **84** can lead to α -amino radical **86**, a highly reactive nucleophilic open shell species. Both the aminium radical cation (**85**) and the α -amino radical **86** can easily be converted to the iminium ion **87**, by hydrogen atom abstraction of the α -amino-C–H or photocatalytic one electron oxidation respectively. Lastly, via simple deprotonation of the acidic α -amino proton, the aminium radical cation can form the α -amino radical **86**. Given the ubiquity of the use of tertiary amines in photoredox chemistry, and the interchangeable nature of the involved amine derived species, it is apparent that the α -amino radical and the iminium both have unique importance in photoredox chemistry as reactive intermediates. Moreover, α -amino alkyl radicals are more easily oxidized than the starting amines, and thus convert rapidly to the respective iminium ion if an excess amount of oxidant is present.^[95] Notably, it should be considered that the aminium radical cation can also undergo a common non-productive process, called back electron transfer reaction, in which the radical cation accepts back one electron from the reduced photocatalyst. This major side reaction is competing against other productive downstream reactions. However, this problem can be circumvented via both photocatalyst and reaction design. Common photoredox catalysts today are intrinsically designed to somewhat mitigate back electron transfer reactions by employing ligands to retard this side reaction.^[96-97] However, reaction design must ensure suitable and rapid downstream pathways are available, such as hydrogen atom abstraction via a good hydrogen atom acceptor.

A less common pathway for the aminium radical cation is β -scission. In this process, the amine radical cation undergoes cleavage of the β -amino C–C bond, leading to concomitant formation of both an iminium ion and α -amino radical (Scheme 18). There are a number of literature examples when this photoinduced process has been exploited in a synthetic fashion.^[93, 98-99]

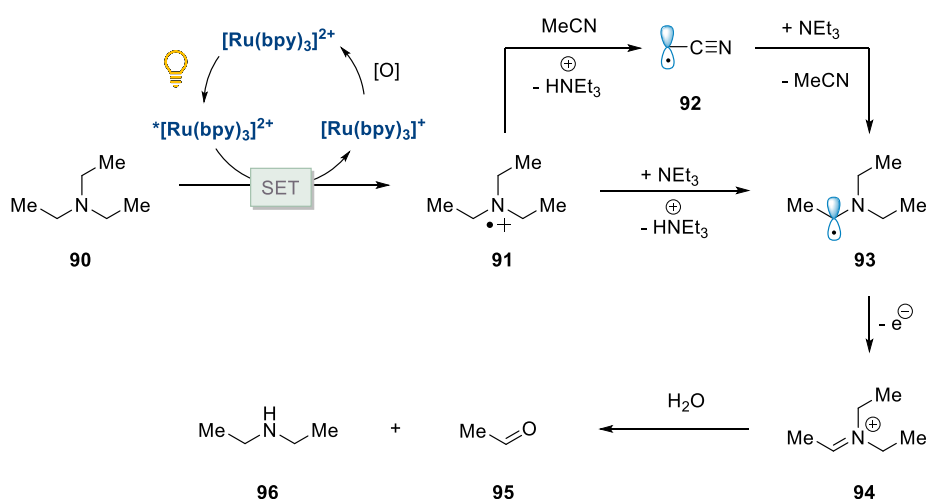


Scheme 18. β -scission of aminium radical cations.

1.2.3 Functionalization of iminium ions

Conversion of amines into their respective, highly electrophilic iminium ions via visible light catalysis is a powerful synthetic method.^[92] In 1980, early studies by the Whitten group explored the conversion of triethylamine to iminium ions (Scheme 19).^[97] Irradiation of triethylamine **90** in the presence of ruthenium polypyridyl complexes, including $[\text{Ru}(\text{bpy})_3](\text{PF}_6)_2$, gave acetaldehyde when the reaction was carried out in the presence of water.

Whitten and Giannotti, 1980

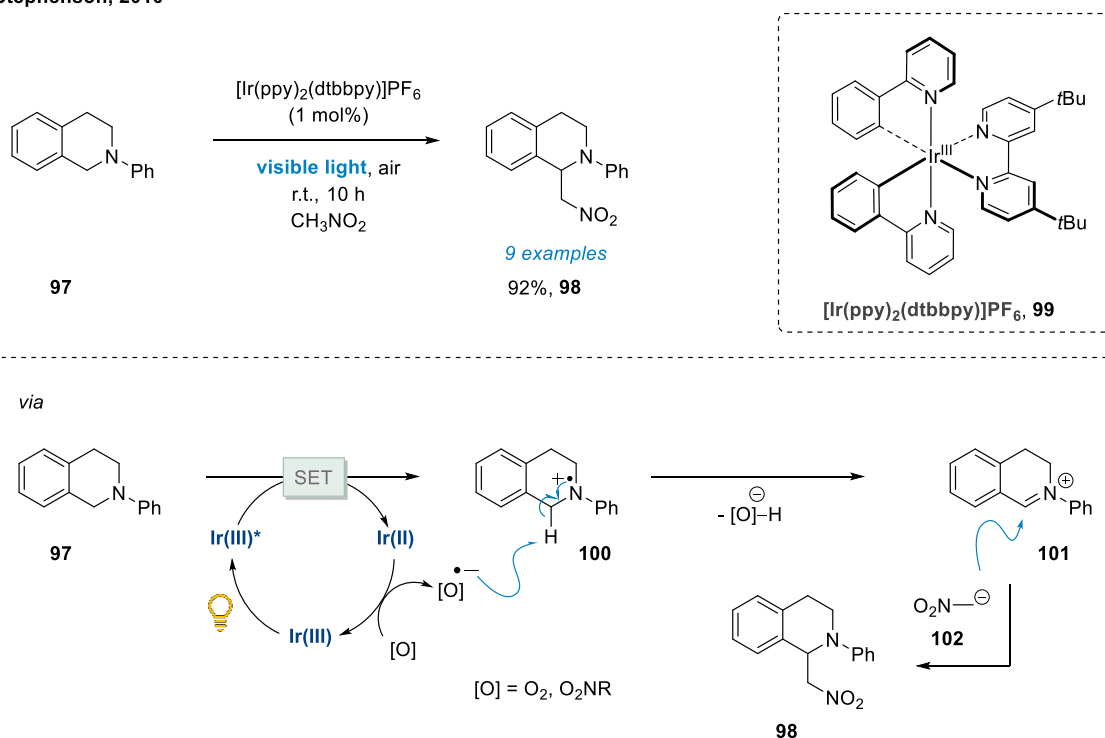


Scheme 19. Whitten's conversion of amine radical cations of triethylamine to iminium ions and acetaldehyde.

Whitten and Giannotti concluded that irreversible oxidation to the iminium ion is taking place. Accordingly, reductive quenching by the of the photoexcited $^*[\text{Ru}(\text{bpy})_3]^{2+}$ state would first produce the radical cation **91**, which could abstract a hydrogen atom from the solvent

acetonitrile, ultimately leading to the generation of α -amino radical **93**. Alternatively, radical cation **91** could undergo deprotonation to form the α -amino radical **93** directly. Subsequent one electron oxidation gives the central iminium ion **94** which in the presence of water is hydrolyzed to acetaldehyde and diethylamine (Scheme 19). Whitten and Giannotti were able to detect the open shell species Ru(I) and α -amino radical **93** via electron spin resonance (ESR) measurements with the aid of the spin-trap nitrosodurene to support their proposed mechanism.

Stephenson, 2010

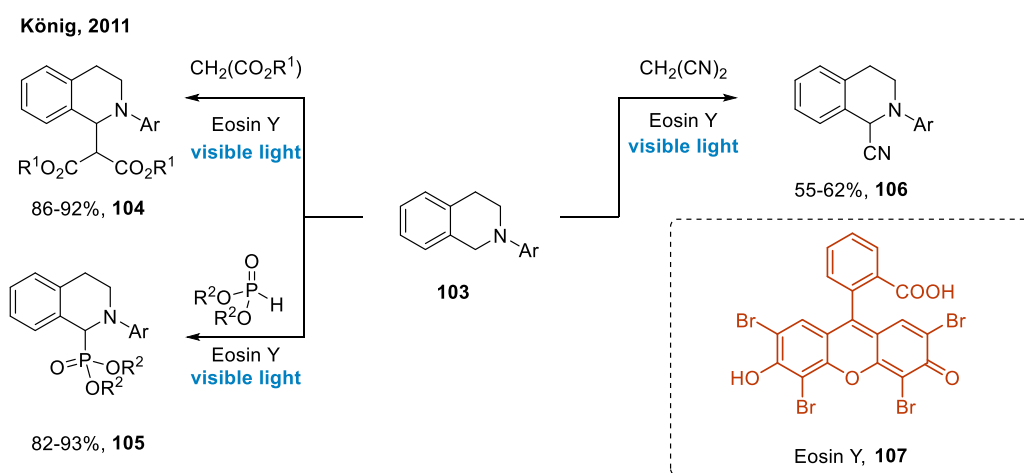


Scheme 20. Stephenson's visible light mediated aza-Henry reaction.

Later, in 2010, Stephenson and co-workers disclosed their photocatalytic functionalization of iminium ions in a visible light mediated aza-Henry reaction.^[100] The oxidative coupling of nitroalkanes and *N*-aryl tetrahydroisoquinolines (**97**) was achieved via irradiation by visible light in the presence of photocatalyst $[\text{Ir}(\text{ppy})_2(\text{dtbbpy})]\text{PF}_6$ (**99**) to provide the aza-Henry products (**98**) in excellent yields (Scheme 20). Mechanistically, Stephenson proposed a reductive quenching cycle is operative, generating a powerful Ir(II) reducing agent ($E_{1/2}^{\text{red}}$ ($[\text{Ir}^{\text{III}}(\text{ppy})_2(\text{dtbbpy})]^+ / [\text{Ir}^{\text{II}}(\text{ppy})_2(\text{dtbbpy})] = -1.51 \text{ V vs SCE}$) via the oxidation of tetrahydroisoquinoline **97**. Control experiments indicated that both oxygen and the nitroalkane (via proposed reduction to nitrosomethane) can be involved in closing the photocatalytic cycle, as for example the vigorously degassed reaction still showed clean formation of the oxidative coupling product. Subsequent hydrogen atom abstraction from the

tetrahydroisoquinoline radical cation **100** furnishes iminium ion **101**, which can be readily trapped by nucleophilic addition of deprotonated nitroalkane **102**. This results in the aza-Henry product **98**. Stephenson and co-workers also reported one example of an *N*-aryl pyrrolidine undergoing the reaction, albeit in low yield.

The transformation was subsequently reported by König using the organic dye Eosin Y (**107**) as photocatalyst,^[101] and pairing the oxidative coupling system with malonate, phosphonate and cyanide nucleophiles (Scheme 21). The nature of the organic dye photocatalyst was further elaborated by Tan and co-workers, who employed Rose Bengal to catalyze the reaction.^[102]



Scheme 21. König's tetrahydroisoquinoline functionalization with organic dye Eosin Y.

Due to the privileged oxidation to the highly stabilized iminium ion, reports of oxidative tetrahydroisoquinoline functionalization sparked a number of further publications describing the oxidative coupling with a wealth of nucleophiles, including allyl silanes (**108**),^[103] indoles (**109**),^[103] enamines (**110**),^[104] various phosphonates (**105**),^[105] silyl enol ethers,^[106] as well as alkynylation (**111**) and trifluoromethylation (**112**),^[103, 107] and intramolecular trapping with alcohols and sulfonamides (**113**, Figure 8).^[108]

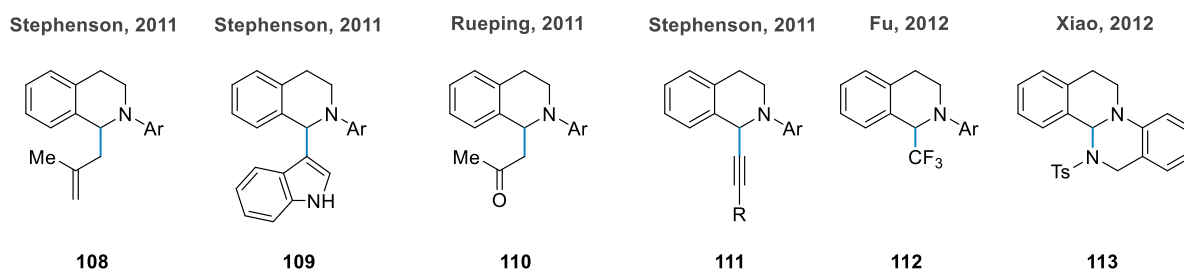
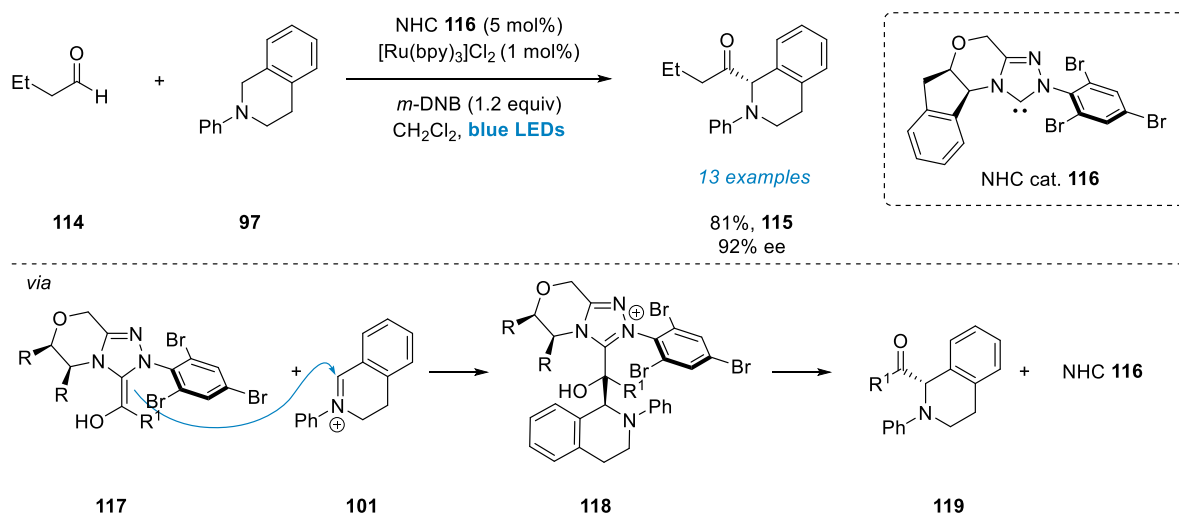


Figure 8. Examples of different nucleophiles in the visible light tetrahydroisoquinoline functionalization.

In 2012, DiRocco and Rovis reported an asymmetric α -acylation strategy for *N*-aryl tetrahydroisoquinolines (**97**), pairing *N*-heterocyclic carbene (NHC) and photoredox catalysis.^[109] Reaction of the NHC-catalyst **116** with an aliphatic aldehyde **114** led to formation of a chiral acyl anion or homoenolate equivalent, the Breslow intermediate **117**, which added to the photocatalytically generated iminium ion **101**, forming a C–C bond (Scheme 22). *m*-Dinitrobenzene (*m*-DNB), a known oxidative quencher of the photocatalyst [Ru(bpy)₃]Cl₂, was employed stoichiometrically in the reaction.

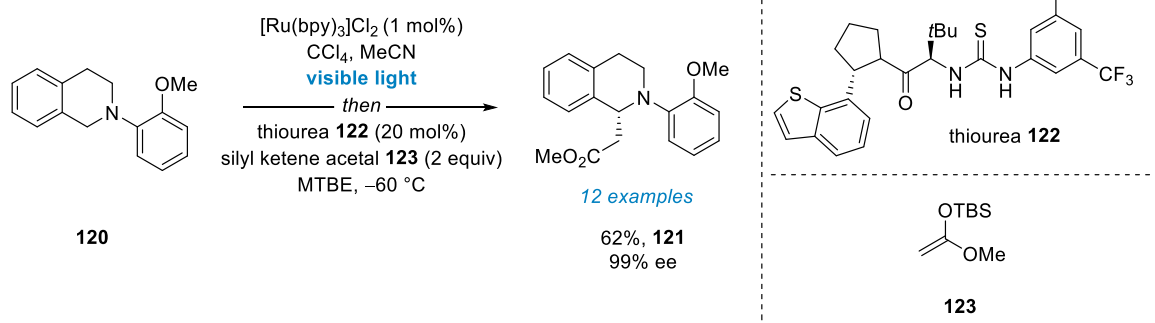
DiRocco and Rovis, 2012



Scheme 22. DiRocco and Rovis' α -acylation of tetrahydroisoquinolines via NHC and photoredox dual catalysis.

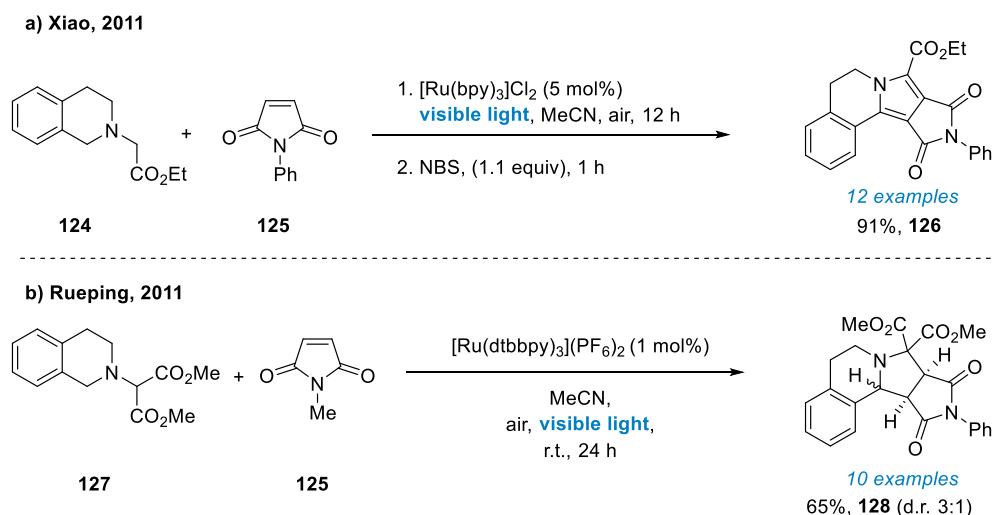
An alternative approach to asymmetric functionalization of photochemically obtained iminium ions using anion binding catalysis was developed by Stephenson and Jacobsen in 2014.^[110] The authors postulated that the formation of halide counterions from oxidants BrCCl₃ or CCl₄ and their association with the oxidized substrate enabled stereoselective nucleophilic addition using thiourea catalysis. Stepwise oxidation to the respective iminium ion and subsequent solvent switch to enable stereocontrol via thiourea catalysis was necessary. Addition of silyl ketene acetal **123** to the photocatalytically pooled iminium ion in the presence of chiral thiourea **122** was achieved in the second step in MTBE, giving the enantioenriched products.

Stephenson and Jacobsen, 2014



Scheme 23. Stephenson and Jacobsen's asymmetric functionalization of photocatalytically generated iminium ions via anion binding and photoredox dual catalysis.

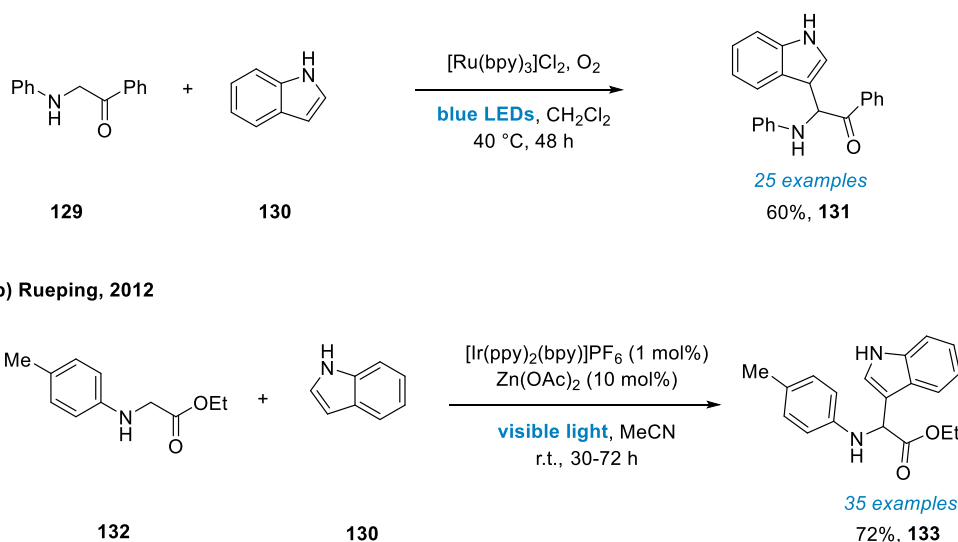
Xiao and Rueping independently reported that for tetrahydroisoquinolines bearing a *N*-methylene group with one or two ester substituents (**124** and **127**), facile formation of the azomethine ylide can take place. Subsequent 1,3-dipolar addition was achieved in both cases with a range of dipolarophiles.^[111-112]



Scheme 24. Visible light mediated 1,3-dipolar addition independently reported by Xiao and Rueping.

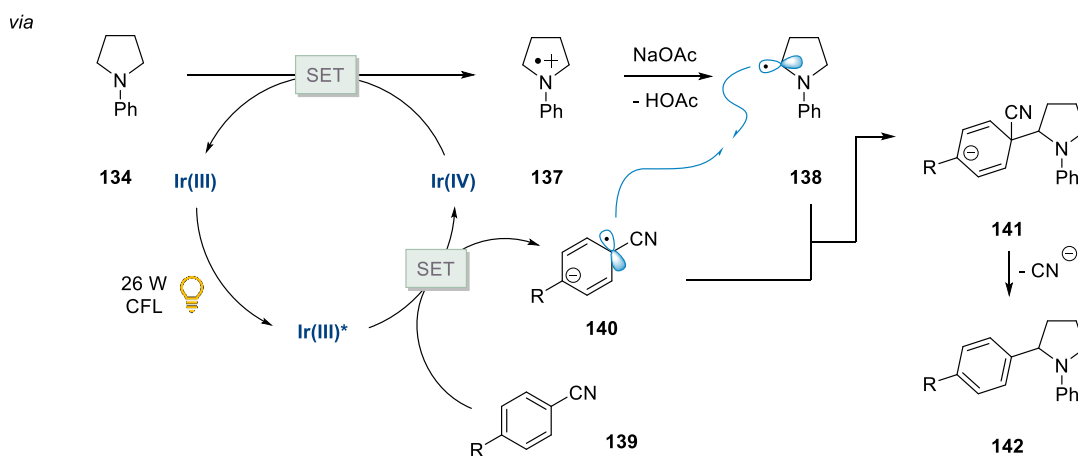
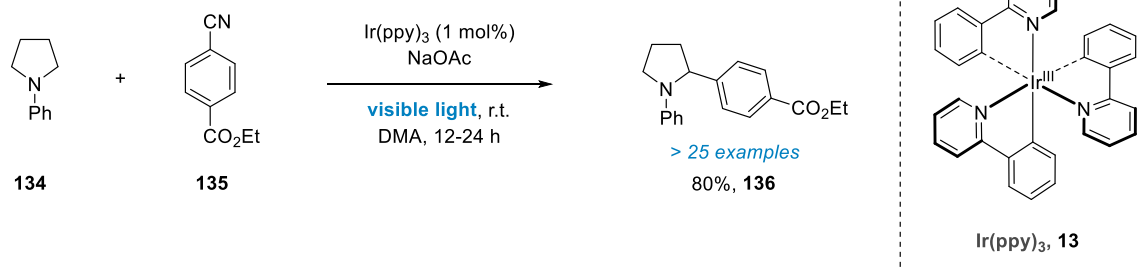
The azomethine ylides were formed from the initially photocatalytically generated iminium ions, by treatment with visible light and [Ru(bpy)₃]Cl₂ or [Ru(dtbbpy)₃](PF₆)₂ and **125**, and gave a series of fused pyrrolidines (Scheme 24a, **126**) and, after oxidation with NBS, pyrrole products (Scheme 24b, **128**), as exemplified by Xiao and co-workers.

While tetrahydroisoquinolines are the most commonly exploited amine for photocatalytic amine functionalization, pioneering efforts by Li^[113] and Rueping^[114] investigated glycine derivatives as substrates for visible light enabled iminium functionalization (Scheme 25). In both cases, a visible light photoredox catalysis strategy for the α -functionalization of glycine



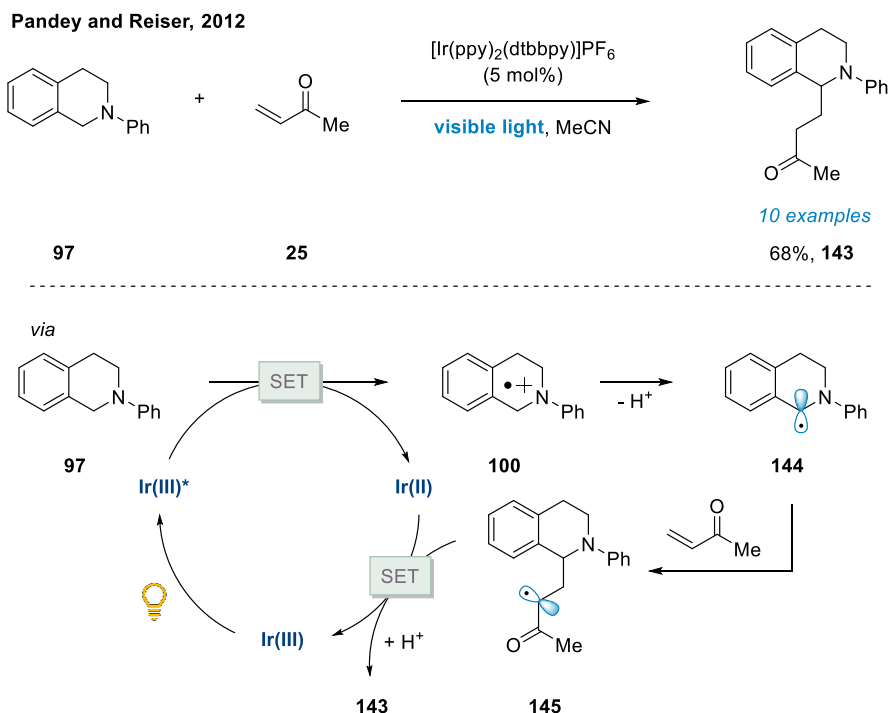
to its radical cation **135**. Radical-radical coupling produced the product **142** after elimination of cyanide.

MacMillan, 2011



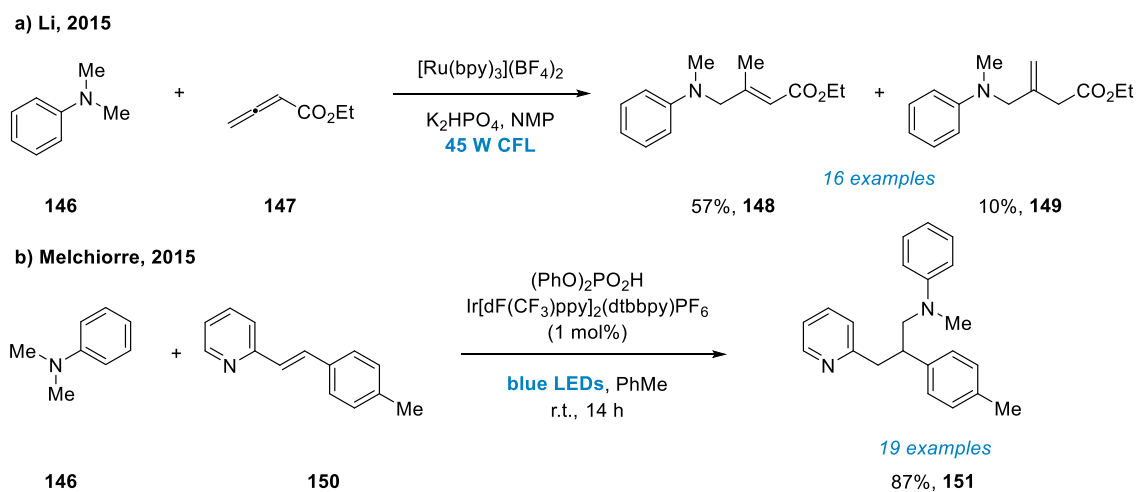
Scheme 26. MacMillan's photoredox α -amino arylation reaction.

In 2012, Pandey and Reiser,^[121] and Nishibayashi^[122] independently reported the first addition of α -amino radicals to α,β -unsaturated carbonyl compounds. In their seminal report, *N*-phenyltetrahydroisoquinolines **97** engage in radical conjugate addition with α,β -unsaturated carbonyl radical acceptors, such as methyl vinyl ketone **25**, to yield the respective α -amino alkylated products **143**. Conceptionally this reaction represented an Umpolung strategy contrary to a number of previous examples employing *N*-aryltetrahydroisoquinolines to furnish the respective highly electrophilic iminium ions. Access to the nucleophilic α -amino radical is further complicated by the fact that the oxidation potential of the generated radicals is lower than those of the starting amines, showing the need for precise control over the single electron transfer events to prevent overoxidation.



Scheme 27. Pandey and Reiser's addition of *N*-aryltetrahydroisoquinoline derived α -amino radicals to Michael acceptors.

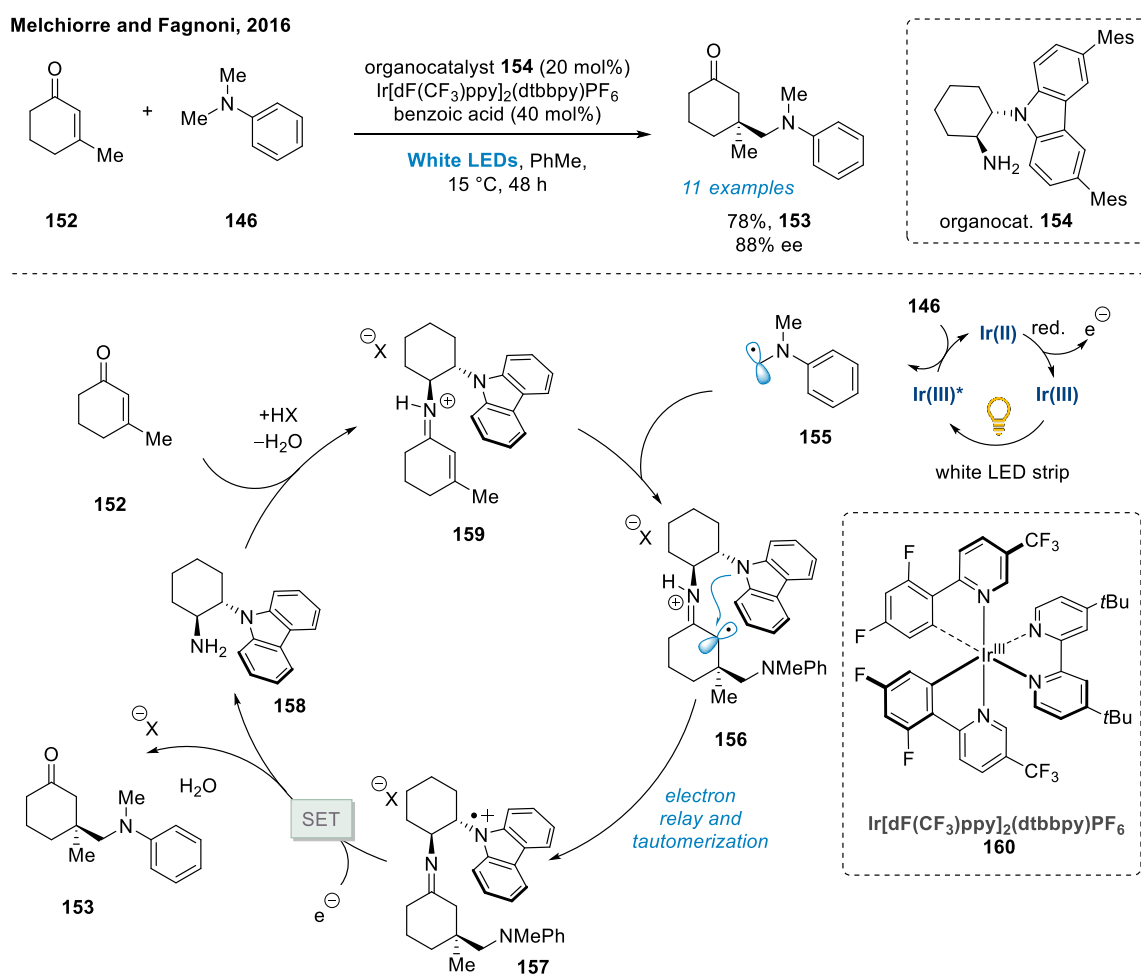
Notwithstanding these challenges, under Pandey and Reiser's conditions, amine **97** underwent facile oxidation under the action of visible light and $[\text{Ru}(\text{bpy})_3]\text{Cl}_2$ or $[\text{Ir}(\text{ppy})_2(\text{dtbbpy})]\text{PF}_6$ (Scheme 27). The authors proposed subsequent facile deprotonation to form key α -amino radical **144**, which adds into radical acceptor **25** to yield the resulting alkyl radical **145**. It was proposed that moderately electron poor **145** could be easily reduced by the photocatalyst, closing the catalytic cycle and forming the alkylated product **143** after protonation.



Scheme 28. Conjugate addition of α -amino radicals into allenates and alkenyl pyridines as reported by Li and Melchiorre respectively.

A number of similar reactions were subsequently published exploiting this pathway, notably by Rueping,^[123] Yoon,^[124] and Li.^[125] Various radical acceptors are compatible with α -amino radical coupling, such as allenates,^[126] and alkenyl pyridines,^[127] as shown by the groups of Li and Melchiorre respectively (Scheme 28).

In 2016, Melchiorre and Fagnoni published an elegant asymmetric radical coupling of α -amino radicals with cyclic enones, utilizing a dual catalysis approach of photoredox and carbazole based organocatalysis (Scheme 29).^[128]



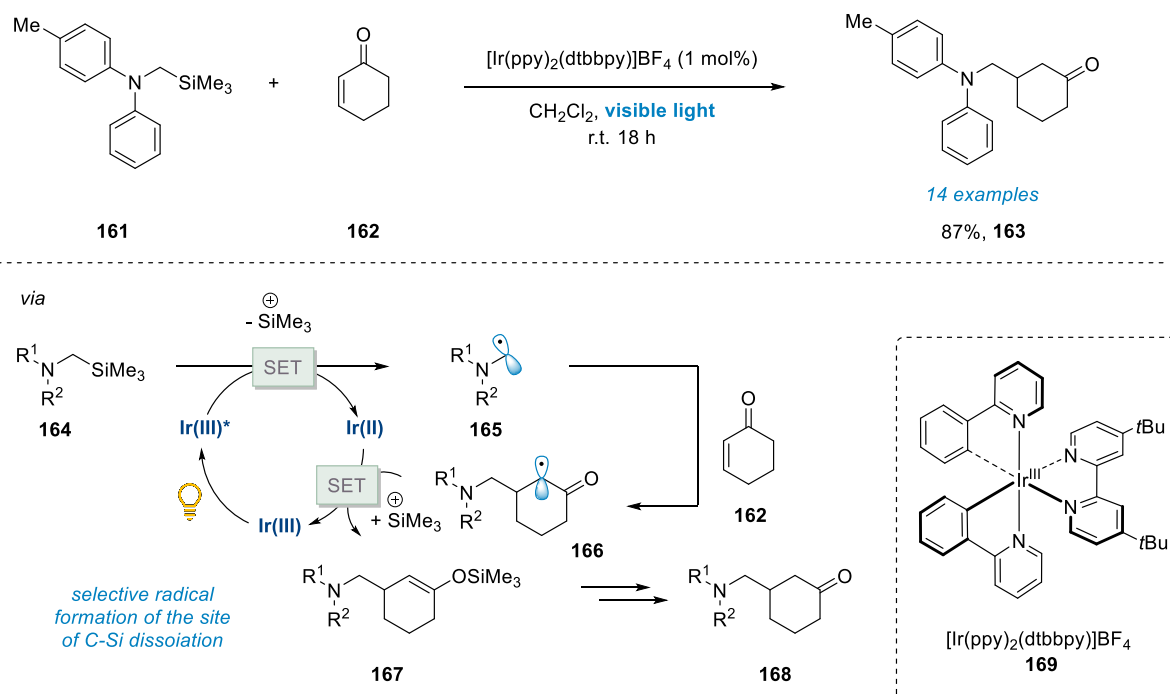
Scheme 29. Melchiorre's enantioselective trapping of α -amino radicals via dual photoredox organocatalytic strategy. (Mes. mesityl-).

In the reaction, cyclic enones **152** and substituted benzodioxoles or anilines **146** were reacted to form cyclic ketones **153** containing a quaternary carbon stereocenter in (Scheme 29). The authors proposed that the reaction is proceeded through initial formation of the protonated imine **159** from cyclic enone **152** and carbazole containing organocatalyst **158**, followed by enantioselective addition of the photocatalytically generated α -amino radical **155**. Remarkably, the resulting radical cation is readily reduced by an intramolecular electron-relay

producing the carbazoliumyl radical cation, and the competing electron back transfer is prevented by fast tautomerization of the resulting enamine to imine **157**. Reduction by the photocatalyst and hydrolysis liberated the product ketones **153**, closing the photocatalytic cycle and regenerating the organocatalyst.

An alternative strategy to access α -amino radicals is the fragmentation of preinstalled functionality leading to radical formation in the desired position.^[119] Pioneering work by Nishibayashi^[129] in 2012, based on studies by Mariano,^[118, 130] enabled utilization of α -amino alkyl radicals generated from α -silylamines via the addition to α,β -unsaturated carbonyl compounds (Scheme 30).

Nishibayashi, 2012

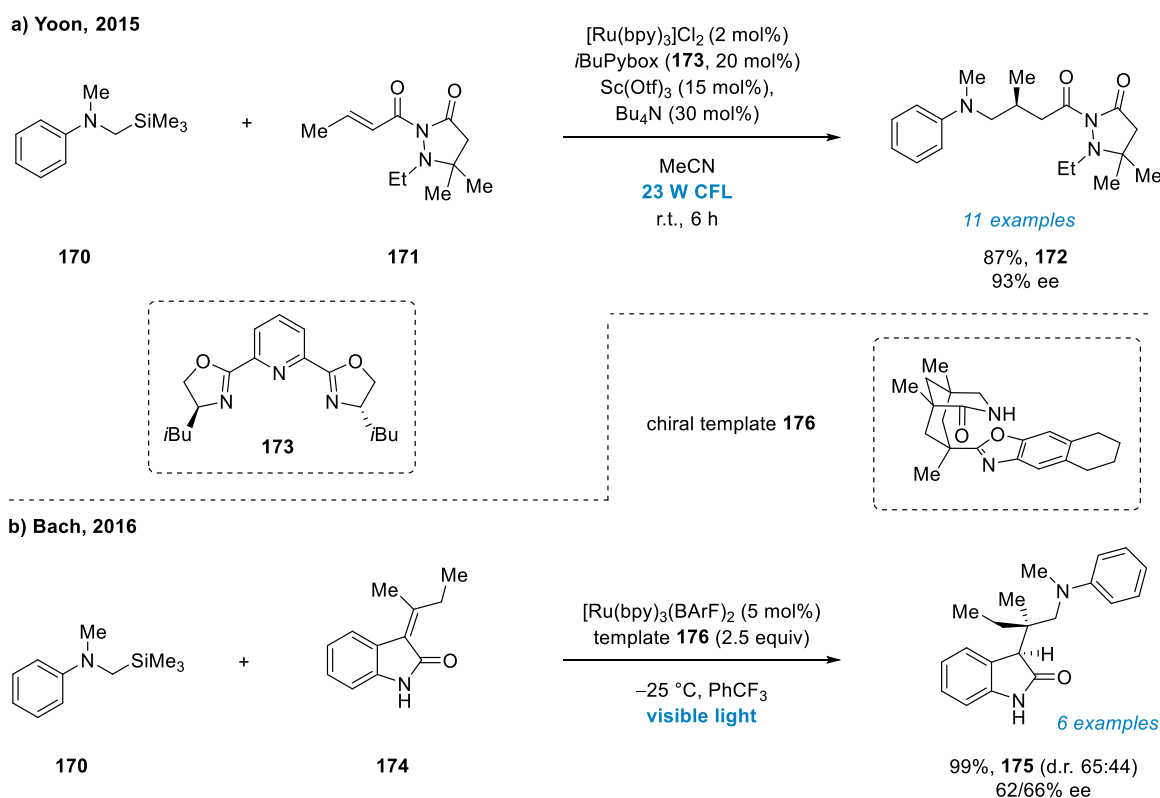


Scheme 30. Nishibayashi's visible light mediated addition of α -aminoalkyl radicals generated from α -silylamines to α,β -unsaturated carbonyl compounds.

This strategy offers superior selectivity in radical generation compared to single electron oxidation and deprotonation due to its regiospecific nature. In the reaction, selective dissociation of C–Si bond in α -silylamine **161** was achieved in the presence of $[\text{Ir}(\text{ppy})_2(\text{dtbbpy})]\text{BF}_4$ (**169**) under irradiation of visible light, and the resulting α -amino radical **165** could be trapped by radical acceptor such as enone **162**. Reduction of the resulting alkyl radical **166** closes the photocatalytic cycle and generates the product **168** after hydrolysis. Notably, the reaction was successfully carried out with trialkyl-derived α -silylamines, with several competing α -C–H bonds available, underpinning the selectivity of

the process. Lastly, the intermediate silyl enol ether was isolated in some cases, leading to higher atom economy and potential synthetic applications. Nishibayashi also reported a variant of this reaction using secondary α -silyl amines in 2014.^[131]

Enantioselective variants of this type of radical addition reaction using α -silylamines and conjugated carbonyl acceptors were subsequently developed by Yoon^[132] and Bach (Scheme 31).^[133]



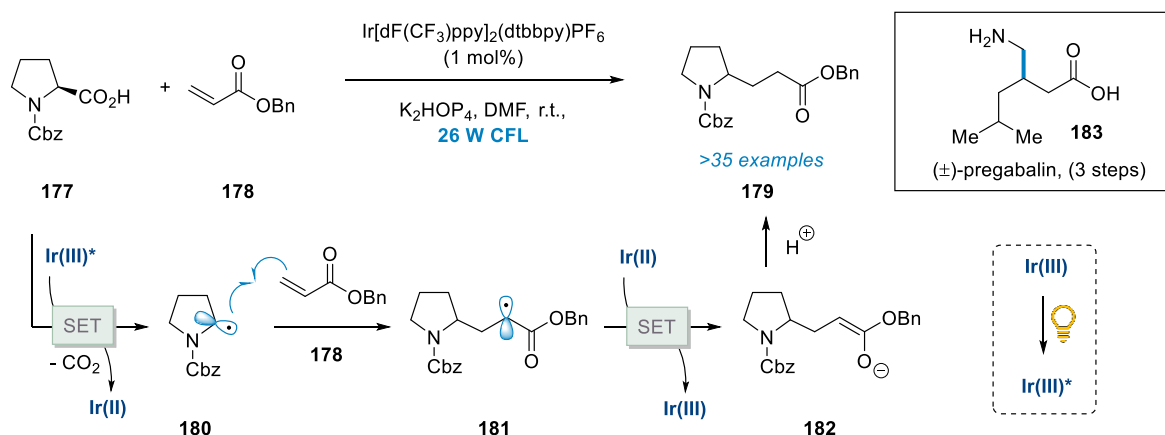
Scheme 31. Yoon's and Bach's enantioselective addition of α -silylamines into α,β -unsaturated carbonyl compounds.

Yoon employed a scandium(III)-pybox derived chiral Lewis acid catalyst in conjunction with $[Ru(bpy)_3]Cl_2$ mediated photoredox catalysis for their enantioselective reaction of α -silylamines **170** with crotonyl dimethylpyrazolidinone **171**. Yoon and co-workers were able to achieve excellent enantioselectivities and yields for this transformation. Bach and co-workers opted for an alternative approach by using chiral template **176** to exert enantiocontrol in the addition of α -silylamines to 3-alkylideneindolin-2-ones (Scheme 31b). Interestingly the reaction was carried out in trifluorotoluene, which entailed the use of tetrakis[3,5-bis(trifluoromethyl)phenyl]borate (BArF) as counterion for the photocatalyst $[Ru(bpy)_3](BArF)_2$ for solubility reasons. Moderate to good levels of stereoinduction could be

achieved via hydrogen bonding between the chiral template and the α,β -unsaturated indolinone **174**.

In 2014, MacMillan and co-workers disclosed multiple reports describing a photocatalyzed pathway to generate α -amino radicals, via the decarboxylation of α -amino carboxylic acids for subsequent arylation, conjugate addition, and vinylation.^[134-136] This pathway was previously explored for UV light by Mariano.^[118, 130] In the conjugate addition reaction, the authors proposed that deprotonation and subsequent oxidation of a carboxylic acid **177** by the Ir[dF(CF₃)ppy]₂(dtbbpy)PF₆ photocatalyst excited state leads to α -carbamate radical **180** via extrusion of CO₂ (Scheme 32).^[134] Addition to radical acceptor furnishes the resulting alkyl radical **181**, whose facile SET reduction closes the photocatalytic cycle to furnish the respective enolate. Protonation yields the α -functionalized products. Notably, MacMillan and co-workers reported the synthesis of (\pm)-pregabalin **183** using this photocatalytic decarboxylative Michael addition method.

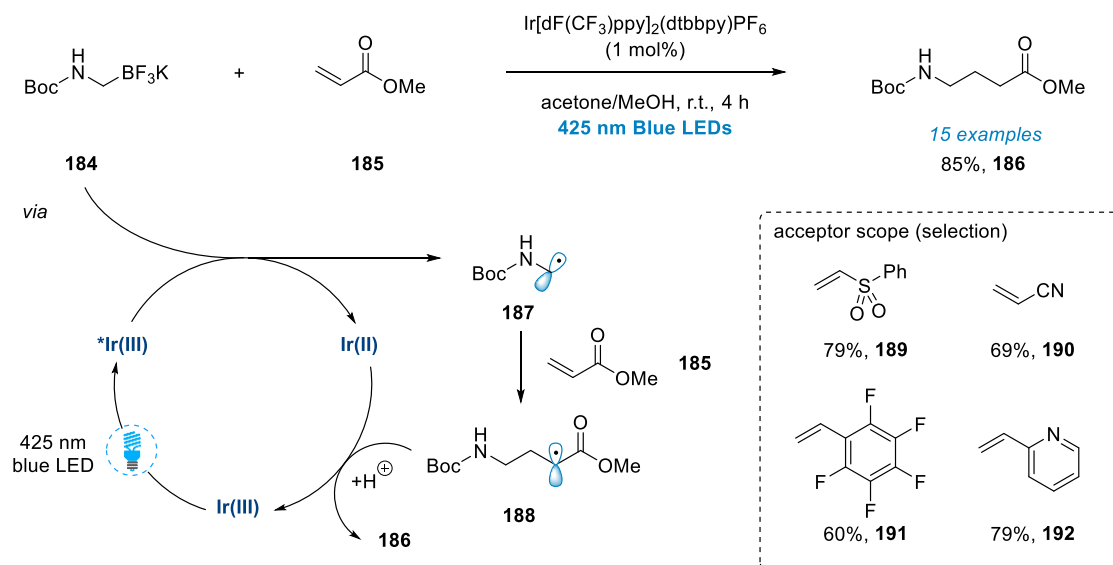
MacMillan, 2014



Scheme 32. MacMillan's visible light photoredox decarboxylative Michael addition, enabling a three step synthesis of (\pm)-pregabalin.

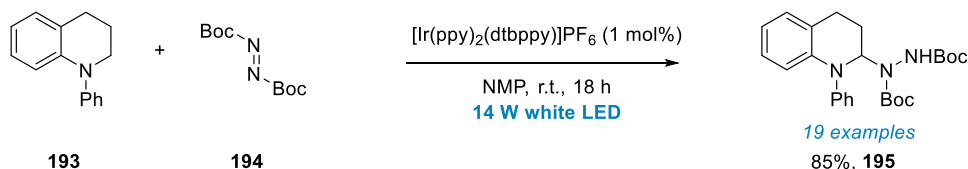
An alternative pathway was described in 2012 by Akita and co-workers with the formation of α -carbamate radicals via direct photoredox mediated oxidation of organoborates.^[137] In a subsequent report in 2014, coupling of potassium trifluoroborate derived α -carbamate radicals with α,β -unsaturated carbonyl compounds was reported.^[138] The reaction utilized photocatalyst Ir[dF(CF₃)ppy]₂(dtbbpy)PF₆ under irradiation of blue LEDs, enabling facile oxidation of potassium trifluoroborate **184** to the respective α -carbamate radical **187**. Radical addition to a number of acceptors, such as perfluorinated arenes **191** and vinyl pyridines **192**, gave the respective addition products in good yields (Scheme 33).

Akita and Koike, 2014

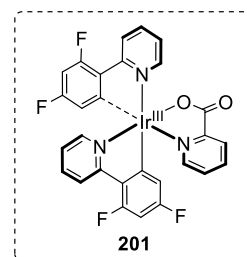
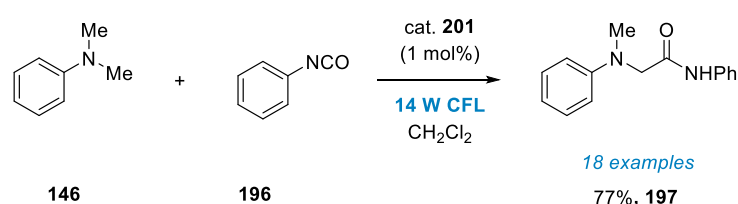
**Scheme 33.** Akita and Koike's hydroaminoalkylation from trifluoroborate derived α -amino radicals.

The general addition of photoredox generated α -amino radicals to radical acceptors is applicable to a wide range of radical-acceptor moieties.^[119] Notable examples include Nishibayashi's report of the addition of α -amino radicals to azadicarboxylate esters (Scheme 34a),^[139] Li's photoredox coupling of dimethylanilines with isocyanates (Scheme 34b),^[140] and Ooi's asymmetric addition of α -aminoalkyl radicals to imines (Scheme 34c).^[141]

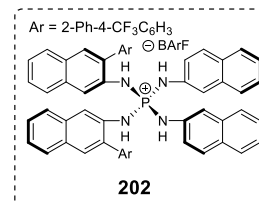
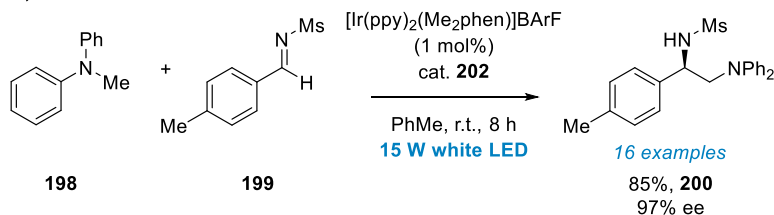
a) Nishibayashi, 2012



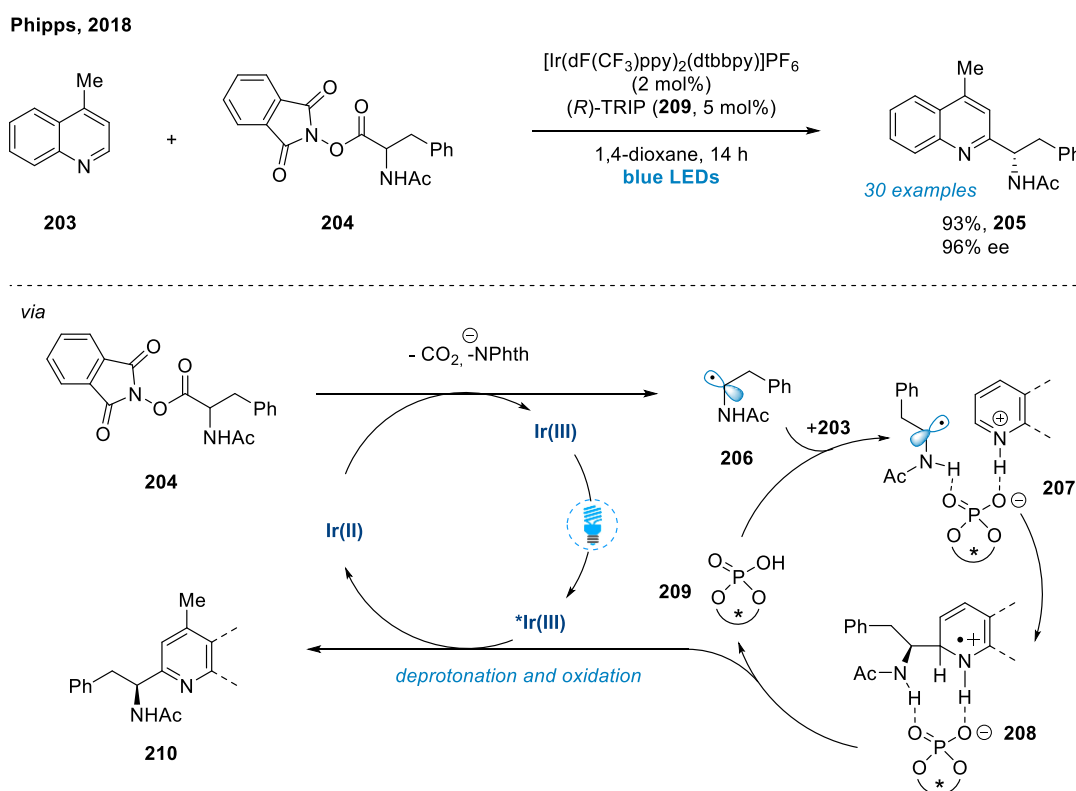
b) Li, 2013



c) Ooi, 2015

**Scheme 34.** Addition of photocatalytically generated α -amino radicals to azadicarboxylates, isocyanates, and imines. (Me_2phen , 2,9-dimethyl-1,10-phenanthroline)

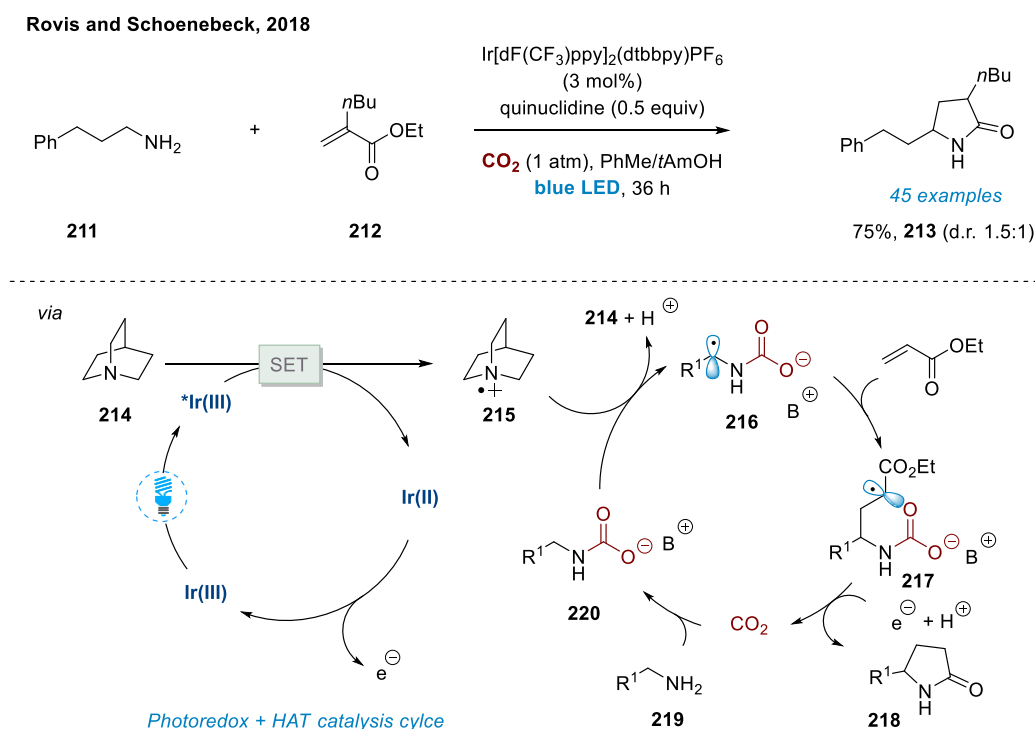
The addition of α -amino radicals to heteroarenes is relatively rare due to challenging control over the oxidation of the initially formed radical.^[119, 142] Pioneering efforts towards the photoredox variant of this reaction were reported by MacMillan.^[135] Additionally, Stephenson successfully carried out heteroaryl functionalization on pharmaceutically relevant scaffolds,^[143] and Fu reported a decarboxylative coupling of amino acid *N*-hydroxyphthalimide esters with heteroarenes.^[144] Based on these studies, Phipps and co-workers recently reported an elegant asymmetric Minisci-type addition of α -amino radicals to a series of heteroaromatics (Scheme 35).^[145]



Scheme 35. Phipps' photocatalytic enantioselective Minisci-type radical addition to heteroarenes.

In the reaction, reduction of a redox-active α -amino *N*-hydroxyphthalimide ester **204** leads to fragmentation and concomitant formation of CO_2 and α -amino radical **206**. The authors proposed an asymmetric radical addition to the heteroarene via chiral Brønsted acid activation, resulting in radical cation **208**. Subsequent deprotonation and oxidation closes the photocatalytic cycle and generates the Minisci product **210**. The reaction exhibited high yields and excellent enantioselectivity, and was applicable for a wide range of amines, quinolines and pyridine acceptors. Phipps and co-workers also demonstrated the applicability of the method in a late-stage functionalization approach for pharmaceuticals.

A hydrogen-atom-transfer (HAT) activation pathway towards the generation of α -aminoalkyl radicals without the use of a dual metal-catalysis approach (*vide infra*) was recently reported by Rovis and Schoenebeck.^[146] Key to the success of this strategy was the electrostatic activation of primary amines by CO₂, which served as a transient protecting group to enable selective HAT to generate the α -carbamate radical. The reaction allowed for a CO₂-promoted α -alkylation/lactamization of primary amines such as **211**, under irradiation with blue LEDs with photocatalyst Ir[dF(CF₃)ppy]₂(dtbbpy)PF₆. Site-selective HAT was achieved through a HAT-catalysis cycle using quinuclidine **214**, whose radical cation **215** was found to engage in hydrogen atom abstraction from the *in situ* formed alkylammonium carbamate **220**. Addition of the α -carbamate radical **216** into an α,β -unsaturated carbonyl acceptor, such as acrylate **212**, furnishes alkyl radical **217**, which after reduction by the photocatalytic system, protonation and dissociation of CO₂ affords the final γ -lactam products **218**. An expansion of this HAT activation strategy for the α -position of primary amine derived trifluoromethanesulfonamides was published by the authors in 2019 (Scheme 36).^[147]



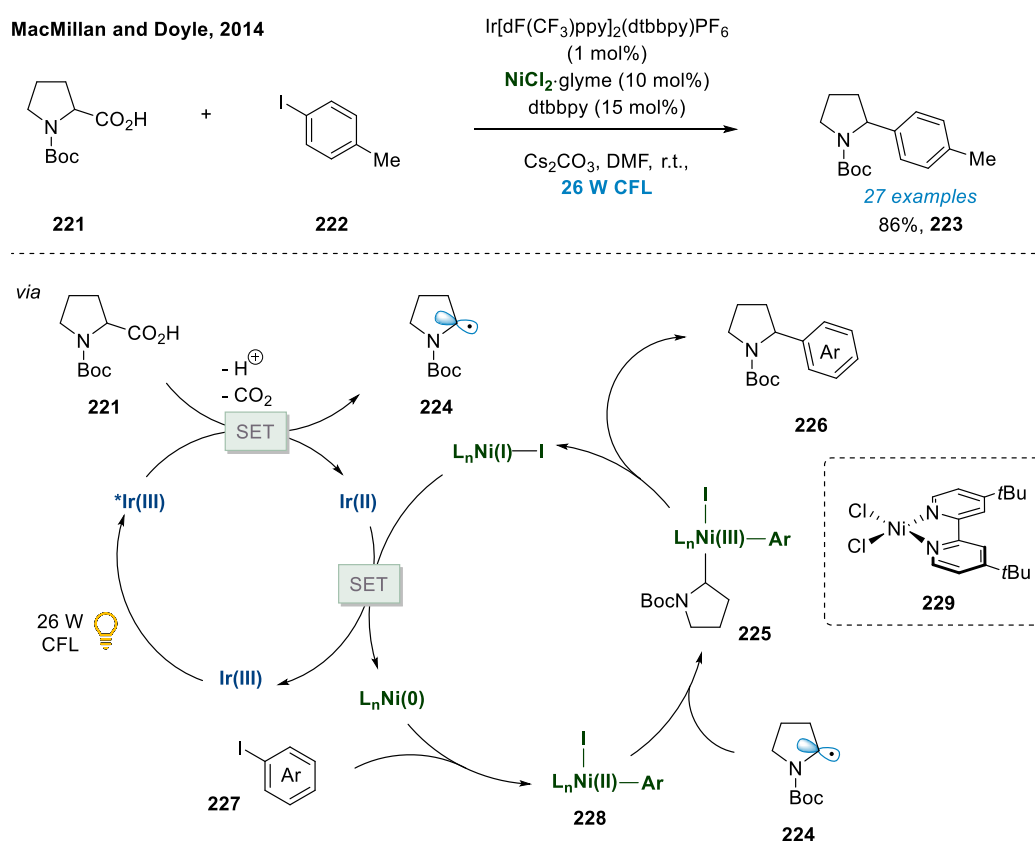
Scheme 36. Rovis and Schoenebeck's α -alkylation of primary aliphatic amines enabled by CO₂ and electrostatics.

1.2.5 α -Aminoalkyl radicals in transition metal – photoredox dual catalysis

Given the interest in novel photoredox transformations over the last decade and the success of the diverse and fruitful field of transition-metal catalysis in organic synthesis, it is perhaps

unsurprising that dual catalytic platforms exploiting both photoredox and alternative modes of catalysis have recently emerged as a particularly promising area of research.^[78, 148-149] The intriguing synergy of photocatalysis with non-photochemical transition-metal catalysis, also termed metallaphotocatalysis, has led to unprecedented control over reactivity of the resulting photogenerated intermediates and contributed to realize a number of challenging, or previously elusive, bond constructions.^[78, 148] Perhaps due to the intrinsic connection of amine redox chemistry with established photoredox methods, this novel mode of dual-catalysis has proven especially useful for the functionalization and cross coupling of α -aminoalkyl and α -amidoalkyl radicals. In the following, a number of seminal reports published in this area will be highlighted.

The first report to employ both photoredox and nickel catalysis in concert was disclosed in 2014 by the groups of Doyle and MacMillan.^[150] In their landmark report, an efficient cross-coupling platform between an aryl halide and an α -carbamate radical using a dual catalytic system was reported (Scheme 37).

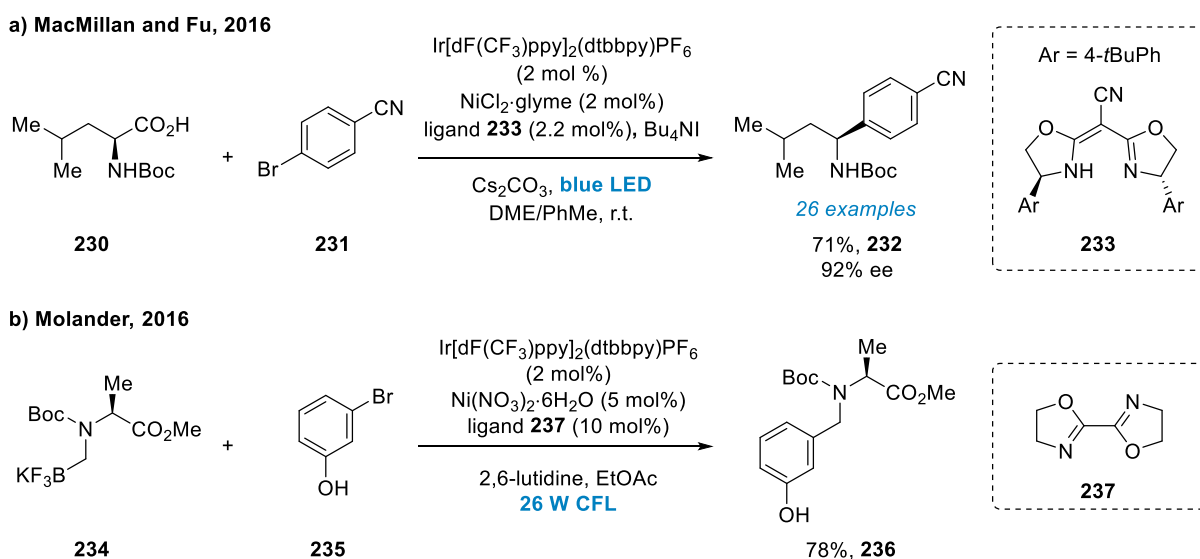


Scheme 37. MacMillan and Doyle's coupling of α -carboxyl sp^3 -carbons with aryl halides.

Due to the ability of Ni(II) complexes to rapidly combine with organic radicals,^[151-152] the authors designed a system in which a photocatalytically generated α -carbamate radical 224

would converge with a Ni(II) complex **228** resulting from oxidative addition to an aryl halide **227**, to form a Ni(III)(Ar)(alkyl) species **225**. Reductive elimination gives rise to the desired C–C bond formation to yield the α -arylated amine product **226** and regenerate the Ni(I)-catalyst. The Ni(I) species is sufficiently oxidizing to receive an electron from the Ir(II) intermediate, regenerating the Ir(III) and Ni(0) catalysts, and closing both the respective catalytic cycles. The reaction was successfully conducted with iodo-, bromo-, and chloroarenes in the presence of Ir[dF(CF₃)ppy]₂(dtbbpy)PF₆, irradiation by a 26 W CFL bulb, and nickel(II) chloride ethylene glycol dimethyl ether complex (NiCl₂·glyme), and proceeded in good yields. Notably, the authors showed in the same report that the catalytic system is also compatible with direct amine oxidation, for example of dimethylaniline, successfully generating the resulting α -aminoalkyl radical.

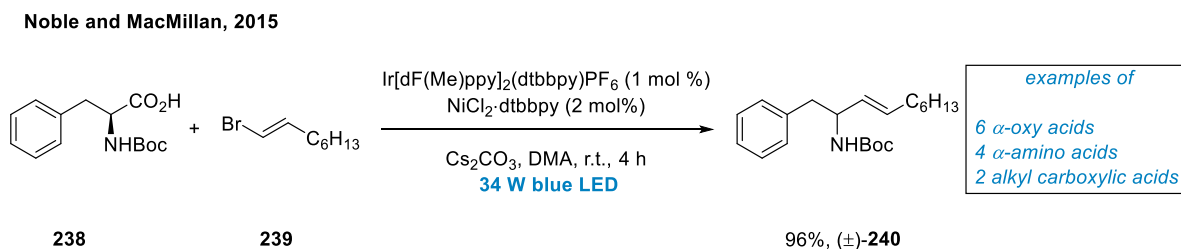
An enantioselective variant of this reaction was subsequently developed by MacMillan and Fu in 2016, by using *in situ* formed chiral Ni(II) complexes to achieve enantioselective arylation in α -position (Scheme 38a).^[153]



Scheme 38. a. Enantioselective decarboxylative arylation via photoredox dual catalysis by MacMillan and Fu; **b.** α -Arylation of chiral α -aminomethyltrifluoroborates via photoredox dual catalysis by Molander.

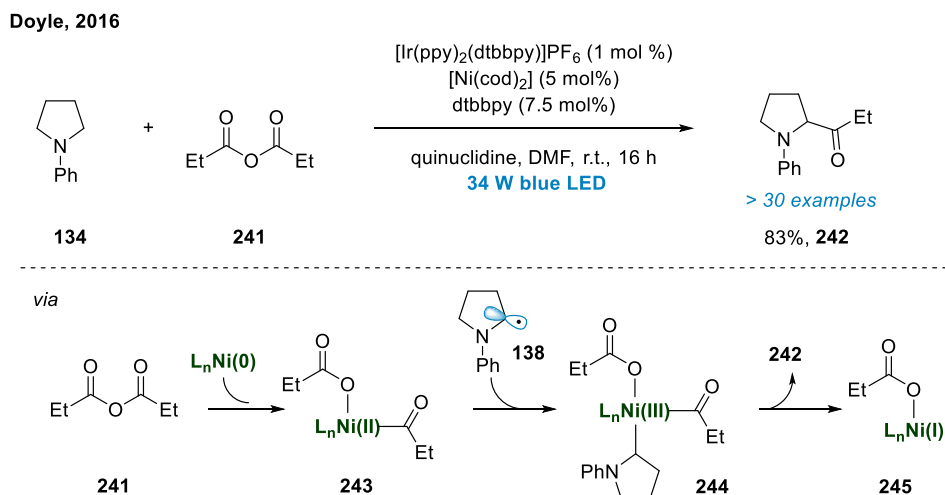
The reaction was reported to furnish high levels of stereoinduction and was applicable to a series of α -amino acids and aryl halides. The authors also demonstrated the utility of this asymmetric coupling by producing two substrates containing known pharmacophores. Furthermore, a similar photoredox nickel dual-catalysis system utilizing potassium alkyltrifluoroborates as radical precursors was disclosed by Molander and co-workers,^[154] enabling the radical cross coupling of chiral α -aminomethyltrifluoroborates (Scheme 38b).^[155]

Following an earlier report from the MacMillan group of the decarboxylative vinylation using vinyl sulfones as radical acceptors (*vide supra*),^[136] in 2015, Noble and MacMillan reported a photoredox and nickel dual catalysis approach for the decarboxylative vinylation of α -amino and α -oxy carboxylic acids.^[156] Instead of vinyl sulfones, the reaction allowed the use of more readily available vinyl halides in the transformation (Scheme 39). A number of α -oxy and α -amino were utilized to generate the respective vinylated products **240**, including *trans*-Rose Oxide, a natural product and widely used fragrance.



Scheme 39. Noble and MacMillan's cross coupling of carboxylic acids with vinyl halides using photoredox dual catalysis.

A photoredox-nickel dual catalysis α -amino acylation method was reported by Doyle and co-workers in 2016, furnishing α -amino ketones (Scheme 40).^[157] The reaction utilizes photocatalyst $[\text{Ir(ppy)}_2\text{(dtbbpy)}]\text{PF}_6$ and bis(1,5-cyclooctadiene)nickel(0) $[\text{Ni(cod)}_2]$ with dtbbpy ligand as a catalytic system and employs quinuclidine as a base.

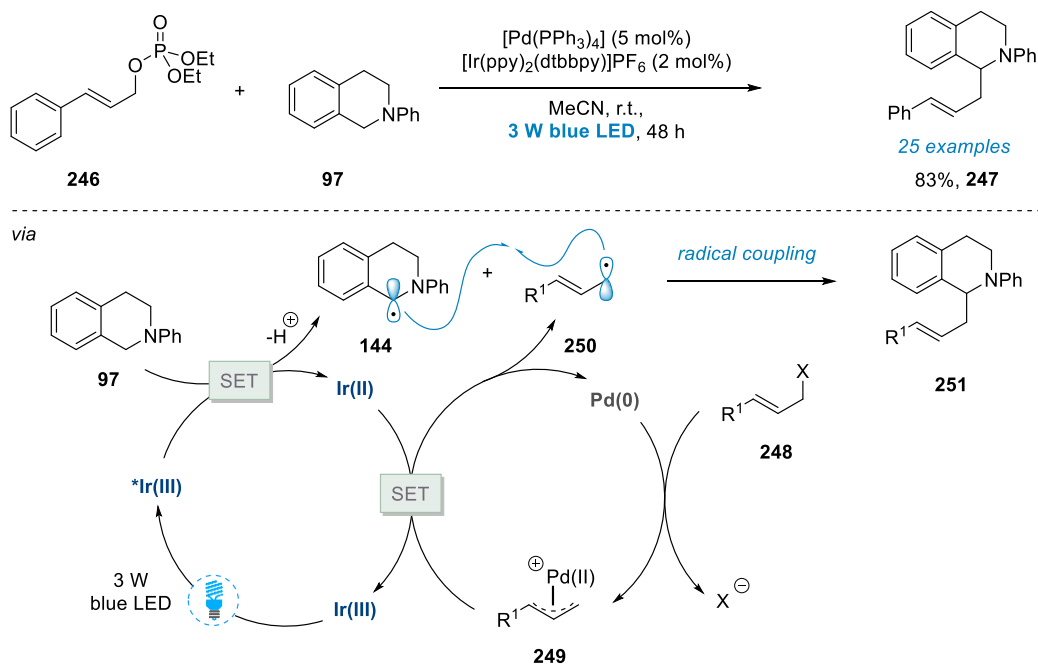


Scheme 40. Doyle's direct acylation of sp^3 α -amino C–H bonds via nickel and photoredox catalysis.

The reaction proceeds from tertiary aryl amines **134** with symmetric anhydrides **241** to produce the respective α -amino ketones **242** in good yields under irradiation of 34 W blue LED. Interestingly, Stern-Volmer quenching studies demonstrated that quinuclidine does not quench the photoexcited state of the photocatalyst in this system.

In 2015, Lu and Xiao reported an allylic substitution reaction using palladium and photoredox dual catalysis (Scheme 41).^[158] The reaction efficiently couples allylic carbonates, esters, bromides, and phosphates (**246**) with a series of tetrahydroisoquinoline (**97**) and secondary amine derived α -amino radicals using a $[\text{Pd}(\text{PPh}_3)_4]$ and $[\text{Ir}(\text{ppy})_2(\text{dtbbpy})]\text{PF}_6$ co-catalytic system. Remarkably, in this redox-neutral transformation, allyl radical **250** is generated from the corresponding π -allylpalladium intermediate **249** via SET from the reduced photocatalyst species Ir(II), which in turn is regenerated by oxidation of the amine to the α -amino radical from the photocatalyst excited state $^*\text{Ir(III)}$. The authors propose that a central SET event closes both catalytic cycles and subsequent radical-radical coupling between allyl radical **250** and α -amino radical **144** affords the α -allyl amine products **251**. An alternative mechanism based on the reaction of nucleophilic α -amino radical **144** and electrophilic π -allylpalladium complex **249** could be considered.

Lu and Xiao, 2016

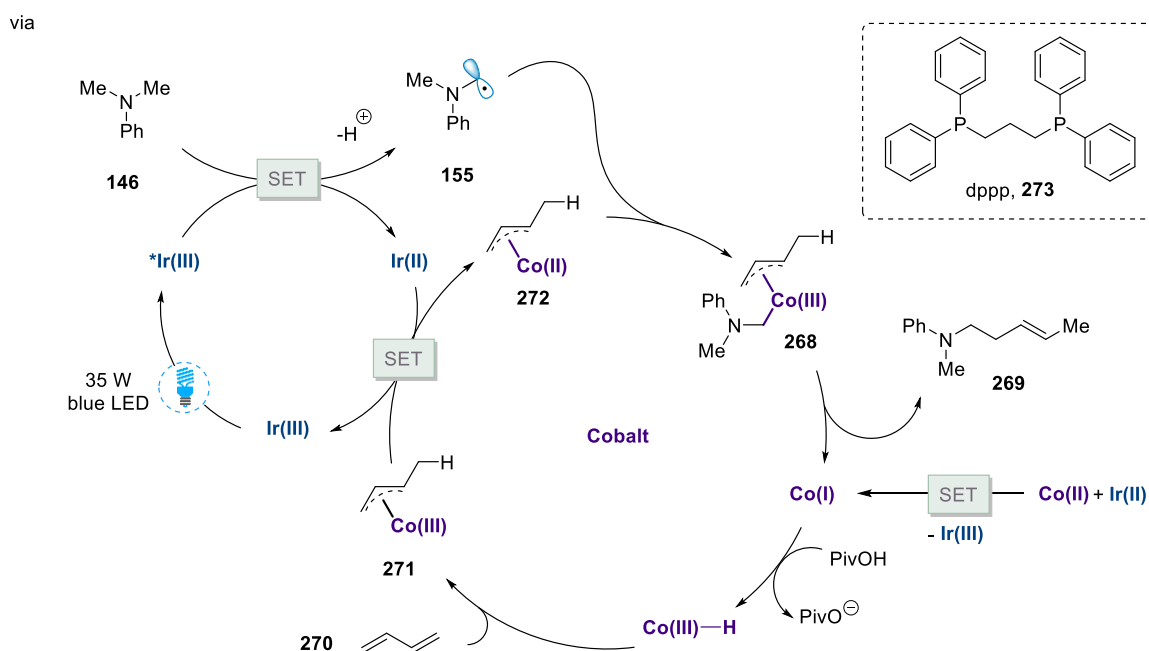
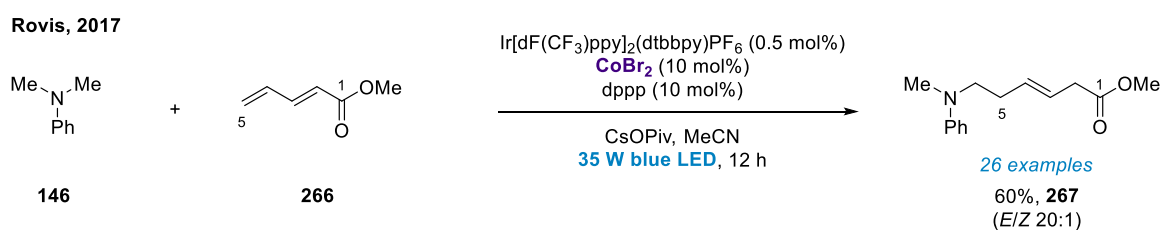


Scheme 41. Lu and Xiao's redox-neutral α -allylation of amines combining palladium and photoredox catalysis.

The merger of photoredox dual catalysis with a third catalytic system, selective HAT catalysis, was reported by MacMillan and co-workers in 2016, achieving selective α -functionalization of amines and amides.^[159] This approach allows formation of the α -carbamate radical via selective hydrogen atom abstraction due to the activated nature of the C–H bond and coupling of the resulting radical species with an electrophile via the established nickel-photoredox dual catalysis platform (Scheme 42a).

employed stoichiometrically. The reaction was applicable to a large scope of substrates and operates with remarkable selectivity, including preference of HAT at methyl over methylene, and methylene over methine. The reaction was further expanded to include alkylation with aliphatic halides as electrophiles, and has been utilized for an elegant late-stage functionalization of the drug derivative *N*-Boc Prozac **263** (Scheme 42b).^[160]

In 2017, the Rovis group reported their hydroaminoalkylation approach using a unified cobalt and photoredox catalytic system. The method enables coupling of photoredox generated α -amino radicals with conjugated dienes to produce useful homoallylic amines, accessing this motif through readily available commercial starting materials (Scheme 43).



Scheme 43. Rovis' hydroaminoalkylation of conjugated dienes via a cobalt photoredox dual catalytic system.

To achieve this transformation, Rovis and co-workers employed photocatalyst Ir[dF(CF₃)ppy]₂(dtbbpy)PF₆ in concert with an *in situ* formed Co(dppp)Br₂ complex (dppp: 1,3-bis(diphenylphosphino)-propane, **273**). Mechanistically, the reaction sets out via oxidation of a tertiary aryl amine **146** by the photocatalytic system, resulting in formation of α -amino radical **155** after deprotonation. The authors propose that the generated Ir(II) species ($E_{1/2}^{\text{red}} = -1.37$ V vs SCE) is reducing enough to engage in single electron transfer with the

formed Co(dppp)(OPiv)_2 ($E_{1/2}^{\text{red}} = -1.29 \text{ V vs SCE}$), to generate a Co(I) species. Reaction with pivalic acid generates a transient Co(III) hydride, which affords a Co(III)-allyl species **271** after migratory insertion of the diene **270** into the Co–H bond.^[161] Reduction to the respective Co(II) allyl system (**272**) closes the photocatalytic system and results in convergence of α -amino radical **155** and **272** to form Co(III)(alkyl)(allyl) complex **268**. Reductive elimination yields the homoallylic amine product **269** and regenerates the Co(I) catalyst.

1.2.6 Summary and outlook

A series of visible light absorbing photocatalysts, developed nearly 50 years ago for water splitting^[162] and solar cell applications,^[163] have, over the course of only the last decade, achieved a paradigm shift promoting the synthetic use of visible light in organic synthetic chemistry. Photoredox chemistry has advanced from an academic curiosity to a modern, indispensable synthetic tool to generate reactive radical intermediates, avoiding the traditionally employed toxic and hazardous chemical reagents. The unique ability to convert visible light into chemical energy, achieving selective activation of bonds and enable the discovery of novel bond forming reactions has led to the rise of photoredox chemistry to the forefront of organic chemistry. The industrial sector is adopting photoredox transformations, allowing for novel discoveries to be rapidly translated into pharmaceutical applications.^[74] The use of visible light as an environmentally benign reagent enables chemists to design synthetic transformations in a safer, more efficient, and less wasteful manner to minimize impact of chemical production and research.^[74] As a part of this development, underpinned by the recent dawn of transition metal and photoredox dual catalysis, metallaphotoredox catalysis,^[78] modern advances in photoredox catalysis have led to a myriad of novel synthetic methodologies. The redox chemistry and synthesis of amines, one of the most important functional groups in organic chemistry,^[164] are intimately interwoven with the field of photoredox chemistry, and a number of elegant amine functionalization pathways have emerged from this new area. However, despite the exponential growth of this field of research since 2008, limitations still exist, and further research is needed to enable environmentally benign photocatalytic pathways for amine functionalization. Due to the numerous pharmaceutical applications and bioactive properties of amines,^[165] there is an ongoing need for versatile methodologies for their general and facile functionalization, which promise to have far-reaching impact in the synthetic and medicinal chemistry community.

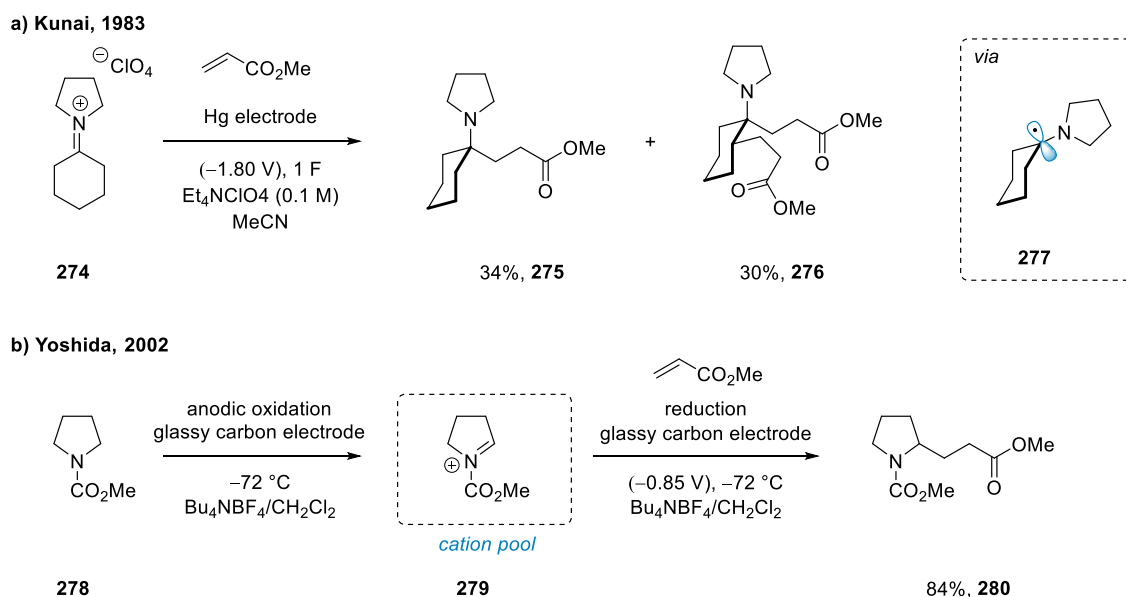
2. Photocatalytic multicomponent olefin-hydroaminoalkylation

2.1 Introduction

2.1.1 α -Aminoalkyl radicals via reductive pathways

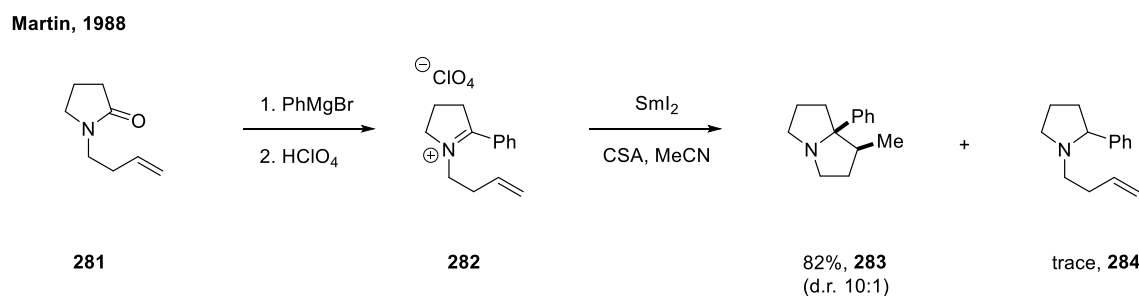
The α -aminoalkyl radical is a synthetically useful intermediate and is involved in numerous photocatalytic protocols for the synthesis of complex amines.^[119] Predominantly, the generation of α -amino radicals for synthetic purposes is achieved via fragmentation of preinstalled functional groups, such as α -aminosilanes and α -amino organoborates (see Section 1.2.4), or via *N*-oxidation and subsequent α -deprotonation of the aminium radical cation. While oxidative methods for α -amino radical generation offer advantages over prefunctionalization and have achieved wide-spread success in the field, the deprotonation of tertiary amine derived radical cations is an inherently unselective process.^[166] This gives rise to significant issues when more than one non-equivalent α -amino C–H bond is available for radical generation, restricting many oxidative methods to the use of symmetric aryl amines^[119] to avoid the resulting product mixtures after α -amino functionalization.^[167] While catalytic HAT processes, pioneered by MacMillan,^[159-160] have shown excellent selectivity for α -amino radical generation in some cases, kinetic selectivity for the desired α -amino position is required. Furthermore, the selectivity of HAT processes is substrate dependent and can lead to the isolation of inseparable regioisomeric mixtures of α -amino functionalized products.^[160]

On the other hand, generation of α -amino radicals through single electron reduction of C=N bonds occurs regiospecifically, but is far less common due to several challenges associated with the method. The generation of α -amino radicals has been achieved using strong stoichiometric reductants, or electrochemical methods, or with UV light.^[168] In an early example, Kunai and co-workers reported the electrochemical reduction of a tetrasubstituted iminium salt on a mercury surface and the subsequent addition of the resulting α -amino radical to Michael acceptors.^[169] Cyclohexylidenepyrrolidinium perchlorate (**274**) was electrochemically reduced at -1.80 V in the presence of methyl acrylate in acetonitrile. Albeit the radical addition product **275** via α -amino radical **277** was observed in Kunai's study, the reaction proved challenging due to polymerization and multiple addition of acrylate (Scheme 44a). A later example by Yoshida^[170] demonstrated the utilization of the cation-pool method at cryogenic temperatures for the electrochemical reduction of pyrrolidine derived acyliminium ions **279**. An excess of olefin was necessary to obtain good yields in the addition of the resulting α -carbamate radicals to electron deficient alkenes (Scheme 44b).



Scheme 44. **a.** Electrochemical reduction of iminium ions by Kunai; **b.** Electrochemical reduction of iminium ions via Yoshida's cation pool method.

The stoichiometric chemical reduction of iminium ions for subsequent radical addition reactions is classically achieved via the use of strong reducing agents, particularly samarium diiodide^[171] and titanocene complexes.^[172] In 1988, Martin and co-workers published an early example of a reduction of an alkyl iminium salt using samarium iodide. Lactam **281** was subjected to phenylmagnesium bromide followed by perchloric acid to yield pyrrolidinium perchlorate **282**. Reduction with samarium diiodide in acetonitrile, in the presence of camphor sulfonic acid (CSA), induces 5-*exo-trig* radical cyclization to yield the bicyclic product **283** and traces of over-reduced tertiary amine **284**. The authors proposed that protonation of the intermediate α -amino radical is beneficial for the reaction to proceed cleanly.



Scheme 45. Martin's generation and cyclization of *N*-homoallyl α -amino radicals.

Starting from the late 1970s, Mariano and co-workers have reported numerous studies on the electron transfer and energy transfer reactivity of the photoexcited state of iminium ions, accessed via irradiation by high energy UV-light.^[173-174] Iminium ions can undergo $\pi \rightarrow \pi^*$ transition, which occur in the wavelength regions of the UV, and, for some conjugated

iminium ions, visible light spectral range. For example, for the iminium ions **285**, **286**, and **287**, the absorption maxima lie at 222 (dioxane),^[175] 275,^[176] and 317 nm^[177] respectively (Figure 9).^[173]

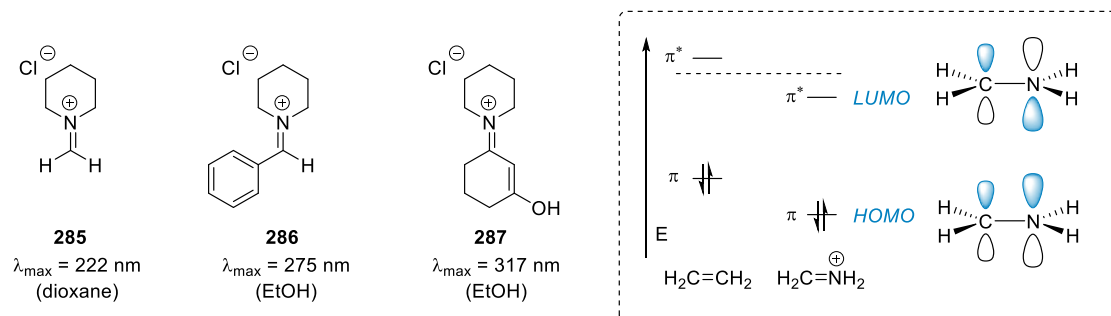
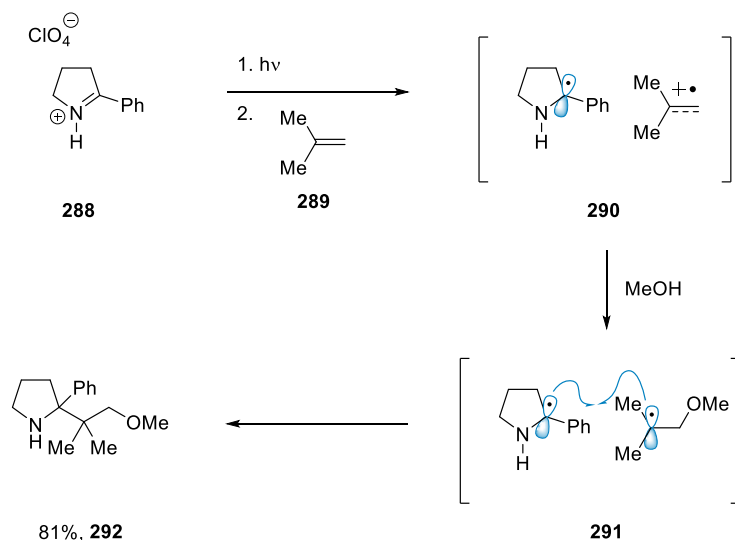


Figure 9. Absorption maxima of iminium ions and photophysical properties of iminium ions.

Calculations confirm that,^[178-179] due to the electronegativity of the nitrogen atom, both HOMO and LUMO energies of the iminium ion are lower than for the respective alkenes (Figure 9). The low lying LUMO in these species thus renders iminium ions particularly susceptible to single electron reduction, resulting in the formation of the stabilized α -amino radical.^[180] Good correlation has been established between the degree of conjugation in iminium ions and the shift of the respective reduction potentials to more positive values.^[181] A comprehensive survey of the electrochemical properties of iminium ions was achieved through a series of reports by Andrieux and Saveant,^[182-185] placing iminium half wave potentials in the range of -1.71 to -0.65 V (vs SCE).

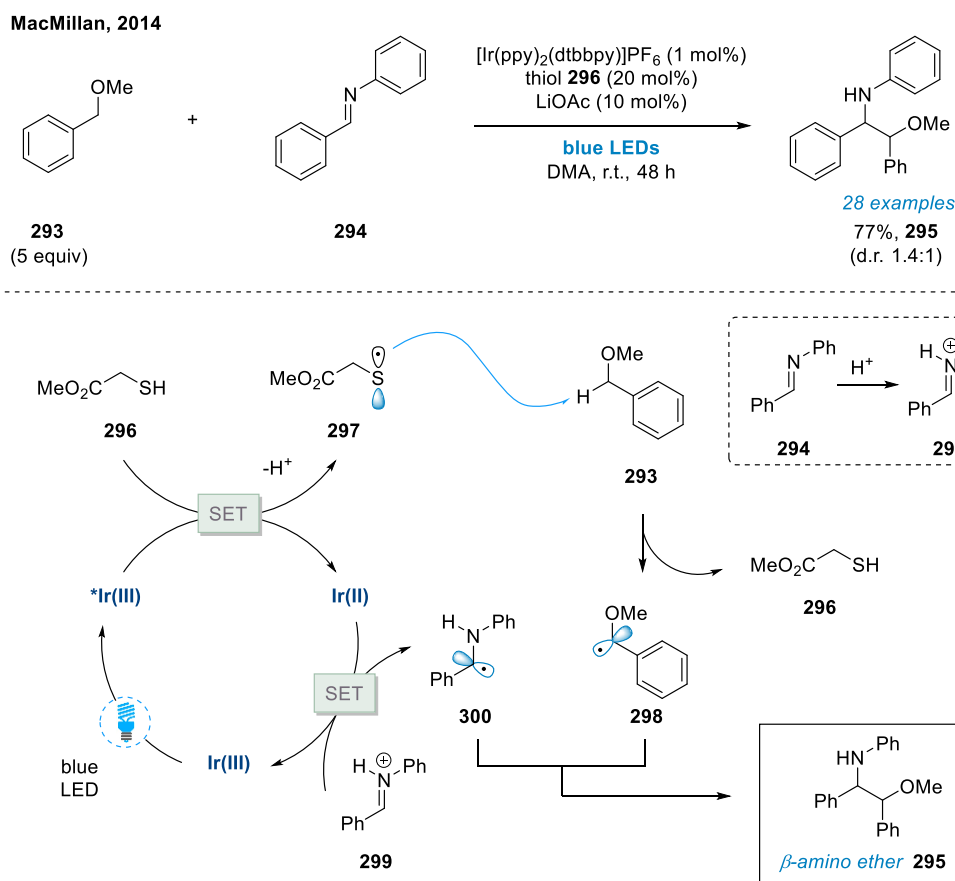
Mariano and co-workers achieved a series of UV light promoted olefin-iminium salt photoaddition reactions.^[186-190] Exemplified by the UV-mediated photoaddition to iminium ion **288** (Scheme 46), electron transfer from electron-rich olefins, such as isobutene (**289**), to the photoexcited state of pyrrolidinium perchlorate type iminium ions is energetically favorable, and can occur under the irradiation of UV light. This is consistent with Mariano's observation that electron-rich olefins are excellent quenchers of the 2-phenyl-1-pyrrolidinium perchlorate (**288**) excited state.^[187] The process is efficient with rate constants near diffusion control. The generated radical pair **290** is readily intercepted by the solvent MeOH, which attacks the isobutene radical cation at the least substituted, charged position, forming adduct **291**. Radical-radical recombination occurs to form the product amine **292** in good yields and exclusive anti-Markovnikov selectivity.



Scheme 46. Olefin-iminium salt photoaddition reaction by Mariano and co-workers.

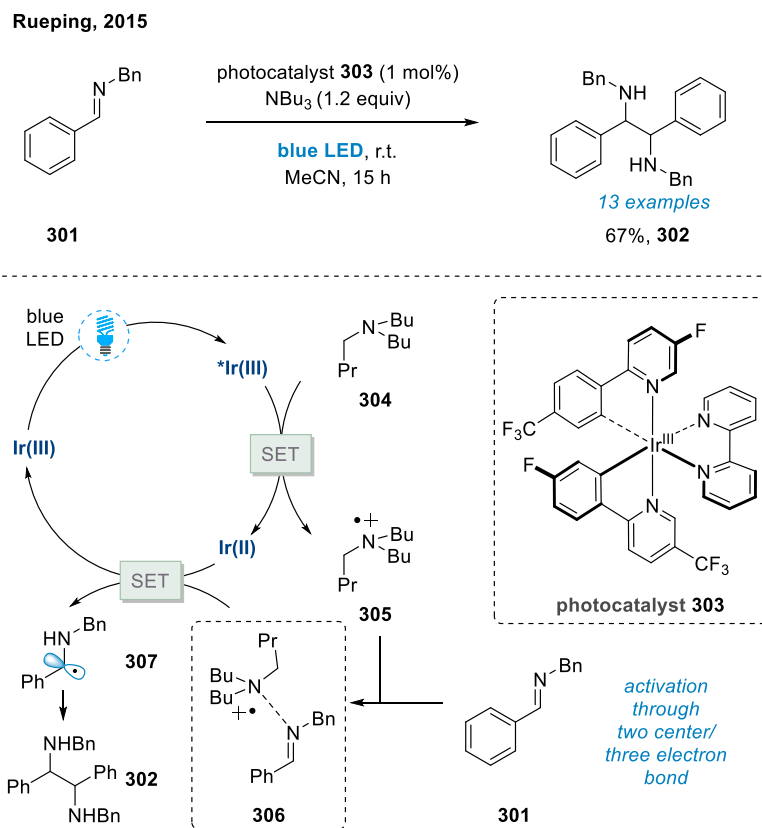
2.1.2 Previous work

With the emergence of visible light photoredox catalysis, a relatively small number of reductive pathways to access α -amino radicals via single electron transfer to C=N double-bonds were reported. In a seminal report in 2014, the MacMillan group detailed the first visible light photoredox mediated reduction of a C=N double-bond in their organocatalytic coupling of benzylic ethers with benzaldimines (Scheme 47).^[191] Benzyl ether **293** and aryl imines **294** generate the β -amino ether products **295** under irradiation with blue LEDs with photocatalyst $[\text{Ir}(\text{ppy})_2(\text{dtbbpy})]\text{PF}_6$ (1 mol%), methyl thioglycolate **296** and catalytic lithium acetate. The catalytic cycle sets out with reductive quenching of the photocatalyst by thiol **296**, generating the thiyl radical **297** and the reducing Ir(II) species ($E_{1/2}^{\text{red}} = -1.51$ V vs SCE). Although the authors propose direct reduction of the imine **294**, due to a significant difference in reduction potential between the Ir(II) reductant and imine **294** ($E_{1/2}^{\text{red}} = \text{ca. } -1.91$ V vs SCE),^[94] it is deemed more likely that imine **294** first undergoes activation through protonation (**299**), lowering the effective reduction potential required.^[168] A proton-coupled electron transfer^[192] pathway can also be considered to mitigate the difference in potentials.^[193] The resulting α -amino radical **300** subsequently undergoes radical-radical coupling with the benzylic radical **298** furnished via HAT with thiyl radical **297**, generating the β -amino ether product and closing the organocatalytic cycle. In 2015, the MacMillan group expanded this methodology to couple aldimine derived, reductively generated α -amino radicals with β -enaminyll radicals to generate γ -aminoketones through the use of $[\text{Ir}(\text{ppy})_2(\text{dtbbpy})]\text{PF}_6$ and DABCO as a HAT catalyst.^[194]



Scheme 47. MacMillan's photoredox coupling of benzylic ethers with imines.

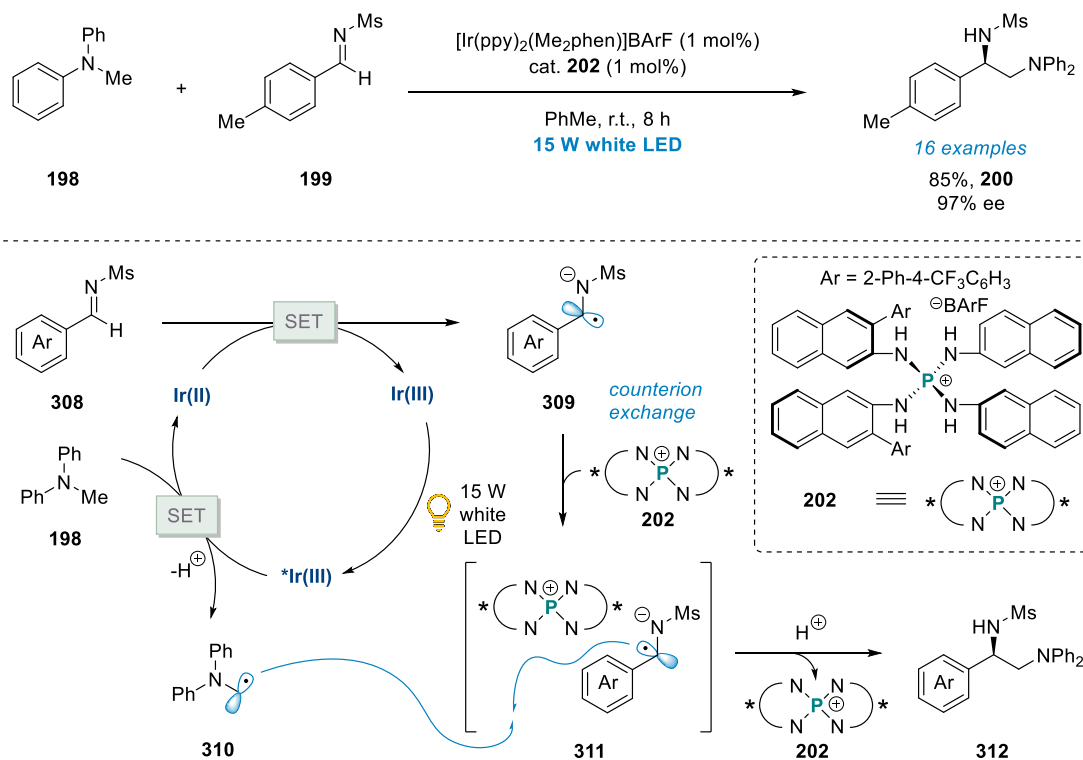
In 2015, Rueping and co-workers reported the homocoupling of reductively generated ketyl- and α -amino radicals to furnish the respective pinacol and imino-pinacol products via visible light photoredox catalysis (Scheme 48).^[195] In the imino-pinacol variant of the reaction, the preformed *N*-benzyl aldimine starting material **301** and Ir-photocatalyst **303** were subjected to irradiation with blue LEDs in the presence of tributylamine. The authors propose that the two α -amino radicals required for the homocoupling are generated via single electron reduction of the respective activated imines by the photocatalytic system. According to the mechanistic hypothesis, the excited state photocatalytic $^*\text{Ir}(\text{III})$ species quenches, reductively, with the amine additive tributylamine (**304**), to generate the respective aminium radical cation **305**. Rueping suggests imines are rendered susceptible to SET via Lewis acid activation by the radical cation **305** through a two-center/three electron bond (**306**),^[196-197] enabling single electron reduction to furnish both the α -amino radical **307** and the ground state Ir(III) species. Radical-radical recombination yields the imino pinacol products **302**.



Scheme 48. Rueping's photoredox reductive homocoupling of imines using visible light.

In 2015, Ooi and co-workers reported a dual catalytic system for the asymmetric coupling of *N*-sulfonyl imine derived α -amino radicals with *N*-arylaminoethanes.^[141] The authors opted for $[\text{Ir}(\text{ppy})_2(\text{Me}_2\text{phen})]\text{BARF}$,^[198] bearing a 2,9-dimethyl-1,10-phenanthroline (Me_2phen) ligand, as a photocatalyst with irradiation by white LEDs and employed a chiral *P*-spiro arylaminophosphonium barfate **202** ($\text{BARF} = [3,5-(\text{CF}_3)_2\text{C}_6\text{H}_3]_4\text{B}$) in their stereoselective protocol (Scheme 49). The mechanistic cycle sets out with the oxidation of the *N*-arylaminoethane **198** by the photoexcited $^*\text{Ir(III)}$ species to generate an Ir(II) species and the α -amino radical **310** after deprotonation. The authors argue that the Ir(II) catalytic species should be sufficiently reducing ($E_{1/2}^{\text{red}} = \text{ca. } -1.40 \text{ V vs SCE}$) to reduce the *N*-sulfonyl imine **308** ($E_{1/2}^{\text{red}} = -1.45 \text{ V vs SCE}$) to form the resulting anionic radical **309**. Prompt ion exchange with the aminophosphonium ion **202** due to its strong H-bond donor ability affords chiral ion pair **311**. A final radical-radical combination reaction between the α -amino radical **310** and chiral ion pair **311** under guidance of chiral ion **202** enantioselectively furnishes the 1,2-diamine product **312**. A conceptionally similar coupling was published in 2016 by the Rueping group.^[199]

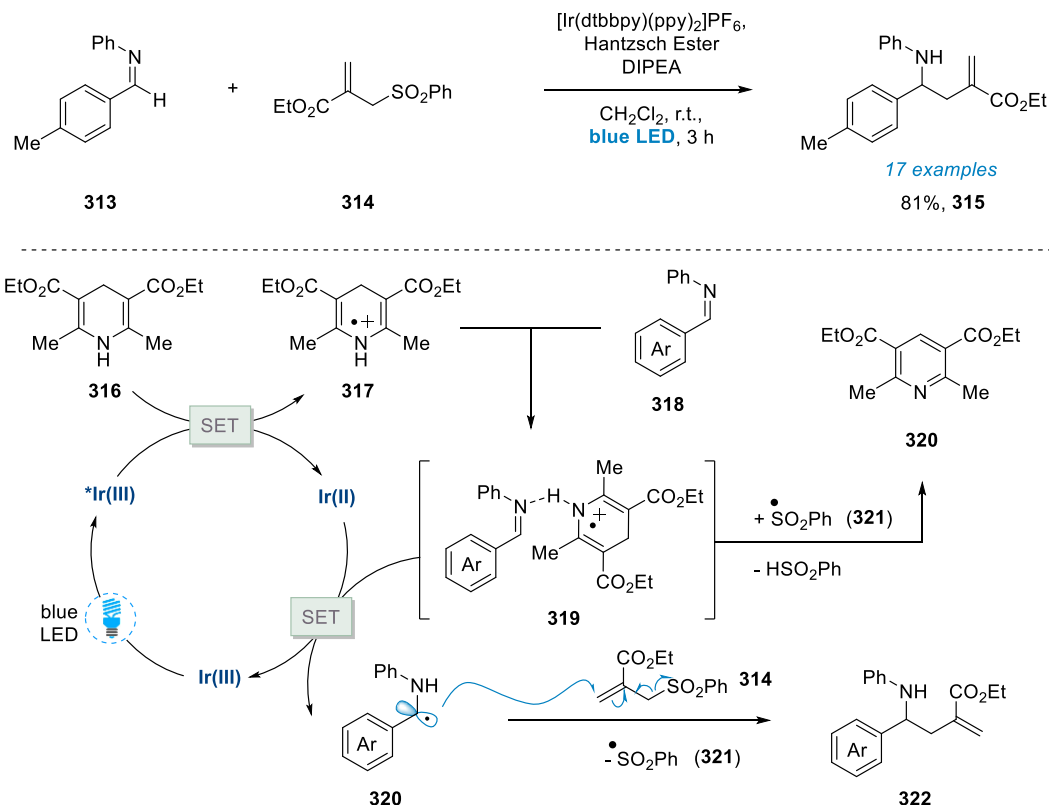
Ooi, 2015



Scheme 49. Ooi's asymmetric coupling of *N*-arylaminoethanes and aldimines (Me₂phen. 2,9- dimethyl-1,10-phenanthroline).

In contrast to radical-radical coupling reactions, the addition of reductively generated, carbonyl derived α -amino radicals into Michael acceptors via visible photoredox chemistry was first reported by Chen and co-workers in 2016.^[200] In their report, allylation of aldehydes, ketones and imines is described, utilizing photocatalyst $[\text{Ir}(\text{dtbbpy})(\text{ppy})_2]\text{PF}_6$ and Hantzsch Ester (**316**) as a terminal reductant (Scheme 50). Mechanistically, the authors propose that the cycle begins with reductive quenching of the excited state photocatalyst through facile oxidation of Hantzsch Ester **316** to its radical cation **317**. The resulting Ir(II) species can then engage in single electron reduction of imine **318**, which is activated by the Hantzsch Ester radical cation (**319**).^[201-202] The resulting α -amino radical **320** adds to the Michael acceptor **314** to furnish the desired addition product **322** and generating sulfur radical **321**, which converges with the Hantzsch Ester radical cation to form the respective pyridine **320**. Notably, a series of alkyl imines tested by Chen and co-workers underwent the reaction smoothly in a multicomponent fashion to produce the respective alkylamine products. A conceptionally very similar multicomponent reaction using organophotocatalyst Eosin Y was subsequently reported by Dixon co-workers.^[203]

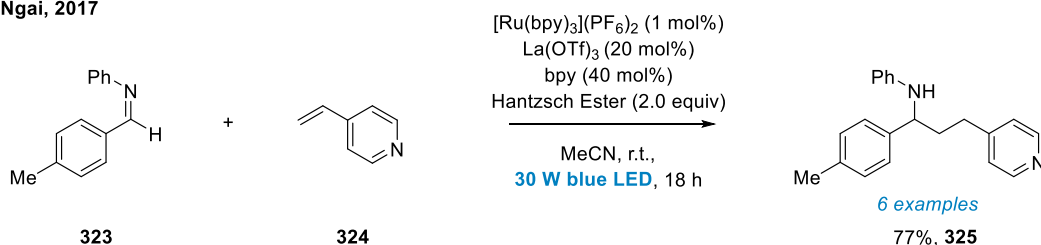
Chen, 2016



Scheme 50. Chen's visible light photoredox allylation of imines enabled by Hantzsch Ester.

In a recent report, Ngai and co-workers detailed the reductive coupling between carbonyl derivatives and alkenylpyridines under Lewis acid and photoredox dual catalysis.^[204] The reaction efficiently couples imines **323** with 4-vinyl pyridine **324** (Scheme 51). The authors propose catalytic generation of the Hantzsch Ester radical cation, which critically activates the imine for single electron reduction. After addition of the α -amino radical to the vinyl pyridine, the resulting benzyl radical undergoes HAT with Hantzsch Ester to form the desired product **325** and regenerate the catalytic Hantzsch Ester radical cation.

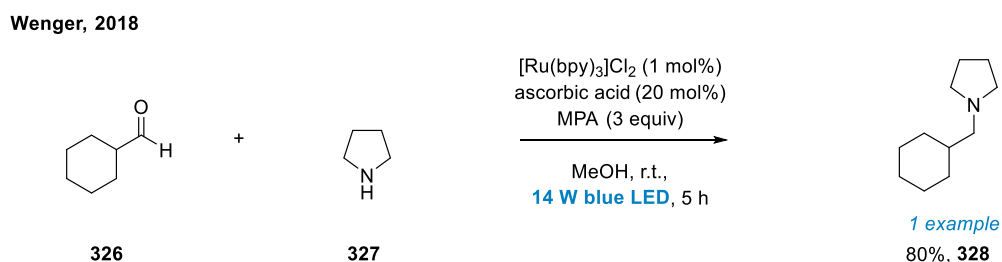
Ngai, 2017



Scheme 51. Ngai's visible light photoredox coupling reaction between imines and 4-vinylpyridines.

While some advances in the reductive generation of α -amino radicals have been achieved through the methods outlined above, it is notable that in contrast to the plethora of oxidative

α -amino radical formation, photocatalytic reduction of C=N bonds remains limited. As outlined by Arnold,^[181] in all cases shown above conjugation of the C=N system with, particularly aromatic, π -systems was necessary to lower the required reduction potentials into the compatible range of the involved photocatalytic systems. Furthermore, protonation of imines, or a PCET mechanism^[192] was often required to overcome the vast potential differences. This renders all-alkyl iminium ions, (alk)₂C=N(alk)₂, particularly challenging candidates for reductive photoredox α -amino radical generation, as these species lack the necessary orbitals to engage in protonation or PCET, and are by definition devoid of any π -system conjugation, resulting in high reduction potentials. To the best of our knowledge, prior to the study outlined below, only a sole example of the reduction of an all-alkyl iminium ion via photoredox existed in the literature, reported by Wenger and co-workers in 2018.^[205] Wenger's reductive amination approach utilizes [Ru(bpy)₃]Cl₂, ascorbic acid, 3-mercaptopropionic acid and methanol under blue LED irradiation, to achieve the photocatalytic reduction of the *in situ* formed imine of cyclohexylcarboxaldehyde **326** and pyrrolidine **327** via a polarity matched HAT (Scheme 52).

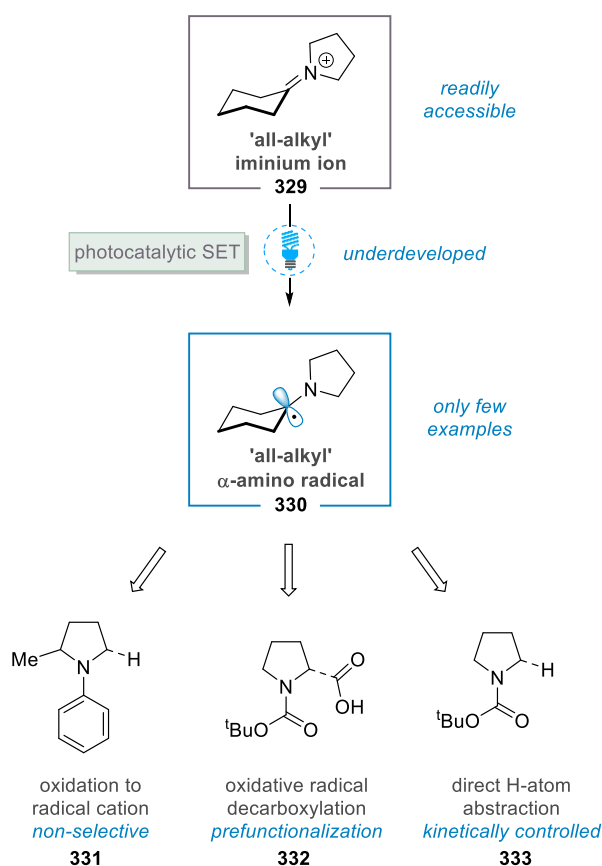


Scheme 52. Wenger's reductive amination by photoredox catalysis via polarity-matched HAT.

2.2 Project Aims

Based on the literature reports outlined above, it was recognized that application of α -amino radicals derived from C=N bond single electron reduction of imines and iminium ions has been hindered by the large reduction potential of these species (*e.g.* $E_{1/2}^{\text{red}} = -1.91$ V vs SCE for *N*-benzylideneaniline,^[94] and up to $E_{1/2}^{\text{red}} = -1.71$ V vs SCE^[182, 206] for alkylidenepyrrolidinium perchlorates) and hence the requirement for toxic reducing agents and/or harsh reaction conditions.^[168] While photoredox enabled C–C bond formation via α -amino radicals derived from heavily conjugated imines and iminium ions is well explored (*vide supra*), our interest was piqued in particular by the class of all-alkyl aldiminium and ketiminium ions, which are readily accessible from feedstock starting materials. The corresponding α -amino radicals of this class of iminium ions were, with the exception of a

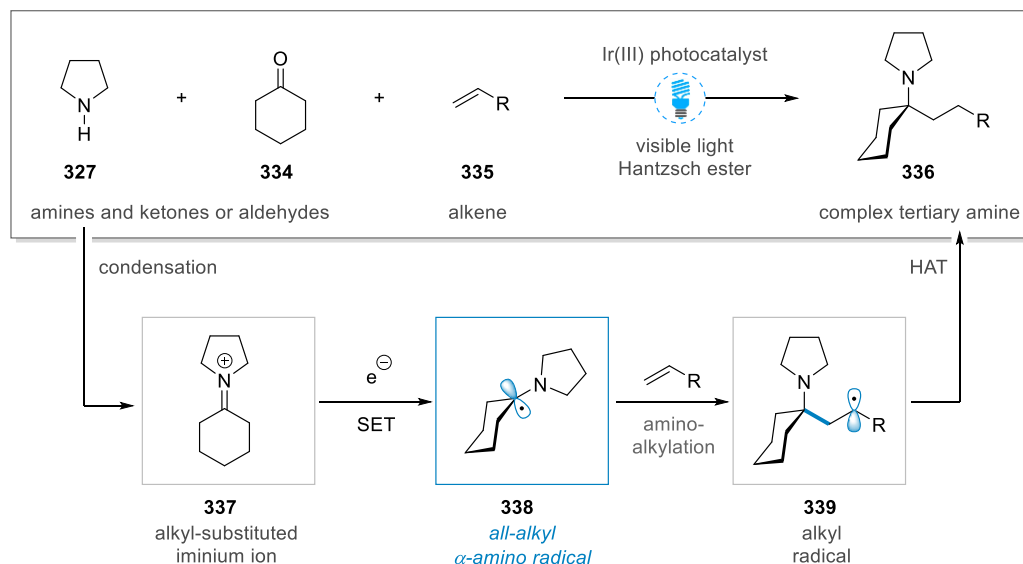
single substrate reported,^[205] hardly explored. Furthermore, C–C bond forming reactions from reductively photoredox generated ‘all-alkyl’ α -amino radicals are unprecedented in the literature. It was envisaged that a visible light mediated reaction via regiospecific C=N bond reduction, should it be realized, would offer significant advantages over oxidative α -amino radical formation, a method inherently plagued by selectivity issues.^[119, 167] Through a multicomponent approach, the site of radical formation could be determined specifically by the location of the C=N double bond, making the system more efficient than prefunctionalization approaches,^[119] and would allow greater site-control than HAT-activation methodologies (Scheme 53).^[159]



Scheme 53. Catalytic photoredox methods for the generation of all-alkyl α -amino radicals.

However, several challenges could impede the development of this desirable technology. Firstly, high reduction potentials of the involved species would require a strongly reducing photocatalyst, while ensuring compatibility with the reaction conditions. Moreover, alkyliminium ions are known to exist in (often unfavorable) equilibrium with the corresponding enamines, which, importantly for photoredox systems, can also undergo SET reactions to form radical species via oxidation.^[207] This can present competing pathways and can lead to the buildup of side-product or prevent the desired catalytic cycle from being

operative. Finally, for the development of a C–C bond forming reaction derived from all-alkyl α -amino radicals, the addition of α -amino radicals to simple alkenes is often known to be low-yielding owing to dimerization of α -amino radicals,^[208] or oligomerization of the resulting alkyl radical.^[125]



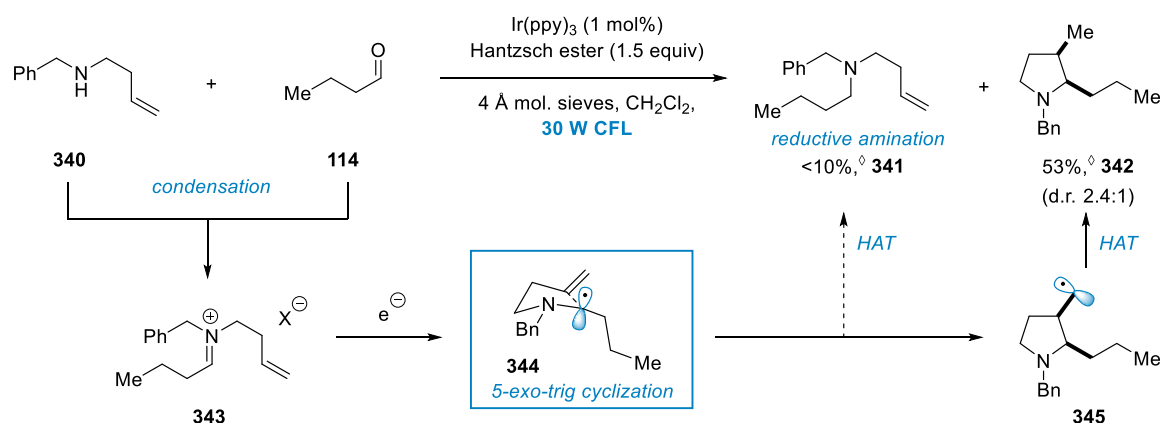
Scheme 54. Design plan for the photoredox catalyzed multicomponent olefin-hydroaminoalkylation.

Notwithstanding these challenges, we were intrigued by the potential gains of a methodology utilizing the reductive generation of all-alkyl α -amino radicals. Accordingly, the aim of the project described in this chapter was to develop a multicomponent approach for the visible light photoredox reduction of *in situ* generated all-alkyl iminium ions. α -Functionalization via radical reactions, such as conjugate addition, of the resulting elusive all-alkyl α -amino radicals **338** is explored (Scheme 54). The resulting complex tertiary amine products **339** belong to a compound class that has become ubiquitous among pharmaceutical agents, small-molecule probes and pre-clinical candidates. It was envisaged that an operationally straightforward photoredox method to enable the construction of complex tertiary amines from simple starting materials would have far-reaching implications both in the synthetic and medicinal chemistry community.

2.3 Results and Discussion

2.3.1 Discovery and early studies

The initial reaction that led to the discovery and design of the multicomponent hydroaminoalkylation reaction described in this chapter was conceived by Dr A. Trowbridge. These initial studies investigated the intramolecular 5-*exo*-trig cyclization of the α -amino radical **344** resulting from the condensation and visible light photoredox reduction of *N*-benzylbut-3-en-1-amine (**340**) and butyraldehyde **114** (Scheme 55). An initial hit was observed when the reaction was conducted with equimolar amounts of amine and aldehyde in the presence of 1.5 equivalents of Hantzsch Ester, activated molecular sieves (4 Å) and strongly reducing photocatalyst Ir(ppy)₃ (1 mol%) in dichloromethane under irradiation of a 30 W CFL light bulb.^[193] Remarkably, substituted pyrrolidine product **342** was observed in 53% (d.r. 2.4:1), which indicated that indeed consecutive condensation, single electron reduction, 5-*exo*-trig cyclization, and HAT reaction of the resulting primary radical **345** occurred in the reaction. Interestingly, only a small amount of reductive amination product **341** was obtained in the reaction. Contrary to Wenger's work,^[205] this suggests that the hydrogen atom donor, a relatively electron rich Hantzsch Ester, may selectively engage in a polarity matched HAT with primary alkyl radical **345** over the electron-rich α -amino radical **344**. The obtained stereoselectivity was consistent with that of Beckwith model for radical cyclizations.^[209]



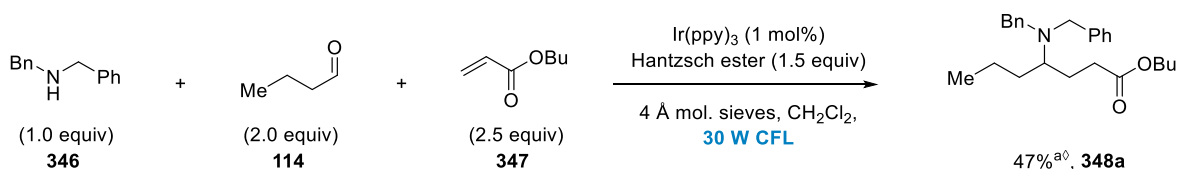
Scheme 55. Initial result of the photoredox catalyzed reductive cyclization of *N*-benzylbut-3-en-1-amine with butyraldehyde. [◊]Reaction conducted by Dr A. Trowbridge.

Dr A. Trowbridge subsequently conducted early studies^[193] investigating different hydrogen atom donors, such as *N*-benzyl-1,4-dihydronicotinamide (BnNADH), and photocatalyst loading, but found that neither variation was superior over the initial conditions. Furthermore,

a brief solvent screen was performed, indicating dichloromethane as favorable solvent for the outlined reaction. Ir(ppy)₃ gave the highest yield in a brief screen of photocatalysts, with [Ru(bpy)₃](PF₆)₂ only giving poor results. A slight increase in yield could be achieved by using 2.0 equivalents of butyraldehyde **114**, resulting in 62% yield of radical cyclization product **342** to be obtained. Raising the equivalents of Hantzsch Ester **316** proved detrimental to the reaction. Finally, a number of control reactions were carried out, demonstrating that no reaction is observed in the absence of either photocatalyst or when the reaction is conducted in the dark. Interestingly, 16% of radical cyclization product were observed when the reaction was carried out without Hantzsch Ester.

This intramolecular cyclization reaction based on this photoredox catalyzed reductive generation of α -amino radicals was then further pursued by N. J. Flodén, Dr D. Willcox, and Dr S. M. Walton, and Y. Kim.^[210]

This photoredox catalyzed reduction of *in situ* formed iminium ions to the respective α -amino radicals was next attempted in a multicomponent fashion. According to the design plan of this reaction, a secondary amine, aldehyde and electron deficient alkene could undergo a photocatalytic three-component coupling in the presence of photocatalyst and a stoichiometric reductant to give the formal olefin-hydroaminoalkylation products as α -amine functionalized tertiary amines. For the reaction, dibenzylamine **346**, due to its synthetic versatility, was selected together with butyraldehyde **114** for the *in situ* formation of the required iminium ion. As the radical acceptor component, *n*-butyl acrylate **347** was employed. Remarkably, under irradiation with a 30 W CFL bulb at room temperature with fan cooling, and in the presence of Ir(ppy)₃ photocatalyst, molecular sieves and Hantzsch Ester (1.5 equiv), the reaction proceeded to yield up to 47% yield of desired coupling product, if a two-fold excess of aldehyde **114** and acrylate **347** was used (Scheme 56).



Scheme 56. Initial conditions for the photoredox catalyzed multicomponent olefin-hydroaminoalkylation. ^aYield determined by ¹H NMR against internal standard 1,1,2,2-tetrachloroethane. [†]Reaction conducted by Dr A. Trowbridge.

2.3.2 Reaction optimization

Encouraged by these promising results, we turned our attention to the optimization of the multicomponent olefin-hydroaminoalkylation reaction. Initial experimentation included investigation of the desiccant, to establish if the condensation step is the limiting factor in the reaction. Indeed, it was found that molecular sieves were integral to the reaction and that no product **348** was obtained in their absence (Table 1, entry 2).

Table 1. Initial study investigating role of desiccant and vessel. ^a Yield determined by ¹H NMR against internal standard 1,1,2,2-tetrachloroethane.

Entry	conditions	reaction time	vessel	yield 348a [%] ^a
1	standard	12 h	10 mL MW tube, round	59
2	no mol. sieves	12 h	10 mL MW tube, round	trace
3	with H ₂ O (2.0 equiv)	12 h	10 mL MW tube, round	70
4	with benzoic acid (1.0 equiv)	12 h	10 mL MW tube, round	trace
5	no mol. sieves, with HOAc (0.1 equiv)	12 h	10 mL MW tube, round	trace
6	standard (various repeats)	12 h	10 mL MW tube, conical	30-65
7	standard (various repeats)	12 h	4 mL scint. vial	69-84
8	in the dark, 45 °C (oil bath)	12 h	4 mL scint. vial	0
9	2 lamps, 54 °C (no fan)	12 h	4 mL scint. vial	66
10	3 lamps, 40 °C (oil bath)	12 h	4 mL scint. vial	74

It was noticed, that under standard conditions, 59% yield was obtained, determined by ¹H-NMR, which was considerably higher as previously observed (Table 1, entry 2). This inconsistency became even more apparent when the reaction was conducted in the presence of two equivalents of water (Table 1, entry 3), in which case a 70% yield was observed. While this led to the conclusion that the reaction was not sensitive to moisture, a reproducibility issue was suspected. Benzoic acid, a common Brønsted acid catalyst to aid condensation in organocatalytic applications, was incompatible with the reaction conditions (Table 1, entry 4). It was suspected that trace acidity of molecular sieves could be crucial for the reaction, and replaced the molecular sieves with catalytic acetic acid, but no product formation was observed (Table 1, entry 5), confirming the initial hypothesis that the desiccant is essential. It was reasoned that the difference in obtained yields could stem from a varying degree of irradiation of the reaction vessels, which would affect the photon-flux and hence the obtained yields. According to the Bouguer–Lambert–Beer law, the penetration of visible light through

a reaction medium decreases exponentially with increasing path length.^[211] Hence, increasing the exposed surface area could increase photon transport into the reaction mixture.^[79] To test this hypothesis, the round bottom microwave (MW) tube reaction vessel was exchanged for a conical MW reaction vessel, which exposes higher surface area to the 30 W CFL bulb. In a series of experiments, yields ranging from 30 to 65% (Table 1, entry 6) were obtained, which confirmed the suspected low reproducibility. Due to its thin glass walls in respect to the round and conical MW tubes, smaller (4 mL) scintillation vials were subsequently employed in the reaction, and, pleasingly, higher yields (69-84%) with slightly increased reproducibility (Table 1, entry 7) were observed. To exclude thermal contributions to the reaction, it was established that no reaction occurred when the reaction was conducted in the dark in a 45 °C oil bath (Table 1, entry 8). If two, or three lamps were used at a time, slightly higher yields were obtained, and the temperature of the reaction mixture was found to have little to no impact (Table 1, entry 9 and 10).

In a further study investigating the photon-flux, the position of the vial in respect to the lamp was shown to considerably affect the ¹H-NMR yield of **348a**, resulting in differences as large as 54% to 71% due to respective position (Figure 10).

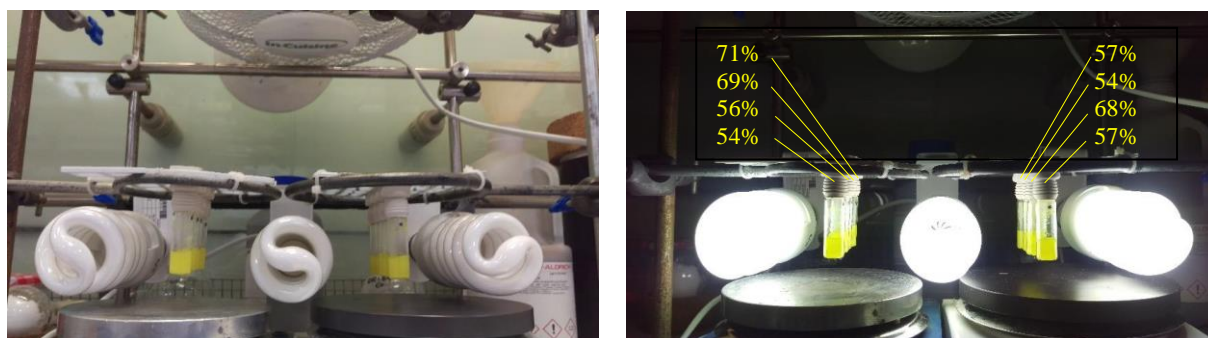


Figure 10. Photon-flux study varying the position of the reaction vessel, a (4 mL) scintillation vial, around the lamp. Yields determined by ¹H NMR against internal standard 1,1,2,2-tetrachloroethane.

On the basis of these studies, it was proposed that poor photon-flux was hampering the reaction, which was potentially further compounded by the heterogenous nature of the reaction mixture itself. It was therefore decided to employ a stronger, focused light source which should have more favorable overlap with the absorption spectrum of the Ir(ppy)₃ catalyst. The Kessil A160WE, a 40 W blue LED lamp commonly used for photoredox applications, was selected.^[212]



Figure 11. Improved reaction setup featuring a 40 W blue LED lamp (Kessil A160WE).

We were delighted to find that, using the new 40 W blue LED lamp distanced 5 cm from the reaction mixture with fan cooling, the reaction furnishes essentially quantitative yield of tertiary amine product **348a** by ^1H -NMR under otherwise unchanged conditions (Table 2, entry 1 and 2).

Table 2. Optimization studies with light source, stoichiometry, catalyst loading and reaction time. ^a Yields determined by ^1H NMR against internal standard 1,1,2,2-tetrachloroethane.

$ \begin{array}{c} \text{Bn} \\ \\ \text{H} - \text{N} - \text{CH}_2 - \text{Ph} \\ \text{346} \end{array} + \begin{array}{c} \text{O} \\ \\ \text{Me} - \text{CH}_2 - \text{CH}_2 - \text{CHO} \\ \text{114} \end{array} + \begin{array}{c} \text{OBu} \\ \\ \text{CH}_2 = \text{CH} - \text{C} = \text{O} \\ \text{347} \end{array} \xrightarrow[\text{4 \AA mol. sieves, CH}_2\text{Cl}_2, \text{40 W Blue LED (Kessil A160WE)}]{\text{Ir(ppy)}_3 \text{ Hantzsch ester}} \begin{array}{c} \text{Bn} \quad \text{Ph} \\ \quad \\ \text{Me} - \text{CH}_2 - \text{CH}_2 - \text{N} - \text{CH}_2 - \text{CH}_2 - \text{C}(=\text{O}) - \text{OBu} \\ \text{348a} \end{array} $									
#	eq. 346	eq. 114	eq. 347	eq. HE	[Ir]	time	lamp distance	vessel	348a [%] ^a
1	1.0	2.0	2.0	1.5	1 mol%	13 h	6 – 8 cm	4 mL scint. vial	88-96
2	1.0	2.0	2.0	1.5	1 mol%	13 h	5.0 cm	4 mL scint. vial	99
3	1.0	1.5	1.5	1.5	1 mol%	14 h	5.0 cm	4 mL scint. vial	99
4	1.0	1.1	1.1	1.5	1 mol%	14 h	5.0 cm	4 mL scint. vial	99
5	1.0	1.1	1.1	1.3	1 mol%	14 h	5.0 cm	4 mL scint. vial	85
6	1.0	1.1	1.1	1.1	1 mol%	14 h	5.0 cm	4 mL scint. vial	79
7	1.0	1.1	1.1	1.5	0.1 mol%	14 h	5.0 cm	4 mL scint. vial	67
8	1.0	1.1	1.1	1.5	-	14 h	5.0 cm	4 mL scint. vial	0
9	1.0	1.1	1.1	1.5	1 mol%	2 h	5.0 cm	VWR 4 mL	98

The new irradiation setup enabled us to increase efficiency by running the reaction in near equimolar stoichiometries of amine **346**, aldehyde **114**, and acrylate **347**, while obtaining near quantitative ^1H -NMR assay yields (Table 2, entry 3 and 4). Reduction of equivalents in Hantzsch Ester resulted in detriment in yield (Table 2, entry 5 and 6). Similarly, with a 0.1 mol% photocatalyst loading, only 67% ^1H -NMR yield was observed, and no reaction

occurred with the LED light source if no photocatalyst was employed (Table 2, entry 7 and 8). The reaction time was reduced to 2 hours, furnishing the reaction product **348a** in 98% assay yield (Table 2, entry 9). In order to increase reproducibility and operational simplicity, the reaction vessel was changed to commercial septum capped 4 mL VWR clear-glass vials (for details see chapter 5.1).

Interestingly, it was found that if the reaction was conducted with freshly distilled butyraldehyde, no formation of tertiary amine product **348a** took place (Table 3, entry 1). This led to the conclusion that a trace amount of butyric acid, likely present as contaminant in butyraldehyde **114**, is functioning as a critical Brønsted acid catalyst in the reaction. To test this hypothesis, known amounts of butyric acid were added as an additive to the reaction mixture using freshly distilled butyraldehyde. Reactivity was restored upon addition of trace butyric acid, and tertiary amine product **348a** was obtained in near quantitative assay yield upon addition of 0.1 equivalents of butyric acid (Table 3, entry 2-4). Propionic acid was tested and provided the same result (Table 3, entry 5).

Table 3. Study to establish the critical Brønsted acid additive. a. Yields determined by ^1H NMR against internal standard 1,1,2,2-tetrachloroethane.

Entry	reaction time	acid additive	amount acid (equiv)	348a [%] ^a
1	14 h	-	-	0
2	4 h	butyric acid	0.05	83
3	4 h	butyric acid	0.1	99
4	2 h	butyric acid	0.1	97
5	2 h	propionic acid	0.1	98

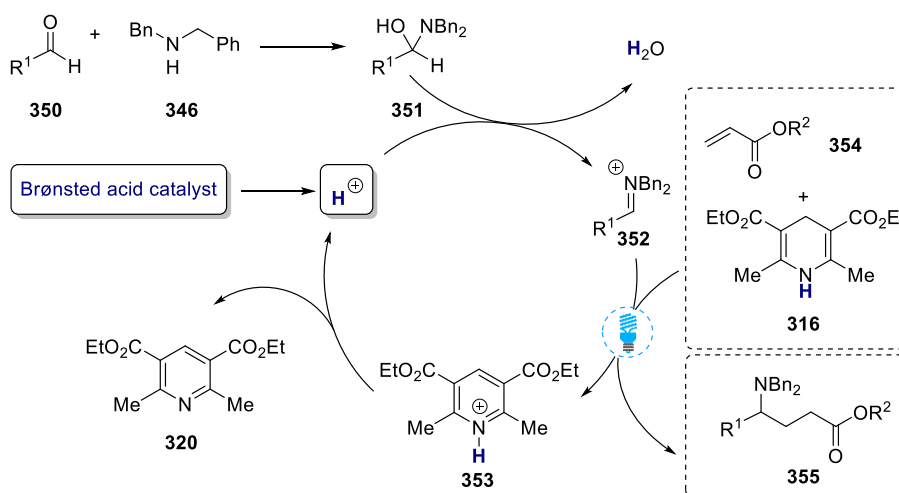
Having established this critical reaction component, a number of Brønsted acid additives were investigated. As the reaction was optimized to quantitative yield with butyraldehyde **114**, freshly distilled cyclohexyl carboxaldehyde **349** was chosen as carbonyl component, which gave moderate yields under standard conditions (Table 4, entry 1). Varying the stoichiometry of propionic acid, it was found that a loading of 0.2 equivalents afforded the optimum yield of 66% tertiary amine product **348m** observed by ^1H -NMR (Table 4, entry 2-4). It is known that the rate of condensation reactions is highly dependent on the pH value of the reaction

medium.^[213] Therefore, a variety of Brønsted acids in the pK_a range from 0.23 (trifluoroacetic acid, TFA) to 7.97 (hexafluoroisopropanol, HFIP) were tested (Table 4, entry 5-10). While product was observed for all tested Brønsted acids, only modest yields were obtained for TFA and (±)-10-camphorsulfonic acid with 47% and 43% yield respectively. Weak acids pyridinium *p*-toluenesulfonate (PPTS, 53% yield) and HFIP (36% yield) also afforded significantly lower yields than the standard conditions with 0.2 equivalents of propionic acid. Carboxylic acids such as octanoic acid and adamantanecarboxylic acid gave better results, 61% and 63% yield respectively, but were not superior to the initially tested propionic acid system. It was concluded that the addition of 0.2 equivalents of propionic acid proved to provide the best results was thus established as part of the standard conditions.

Table 4. Reaction optimization: Brønsted acid screen. ^a Yields determined by ¹H NMR against internal standard 1,1,2,2-tetrachloroethane.

Entry	acid additive	amount acid (equiv)	acid pK_a (H ₂ O)	yield 348m [%] ^a
1	propionic acid	0.1	4.88 ^[214]	55
2	propionic acid	0.2	“	66
3	propionic acid	0.5	“	62
4	propionic acid	1.0	“	57
5	TFA	0.1	0.23 ^[215]	47
6	CSA (±)	0.1	1.2 ^[216]	43
7	octanoic acid	0.2	4.89 ^[217]	61
8	adamantanecarboxylic acid	0.2	4.8-4.9	63
9	PPTS	0.2	5.21	53
10	HFIP	0.2	7.97	36

The requirement of an external Brønsted acid catalyst provided some mechanistic insight at an early stage of the investigation. It is predicted that the Brønsted acid is an initial proton source, aiding the condensation of secondary amine **346** and aldehyde **350** to give hemiaminal **351** (Scheme 57).



Scheme 57. Proposed Brønsted acid catalysis operative in the reaction.

Protonation of the hemiaminal intermediate **351** then allows an equivalent of water to be liberated to form iminium ion **352**. Furthermore, after reductive quenching and subsequent HAT of the starting Hantzsch Ester **316**, Hantzsch Ester pyridinium salt **353** is formed which serves as a proton source for the reaction.

2.3.3 Scope of the reaction

With the optimized conditions in hand, the generality of the reaction was investigated. Due to the multicomponent nature of the reaction, each of the three starting materials, aldehyde, amine, and radical acceptor can be varied to provide a comprehensive study of the scope of the reaction. To aid purification, some of the reactions in the substrate screen were carried out using modified Hantzsch Ester **356** bearing 2-methoxyethyl esters, rather than ethyl esters (**316**), as this led to the generation of more polar pyridine derivatives which could be separated more easily (Figure 12).

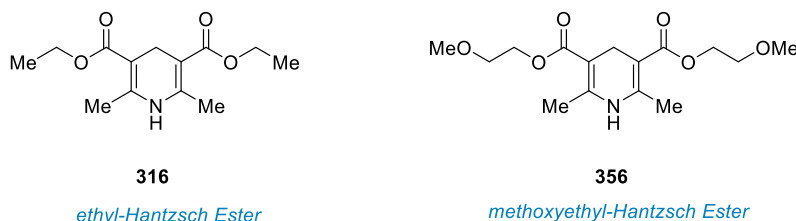
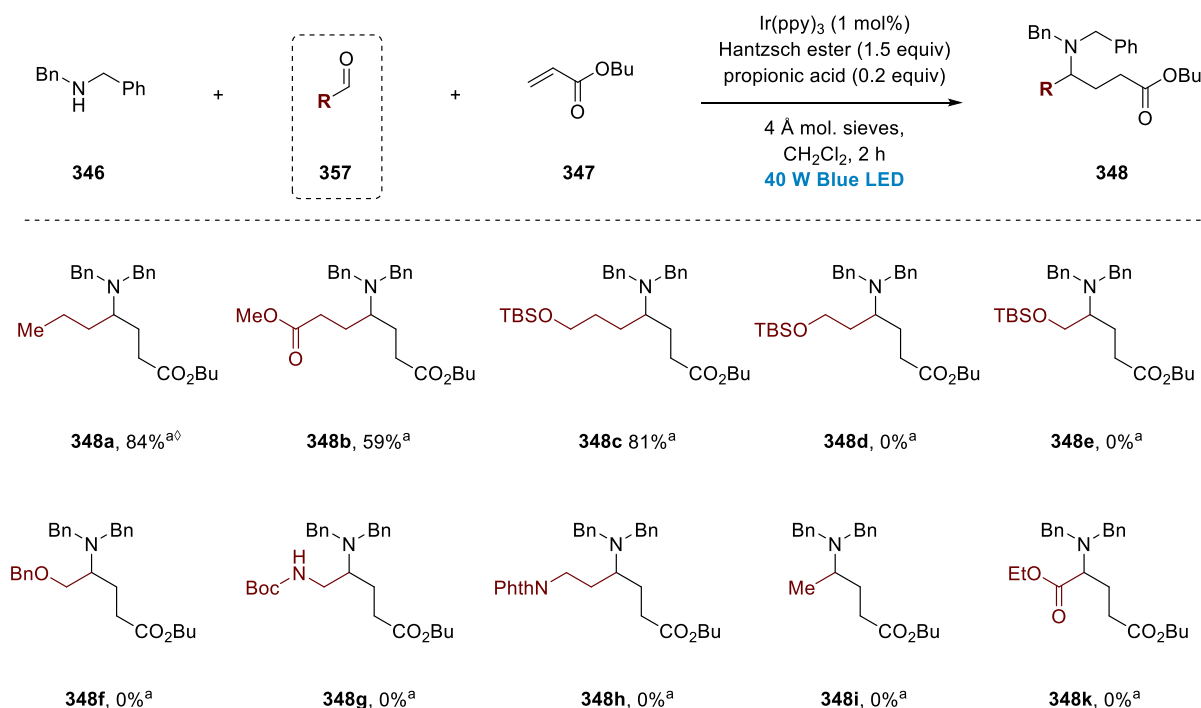


Figure 12. Hantzsch Esters **316** and **356** used in this substrate scope.

First, the aldehyde component was investigated. It was found that a series of aliphatic aldehydes could be accommodated under the reaction conditions, such as butyraldehyde (**114**), giving resulting amino ester **348a** in isolated in 84% yield (Scheme 58). Furthermore, methyl 4-oxobutanoate (**357b**), and 4-((*tert*-butyldimethylsilyl)oxy)butanal (**357c**), afforded

the corresponding complex tertiary amines **348b** and **348c** in 59% and 81% yield respectively. TBS-Protected 3-hydroxy propanal **357d** and 2-hydroxy acetaldehyde **357e** were unproductive under the reaction conditions, potentially due to the activation of the β - and γ -amino positions after condensation, promoting side reactions. Similarly, benzoxyacetaldehyde **357f**, *N*-Boc protected 2-amino acetaldehyde **357g** and 3-phthalimidopropionaldehyde **357h** did not yield the desired product under the reaction conditions due to decomposition. Acetaldehyde **357i** proved too reactive, forming a black precipitate upon addition to the reaction mixture, presumably from polymerization of the *in situ* formed enamine. Additionally, ethyl glyoxylate **357k**, employed as a freshly distilled solution in toluene, also did not lead to product formation. It was concluded that despite broad functional group tolerance, the reaction is sensitive to heteroatom substitution of the aldehyde in the α or β -position.

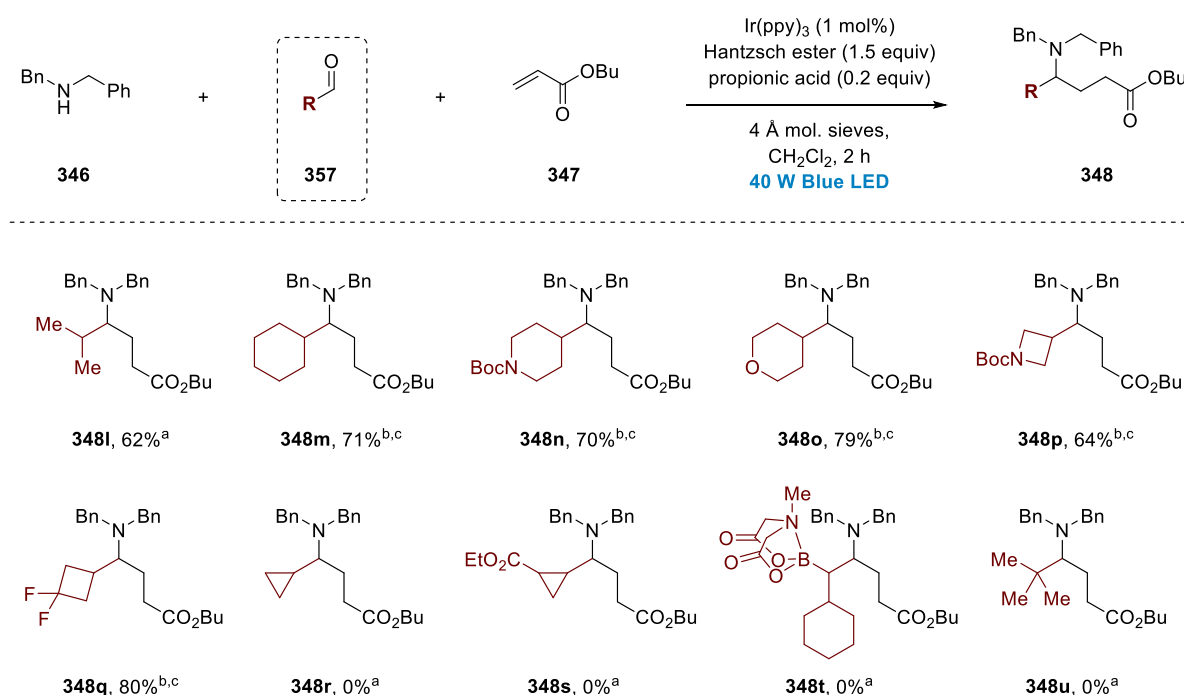


Scheme 58. Aliphatic aldehyde scope for photocatalytic multicomponent synthesis of alkyl tertiary amines.

^aamine:aldehyde:acceptor (1:1.1:1.1). [†]Reaction conducted by Dr A. Trowbridge.

Next, a number of α -branched aldehydes was tested to study the effect of the steric encumbrance of this center on the reaction (Scheme 59). Good yields were obtained with isobutyraldehyde **357l** and cyclohexylcarboxaldehyde **357m** under the standard conditions, with the desired tertiary amine products **348l** and **348m** isolated in 62% and 71% yield respectively. 4-*N*-Boc-piperidine- and 4-tetrahydropyrane carboxaldehyde (**357n** and **357o**) afforded similar yields, with 70% for tertiary amine **348n**, and 79% for tertiary amine **348o**,

albeit with 2 equivalents of aldehyde and radical acceptor used. Four-membered ring systems have become a prominent structural feature for drug discovery and medicinal chemistry applications, and can lead to enhanced pharmaco-kinetic properties of drugs.^[218-220] Accordingly, the four membered ring containing aldehydes *N*-Boc-azetidine carboxaldehyde (**357p**) and 3,3-difluoro-cyclobutane carboxaldehyde (**357q**) were subjected to the reaction conditions, furnishing the corresponding products **348p** and **348q** in 64% and 80% yield respectively.



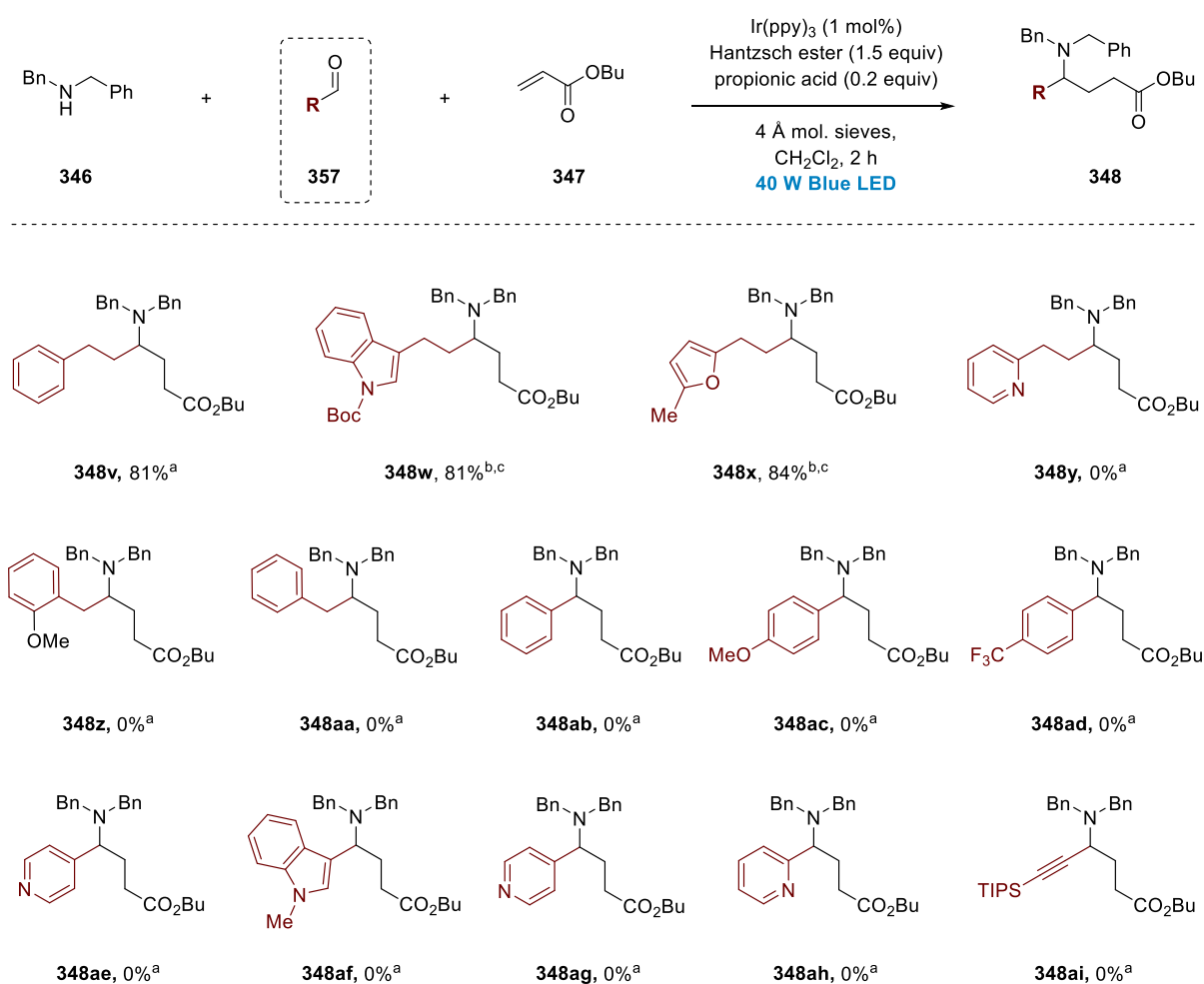
Scheme 59. α -Branched aldehyde scope for photocatalytic multicomponent synthesis of alkyl tertiary amines.

^aamine:aldehyde:acceptor (1:1.1:1.1); ^b amine:aldehyde:acceptor (1:2:2); ^c methoxyethyl-Hantzsch ester **356** used (1.5 equiv.).

If cyclopropane derived carboxaldehydes **357r** and **357s** were used, no product formation was observed, likely due to fragmentation of the three membered rings from the α -amino radical intermediate and the subsequent side reactions. Furthermore, MIDA-boronate ester **357t** proved unproductive under the reaction conditions, potentially due to the large steric demand of the aldehyde α -position in this substrate. Lastly, no product formation was observed if pivaldehyde **357u** was employed as the carbonyl component. Overall, α -branched aldehydes were amenable to the reaction, albeit in slightly lower yields.

Having established the reactivity for aliphatic aldehydes, aryl containing aldehydes, both remote and in conjugation with the aldehyde, were investigated (Scheme 60). Dihydrocinnamaldehyde **357v** gave complex tertiary amine product **348v** in excellent 81%

isolated yield. Other β -aryl substituted aldehydes also were good substrates for the reaction, such as 3-(*N*-Boc-3-indolyl)propional **357w** and 3-(5-methylfuran-2-yl)propanal **357x**, resulting in formation of products **348w** and **348x** in impressive 81% and 84% yield respectively. However, the reaction proved incompatible with the analogous 2-pyridine substrate **357y**, which failed to undergo the desired transformation. Moving the aryl group to the α -position of the aldehyde, such as in arylacetaldehydes **357z** and **357aa** resulted in complete suppression of product formation. Arguably, this effect may have been caused by the vastly increased stability of the respective enamine, which is in an (proton loss induced) equilibrium with the iminium ion.

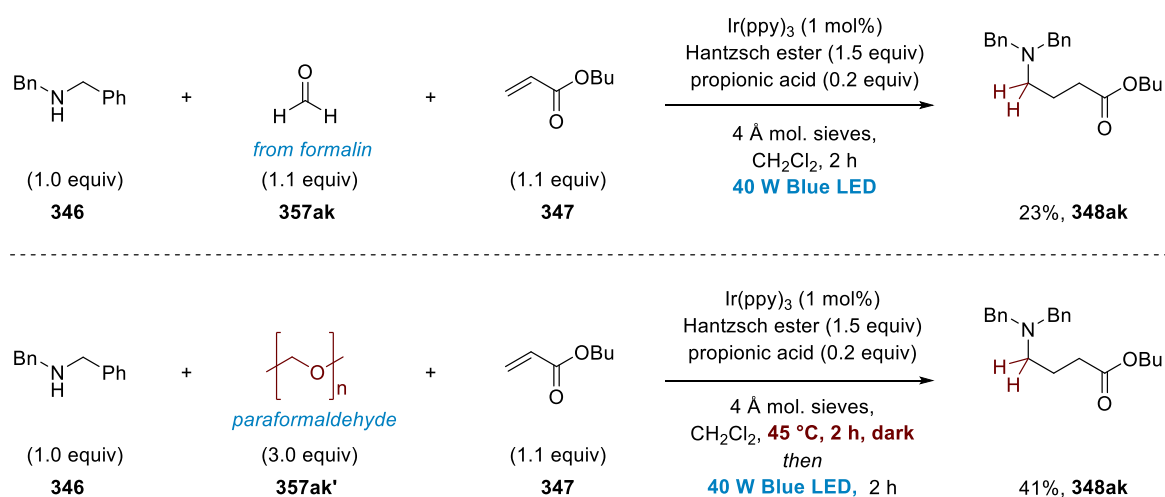


Scheme 60. Aryl containing aldehyde scope for photocatalytic multicomponent synthesis of alkyl tertiary amines. ^a amine:aldehyde:acceptor (1:1.1:1.1); ^b amine:aldehyde:acceptor (1:2:2); ^c methoxyethyl-Hantzsch ester **356** used (1.5 equiv.).

A number of aromatic aldehydes such as benzaldehydes **357ab**, **357ac** and **357ad** were tested but did not result in formation of the desired products. The fact that aromatic aldehydes in general were unsuitable substrates for the reaction was contrary to some literature protocols

involving benzaldimines, but was corroborated further by the failure of nitrogen-heteroaromatics-containing aldehydes **357ae**, **357af**, **357g**, and **357ah** to lead to the desired products. Although the reaction with aryl aldehydes is subject to ongoing studies in our laboratory, we hypothesize that the resulting benzylic α -amino radicals are less nucleophilic due to conjugation with the aromatic system and do not undergo the subsequent radical addition to acrylates. Finally, when propargylic aldehyde **357ai** as was tested, no product formation was observed.

Our interest was piqued by the possibility of developing a hydroaminomethylation procedure from this protocol, which could be realized if formaldehyde could be used as carbonyl source in the present reaction. A hydroaminomethylation system was tested using dibenzylamine **346**, formaldehyde **357ak** and *n*-butyl acrylate **347** as a potentially useful modular reaction platform. We were mindful of the high reactivity of formaldehyde derived iminium ions, particularly towards reductive processes and polymerization. When simple formalin solution (37% formaldehyde in H₂O, stabilized with 10-15% MeOH) was employed, the aminomethylation product **348ak** was observed in low but significant 23% yield (Scheme 61). Extensive studies were performed to identify the ideal delivery method for the formaldehyde gas to be available under the reaction conditions. Unfortunately, the efforts were complicated by the fact that gaseous formaldehyde would polymerize to form paraformaldehyde precipitate in the reaction solvent, dichloromethane.

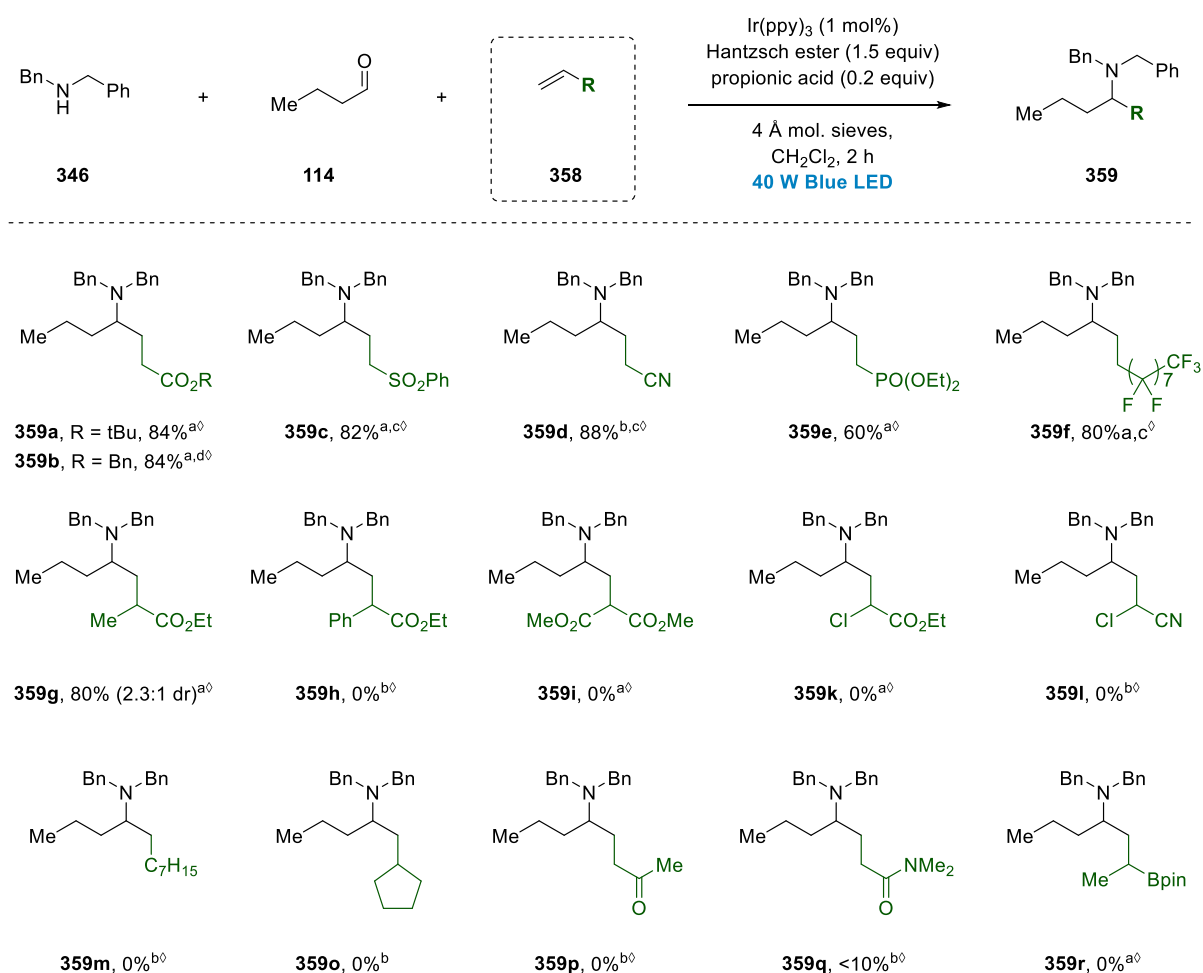


Scheme 61. Photocatalytic multicomponent hydroaminoalkylation using different formaldehyde sources.

Nonetheless, a suitable protocol was identified, when solid paraformaldehyde was used as formaldehyde source. The best results were obtained using a two-step procedure, in which the reaction mixture containing excess paraformaldehyde was first heated to 45 °C in the dark,

followed by immediate irradiation of the reaction mixture at room temperature. Using this method, aminomethylation product **348ak** was obtained in 41% isolated yield (Scheme 61).

Having established the aldehyde part of the reaction scope, we turned our attention to the alkene coupling partners **358**. A number of potentially suitable alkenes and known radical acceptors were tested in this study led by Dr A. Trowbridge (Scheme 62).

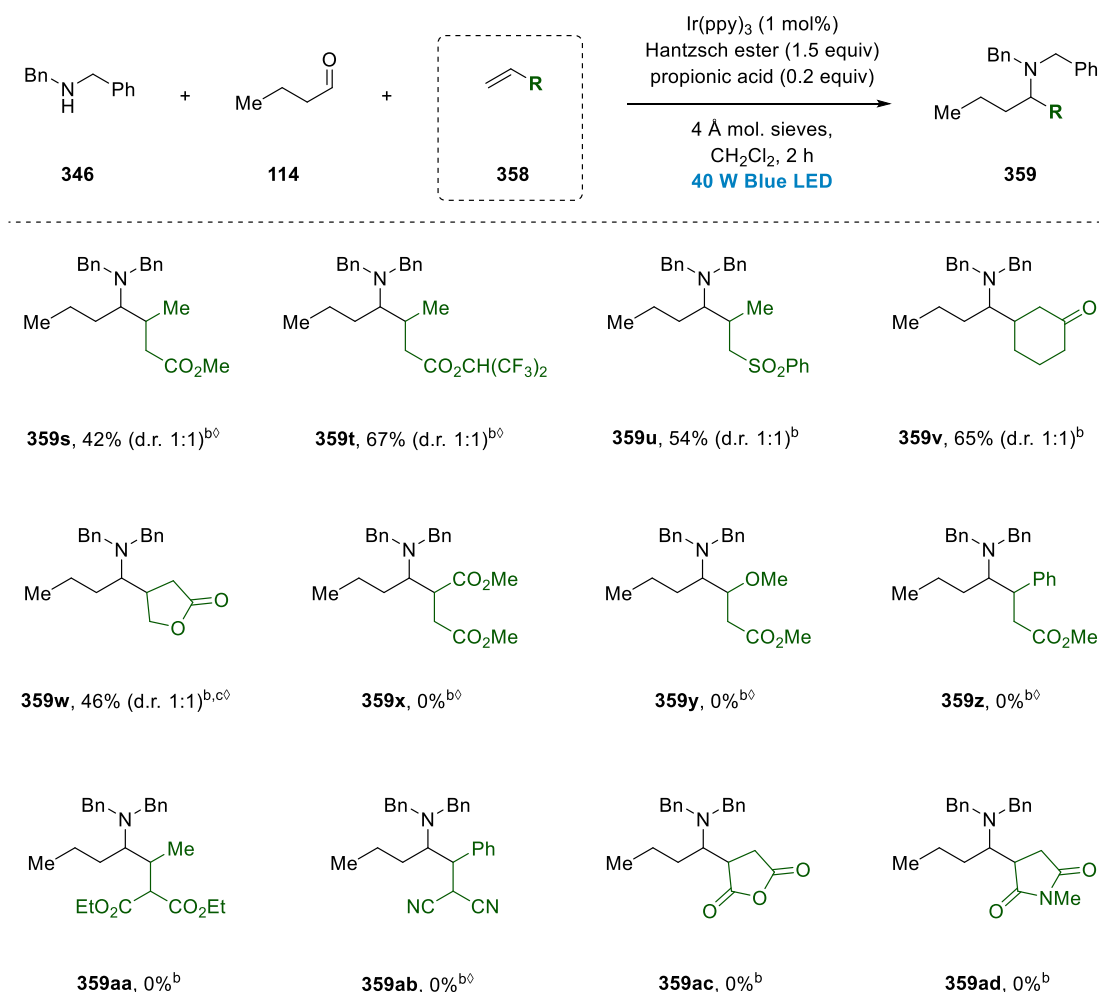


Scheme 62. Radical acceptor scope for photocatalytic multicomponent synthesis of alkyl tertiary amines. ^a amine:aldehyde:acceptor (1:1.1:1.1); ^b amine:aldehyde:acceptor (1:2:2); ^c methoxyethyl-Hantzsch ester **356** used (1.5 equiv); ^d performed on gram-scale. ^oReaction conducted by Dr A. Trowbridge.

It was established that simple acrylates, such as *t*-butyl- or benzyl acrylate **358a** and **358b** functioned as excellent radical acceptors in the reaction, both affording yields of 84%. Importantly, despite the often problematic scale up of photoredox protocols, the reaction involving benzyl acrylate could be performed on gram-scale giving the same result with a catalyst loading of 0.5 mol% Ir(ppy)_3 . Several common radical acceptors were subsequently tested, such as vinyl sulfone **358c**, acrylonitrile **358d** and vinyl phosphonate **358e** and were well tolerated with 82%, 88%, and 60% yield obtained respectively. Perfluorinated alkenes

such as **358f** afforded excellent yield of coupled product **359f** (80%), enabling the multicomponent incorporation of perfluorinated alkane chains through this methodology. Furthermore, a number of α -substituted acrylates and acrylonitriles **358g-l** were screened, of which only ethyl methacrylate **358g** gave satisfying results with an 80% yield of coupling product **359g** in 2.3:1 diastereomeric ratio. Phenyl, malonyl, and chloro substituents were unsuccessful under the reaction conditions (**358h-l**) due to high reactivity towards polymerization-type side reactions. Unsurprisingly, non-activated alkenes 1-octene **358m** and methyldiene cyclopropane **358o** did not deliver the respective products due to their low rate for radical additions.^[221] Moreover, methyl vinyl ketone **358q** led to polymerization without product formation, and dimethyl-acrylamide **358q** proved a poor radical acceptor for the reaction with only trace product observed. Finally, using vinyl boronate **358r**, no product formation was observed.

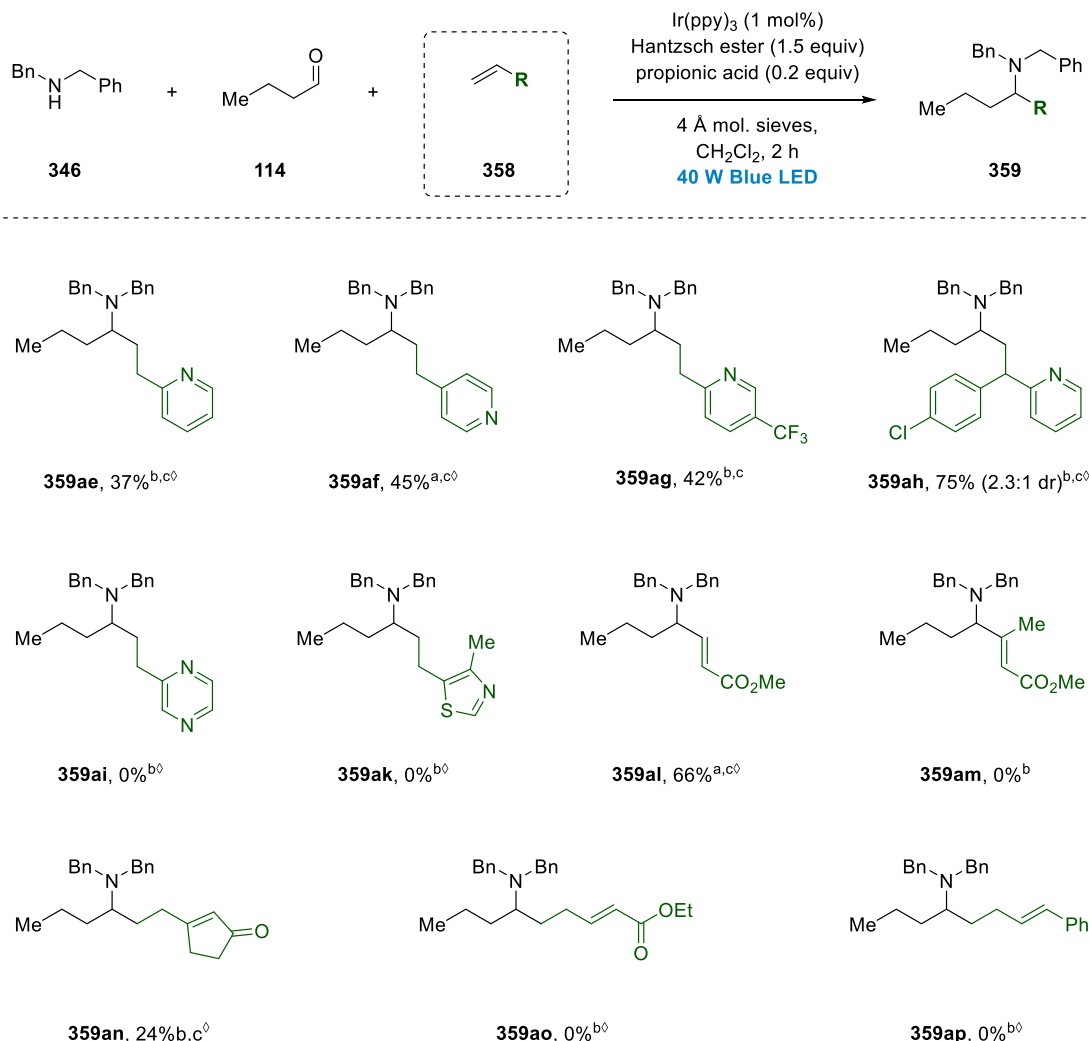
Moreover, internal alkene radical acceptors were investigated (Scheme 63).^[193] Crotonic acid derived internal alkenes **358s** and **358t** were viable substrates, delivering the coupling products **359s** and **359t** in 42% and 67% yield (d.r. 1:1). Similar reactivity was observed for internal vinyl sulfone **358u**, cyclohexenone **358v** and butenolide **358w**, with moderate yields of 54%, 65% and 46% in coupling products **359u-w** obtained respectively (1:1 d.r.). The ketone in cyclohexanone product **359v** was well tolerated, with excellent selectivity of the reaction for the aldehyde. Fumarates, 3-methoxyacrylates and cinnamates **358x-z** all proved unreactive under the reaction conditions. Additionally, highly reactive alkylidene malonates and malonitriles **358aa** and **358ab** were incompatible and did not deliver the respective coupling products. Lastly, maleic acid derivatives **358ac** and **358ad** were subjected to the reaction conditions but did not afford the desired amine products.



Scheme 63. Internal alkene radical acceptor scope for photocatalytic multicomponent synthesis of alkyl tertiary amines. ^a amine:aldehyde:acceptor (1:1.1:1.1); ^b amine:aldehyde:acceptor (1:2:2); ^c methoxyethyl-Hantzsch ester **356** used (1.5 equiv); ^d performed on gram-scale. ^oReaction conducted by Dr A. Trowbridge.

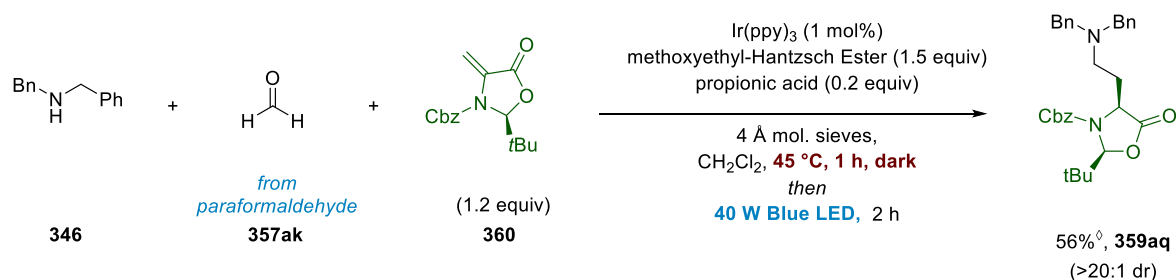
Next, due to their ubiquity of aromatic and heteroaromatic moieties in medicinal chemistry,^[220] possible vinyl arene acceptors were studied (Scheme 64). Gratifyingly, vinyl pyridines **358ae-358ag** were compatible with the reaction, producing the respective pyridine products **359ae-359ag** in 47%, 45% and 42% yield. Notably, vinyl pyridine **358ah** was used to directly access coupling product **359ah** in 75% yield (d.r. 2.3:1), a derivative of the first generation antihistamine chlorphenamine. Unfortunately, it was found that both vinyl pyrazine **358ai** and vinyl thiazole **358ak** are less amenable as coupling partners, not delivering the desired product scaffolds. The addition of α -amino radicals into alkynes is underdeveloped,^[222] therefore we were pleased to find that radical addition with alkyne **358al** proceeded smoothly under the standard conditions, giving the product **359al** in 66% yield. Regrettably, analogous internal alkyne 2-butyne (358am) only gave trace product in a complex mixture. It was established that 1,4 addition under the reaction conditions is feasible using vinylcyclopentenone **358an**, which furnished the unsaturated product **359an**, albeit in

low yield of 24%. However, the reaction proved unsuccessful for related ethyl sorbate **358ao** and phenylbutadiene **358ap**.



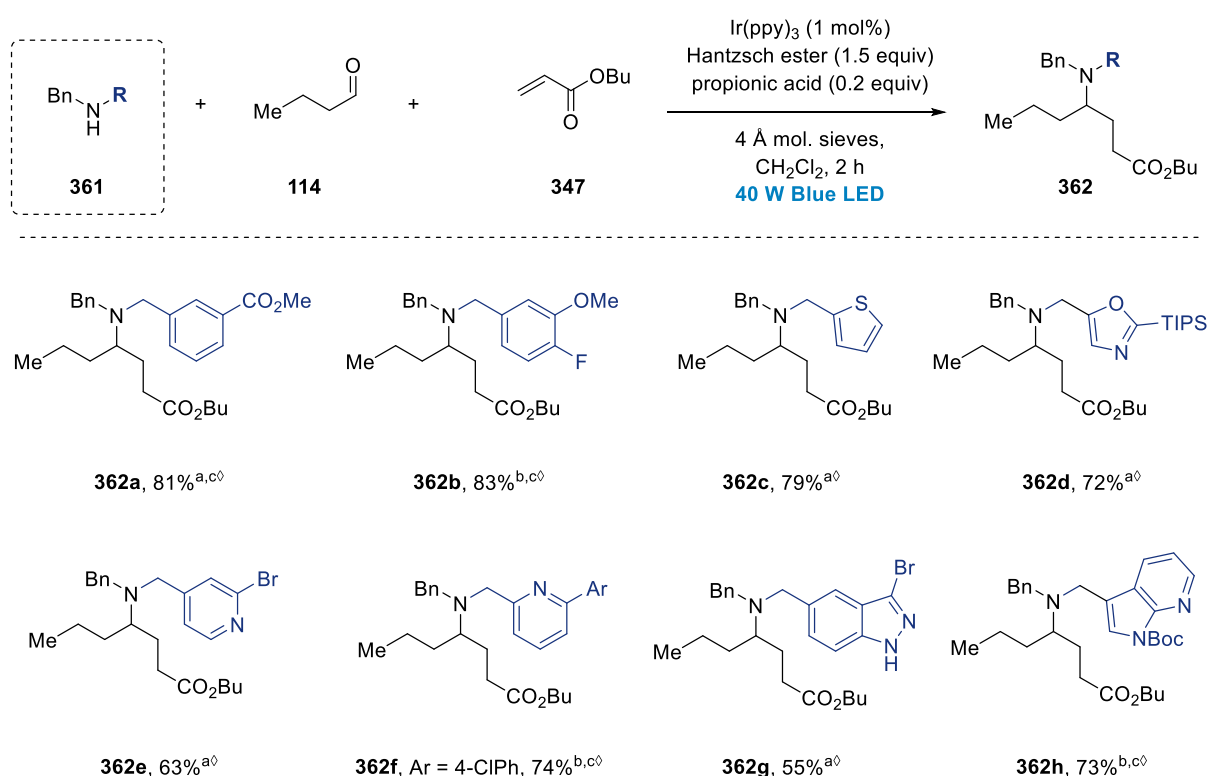
Scheme 64. Aryl and alkyne conjugated radical acceptor scope for photocatalytic multicomponent synthesis of alkyl tertiary amines. ^a amine:aldehyde:acceptor (1:1.1:1.1); ^b amine:aldehyde:acceptor (1:2:2); ^c methoxyethyl-Hantzsch ester **356** used (1.5 equiv); ^d performed on gram-scale. ^oReaction conducted by Dr A. Trowbridge.

The synthesis of enantioenriched non-natural amino acids is a longstanding area of interest in the synthetic community and can be a formidable challenge, depending on the desired side chain to be installed.^[223] To this end, it was reasoned that the use of a suitable chiral radical acceptor to access this desirable class of compounds via the modular multicomponent reaction would be a valuable protocol. Accordingly, chiral cyclic dehydroalanine **360**, first described by Beckwith^[224-225], based on work by Karady^[226] and Seebach,^[227] was identified as a privileged acceptor towards the synthesis of chiral α -amino acid. **360** is readily accessible from *S*-benzyl cysteine^[228] and was produced on a multi-gram scale in our laboratory (see Section 3.3.2, Scheme 137).



Scheme 65. Synthesis of enantioenriched non-canonical amino acids via multicomponent photocatalytic olefin-hydroaminoalkylation of dehydroalanine **360**. [◊]Reaction conducted by Dr A. Trowbridge.

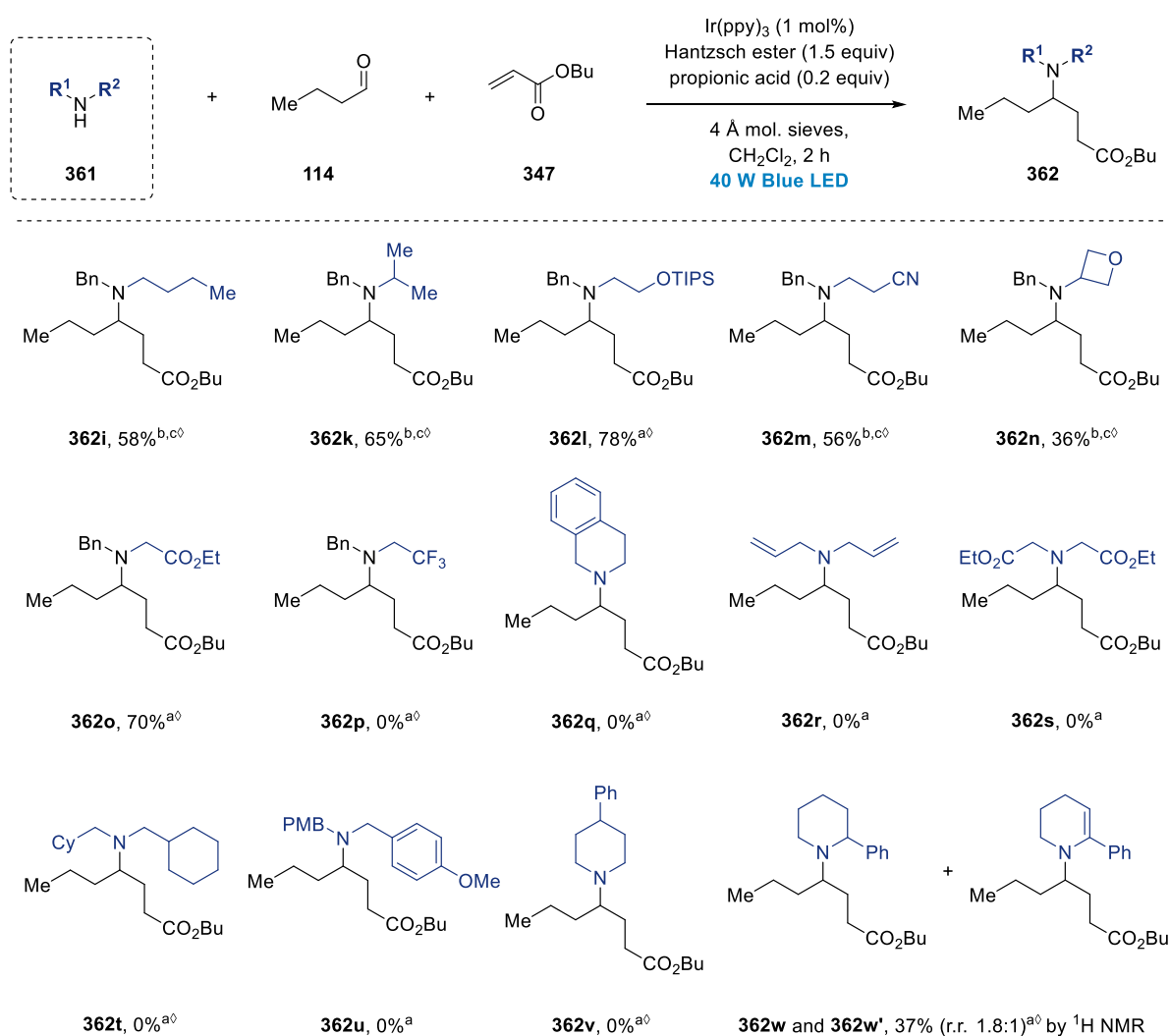
Gratifyingly, dehydroalanine **360** proved an amenable radical acceptor for the reaction. Reaction with dibenzylamine **346** and formaldehyde **357ak** under the standard conditions afforded protected 2,4-diamino butyric acid product **359aq** in 56% in excellent diastereomeric ratio (Scheme 65). As previously explored for this compound by Beckwith,^[224] diastereoselective HAT is occurring from the *re*-face due to steric control exerted by the *tert*-butyl substituent (see also Scheme 133).



Scheme 66. Benzylamine scope for the photocatalytic multicomponent synthesis of alkyl tertiary amines. ^a amine:aldehyde:acceptor (1:1.1:1.1); ^b amine:aldehyde:acceptor (1:2:2); ^c methoxyethyl-Hantzsch ester **356** used (1.5 equiv.); [◊]Reaction conducted by Dr A. Trowbridge.

With the scope of aldehydes and electron deficient alkenes firmly established, we turned our attention to the secondary amine scope. A study led by Dr A. Trowbridge investigated a

number of benzylic and aliphatic secondary amines under the established reaction conditions (Scheme 66).^[193] It was found that ester, fluorine and phenol ether substituent containing dibenzylamines **361a** and **361b** are excellent substrates, giving the corresponding products **362a** and **362b** in 81% and 83% yield respectively. Thiophene **361c** and silyl-oxazole **361d** were tolerated well under the reaction conditions affording similarly high product yields. A series of heteroaromatic benzyl surrogates **361e-h** were tested, containing 4-pyridine, 2-pyridine, bromo-indazole and 7-azaindole moieties, which all proved amenable under the reaction conditions, affording moderate to high yields. Remarkably, bromine substituents commonly undergoing dehalogenation and radical coupling side reactions under similar conditions were stable under the reaction conditions.



Scheme 67. Further amine scope for the photocatalytic multicomponent synthesis of alkyl tertiary amines. ^a amine:aldehyde:acceptor (1:1.1:1.1); ^b amine:aldehyde:acceptor (1:2:2); ^c methoxyethyl-Hantzsch ester **356** used (1.5 equiv.); [◊]Reaction conducted by Dr A. Trowbridge.

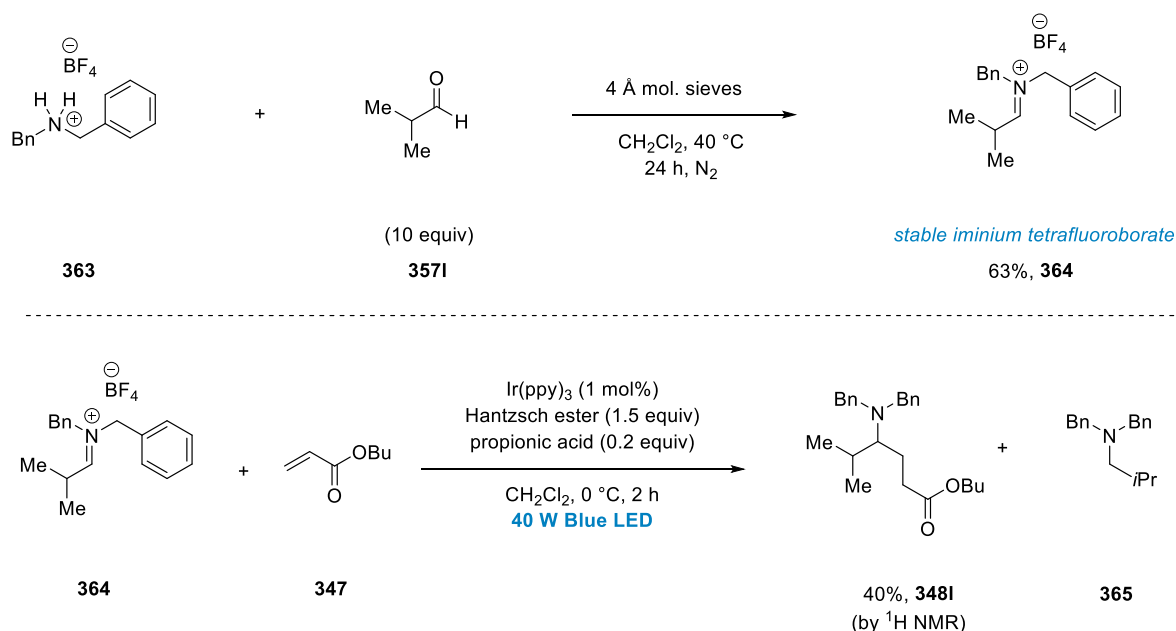
To expand the secondary amine scope beyond dibenzylamines, a series of *N*-benzyl alkylamines and *N,N*-dialkylamines were tested. Butyl-benzylamines **361i** and **361k** gave good conversion to the respective products **362i** and **362k** 58% and 65% yield. Silylether- and nitrile functionalized *N*-benzyl alkylamines **361l** and **361m** were compatible with the reaction conditions and delivered the target amines in good yields. Despite its sensitivity towards acid, oxetane bearing *N*-benzylamine **361n** delivered the desired product **362n**, albeit in decreased yield of 36%. Furthermore, glycine derived benzylamine **361o** cleanly generated the desired coupling product **362o** in 70% yield. 2,2,2-Trifluorobenzylamine **361p** failed to deliver desired product, arguably due to the low nucleophilicity of the secondary amine towards the necessary condensation step.^[229] It was noted that tetrahydroisoquinoline **361q** showed significant decomposition under the reaction conditions due to facile oxidative aromatization. Given the established reactivity of benzylamines in the reaction, a number of symmetric dialkylamines such as diallylamine **361r**, diethyl iminodiacetate **361s**, and bis(cyclohexylmethyl)amine **361t** were investigated, but regrettably none of the *N,N*-dialkyl amines afforded the desired amine products. It was found that bis(*para*-methoxybenzyl) amine **361u** was also incompatible with the reaction conditions. In line with other *N,N*-dialkylamines, 4-phenyl piperidine **361v** proved incompatible with the methodology, underpinning the apparent requirement of a benzylamine. Before concluding, 2-phenylpiperidine **361w** was investigated as a substrate, but it produced an inseparable mixture of tertiary amine products **362w** and **362w'**, and attempts to isolate the material failed.

2.3.4 Mechanistic studies

Given the requirement for a benzylic substituent on the starting nitrogen of the amine substituent, the underlying mechanistic explanation for this unexpected outcome was investigated. Firstly, it was important to confirm that the single electron reduction of the iminium ion (rather than an enamine oxidation-type mechanism) is indeed the operative pathway to arrive at the initial α -amino radical. Some evidence had already been obtained at this point, given that formaldehyde, which is unable to form enamines, is a suitable substrate for the reaction. This suggested that the single electron reduction of the Eschenmoser-like iminium salt is indeed operative, at least when formaldehyde is the substrate. Furthermore, MacMillan reported that similar enamines from condensation of secondary amines and aldehydes are not quenching the photoexcited state of catalyst *fac*-Ir(ppy).^[230]

To unambiguously demonstrate the iminium ion as immediate precursor of the α -amino radical, the reaction was performed from an isolated preformed dibenzyl iminium salt.

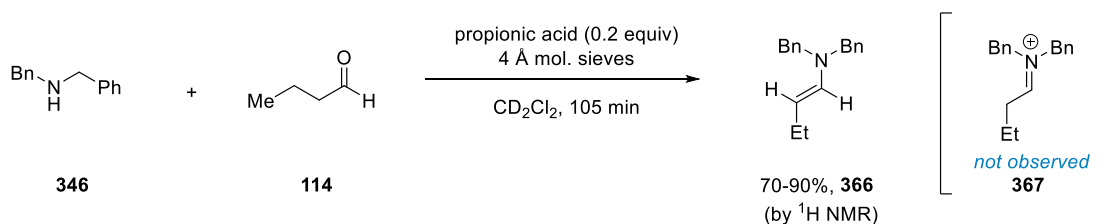
Ultimately, the iminium tetrafluoroborate salt **364**, derived from dibenzylammonium tetrafluoroborate **363** and isobutyraldehyde **357I**, was successfully obtained following a modified procedure based on work by Melchiorre and co-workers (Scheme 68).^[231] The preformed iminium tetrafluoroborate **364**, which was highly moisture sensitive but exhibited sufficient stability in solution under strictly anhydrous conditions, afforded the desired coupling product **348I** with butyl acrylate **347** when subjected to the standard reaction conditions, albeit in low quantities. The main reaction product **365** was generated by polar reduction of the iminium ion with Hantzsch Ester (evidenced by GC-MS), which occurred in the dark. Critically, this pathway could largely be mitigated by conducting the reaction at 0 °C, affording the desired product in 40% yield by ¹H-NMR.



Scheme 68. Synthesis of iminium tetrafluoroborate and stoichiometric control reaction yielding desired coupling product **348I**.

While this experiment proved the involvement of the iminium ion as the precursor for the single electron reduction, the fast polar reduction of the iminium with Hantzsch Ester was somewhat surprising as these reduction products were not observed under the standard conditions. It was suspected that the iminium ion may only be formed in small quantities and replenished by protonation of the enamine. An investigation of the crude reaction mixture of dibenzylamine **346**, butyraldehyde **114**, propionic acid and molecular sieves in *d*₂-dichloromethane was performed to identify the predominant species in the reaction. Interestingly, it was found that after a 105 minutes incubation period, 70-90% of the starting materials were converted to the respective enamine **366**, which was the dominant species in

the reaction mixture at the recorded time (Scheme 69, for data see *Appendix II*, Figure 24). Respective transient iminium ion **367** was not observed under the reaction conditions within the sensitivity of ^1H -NMR. In agreement with MacMillan's findings that **366**-type enamines do not quench the $\text{Ir}(\text{ppy})_3$ excited state,^[230] it was proposed that the majority of condensation product generated by secondary amine and aldehyde resides in the reaction mixture as the corresponding enamine, inert to the photocatalytic cycle, thus precluding the polar reduction of the respective iminium ion by Hantzsch Ester.



Scheme 69. ^1H NMR study showing enamine **366** as predominant species in the reaction mixture. Crude mixture of dibenzylamine, butyraldehyde, propionic acid (0.2 equiv) in CD_2Cl_2 . Yields determined by ^1H NMR against internal standard 1,1,2,2-tetrachloroethane.

To further investigate the role of the iminium ion in the reaction mechanism, Stern-Volmer quenching studies between the $\text{Ir}(\text{ppy})_3$ photocatalyst and preformed iminium tetrafluoroborate **364** were performed (Figure 13, for details and data see *Appendix II*). It was found that the excited photocatalyst was effectively quenched by the iminium ion with a quenching rate constant of $k_q = 6.2 \times 10^5 \text{ L} \cdot \text{mol}^{-1} \text{ s}^{-1}$. This quenching could either result from an energy-transfer mechanism between the photoexcited $^*\text{Ir}(\text{ppy})_3$ to the iminium ion, or from single electron reduction of the iminium ion. Although the $^*\text{Ir}(\text{III})$ species would be potentially reducing enough ($\text{Ir}(\text{IV})/^*\text{Ir}(\text{III})$, $E_{1/2}^{\text{red}} = -1.73 \text{ V vs SCE}$)^[37] to induce SET to some all-alkyl iminium ions,^[182] it was reasoned that quenching with the Hantzsch Ester would occur far more likely due to its higher relative concentration in the reaction mixture and significantly larger quenching rate constant ($k_q = 1.7 \times 10^7 \text{ L} \cdot \text{mol}^{-1} \text{ s}^{-1}$).^[193] Overall, in line with a number of literature reports,^[232] the results indicate that a reductive quenching cycle through initial oxidation of Hantzsch Ester is operative. UV-Vis analysis performed by Dr A. Trowbridge on Hantzsch Ester **316** and iminium tetrafluoroborate **364** further excluded the presence of a donor-acceptor complex (for details see *Appendix II*).

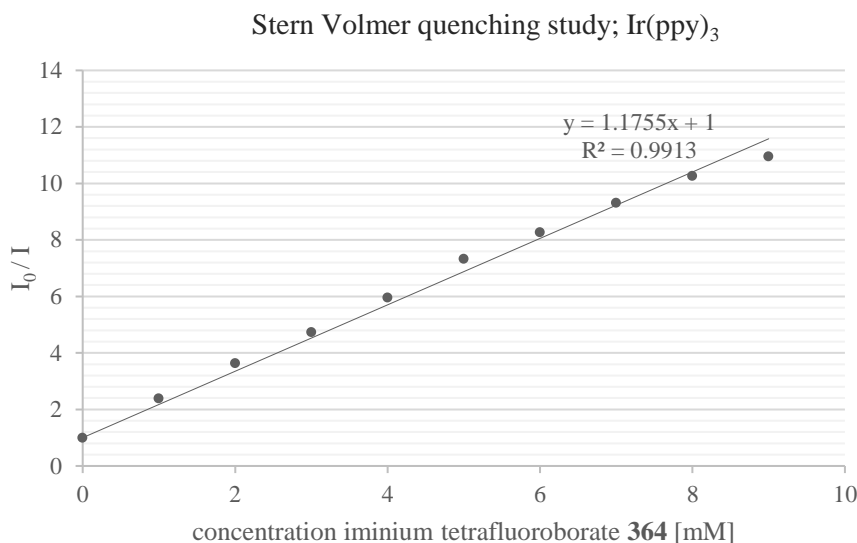
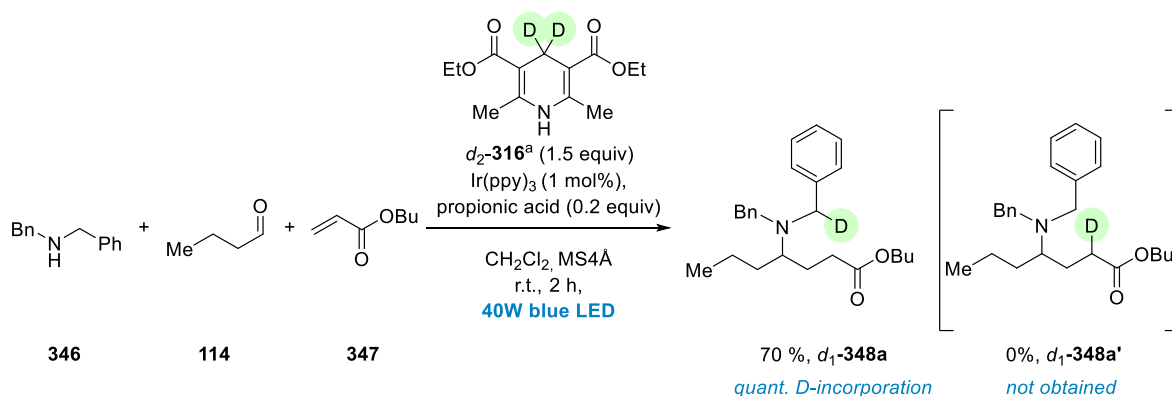


Figure 13. Stern Volmer quenching study demonstrating quenching of the photoexcited *Ir(ppy)₃ by iminium tetrafluoroborate **364**.

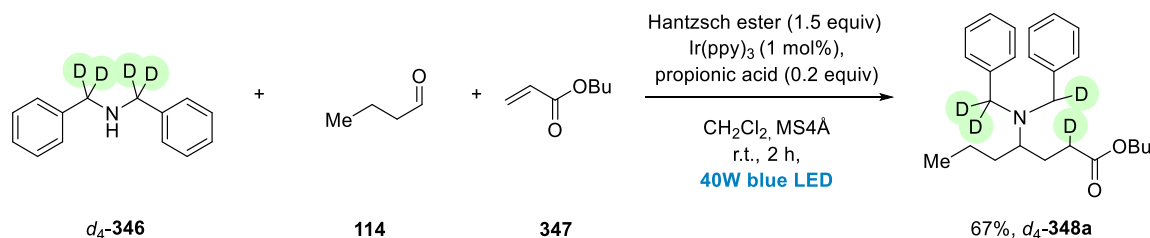
Next, an investigation into the mechanistic role of the *N*-benzyl substituent was performed. Therefore, a deuterium labelling study with *d*₂-4,4-Hantzsch Ester (*d*₂-**316**) was pursued to reveal possible intramolecular HAT events. When the reaction was performed with dibenzylamine **346**, butyraldehyde **114**, butyl acrylate **347**, and deuterated Hantzsch Ester *d*₂-**316**, mono-deuterated product *d*₁-**348a** was exclusively obtained as single regioisomer (rather than expected regioisomer *d*₁-**348a'**), with quantitative deuterium incorporation (Scheme 70, for data see Appendix II, Figure 27).



Scheme 70. Deuterium labelling studies indicating a 1,5 HAT process. ^aprepared by Dr M. Taylor.

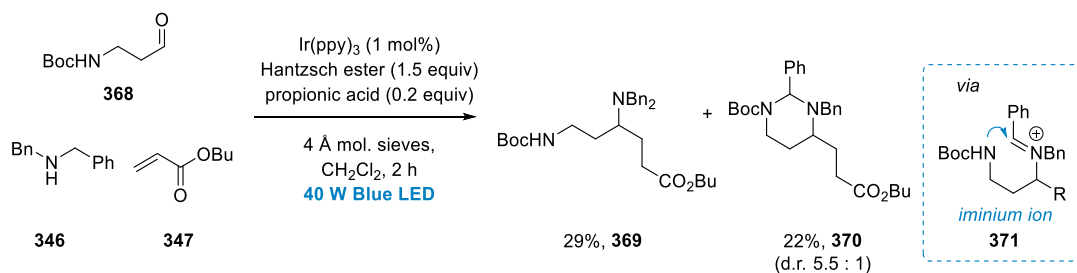
The results strongly indicated a 1,5-HAT process was operative subsequent to the radical addition, migrating the alkyl radical from the α-ester position to the benzylic position, where it undergoes HAT with Hantzsch Ester to furnish the product. To corroborate this result, *d*₄-dibenzylamine *d*₄-**346** was prepared. Using the standard conditions, the reaction between *d*₄-

dibenzylamine **d₄-346**, butyraldehyde **114**, butyl acrylate **347**, and Hantzsch Ester **316** led to exclusive formation of respective deuterated product **d₄-348a** (Scheme 71, for data see Appendix II, Figure 28), confirming the 1,5-HAT pathway.



Scheme 71. Deuterium labelling studies using **d₄-dibenzylamine d₄-348a**, confirming a 1,5-HAT process.

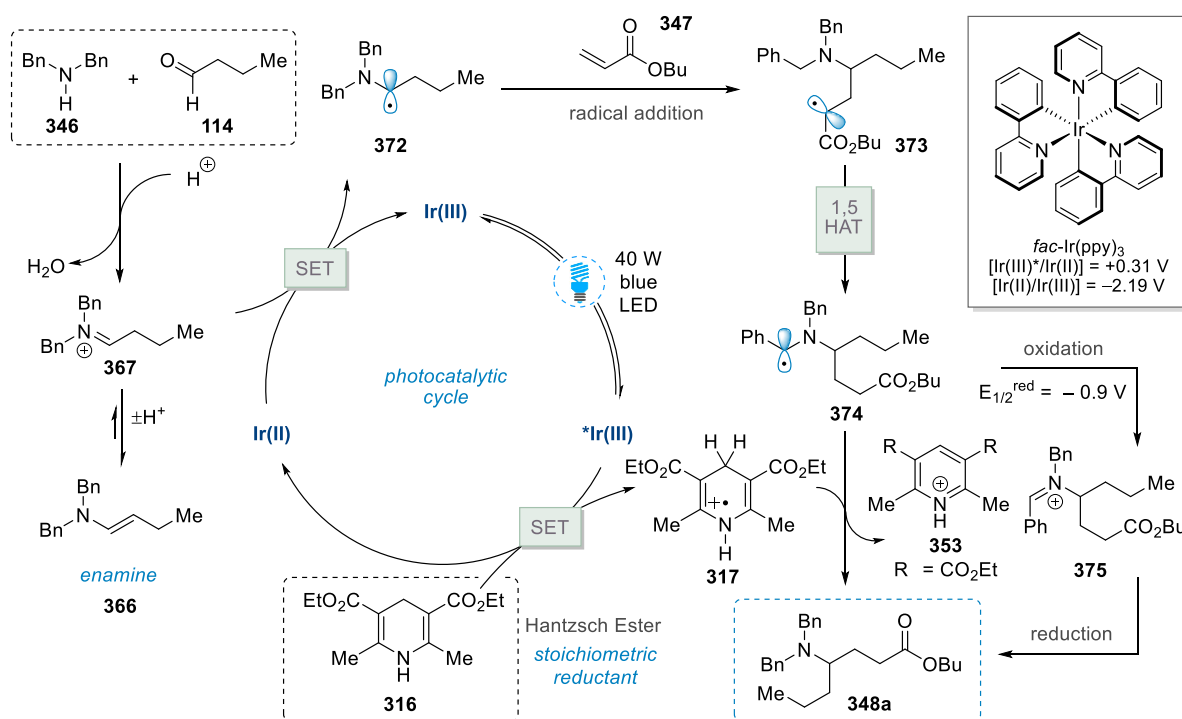
Lastly, a mechanistically relevant observation was made when *N*-Boc-3-aminopropionaldehyde **368**, bearing the pendant nucleophilic *N*-Boc group in 3-position, was employed as aldehyde component in the reaction. Unexpectedly, along with formation of the desired product **369** (29% yield), we observed generation of unusual cyclic aminal **370** in 22% yield (d.r. 5.5:1) (Scheme 72). While this result gave further proof that the benzylic amine substituent is non innocent in the reaction, the observed reaction was unlikely the result of a cyclization of the benzylic radical. It was reasoned that this interesting C–N bond formation would most probable be caused by nucleophilic addition of the carbamate nitrogen into benzyldene iminium ion **371**. Iminium ion **371** could in turn be derived from the respective benzylic radical via single electron oxidation.



Scheme 72. Iminium ion cyclization to form cyclic aminal **370**.

Based on the results from these mechanistic studies, a proposed mechanism was outlined for the photocatalytic multicomponent olefin-hydroaminoalkylation (Scheme 73). The catalytic cycle begins with visible light excitation to afford the photoexcited $^*\text{Ir(III)}$ species. Efficient reductive quenching with Hantzsch Ester **316** ($^*\text{Ir(III)}/\text{Ir(II)}$, $E_{1/2}^{\text{red}} = +0.31 \text{ V vs SCE}$)^[37] generates the radical cation **317** and the highly reducing Ir(II) species. Brønsted acid mediated condensation of amine **346** and aldehyde **114** leads to formation of iminium ion **367**. The equilibrium is predominantly on the side of the enamine form **366**, which is inert under the

reaction conditions.^[230] It is proposed that the enamine is thus an off-cycle precursor to the iminium ion **367**, with the acid maintaining a low concentration of iminium ion **367** by protonation of the enamine **366**. Importantly, the generated Ir(II) species is sufficiently reducing (Ir(III)/Ir(II), $E_{1/2}^{\text{red}} = -2.19$ V vs SCE)^[37] to undergo SET with the full range of alkyliminium ions,^[182] leading to α -amino radical **372**. α -Amino radical **372** now engages in addition to acrylate **347**, furnishing alkyl radical **373**. Stabilization via 1,5-HAT reaction to form the respective benzylic radical **374** precludes the propensity of alkyl radical **373** to undergo oligomerization,^[125] and serves as a thermodynamic driving force^[180] to promote the reversible radical addition process. Similar 1,5-HAT assisted approaches to aid radical addition processes have been reported by Tan and Liu,^[233-234] as well as Chiba and Gagosz.^[235]



Scheme 73. Proposed mechanism for the photocatalytic olefin-hydroaminoalkylation.

Intermolecular HAT between benzylic radical **374** and Hantzsch Ester **316** or its radical cation **317** then affords the product tertiary amine **348a** alongside protonated Hantzsch pyridine **353**, which serves as a proton source. However, facile oxidation of benzylic radical **374** ($E_{1/2}^{\text{red}} = -0.9$ V vs SCE)^[95] can lead to formation of benzyldene iminium ion **375**, which can in turn undergo photocatalytic or polar reduction by Hantzsch Ester **316** to produce the tertiary amine product **348a**. Notably, this formal redox-relay process in which the starting iminium ion is translated into a new iminium ion in a redox-neutral fashion, is, to the best of our knowledge, unprecedented.

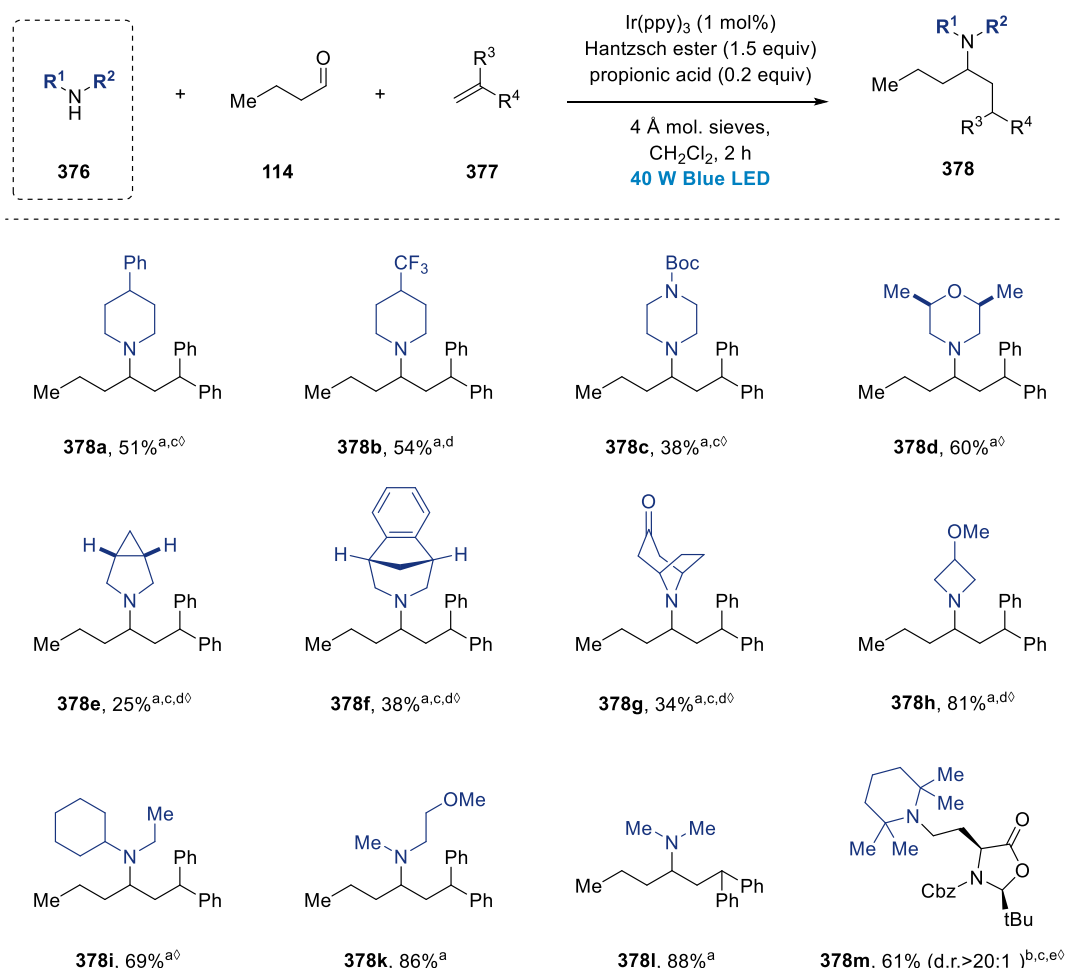
While the outlined mechanism is proposed as the most likely mechanistic pathway, a minor oxidative pathway originating from the oxidative quenching of the photoexcited $^*\text{Ir(III)}$ with iminium ion **367** cannot be ruled out. Furthermore, energy transfer processes, such as from photoexcited $^*\text{Ir(III)}$ to Hantzsch Ester **316**, cannot be entirely discounted. This could be exemplified by an energy-transfer process leading to the photoexcited Hantzsch Ester species, which has been shown to act as a powerful reductant with reduction potentials up to $E_{1/2}^{\text{red}} = -2.28 \text{ V}$,^[236] formally capable to engage in iminium reduction. Finally, a possible chain propagation mechanism involving **317** cannot be excluded.

2.3.5 Extended scope and functionalization of enamines

The intriguing mechanistic results obtained from the studies, in particular in regard to the operative 1,5-HAT process, showed the serendipitously placed benzyl group as crucial promoter for the radical addition, overcoming the inherent challenges of this addition reaction. Fortuitously, the benzyl group can be easily removed via hydrogenolysis and thus acts as a protecting group, enabling for example later functionalization on the nitrogen after selective deprotection.^[237] However, it was reasoned that the use of an alkene that would produce a less-electrophilic radical should favor direct reaction with the Hantzsch ester **316** or its radical cation **317**, obviating the need for the 1,5-HAT process, and hence permitting the use of various dialkylamines and expanding the methodology to a wealth of non-benzylic amines.

Accordingly, for this extended amine substrate scope, 1,1-diphenylethylene was selected as radical acceptor under otherwise unchanged reaction conditions. This hypothesis was tested in a photocatalytic coupling of non-benzylic amine 4-phenyl piperidine **361v** (an unsuccessful substrate in the previous addition to acrylates), butyraldehyde **114** and diphenylethylene radical acceptor **377a** using standard conditions. Pleasingly, it was found that the desired tertiary amine product **378a** was obtained in 51% yield. Notably, the resulting 3,3-diarylpropylamines are of significant importance as part of the first-generation family of H_1 antihistaminic agents.^[238-240] Continued investigation showed that substituted heterocyclic aliphatic amines such as trifluoromethyl substituted piperidine **376b**, Boc-piperazine **376c** and dimethyl morpholine **376d** afforded the desired products **378b**, **378c**, and **378d** in 54%, 38%, and 60% respectively. Azabicyclo[3.1.0]hexanes, azepines, tropinones and azetidines all were amenable substrates for the reaction furnishing the desired substituted 3,3-diarylpropylamines **378e-h** in moderate to good yields. Non-cyclic aliphatic secondary amines such as *N*-cyclohexyl-ethylamine **376i**, 2-(methoxyethyl)methylamine **376k** and dimethylamine **376l**

delivered high yields of the respective products. Importantly, coupling between hindered secondary tetramethylpiperidine **376m**, formaldehyde **357ak**, and dehydroalanine acceptor **360** gave the desired product **378m** in 61% yield (d.r. >20:1), demonstrating that dehydroalanine acceptor **360** does not require the 1,5-HAT process to be operative. The product **378m** can be deprotected to the enantioenriched amino acid.^[193]

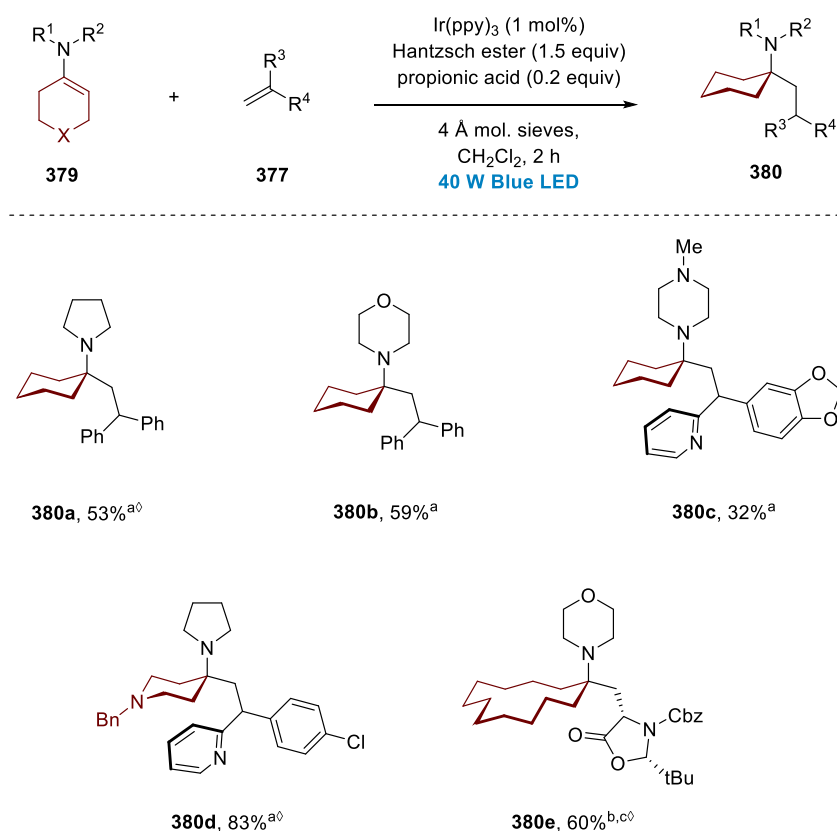


Scheme 74. Extended non-benzylic amine scope for the photocatalytic multicomponent synthesis of alkyl tertiary amines. ^a amine:aldehyde:acceptor (1:2:2); ^b acceptor (1.5 equiv); ^c methoxyethyl-Hantzsch ester **356** used (1.5 equiv.); ^d amine hydrochloride and NEt_3 (1.0 equiv) used. ^e paraformaldehyde (5 equiv) used, preheated for 1 h; ^d Reaction conducted by Dr A. Trowbridge.

While this process successfully extended the amine scope beyond benzylamines, we were intrigued by the opportunity to employ dialkylketones in the reaction to produce a number of synthetically intractable, α -tertiary amines. This prospect is particularly promising due to the high desirability of the α -tertiary amine motif, which is present in a large number of naturally occurring bioactive compounds,^[241] but also due to the fact that this class C–N bond is inaccessible via traditional reductive amination^[242] approaches due to the α -tertiary center. Despite our extensive efforts, dialkylketones proved entirely unreactive in the

multicomponent approach, arguably due to the considerably slower condensation rates of ketones compared to aldehydes with the only moderately nucleophilic benzylamines.

It was reasoned that due to the more forcing conditions required to access ketiminium ions, protonation of preformed alkylenamines, which can be readily prepared^[243-244] and commercially available, could provide a more accessible source of the necessary ketiminium ion intermediate. Indeed, under standard conditions, a number of alkylenamines **379** underwent smooth coupling with alkene acceptors **377** to form the desired α -tertiary amine products **380** (Scheme 75).

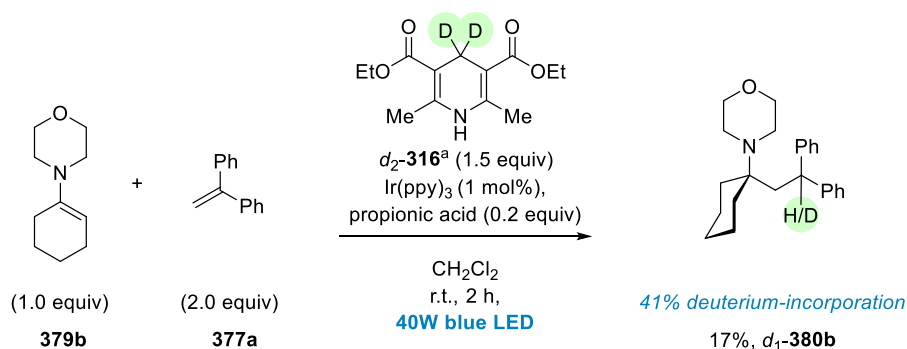


Scheme 75. Enamine scope for the photocatalytic multicomponent synthesis of alkyl tertiary amines. ^a Reaction conducted using enamine:acceptor (1:2 equiv); ^b Reaction conducted using enamine:acceptor (1:1.1 equiv); ^c methoxyethyl-Hantzsch ester **356** used (1.5 equiv.); [‡]Reaction conducted by Dr A. Trowbridge.

The coupling of 1-cyclohexenyl pyrrolidine **379a** with 1,1-diphenylethylene **377a** was established to give the target α -tertiary amine product **380a** in 53% yield. Encouraged by this result, cyclohexenyl morpholine **379b** was subjected to the same conditions, affording 59% yield. Methyl-piperazine derived enamine **379c** was coupled successfully with aryl substituted vinyl pyridine acceptor **377c**, furnishing the highly polar complex α -tertiary amine product **380c** in synthetically useful 32% yield. Moreover, coupling of *N*-benzyl enamine **379d** and

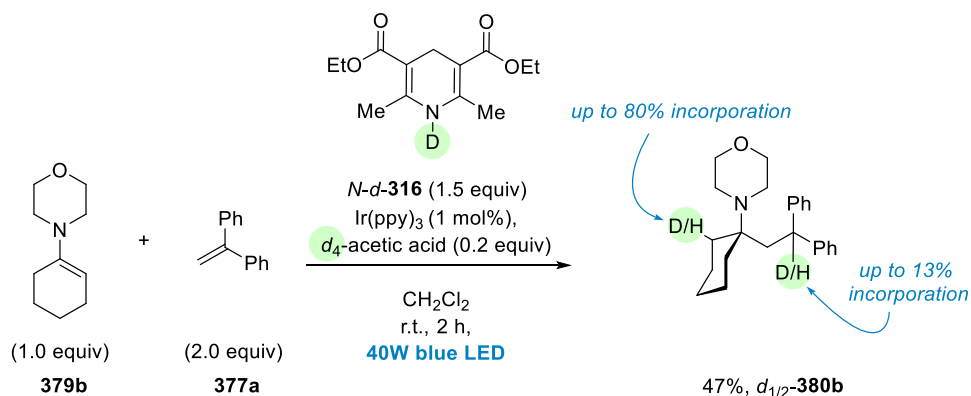
cyclohexenone derived enamine **379e** with vinyl pyridine **377d** and chiral dehydroalanine acceptor **360** were achieved in good yields.

Given this novel mode of reactivity, it was decided to briefly investigate the mechanistic aspect of the enamine reaction in a deuterium labeling experiment. Firstly, cyclohexenyl morpholine **379b** was subjected to standard reaction conditions using d_2 -Hantzsch Ester d_2 -**316**. Only a low yield of 17% product d_1 -**380b** was isolated under these conditions (Scheme 76, for data see *Appendix II*). In line with the hypothesis that an alkene producing a less electrophilic radical should favor direct reaction with Hantzsch ester **316** or its radical cation **317** (and their deuterated analogues), obviating the need for the 1,5-HAT process, 41% deuterium incorporation was observed (by ^1H -NMR) in the bis-benzylic position. It is likely that H/D scrambling occurs from this position either under reaction conditions or during purification.^[245]



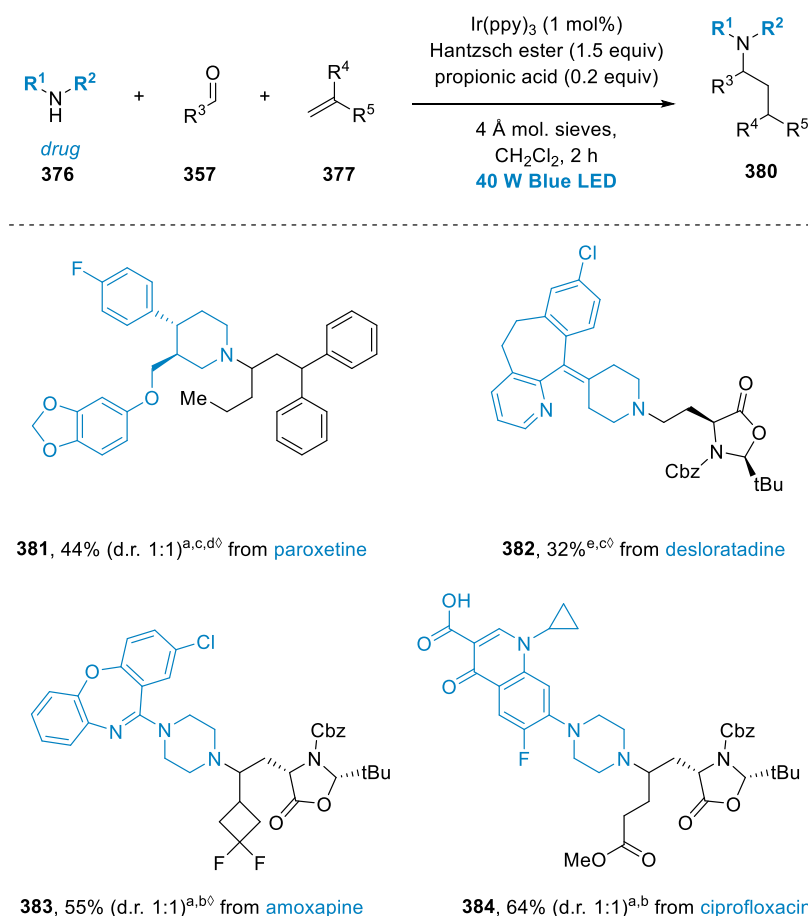
Scheme 76. 1,1-Diphenylethylene acceptor deuterium labeling study with enamines. ^aprepared by Dr. M. Taylor.

Given the reduction potential of the bis-benzylic radical ($E_{1/2}^{\text{red}} = -1.34 \text{ V vs. SCE}$)^[246] was likely to be in the range of the photoexcited state of the catalyst, it was investigated if deuterium incorporation in bis-benzylic position would occur using d - N -Hantzsch Ester^[247-248] d - N -**316** and d_4 -acetic acid (Scheme 77, for data see *Appendix II*). Under these conditions, major deuterium incorporation was observed at the enamine β -carbon, confirming the protonation-reduction pathway. Only minor incorporation was observed in the bis-benzylic position, suggesting HAT with Hantzsch Ester or its radical cation is the major reaction pathway for the bis-benzylic radical.



Scheme 77. 1,1-Diphenylethylene acceptor deuterium labeling study with enamines using deuterium-labelled Brønsted acids.

2.3.6 Functionalization of pharmaceutical agents



Scheme 78. Functionalization of pharmaceutically active compounds via photocatalytic multicomponent olefin-hydroaminoalkylation. ^a amine:aldehyde:acceptor (1:2:2); ^b acceptor (1.5 equiv.); ^c methoxyethyl-Hantzsch ester used (1.5 equiv.); ^d amine hydrochloride and Et_3N (1 equiv.) used; ^e paraformaldehyde (5 equiv.), preheated for 1 h; ^f Reaction conducted by Dr A. Trowbridge.

Lastly, with a non-benzylic amine scope established, we were interested in demonstrating the utility, mild conditions, and broad functional group tolerance of the developed photocatalytic olefin-hydroaminoalkylation on a small number of pharmaceuticals featuring a free secondary amine group. Subjecting the pharmaceutical agents paroxetine, desloratadine, amoxapine and ciprofloxacin to the reaction conditions, it was found that the corresponding complex tertiary amines **381**, **382**, **383**, and **384** were formed in moderate to good yields, demonstrating the potential to construct ‘drug-like’ molecules in a single step from readily available materials (Scheme 78). Notably, the dehydroalanine acceptor **360** proved especially useful in these transformations, without a 1,5-HAT pathway operative.

2.4 Summary

In summary, this chapter details the development of a visible light photoredox reductive processes to access α -amino radicals from all-alkyl C=N double-bonds. Several challenges complicate this type of reaction, such as the high reduction potentials and competing single-electron reactivity of the corresponding enamines. A stark contrast exists to reported work to date in the field, which utilizes conjugated and functionalized imines and iminium ions. A versatile and general approach for a photocatalytic olefin-hydroaminoalkylation was developed, based on the coupling of reductively, and hence regiospecifically generated α -amino radicals from all-alkyl iminium ions.^[249] After optimization of the reaction conditions, a broad range of amine, aldehyde and electron deficient alkene coupling partners was explored. The reaction proved compatible with a large number of functional groups due to mild conditions, enabling the one-step generation of complex tertiary amine products from readily available feed-stock starting materials. Aromatic aldehydes proved incompatible with the reaction. A series of mechanistic experiments were performed, including Stern-Volmer quenching studies and deuterium labelling studies, leading to a proposed mechanism featuring a 1,5-HAT process and a unprecedented iminium redox-relay. Due to the mechanistic rationalization, the substrate scope of the reaction could be significantly expanded to include simple cyclic and acyclic alkylamines. Furthermore, alkyl-enamine starting materials yielded complex α -tertiary amines in a single step. Finally, we utilized the novel photocatalytic olefin-hydroaminoalkylation approach to successfully functionalize a small number of pharmaceutical agents.

3. Total synthesis of alkaloids FR901483 and TAN1251C

3.1 Introduction

3.1.1 FR901483 – Structure, isolation, bioactivity and proposed biosynthesis

(-)-FR901483 (**1**, Figure 14) is an immunosuppressant indolizine alkaloid first isolated from a fermentation broth of *Cladobotryum* in 1996 by chemists of the Fujisawa Chemical Co (now Astellas).^[250-251] Structural determination was achieved by X-ray crystallography, however the absolute stereoconfiguration of FR901483 was not established until Snider and co-workers achieved its first enantiocontrolled total synthesis in 1999.^[252]

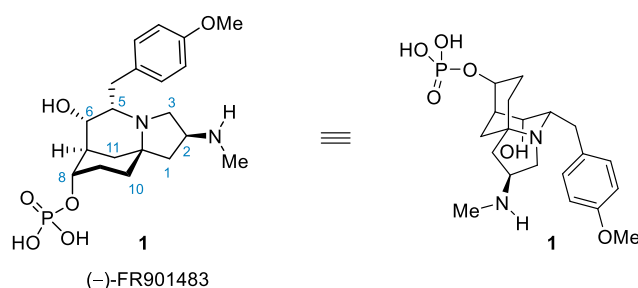


Figure 14. Two equivalent representations of the structure of (-)-FR901483, including the numbering used in this work featured in the left structure.

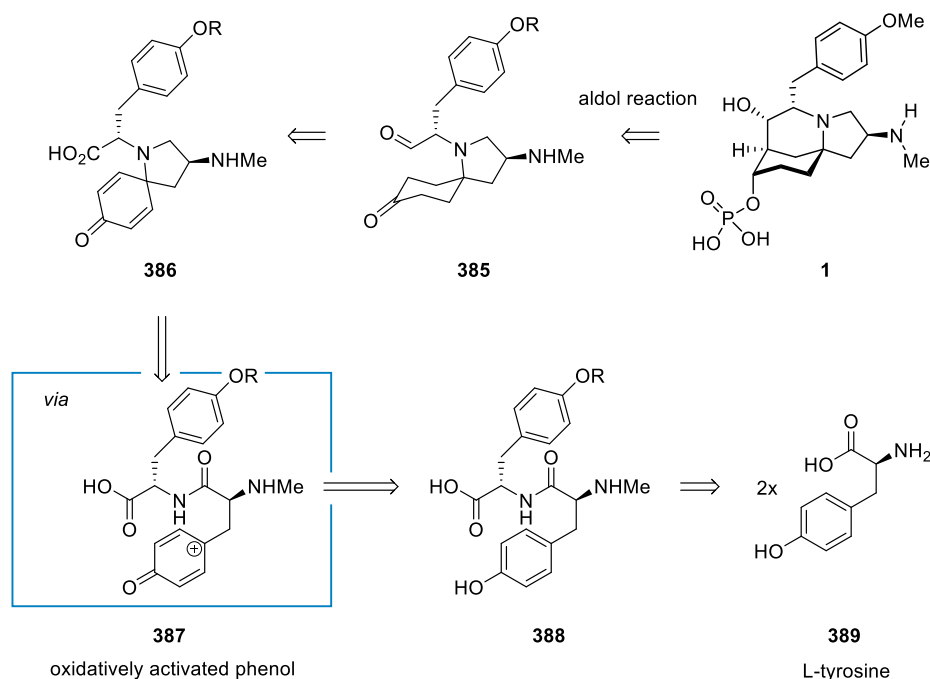
The isolation work by the Fujisawa group investigated *Cladobotryum* sp. No. 11231, a fungal strain obtained from litter collected at Iwaki city, Fukushima, Japan. Fermentation of the organism was carried out on large scale for 96 hours, yielding 160 liter of fermentation broth (max. yield 50 µg/mL).^[250] After filtration, extraction, and several sequential purification steps concluded by crystallization, 230 mg of FR901483 were obtained as colorless needles. The molecular formula was first established by FAB-MS and elemental analysis. Structural elucidation was achieved by combination of spectral (IR, NMR, UV-Vis) and chemical methods and was confirmed by X-ray crystallographic analysis, which also revealed the relative stereochemistry present in the natural product.^[250]

From a structural perspective, FR901483 exhibits a unique azatricyclic core structure, with a morphan and indolizidine moiety sharing a central piperidine ring system. The 5-azatricyclo[6.3.1.0^{1,5}]dodecane system carries an unusual phosphate ester residue located on the morphan ring.^[253] Further notable features are the presence of a synthetically challenging α -tertiary amine moiety in the skeleton,^[241] a total of 6 stereocenters, and the presence of a *N*-secondary, *N*-tertiary diamino alcohol.

FR901483 was discovered in efforts of Fujisawa Chemical Co to identify immunosuppressant agents following the discovery of tacrolimus^[254-255] and asomycin,^[256-257] two successful immunosuppressant drugs, both isolated by the same team in 1987 and 1988. Significant effort was placed in the assessment of the immunosuppressant activity of FR901483 in its isolation reports.^[250-251] FR901483 possesses immunosuppressant activity useful for the treatment of immune-mediated diseases such as the resistance to organ and tissue transplant and graft-vs-host disease, and autoimmune diseases such as rheumatoid arthritis, lupus, multiple sclerosis and type I diabetes. While the compound has not been employed as a drug to date, it is also seen as potentially useful for the treatment and prophylaxis of inflammatory and hyperproliferative skin diseases and immunologically-mediated illnesses (such as psoriasis, dermatitis, eczema, and acne), asthma, bronchitis, inflammatory bowel disease, intestinal inflammations and allergies (such as Coeliac disease and Crohn's disease), and Guillain–Barré syndrome.^[251] In the initial studies, FR901483 was found to have a highly potent inhibitory effect on lymphocyte proliferation, up to 100 times more potent on a molar basis than cyclosporin.^[250, 258] Importantly, FR901483 exhibits a different mechanism of action than the immunosuppressants cyclosporin and tacrolimus, which both directly or indirectly interfere with interleukin-2 (IL-2) pathways, a signaling molecule responsible for regulating activity of white blood cells. The possible mode of FR901483's immunosuppression is considered to be via inhibition of a purine biosynthesis pathway by interference with adenylosuccinate synthetase and/or adenylossuccinase.^[250] Two studies confirmed immunosuppressant activity of FR901483 in-vivo, including a skin allograft survival study in rats, in which FR901483 showed significantly increased graft survival time. Oral administration of FR901483 has failed to lead to effective immunosuppression, this is supposedly due to deactivation of the active form by hydrolysis of the phosphate ester. This result is supported by the fact that the dephosphorylated form of FR901483 has been found to be entirely inactive, suggesting an essential role of the phosphate ester in FR901483's bioactivity.^[250] The labile C-8 phosphate ester and its propensity to undergo hydrolysis has reportedly hampered the development of FR901483 as a drug.^[259]

There is widespread consensus considering the presumed biosynthesis of FR901483. Retrosynthetic analysis reveals that FR901483 is most likely derived from a tyrosine-tyrosine dipeptide (Scheme 79).^[252, 260] Intramolecular oxidative amidation of tyrosinyl-tyrosin **388** is envisioned to form spiro lactam **386** followed by appropriate redox-modulations to give aldehyde **385**. The intramolecular coupling presumably proceeds first with an oxidative activation of the tyrosine phenol, giving a highly electrophilic activated phenol species,

shown in Scheme 79 simplified as **387**, which is intercepted by nucleophilic attack of the amide to form **386**.



Scheme 79. Likely biosynthetic pathway for the generation of FR901483.

The tricyclic core structure in **1** is then most likely generated via an intramolecular aldol reaction of **385** to form the C6–C7 bond. In accordance with this biosynthetic pathway, many reported synthetic approaches to FR901483 are hence, at least in part, biomimetic. The aldol step has been employed in Snider's initial synthesis,^[252] but also by Sorensen^[261] and Ciufolini.^[262-263] Ciufolini and co-workers, given their prior work on oxidative amidation chemistry,^[264] have extensively reviewed the biosynthesis of FR901483^[258-260] and achieved a biomimetic approach utilizing both aldol and oxidative coupling key transformations. The Sorensen synthesis also uses a similar biomimetic approach.^[261]

3.1.2 FR901483 – Previous syntheses

3.1.2.1 Overview

Due to its favorable bioactive properties and unique structural features, significant synthetic effort has been placed in the total synthesis of FR901483 since its isolation.^[265] The first enantiocontrolled total synthesis was achieved by Snider in 1999, and a considerable number of other elegant and inventive accounts have been dedicated to the total synthesis of the alkaloid since. At the time of this work, a total of 10 total syntheses of FR901483 are

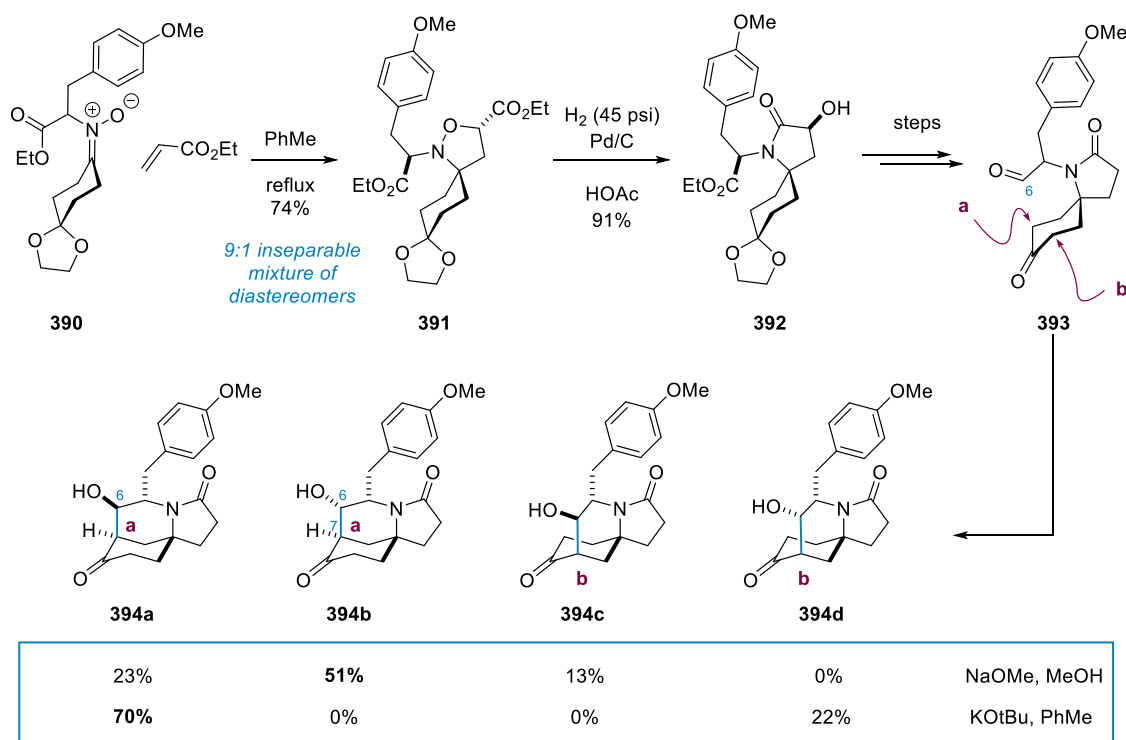
reported, comprising of six enantiocontrolled syntheses, two racemic syntheses, and two enantiocontrolled formal syntheses. An overview is given in Table 5.

Table 5. Overview of syntheses of FR901483.

Main author	Year	Ref	Enantiocontrol	note
Snider	1999	[252]	(–)	first
Sorensen	2000	[261]	(–)	-
Ciufolini	2001	[262-263]	(–)	-
Fukuyama	2012	[266]	(–)	-
Tu	2012	[267]	(–)	-
Huang	2013	[268-269]	(–)	-
Funk	2001	[270]	rac	-
Fukuyama	2004	[271-272]	rac	-
Brummond	2005	[273]	(–)	formal
Kerr	2009	[274]	(–)	formal

3.1.2.2 Snider's desmethylamino-FR901483 study

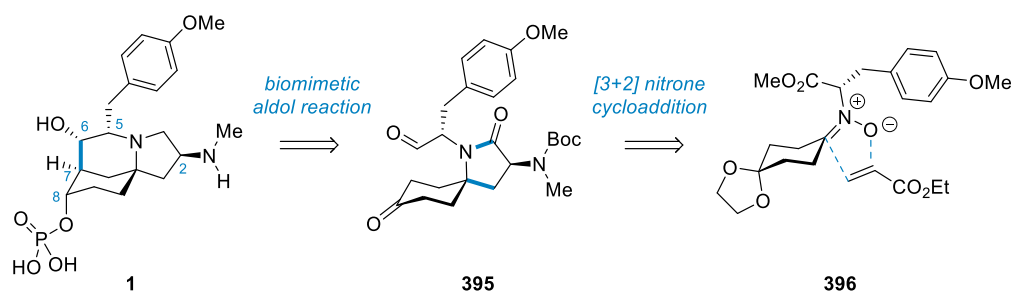
Prior to their pioneering total synthesis of FR901483, Snider and co-workers published their first study on the subject with the synthesis of desmethylamino-FR901483 in 1998.^[275]



Scheme 80. Snider's desmethylamino FR901483 model study on formation of the spirolactam **393** and the biomimetic aldol reaction.

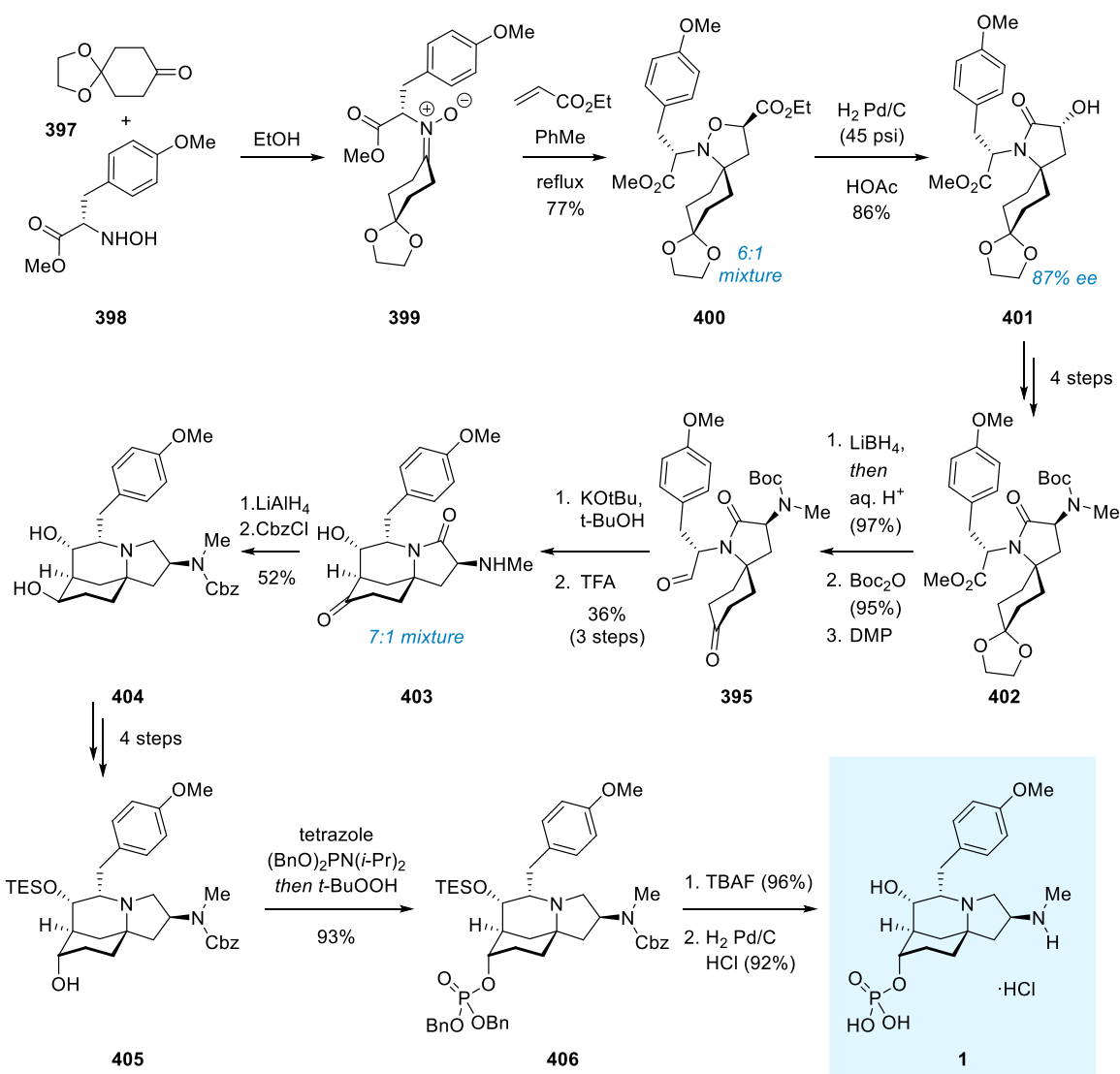
The work investigated the stereochemical outcome of the construction of the spirolactam scaffold via [3+2] cycloaddition between racemic nitron **390** and ethyl acrylate,^[276-277] and displays one of the most significant contributions probing the stereochemical outcome of the biomimetic aldol reaction forming the C6–C7 bond (Scheme 80). After a sequence of steps, Snider and co-workers opted for defunctionalization on the C2 position and established a simplified model system with keto aldehyde **393** to probe the aldol reaction (Scheme 80). The reaction gave a satisfactory yield (51%) of the desired diastereomer **394b** under basic conditions (sodium methoxide) in methanol. Potassium *tert*-butoxide in toluene, however, failed to give any desired product and yielded predominantly diastereomer **394a**, with opposite stereoconfiguration at the C6 alcohol in regard to the natural product. Importantly, it was determined that the aldol reaction seems to preferably occur from carbon *a* (Scheme 80), which might be due to the stabilizing effect of the equatorial *p*-methoxy benzyl group in the products **394a** and **394b**.

3.1.2.3 First total synthesis of (–)-FR901483 by Snider



Scheme 81. Snider's retrosynthetic strategy.

In continuation of the positive results of their model study, Snider and coworkers proceeded to publish the first report of the enantiocontrolled total synthesis of FR901483 in 1999, which also established the until then unknown absolute stereoconfiguration of the compound.^[252] It was hypothesized that, in the biosynthesis, stereocenters at C2 and C5 were both L-tyrosine derived, and Snider's retrosynthetic strategy was laid out accordingly (Scheme 81). Condensation of optically active hydroxylamine **398** with ketone **397** followed by [3+2] cycloaddition with ethyl acrylate yielded an inseparable 6:1 mixture of diastereomers of spirolactam **400**. Unfortunately, the selectivity was slightly lower than in the model study (9:1 d.r.). Hydrogenolysis gave chiral spirolactam **401**, which unfortunately was also inseparable from its diastereomer, resulting in a 6:1 mixture. Furthermore, due to partial racemization in the cycloaddition step, enantiomeric excess in **401** was found diminished to 87% ee.

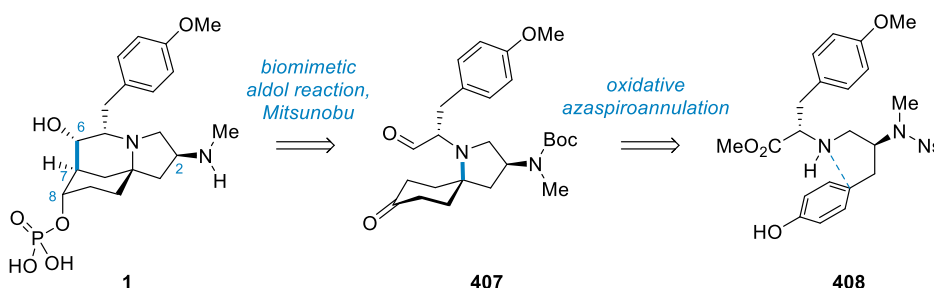
Scheme 82. Snider's total synthesis of (-)-FR901483.^[252]

The 6:1 mixture was carried forward in the synthesis, and after displacement of the tosylated C2 alcohol with azide easily separated. Consecutive reduction, Boc-protection and methylation installed the challenging C2-amine functionality in the correct stereoconfiguration resulting in Boc-amine **402**. This was followed by reduction of the methyl ester and treatment with aqueous acid, revealing the C8 ketone but also removing the desired Boc-group, which had to be reinstalled in the next step. Dess Martin oxidation then set the stage for the key step from keto aldehyde **395**, intramolecular aldol addition to form the azatricyclic framework. The aldol reaction gave similar results in regards to the model system,^[275] however slightly better selectivity was observed using KOtBu in *tert*-butanol in place of NaOMe in methanol, yielding an inseparable 7:1 mixture of the desired aldol product **403**. Reduction to the equatorial alcohol and Cbz protection gave carbamate **404**, which could be cleanly separated from the mixture. Inversion of the C8 alcohol was achieved through C8 nosylation, TES-protection of the alcohol at C6, nucleophilic substitution of the C8 nosylate

by treatment with cesium acetate and 18-crown-6, and finally basic solvolysis of the resulting acetate to yield axial alcohol **405**. Installation of the phosphate was achieved through phosphoramidite addition and subsequent oxidation to the phosphate furnishing dibenzylphosphate ester **406**. TES deprotection and consecutive hydrogenation under acidic conditions gave the first fully synthetic sample of (–)-FR901483 (**1**) as its HCl salt, confirming Snider's hypothesis regarding the absolute stereoconfiguration.

In conclusion, Snider elegantly achieved the first synthesis of the natural product in ca. 22 steps in the longest linear sequence. Highlights of the synthesis are its inventive [3+2] nitronc cycloaddition, the biomimetic intramolecular aldol step, and the resulting brevity of the approach. Snider's basic intramolecular aldol conditions are still the standard method to directly obtain significant amounts of the desired aldol product to date, and despite vast efforts by many authors could not be significantly improved upon in the 20 years since Snider's report. The main challenges of Snider's approach include difficulties in obtaining the central spiro lactam **401**, both in sufficient diastereomeric and enantiomeric purity, the problematic inseparable 7:1 aldol product mixture, and a variety of necessary inversion operations at the C2 and C8 centers.

3.1.2.4 Sorensen's synthesis

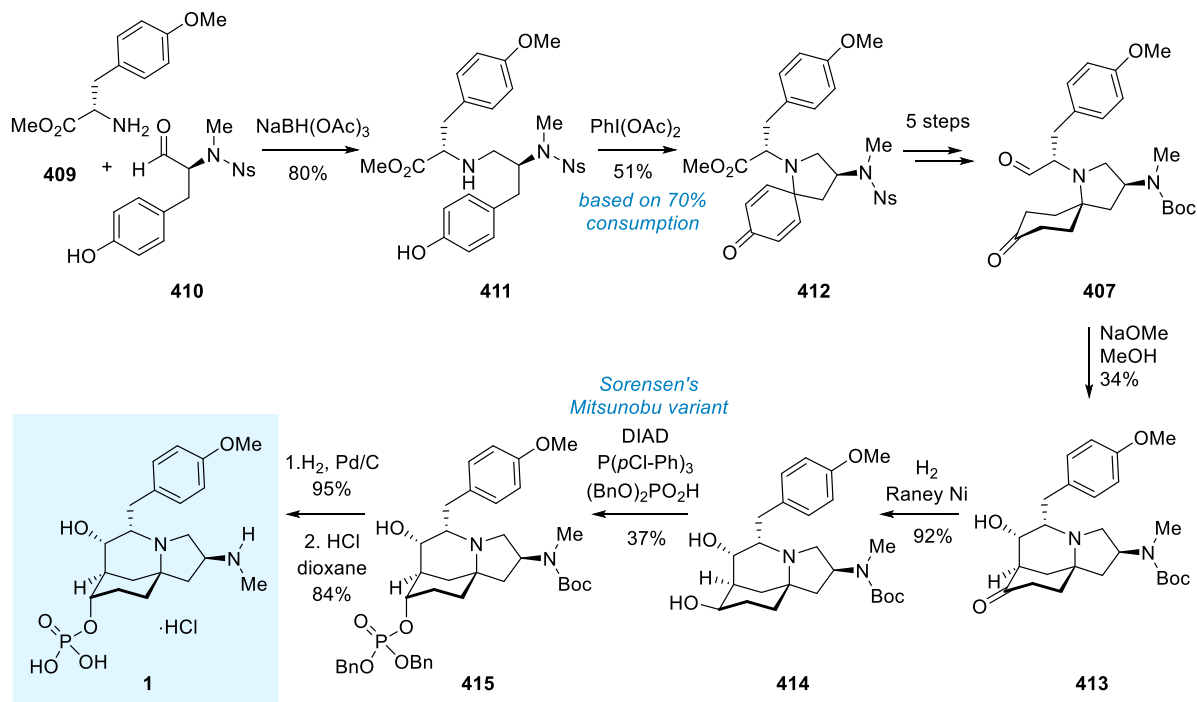


Scheme 83. Sorensen's retrosynthetic strategy.

In 2000, the Sorensen group reported their total synthesis of (–)-FR901483.^[261] The general approach was biomimetic, starting from a tyrosine-tyrosine dimer which could undergo oxidative cyclisation to generate the central spirocycle **407**. The route also featured the Snider-type aldol addition to assemble the tricyclic scaffold of **1** (Scheme 83).

The central oxidative azaspiroannulation step of tyrosine-tyrosine dimer **411** proceeded under remarkably simple conditions, using hypervalent iodine oxidant $\text{PhI}(\text{OAc})_2$ at ambient temperature, to yield **412** (Scheme 84). After a sequence of standard operations, intramolecular aldol reaction was carried out in a similar fashion to Snider's work, resulting in 34% of the isolated desired stereoisomer **413**. To invert the C8 alcohol in **414** Sorensen's

team developed a useful Mitsunobu reaction to install the dibenzyl phosphate in the correct stereoconfiguration in the presence of the free C6 hydroxyl group.^[278] Although the reaction gave only modest yield of **415**, the direct transformation is advantageous and has been used by a number of later syntheses of FR901483. Finally, hydrogenation and Boc-deprotection with HCl-dioxane yielded the natural product **1**, concluding the total synthesis.

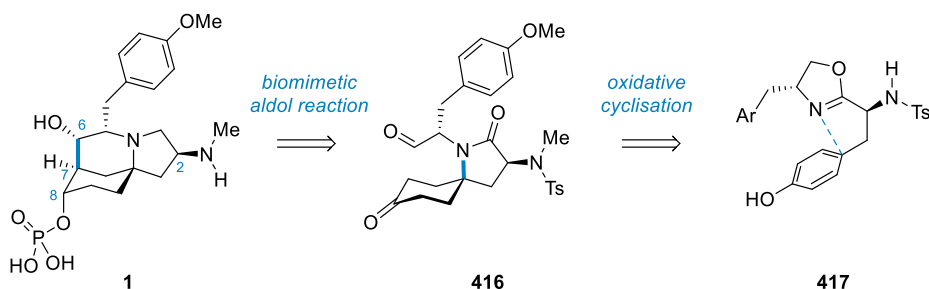


Scheme 84. Sorensen's synthesis of (-)-FR901483.

In summary, Sorensen and co-workers deliver an efficient enantiocontrolled total synthesis, significantly shorter than Snider's initial report. Sorensen's work still displays one of the most efficient approaches to FR901483. The main challenges of the route are the protecting group strategy and the moderate yield of the azaspiroannulation step.

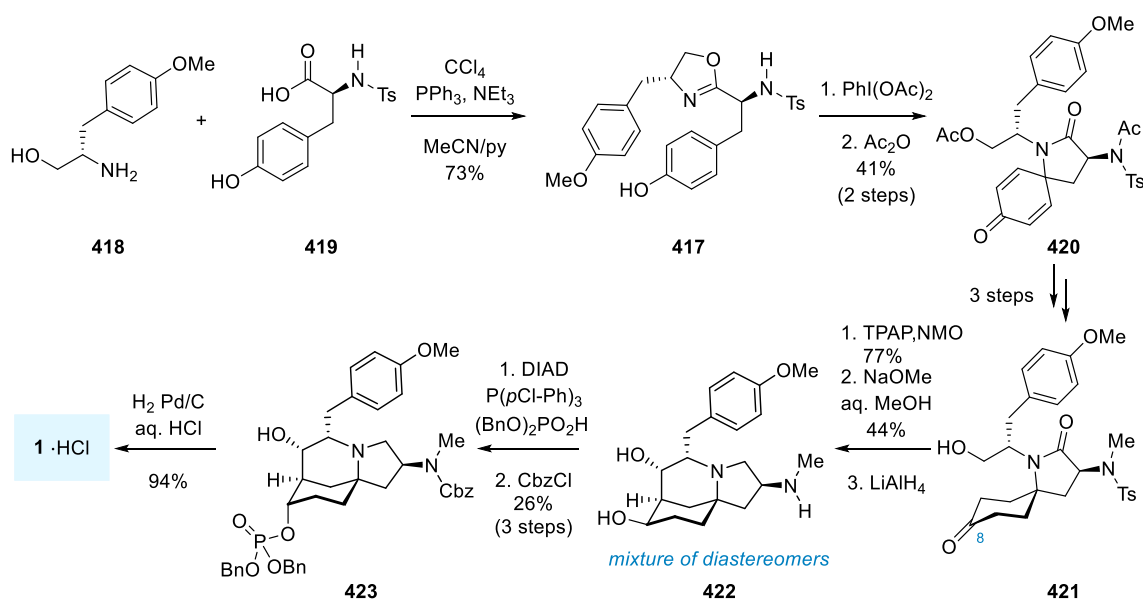
3.1.2.5 Ciufolini's synthesis

In 2001, the Ciufolini group published their total synthesis of (-)-FR901483,^[262-263] taking an approach similar to Sorensen's work. The strategy includes an oxidative cyclisation step from oxazoline **417** and makes use of the biomimetic aldol reaction (Scheme 85).



Scheme 85. Ciufolini's retrosynthetic strategy.

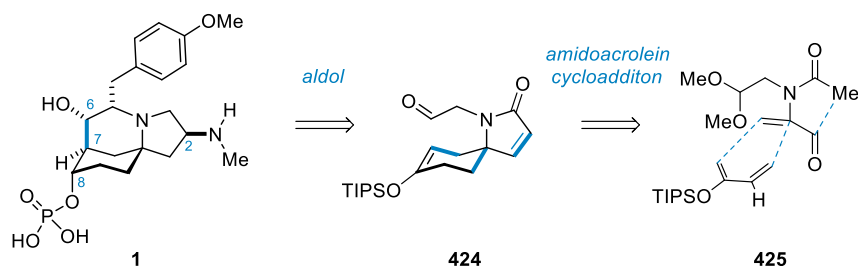
Oxazoline **417** was prepared using the Vorbrüggen method from amino alcohol **418** and acid **419** (Scheme 86).^[279] Exposure to hypervalent iodine oxidant achieved oxidative cyclisation, which after acetalization resulted in spirocycle **420**. The tosyl protecting group was necessary to suppress side reactions in the cyclisation step.^[280] After a brief sequence of operations, the aldol reaction was carried out in aqueous methanol, affording 44% of the desired diastereomer **422**. The authors proposed that this slightly increased selectivity of the aldol reaction compared to previous work was due to the polar nature of the aqueous methanolic solvent. The reaction product was subjected to vigorous metal hydride reduction, which resulted in a mixture of diastereomers on the C8 alcohol in **422**. The mixture was carried forward using Sorensen's Mitsunobu reaction. The difficulty in handling the products due their high polarity could be remedied by conversion into the respective benzyl carbamates **423**, at which point the mixture could be readily separated. Hydrogenation under acidic conditions then concluded the synthesis of **1**.



Scheme 86. Ciufolini's synthesis of (-)-FR901483.

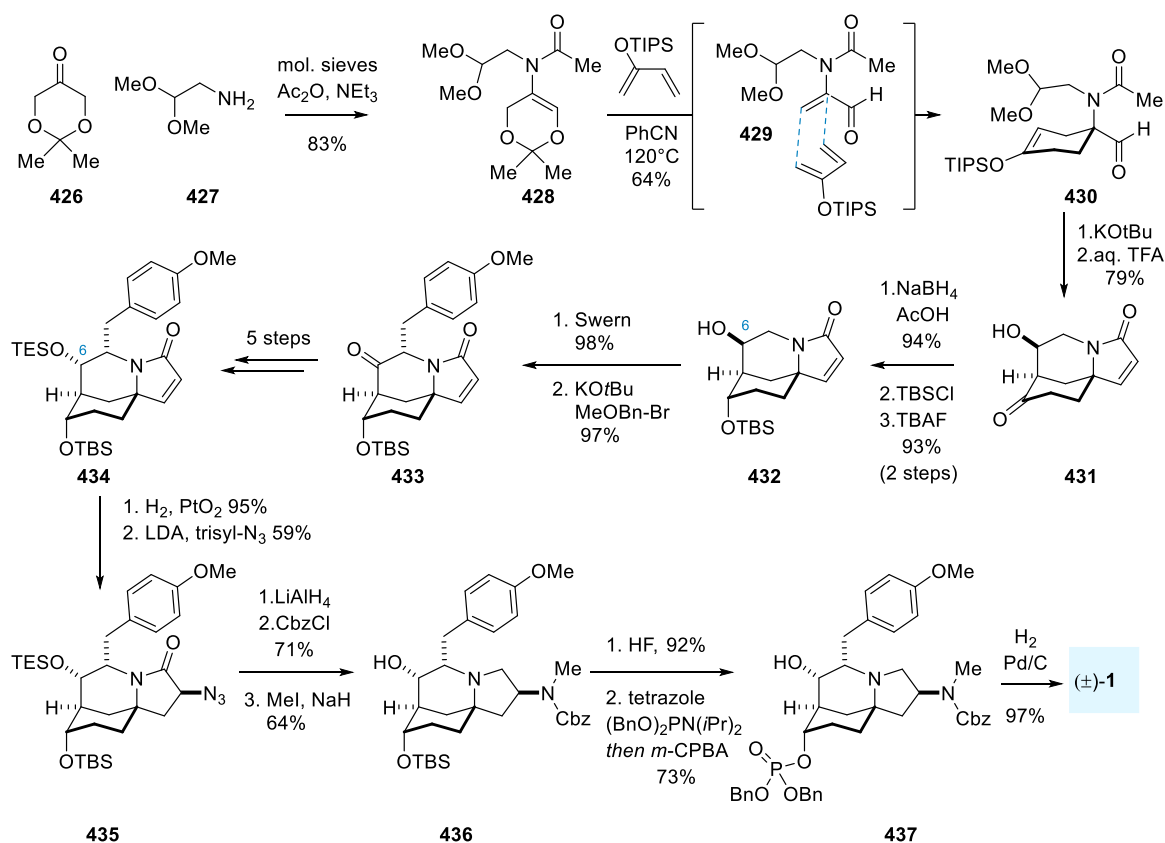
Ciufolini and co-worker's enantiocontrolled synthesis of FR901483 is similar to the Sorensen approach in its successful biomimicry leading to a concise synthesis. Furthermore, Ciufolini's aldol reaction featuring the C2 sulfonamide group seems to be slightly less problematic and allows slightly higher yield in comparison to Snider and Sorensen. With the use of Sorensen's Mitsunobu reaction Ciufolini achieved a synthesis similar in efficiency and brevity to the Sorensen synthesis.

3.1.2.6 Funk's synthesis of (±)-FR901483



Scheme 87. Funk's retrosynthetic strategy.

Funk and co-workers published their contribution to the racemic series in 2001.^[270] In a novel approach to the triazacyclic system, an amidoacrolein cycloaddition delivered the starting material for two concomitant biomimetic aldol reactions, rapidly giving rise to the FR901483 scaffold (Scheme 87).



Scheme 88. Funk's racemic synthesis of FR901483.

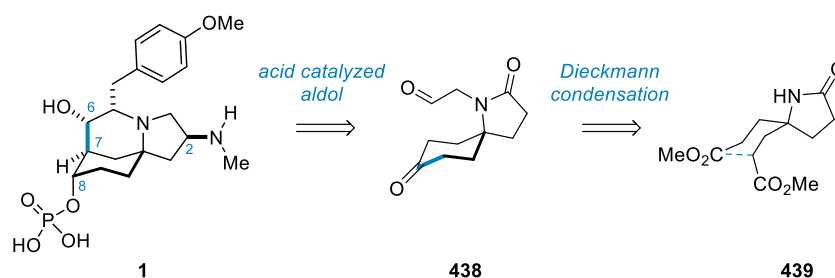
In the key step, dioxin enamine **428** underwent retro Diels Alder reaction to generate amidoacrolein **429** (Scheme 88), which was reacted *in situ* with 2-triisopropylsiloxybutadiene to afford silylenolether **430**. After ring closure, Evans-Saksena reaction^[281-282] installed the axial C8 alcohol, which was silyl protected. Funk achieved selective deprotection of the C6 silylether with TBAF to afford **432**. Subsequent oxidation of the C6 alcohol was followed by α -benzylation of the ketone to install the *para*-methoxy benzyl group selectively

in equatorial position of **433**. Inversion at the C6 position similar to Snider's work,^[252] yielded the silylether **434** in correct relative stereoconfiguration. The conjugated lactam was then hydrogenated, and azidation of the resulting lactam furnished azide **435**. The diastereomeric ratio of the azidation step was moderate (2.5:1) in favor of the desired diastereomer. After a series of standard operations, deprotection of the C8 alcohol followed by phosphorylation gave dibenzylphosphate **437**, which was readily converted to the racemic natural product **1** via hydrogenolysis.

Funk and co-workers assembled the challenging aza-tricyclic skeleton in only four steps using two (retro)-cycloaddition and two aldol steps. Challenges of the synthesis are the stereoinversion at C6, a number of redox fluctuations and the low diastereomeric control for the installation of the C2 nitrogen.

3.1.2.7 Fukuyama's first generation synthesis of FR901483

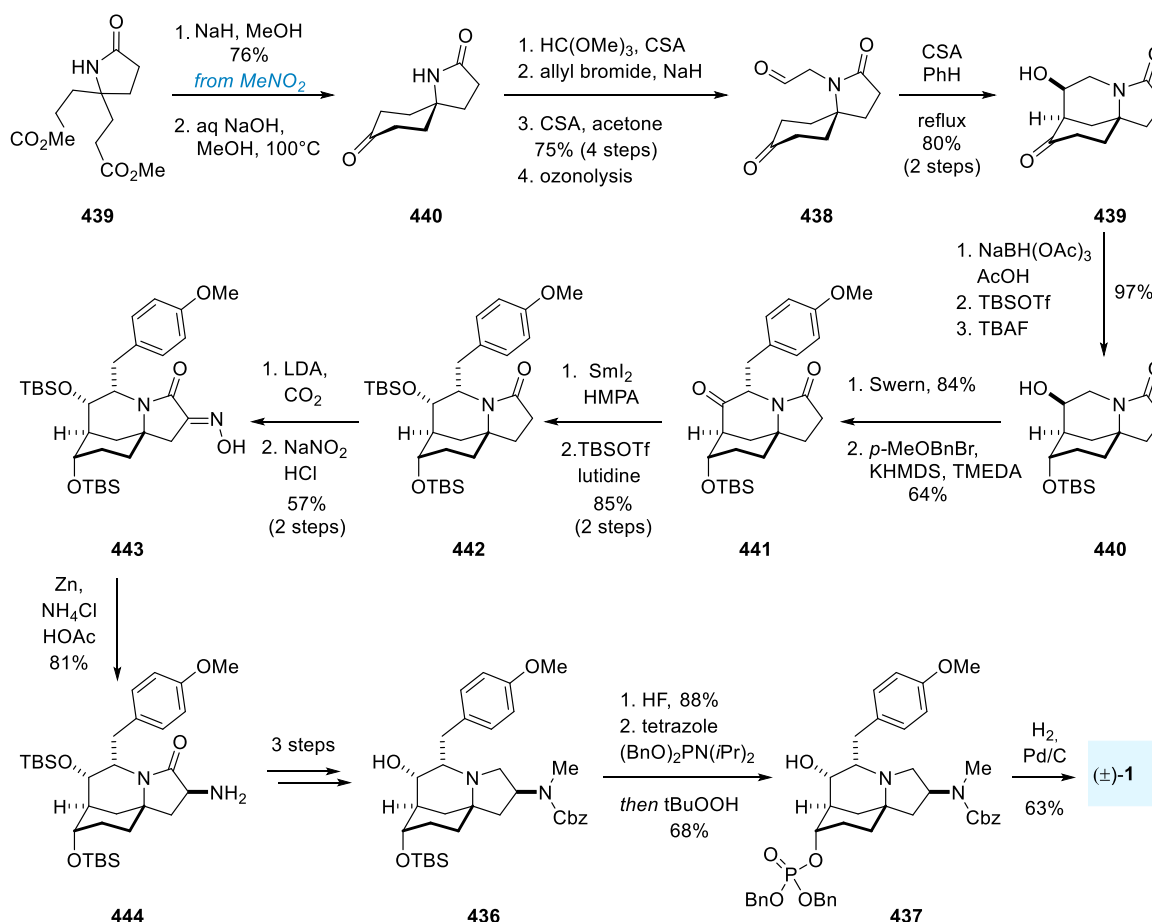
Fukuyama and co-workers published their first racemic total synthesis of **1** in 2004.^[271-272] Fukuyama's approach features the synthesis of the starting spirocycle via Dieckmann condensation to enable an biomimetic intramolecular aldol reaction (Scheme 89).



Scheme 89. Fukuyama's first generation retrosynthetic strategy.

At the beginning of the synthesis, Dieckmann condensation and consecutive decarboxylation gave rise to spiro lactam **440**. Following allylation of the amide, ozonolysis gave access to keto aldehyde **438**. Fukuyama's acidic aldol conditions were similar to Funk's,^[270] and offered excellent yield of single isomer **439**, albeit with the incorrect stereochemistry on the C6 alcohol center. Fukuyama also employed the Evans-Saksena reduction^[281-282] to set the axial C8 alcohol successfully, followed by silylation and Funk's selective deprotection of the C6 silylether resulting in alcohol **440**. Further similarities between the two syntheses followed with Swern oxidation and α -benzylation to install the equatorial *para*-methoxy benzyl group. Fukuyama elegantly reduced resulting ketone **441** to the desired alcohol in correct stereoconfiguration, overcoming the steric demand of the encumbered ketone at C6 by using samarium iodide and HMPA. Installation of the C2 nitrogen was carried out via oxime **443**.

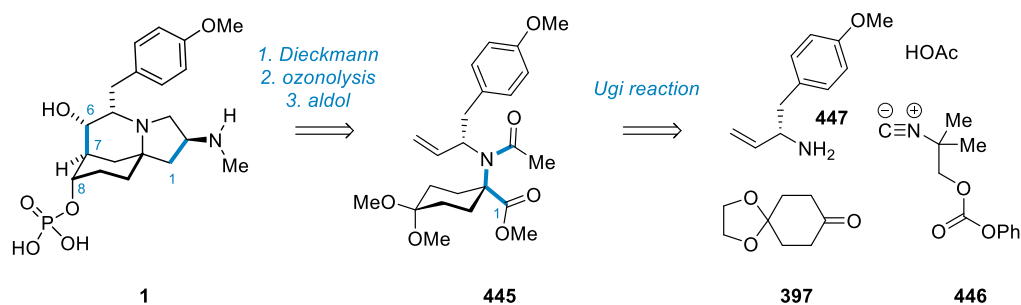
Reduction with zinc metal occurred selectively to yield amine **444** as a single isomer in excellent yield. After a series of standard operations, palladium catalyzed hydrogenolysis of **437** gave the racemic natural product **1**.



Scheme 90. Fukuyama's first generation synthesis of (±)-FR901483.

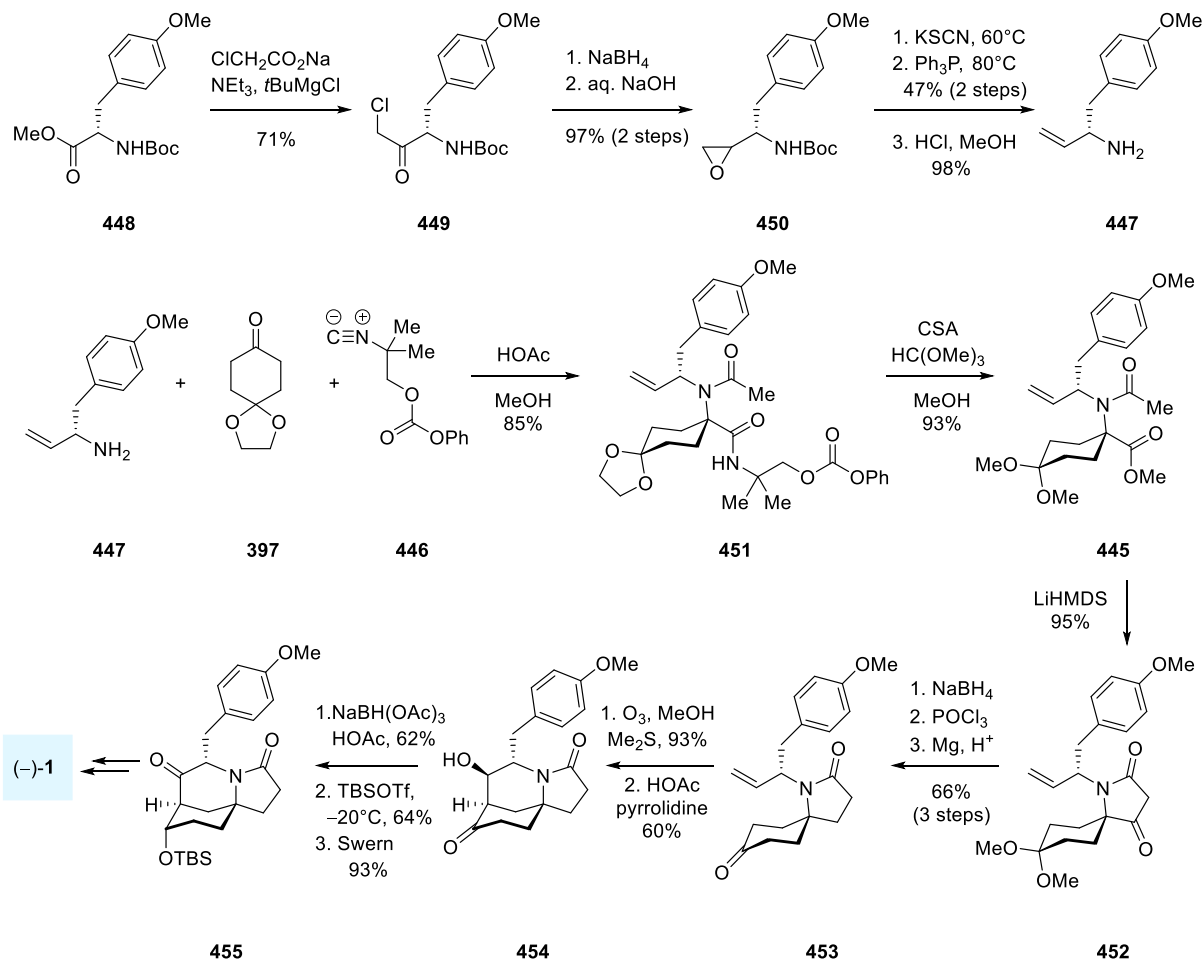
The first generation Fukuyama synthesis is similar to the Funk synthesis, however, significant improvements were achieved over the established steps. Highlights of the synthesis include the inventive formation of the starting spirocycle via Dieckmann condensation, the excellent aldol yield and efficacy in their stereoselective reductions with SmI_2 and Zn metal, leading to a more concise route without the need for inversion.

3.1.2.8 Fukuyama's second generation enantiocontrolled synthesis



Scheme 91. Fukuyama's second generation retrosynthetic strategy.

In 2012, the Fukuyama group reported a second generation, enantiocontrolled approach to FR901483,^[266, 283] realizing the synthesis of optically active **445** via an Ugi reaction,^[284] as earlier reported by the Sorensen group.^[285] Dieckmann condensation and established steps from the racemic synthesis led to completion of the synthesis (Scheme 91).^[272]



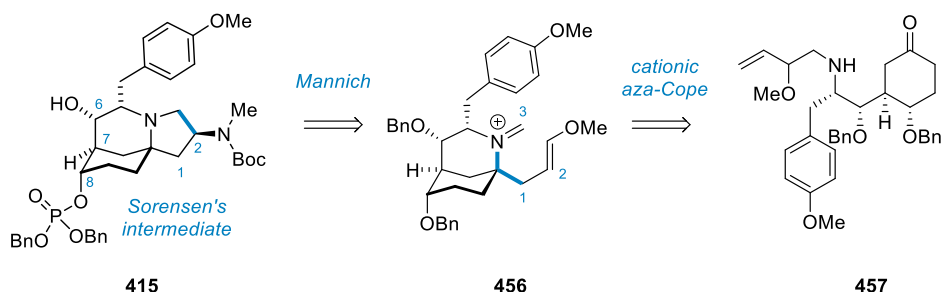
Scheme 92. Fukuyama's second generation synthesis of (-)-FR901483.

The second generation sequence started with the synthesis of the allyl amine **447** for the Ugi reaction (Scheme 92).^[266, 286] Combination of the optically active amine **447**, ketone **397**, isonitrile **446** and acetic acid in Fukuyama's four-component Ugi reaction assembled allyl amine **451** in a single step with an impressive 85% yield. Methyl ester **445** was generated by methanolysis with CSA and HC(OMe)₃, which also led to transacetalization. Dieckmann condensation closed the lactam ring to furnish spiro lactam **452**, followed by a series of reductive operations resulting in ketone **453**. Oxidative cleavage of the aldehyde by ozonolysis was followed by aldol reaction with pyrrolidine in acetic acid.^[261, 287-288] Similarly to Fukuyama's prior work, a yield of 60% was obtained for diastereomer **454** featuring the epimeric alcohol at C6. Again, Evans-Saksena reduction^[281-282] was employed, followed by a selective silyl protection of the C8 alcohol. Swern oxidation lead to key intermediate **455**,

which was carried forward successfully according to the racemic synthesis, to arrive at the optically active natural product **1**.

In conclusion, the Fukuyama group complemented their racemic variant with an elegant enantiocontrolled synthesis. Fukuyama's four component, high yielding Ugi reaction efficiently accessed the optically active spirolactam. Unfortunately, the starting chiral amine is difficult to obtain via a 7 step synthesis. The outcome of the aldol reaction, is slightly lower yielding than in the previous Fukuyama synthesis, illustrating the substrate dependence of the intramolecular aldol ring closure.

3.1.2.9 Brummond's formal synthesis of FR901483

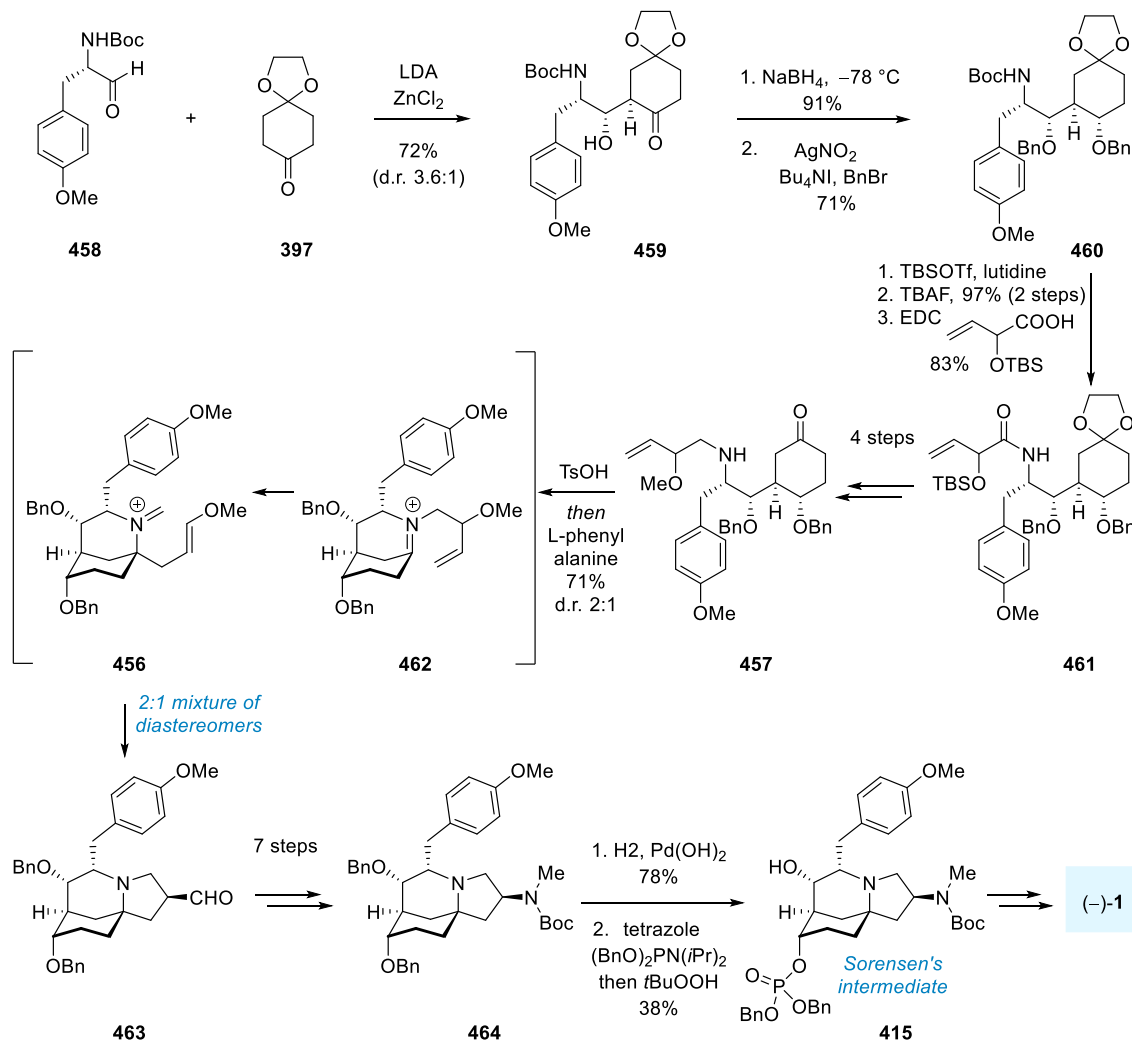


Scheme 93. Brummond's retrosynthetic strategy.

Brummond and co-workers reported a formal synthesis of (–)-FR901483 in 2005 featuring a cascade of a cationic aza-Cope rearrangement and Mannich reaction to generate the tricyclic scaffold in a single step,^[273, 289] with all stereocenters except C2 pre-installed in the precursor prior to the key step (Scheme 93).

The synthesis began with synthesis of hydroxy ketone **459** via aldol reaction (Scheme 94).^[290] Reduction and benzylation yielded dibenzylether **460**, which was elaborated to ketone **457**, the immediate precursor for the tandem reaction, through a series of standard operations. Consecutive treatment with tosylic acid and (*S*)-phenylalanine triggered the cascade of aza-Cope rearrangement to yield intermediate **456** via bridgehead iminium ion **462**, from which Mannich reaction occurred to give aldehyde **463** in a single step. Unfortunately, a 2:1 mixture of diastereomers was obtained which could only be separated after reduction to the alcohol. Installation of the C2-nitrogen via the acyl azide led to *N*-Boc methylamine **464**. Palladium catalyzed hydrogenation and phosphorylation gave Sorensen's intermediate **415**,^[261] concluding the formal synthesis. In summary, the Brummond formal synthesis takes a novel, non-biomimetic approach with their splendid aza-Cope rearrangement / Mannich cascade reaction. Assembly of the precursor featuring a rare aldol reaction is rapid and efficient. Challenges arose later in the synthesis, when the installation of the C2 amine is slowed down

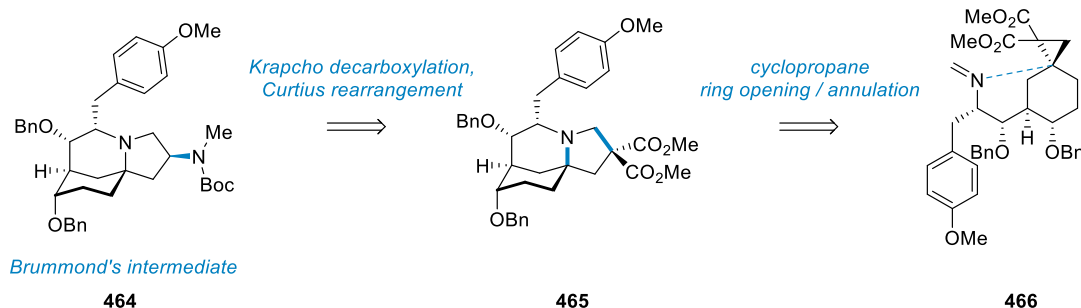
by a mixture of diastereomers obtained from the cascade, necessitating a detour via the alcohol to allow separation.



Scheme 94. Brummond's formal synthesis of FR901483.

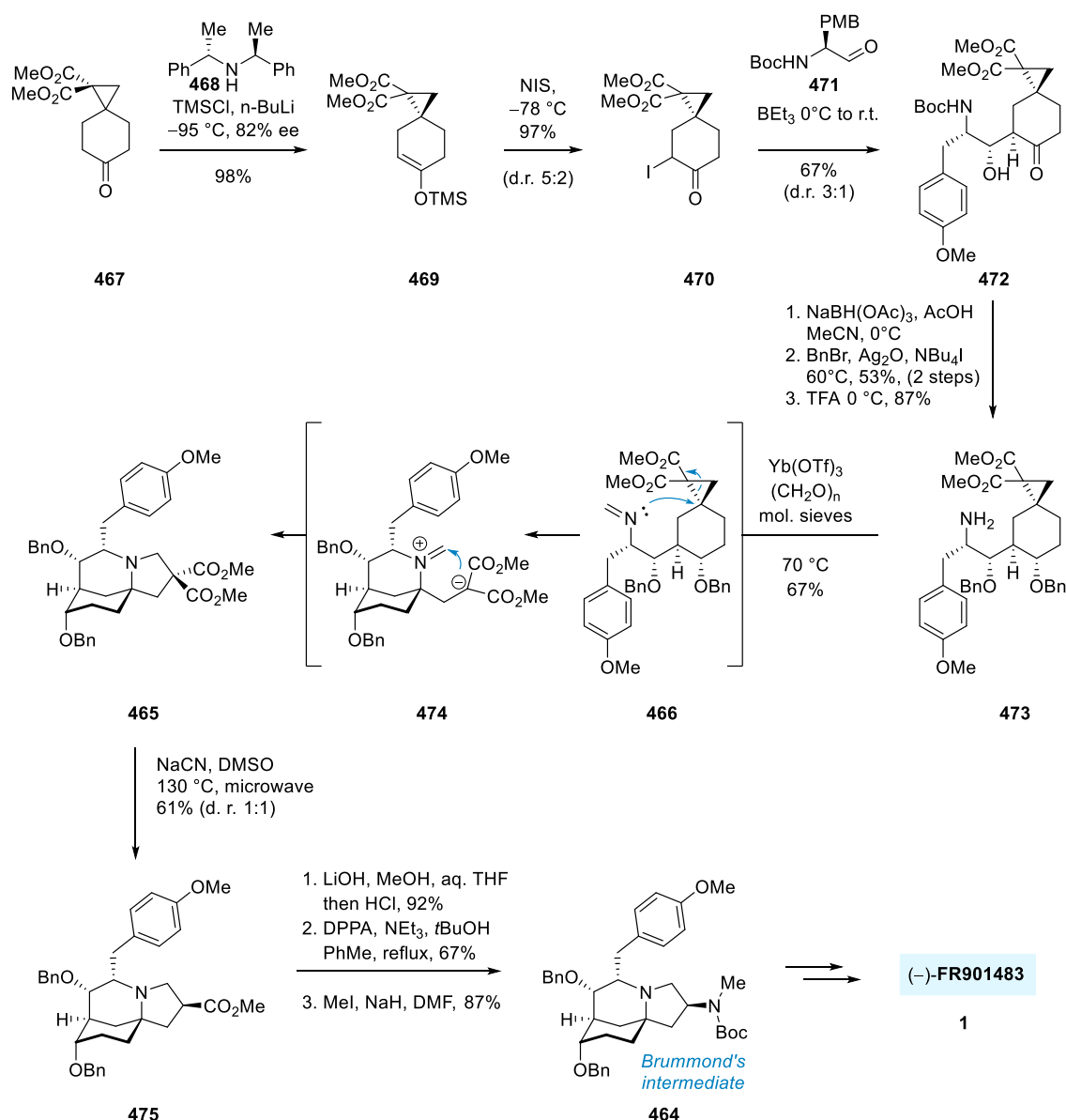
3.1.2.10 Kerr's formal synthesis of FR901483

The Kerr group published a formal synthesis of (-)-FR901483 in 2009, featuring a cyclopropane ring-opening annulation reaction.^[274] The approach started from a precursor similar to Brummond's synthesis with pre-installed stereocenters.



Scheme 95. Kerr's retrosynthetic strategy.

The synthesis commenced with desymmetrization of **467**,^[291-292] leading to β -hydroxy ketone **472** in a short sequence including a Reformatsky reaction with aldehyde **471**. Brummond's method was used to obtain dibenzyl ether **473**.^[273] Addition of **473** to a heated solution of ytterbium triflate and paraformaldehyde triggered formation of imine **466** and initiated the cascade of cyclopropane opening and annulation through resulting enolate **474**.^[293-295] Krapcho decarboxylation^[296-297] of diester **465** resulted in ester **475** and was followed by saponification to the corresponding acid. Reaction with diphenylphosphoryl azide (DPPA) induced Curtius rearrangement of the acyl azide in the presence of *tert*-butanol. The generated carbamate was directly methylated to yield Brummond's intermediate **464**, concluding the formal synthesis.

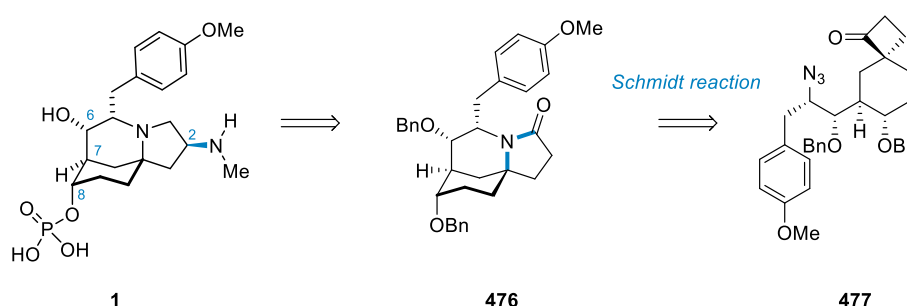


Scheme 96. Kerr's formal synthesis of FR901483.

In summary, Kerr and co-workers demonstrated the utility of the cyclopropane opening/annulation cascade in their formal synthesis of FR901483. The cascade reaction offered an alternative to the bridgehead iminium – aza cope reaction employed in the Brummond route. Kerr obtains high yield with exclusive formation of the desired isomer **465**, albeit without the C2 stereocenter in place. However, challenges arose for Kerr with unselective Krapcho decarboxylation (d.r. 1:1) of the cascade product. An alternative mono-saponification strategy was offered to increase the yield marginally.^[274] In the final steps, Kerr and co-workers efficiently obtain the methylated N-Boc derivative in significantly fewer steps than required by Brummond from their cascade product,^[273] completing an elegant formal synthesis.

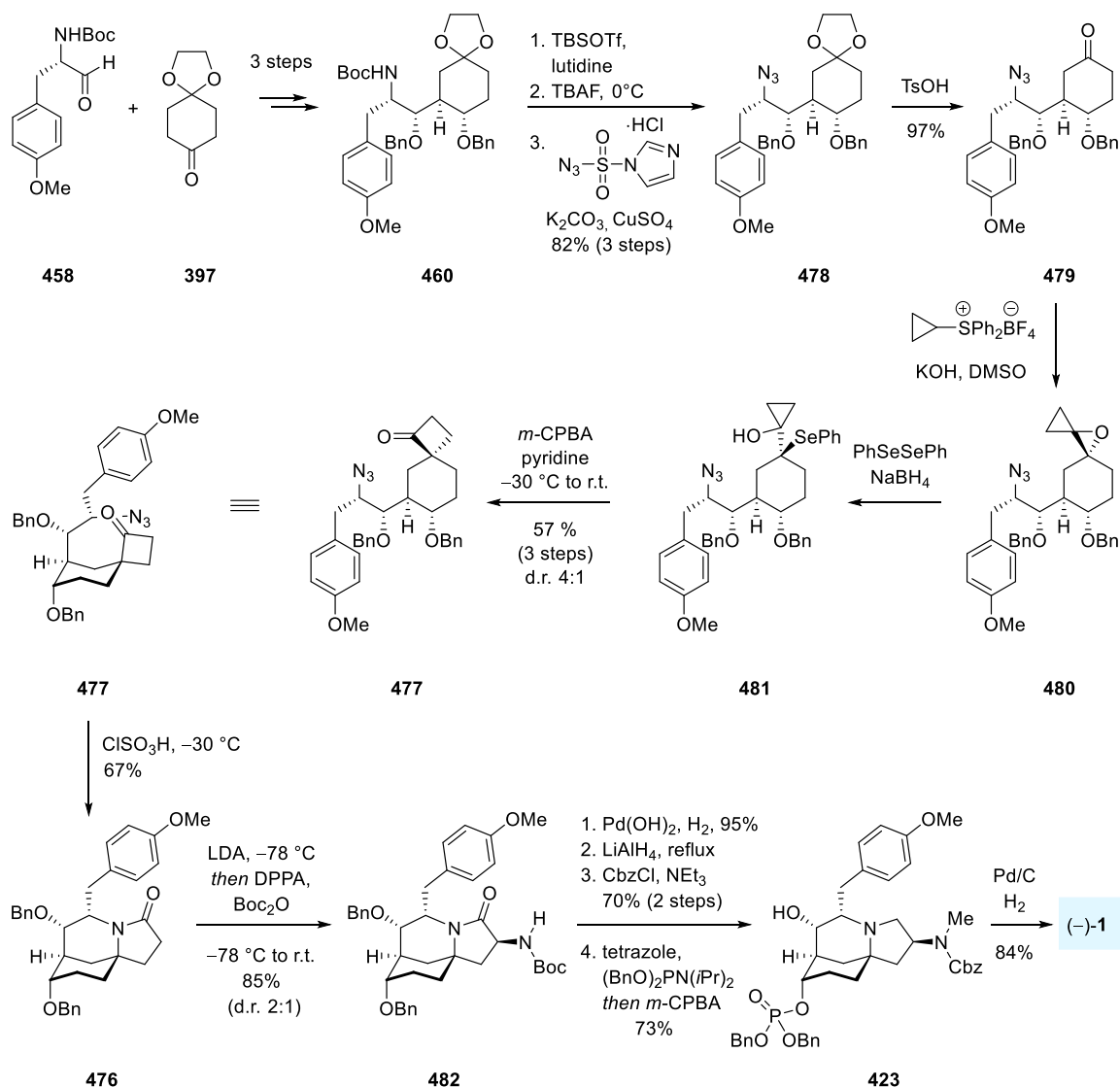
3.1.2.11 Tu's total synthesis of FR901483

In 2012 the Tu group published their approach to (–)-FR901483 (Scheme 97).^[267] A Schmidt reaction of an alkyl azide, as explored by Aubé,^[298-299] assembled the tricyclic scaffold selectively from a cyclobutanone precursor, which, similar to the approaches of Brummond^[273] and Kerr,^[274] featured all stereocenters except the C2 amine.



Scheme 97. Tu's retrosynthetic strategy.

The total synthesis commenced with synthesis of dibenzylether **460** following the protocol of Brummond (Scheme 98).^[273] An established sequence^[273, 300] gave access to azido compound **479**. Epoxide **480**^[301] was readily translated to key cyclobutanone **477**, the precursor for the Schmidt reaction. Tu found the Schmidt reaction^[298-299] to be promoted most suitably by chlorosulfonic acid at –30 °C to generate aza-tricyclic product **476** in 67% yield as a single isomer.^[267] Efficient installation of the C2 nitrogen followed via treatment with LDA, diphenyl phosphoryl azide (DPPA),^[302-303] and Boc₂O, resulting in carbamate **482** in a 2:1 mixture of diastereomers. In a final sequence of reductive transformations, Cbz protection and phosphitylation/oxidation, dibenzylphosphate ester **423** was obtained. Established hydrogenolysis yielded the natural product **1**.



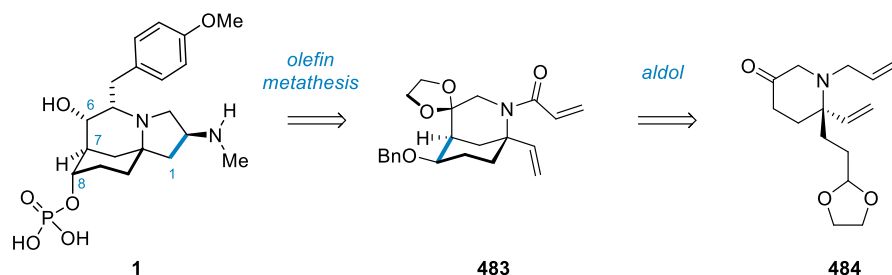
Scheme 98. Tu's total synthesis of FR901483.

In conclusion Tu and co-workers have provided one of the most efficient approaches to FR901483 to date, with its brevity only paralleled by the Sorensen group synthesis.^[261, 265] Selectivity issues in the semi-pinacol type rearrangement as well as in the installation of the amino group pose a challenge in this otherwise high yielding synthesis. Highlight of the synthesis is Tu's highly selective Schmidt reaction giving rapid access to the triazacyclic scaffold. Notably, a similar study on the core fragment investigating the Schmidt reaction was published concurrently.^[304]

3.1.2.12 Huang's Synthesis of FR901483

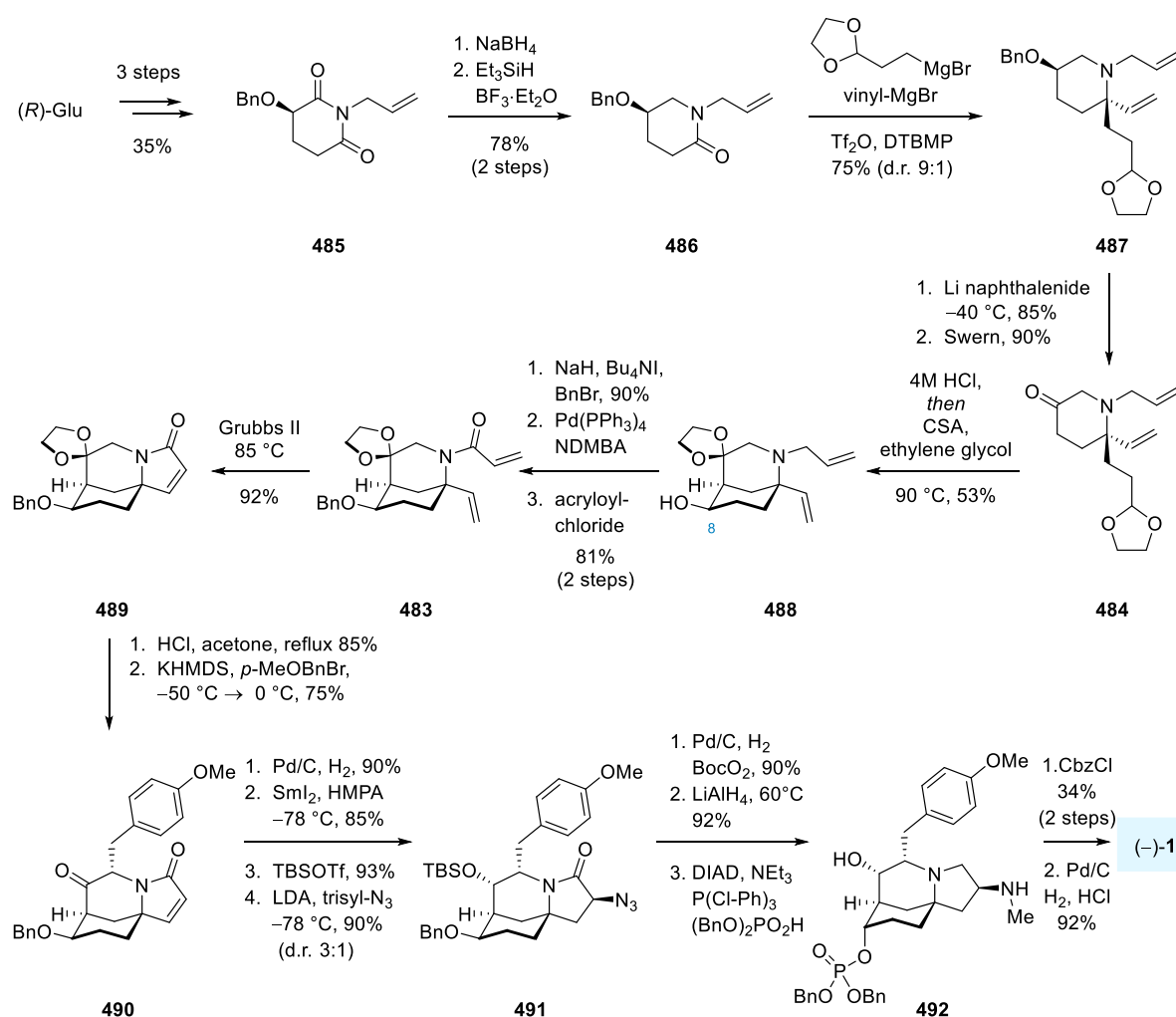
In 2012 and 2013 the Huang group reported first their formal synthesis, followed by the completed enantioselective total synthesis of FR901483.^[268-269] Huang's approach accessed a

cyclic α -tertiary amine precursor for an aldol reaction to establish an morphan system. Ring closing metathesis then completed the FR901483 scaffold (Scheme 99).



Scheme 99. Huang's retrosynthetic strategy.

The synthesis started from optically active *N*-allyl 3-benzyoxy glutarimide **485**.^[305-309] Defunctionalization to chiral lactam **486** was achieved by reduction to the hemi-aminal followed by treatment with triethyl silane and Lewis acid. Generation of the α -tertiary amine **487** was carried out by double Grignard addition in the presence of triflic anhydride and DTBMP in good yields and good diastereoselectivity (9:1).^[310-311]



Scheme 100. Huang's total synthesis of FR901483.

Intramolecular aldol addition was carried out from **484** using acidic conditions with ethylene glycol as an additive, steering the selectivity towards desired dioxolane **488**. **488** was converted into its benzyl analogue,^[270] and the *N*-allyl group replaced with an acryloyl substituent,^[312-313] furnishing **483**. After ring closure and deprotection of the ketone, α -benzylation to incorporate the *para*-methoxybenzyl group gave ketone **490**. A final sequence including Fukuyama's samarium iodide reduction,^[266, 272] and Sorensen's Mitsunobu reaction^[261] led to dibenzyl phosphate ester **492**. Introduction of the Cbz-group followed by immediate hydrogenolysis gave the natural product.

Huang's synthesis used a novel approach with the early and efficient installation of the α -tertiary amine center. The *N*-allyl group had to be exchanged to the acryloyl group to enable the use of Fukuyama's samarium iodide method. In conclusion, Huang's aldol reaction is an important contribution to the selective generation of the aza-tricyclic scaffold.

3.1.2.13 Other approaches towards the FR901483 core structure

Additionally to these elegant syntheses, a number of synthetic studies towards the core structure of FR901483 have been reported.^[265] In 1997, Kibayashi and co-workers reported the synthesis of the 5-azatricyclo[6.3.1.0^{1,5}]-dodecane core structure of FR901483 using Lewis acid mediated opening of an *N,O*-acetal followed by alkylation of an *anti*-Bredt iminium ion.^[314-316] In 2001, the Kibayashi group reported a modified strategy of this approach.^[317] In the same year, Wardrop and co-workers disclosed their formal synthesis of racemic desmethylamino FR901483^[275] featuring a 6-*exo-trig* radical cyclisation.^[318] Both Bonjoch and Hayes reported studies towards the synthesis of FR901483,^[253, 319-320] utilizing a palladium catalyzed cyclization of tethered vinyl bromides.^[321-327] Bonjoch later expanded the work implementing an intramolecular Kharasch-type^[328] cyclization.^[329] In 2006, Weinreb and co-workers reported their approach towards racemic FR901483 via cyclisation of an iodoacetamide ketone.^[330-331] The Martin group disclosed their approaches to the azatricyclic core of FR901483 via nucleophilic addition to a *N*-acyl iminium ion in 2006 and 2007.^[332-333] Another approach towards FR901483 was published by the Reissig group in 2006 featuring an intramolecular aldol reaction of a spiroketone.^[334] Sorensen and co-workers developed a second generation approach to FR901483 in 2008,^[285] featuring a multicomponent Ugi reaction, later utilized by Fukuyama,^[266] to access a spirolactam precursor and a highly selective sulfonate ester elimination in order to desymmetrize the cyclohexane ring. Rovis published an efficient enantioselective approach to the chiral tricyclic scaffold of FR901483 in 2014 using a rhodium catalyzed [2+2+2] cycloaddition.^[335-337] Recently, Jia reported an enantioselective methodology to access the azatricyclic core skeleton of FR901483.^[338]

3.1.3 TAN1251C – Structure, isolation, bioactivity and proposed biosynthesis

The TAN1251 alkaloids, namely TAN1251A (**493a**), TAN1251B (**493b**), TAN1251C (**2**), and TAN1251D (**493d**), are a series of anticholinergic alkaloids first isolated in 1991 from a *penicillium thomii* RA-89 fermentation broth by Takeda Chemical Industries, Osaka, Japan (Figure 15).^[339]

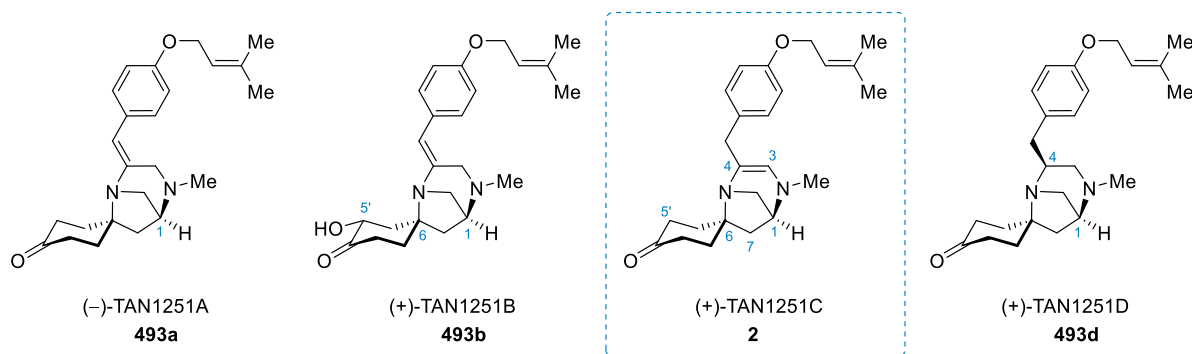


Figure 15. The TAN1251 series of alkaloids with TAN1251C (this work) highlighted.

In their isolation work,^[339] the Takeda team prepared a seed culture of the *penicillium thomii* RA-89 strain, obtained from soil in the Miyagi prefecture, Japan, which was incubated in an aerated reactor with 3600 liter fermentation medium for 90 hours. The broth was filtered, and multistep acid/base treatment of the filtrate followed by extraction gave crude material. Purification by column chromatography, and crystallization if applicable, furnished the alkaloids TAN1251A (925 mg), TAN1251B (1.2 g), TAN1251C (5.1 g), and TAN1251D (7.6 g) as their respective free bases. Elucidation of molecular structure and relative stereochemistry of TAN1251B was achieved via X-ray crystallographic analysis, complemented by spectroscopic (NMR, IR), chemical, and elemental analysis. Absolute configuration of TAN1251 B was established via circular dichroism (CD) spectroscopic analysis of the dibenzoate of the diol reduction product of TAN1251B.^[340] Interestingly, resubjection of isolated TAN1251A to fresh seeded fermentation broth showed that ca. 60% of TAN1251A was converted to TAN1251B after 72 hours, which suggested that the absolute stereoconfiguration of the stereocenter in TAN1251A and TAN1251B were identical. The absolute stereochemistry of TAN1251C and TAN1251D was unambiguously determined through total synthesis by Snider and co-workers in 1999.^[340]

Structurally, the four natural products from the TAN1215 family share an interesting common diaza-tricyclic core structure featuring a 1,4-biazabicyclo[3.2.1]octane with a spiro-fused cyclohexanone.^[253] All compounds but TAN1251D contain an enamine functionality

originating from the α -tertiary amine, which in case of TAN1251C constitutes an unusual dienamine moiety. TAN1251A and TAN1251C have a single stereocenter at the C1 position, whereas TAN1251D contains two stereocenters, in C1 and C4 position. TAN1251B bears three chiral centers, at the C1, C6, and C5' carbons.

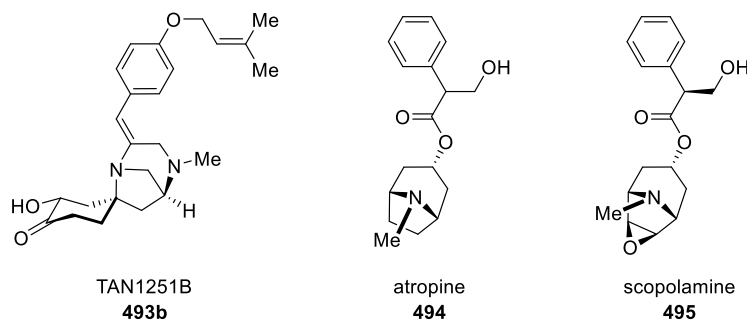
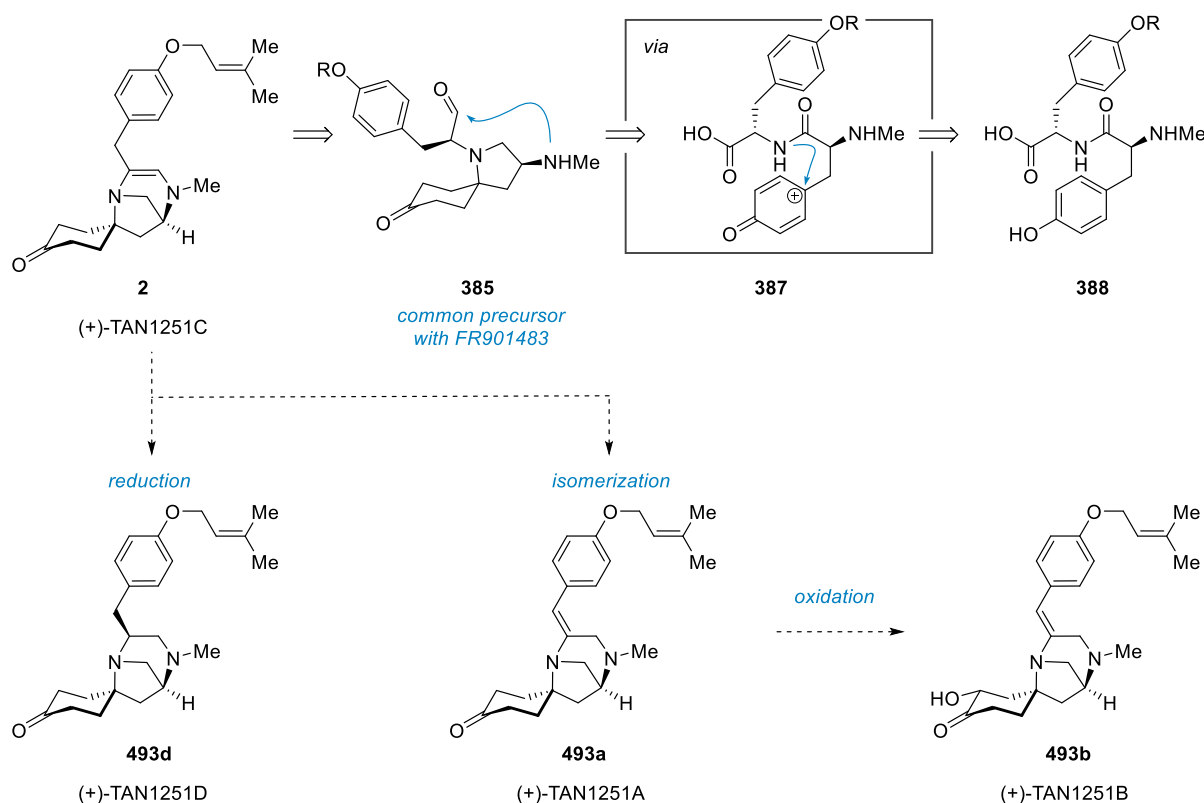


Figure 16. Comparison of TAN1251B with known muscarinic antagonists atropine and scopolamine.

The bioactivity of the TAN1251 series was assessed in the isolation report.^[339] TAN1251A and TAN1251B are potent muscarinic antagonists, with potential use as mydriatic agents, antispasmodic and antiulcer agents. Muscarinic antagonists, such as atropine and scopolamine (Figure 16), have been employed for the treatment of nervous diseases (such as Parkinson's and motion sickness), disorders of the digestive tract (such as peptic ulcer and irritable bowel syndrome), and respiratory illnesses (such as chronic obstructive pulmonary disease, and asthma). However, their unpleasant side effects (blurred vision, dry mouth, dizziness) has driven the search for newer, synthetic antimuscarinics.^[341] TAN1251A and TAN1251B exhibited strong anticholinergic activity on the basis of a radio ligand receptor binding assay with ^3H -quinuclidinyl benzilate and microsomal fractions of rat cerebral cortex.^[339] The affinity of TAN1251B to muscarinic acetylcholine acceptors exceeds that of atropine, making it an attractive target for drug development.^[342] TAN1251A was selective towards the M_1 subtype of the muscarinic receptor. Moreover, an animal study in the isolation work shows that TAN1251A and TAN1251B inhibit the acetylcholine-induced contraction of Guinea pig ileum quoting ED_{50} values of 8.0 and 10.0 nM respectively. Assessment of the acute toxicity of TAN1251A and TAN1251B, performed in mice showed no signs of toxicity at doses of up to 100 mg/kg for either of the two substances.^[339]

Similar to FR901483 (see Scheme 79), the TAN1251 series of alkaloids appear to be biosynthetically derived from a tyrosine-tyrosine dipeptide unit. In fact, it is likely that the TAN1251 alkaloids and FR901483 share a common biosynthetic precursor in the form of spirocycle **385** (Scheme 101). In the purported biosynthesis pathway,^[260, 262, 340] tyrosinyl-

tyrosine **388** undergoes intramolecular oxidative amidation to form the common antecedent spirocycle **385**. The biosynthesis continues via attack of the C2 amine at the tyrosine aldehyde, to form the dienamine natural product TAN1251C (**2**). TAN1251C is of central importance as it is likely to serve as the precursor for the three other TAN1251 series alkaloids.^[258] TAN1251D (**493d**) could be formed by reduction, while TAN1251A (**493a**) is the product of isomerization of the enamine double bond, notably eroding stereochemistry at C4. Lastly, the results from the isolation work indicate that TAN1251B (**493b**) is an oxidation product of TAN1251A (**493a**).



Scheme 101. Purported biosynthetic pathway for the TAN1251 series of alkaloids.

3.1.4 TAN1251 series – Previous syntheses

3.1.4.1 Overview

The TAN1251 alkaloid series has attracted considerable synthetic interest since its isolation in 1991. To date, 13 total and formal syntheses have been dedicated to the TAN1251 series, with the first report in 1998 and the latest contribution in 2017. Starting with TAN1251A (**493a**), 6 syntheses of the compound are reported, comprising of 2 enantiocontrolled total syntheses, 3 formal syntheses, and one racemic total synthesis. Only one instance of the total synthesis of

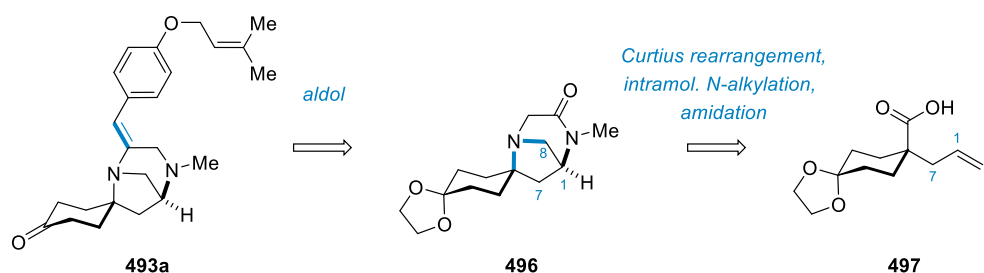
TAN1251B (**493b**) has been reported. (+)-TAN1251C (**2**) has received significant synthetic attention with four reported total syntheses of the optically active natural compound. Finally, two contributions report the enantiocontrolled synthesis of TAN1251D (**493d**). An overview of the synthetic work on the series is provided in Table 6.

Table 6. Total syntheses of the TAN1251 series of alkaloids.

Main authors	Year	Ref	Enantiocontrol	Note
TAN1251A				
Kawahara-Nagumo	1998	[343-344]	rac.	first rac.
Snider	2000	[340]	(-)	first
Wardrop	2001	[345]	(-)	
Honda	2002	[346-347]	(-)	formal
Kawahara-Nagumo	2002	[348]	(-)	formal
Hayes	2004	[349]	(-)	formal
TAN1251B				
Snider	2000	[340]	(+)	
TAN1251C				
Snider	2000	[340]	(+)	
Ciufolini	2001	[262]	(+)	
Honda	2005	[350]	(+)	
Kan	2017	[351]	(+)	
TAN1251D				
Snider	2000	[340]	(+)	
Honda	2005	[350]	(+)	

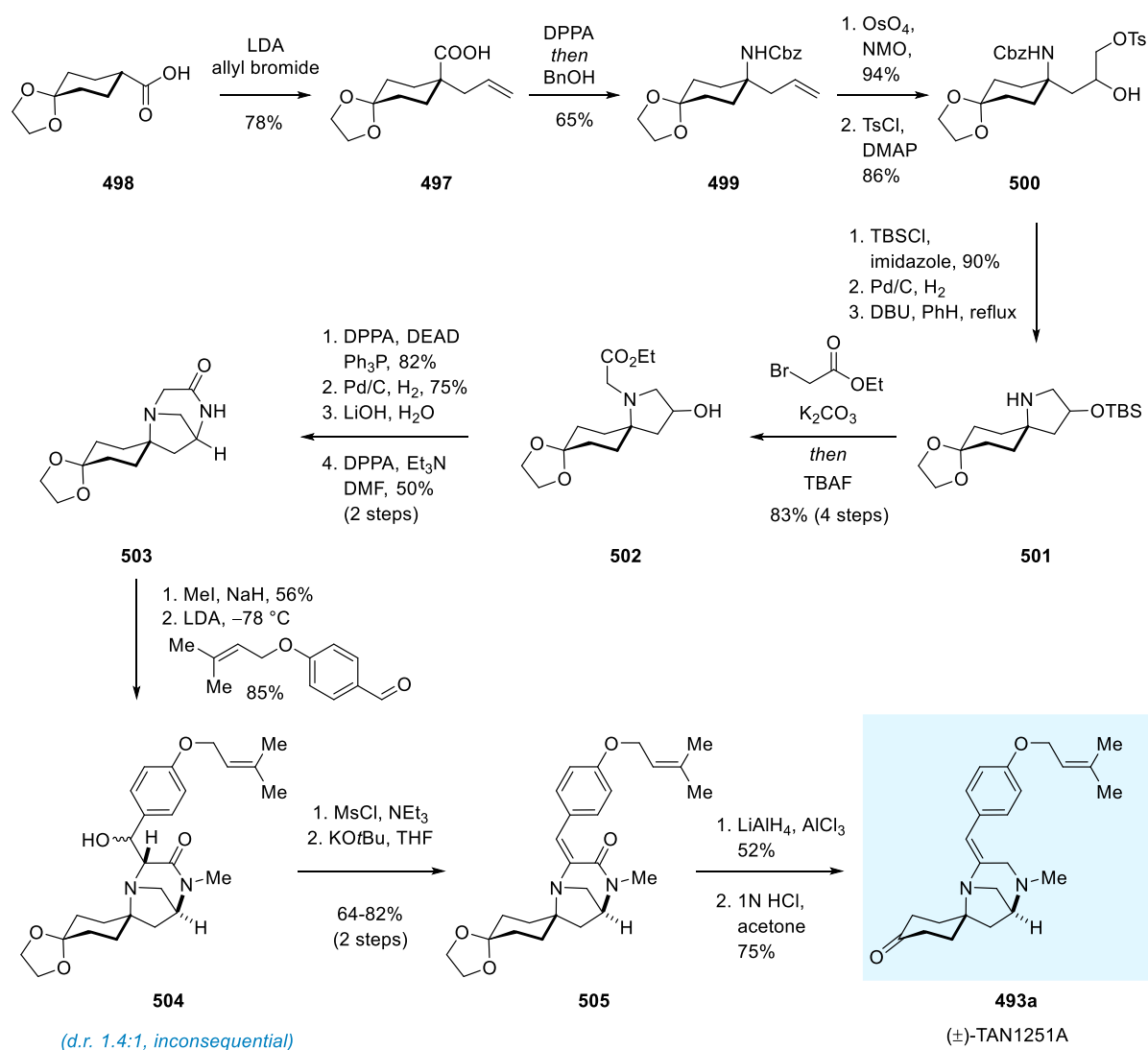
3.1.4.2 Kawahara and Nagumo's first generation synthesis of TAN1251A

In 1998, Kawahara and Nagumo published the first total synthesis of (\pm)-TAN1251A.^[343-344] In their retrosynthetic strategy, Kawahara, Nagumo and co-workers utilized a Curtius rearrangement to install the key spiro α -tertiary amine. The plan included generation of the pyrrolidine ring via an intramolecular alkylation reaction (Scheme 102).



Scheme 102. Kawahara and Nagumo's retrosynthetic strategy.

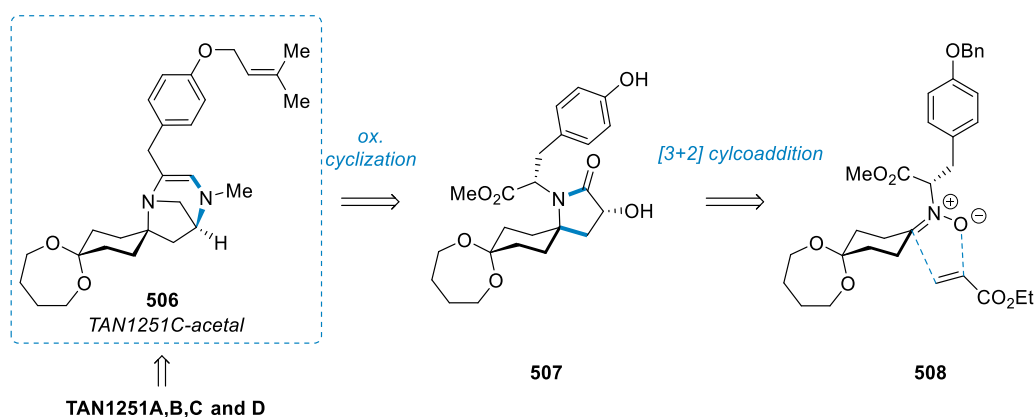
The racemic synthesis starts from known carboxylic acid **498**, which is converted to tosylate **500** through a series of standard operations including a Curtius rearrangement (Scheme 103). Intramolecular *N*-alkylation resulted in aza-spirocycle **501**, which was alkylated and the silylether cleaved with TBAF to furnish secondary alcohol **502**. Installation of the C2 nitrogen via Mitsunobu reaction with DPPA and subsequent cyclisation delivered tricyclic lactam **503**. Methylation and aldol reaction with LDA at low temperature gave an inconsequential diastereomeric mixture of alcohols **504** (d.r. 1.4:1). Finally, reduction of the derived conjugated lactam **505** with LiAlH_4 and AlCl_3 followed by transacetalization with acetone gave racemic TAN1251A (**493a**). In their early contribution, Kawahara and Nagumo present the first total synthesis of (\pm)-TAN1251A, employing an elegant and effective route.



Scheme 103. The Kawahara-Nagumo Synthesis of racemic TAN1251A.

3.1.4.3 Snider's synthesis of TAN1251A, B, C and D

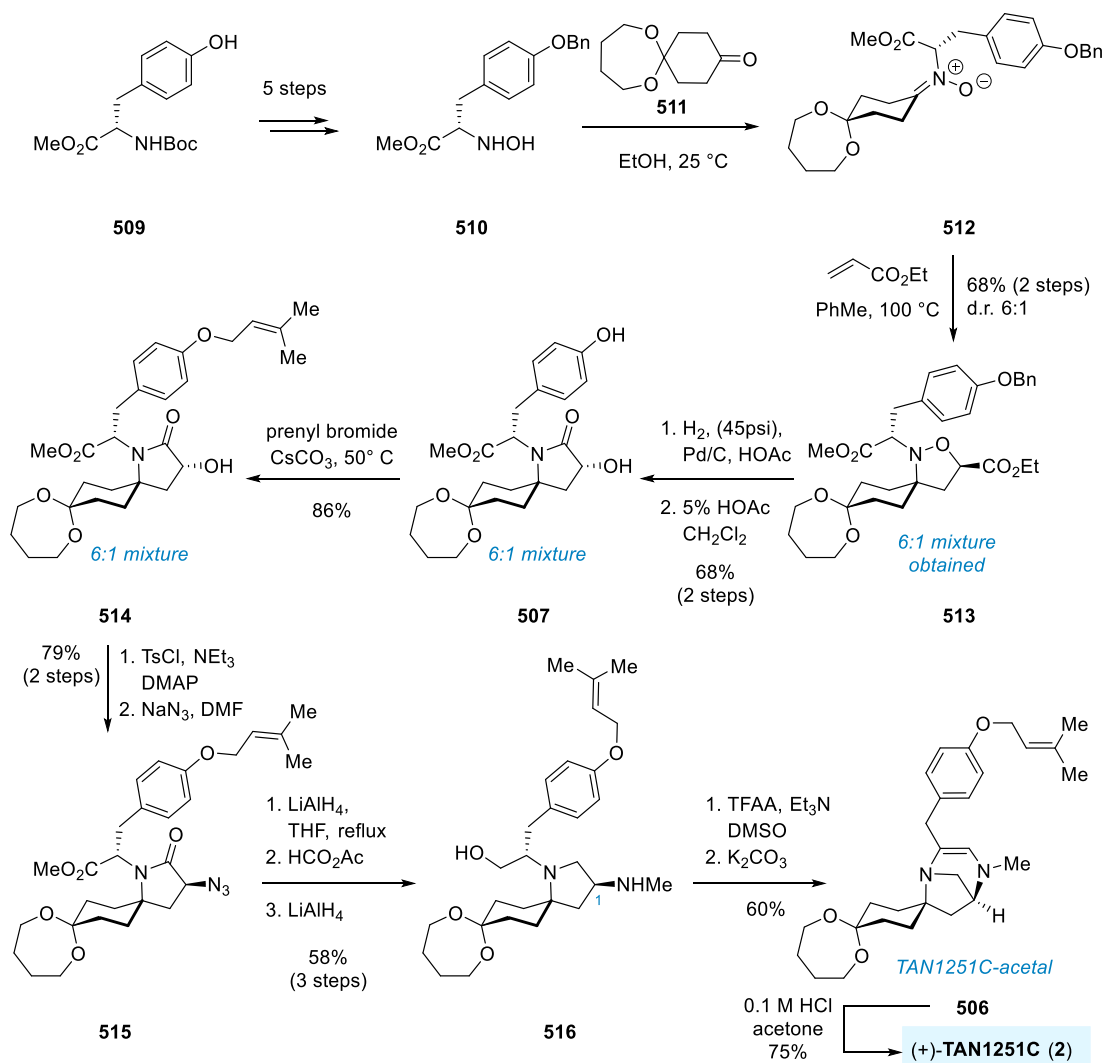
In a landmark paper in 2000, Snider and co-workers reported the synthesis of all members of the TAN1251 series, TAN1251A-D, all in their enantiopure form.^[340] The four natural products were obtained via a common precursor **506**, the acetal protected form of (+)-TAN1251C. Snider and co-workers were able to employ methodology previously developed for their synthesis of FR901483. The retrosynthetic strategy to access key acetal **506** utilized a nitron [3+2] dipolar cycloaddition to construct the pyrrolidine ring, and a biomimetic oxidative cyclization reaction (Scheme 104).



Scheme 104. Snider's retrosynthetic strategy towards acetal **506**.

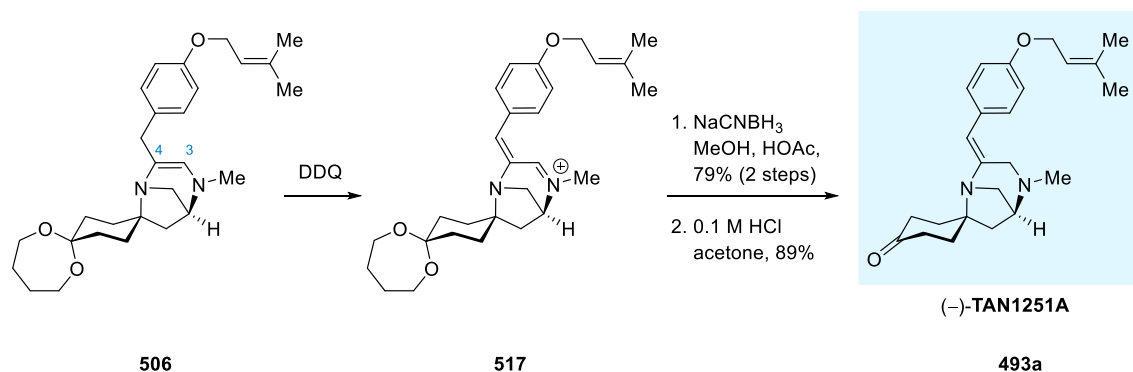
The synthesis of precursor **506** sets out from *O*-benzyl tyrosine methyl ester which was accessed from commercial *L*-*N*-Boc-tyrosine (**509**) by simple benzylation and Boc-deprotection in quantitative yield (Scheme 105).^[340] The respective hydroxylamine **510** was obtained via Grundke's procedure,^[352] and subsequent condensation with monoketal **511** afforded nitron **512**. Originally, the strategy was carried out with the mono dioxolane ketal instead of **511**, however, while cleavage could be achieved in the synthesis TAN1251A, analogous deprotection protocols for TAN1251C and TAN1251D were unsuccessful. Hence the dioxepane ketal, which is easier to cleave,^[353] was chosen. Nitron **512** was treated with ethyl acrylate in toluene at reflux to afford an inseparable 6:1 diastereomeric mixture in favor of desired spiro-isoxazolidine **513**. Conversion to **507** was achieved via hydrogenation followed by acid catalyzed lactam formation with a catalytic amount of acetic acid. Treatment with cesium bromide and cesium carbonate in acetone gave phenolic prenyl ether **514**. The installation of the C1 nitrogen could be achieved via tosylation followed by azide substitution. At the stage of azide **515**, separation of the diastereomeric mixture was achieved and yielded 79% yield of the desired compound, and 12% of the unwanted diastereomer. The authors propose that Omura–Sharma–Swern oxidation^[354] of the derived primary alcohol **516**

concomitantly formed the trifluoroacetamide at the C1 methylamine, which was readily hydrolyzed under basic conditions to afford TAN1251C-acetal **506**. Transacetalization in acidified acetone proceeded smoothly to give the first natural product of the series, TAN1251C (**2**).



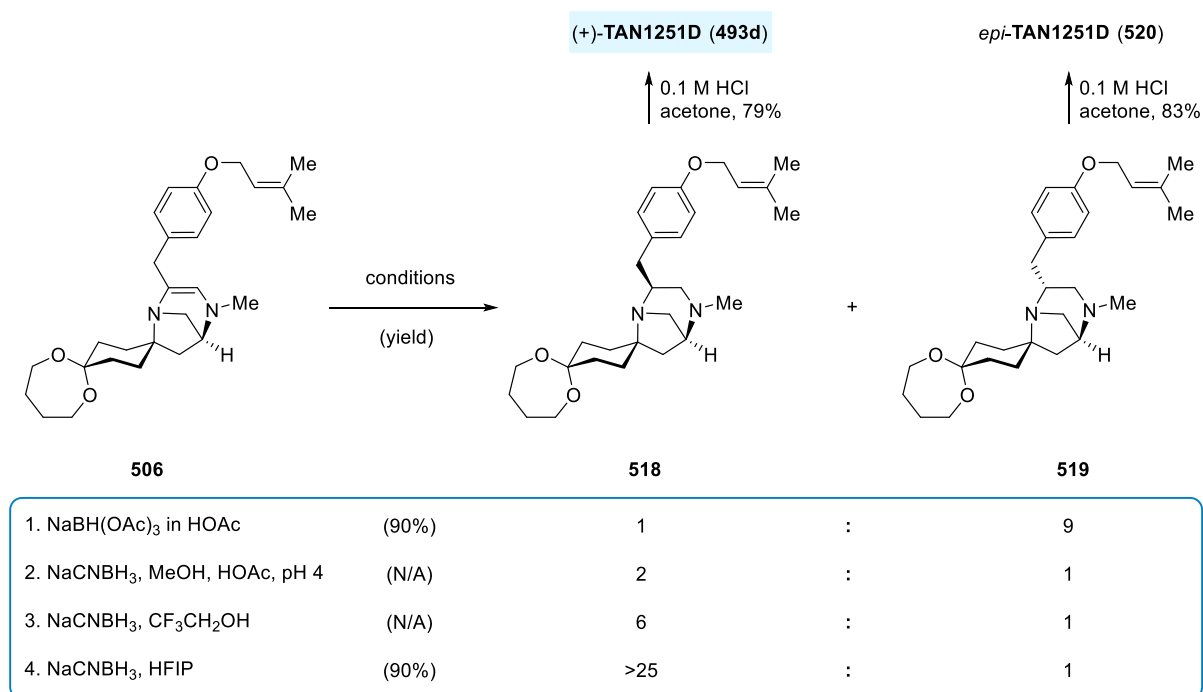
Scheme 105. Snider's synthesis of key precursor acetal **506** and (+)-TAN1251C (**2**).^[340]

The synthesis of TAN1251A required the isomerization of the C3–C4 double bond. To this end, Snider opted for slow addition of DDQ to precursor acetal **506** in dry dichloromethane to obtain highly conjugated eniminium salt **517** (Scheme 106). The product was immediately reduced using sodium cyanoborohydride, and the isomerized TAN1251A-acetal deprotected in acidic acetone to afford TAN1251A (**493a**).

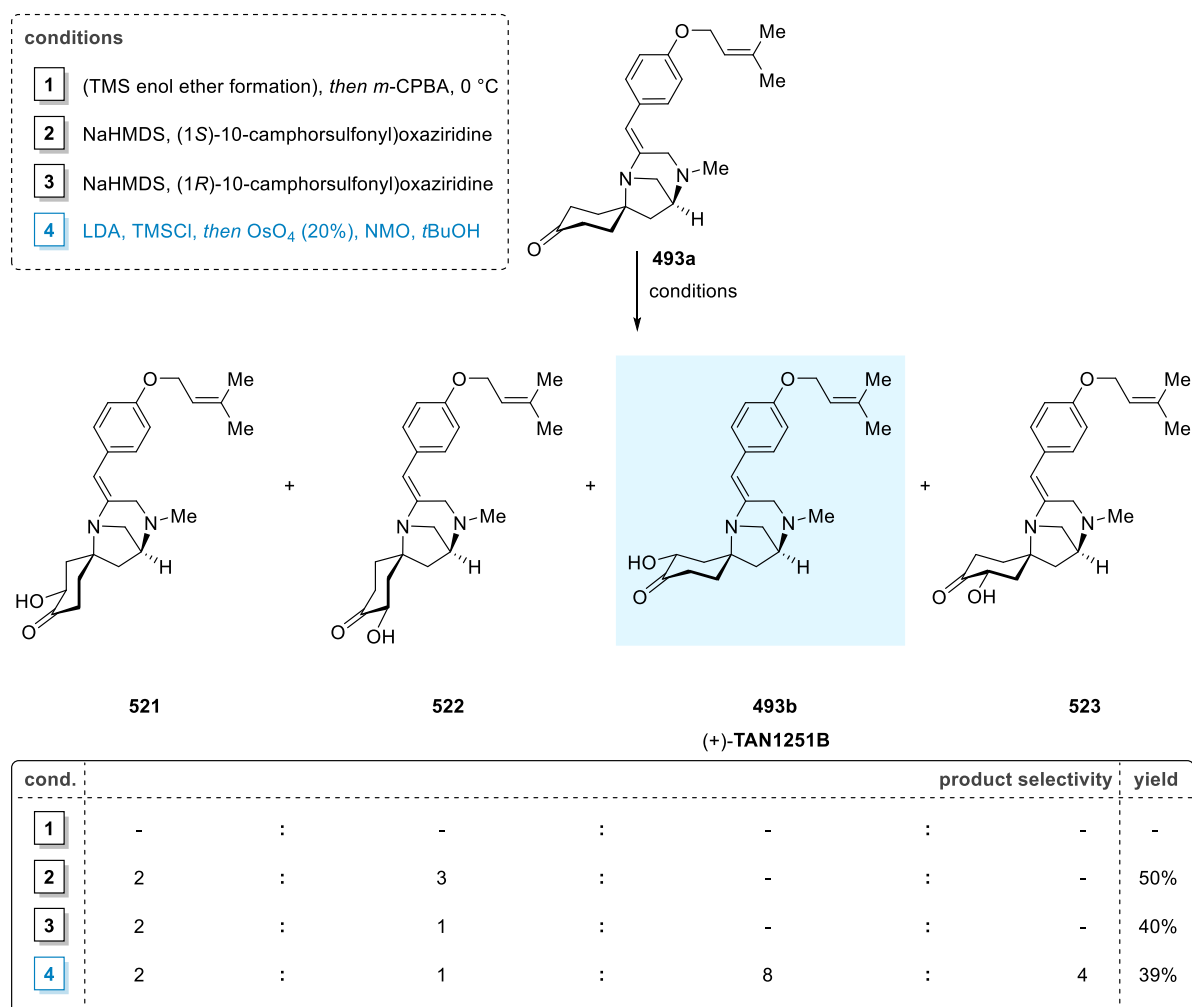


Scheme 106. Snider's synthesis of TAN1251A.

It was considered likely that the biosynthesis of TAN1251D proceeded via the reduction of the protonated iminium ion of TAN1251C. Thus, Snider and co-workers decided to pursue a similar synthetic strategy. Initial reduction of TAN1251C-acetal **506** with sodium triacetoxy borohydride in acetic acid yielded a 1:9 mixture of products, of which the major component was found to be **519**, the acetal of 4-*epi*-TAN1251D (**520**). By optimization of the reaction conditions, Snider and co-workers successfully inverted the selectivity of the reduction, a parameter which was most significantly influenced by the polarity of the solvent used. Under optimized conditions, reduction of **506** with NaCNBH₃ in hexafluoroisopropanol (HFIP) proceeded smoothly, yielding TAN1251D-acetal **518** in 90% yield (d.r. >25:1). Facile transacetalization was achieved in acidified acetone to reveal the natural product (+)-TAN1251D (**493d**), confirming its absolute stereoconfiguration (Scheme 107).

Scheme 107. Snider's reduction study of **506** and synthesis of (+)-TAN1251D (**493d**).

The first, and to date only synthesis of TAN1251B (**493b**) was achieved by Snider in the same report.^[340] The transformation of the enolate of TAN1251A (**493a**) to TAN1251B (**493b**) presented a formidable challenge since four α -hydroxy ketones could be formed from **493a**. Furthermore, any oxidant employed needed to be compatible with readily oxidizable functionality in **493a** such as amines and olefins. At the outset of Snider's investigation into the synthesis of TAN1251B, oxidation of the trimethylsilyl enol ether prepared from TAN1251A (**493a**) with *m*-CPBA at 0 °C resulted in formation of the *N*-oxide of the C1 amine and no formation of the desired isomer was observed (Scheme 108).



Scheme 108. Snider's oxidation study of TAN1251A (**493a**) and synthesis of (+)-TAN1251B (**493b**).

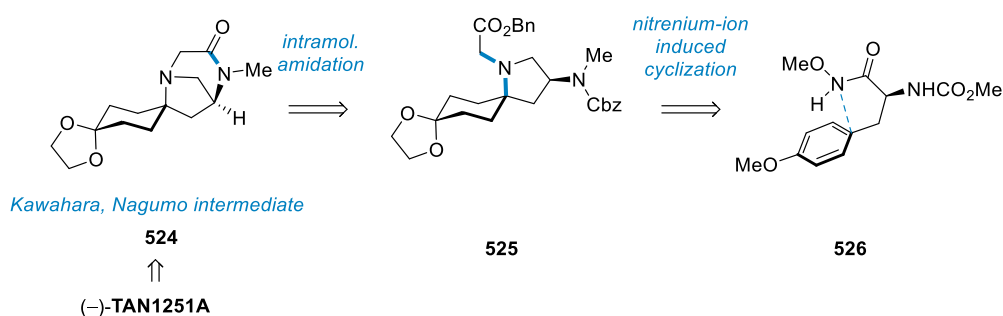
Formation of the enolate with NaHMDS followed by treatment with (1*S*)-10-(camphorsulfonyl)oxaziridine, as pioneered by Davis,^[355-356] led to a 2:3 mixture of undesired isomers **521** and **522** respectively. Hydroxylation of the enolate with the opposite enantiomer, (1*R*)-10-(camphorsulfonyl)oxaziridine resulted in a 2:1 mixture of **521** and **522**. The preference for hydroxylation on this undesired face of the six membered ring could only be

overcome when the mixture of pre-formed trimethylsilyl enol ethers was reacted with OsO₄ (20%) and NMO in aq. *tert*-butanol, resulting in a 2:1:8:4 mixture of **521**, **522**, TAN1251B (**493b**), and **523**. Purification proved challenging and furnished a mixture of TAN1251B and **523** which was inseparable by conventional methods. However, separation was ultimately achieved on a Chiralpak AD column, leading to an isolated sample of (+)-TAN1251B (**493b**).

In summary, Snider's report employs methodology originally developed for FR901483 and expanded the work significantly in this tour-de-force synthesis of the TAN1251 alkaloid family. This led to the elegant synthesis of all four members of the TAN1251 family in an enantiocontrolled fashion in a single report. To date, Snider's study is the only report achieving the synthesis of the complete series. The work demonstrates the key role of TAN1251C in the synthesis of the series, and supports the purported biosynthesis. Access to TAN1251A,C and D was established readily, while synthesis of TAN1251B was most challenging, with a selective method for its generation yet to be achieved.

3.1.4.4 Wardrop's synthesis of TAN1251A

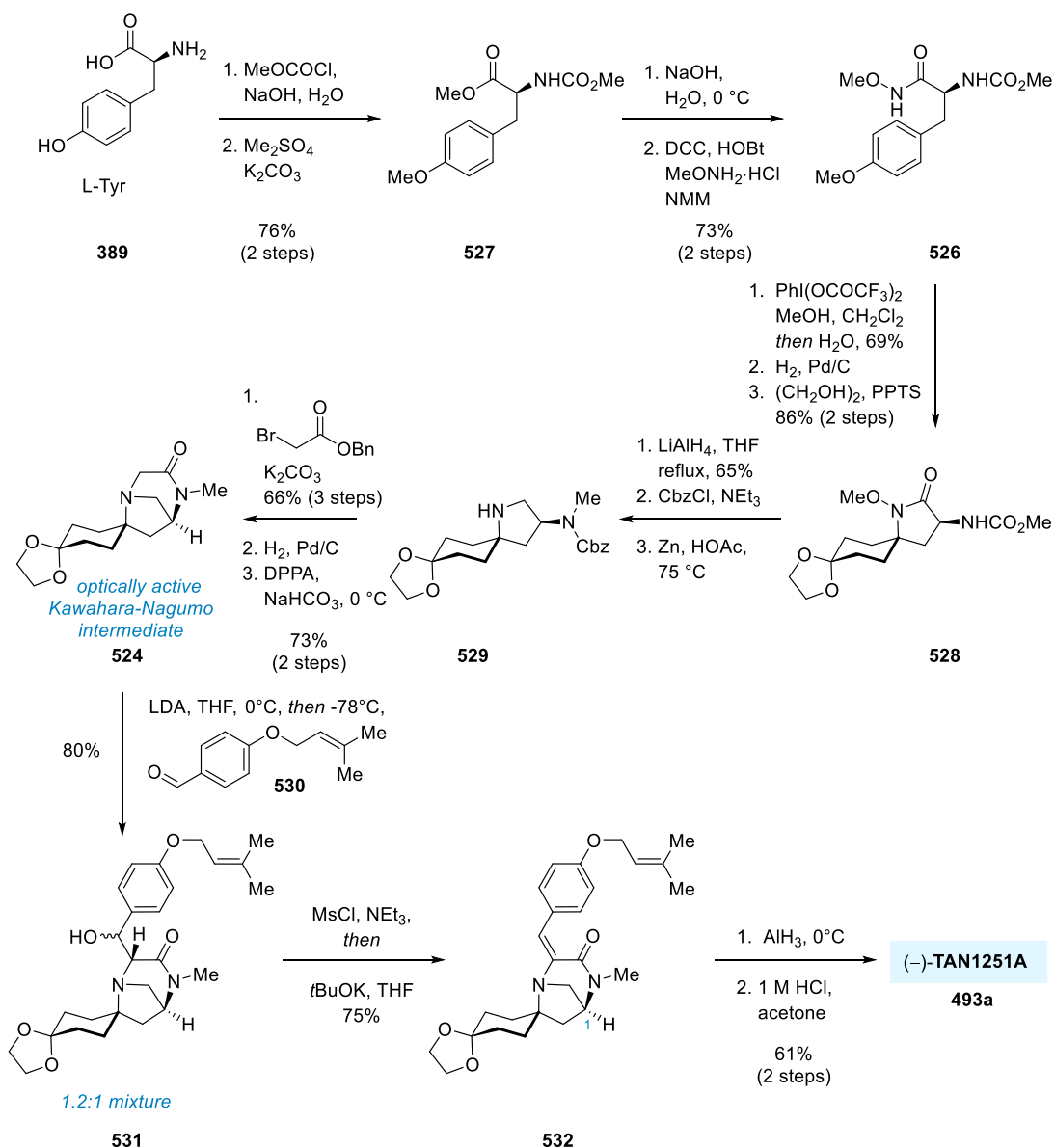
In 2001, the Wardrop group published their approach to TAN1251A,^[345] detailing an elegant *N*-methoxy-*N*-acylnitrenium ion-induced spirocyclization to generate the α -tertiary amine center (Scheme 109). The enantiocontrolled synthesis was merged with Kawahara and Nagumo's first generation (racemic) route.^[343]



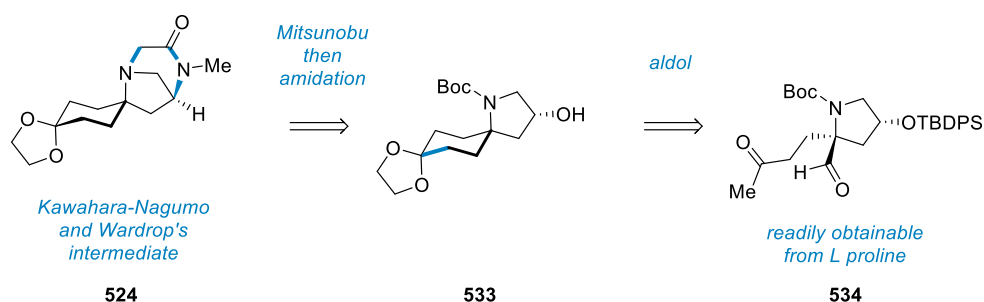
Scheme 109. Wardrop's retrosynthetic strategy to TAN1251A.

The key aza-spirocyclization was initiated from **526** (accessible from L-tyrosine)^[357-358] by treatment with bis(trifluoroacetoxy)iodobenzene, readily providing the resulting dienone in 69% yield (Scheme 110). Hydrogenation of the dienone followed by ketal protection of the generated ketone led to spirocycle **528**. Lithium aluminium hydride reduction unexpectedly generated the desired methyl amine selectively, which enabled differentiation between the two amines and consecutive protection of the C1 amine as the benzyl carbamate.

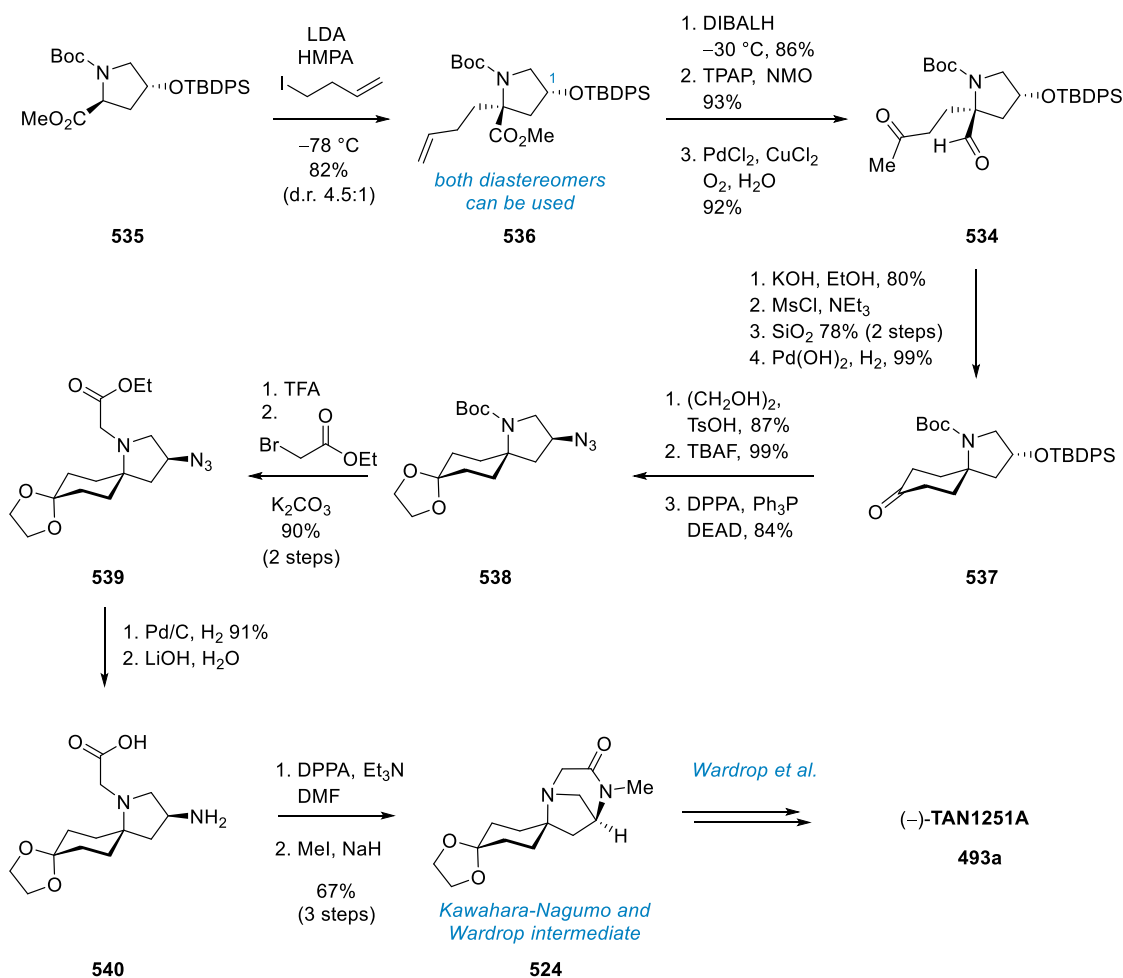
Zinc-mediated reduction of the N–O bond then afforded secondary amine **529**. Kawahara-Nagumo intermediate **524** was accessed via established steps. The benzyl group was introduced via aldol reaction with *para*-prenyloxybenzaldehyde, to give an inconsequential 1.2:1 mixture of products **531** in a combined yield of 80%. The mixture was treated with mesyl chloride, and the resulting mesylates submitted to basic elimination conditions, destroying two of the three stereocenters and converging the mixture into resulting α,β -unsaturated amide **532**. Reduction of **532** with AlH_3 in ether followed by transacetalization in a mixture of HCl and acetone completed Wardrop's total synthesis of (–)-TAN1251A (**493a**).



Scheme 110. Wardrop's synthesis of (–)-TAN1251A (**493a**).

3.1.4.5 Kawahara and Nagumo's 2nd generation synthesis of TAN1251A**Scheme 111.** The Kawahara-Nagumo second generation retrosynthetic strategy towards TAN1251A.

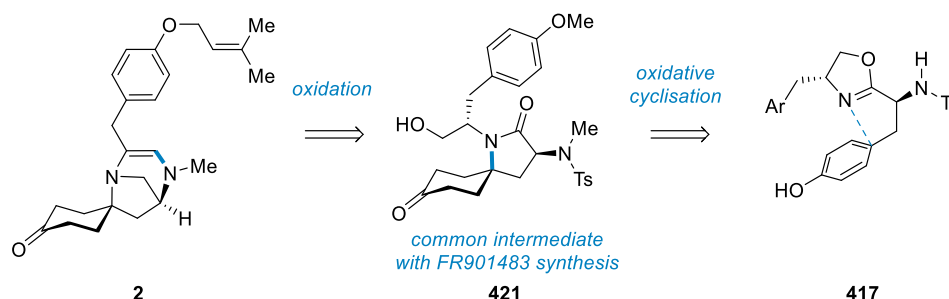
In 2002, Kawahara, Nagumo and co-workers published their second generation synthesis of optically active (–)-TAN1251A (Scheme 111).^[348] The formal synthesis centers around chiral intermediate **524**.^[343, 345] In contrast to prior work, Kawahara and Nagumo chose a proline derivative as the starting material in their synthesis. Aldol reaction to close the cyclohexanone ring was followed by Mitsunobu reaction to install the C1 nitrogen, allowing the completion of the core scaffold via intramolecular amidation.

**Scheme 112.** Kawahara and Nagumo's second generation formal synthesis of TAN1251A (**493a**).

The synthesis commences with alkylation of *trans*-4-hydroxy-L-proline derivative **535** with LDA to afford α -tertiary amine product **536** (67%) and its epimer (15%) (Scheme 112). Both diastereomers could be used for the outlined route to access methyl ketone **537**. Closure of the cyclohexanone ring was followed by a series of standard operations to arrive at aza-spirocyclic ketone **537**. Acetal protection of the ketone followed by cleavage of the silylether delivered the secondary alcohol, which was transformed into azide **538** with the correct stereoconfiguration on C1 via established Mitsunobu reaction.^[343] Removal of the Boc group was followed by *N*-alkylation to give ester **539**. The azide was reduced via catalytic hydrogenation and the resulting amino ester hydrolyzed to give acid **540**. DPPA induced cyclisation followed by methylation delivered the optically active first-generation intermediate **524** with the complete core structure in place. As **524** has been transformed into (–)TAN1251A by Wardrop, the second-generation synthesis of **524** by Kawahara and Nagumo constitutes a enantiocontrolled formal synthesis of TAN1251A.

3.1.4.6 Ciufolini's synthesis of TAN1251C

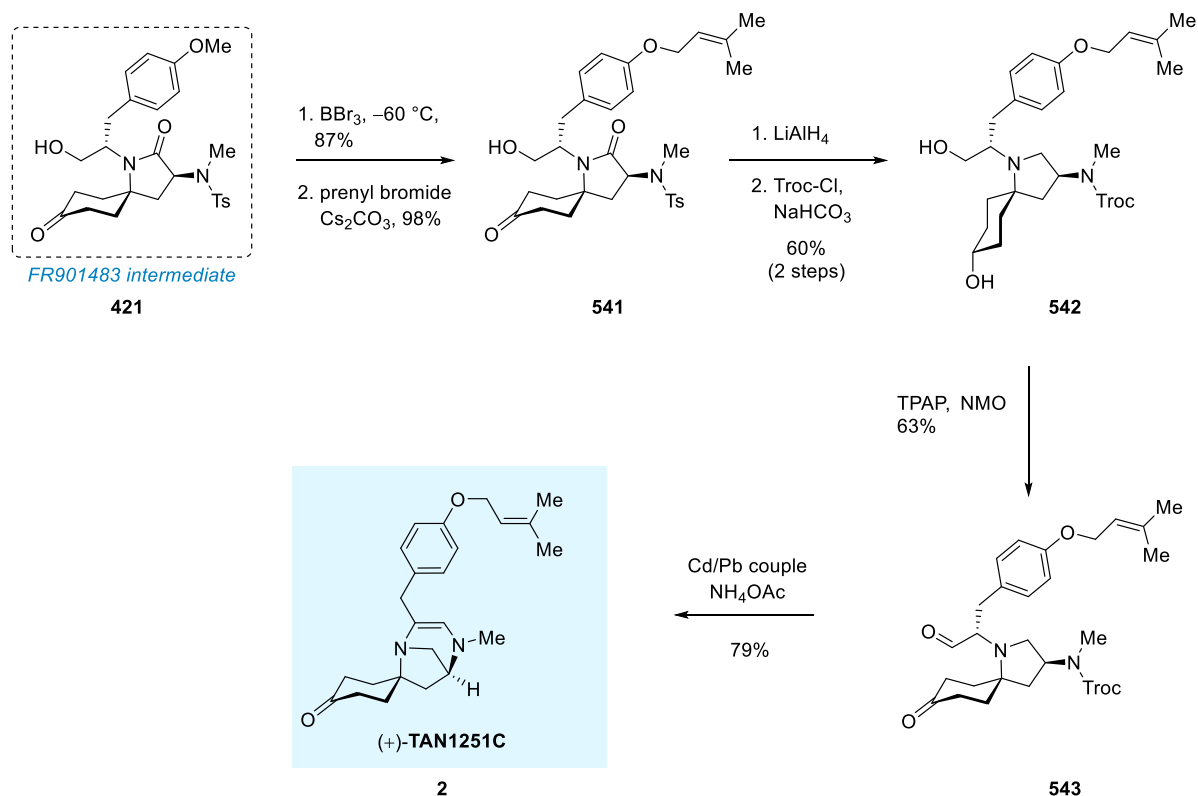
In 2001, Ciufolini and co-workers published their approach to TAN1251C together with their synthesis of FR901483.^[262] The Ciufolini group used a divergent approach, in which an intermediate from their FR901483 synthesis could be directly used as a late stage precursor in the synthesis of TAN1251C. The central intermediate **421** was obtained through the same methodology as in the synthesis of FR901483 (Scheme 113, see also Section 3.1.2.5).



Scheme 113. Ciufolini's divergent retrosynthetic strategy to TAN1251C.

The advanced intermediate **421** was first converted into the free phenol by treatment with BBr_3 , followed by prenylation under standard conditions to furnish prenyl ether **541** (Scheme 114). Subsequent global reduction with lithium aluminium hydride gave the respective diol. Ciufolini and co-workers opted for 2,2,2-trichloro-ethoxycarbonyl (Troc) protection of the secondary amine to obtain carbamate **542**. The diol could be successfully oxidized using Ley-oxidation conditions with TPAP and NMO, resulting in keto aldehyde **543**. Deprotection

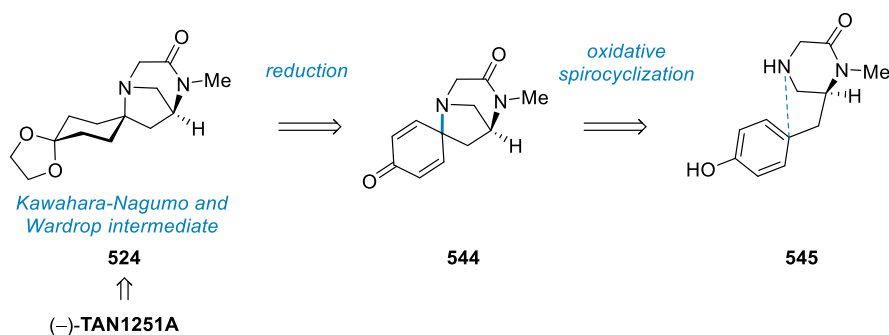
using the cadmium-lead couple led to intramolecular condensation forming the desired natural product TAN1251C in good yield (79%).



Scheme 114. Ciufolini's synthesis of (+)-TAN1251C.

Overall, Ciufolini's elegant approach was the first to allow construction of both the FR901483 and TAN1251C scaffolds divergently, featuring a late stage common intermediate, albeit with the necessary removal of the phenolic methyl group. Suppression of the aldol reaction in the final oxidation step as encountered by the Ciufolini group remains an unsolved problem requiring protecting group manipulations late in the synthesis.

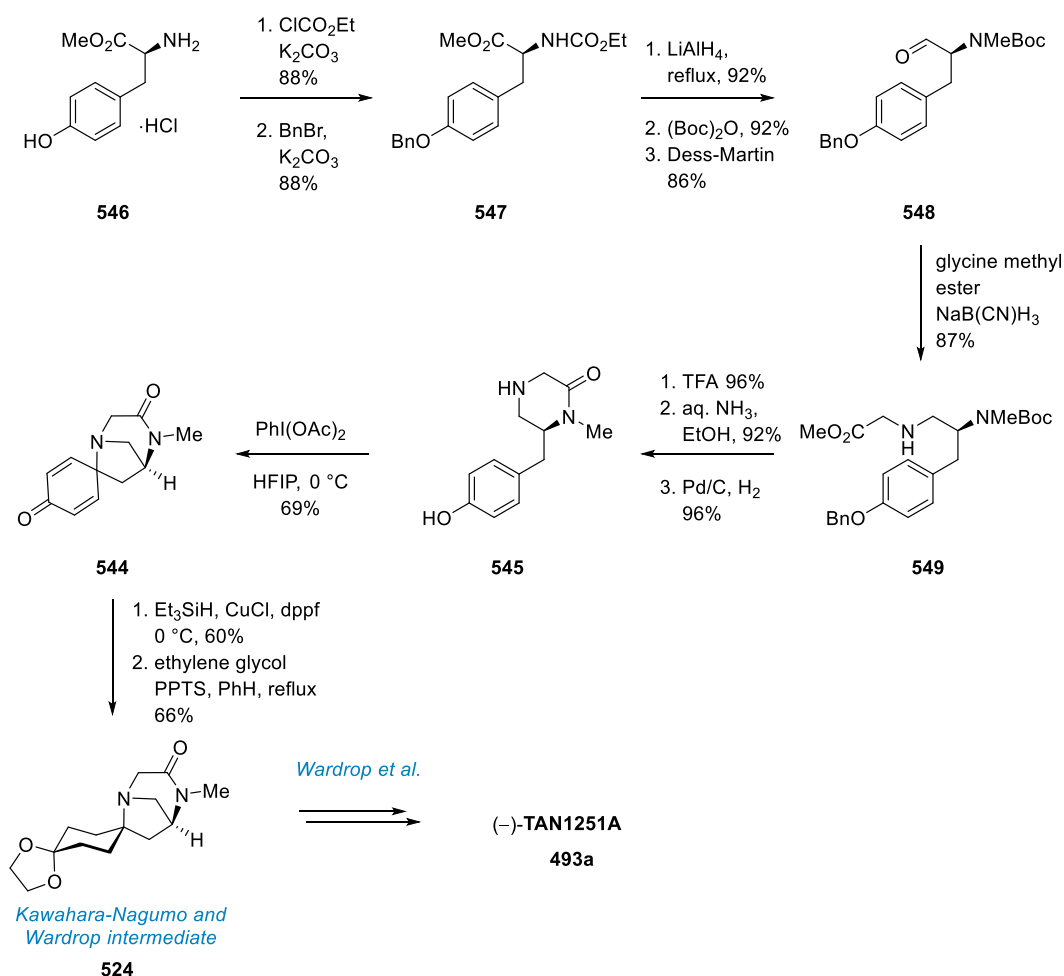
3.1.4.7 Honda's formal synthesis of TAN1251A



Scheme 115. Honda's retrosynthetic strategy to TAN1251A.

In 2002, Honda^[346-347] developed a novel approach to the formal synthesis of (–)-TAN1251A, targeting synthetic intermediate **524** previously reported in the Kawahara-Nagumo^[343-344, 348] and Wardrop^[345] syntheses. The synthesis employed a oxidative spirocyclization mediated by hypervalent iodine reagents, as previously reported in the syntheses of Wardrop^[345] and Ciufolini^[262], however on a more challenging piperazinone ring system (**545**) (Scheme 115).

Benzyl phenylether **547** (accessible from tyrosine methyl ester hydrochloride **546**) was subjected to a series of standard operations to deliver amine **549**, which in turn was cyclized to the respective piperazinone ring system after Boc-deprotection. Hydrogenolysis of the phenolic benzyl group gave the resulting piperazinone **545**. In the key step of the synthesis, oxidative cyclization employing bis(acetoxy)iodobenzene in hexafluoroisopropanol (HFIP) proved particularly successful, delivering the desired diazabicyclic dienone product **544** in 69% yield, which could be readily advanced to the Kawahara-Nagumo and Wardrop intermediate **524**.

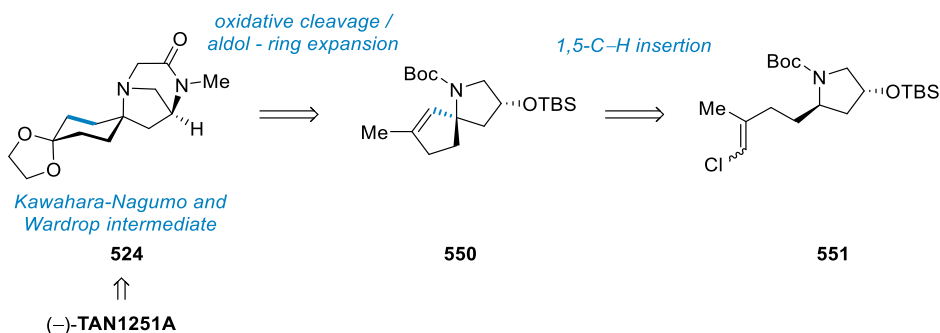


Scheme 116. Honda's formal synthesis of (–)-TAN1251A.

Honda detailed a concise formal route to TAN1251A employing the commonly used oxidative cyclization chemistry efficiently to access the diazabicyclic ring system of the TAN1251 series. Although the synthesis presents selectivity challenges in the reduction of dienone **544**, the approach is appealing due to its brevity.

3.1.4.8 Hayes' formal synthesis of TAN1251A

In 2004, the Hayes group published their formal synthesis of TAN1251A, utilizing an alkylidene carbene 1,5-C–H insertion approach^[359] to access a [5,5]-spirocyclic precursor.^[349] The synthesis involves ring expansion via an oxidative cleavage / aldol sequence to generate the cyclohexanone ring fragment, and an intramolecular amidation previously reported in Kawahara and Nagumo's second generation approach (Scheme 117).^[348]

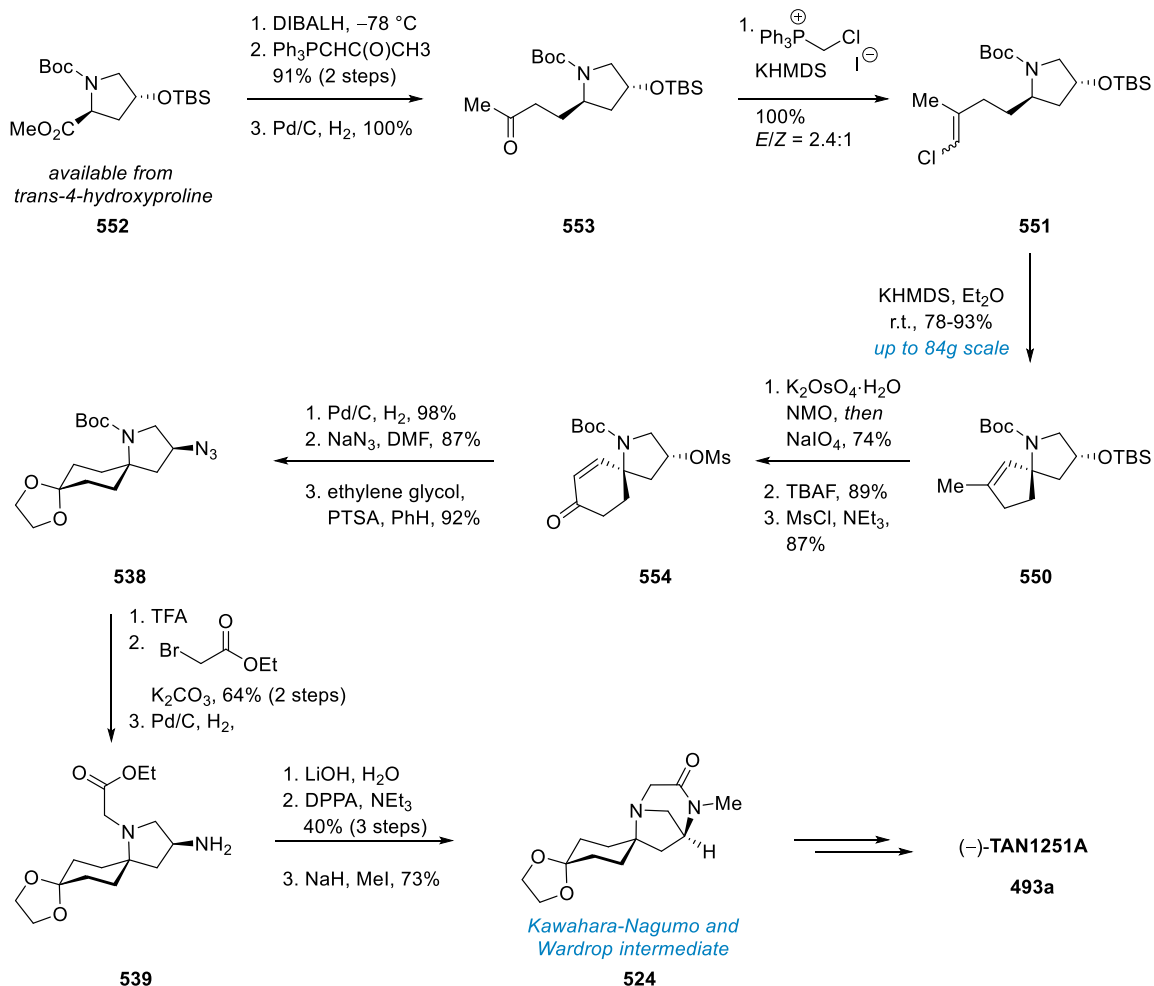


Scheme 117. Hayes' retrosynthetic strategy towards TAN1251A.

The Hayes synthesis commenced from proline derivative **552** (Scheme 118). Derived ketone **553** was employed in the key 1,5-C–H insertion, following a procedure reported by Ohira,^[360] delivering the desired [5,5]-spirocycle **550** in 40-86%. Due to reproducibility concerns, the reaction was optimized to start from vinyl chloride **551**, obtained quantitatively from **553** via Wittig reaction, to produce the desired spirocyclic product **550** in improved 78-93% yield. The double bond in spirocycle **550** was cleaved following the Lemieux-Johnson protocol,^[361] allowing ring expansion and elaboration to spirocycle **538**. Removal of the Boc-group followed by treatment with ethyl bromoacetate under basic conditions installed the tether for subsequent intramolecular cyclization. Reduction of the azide gave known amine **539**.^[348] Conversion of amine **539** to the targeted Kawahara-Nagumo and Wardrop intermediate **524** completed the formal synthesis.

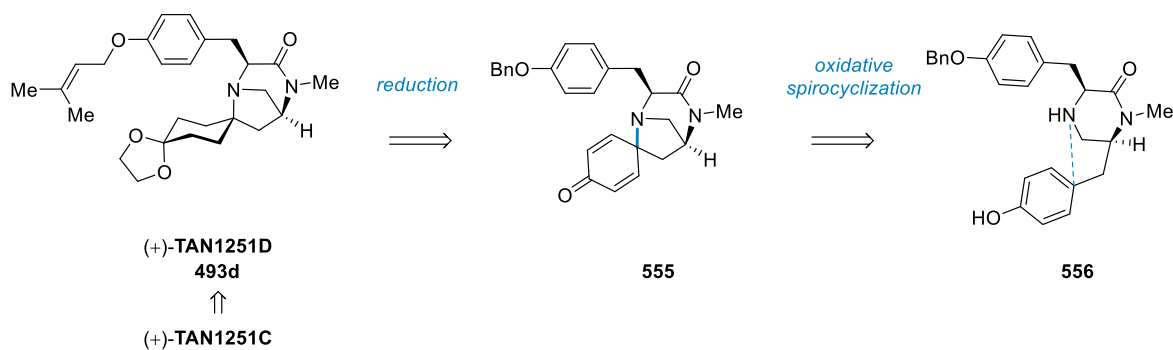
The Hayes group contributed a valuable methodology for construction of the challenging chiral α -tertiary amine spirocenter, present in all TAN1251 alkaloids. The method could also allow access to the related FR901483 scaffold. The reaction displays high levels of

diastereoselectivity and the chiral information in the precursor is derived from a readily available proline derivative. Notably, the total synthesis of TAN1251A was completed by the Hayes group via the established protocol in the same report.



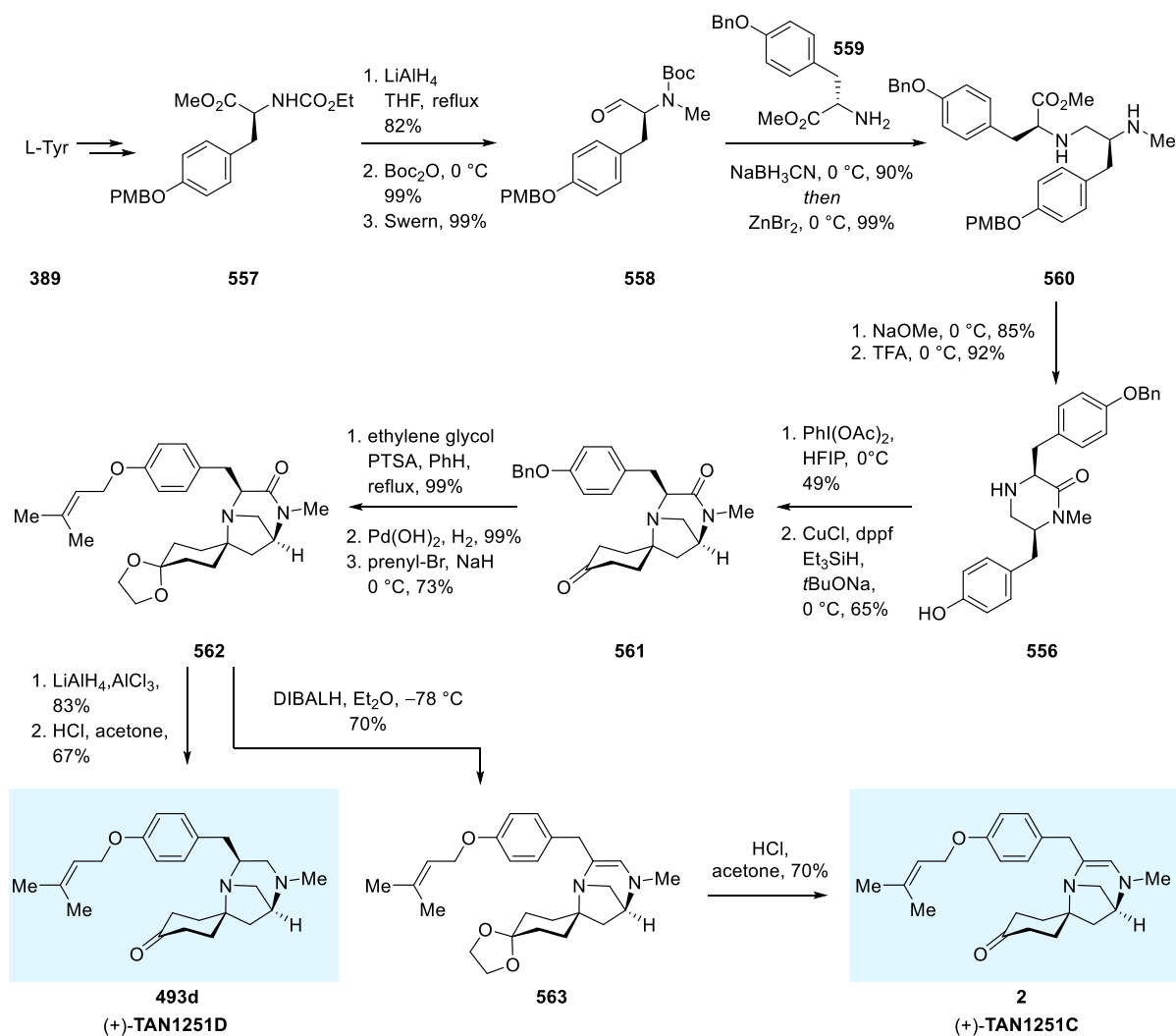
Scheme 118. Hayes formal synthesis of (-)-TAN1251A.

3.1.4.9 Honda's synthesis of TAN1251C and TAN1251D



Scheme 119. Honda's retrosynthetic strategy towards TAN1251D and TAN1251C.

In 2005, the Honda group published their second report on the synthesis of TAN1251-series compounds, achieving the synthesis of (+)-TAN1251C and (+)-TAN1251D.^[350] Honda employed a similar method to that reported in their previous synthesis of TAN1251A,^[346-347, 362] relying on an oxidative cyclization of a piperazinone through treatment with hypervalent iodine reagents (Scheme 119). In the new approach, the cyclization precursor was derived from a di-tyrosine unit, rather than tyrosinyl-glycine, precluding the need for late-stage installation of the benzyl group.



Scheme 120. Honda's total synthesis of TAN1251D and TAN1251C.

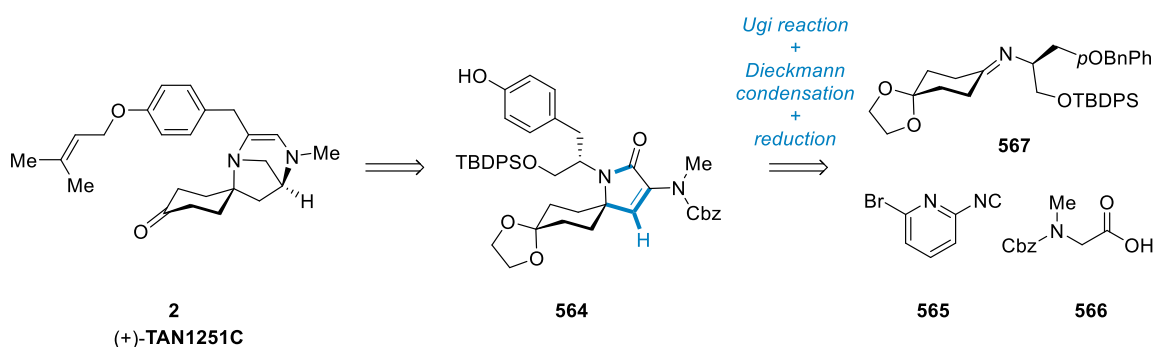
The synthesis began from the diamine **560**, which was readily accessible from *O*-para-methoxybenzyl (PMB) protected carbamate **557** (Scheme 120). Cyclization induced by sodium methoxide delivered the piperazinone, in which the PMB-group was removed by treatment with TFA to afford the key precursor piperazinone **556**. Oxidative spirocyclization proceeded in moderate yield employing conditions from Honda's previous study.^[346] Established copper hydride reduction afforded cyclohexanone **561**. After a sequence of

standard operations, prenyl ether **562** was obtained. Reduction followed by transacetalization in acetone gave the natural product (+)-TAN1251D (**493d**). Alternatively, **562** was subjected to DIBALH reduction to give dienamine **563**, which was readily converted to the natural product TAN1251C (**2**) via transacetalization.

With the synthesis of TAN1251C (**2**) and TAN1251D (**493d**), the Honda group expanded their methodology employed for the synthesis of TAN1251A. The study underpins the unusual piperazinone oxidative spirocyclization as an effective strategy to access the TAN1251-azabicyclic scaffold. To date, the Honda group is the second laboratory to achieve the total synthesis of TAN1251D, along with Snider.^[340]

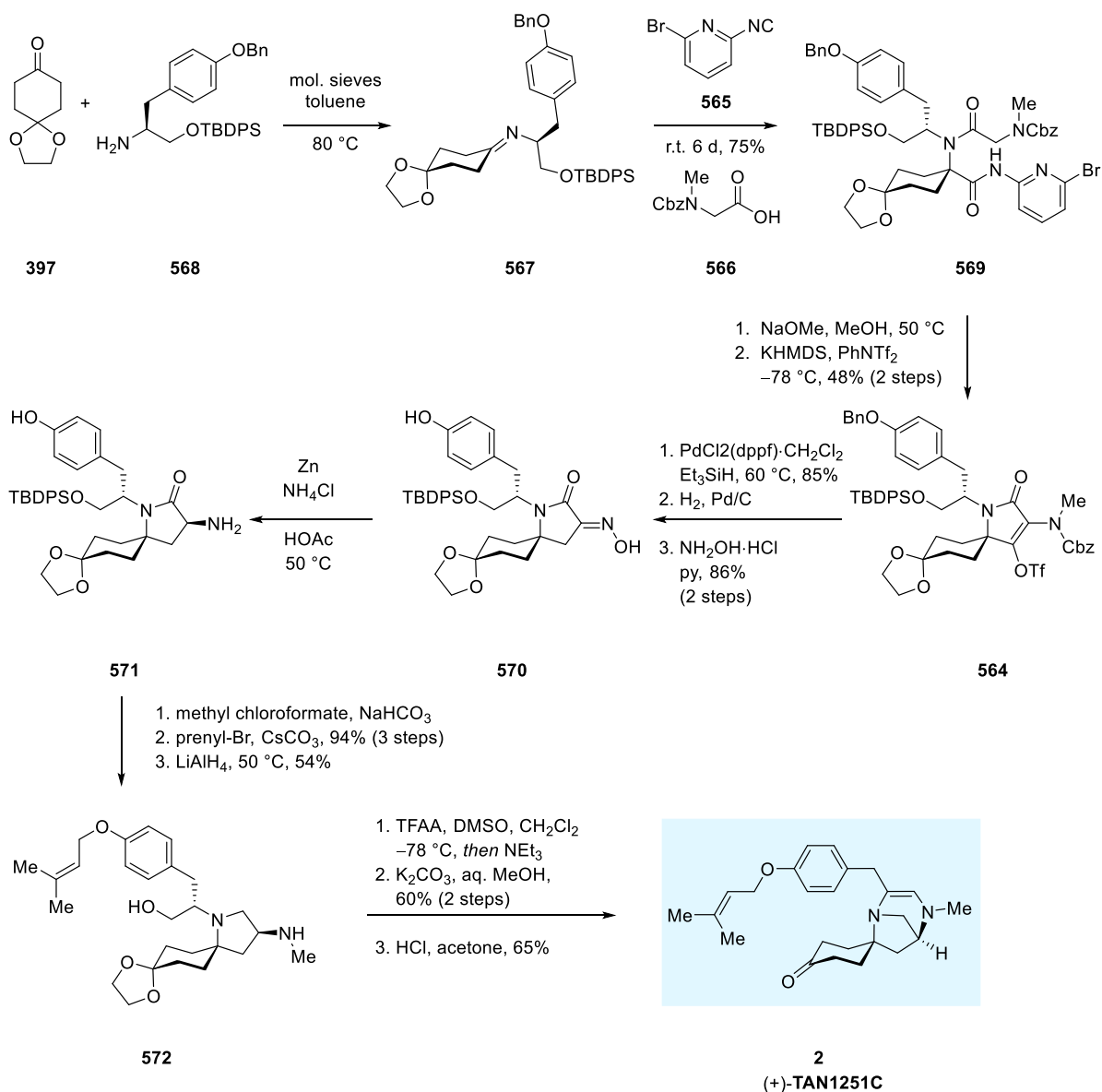
3.1.4.10 Kan's total synthesis of TAN1251C

In a recent contribution by the Kan group in 2017,^[351] a four-component Ugi reaction previously employed by Sorensen^[285] and Fukuyama and Kan^[266] is used to quickly access the TAN1251C core structure via a subsequent Dieckmann condensation / reduction sequence (Scheme 121).



Scheme 121. Kan's synthetic approach to TAN1251C.

The synthesis commenced from imine **567**, which was subjected to the four component Ugi reaction with isonitrile **565** and glycine derived acid **566** (Scheme 122). Ugi-product bromopyridine amide **569** underwent smooth Dieckmann condensation and conversion to the corresponding enol triflate **564**. After defunctionalization of the triflate, hydrogenolysis of the phenolic benzyl ether and the Cbz-group was followed by conversion of the resulting methyl enamine to oxime **570**. Remarkable stereoinduction was observed upon treatment of oxime **570** with zinc and ammonium chloride in acetic acid,^[271-272] delivering primary amine **571** as single diastereomer. Intermediate **572** was obtained after a series of standard operations. The natural product (+)-TAN1251C (**2**) was obtained following Snider's protocol.^[340]



Scheme 122. Kan's synthesis of TAN1251C.

Kan's recent approach offers the possibility of conducting this type of Ugi reaction with the respective glycine derivatives, omitting the late stage installation of the C2 nitrogen, which has the potential to significantly shorten the synthesis of related scaffolds. Unfortunately, challenges in the reduction of the Dieckmann product made a moderately yielding conversion to the enol triflate necessary. Furthermore, planned stereoselective reduction of the conjugated lactam failed due to difficulties in separating the reduction products. This forced the authors to entirely abandon the installed, glycine derived C2 carbamate, and proceed with transformation to oxime **570**, a pathway only made palatable by the subsequent astonishingly stereoselective zinc reduction. Overall, this recent approach constitutes an elegant contribution to access the TAN1251 scaffold via a versatile new multicomponent reaction.

3.2 Summary and Project aims

Despite the wealth of elegant and efficient reports that has been published on both FR901483 (**1**) and the TAN1251 alkaloid series, the construction of their unique azatricyclic molecular architectures remains a formidable challenge. Previous work on the construction of the azabicyclic scaffold of the two natural products (*vide supra*) suggests that two factors are of particular importance for a successful and succinct synthesis: (i) a rapid and efficient pathway to construct the α -tertiary amine spirocenter and (ii) incorporation of the two amino acid derived stereocenters, preferably from precursors from the chiral pool, such as L-tyrosine.

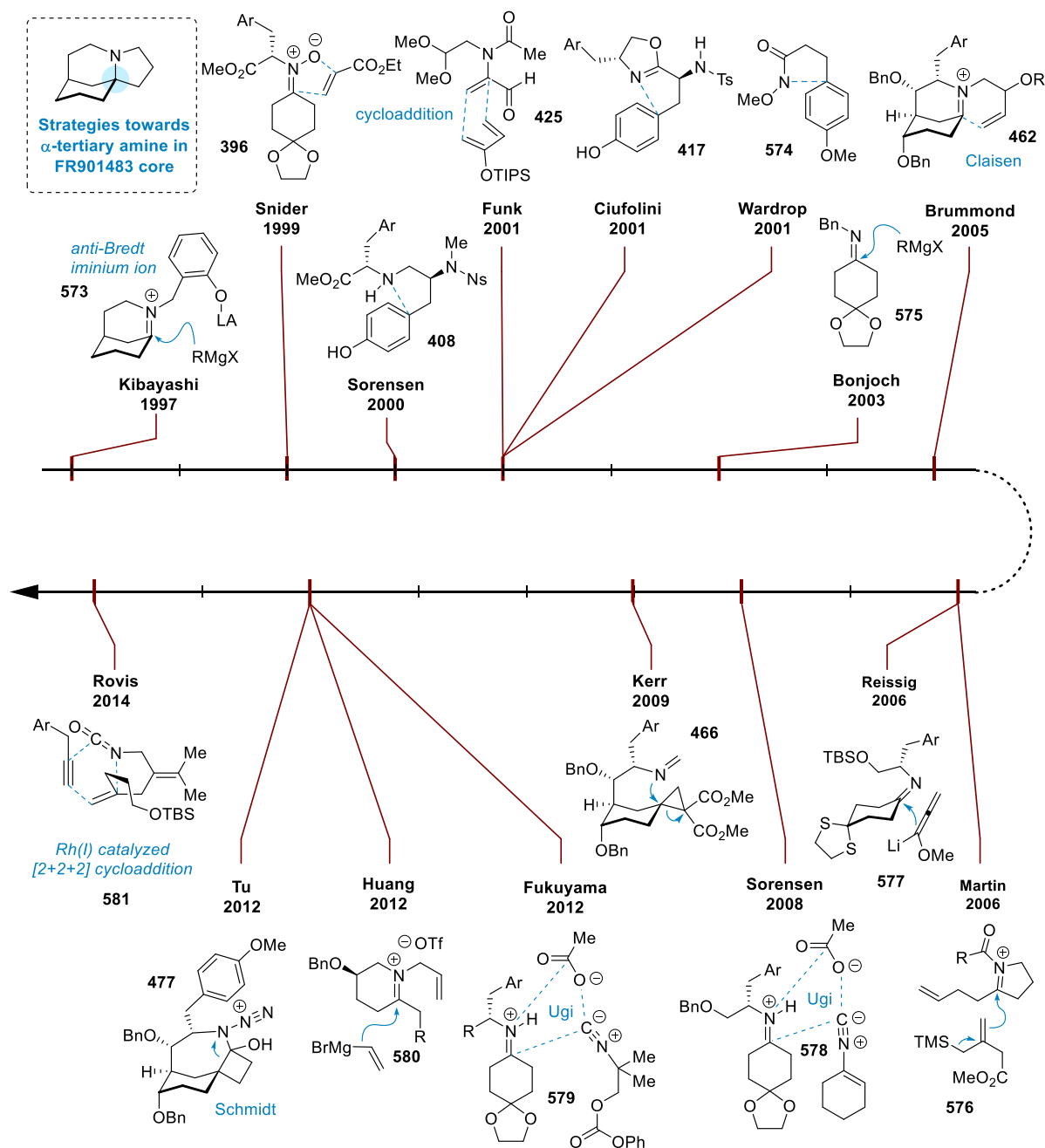


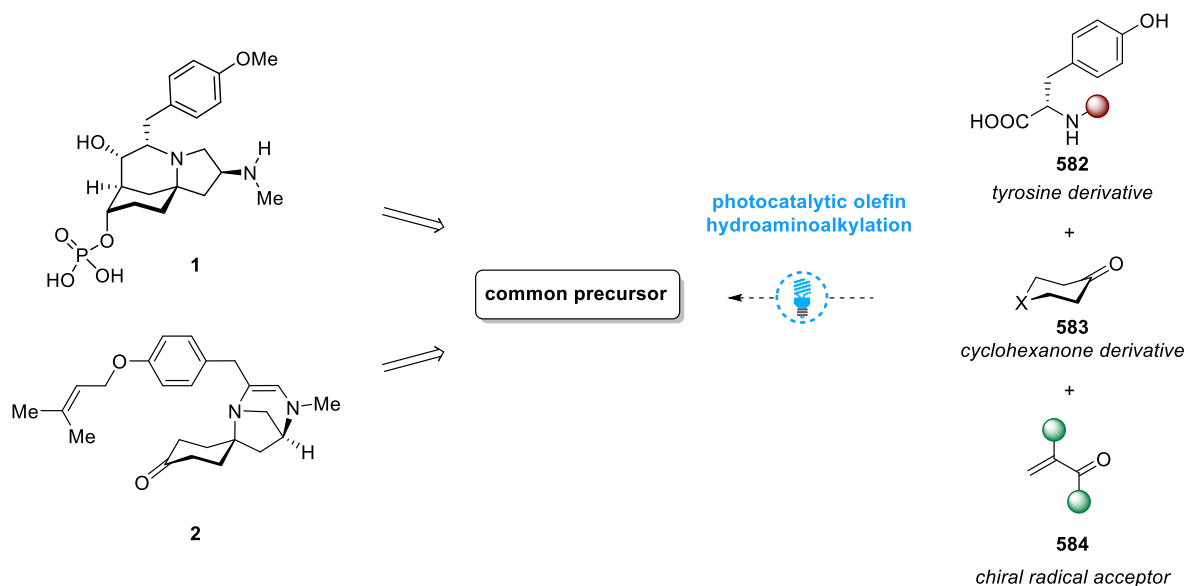
Figure 17. Timeline of synthetic approaches towards the α -tertiary amine spirocenter in the FR901483 core scaffold.

A chronological summary of synthetic methods for the generation of the α -tertiary amine center in FR901483 is shown in Figure 17. Due to the structural similarity between FR901584 and the TAN1251 family, methods in the construction of the spirocyclic α -tertiary amine center in TAN1251 alkaloids are oftentimes derived from approaches towards FR901483, with the oxidative spirocyclization in the case of Snider,^[252, 340] Ciufolini,^[262-263] Wardrop,^[318, 345] and Honda^[362] being the by far most commonly employed method. Kawahara and Nagumo^[343-344, 348] utilized a stereoselective alkylation, while Kan^[351] used a variant of the Ugi reaction from earlier work on FR901483. Notably, a novel approach was pioneered by the Hayes group^[327, 349] with their alkylidene carbene 1,5-C–H insertion followed by ring expansion.

The use of a common precursor between the TAN1251 series and the FR901483 scaffold was only capitalized on by a small number of reports, most efficiently by Ciufolini,^[262] and notably in some regards also by the work of Snider,^[252, 340] as well as Fukuyama and Kan.^[266, 271-272, 283, 351] Indeed, an operationally simple, multicomponent approach to access a common, and possibly advanced, precursor for both syntheses still remained elusive in the literature. Based on this assessment, the goal of this project was set to develop a significantly shorter route to the two alkaloids **1** and **2**, potentially accelerating the development of new therapeutic agents based on their highly bioactive profiles. In line with the previous work,^[249] we recognized the photocatalytic multicomponent olefin-hydroaminoalkylation as a powerful method for construction of α -tertiary amine spirocenters.^[249] It was envisaged to utilize this chemistry to generate the respective spirocenters in the FR901483 and TAN1251 scaffolds in a facile and efficient way.

This multicomponent approach would allow installation of most of the functionality of the natural products in a single step. The only multicomponent strategy towards **1** and **2** to date was reported by Fukuyama and Kan,^[266, 351] which required two different Ugi reactions for the construction of FR901483 and TAN1251C in the respective synthetic studies. While the Ugi reaction is a powerful tool, the required precursors were often not commercial, sometimes difficult to synthesize (*e.g.* 7 steps to synthesize the amine precursor in the Ugi reaction in Fukuyama's second generation synthesis of FR901483),^[266] and would require extensive functional group modifications after the multicomponent reaction, such as hydrolysis, transacetalization and protecting group operations. In contrast, the outlined strategy was designed to be capable of incorporating an easily accessible tyrosine precursor as amine component, a commercially obtainable ketone, and a radical acceptor containing the second

chiral center (Scheme 123). If realized, this idea would allow a more rapid and efficient assembly of the core structure of both natural products in a modular fashion, streamlining the syntheses and decreasing the number of synthetic operations.



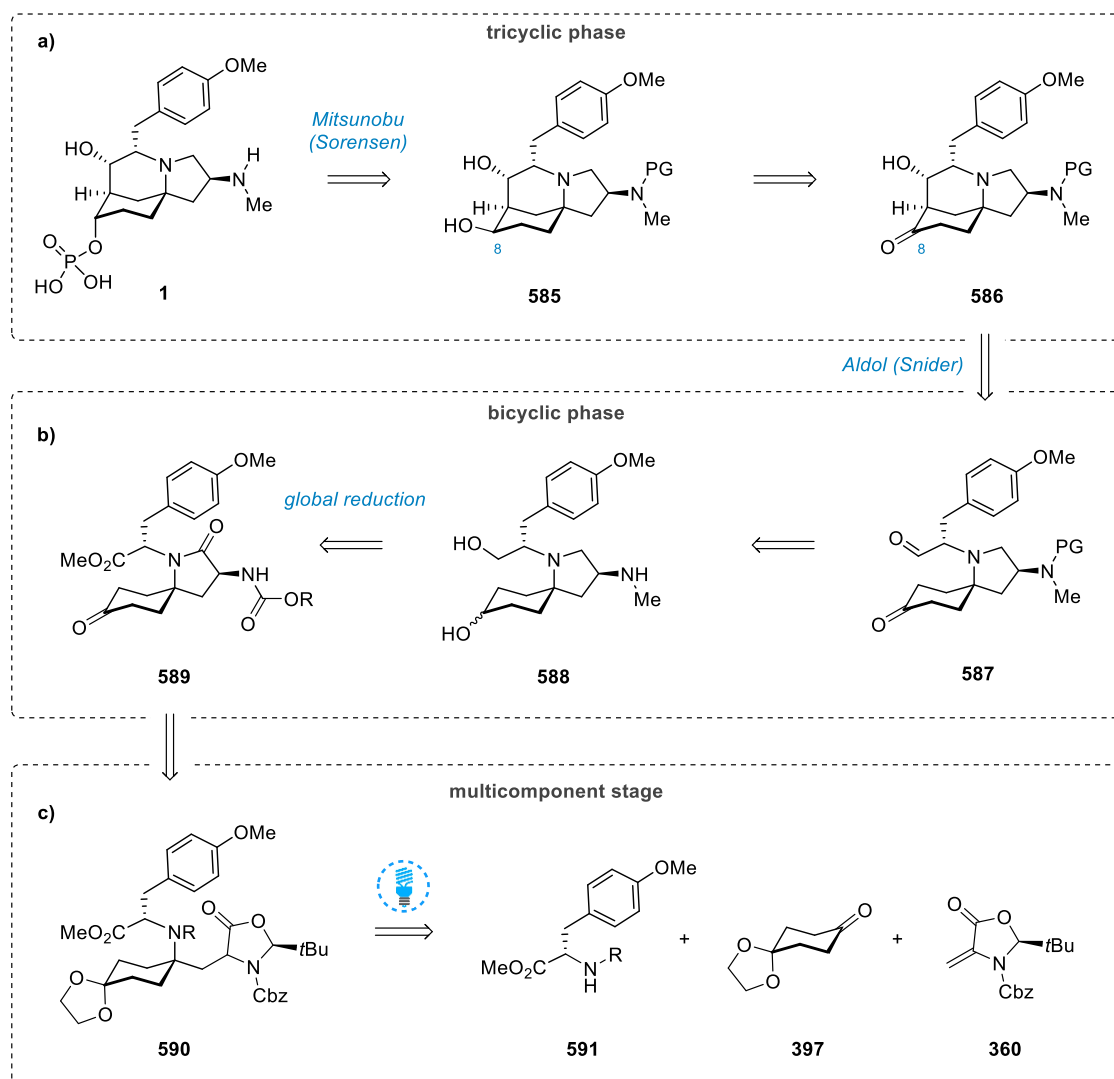
Scheme 123. Project outline for the total synthesis of FR901483 and TAN1251C.

In line with this strategy, a common precursor, from which both the synthesis of FR901483 and TAN1251C could be achieved in an efficient fashion, had to be proposed (Scheme 123). From this common intermediate, it was planned to establish two chemically distinct and efficient routes leading to the respective syntheses of FR901483 (**1**) and TAN1251C (**2**).

3.3 Results and Discussion

3.3.1 Strategy for the total synthesis of (-)-FR901483 and (+)-TAN1251C

A retrosynthetic analysis of FR901483 (**1**) and TAN1251C (**2**) was conducted, focused on utilizing a multicomponent photocatalytic olefin-hydroaminoalkylation approach (Scheme 124).

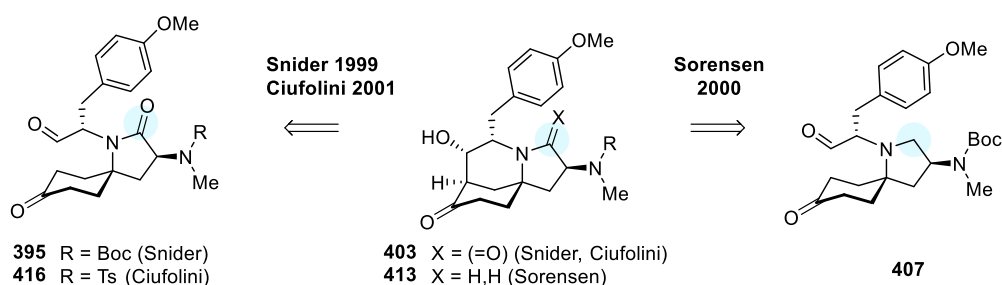


Scheme 124. Initial retrosynthesis analysis of FR901483.

The retrosynthesis of FR901483 (**1**) can be divided into three fundamental stages, the tricyclic phase, in which functionalization of the established core scaffold is achieved, the bicyclic phase, an intermediate phase leading up to the completion of the core fragment, and the multicomponent stage, in which a precursor for the bicyclic phase is assembled. According to the initial strategy, in the tricyclic phase (Scheme 124a), the natural product **1** could be obtained from a secondary alcohol such as **585** via the Mitsunobu reaction developed by

Sorensen^[261] followed by hydrogenation. This pathway was based on the known predicament that reductions of a C8 ketone would strongly favor the equatorial C8 alcohol.^[252, 261-262] We hence chose to access **585** from ketone precursor **586**, completing the tricyclic phase of the retrosynthesis.

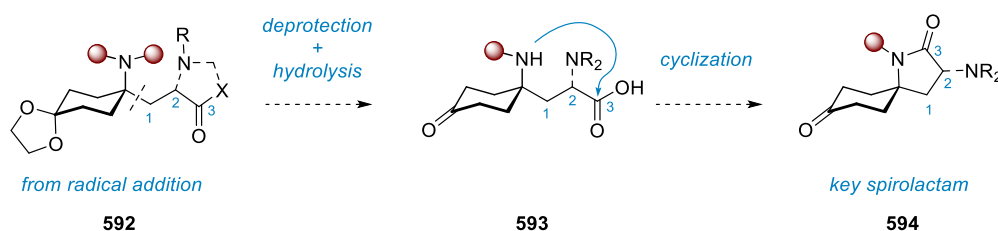
Pioneered by the studies of Snider,^[252, 275] the azatricyclic scaffold is commonly constructed via intramolecular biomimetic aldol reaction. Reported instances of this aldol reaction have shown to be relatively unselective (*vide supra*), and sensitive to small changes in the substrate scaffold.^[334] The groups of Ciufolini^[262] and Sorensen^[261] have also used Snider's approach, albeit modified, and were able to obtain sufficient material from this challenging step to complete the respective total syntheses. In contrast to the work of Snider, in the retrosynthetic plan, it was envisaged to induce aldol reaction from the pyrrolidine tertiary amine, the reduced form of the spirolactam motif. Advantageously, this aspect is well reflected in the literature by the work of the Sorensen group (Scheme 125). Sorensen conducted the aldol reaction with the respective pyrrolidine precursor **407**, bearing a carbamate on the C2 nitrogen, albeit with limited experimental data available. Given this precedent, we were hopeful to obtain **586** in acceptable selectivity from keto aldehyde **587** (Scheme 124b), allowing access to the final tricyclic stage in the outlined synthesis.



Scheme 125. Biomimetic aldol reactions towards FR901483 in the literature.

Leading up to the aldol reaction in the bicyclic phase (Scheme 124b), access to aldol precursor keto aldehyde **587** was proposed via concomitant oxidation of both the secondary C8 alcohol and the primary alcohol on the tyrosine tether. A similar oxidation on the scaffold has been previously reported by Sorensen.^[261] To avoid condensation of the resulting aldehyde with the secondary C2 amine, the amine functionality needed to be protected, precluding oxidative cyclization to the TAN1251 scaffold. The benzyl carbamate was selected as a preferred protecting group, due to its facile removal via a naturally occurring hydrogenolysis step later on in the synthesis. Moreover, it became clear that the protecting group strategy at this step would be the pivotal point of divergence between the FR901483

and TAN1251C syntheses. Diol **588** would then be readily available via global reduction from precursor **589**, which in turn would stem from the photocatalytic multicomponent approach. It was envisaged that in the global reduction step, introduction of the methyl group on the C2 nitrogen could occur via reduction of a carbamate, concomitantly with the generation of the diol from the ester and ketone motifs, and reduction of the lactam to the tertiary amine. Accordingly, key bicyclic spirolactam **589** would be generated from the product of the multicomponent step (**590**) by intramolecular condensation of the amine with the carbonyl group of a suitable radical acceptor (Scheme 126).

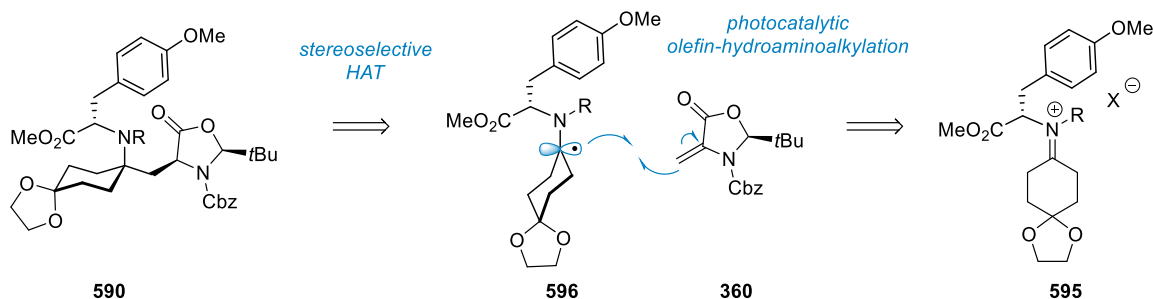


Scheme 126. Design plan for construction of pyrrolidinone ring system.

Therefore, it was envisioned that a product such as **592** from the multicomponent photocatalytic radical reaction had to be deprotected at the nitrogen, as, in the previous studies,^[249] *N*-benzyl groups were required for the reaction to proceed. The free secondary nitrogen in **593** could then cyclize under action of activating reagents^[363] with the available carbonyl (i.e. carboxylic acid) to close the pyrrolidinone ring system in **594**.

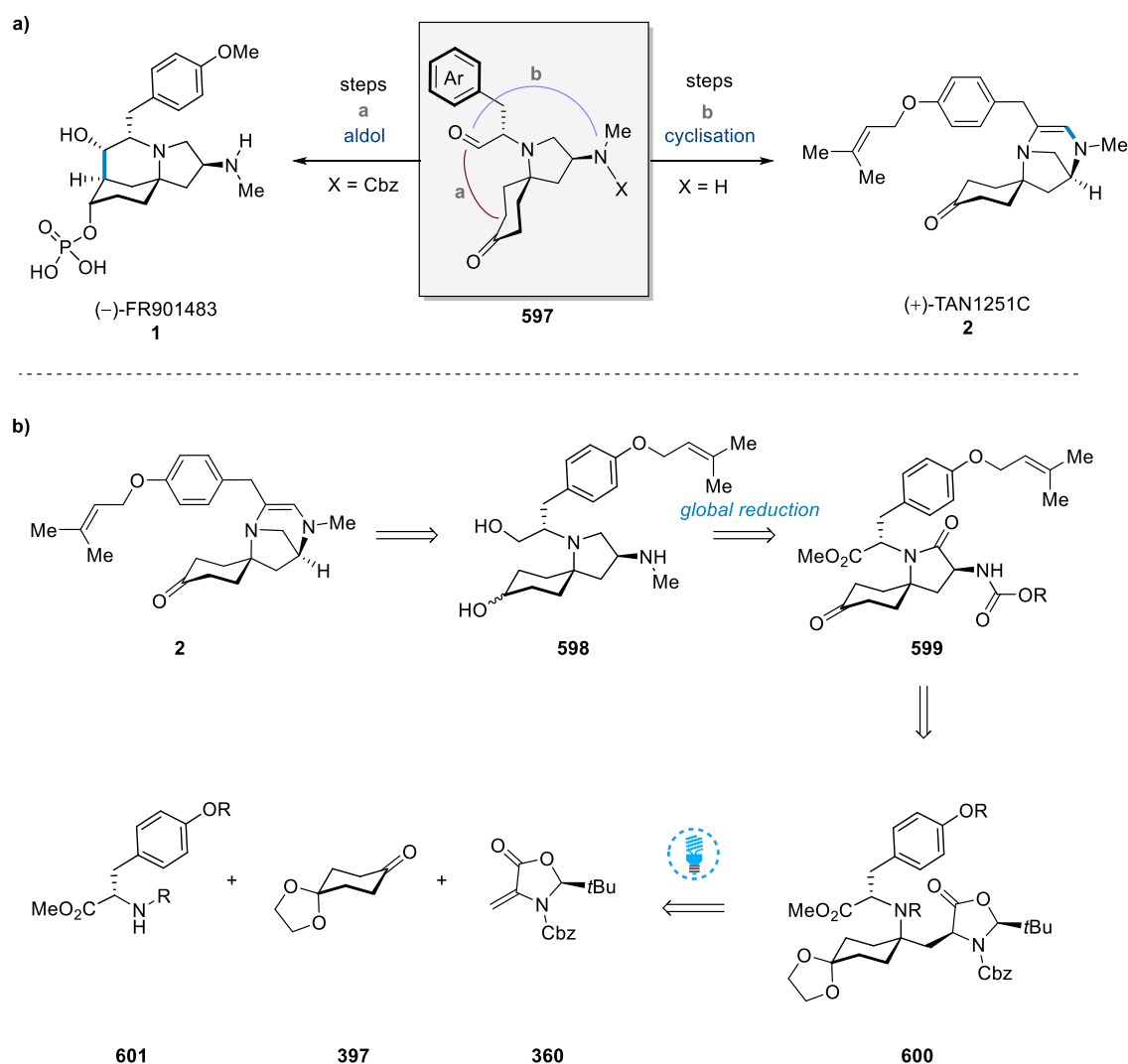
In the multicomponent stage (Scheme 124c) it was proposed to obtain the photocatalytic olefin-hydroaminoalkylation product via the previously established methodology.^[249] A variant of this reported olefin-hydroaminoalkylation reaction enabled the generation of an α -tertiary from a respective enamine. Accordingly, the retrosynthetic strategy proceeded from the respective iminium ion **595** (Scheme 127), which had to be obtained from condensation of a tyrosine derivative with 1,4-cyclohexanedione monoethylene ketal. After the iminium ion **595** has formed either through condensation, or protonation of the respective enamine, single electron transfer would occur to generate the α -amino radical **596**. The use of chiral dehydroalanine **360** as radical acceptor was proposed. The compound, initially introduced by Beckwith,^[224] displays the ideal coupling partner for this multicomponent reaction, providing (i) an intermediate lactone for subsequent functionalization, (ii) a masked methyl group on the nitrogen in the form of a benzyl carbamate, accessible by reduction, and (iii) facile introduction of the stereocenter on C2 through a known stereoselective HAT process. Alkene **360** is readily available in a three step sequence from *S*-benzyl cysteine and can be obtained in

high optical purity and on large scale (*vide infra*). Stereoselective HAT with a stoichiometric reductant, which has been demonstrated to proceed in high diastereoselectivity in the previous methodology, would give access to desired radical addition product **590**.



Scheme 127. Initial plan for the photocatalytic hydroaminoalkylation step.

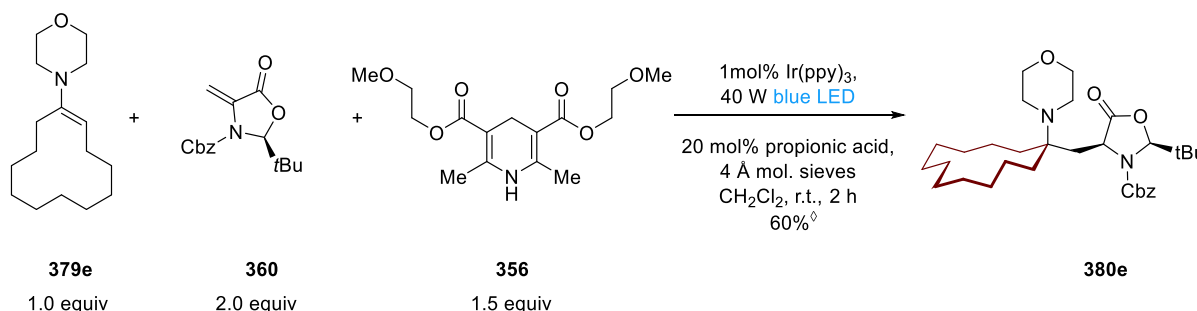
Given the divergent nature of the strategy, diversification of the scaffold accessible via the photocatalytic multicomponent reaction could give facile access to both FR901483 (**1**) and TAN1251C (**2**). It was envisaged that TAN1251C (**2**) could be accessed from a suitable ketoaldehyde **597**, which could undergo either aldol reaction to form the FR901483 (**1**) scaffold or condensation between the aldehyde and the free amine to TAN1251C (**2**) (Scheme 128a).^[252, 260, 262] This strategy would also give formal access to the full TAN1251 series, as TAN1251C (**2**) serves as a synthetic gateway to the three other congeners of the family.^[340] Consequently, the retrosynthesis followed the disconnection of a oxidative cyclization to dienamine TAN1251C from diol **598** (Scheme 128b), which corresponds to the respective diol **588** in the FR901483 synthesis, only differing in the *O*-alkylation on the phenol, as a phenolic prenyl ether is present. It was proposed that diol **598** can in turn be generated via global reduction of spirocyclic lactam **599**, including the introduction of a *N*-methyl group through reduction of the benzyl carbamate. The remainder of the synthetic pathway to obtain **599** would be equivalent to that laid out for the synthesis of FR901483, with a possible divergent introduction of the *O*-prenyl group present at the phenol, and would proceed via a photocatalytic multicomponent reaction to obtain spirocyclic lactam **600**.



Scheme 128. **a.** Divergent strategy to access natural compounds **1** and **2**; **b.** Retrosynthetic analysis for the synthesis of **2**.

3.3.2 Development of the primary amine multicomponent reaction

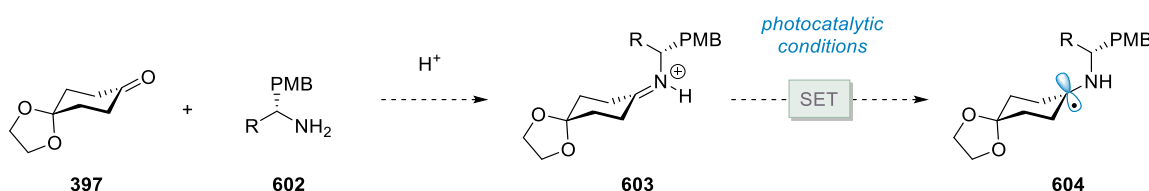
With the synthetic plan in hand, the synthesis of both natural products **1** and **2** commenced with the multicomponent photocatalytic olefin-hydroaminoalkylation method previously developed.^[249] The closest example to the proposed reaction stemmed from the previous studies. Therein, commercial enamine **379e** and chiral dehydroalanine acceptor **360** were reacted with *O*-methoxyethyl Hantzsch Ester **356** as stoichiometric reductant, with catalytic Ir(ppy)₃ (1 mol%), propionic acid (20 mol%) and molecular sieves in dichloromethane under irradiation of blue light for two hours to obtain α -tertiary amine **380e** in 60% yield (see Section 2.3.5, Scheme 75).



Scheme 129. Enamine photocatalytic olefin-hydroaminoalkylation. [◇]Reaction conducted by Dr A. Trowbridge.

Although the reaction stereoselectively incorporated the dehydroalanine fragment, and led to formation of the α -tertiary amine center, several challenges had to be met to render the reaction synthetically valuable in the proposed synthesis. Firstly, the used commercial enamine **379e** was easily accessible from morpholine and cyclododecanone. However, while enamine generation from pyrrolidine, piperidine and morpholine and carbocyclic ketones is facile due to privileged stability, enamine formation can be challenging from less nucleophilic, acyclic amines.^[243-244] This was problematic due to the fact that the enamine had to feature an electron withdrawing, sterically demanding *N*-benzyl tyrosine derivative as the amine component to be a suitable substrate. Furthermore, the carbocyclic ketone component had to be altered to 1,4-cyclohexanedione monoethylene ketal **397**.

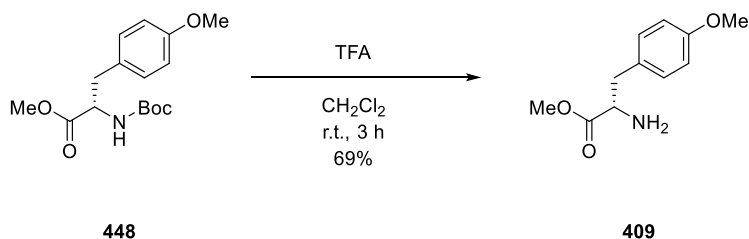
While the generation of enamines from hindered non-cyclic secondary amines and ketones can be very challenging,^[244] imine formation from primary amines and ketones is common place,^[364-365] and this feature is used frequently for their transient formation in organocatalysis.^[366] We thus turned our attention to a possible *in situ* condensation reaction of a primary amine tyrosine derivative **602** with ketone **397** to form the respective imine. This species could potentially undergo protonation to iminium **603** followed by single electron reduction to the α -amino radical **604** (Scheme 130), which could be trapped by a suitable olefin.



Scheme 130. *In situ* imine formation strategy to access α -amino radical **604**.

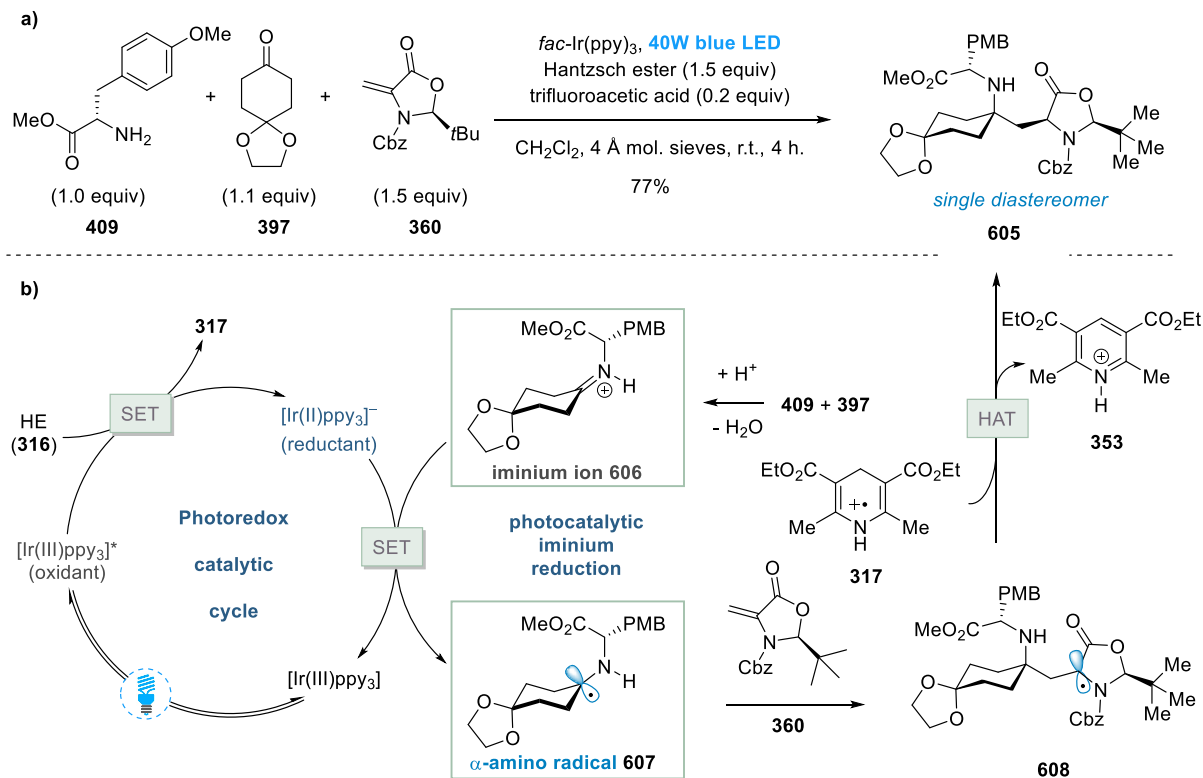
In contrast to the previous methodology, this reaction would require the use of ketones (rather than aldehydes or enamines), and the resulting α -amino radical and thus α -tertiary secondary

amine products could serve as a valuable extension to the existing methodology. To trial the reaction, starting primary amine **409** was synthesized from **448**.



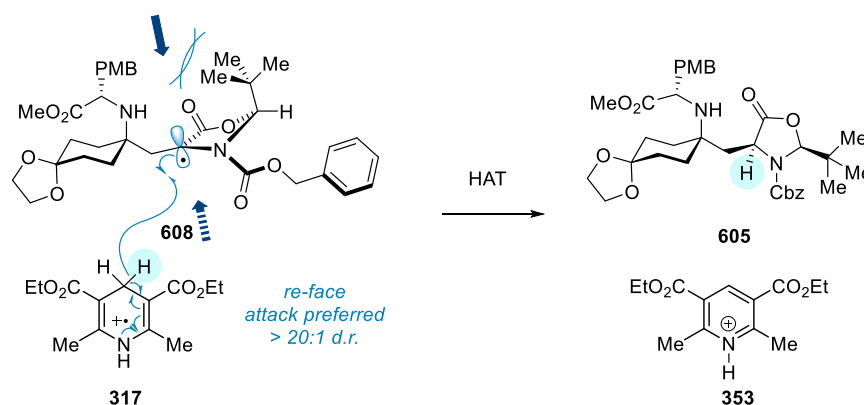
Scheme 131. Synthesis of primary amine **409**.

The initial test reaction used the *O*-methyl tyrosine ester **409**, 1,4-cyclohexanedione monoethylene ketal (1.1 equiv, **397**), chiral dehydroalanine (1.5 equiv, **360**), Hantzsch Ester (1.5 equiv, **316**), and a 1 mol% loading of photocatalyst *fac*-Ir(ppy)₃ under irradiation of a 40W Kessil blue LED lamp. Trifluoroacetic acid (TFA) was chosen as catalytic acid (20 mol%). The reaction was carried out on a 0.1 mmol scale in dry dichloromethane under the addition of activated 4 Å molecular sieves. We were delighted to observe the formation of the desired olefin-hydroaminoalkylation product **605** in 77% isolated yield as a single diastereomer (Scheme 132a).



Scheme 132. a. Initial test reaction for the generation of **605** via photocatalytic olefin-hydroaminoalkylation using primary amine **409**. **b.** Proposed mechanism for the transformation based on prior work^[249] (PMB, *para*-methoxybenzyl).

The proposed mechanism (Scheme 132b) for the transformation is in accordance with the previous findings on the photocatalytic olefin-hydroaminoalkylation, which were confirmed with mechanistic studies. The photocatalytic cycle starts with excitation of *fac*-Ir(ppy)₃, generating the photoexcited [Ir(III)ppy₃]*, a mild oxidant (*Ir(III)/Ir(II), $E_{1/2}^{\text{red}} = +0.31$ V versus SCE in acetonitrile).^[37] Although this species would be reducing enough (Ir(IV)/*Ir(III), $E_{1/2}^{\text{red}} = -1.73$ V versus SCE in acetonitrile)^[37] for SET to occur with protonated imine **606** (which could be as facile as $E_{1/2}^{\text{red}} = -1.14$ V vs SCE)^[182], in line with the previous study, SET with Hantzsch Ester (**316**) was proposed, which efficiently quenches [Ir(III)ppy₃]* and is available in greater relative concentrations than the protonated imine, generating its radical cation **317** and the strongly reducing [Ir(II)ppy][−]. This powerful reductant in turn undergoes SET with protonated imine **606** to generate α -amino radical **607** and the ground-state photocatalyst *fac*-Ir(ppy)₃. Radical **607** is efficiently trapped by radical acceptor dehydroalanine **360** resulting in radical **608**. Importantly, due the strong stabilization of this radical by the neighboring heteroatom and carbonyl, a 1,5-HAT process to preclude polymerization processes is not necessary with this acceptor. Lastly, stereoselective HAT occurs from the sterically more available *re*-face (*si*-face is encumbered by *tert*-butyl substituent, Scheme 133) with a high degree of stereoselectivity (in this case only one diastereomer was obtained, generally the diastereoselectivity of the process is >20:1 d.r.),^[228] affording the α -tertiary amine **605**. The protonated Hantzsch pyridine **353** is the main reaction by-product and serves as proton source required to protonate the imine. Crucially, in a control experiment, it was found that the addition of trifluoroacetic acid (TFA) was instrumental in achieving high conversion to the intermediate secondary amine **605**; presumably, protonation of the imine facilitates SET by lowering the reduction potential or via proton coupled electron transfer (PCET).

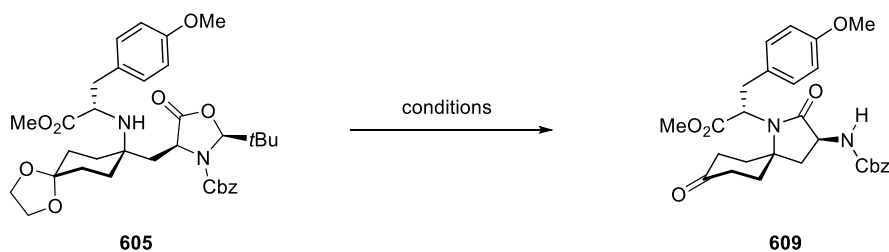


Scheme 133. Diastereoselective HAT between α -carbonyl radical **608** and Hantzsch ester radical cation **317**.

With **605** in hand, the total syntheses of **1** and **2** were deemed achievable, as all of the scaffold atoms of FR901483 (**1**) and TAN1251C (**2**) were already in place after this key step. The direct access to the secondary amine **605** from primary amine **409** also potentially reduced the number of necessary steps of the synthesis, as the expected removal of *i.e.* a *N*-benzyl group was not required. The closure of the spiro-piperidinone ring system would be the first required transformation towards the two natural product scaffolds.

An investigation of the closure of the pyrrolidinone ring was carried out next (see Scheme 126). The initial plan foresaw cleavage of the 5-oxazolidinone and concomitant removal of an *N*-benzyl group, for example through hydrogenolysis of the Cbz group reported by Beckwith.^[224] Through direct access to secondary amine **605**, the possibility emerged to conserve the *N*-Cbz group for later transformation into the native *N*-Me substitution of the natural product via reduction. This ‘masked methyl’ approach was desirable as it would further reduce the step count of the proposed synthesis, but it required direct pyrrolidinone ring closure through attack of the secondary nitrogen in **605** onto the 5-oxazolidinone carbonyl, forming spiro lactam **609**. Accordingly, cyclization conditions were screened to achieve this, on this scaffold, unprecedented transformation.

Table 7. Exploration of different conditions for the cyclization of **605**. ^aisolated yield.

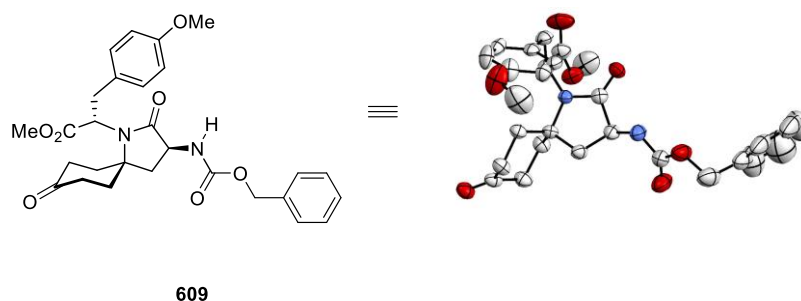


Entry	Conditions	reaction time	yield 609 ^a	note
1	80 °C, toluene	1 h	-	<i>no reaction</i>
2	80 °C, toluene	2 h	-	<i>no reaction</i>
3	80 °C, toluene, NEt ₃	2 h	-	<i>no reaction</i>
4	excess LiAlH ₄ , 0 °C	16 h	-	<i>complex mixture</i>
5	amberlyst-15, CHCl ₃ , r.t.	15 h	observed	<i>slow conversion</i>
6	PPTS, wet acetone, 60 °C	1 h	-	<i>selective ketal cleavage</i>
7	1 M aq. HCl in THF, r.t.	4 d	63 %	-

Given the presence of trace amounts of spiro lactam ester **609** during the isolation of 5-oxazolidinone **605** from the crude multicomponent reaction mixture, it was surprising that heating of **605** in toluene did not result in cyclization, and instead no reaction was observed (Table 7, entries 1,2). Addition of triethylamine led to no improvement. Next, treatment with

lithium aluminium hydride to cleave the oxazolidinone or increase the nucleophilicity of the secondary nitrogen resulted in a complex mixture. Pleasingly, acidic conditions were more favorable, and product (**609**) formation was observed when **605** was reacted with amberlyst-15 resin in chloroform at room temperature for 15 h (Table 7, entry 5).^[367] However reaction performance was sluggish, and a mixture of products was observed, mainly stemming from the incomplete hydrolysis of the dioxolane. Furthermore, in line with one literature report of a 8 day reaction time,^[367] conversion only reached an estimated 25% after 15 hours (LC-MS). Interestingly, it was observed that PPTS in wet acetone at 60 °C selectively deprotected the ketal when reaction times are kept relatively short (1 hour).^[368] Finally, it was found that classic conditions for removal of the dioxolane-ketal,^[369] treatment with aq. 1 M HCl in THF (15:85), gave the best results. Full conversion to the cyclized product **609** (including ketal deprotection) was observed after 4 days at room temperature. After purification, an isolated yield of 63% of spirolactam **609** was obtained. Despite the long reaction time, the mild conditions allowed cyclization, concomitant removal of the dioxolane, and conservation of the Cbz-group, delivering the chiral azaspiro-scaffold of **609** in a facile manner.

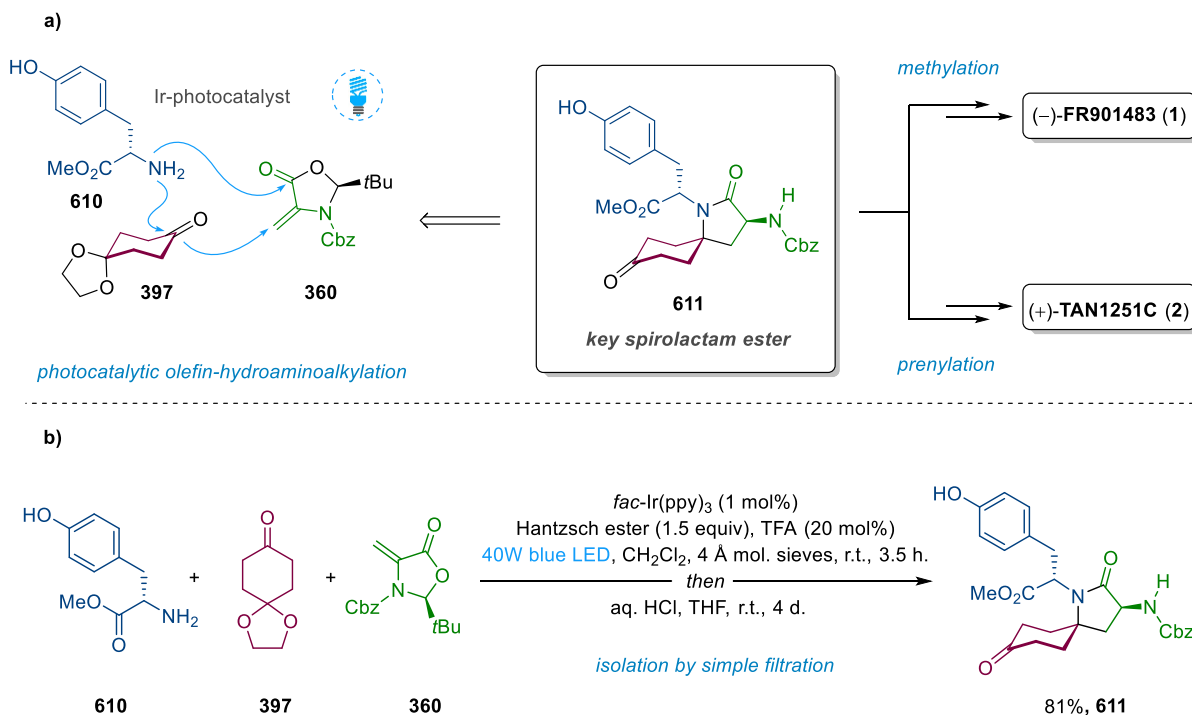
With spirolactam **609** in hand, the relative stereoconfiguration of the two chiral centers was confirmed via X-ray crystallography (performed by A. Bond). Pleasingly, the data obtained showed the correct stereoconfiguration of both centers in regard to the natural product, and furthermore established the compound as a single enantiomer. While the absolute stereochemistry could not be determined with statistical certainty from the data, all evidence obtained from the X-ray crystallographic analysis indicated the proposed absolute stereoconfiguration was correct. Given that the synthesis started from L-tyrosine, the relative and absolute stereoconfiguration of the obtained scaffold was considered to be established with high confidence.



Scheme 134. Crystal structure of **609**.

It was reasoned that the efficiency of the reaction could be increased if the reaction was run from commercial starting materials, (except for necessary alkene **360**), with L-tyrosine methyl ester **610** as a suitable starting point. Furthermore, this would implement the desired divergent

synthesis strategy for FR901483 (**1**) and TAN1251C (**2**), by providing a common synthetic precursor in form of the resulting spirolactam ester **611**, featuring a free phenol motif, from which rapid synthesis of both **1** and **2** could be achieved. *O*-Alkylation of the phenol with either methyl or prenyl would constitute the next step from the common spirolactam ester **611** (Scheme 135a).



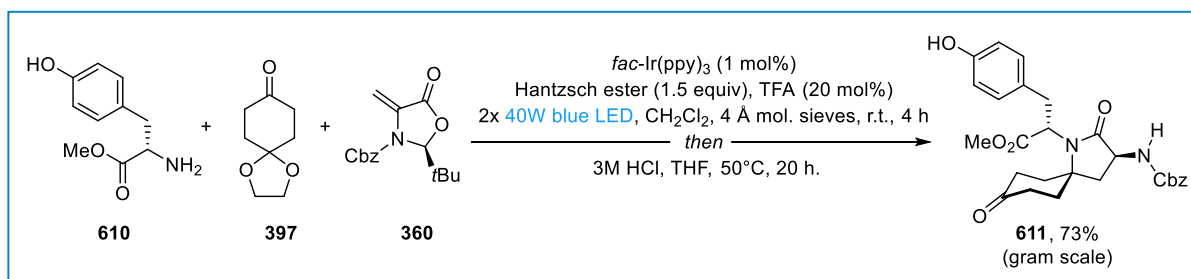
Scheme 135. a. Divergent strategy from commercially available L-tyrosine methyl ester (**610**) followed by alkylation of the phenol, which displays the point of divergence (OMe → FR901483, O-prenyl → TAN1251C).

b. Initial one-pot synthesis of key spirolactam ester **611**.

It was envisioned that the photocatalytic multicomponent reaction and subsequent cyclization could be streamlined into a one-pot process, by simple filtration and swapping the solvent to a mixture of aqueous HCl and THF. By applying these changes, it was found that commercial L-tyrosine methyl ester (**610**) was indeed a suitable substrate for the reaction, with the unprotected phenol side chain being well tolerated under the reaction conditions. The preliminary one-pot approach involved 3.5 hours of irradiation followed by treatment with a 1:1 mixture of aq. HCl and THF (4 days), and delivered key spirolactam ester **611** in 81% yield (Scheme 135b). Furthermore, it was serendipitously discovered during the workup of the cyclization step, that the spirolactam product **611** is poorly soluble in most organic solvents and precipitates upon basification from the reaction mixture. A purification procedure by simple filtration and washing was thus developed. Using this procedure, pure

(within sensitivity of $^1\text{H-NMR}$) spirolactam ester **611** could be obtained, importantly omitting the need for chromatographic purification.

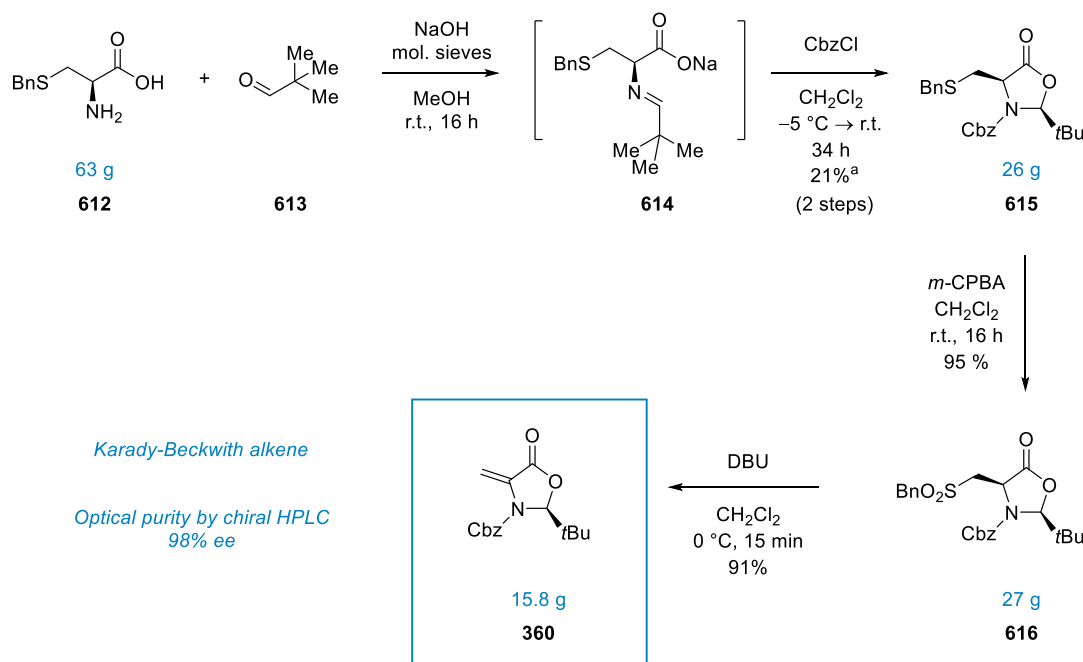
Despite initial success of this approach, the long overall reaction time of the cyclization step was considered unsatisfactory. It was found that by increasing the concentration of HCl and conducting the reaction at a temperature of 50 °C, the reaction time of the cyclization step could be shortened to 20 h. Importantly, the reaction could be successfully conducted on gram-scale, although irradiation with two 40 W Kessil blue LED lamps was found to be necessary. Furthermore, reducing the loading of alkene **360** to 1.3 equivalents (rather than 1.5 equiv) could be achieved without appreciable deterioration in yield. Under these optimized scaled-up conditions (4 mmol), irradiation of the reaction mixture for 4 hours, followed by 20 h stirring in a 1:1 mixture of 3 M HCl and THF afforded the key spirolactam ester **611** in 73% yield on gram-scale. The reaction could be run in parallel (2 x 4 mmol) and combined at the cyclization stage to obtain up to 2.83 g (72%) per batch.



Scheme 136. Optimized one-pot gram-scale synthesis (4 mmol) of key spirolactam ester **611**.

Subsequently, a large-scale synthesis of dehydroalanine radical acceptor **360** was established. With only few methods available in the literature,^[370-371] the approach is based on recent work by Jui.^[228] The synthesis commences from *S*-benzyl-L-cysteine (**612**), providing the stereocenter from the chiral pool (Scheme 137). The optimized sequence began with the deprotonation of 63 g (0.3 mol) of **612**, and subsequent formation of the respective imine with pivaldehyde (**613**), forming the intermediate carboxylate **614**. Intramolecular attack by the carboxylate is induced by addition of benzyl chloroformate, likely resulting in a reactive acyl-iminium species from which cyclization occurs. The reaction temperature has to be carefully controlled to obtain good selectivity for the *syn*-diastereomer **615**. Under the shown conditions the reaction usually exhibited good selectivity (>12:1 d.r.). Although the reaction is reported with slightly higher yields by the Jui group,^[228, 372] the reaction was notoriously low yielding in the synthetic studies, and despite considerable efforts, no significant increase in efficiency could be achieved. Ultimately, sufficient amounts of 5-oxazolidinone **615** could

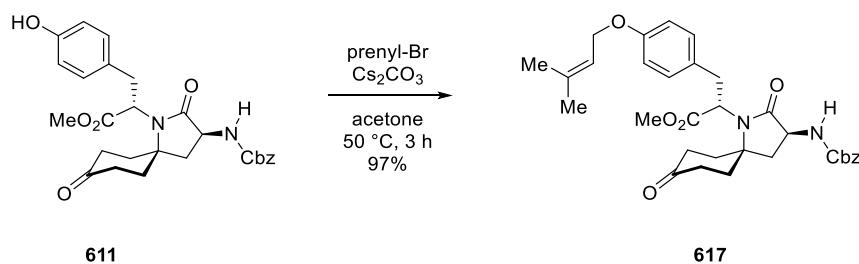
be obtained via this approach. Completion of the synthesis was achieved via oxidation of the thioether to the respective sulfone **616**, followed by elimination under basic conditions, delivering chiral dehydroalanine acceptor **360** in high optical purity (98% ee) on 15 gram-scale.



Scheme 137. Large scale synthesis of dehydroalanine acceptor **360**. a. Large scale reaction carried out together with Dr A. Trowbridge.

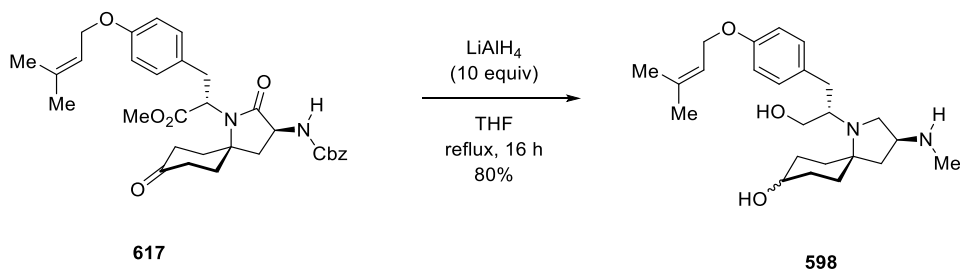
3.3.3 Completion of the total synthesis of (+)-TAN1251C

With key spirolactam ester **611** available, we turned our attention to the total synthesis of (+)-TAN1251C (**2**). Prenylation of the phenol in spirolactam ester **611** was carried out under established conditions^[340] with prenyl bromide and cesium carbonate in acetone at 50 °C (Scheme 138). The reaction proceeded smoothly and afforded phenolic prenyl ether **617** in 97% yield after purification.



Scheme 138. Synthesis of prenyl phenolic ether **617**.

With **617** in hand, the subsequent global reduction step was attempted. Ideally, lithium aluminium hydride reduction would concomitantly reduce (i) the methyl ester to the primary alcohol, (ii) the ketone to the secondary alcohol, (iii) the lactam to the respective tertiary amine, and (iii) the benzyl carbamate to a methyl group. Pleasingly, full conversion was observed after treatment with an excess of lithium aluminium hydride in refluxing THF for 16 hours. The resulting benzyl alcohol side-product had to be removed either during workup, or through column chromatography. Despite the high polarity of the resulting amino diol motif, perhaps surprisingly, chromatographic separation was found to give the best results, affording the product amino diol **598** in 80% yield (Scheme 139). The product was obtained as a single diastereomer within the limits of ^1H -NMR spectroscopy.



Scheme 139. Synthesis of diol **598**.

The geometrical configuration of the nitrogen and oxygen substituents on the cyclohexane ring can be either *O-N-syn* or *O-N-trans*. Unfortunately, it was found that this determination was non-trivial in the present case due the absence of indicating correlations in the ^1H - ^1H -NOESY data. The compound exhibited hygroscopic properties which prevented a crystalline sample to be obtained. Hence, the geometrical configuration, albeit inconsequential for the further synthesis, had to remain unassigned. However, a tentative assignment is possible based on the analogous compound from the FR901483 synthesis, in which NOESY correlation did occur (*vide infra*), suggesting the geometrical configuration is *O-N-trans* (Figure 18).

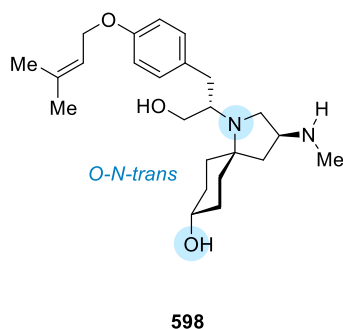
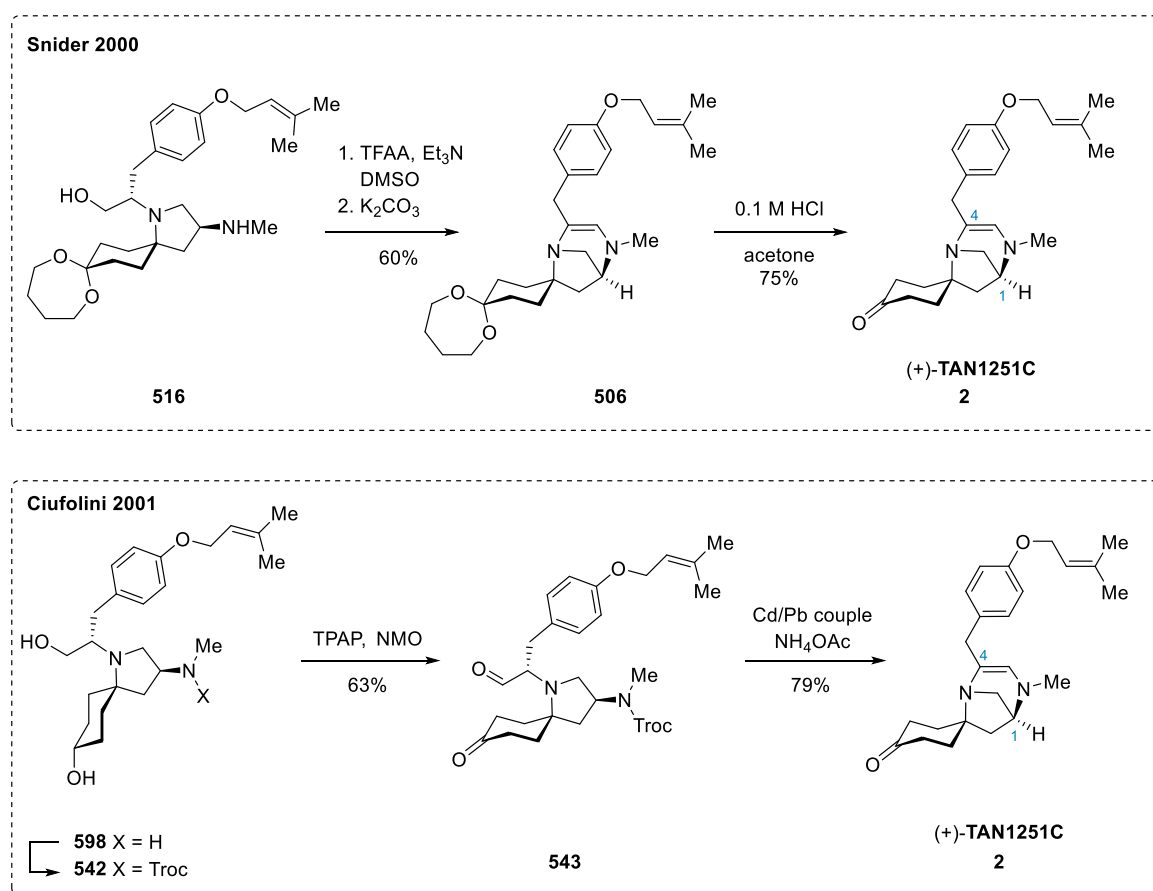


Figure 18. Tentative assignment of the geometrical configuration of **598**.

One step formation of the natural product **2** from obtained diol **598** would be desirable as it provided a synthesis of TAN1251C (**2**) of unprecedented brevity (4 steps from known alkene **360**). It was reasoned that this task should be achievable via concurrent oxidation of the primary and secondary alcohol to their respective carbonyl compounds. This would induce intramolecular cyclization of the formed aldehyde with the C1 nitrogen, followed by dehydration to form the unusual dienamine moiety, and thus the natural product (**2**). Notably, this synthetic step destroys the chiral center at C4. Crucially, the chosen oxidation conditions needed to be compatible with the free methyl amine at C1. Two similar literature examples have been reported by Snider^[340] and Ciufolini,^[262] shown in Scheme 140.

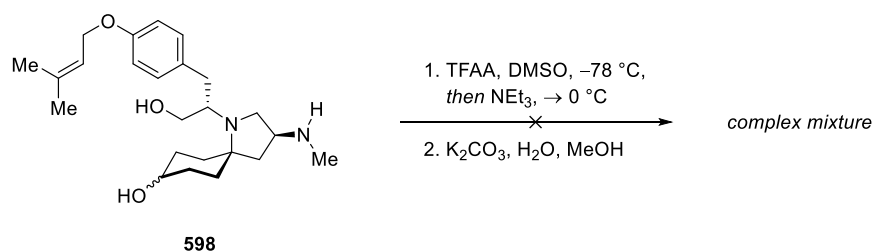


Scheme 140. Snider's and Ciufolini's endgame in their syntheses of TAN1251C.

Snider developed arguably the most important method to date for the oxidative cyclization to the TAN1251 scaffold. By using Omura–Sharma–Swern oxidation of **516**,^[354] the free methyl amine is protected under the reaction conditions by *in situ* formation of the trifluoroacetamide. Methanolic potassium carbonate then liberates the amine, which immediately condenses under basic conditions. Importantly, this oxidation is carried out while the ketone in the molecule is protected as a ketal. Due to the absence of this ketone protection, Ciufolini's attempts of an Omura–Sharma–Swern oxidation of substrate **598** essentially

failed, reporting only a 10% yield of the Snider sequence to the natural product. Ciufolini accordingly suspected that the starting material is diverted to aldol products, and opted for 2,2,2-trichloro-ethoxycarbonyl (Troc) protection and subsequent Ley oxidation.^[262] Deprotection with Cd/Pb then yielded the natural product **2**.

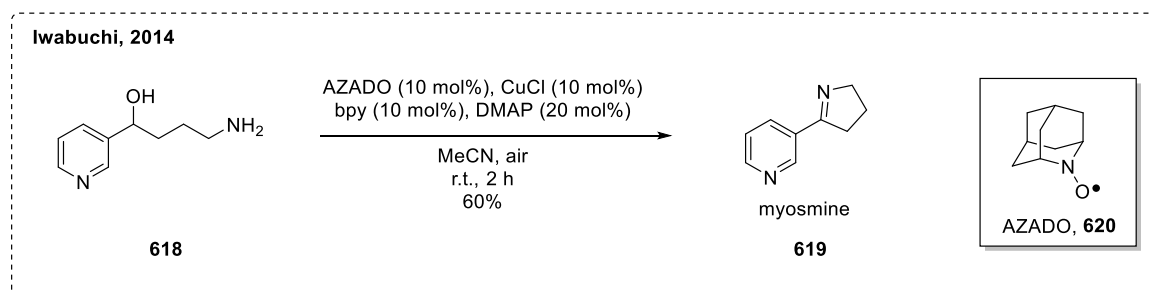
In line with Ciufolini's findings, attempts to use Snider's Omura–Sharma–Swern oxidation were unsuccessful. Treatment with trifluoroacetic acid anhydride (TFAA), DMSO and triethylamine at $-78\text{ }^{\circ}\text{C}$ followed by addition of triethylamine and basic work-up yielded a complex mixture (Scheme 141).



Scheme 141. Attempted Omura–Sharma–Swern oxidation of **598**.

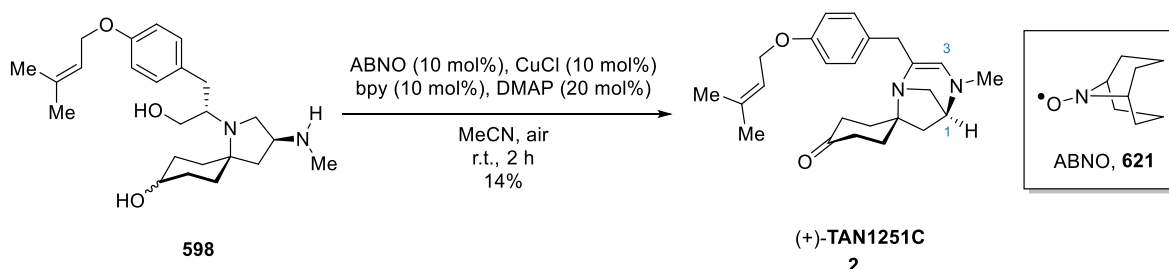
It was reasoned that an alternative 3-step sequence of protection-oxidation-deprotection as pioneered by Ciufolini would be undesirable due to the use of the toxic and potentially carcinogenic Cd/Pb couple in the last step of the synthesis. However, when trialing other standard oxidation methods such as direct oxidation with Dess–Martin–Periodinane or catalytic tetrapropylammonium perruthenate, a large degree of decomposition was obtained, most likely due to the unprotected amine intercepting electrophilic intermediate species.

To this end, a compelling aerobic oxidation developed by Iwabuchi,^[373] based on work by Stahl,^[374] was considered. The method is one of few reported methodologies allowing conversion of primary and secondary alcohols to the respective aldehyde/ketone oxidation state in the presence of unprotected amines. The method using a 2-azaadamantane *N*-oxyl (AZADO, **620**)/copper catalysis platform would be uniquely suited for the proposed one-step oxidation of diol **598** to the natural product **2**. A similar oxidative cyclization was featured in Iwabuchi's seminal work; aminoalcohol **618** was oxidized to imine myosmine (**619**) with AZADO, CuCl, 4,4'-bipyridine (byp) and DMAP in the presence of air at room temperature for 2 hours. Using this procedure, bioactive myosmine **619** was obtained by Iwabuchi in 60% yield (Scheme 142).



Scheme 142. Iwabuchi's aerobic oxidation of amino alcohol **618** to myosmine (**619**).^[373]

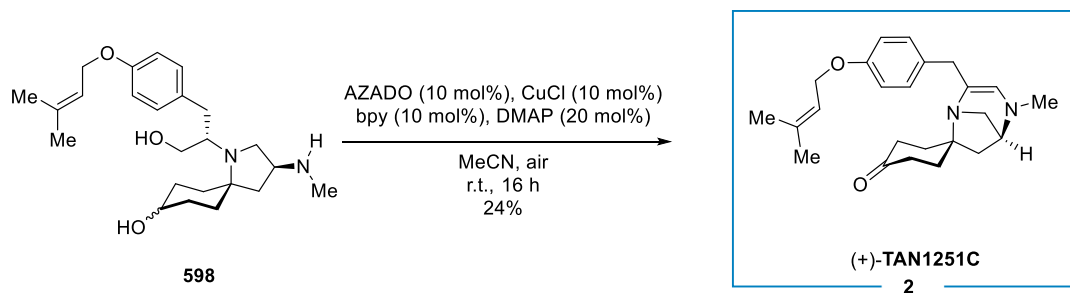
The oxidation of diol **598** was trialed accordingly. In line with seminal work by Stahl,^[374] the investigation started with 9-azabicyclo[3.3.1]nonane *N*-oxyl (ABNO) instead of AZADO. To our delight, the natural product (+)-TAN1251C (**2**) was formed (by LC-MS) after stirring a mixture of diol **598**, ABNO (10 mol%), copper(I) chloride (10 mol%), DMAP (20 mol%) and bpy (10 mol%) for two hours at room temperature under air. Purification proved challenging and isolation via preparative TLC delivered a low yield of 14% natural product (+)-TAN1251C (**2**) (Scheme 143). Despite the low yield, the sample allowed us to confirm the identity of the natural product via NMR, IR and mass spectrometry. The data obtained was identical with those of the natural product. Importantly, the optical rotation exhibited by the fully synthetic natural product sample matched the reported literature,^[339] confirming the correct absolute stereochemistry and enantiopurity.



Scheme 143. Initial ABNO catalyzed Iwabuchi oxidation of diol **598** to (+)-TAN1251C (**2**).

Given the low yield of the transformation, possible causes were investigated. Interestingly, ¹H-NMR of the crude reaction mixture revealed that the enamine product **2** was only present in 4% yield, indicating that the product might only be liberated in the work-up. Importantly, the intermediate aldehyde was not observed. Different work-up conditions were tested and basic aqueous conditions were found to be most suitable. A large degree of highly polar side products was observed, including the incomplete oxidation product, with the secondary alcohol of diol **598** intact.

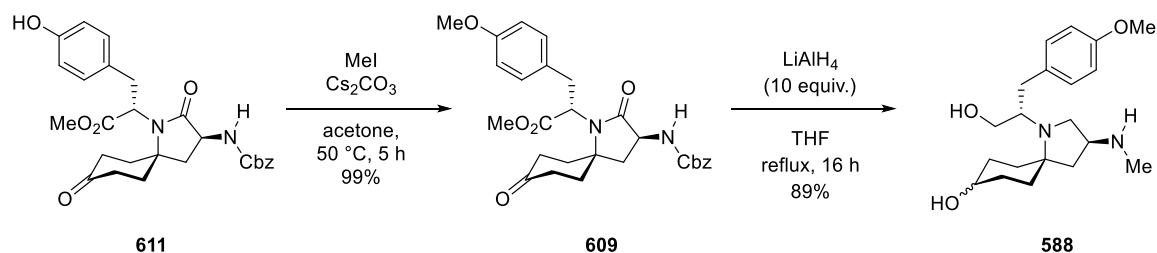
Furthermore, as reported by Hayes and co-workers for (–)-TAN1251A,^[349] purification of TAN1251C by silica-based chromatography seemed to incur significant losses of material. It was speculated that this behavior might be caused by the dienamine, suggesting that a more basic stationary phase would be more desirable. Indeed, better results were obtained with aluminium oxide based purification. Notwithstanding the challenges, having implemented these changes in conjunction with the use of more active AZADO (**620**), and a longer reaction time to decrease incomplete oxidation, the natural product TAN1251C (**2**) was obtained in 24% yield after purification (Scheme 144). Despite its modest yield, the conversion of the *N*-unprotected amino diol **598** to the natural product in a single step is unprecedented, avoids the use of protecting group manipulations in the synthesis, and is operationally simple. Ultimately, the reaction proved to be synthetically valuable, enabling facile access to sufficient amounts of **2**.



Scheme 144. Optimized Iwabuchi's^[373] conditions for the synthesis of (+)-TAN1251C (**2**).

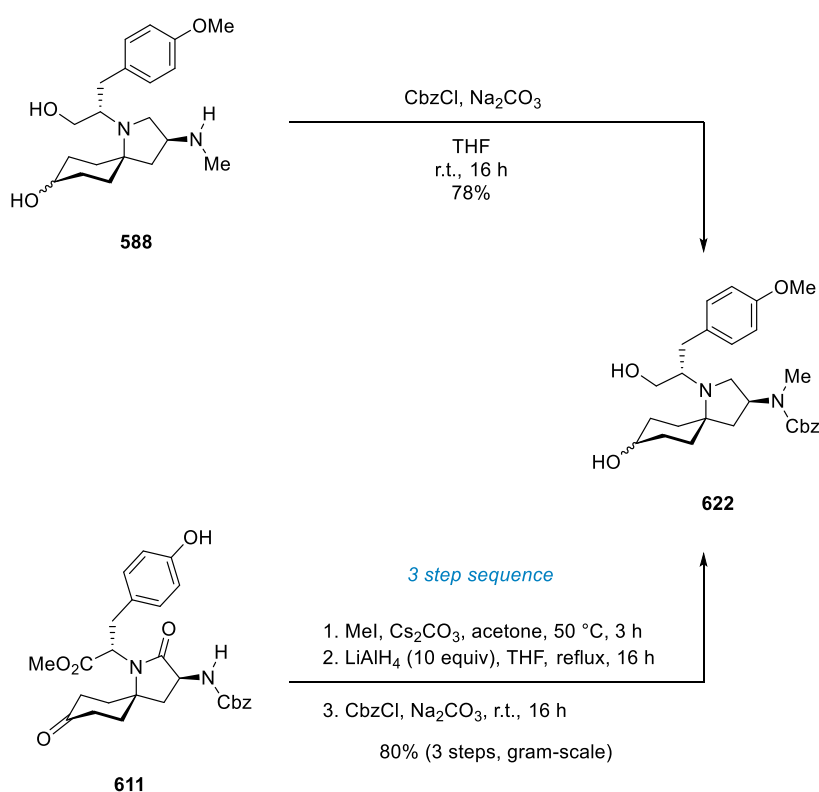
3.3.4 Synthesis of the keto-aldehyde towards FR901483

With the synthesis of TAN1251C (**2**) completed, we turned our attention to the synthesis of FR901483. Given the divergent approach, the synthesis resumed from the common precursor key spirolactam ester **611**. Analogous to the initial prenylation in the synthesis of TAN1251C, methylation is required at the free phenol on the tyrosine side chain. Treatment of spirolactam ester **611** with methyl iodide and cesium carbonate in acetone at 50 °C proceeded smoothly to afford the product phenolic methyl ether **609** in 99% yield. The synthesis proceeded with a global reduction of phenolic methyl ether **609** with lithium aluminium hydride. Concomitant reduction of the ester, ketone, lactam and benzyl carbamate gave amino diol **680**. Despite its high polarity, amino diol **680** could be efficiently separated in good yields from by-product benzyl alcohol via chromatographic purification to afford the product in 89% yield (Scheme 145).



Scheme 145. Synthesis of amino diol **588** towards FR901483.

Although, within the limits of $^1\text{H-NMR}$, a single geometric isomer was obtained, in line with the work on TAN1251C, unambiguous determination of the configuration of the secondary alcohol in **588** could not be achieved. Subsequent protection of the secondary methylamine to the benzyl carbamate **622** was necessary to preclude oxidative condensation towards the TAN1251 scaffold during the oxidation of the primary alcohol. The Cbz group was selected as its deprotection could occur concomitantly with the hydrogenation step later in the synthesis, without the need for a dedicated deprotection step. Accordingly, treatment of amino-diol **588** with benzyl chloroformate in the presence of sodium carbonate^[375] gave smooth conversion to benzyl carbamate **622** (Scheme 146) in 78% yield.



Scheme 146. Synthesis of benzyl carbamate **622** from amino diol **588**, or via 3-step sequence from key spirolactam ester **611**.

In an effort to further streamline the synthesis of benzyl carbamate **622**, a three-step sequence was employed. Methylation of key spirolactam ester **611**, followed by lithium aluminium hydride reduction, and finally Cbz protection of the crude reaction products required only a single chromatographic purification step to afford of benzyl carbamate **622** in 80% yield (3 steps from **611**, Scheme 146). Pleasingly, analysis of benzyl carbamate **622** by 2D-NMR revealed spatial correlation in the ^1H - ^1H -NOESY experiment (Figure 19). The data allowed the tentative relative assignment of the geometric configuration of the heteroatom substituents at the cyclohexane ring fragment as *O,N-trans*.

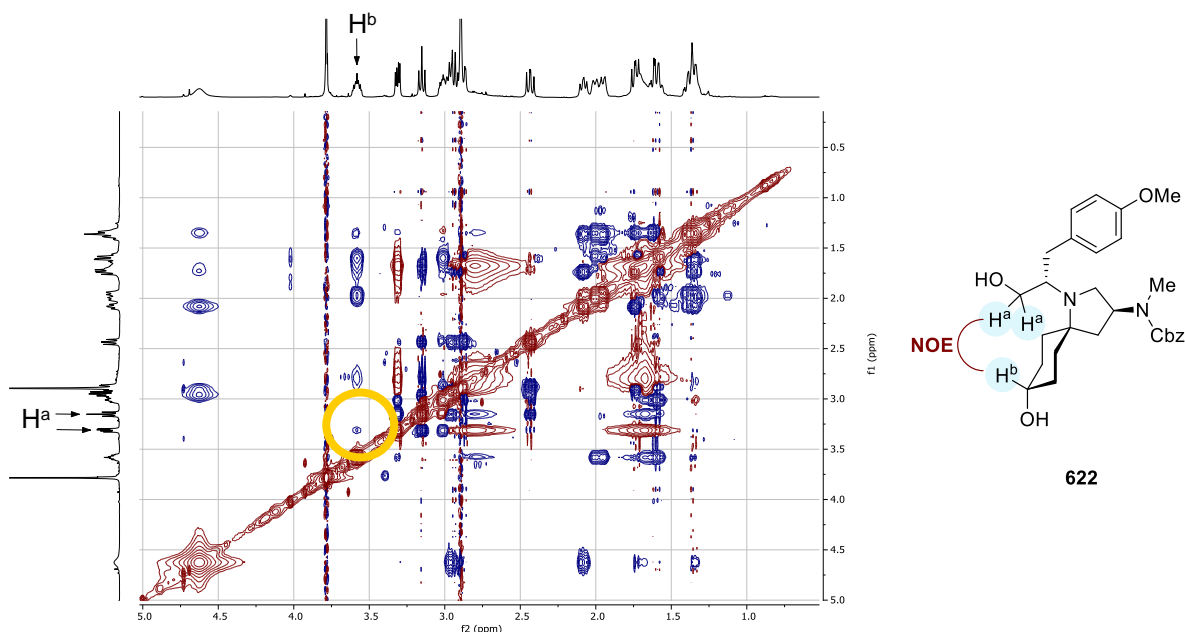
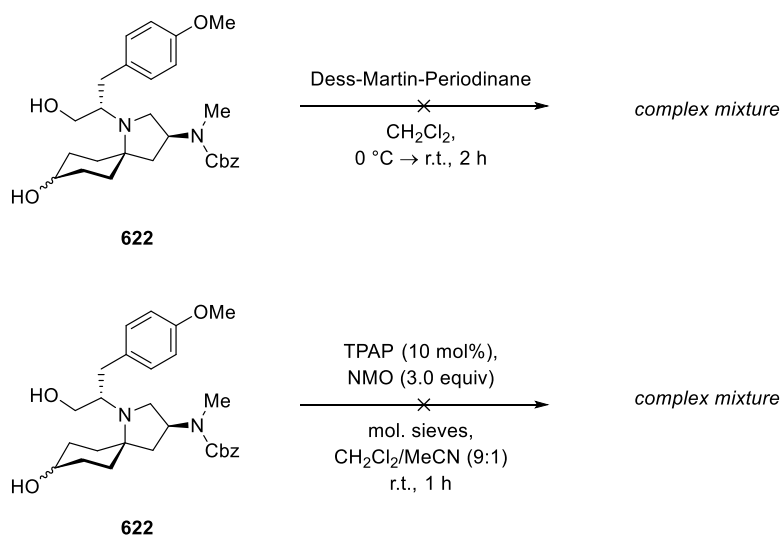


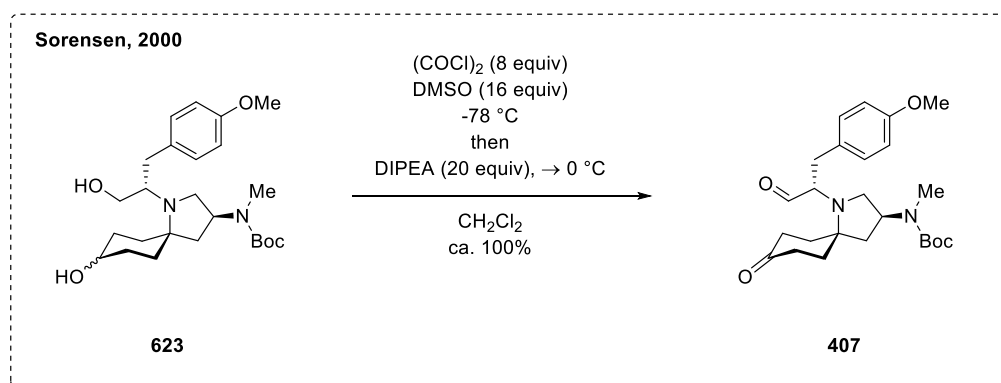
Figure 19. ^1H - ^1H -NOESY correlation in compound **622**, allowing tentative assignment of the geometric isomer of the cyclohexane ring as *O,N-trans*.

Subsequently, the oxidation of the primary and secondary alcohols in benzyl carbamate **622** was investigated. It was surprising to find that this supposedly standard operation proved challenging. Both oxidation with Dess-Martin-Periodinane and Ley oxidation^[376] using freshly prepared^[377] TPAP (10 mol%) and NMO as stoichiometric oxidant resulted in decomposition. While there was a possibility that during these oxidations an aldol reaction would be initiated, *e.g.* though mild Brønsted acid catalysis, aldol products could not be isolated from the complex mixtures.



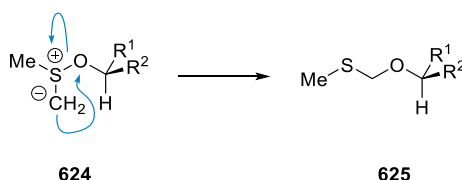
Scheme 147. Failed attempts for the oxidation of benzyl carbamate **622**.

In the search for further oxidation conditions, conditions reported by Sorensen for a similar intermediate in their synthesis of FR901483 were tested.^[261] In this modified Swern-oxidation, an excess of oxalyl chloride and DMSO is used with *N,N*-diisopropylethylamine (DIPEA) as amine base (Scheme 148).



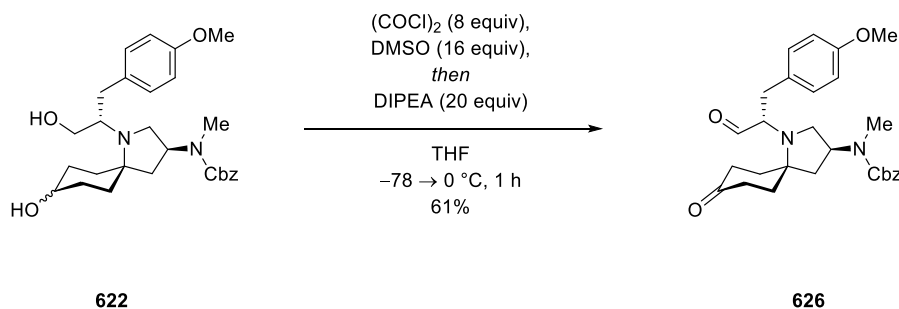
Scheme 148. Sorensen's modified Swern oxidation of diol **623**.^[261]

Starting from benzyl carbamate **622**, the reaction proceeded with a significantly cleaner reaction profile than other tested oxidation conditions, and the formation of keto-aldehyde **626** could be observed by ¹H-NMR from the crude reaction mixtures. However, only moderate yields were obtained, possibly caused by formation of a side-product. The identity of the side product could not be determined with certainty. Initially we suspected the respective methyl thiomethyl ether, a common side product in Swern-type oxidations (Scheme 149).^[378]



Scheme 149. Mechanism for formation of methyl thiomethyl ethers in the Swern reaction.

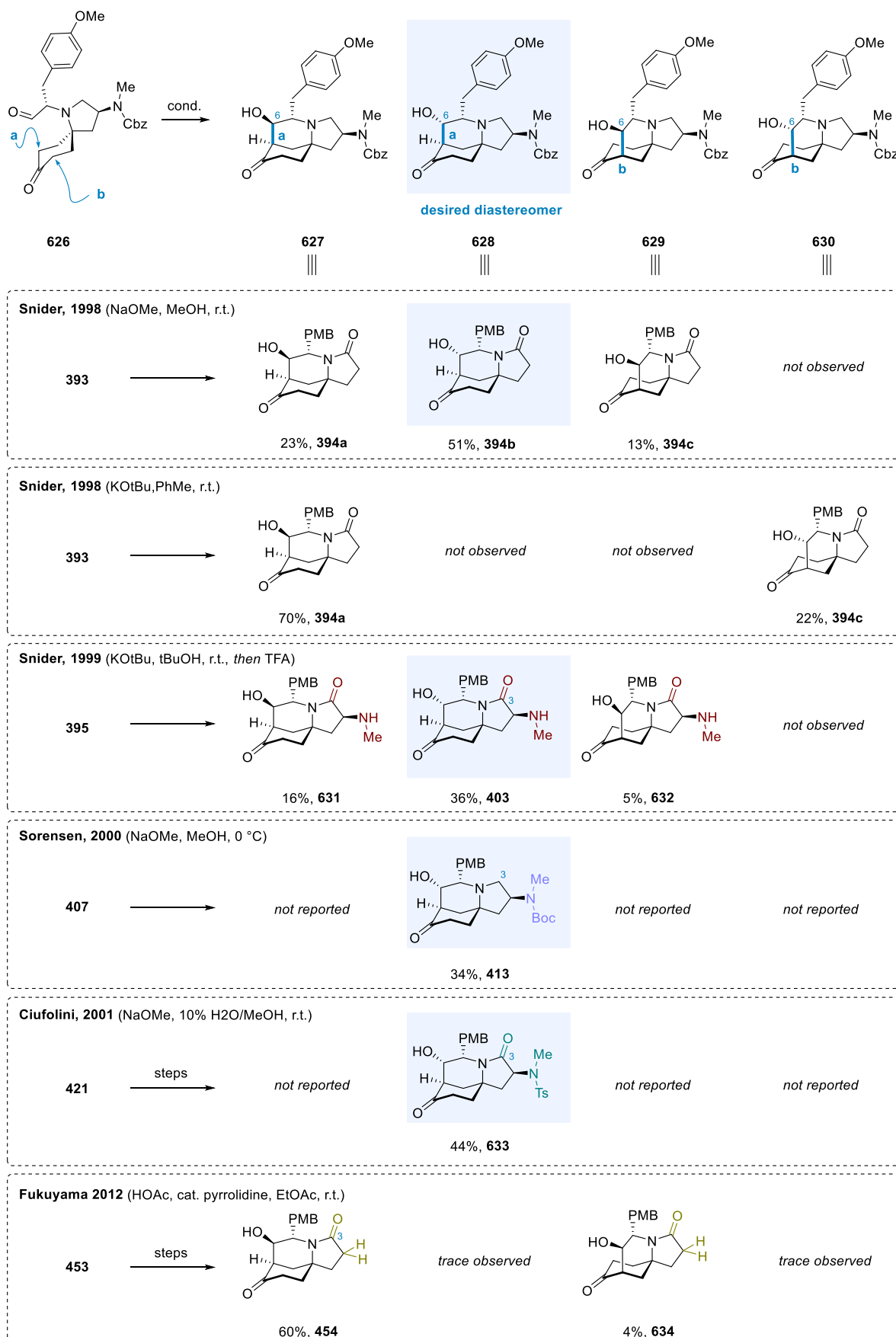
The formation of this type of side product is usually caused by exposure of the Swern intermediate ylide **624** to temperatures significantly greater than $-78\text{ }^{\circ}\text{C}$, leading to cyclization and formation of the respective mixed thioacetal **625**. However, conducting the reaction on small scale with rigorous temperature control did not improve the obtained yield. However, the reaction could be performed on gram-scale in moderate yields with good reproducibility. In line with literature observations of stability of similar chiral aldehydes towards epimerization by Snider,^[252, 275] but also earlier by Garner,^[379] the keto aldehyde **626** exhibited sufficient stability to be purified via column chromatography and stored at low temperature without appreciable decomposition. Under the optimized conditions, Swern-oxidation of diol **622** afforded key intermediate keto-aldehyde **626** in 61% on gram-scale after purification.



Scheme 150. Synthesis of keto aldehyde **626** via modified Swern oxidation.^[261]

3.3.5 Biomimetic aldol-reaction

With keto-aldehyde **626** in hand, the biomimetic aldol reaction pioneered by Snider,^[252] and later used in a modified version by Ciufolini^[262] and Sorensen,^[261] was investigated. Selectivity and separation was anticipated to be problematic from literature reports. Relevant literature reactions and their obtained products with yields are shown in Scheme 151.

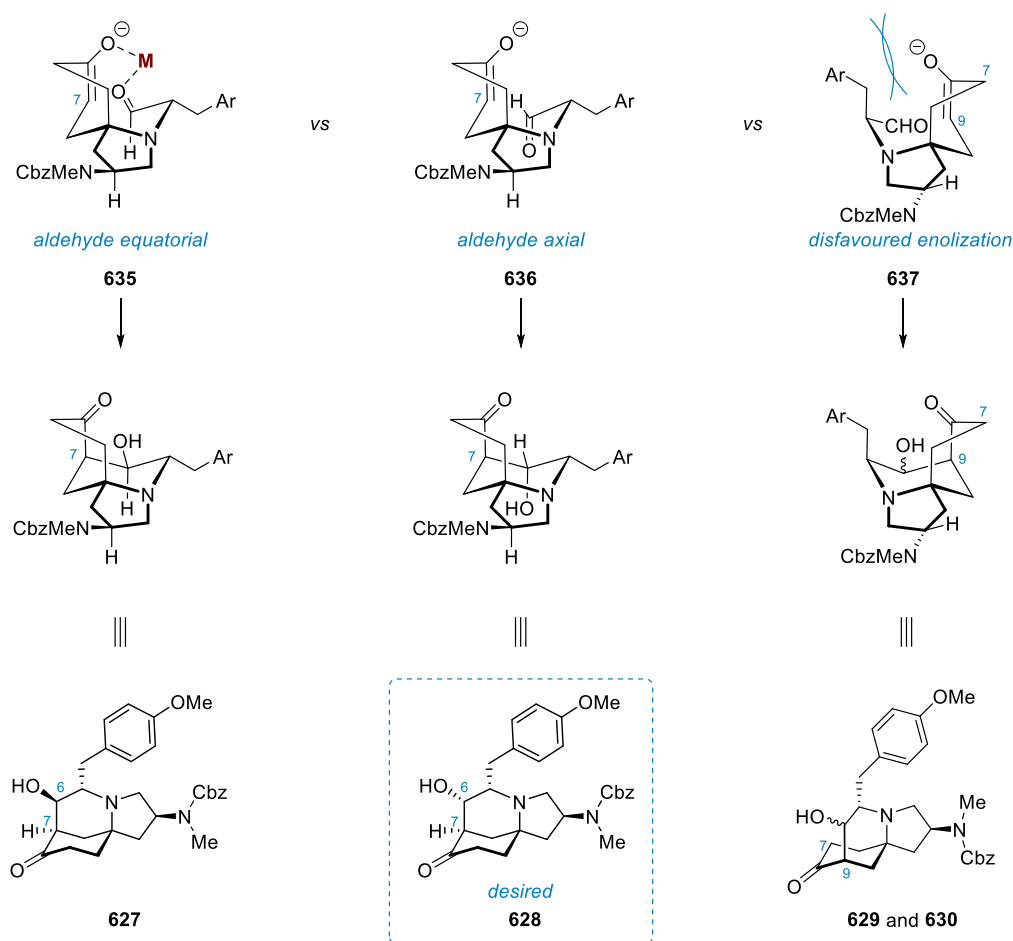


Scheme 151. Possible four diastereomers for the proposed biomimetic aldol reaction with examples of similar aldol reaction from previous literature syntheses, and Snider's studies (PMB, *para*-methoxybenzyl).

As shown in Scheme 151, four different stereochemical outcomes (hydroxy ketones **627**, **628**, **629**, and **630**) are possible for the aldol reaction of keto-aldehyde **626** due to (i) two enolizable carbons at the ketone (*a* and *b*, Scheme 151), and (ii) two possible configurations of the resulting C6 secondary alcohol in the aldol product. It has been shown that inherent selectivity for the desired diastereomer **628**, exhibiting the identical configuration as the natural product, is generally low. Thus, only modest isolated yields are usually obtained for this diastereomer. The highest yield of a ‘desired’ diastereomer obtained as part of a total synthesis is reported by Ciufolini with 44% on a C2 sulfonamide protected lactam substrate (**633**).^[262] Intramolecular asymmetric organocatalytic aldol cyclizations^[380] were investigated by Fukuyama^[266] and Reissig,^[334] but did not lead to improved selectivities. Ultimately, Fukuyama and co-workers employed an acid-catalyzed aldol reaction to promote a different stereo-outcome (60% yield), albeit on a scaffold with less substitution.^[266] This approach however requires subsequent inversion of the resulting C6 alcohol. Additionally to these challenges, small changes in the starting keto-aldehyde have been observed to have significant effects on the stereochemical outcome, such as reported by Reissig,^[334] and Snider.^[275] Although the planned transformation from the synthesized keto-aldehyde **626** was unprecedented, Sorensen’s work is closely similar in having a methylene group in C3 position (rather than a lactam), and featuring a carbamate protecting group (Boc) on the C2 nitrogen. Sorensen reported an isolated yield of 34% of the desired diastereomer **413** with a total yield of aldol products of 74%.

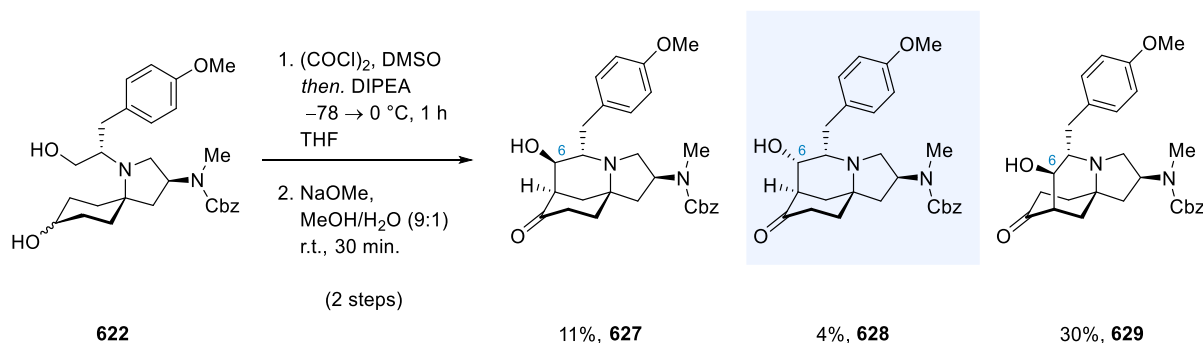
The hypothesis for the transition state model for the transformation is depicted in Scheme 152. Empirically, it is known from Snider’s studies that there is a preference for the desired carbon (C7, *a* in Scheme 151) to undergo enolization,^[275] presumably due to equatorial position of the *para*-methoxy benzyl group (see Scheme 152, **635** and **636** vs **637**). Possible factors for the selectivity of the reaction have also been discussed by Ciufolini and co-workers^[259-260] in order to explain the stereochemistry of the transformation.^[381] In line with literature reports on the mechanistic origin of the diastereoselectivity of the reaction,^[252, 259-260, 266] a 6-membered chair-like transition-state is proposed. Importantly, the *para*-methoxy benzyl group preferably is in the equatorial position, allowing favorable enolization at C7 (Scheme 152, **635** and **636**). Attack of the enolate at the aldehyde closes the central piperidine ring. During the attack, the aldehyde can either reside in equatorial (**635**) or axial (**636**) conformation, determining the configuration of the resulting C6 alcohol in the aldol product, to form either the undesired C6-epimer **627**, or desired product **628**. It has been found that under acidic (HOAc, pyrrolidine),^[261, 266] or apolar basic conditions, such as KO^{*t*}Bu in toluene

(Snider)^[275] or DBU in CH₂Cl₂ (Ciufolini),^[259-260] the C6-epimer **627** is formed with relatively high selectivity. This might result from the energetically more favorable equatorial conformation of the aldehyde, but also from stabilizing metal chelation, as shown in **635**, increasing the stability of this undesirable conformation. At the same time, it has been detailed by Snider, Sorensen, and Ciufolini that formation of the desired diastereoconfiguration, presumably originating from axial aldehyde configuration **636**, is more favorable in highly polar solvents, such as methanol,^[261, 275] aqueous methanol,^[262] and *t*BuOH.^[252] This might be caused by two factors, (i) the increased solvatization of metal ions, reducing their propensity to chelate (and thus makes entering transition state **635** less likely), and (ii) stabilization of the native, non-chelated transition state **636** by the solvent due to interaction with a larger dipole moment solvent-cage.



Scheme 152. Hypothesis for the transition state of biomimetic aldol reaction.

Given the literature precedent, the reaction was first trialed in a polar reaction medium, a mixture of water and methanol (1:9), using sodium methoxide as a base at room temperature (Scheme 153).



Scheme 153. Results from the initial study of intramolecular aldol reaction.

Three diastereomeric products were obtained from the reaction and, pleasingly, isolation via preparative thin layer chromatography (TLC) was feasible for each diastereomer. Structural elucidation was achieved through 2D-NMR studies of each of the products. ^1H - ^1H -NOESY and ^1H - ^1H -ROESY studies were able to give important spatial correlations, on which the final structural assignment could be carried out. Interestingly, ^1H - ^1H -NOESY experiments exhibited relatively low sensitivity for the compound, a known effect for intermediate sized compounds,^[382] and in some instances ^1H - ^1H -ROESY experiments gave better results. The study was aided by structural assignment using standard COSY, HSQC, HMBC, and TOCSY experiments. The results of the 2D-NMR study are summarized in (Figure 20).

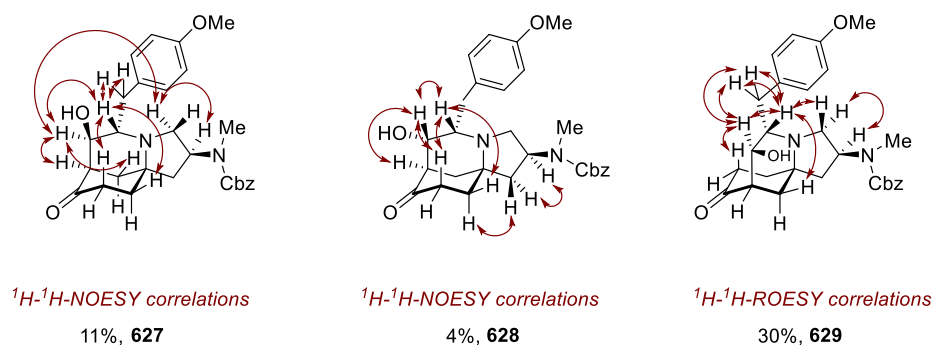
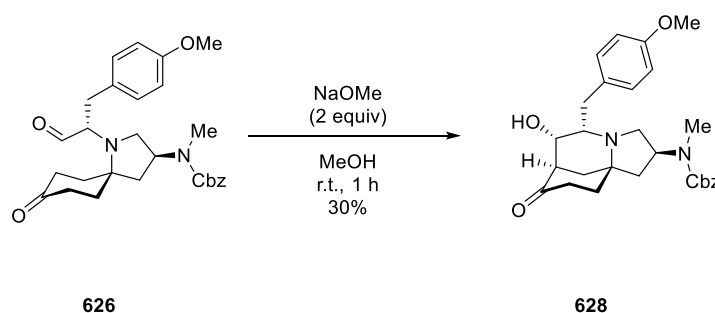


Figure 20. NOESY and ROESY correlations of compounds **627**, **628** and **629**.

Based on these NMR studies, the structures of all three isolated diastereomers, including the desired diastereomer **628** could be confidently assigned. Unexpectedly, and contrary to literature precedent, the yield for the desired diastereomer was modest, with 4% isolated by preparative TLC. Furthermore, the total isolated yield of all aldol products was low with 45%. It was speculated that significant losses of material might have occurred during purification, especially for desired diastereomer **628**, which exhibited the highest polarity of the three compounds. The purification method was subsequently changed to silica flash-column chromatography, which improved the obtained total yield of aldol products to 79% (2 steps

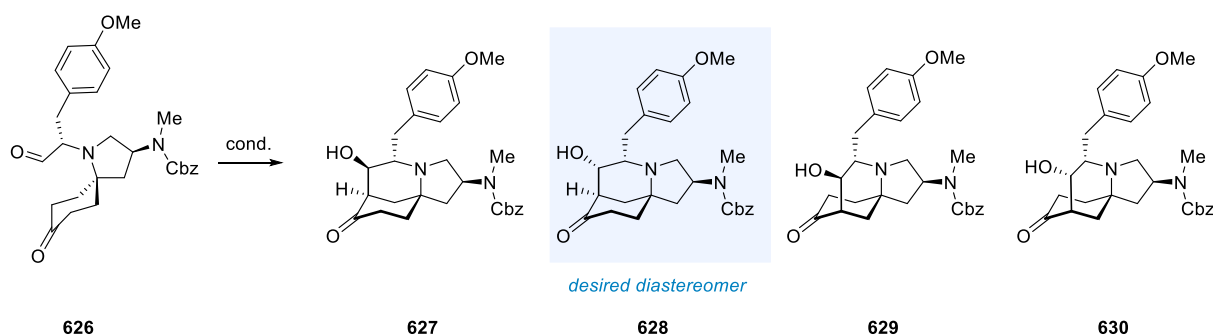
from diol **622**). Encouragingly, this entailed a higher isolated yield of the desired diastereomer **628** of 23%. Unfortunately, a series of inseparable mixed fractions were also obtained using this purification method. It was furthermore determined that the reaction exhibited poor reproducibility if crude starting aldehyde **626** was used. To overcome these problems, the two-step sequence strategy was abandoned, and isolated aldehyde **626**, reasonably stable to purification and storage, was used as starting material for the aldol reaction. Moreover, it was found that the reaction could be carried out with improved reproducibility if the reaction was conducted in anhydrous methanol. After some optimization of the purification procedure, preparative TLC remained the purification method of choice, affording isolated yields of 30% of **628**. In this fashion, significant amounts of desired hydroxy ketone **628** (Scheme 154) were routinely produced using this optimized procedure.



Scheme 154. Optimized conditions for the intramolecular aldol reaction.

With the prospect of uncovering conditions exhibiting superior selectivity, a set of aldol conditions was screened. However, due to the complexity of the product mixture, $^1\text{H-NMR}$ based yield determination could not be employed. Due to high polarity of the hydroxy ketones and the extreme sensitivity of their chromatographic properties towards changes in pH and concentration, no suitable assay could be developed on HPLC and LC-MS instruments. In lieu of a suitable assay, conditions were screened and qualitatively monitored product generation via TLC. The results are summarized in Table 8.

In this study, it was found that the generally favored product, in line with literature findings, was C6 epimer hydroxy ketone **627**. HMPA was employed as solvent (Table 8, entry 2) in order to suppress chelating effects. This indeed changed product distribution but still provided diastereomer **627** as the major component of the product mixture. Analogously, 18-crown-6 was employed with potassium *tert*-butoxide in order to mask the potassium cation (Table 8, entry 4), however with little effect on the product ratio in regards to the same conditions without the crown ether (Table 8, entry 3).

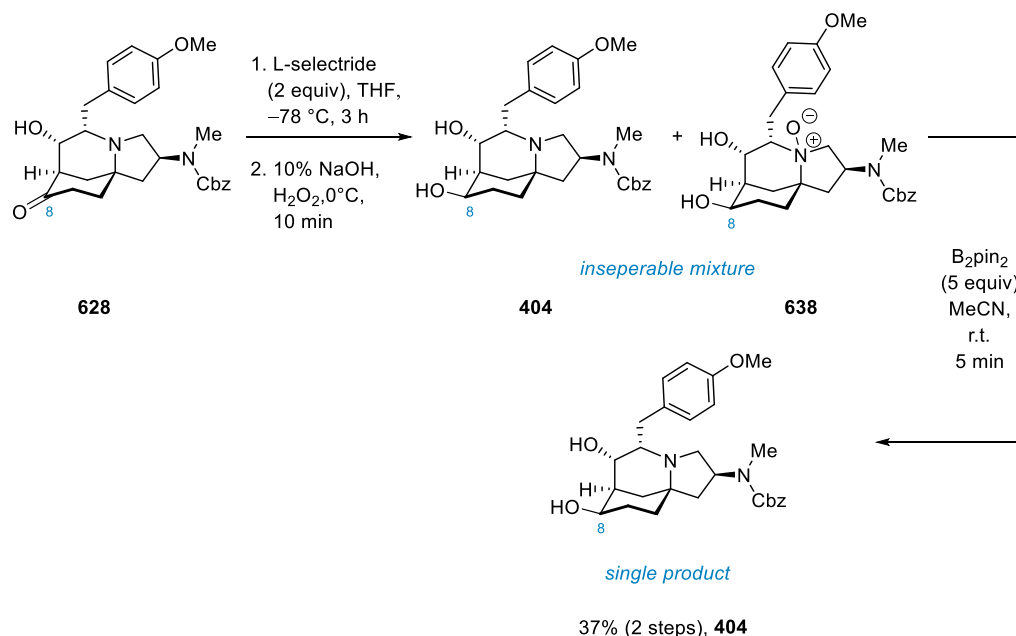
Table 8. Screen of different aldol conditions and the qualitative tentative product ratios (TLC). ^a not determined.

Entry	Conditions	Yield:	627	628	629	630
1	NaOMe (2 eq.), MeOH, r.t., 1 h	- ^a	- ^a	30%	- ^a	- ^a
2	KOtBu (1.2 eq.), HMPA (solvent), r.t., 24 h	major	major	minor	-	-
3	KOtBu (1.2 eq.), THF, r.t., 1 h,	major	major	-	minor	-
4	KOtBu (1.2 eq.), 18-crown-6, THF, r.t., 1 h	major	major	-	minor	-
5	KOtBu (3.0 eq.), HFIP, r.t., 3 h		<i>no reaction</i>			
6	Aq. NaOH (10%), HFIP, r.t., 12 h	major	major	-	-	-
7	DBU (1.2 eq.), DCM, r.t., 1 h	major	major	minor	minor	-
8	KHMDS (1.2 eq.), THF, -78°C, 1.5 h	major	major	-	-	-
9	KHMDS (1.2 eq.), HMPA (6 eq.), THF, -78°C, 1.5 h	major	major	-	-	-
10	DIPEA (1.1 eq.), Bu ₂ BOTf (1.1 eq.), -78°C to 0°C, 2 h		<i>complex mixture</i>			

In Ciufolini's synthesis, fluorinated alcoholic solvents were suggested to increase the propensity of the solvent to hydrogen-bond. However, hexafluoroisopropanol (HFIP) did not give any conversion unless it was thoroughly basified with an excess of aq. sodium hydroxide (Table 8, entry 5+6), potentially due to the acidity of HFIP. Treatment with DBU in dichloromethane confirmed Ciufolini's findings^[259] for the present substrate (Table 8, entry 7). Finally, the reaction was attempted under cryogenic temperatures (Table 8, entry 8-10) with potassium hexamethyldisilazide (KHMDS), but it was found that predominantly C6-epimer **627** was formed, with the addition of HMPA ineffective of altering the diastereomeric ratio. DIPEA and Bu₂BOTf gave decomposition resulting in a complex mixture.

3.3.6 Completion of the total synthesis of FR901483

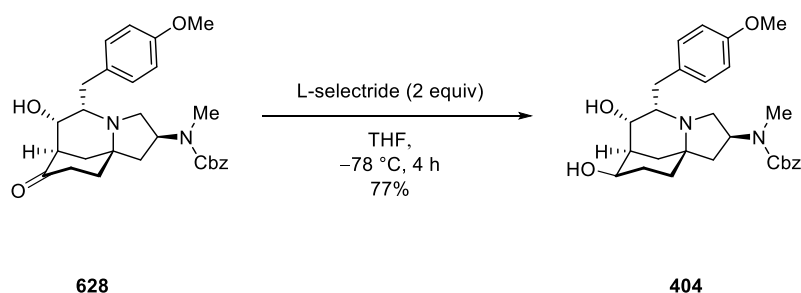
With significant amounts of hydroxy ketone **628** in hand, and the tricyclic scaffold in place, we turned our attention to the completion of the synthesis of the natural product **1**. Reduction of the C8 ketone has previously been reported to favor the equatorial C8 alcohol, opposite to the configuration in the natural product. This preference can be explained by the obstruction of the *re*-face by the concave tricyclic scaffold. Excellent hydrogenative conditions developed by Sorensen are available for the selective transformation to the equatorial alcohol,^[261] but this method could not be applied to hydroxy ketone **628** due to the incompatibility with the Cbz group. Ciufolini reported reduction of the ketone with L-selectride, albeit with acetyl protection employed on the C6 alcohol and on Ciufolini's lactam (rather than tertiary amine) sulfonamide protected scaffold.^[262] Despite the free alcohol and tertiary amine in starting material **628**, direct reduction of keto aldehyde **628** was attempted with 2.5 equivalents of L-selectride, taking into account the necessary deprotonation of the C6 alcohol. After conventional work up with sodium hydroxide and hydrogen peroxide (at 0 °C), an inseparable mixture of products was obtained, which through mass spectrometry were tentatively identified as the desired product **404** and its *N*-oxide **638** (Scheme 155). Despite being sterically highly encumbered, brief exposure to hydrogen peroxide seemed incompatible with the tertiary amine contained in the substrate.



Scheme 155. Initial studies for the L-selectride reduction of **628**.

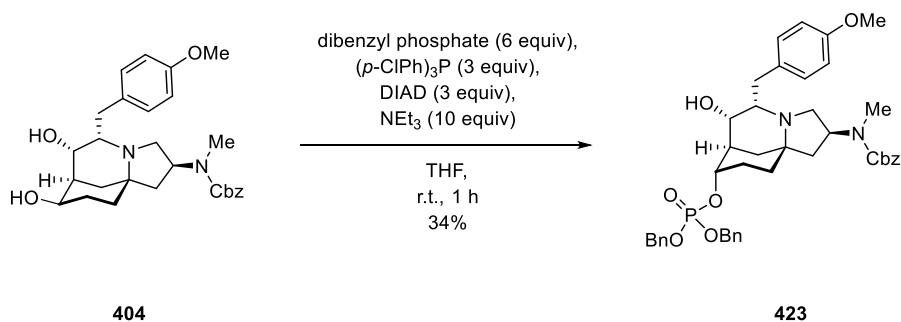
However, to confirm the identity of the product, conversion of the *N*-oxide portion of the mixture to the desired product was attempted via treatment with bis(pinacolato)diboron (B₂pin₂). To our delight, the remarkably efficient procedure by Lakshman^[383] converted the

mixture to single desired product **404** via treatment with an excess of B₂pin₂ in acetonitrile in less than 5 minutes. After purification, a 37% yield of equatorial alcohol **404** was obtained, which after analysis proved to be identical to the reported compound from Huang's work.^[269] Encouraged by these results, the reduction step was optimized by altering the oxidative work-up to treatment with sodium hydroxide, allowing isolation of the desired equatorial alcohol **404** in 77% yield.



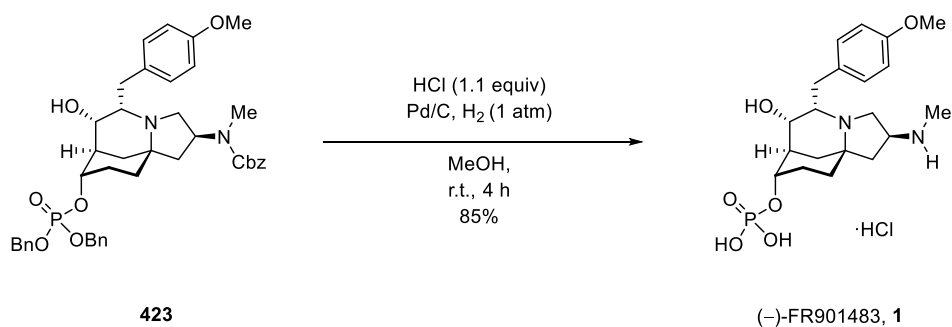
Scheme 156. Optimized synthesis of equatorial alcohol **404**.

Next, the inversion of the C8 alcohol was necessary. Sorensen's efficient Mitsunobu conditions^[261] allow for inversion and installation of the dibenzyl phosphate ester in a single step. We were mindful of the fact that in contrast to the Sorensen synthesis, the reaction was conducted in the presence of a carbamate instead of the free C2 amine. The reaction proceeded smoothly under the adapted conditions, employing dibenzyl phosphate, tris(4-chlorophenyl)phosphine, diisopropyl azodicarboxylate (DIAD) and triethylamine in THF, affording the desired axial dibenzylphosphate ester **423** in 34% after purification via preparative TLC (Scheme 157).



Scheme 157. Synthesis of dibenzyl ester **423**.

The last step of the total synthesis was identical to Snider's reported hydrogenolysis of the dibenzyl phosphate ester and concomitant removal of the benzyl carbamate.^[252] The reaction was carried out accordingly from **423**, with the addition of 1.1 equivalents of hydrochloric acid, delivering the natural product (**1**). Conversion to the natural product proceeded as planned, and (–)-FR901483 (**1**) was isolated as the respective hydrochloride salt in 85% yield from the reaction mixture without the need of further purification (Scheme 158).



Scheme 158. Final step of the synthesis affording natural product **1**.

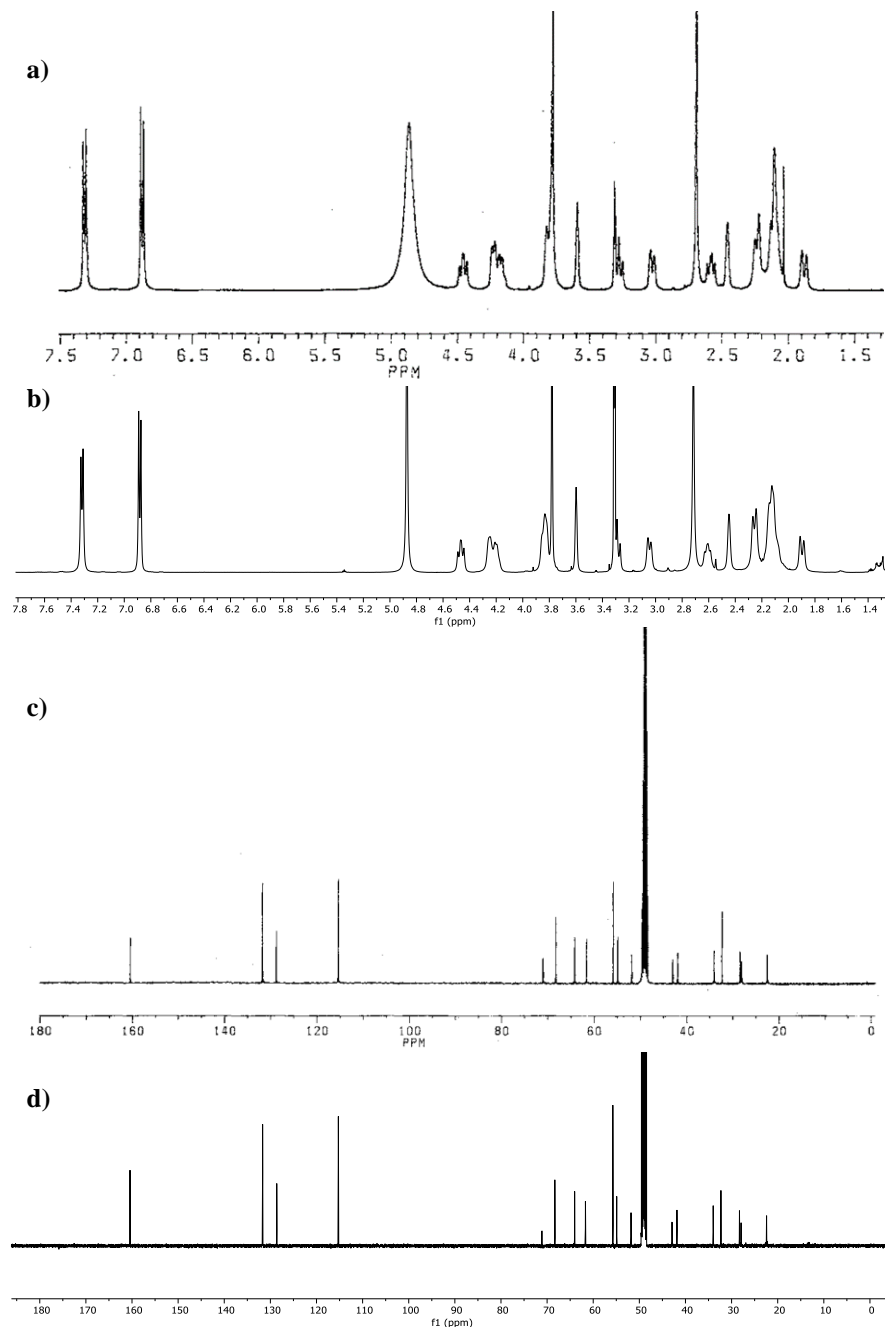


Figure 21. **a.** ^1H NMR spectrum (CD_3OD , 400 MHz) from the isolation report of FR901483^[250]; **b.** ^1H NMR spectrum (CD_3OD , 500 MHz) of fully synthetic sample of (-)-FR901483 prepared in this work. **c.** ^{13}C NMR spectrum (CD_3OD , 100 MHz) from the isolation report of FR901483^[250]; **d.** ^{13}C NMR spectrum (CD_3OD , 126 MHz) of fully synthetic sample of (-)-FR901483 prepared in this work.

The fully synthetic sample of (–)-FR901483 (**1**) was identical in all respects with the spectroscopic data reported in the literature (*e.g.* see Figure 21). The measured optical rotation was near-identical to the reported values (measured $[\alpha]_{\text{D}}^{22} = -10.7$ ($c = 0.28$, MeOH) [lit. $[\alpha]_{\text{D}}^{25} = -11$ ($c = 0.74$, MeOH)].^[250] It is notable that slow solvolysis of the phosphate ester in the natural product was observed in CD₃OD solution at room temperature.

3.3.7 Additional studies

In a complementing study carried out by Dr A. Trowbridge, the substrate scope of the novel multicomponent photocatalytic olefin-hydroaminoalkylation reaction was investigated, showing the broad applicability and functional group tolerance of the reaction. Therein, the modularity of the method was showcased through facile synthesis of natural product analogue 4',4'-difluoro-(+)-TAN1251C from 4,4-difluorocyclohexanone (Figure 22).

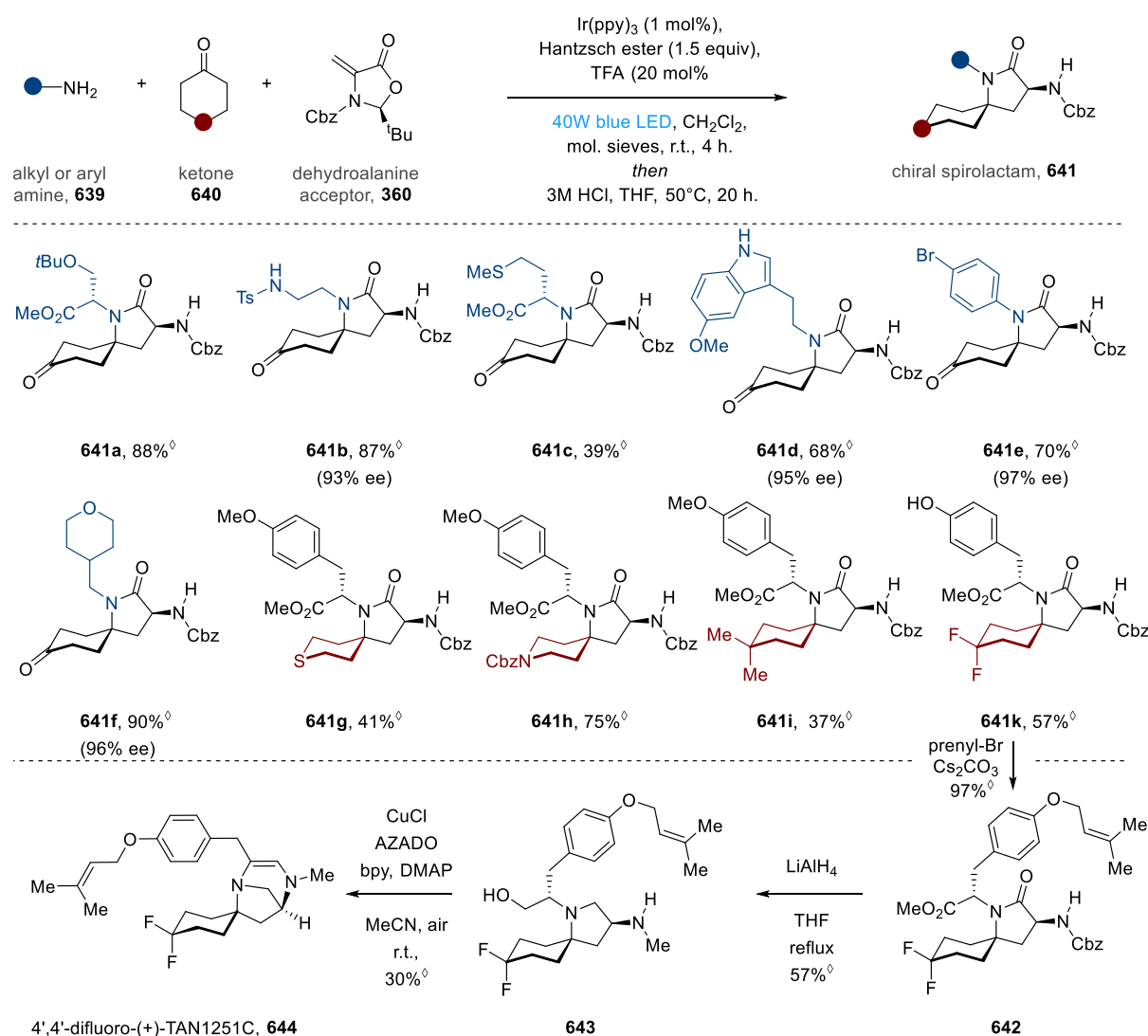
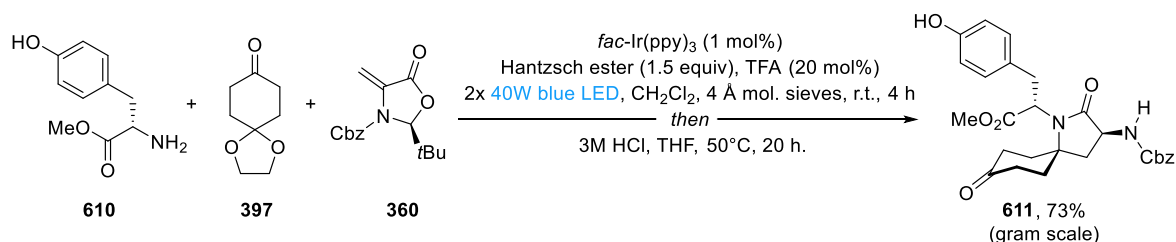


Figure 22. Substrate scope study and synthesis of 4',4'-difluoro-(+)-TAN1251C by Dr A Trowbridge. [◇]Reaction conducted by Dr A. Trowbridge.

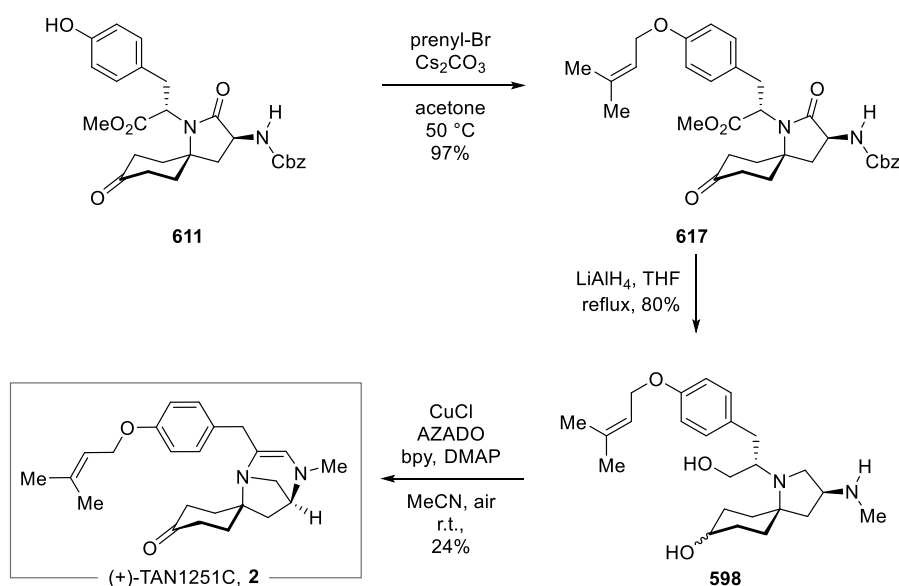
3.4 Summary

In summary, this chapter describes the development of an efficient photocatalytic multicomponent olefin-hydroaminoalkylation procedure utilizing abundant primary amines, in particular amino acids, to generate chiral spirolactam building blocks. The synthesis of key spirolactam precursor **611** was developed, from which the total syntheses of both natural products FR901483 (**1**) and TAN1251C (**2**) were successfully carried out (Scheme 159).



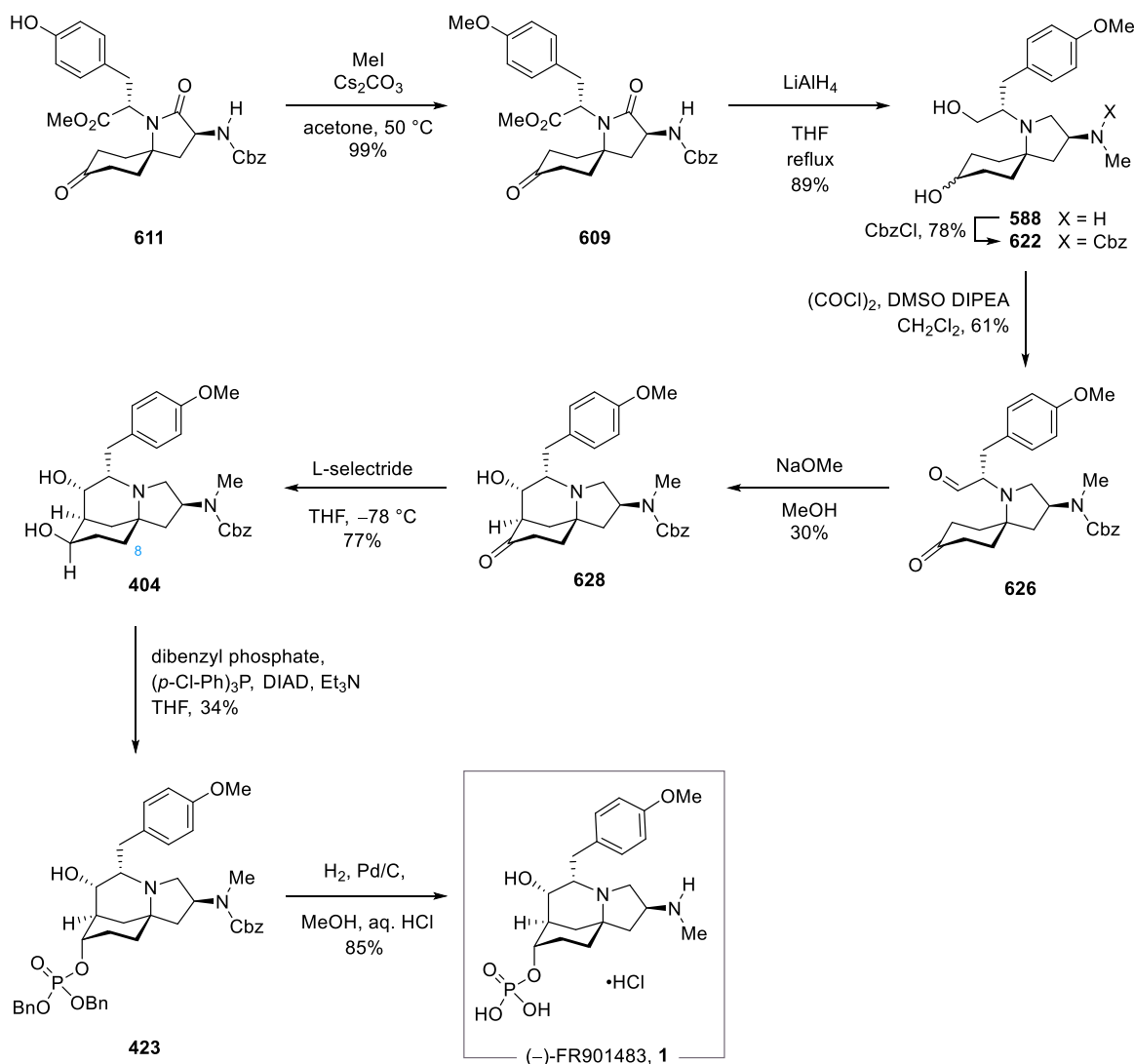
Scheme 159. Synthesis of key spirolactam precursor **611** via primary amine photocatalytic multicomponent olefin-hydroaminoalkylation from tyrosine methyl ester **610**.

Commencing from spirolactam **611** (Scheme 160), the total synthesis of TAN1251 began with prenylation to generate the phenolic prenyl ether **617**. Global reduction of the methyl ester, ketone, spirolactam and benzyl carbamate with an excess of lithium aluminium hydride in refluxing THF gave rise to diol **598**, containing a free methyl amino group at C2. Oxidative intramolecular condensation to the dienamine was achieved under Iwabuchi's aerobic oxidation conditions,^[373] generating the natural product (+)-TAN1251C (**2**) directly from diol **598** in synthetically useful yield.



Scheme 160. Total synthesis of (+)-TAN1251C (**2**).

The synthesis of natural product FR901483 (**1**) started with methylation of key spirolactam **611**, delivering methyl ether **609**, followed by global reduction resulting in diol **588**. After Cbz protection of the generated C2 methyl amine with benzyl chloroformate, Swern oxidation afforded key keto aldehyde **626** (Scheme 161).



Scheme 161. Total synthesis of (-)-FR901483 (**1**).

A biomimetic intramolecular aldol reaction, similar as previously explored by Snider,^[275] furnished hydroxy ketone **628**, and two other diastereomers, which were fully characterized in a 2D NMR study. The reaction had sufficient selectivity for the desired diastereomer (30% yield) to produce significant amounts of material, and completed assembly of the tricyclic core structure of the natural product **1** with the C6 alcohol in the correct stereoconfiguration. Preliminary studies were conducted to improve the selectivity of the intramolecular aldol reaction but no results superior to Snider's conditions could be obtained. Subsequent reduction of the ketone with L-selectride occurred from the open *si*-face resulting in

equatorial C8 alcohol **404**. Sorensen's conditions for an Mitsunobu-type reaction gave efficient inversion of the C8 alcohol with concomitant installation of a dibenzylphosphate ester delivering **423**. In the final step, removal of the benzyl esters and benzyl carbamate via hydrogenolysis under acidic conditions yielded the natural product (–)-FR901483 (**1**) as its hydrochloride salt.

In a complementing study by Dr A. Trowbridge, the broad applicability and functional group tolerance of the primary amine photocatalytic multicomponent olefin-hydroaminoalkylation has been demonstrated, and the synthesis of natural product analogue 4',4'-difluoro-(+)-TAN1251C was achieved.

4. Conclusions and Future Outlook

In the last decade, the field of visible light photoredox chemistry has experienced exponential growth and risen to the forefront of synthetic organic chemistry. The emergence of a host of novel, valuable light-mediated photoredox transformations has reinvigorated the interest in single electron redox and radical chemistry. This development has caused practitioners of organic chemistry to move away from the use of hazardous radical initiators, a number of toxic reagents, and high temperatures or harmful ultra-violet light.^[74] Due to their unique properties, the single electron chemistry of amines is intimately connected to the field of photoredox chemistry. A wealth of chemical transformations began to exploit these electron-rich compounds through novel photoredox pathways, and due to the ubiquity of amine functionality in biologically active compounds, soon amines surpassed their use as mere reductive additives. The functionalization and synthesis of amines through visible light photoredox methods has since become a major point of interest for the synthetic community.

Along these lines, visible light photoredox generated α -amino radicals have proven a uniquely useful and versatile synthetic tool for amine synthesis and functionalization. This avenue of reactivity has been extensively studied and combined with organocatalysis, transition metal catalysis, and Brønsted or Lewis acid catalysis to achieve a plethora of complex transformations via addition of the resulting α -amino radical into alkenes, nitrogen-containing double bonds or aromatic rings.^[119] Most commonly, α -amino radicals are accessed via single electron oxidation or fragmentation of redox-active preinstalled groups. In the case of amine oxidation, single electron transfer with susceptible amines can lead to the formation of the respective radical cation, from which fragmentation can occur to directly afford the desired α -amino radicals. Problematically, the fragmentation is inherently unselective and only gives poor control over the site of radical generation. On the other hand, α -silylamines, redox active esters and carboxylic acids are common examples for preinstalled functional groups which have been used heavily to induce radical generation in α -amine position.

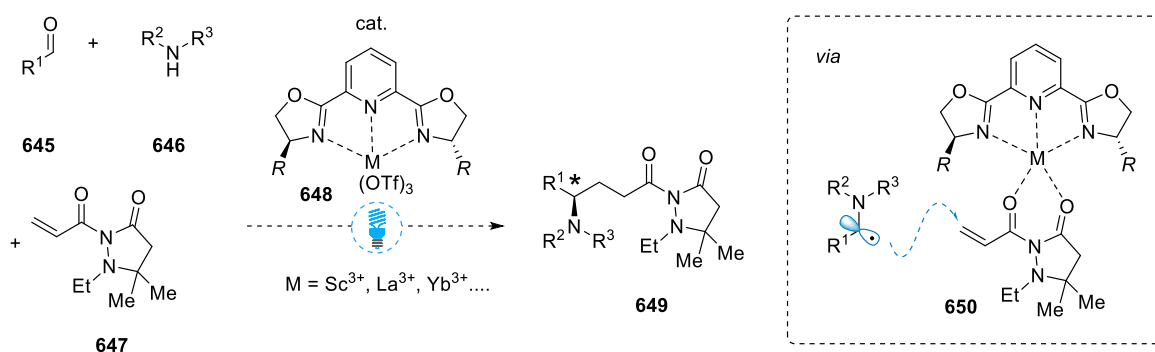
The uncommon reductive generation of α -amino radicals from the respective C=N double bonds is regiospecific, does not require prefunctionalization and is convergent. This desirable process, however, is hampered by high reduction potentials of alkyl iminium ions, interference of the respective enamines, and the generally poor outcome of additions of reductively generated α -amino radicals to radical acceptors. These factors rendered reductive α -amino radical generation both underexploited and underappreciated in chemical synthesis.

Prior to the work detailed in this thesis, only a single example of a visible light photoredox reduction of an all-alkyl iminium ion was reported in literature.^[205]

Overcoming these limitations, a general visible light photoredox reduction of all-alkyl iminium ions for the synthesis of complex tertiary amines was developed.^[249] The multicomponent photocatalytic olefin-hydroaminoalkylation approach enables the union of amines, aldehydes and electron deficient olefins to furnish pharmaceutically relevant complex tertiary amine products via the single-electron reduction of an *in situ* formed iminium ion. The reaction proceeds under mild conditions, exhibits broad substrate scope, and is environmentally benign. Preliminary mechanistic studies revealed an enabling 1,5-HAT process and an unprecedented redox relay of iminium ions. An expansion of the methodology enabled the use of dialkylamines and alkylenamines as starting materials in the reaction, giving access to a series of α -tertiary amine products, an important substance class in bioactive natural compounds.^[241]

Although the biosynthetically related (–)-FR901483 and (+)-TAN1251C alkaloids have attracted significant attention from the synthetic community in the last 20 years due to their biological activity and architecturally complex structures. The concise construction of the amino-substituted, α -tertiary amine containing, azaspirocyclic scaffold of these natural products remains a formidable synthetic challenge. In line with the previous work, a variant of the photocatalytic olefin-hydroaminoalkylation methodology was developed, employing primary amines and ketones to specifically target α -tertiary amine products. The new methodology was identified to give rapid access to a series of chiral spirolactam building blocks, including a chiral spirolactam precursor, which served as starting point for a divergent, enantiocontrolled total synthesis strategy accessing both immunosuppressant (–)-FR901483 and muscarinic antagonist (+)-TAN1251C. Demonstrating the utility of the olefin-hydroaminoalkylation approach, the reaction was optimized to access the common spirolactam precursor on gram-scale with only a simple filtration as the single purification step. From this advanced precursor, both total syntheses of (–)-FR901483 and (+)-TAN1251C were completed significantly more rapid and efficient than previously reported in the literature. The novel multicomponent approach furthermore enables a modular synthetic strategy for the facile construction of chiral 3-amino-1-azaspiro[4.5]decane fragments. This modularity can significantly facilitate the generation of derivatives or library of these, previously elusive structural motives.

A possible future expansion of the photocatalytic olefin-hydroaminoalkylation could be achieved via enantioselective control over the generated α -amino stereocenter. A potentially valuable avenue to realizing this aim could be taken by investigating the face preference of attack on the radical acceptor by using chiral Lewis acid catalysis (Scheme 162). Similarly to a method reported by Yoon and co-workers,^[132] enantioselective conjugate addition may be achieved by activation of an acryloyl dimethylpyrazolidin-3-one **647** with a lanthanide triflate complex aided by a suitable Pybox ligand **648**, potentially leading to enantiomerically enriched tertiary amine products **649**.



Scheme 162. Concept for an enantioselective conjugate α -amino radical addition via Lewis acid catalysis.

The primary amine variant of the olefin-hydroaminoalkylation generates the deceptively simple 1-azaspiro[4.5]decane structure, present in a large number of bioactive natural compounds. Further development of the radical acceptor by modulating the pivotal stability of the resulting alkyl radical may allow for a general method for the generation of these scaffolds without the incorporation of the chiral 3-amino group. This approach may enable the total synthesis of *Lycopodium* (lycojaponicumins) and *Clavelina* (cylindricines and lepadiformines) alkaloids (Figure 23), which are renowned for their unique molecular architectures and potent bioactive properties.

In conclusion, the two multicomponent photocatalytic olefin-hydroaminoalkylation methodologies detailed in the present thesis are of significant interest for chemical synthesis due to their utility, operational simplicity and environmentally benign conditions. They grant access to a number of challenging tertiary amine products, as well as previously elusive α -tertiary amines and chiral spirolactam precursors. In line with the herein described rapid synthesis of two natural products featuring the important 1-azaspiro[4.5]decane core fragment, (–)-FR901483 and (+)-TAN1251C, further development of the olefin-hydroaminoalkylation could significantly facilitate access to a number of architecturally challenging bioactive natural products.

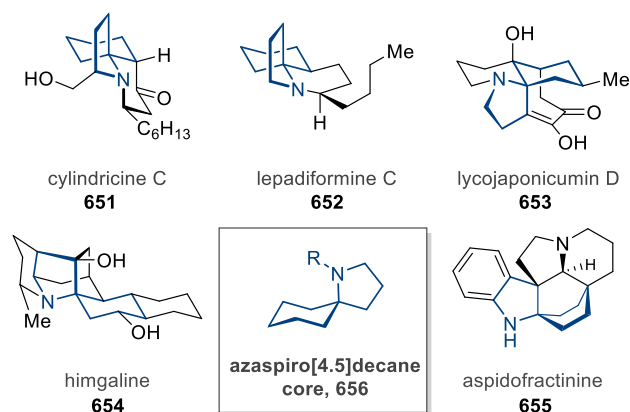


Figure 23. Selection of alkaloids featuring the 1-azaspiro[4.5]decane core.

Finally, it is hoped that the described, facile reductive generation of alkyl-substituted α -amino radicals from alkyl iminium ions, and their use towards the synthesis of increasingly complex tertiary amine scaffolds, will inspire novel advances in the area in both academia and industry.

5. Experimental Section

5.1 Materials and Methods

All reactions were run under an inert atmosphere (N_2) unless otherwise stated, with oven-dried glassware, using standard techniques. Anhydrous solvents were obtained from solvent stills (Et_2O and THF was distilled from $LiAlH_4$; MeCN, dichloromethane, hexane and toluene from CaH_2). Dichloromethane for use in the photocatalytic reaction in Chapter 2 was dried using 4Å MS (beads), degassed (freeze-pump-thaw) and stored in a Schlenk flask under N_2 . No appreciable deterioration in yield was observed after use for 3 months. Anhydrous dichloromethane for the photocatalytic reaction in Chapter 3 was used as described without further drying or degassing. Identical results were obtained using commercial anhydrous dichloromethane (Acros Organics, 348461000). Commercially available activated powdered 4Å molecular sieves (MS) were used as supplied (Alfa Aesar, A11535). $Ir(ppy)_3$ was obtained from Sigma-Aldrich and used as supplied. Hantzsch ester was obtained from Matrix Scientific and used without further purification. All other commercial reagents were used as supplied unless otherwise stated.

Irradiation of the reaction mixture was achieved using 40 W Kessil A160WE LED – Tuna Blue lights (setup: max blue, max intensity). Two lamps were used for larger scale experiments as specified. Small scale reactions were carried out in clear glass vials (4 mL) with PTFE/silicon septum lined screw caps (VWR, 548-0521). The Kessil lamps were positioned 5 cm from the reaction vessel, with a desk-fan provided for cooling.

Analytical thin-layer chromatography (TLC) was performed on Merck Kieselgel 60 F₂₅₄ 0.20 mm precoated, glass backed silica gel plates. Visualization of the developed chromatogram was performed by UV absorbance ($\lambda_{max} = 254$ nm), and/or by using aq. $KMnO_4$ TLC stain solution. Preparative thin-layer chromatography was performed on Merck PLC Silica gel 60 F₂₅₄ 1 mm plates using visualization by UV absorbance ($\lambda_{max} = 254$ nm). Flash column chromatography was performed using silica gel (Merck Geduran Si 60 [40-63 μm]) or aluminium oxide (EMD Millipore aluminium oxide 90, standardized) as specified with the indicated solvent system.

Nuclear magnetic resonance (NMR) spectra were recorded on a Bruker DPX 400 or DPX 500 spectrometer, generally equipped with a cryoprobe. Data is reported as follows: chemical shift [integration, multiplicity (s = singlet, d = doublet, t = triplet, q = quartet, quint = quintet, sext

= sextet, spt = septet, m = multiplet, br = broad), coupling constant and molecular assignment]. Coupling constants (J) are quoted to the nearest 0.1 Hz. Chemical shifts (δ) for ^1H NMR spectra are recorded in ppm from Me_4Si with the solvent resonance as the internal standard ($\text{CDCl}_3 = 7.26$ ppm, $\text{DMSO}-d_6 = 2.50$, $\text{CD}_3\text{OD} = 3.31$ ppm, $\text{C}_6\text{D}_6 = 7.16$ ppm, $\text{CD}_3\text{CN} = 1.94$ ppm). ^{13}C NMR spectra are reported in ppm from Me_4Si with the solvent resonance as the internal standard ($\text{CDCl}_3 = 77.16$ ppm, $\text{DMSO}-d_6 = 39.52$, $\text{CD}_3\text{OD} = 49.00$ ppm, $\text{C}_6\text{D}_6 = 128.06$ ppm, $\text{CD}_3\text{CN} = 118.26$ ppm). ^{19}F NMR spectra are reported in ppm from CFCl_3 and are uncorrected. ^{35}P NMR spectra are reported in ppm from 85% H_3PO_4 and are uncorrected. Where applicable, assignment was carried out using DEPT135 and 2-dimensional experiments (COSY, TOCSY, HMBC, HMQC, NOESY, ROESY). Atom numbering for assignment is provided for each assigned compound individually.

Stern-Volmer quenching was performed using a Shimadzu RF-6000 spectrofluorometer. Experiments were recorded using a quartz cell equipped with septa-lined screw cap under Ar. UV-Vis analysis was performed on a Shimadzu UV-1800 spectrophotometer.

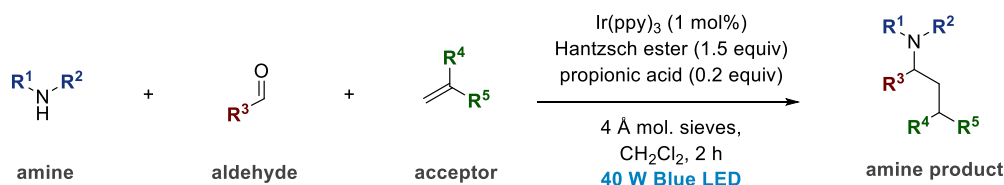
Infrared spectra (FT-IR) were recorded using a Perkin-Elmer Paragon 1000 Fourier transform Spectrometer equipped with ATR, with absorption maxima (ν_{max}) being quoted in wavenumbers (cm^{-1}) and characteristic peaks being defined (br = broad). High Resolution Mass spectrometry (HRMS) was carried out on a Waters XEVO GII-S Q-TOF equipped with an ESI probe, by the Mass Spectrometry Service of the Department of Chemistry, University of Cambridge, and by ESPRC Mass Spectrometry Service at the University of Swansea using an LTQ Orbitrap XL spectrometer with positive ion nano-electrospray. Melting points (m.p.) were recorded using a Gallenkamp melting point apparatus and are reported uncorrected.

Optical rotations were measured on a Perkin Elmer 343 Polarimeter and a Anton Paar MCP 100 Polarimeter, using a sodium lamp (λ 589 nm, D-line). $[\alpha]_{\text{D}}$ values (sodium D line) are reported at a given temperature ($^{\circ}\text{C}$) in $\text{deg cm}^2 \text{g}^{-1}$ with concentration (c) reported in g / 100 mL. Chiral HPLC analysis was performed on a Shimadzu XR-LC apparatus with Chiralpak[®] columns in a mixed solvent system of *n*-hexane and *iso*-propanol. X-ray crystallography was performed by Dr Andrew Bond on a Bruker D8-QUEST PHOTON-100 diffractometer using CuK α radiation ($\lambda = 1.5418 \text{ \AA}$) at the Cambridge University Chemistry X-Ray Laboratory.

5.2 Experimental procedures

5.2.1 Photocatalytic olefin-hydroaminoalkylation

General Procedure A: Photocatalytic olefin-hydroaminoalkylation



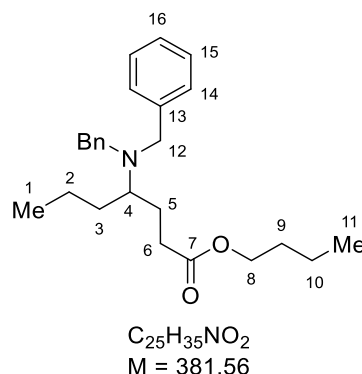
A 4 mL PTFE/Silicone-lined septa screw cap (PP) clear glass vial equipped with magnetic stirrer bar (10 mm, cylindrical) was charged with all solid reagents [typically Ir(ppy)₃, 4 Å MS and Hantzsch ester] under air. The vial was sealed and a needle was inserted through the septa and the contents evacuated/backfilled with N₂ (3 cycles). Anhydrous dichloromethane was added followed by the remaining liquid reagents [typically dialkylamine, aldehyde, acceptor and propanoic acid] using a micro-syringe. The vial was sealed with additional parafilm™ and secured upon an upturned crystallizing basin using double-sided tape, in the center of a stirrer/hotplate. The Kessil lamp was positioned 5 cm from the vial along with a desk-fan for cooling. The vial was irradiated for a period of 2 hours with vigorous stirring (600-800 rpm), over which time the color of the reaction mixture (under light) typically turned from dark red/brown to bright yellow, indicating the consumption of the Hantzsch ester and completion of the reaction. Upon completion, the reaction mixture was analyzed by TLC and either directly loaded onto the column (in the case of dichloromethane/Et₃N as an eluent) or filtered and the solvent removed *in vacuo* for purification using EtOAc/P.E. as an eluent. For non-polar compounds purified by flash column chromatography using dichloromethane/Et₃N as an eluent, the product regularly co-elutes with either the Ir(ppy)₃ photocatalyst and/or the starting aldehyde. In this instance the column fractions were combined, the solvent removed *in vacuo* and the residue dried under hi-vac. The residue was dissolved in P.E. (Ir(ppy)₃ insoluble) and filtered over celite® to afford the pure product. For non-volatile aldehydes, the product can be obtained either by purification using an SCX cartridge or acid/base workup.

From enamines: The amine and aldehyde components can be replaced by the preformed enamine.

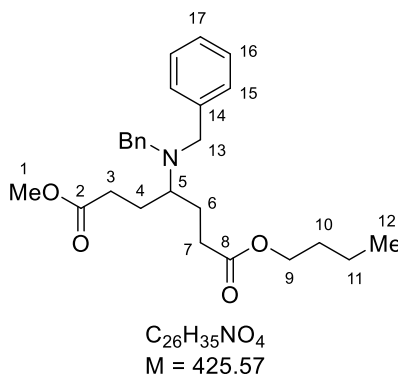
From amine hydrochloride salts: If amine hydrochloride salts are used, one equivalent of triethylamine was added to the reaction prior to irradiation.

General Procedure B: *Photocatalytic olefin-hydroaminoalkylation using paraformaldehyde*

The reaction is conducted as in General Procedure A, but solid paraformaldehyde (5 equiv) is used as the carbonyl component, and the reaction is heated in an oil bath at 45 °C for 1 h in the dark (covered in aluminium foil) prior to irradiation.

butyl 4-(dibenzylamino)heptanoate (348a)

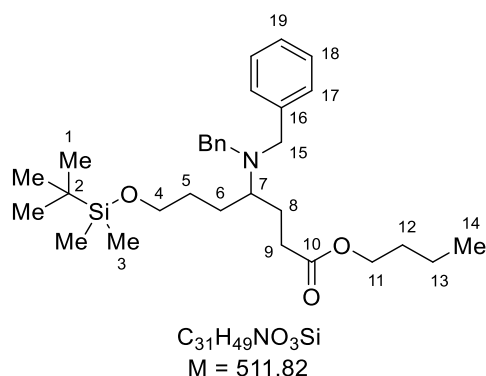
Prepared according to general procedure A using dibenzylamine (39 μL , 0.2 mmol), butyraldehyde (20 μL , 0.22 mmol), *n*-butyl acrylate (32 μL , 0.22 mmol), ethyl-Hantzsch Ester (76 mg, 0.3 mmol), 4Å MS (100 mg), propanoic acid (3 μL , 40 μmol) and *fac*-Ir(ppy)₃ (1.4 mg, 2 μmol) in anhydrous degassed dichloromethane (2 mL). The crude reaction mixture was purified by flash column chromatography (0.5% Et₃N in dichloromethane) to afford the product as a colorless oil (64 mg, 84%). **R_f** (5% EtOAc in P.E.): 0.21; **IR** $\nu_{\text{max}}/\text{cm}^{-1}$ (film): 3027, 2957, 2932, 2870, 1732, 1602, 1494, 1453, 1360, 1244, 1170, 1141, 1072, 951, 744, 697. **¹H NMR** (400 MHz, CDCl₃) δ : 7.40 – 7.18 (10 H, m, H_{14,15,16}), 4.07 – 3.96 (2 H, m, H₈), 3.69 (2 H, d, $J = 13.7$ Hz, H_{12a}), 3.49 (2 H, d, $J = 13.7$ Hz, H_{12b}), 2.56 – 2.43 (2 H, m, H_{6a,4}), 2.33 – 2.23 (1 H, m, H_{6b}), 1.89 – 1.78 (1 H, m, H_{5a}), 1.75 – 1.64 (2 H, m, H_{5b,3a}), 1.63 – 1.54 (2 H, m, H₉), 1.44 – 1.32 (4 H, m, H_{2,10}), 1.28 – 1.16 (1 H, m, H_{3b}), 0.96 (3 H, t, $J = 7.4$ Hz, H₁₁), 0.89 (3 H, t, $J = 7.4$ Hz, H₁); **¹³C NMR** (101 MHz, CDCl₃) δ : 174.1 (C₇), 140.4 (C₁₃), 128.9 (C₁₄), 128.1 (C₁₅), 126.7 (C₁₆), 64.1 (C₈), 56.5 (C₄), 53.3 (C₁₂), 31.8 (C₆), 30.9 (C₃), 30.7 (C₉), 25.5 (C₅), 20.4 (C₂), 19.2 (C₁₀), 14.3 (C₁), 13.8 (C₁₁). ***m/z* HRMS** found [M + H]⁺ 382.2739, C₂₅H₃₆NO₂⁺ requires 382.2741.

1-butyl 7-methyl 4-(dibenzylamino)heptanedioate (348b)

Prepared according to general procedure A using dibenzylamine (39 μL , 0.2 mmol), methyl 4-oxobutanoate (23 μL , 0.22 mmol), *n*-butyl acrylate (32 μL , 0.22 mmol), ethyl-Hantzsch Ester

(76 mg, 0.3 mmol), 4Å MS (100 mg), propanoic acid (3 µL, 40 µmol) and *fac*-Ir(ppy)₃ (1.4 mg, 2 µmol) in anhydrous degassed dichloromethane (2 mL). The crude reaction mixture was purified by flash column chromatography (1% EtOAc in dichloromethane) to afford the product as a colorless oil (50 mg, 59%). **R_f** (10% EtOAc in heptane): 0.44; **IR** $\nu_{\text{max}}/\text{cm}^{-1}$ (film): 3028, 2958, 2872, 1731, 1453, 1362, 1171, 1117, 1074, 1027, 952, 745, 697. **¹H NMR** (500 MHz, CDCl₃) δ : 7.35 – 7.18 (10 H, m, H_{15,16,17}), 4.06 – 3.95 (2 H, m, H₉), 3.60 (3 H, s, H₁), 3.57 (4 H, s, H₁₃), 2.47 – 2.34 (3 H, m, H_{3/7a,5}), 2.33 – 2.26 (2 H, m, H_{3/7b}), 1.99 – 1.88 (2 H, m, H_{4/6a}), 1.64 – 1.53 (4 H, m, H_{4/6b,10}), 1.36 (2 H, sext, *J* = 7.7 Hz, H₁₁), 0.93 (3 H, t, *J* = 7.5 Hz, H₁₂); **¹³C NMR** (126 MHz, CDCl₃) δ : 174.2 (C_{2/8}), 173.8 (C_{2/8}), 140.1 (C₁₄), 129.0 (C₁₅), 128.3 (C₁₆), 126.9 (C₁₇), 64.4 (C₉), 56.4 (C₅), 53.3 (C₁₄), 51.6 (C₁), 31.8 (C_{3/7}), 31.6 (C_{3/7}), 30.8 (C₁₀), 24.6 (C_{4/6}), 24.5 (C_{4/6}), 19.3 (C₁₁), 13.8 (C₁₂). ***m/z* HRMS** found [M]⁺ 425.2560, C₂₆H₃₅NO₄⁺ requires 425.2561.

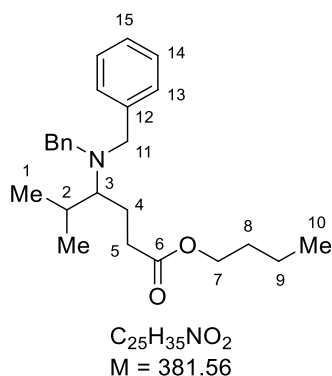
butyl 7-((tert-butyldimethylsilyl)oxy)-4-(dibenzylamino)heptanoate (348c)



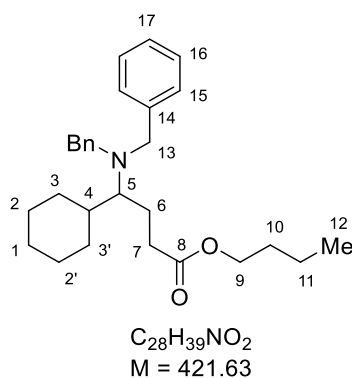
Prepared according to general procedure A using dibenzylamine (39 µL, 0.2 mmol), 4-((tert-butyldimethylsilyl)oxy)butanal (45 mg, 0.22 mmol), *n*-butyl acrylate (32 µL, 0.22 mmol), ethyl- Hantzsch Ester (76 mg, 0.3 mmol), 4Å MS (100 mg), propanoic acid (3 µL, 40 µmol) and *fac*-Ir(ppy)₃ (1.4 mg, 2 µmol) in anhydrous degassed dichloromethane (2 mL). The crude reaction mixture was purified by flash column chromatography (1% EtOAc in P.E.) to afford the product as a colorless oil (82 mg, 81%). **R_f** (20% EtOAc in P.E.): 0.64; **IR** $\nu_{\text{max}}/\text{cm}^{-1}$ (film): 3029, 2954, 2928, 2856, 1732, 1494, 1454, 1360, 1252, 1167, 1094, 1027, 939, 833, 774, 742, 697. **¹H NMR** (400 MHz, CDCl₃) δ : 7.40 – 7.21 (10 H, m, H_{17,18,19}), 4.07 – 3.98 (2 H, m, H₁₁), 3.70 (2 H, d, *J* = 14.0 Hz, H_{15a}), 3.66 – 3.56 (2 H, m, H₄), 3.52 (2 H, d, *J* = 14.0 Hz, H_{15b}), 2.55 – 2.45 (2 H, m, H_{7,9a}), 2.35 – 2.25 (1 H, m, H_{9b}), 1.94 – 1.76 (2 H, m, H_{6a,8a}), 1.75 – 1.66 (1 H, m, H_{8b}), 1.65 – 1.50 (4 H, m, H_{5,12}), 1.40 (2 H, sext, *J* = 7.8 Hz, H₁₃), 1.35 –

1.24 (1 H, m, H_{6b}), 0.97 (3 H, t, $J = 7.4$ Hz, H₁₄), 0.95 (9 H, s, H₁), 0.09 (6 H, s, H₃); ¹³C NMR (101 MHz, CDCl₃) δ : 174.0 (C₁₀), 140.3 (C₁₆), 128.9 (C₁₇), 128.2 (C₁₈), 126.8 (C₁₉), 64.2 (C₁₁), 63.1 (C₄), 56.7 (C₇), 53.3 (C₁₅), 31.8 (C₉), 30.7 (C₁₂), 30.6 (C₅), 26.0 (C₁), 25.4 (C₈), 24.8 (C₆), 19.2 (C₁₃), 18.4 (C₂), 13.8 (C₁₄), -5.2 (C₃). m/z HRMS found $[M + H]^+$ 512.3560, C₃₁H₅₀NO₃Si⁺ requires 512.3560.

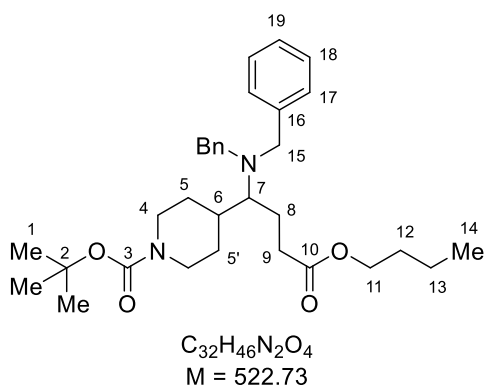
butyl 4-(dibenzylamino)-5-methylhexanoate (348I)



Prepared according to general procedure A using dibenzylamine (39 μ L, 0.2 mmol), isobutyraldehyde (20 μ L, 0.22 mmol), *n*-butyl acrylate (32 μ L, 0.22 mmol), ethyl- Hantzsch Ester (76 mg, 0.3 mmol), 4Å MS (100 mg), propanoic acid (3 μ L, 40 μ mol) and *fac*-Ir(ppy)₃ (1.4 mg, 2 μ mol) in anhydrous degassed dichloromethane (2 mL). The crude reaction mixture was purified by flash column chromatography (1% EtOAc in P.E.) to afford the product as a colorless oil (47 mg, 62%). **R_f** (20% EtOAc in P.E.): 0.77; **IR** $\nu_{\text{max}}/\text{cm}^{-1}$ (film): 3063, 3029, 2958, 2872, 1731, 1602, 1494, 1453, 1360, 1257, 1173, 1103, 1070, 1027, 954, 744, 697. ¹H NMR (400 MHz, CDCl₃) δ : 7.40 – 7.20 (10 H, m, H_{13,14,15}), 4.11 – 4.01 (2 H, m, H₇), 3.74 (2 H, d, $J = 13.6$ Hz, H_{11a}), 3.64 (2 H, d, $J = 13.6$ Hz, H_{11b}), 2.57 – 2.47 (1 H, m, H_{5a}), 2.36 – 2.24 (2 H, m, H_{3,5b}), 2.13 – 2.02 (1 H, m, H₂), 1.97 – 1.84 (1 H, m, H_{4a}), 1.76 – 1.66 (1 H, m, H_{4b}), 1.65 – 1.57 (2 H, m, H₈), 1.47 – 1.35 (2 H, m, H₉), 1.03 – 0.92 (9 H, m, H_{1,10}); ¹³C NMR (101 MHz, CDCl₃) δ : 174.1 (C₆), 140.4 (C₁₂), 129.0 (C₁₃), 128.1 (C₁₄), 126.7 (C₁₅), 64.2 (C₇), 61.9 (C₃), 54.2 (C₁₁), 32.7 (C₅), 30.7 (C₈), 28.2 (C₂), 22.2 (C₄), 22.1 (C_{1a}), 19.9 (C_{1b}), 19.2 (C₉), 13.8 (C₁₀). m/z HRMS found $[M + H]^+$ 382.2742, C₂₅H₃₆NO₂⁺ requires 382.2741.

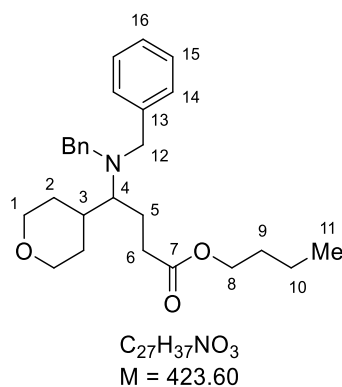
butyl 4-cyclohexyl-4-(dibenzylamino)butanoate (348m)

Prepared according to general procedure A using dibenzylamine (39 μL , 0.2 mmol), cyclohexanecarboxaldehyde (48 μL , 0.40 mmol), *n*-butyl acrylate (57 μL , 0.40 mmol), methoxyethyl- Hantzsch Ester (94 mg, 0.3 mmol), 4Å MS (100 mg), propanoic acid (3 μL , 40 μmol) and *fac*-Ir(ppy)₃ (1.4 mg, 2 μmol) in anhydrous degassed dichloromethane (2 mL). The crude reaction mixture was purified by flash column chromatography (0.5% Et₃N in dichloromethane) to afford the product as a colorless oil (60 mg, 71%). **R_f** (10% EtOAc in P.E.): 0.27; **IR** $\nu_{\text{max}}/\text{cm}^{-1}$ (film): 3063, 3028, 2924, 2851, 1732, 1602, 1494, 1452, 1261, 1167, 1112, 1070, 1027, 958, 744, 697. **¹H NMR** (500 MHz, CDCl₃) δ : 7.36 – 7.17 (10 H, m, H_{15,16,17}), 4.06 – 3.97 (2 H, m, H₉), 3.66 (2 H, d, $J = 13.7$ Hz, H_{13a}), 3.60 (2 H, d, $J = 13.7$ Hz, H_{13b}), 2.49 – 2.40 (1 H, m, H_{7a}), 2.30 – 2.16 (2 H, m, H_{5,7b}), 1.93 – 1.78 (2 H, m, H_{3a,6a}), 1.76 – 1.62 (6 H, m, H_{1a,2a,2'a,3'a,5,6b}), 1.58 (2 H, quint, $J = 7.3$ Hz, H₁₀), 1.36 (2 H, sext, $J = 7.5$ Hz, H₁₁), 1.31 – 1.18 (2 H, m, H_{2b,2'b}), 1.16 – 0.97 (3 H, m, H_{1b,3b,3'b}), 0.93 (3 H, t, $J = 7.5$ Hz, H₁₂); **¹³C NMR** (125.8 MHz, CDCl₃) δ : 174.2 (C₈), 140.6 (C₁₄), 129.1 (C₁₅), 128.2 (C₁₆), 126.8 (C₁₇), 64.3 (C₉), 61.8 (C₅), 54.4 (C₁₃), 38.8 (C₄), 33.1 (C₇), 32.1 (C₃), 30.8 (C₁₀), 30.7 (C_{3'}), 27.0 (C₂), 26.8 (C_{2'}), 26.7 (C₁), 22.6 (C₆), 19.3 (C₁₁), 13.9 (C₁₂). ***m/z* HRMS** found [M + H]⁺ 422.3060, C₂₈H₄₀NO₂⁺ requires 422.3059.

tert-butyl 4-(4-butoxy-1-(dibenzylamino)-4-oxobutyl)piperidine-1-carboxylate (348n)

Prepared according to general procedure A using dibenzylamine (39 μL , 0.2 mmol), 1-Boc-piperidine-4-carboxaldehyde (85 mg, 0.40 mmol), *n*-butyl acrylate (57 μL , 0.40 mmol), methoxyethyl-Hantzsch Ester (94 mg, 0.3 mmol), 4Å MS (100 mg), propanoic acid (3 μL , 40 μmol) and *fac*-Ir(ppy)₃ (1.4 mg, 2 μmol) in anhydrous degassed dichloromethane (2 mL). The crude reaction mixture was purified by flash column chromatography (0.5% Et₃N in dichloromethane) to afford the product as a colorless oil (73 mg, 70%). **R_f** (20% EtOAc in P.E.): 0.22; **IR** $\nu_{\text{max}}/\text{cm}^{-1}$ (film): 2930, 2853, 1731, 1688, 1452, 1421, 1364, 1245, 1162, 1069, 1027, 961, 869, 746, 698. **¹H NMR** (400 MHz, CDCl₃) δ : 7.39 – 7.20 (10 H, m, H_{17,18,19}), 4.13 (2 H, br s, H_{4a}), 4.08 – 4.00 (2 H, m, H₁₁), 3.67 (4 H, s, H₁₅), 2.68 (2 H, br t, *J* = 11.3 Hz, H_{4b}), 2.50 – 2.40 (1 H, m, H_{9a}), 2.38 – 2.24 (2 H, m, H_{7,9b}), 2.01 – 1.91 (1 H, m, H_{8a}), 1.87 (1 H, br d, *J* = 12.0 Hz, H_{5a}), 1.83 – 1.66 (2 H, m, H_{6,8b}), 1.65 – 1.56 (3 H, m, H_{5'a,12}), 1.48 (9 H, s, H₁), 1.40 (2 H, sext, *J* = 7.5 Hz, H₁₃), 1.28 – 1.08 (2 H, m, H_{5b,5'b}), 0.97 (3 H, t, *J* = 7.4 Hz, H₁₄); **¹³C NMR** (101 MHz, CDCl₃) δ : 173.7 (C₁₀), 154.8 (C₃), 140.0 (C₁₆), 128.9 (C₁₇), 128.2 (C₁₈), 126.9 (C₁₉), 79.3 (C₂), 64.3 (C₁₁), 61.0 (C₇), 54.3 (C₁₅), 44.0 (br s, C₄), 37.9 (C₆), 32.9 (C₉), 30.69 (C₅), 30.68 (C₁₂), 29.7 (br s, C_{5'}), 28.5 (C₁), 22.4 (C₈), 19.2 (C₁₃), 13.8 (C₁₄). ***m/z*** **HRMS** found [M + H]⁺ 523.3522, C₃₂H₄₇N₂O₄⁺ requires 523.3522.

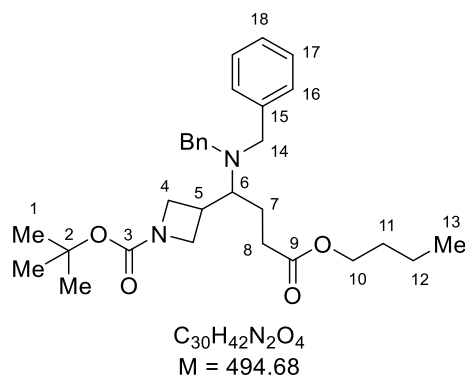
butyl 4-(dibenzylamino)-4-(tetrahydro-2*H*-pyran-4-yl)butanoate (348o)



Prepared according to general procedure A using dibenzylamine (39 μL , 0.2 mmol), tetrahydro-2*H*-pyran-4-carbaldehyde (45.6 mg, 0.40 mmol), *n*-butyl acrylate (57 μL , 0.40 mmol), methoxyethyl-Hantzsch Ester (94 mg, 0.3 mmol), 4Å MS (100 mg), propanoic acid (3 μL , 40 μmol) and *fac*-Ir(ppy)₃ (1.4 mg, 2 μmol) in anhydrous degassed dichloromethane (2 mL). The crude reaction mixture was purified by flash column chromatography (0.5% Et₃N in dichloromethane) to afford the product as a colorless oil (67 mg, 79%). **R_f** (20% EtOAc in P.E.): 0.42; **IR** $\nu_{\text{max}}/\text{cm}^{-1}$ (film): 3029, 2955, 2843, 1730, 1602, 1494, 1453, 1361, 1264, 1238,

1171, 1115, 1094, 1027, 966, 823, 733, 697. **¹H NMR** (400 MHz, CDCl₃) δ : 7.35 – 7.16 (10 H, m, H_{14,15,16}), 4.02 (2 H, dt, J = 2.1, 6.8 Hz, H₈), 3.99 – 3.91 (2 H, m, H_{1a,1'a}), 3.67 (2 H, d, J = 13.7 Hz, H_{12a}), 3.63 (2 H, d, J = 13.7 Hz, H_{12b}), 3.42 – 3.33 (2 H, m, H_{1b,1'b}), 2.48 – 2.39 (1 H, m, H_{6a}), 2.35 – 2.22 (2 H, H_{4,6b}), 1.97 – 1.81 (2 H, m, H_{5a,3}), 1.81 – 1.74 (1 H, m, H_{2a}), 1.73 – 1.63 (1 H, m, H_{5b}), 1.58 (2 H, quint, J = 6.9 Hz, H₉), 1.54 – 1.47 (1 H, m, H_{2b}), 1.44 – 1.29 (4 H, m, H_{2'a,2'b,10}), 0.93 (3 H, t, J = 7.4 Hz, H₁₁); **¹³C NMR** (101 MHz, CDCl₃) δ : 173.8 (C₇), 140.0 (C₁₃), 128.9 (C₁₄), 128.2 (C₁₅), 126.9 (C₁₆), 68.4 (C₁), 68.1 (C_{1'}), 64.3 (C₈), 61.1 (C₄), 54.2 (C₁₂), 36.9 (C₃), 32.9 (C₆), 31.7 (C₂), 30.8 (C_{2'}), 30.7 (C₉), 22.4 (C₅), 19.2 (C₁₀), 13.8 (C₁₁). ***m/z* HRMS** found [M + H]⁺ 424.2849, C₂₇H₃₈NO₃⁺ requires 424.2852.

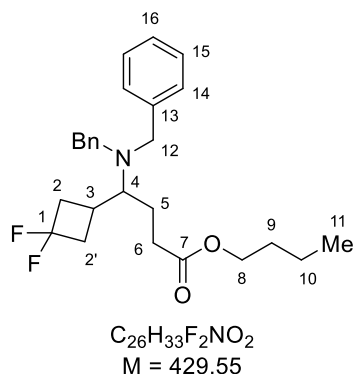
***tert*-butyl 3-(4-butoxy-1-(dibenzylamino)-4-oxobutyl)azetidine-1-carboxylate (348p)**



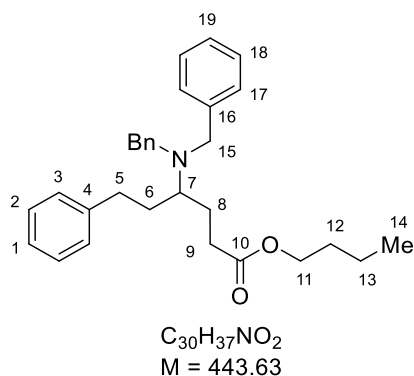
Prepared according to general procedure A using dibenzylamine (39 μ L, 0.2 mmol), 1-Boc-azetidine-3-carboxaldehyde (74 mg, 0.4 mmol), *n*-butyl acrylate (57 μ L, 0.4 mmol), methoxyethyl-Hantzsch Ester (94 mg, 0.3 mmol), 4Å MS (100 mg), propanoic acid (3 μ L, 40 μ mol) and *fac*-Ir(ppy)₃ (1.4 mg, 2 μ mol) in anhydrous degassed dichloromethane (2 mL). The crude reaction mixture was purified by flash column chromatography (0.5% Et₃N in dichloromethane) to afford the product as a colorless oil (63 mg, 64%). **R_f** (20% EtOAc in P.E.): 0.29; **IR** ν_{max} /cm⁻¹ (film): 2960, 2881, 1695 (br), 1453, 1391, 1365, 1253, 1134, 939, 859, 748, 699. **¹H NMR** (400 MHz, CDCl₃) δ : 7.37 – 7.21 (10 H, m, H_{16,17,18}), 4.09 – 3.98 (3 H, m, H_{4a,10}), 3.93 (1 H, t, J = 7.7 Hz, H_{4b}), 3.88 – 3.77 (1 H, m, H_{4c}), 3.70 – 3.61 (3 H, m, H_{4d,14a}), 3.51 (2 H, d, J = 13.6 Hz, H_{14b}), 2.94 – 2.82 (1 H, m, H₅), 2.81 – 2.72 (1 H, m, H₆), 2.52 – 2.42 (1 H, m, H_{8a}), 2.37 – 2.26 (1 H, m, H_{8b}), 1.97 – 1.95 (1 H, m, H_{7a}), 1.71 – 1.53 (3 H, m, H_{7b,11}), 1.45 (9 H, s, H₁), 1.39 (2 H, sext, J = 7.6 Hz, H₁₂), 0.96 (3 H, t, J = 7.6 Hz, H₁₃); **¹³C NMR** (101 MHz, CDCl₃) δ : 173.4 (C₉), 156.2 (C₃), 139.6 (C₁₅), 128.9 (C₁₆), 128.3 (C₁₇), 127.1 (C₁₈), 79.3 (C₂), 64.4 (C₁₀), 59.3 (C₆), 54.2 (C₁₄), 53.2 (br s, C₄), 31.6 (C₈), 30.7 (br s,

C₅), 30.6 (C₁₁), 28.4 (C₁), 23.1 (C₇), 19.2 (C₁₂), 13.7 (C₁₃). **m/z HRMS** found [M + H]⁺ 495.3209, C₃₀H₄₃N₂O₄⁺ requires 495.3217.

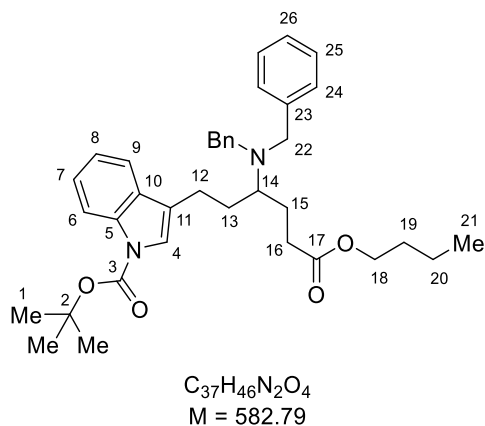
butyl 4-(dibenzylamino)-4-(3,3-difluorocyclobutyl)butanoate (348q)



Prepared according to general procedure A using dibenzylamine (39 μ L, 0.2 mmol), 3,3-difluorocyclobutane-1-carbaldehyde (48 mg, 0.4 mmol), *n*-butyl acrylate (57 μ L, 0.4 mmol), methoxyethyl-Hantzsch Ester (94 mg, 0.3 mmol), 4Å MS (100 mg), propanoic acid (3 μ L, 40 μ mol) and *fac*-Ir(ppy)₃ (1.4 mg, 2 μ mol) in anhydrous degassed dichloromethane (2 mL). The crude reaction mixture was purified by flash column chromatography (0.5% Et₃N in dichloromethane) to afford the product as a colorless oil (69 mg, 80%). **R_f** (20% EtOAc in P.E.): 0.47; **IR** ν_{max} /cm⁻¹ (film): 3029, 2958, 1731, 1494, 1454, 1374, 1294, 1238, 1169, 1123, 1072, 1027, 900, 746, 699. **¹H NMR** (400 MHz, CDCl₃) δ : 7.41 – 7.22 (10 H, m, H_{14,15,16}), 4.11 – 3.97 (2 H, m, H₈), 3.72 (2 H, d, *J* = 13.5 Hz, H_{12a}), 3.57 (2 H, d, *J* = 13.5 Hz, H_{12b}), 2.81 – 2.68 (1 H, m, H_{2a}), 2.66 – 2.54 (2 H, m, H_{2'a,4}), 2.54 – 2.31 (4 H, m, H_{2b,6a,6b,3}), 2.30 – 2.15 (1 H, m, H_{2'b}), 1.91 – 1.80 (1 H, m, H_{5a}), 1.70 – 1.57 (3 H, m, H_{5b,9}), 1.40 (2 H, sext, *J* = 7.5 Hz, H₁₀), 0.97 (3 H, t, *J* = 7.5 Hz, H₁₁); **¹³C NMR** (101 MHz, CDCl₃) δ : 173.5 (C₇), 139.7 (C₁₃), 128.8 (C₁₄), 128.3 (C₁₅), 127.1 (C₁₆), 119.7 (dd, *J* = 269.1, 287.4 Hz, C₁), 64.4 (C₈), 60.7 (C₄), 54.1 (C₁₂), 40.3 (dd, *J* = 21.3, 23.1 Hz, C₂), 39.7 (dd, *J* = 21.2, 23.4 Hz, C_{2'}), 31.6 (C₆), 30.7 (C₉), 25.5 (dd, *J* = 2.7, 14.3 Hz, C₃), 23.7 (C₅), 19.2 (C₁₀), 13.7 (C₁₁); **¹⁹F [¹H] NMR** (376 MHz, CDCl₃) δ : -80.7 (d, *J* = 192.6 Hz), -101.1 (d, *J* = 192.2 Hz). **m/z HRMS** found [M + H]⁺ 430.2556, C₂₆H₃₄F₂NO₂⁺ requires 430.2558.

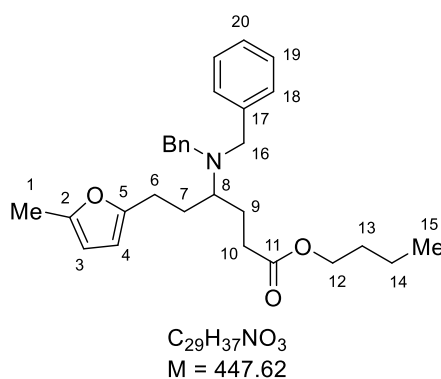
butyl 4-(dibenzylamino)-6-phenylhexanoate (348v)

Prepared according to general procedure A using dibenzylamine (39 μ L, 0.2 mmol), 3-phenylpropionaldehyde (29 μ L, 0.22 mmol), *n*-butyl acrylate (32 μ L, 0.22 mmol), ethyl-Hantzsch Ester (76 mg, 0.3 mmol), 4Å MS (100 mg), propanoic acid (3 μ L, 40 μ mol) and *fac*-Ir(ppy)₃ (1.4 mg, 2 μ mol) in anhydrous degassed dichloromethane (2 mL). The crude reaction mixture was purified by flash column chromatography (gradient elution: 100% P.E. to 4% EtOAc in P.E.) to afford the product as a colorless oil (71 mg, 81%). **R_f** (10% EtOAc in P.E.): 0.39; **IR** ν_{max} /cm⁻¹ (film): 3063, 3028, 2930, 2871, 1730, 1602, 1494, 1453, 1360, 1244, 1176, 1116, 1070, 1027, 949, 908, 744, 696. **¹H NMR** (400 MHz, CDCl₃) δ : 7.33 – 7.09 (15 H, m, H_{1,2,3,17,18,19}), 4.05 – 3.94 (2 H, m, H₁₁), 3.65 (2 H, d, *J* = 13.6 Hz, H_{15a}), 3.45 (2 H, d, *J* = 13.6 Hz, H_{15b}), 2.68 – 2.55 (2 H, m, H₅), 2.53 – 2.40 (2 H, m, H_{7, 9a}), 2.29 – 2.17 (1 H, m, H_{9b}), 2.05 – 1.94 (1 H, m, H_{6a}), 1.93 – 1.81 (1 H, m, H_{8a}), 1.79 – 1.68 (1 H, m, H_{8b}), 1.61 – 1.50 (3 H, m, H_{6b,12}), 1.36 (2 H, sext, *J* = 7.6 Hz, H₁₃), 0.94 (3 H, t, *J* = 7.5 Hz, H₁₄); **¹³C NMR** (101 MHz, CDCl₃) δ : 174.0 (C₁₀), 142.6 (C₄), 140.2 (C₁₆), 129.0 (C₁₇), 128.43 (C₃), 128.40 (C₂), 128.2 (C₁₈), 126.8 (C₁₉), 125.8 (C₁), 64.2 (C₁₁), 56.4 (C₇), 53.3 (C₁₅), 33.5 (C₅), 31.7 (C₉), 31.1 (C₆), 30.7 (C₁₂), 25.2 (C₈), 19.2 (C₁₃), 13.8 (C₁₄). ***m/z* HRMS** found [M + H]⁺ 444.2892, C₃₀H₃₈NO₂⁺ requires 444.2897.

***tert*-butyl 3-(6-butoxy-3-(dibenzylamino)-6-oxohexyl)-1*H*-indole-1-carboxylate (348w)**

Prepared according to general procedure A using dibenzylamine (39 μL , 0.2 mmol), 1-Boc-3-(3-oxopropyl)indole^[384] (109 mg, 0.4 mmol), *n*-butyl acrylate (57 μL , 0.4 mmol), methoxyethyl- Hantzsch Ester (94 mg, 0.3 mmol), 4Å MS (100 mg), propanoic acid (3 μL , 40 μmol) and *fac*-Ir(ppy)₃ (1.4 mg, 2 μmol) in anhydrous degassed dichloromethane (2 mL). The crude reaction mixture was purified by flash column chromatography (0.5% Et₃N in dichloromethane) to afford the product as a colorless oil (95 mg, 81%). **R_f** (20% EtOAc in P.E.): 0.48; **IR** $\nu_{\text{max}}/\text{cm}^{-1}$ (film): 3029, 2930, 1727, 1603, 1494, 1452, 1368, 1252, 1155, 1080, 1018, 910, 857, 766, 743, 697. **¹H NMR** (400 MHz, CDCl₃) δ : 8.17 (1 H, br s, H₆), 7.53 (1 H, d, J = 7.7 Hz, H₉), 7.35 (1 H, t, J = 7.8 Hz, H₇), 7.30 – 7.18 (12 H, m, H₄, 8, 24,25,26), 4.09 – 3.95 (2 H, m, H₁₈), 3.68 (2 H, d, J = 13.6 Hz, H_{22a}), 3.42 (2 H, d, J = 13.6 Hz, H_{22b}), 2.71 (2 H, t, J = 7.6 Hz, H₁₂), 2.60 – 2.46 (2 H, m, H_{14,16a}), 2.36 – 2.26 (1 H, m, H_{16b}), 2.19 – 2.08 (1 H, m, H_{13a}), 1.97 – 1.76 (2 H, m, H₁₅), 1.69 (9 H, s, H₁), 1.65 – 1.54 (3 H, m, H_{13b,19}), 1.38 (2 H, sext, J = 7.6 Hz, H₂₀), 0.96 (3 H, t, J = 7.4 Hz, H₂₁); **¹³C NMR** (101 MHz, CDCl₃) δ : 174.0 (C₁₇), 149.8 (C₃), 140.1 (C₂₃), 135.7 (C₅), 130.6 (C_{4/8/10/11}), 128.8 (C₂₄), 128.1 (C₂₅), 126.8 (C₂₆), 124.3 (C₇), 122.5 (C_{4/8/10/11}), 122.3 (C_{4/8/10/11}), 120.8 (C_{4/8/10/11}), 118.9 (C₉), 115.4 (C₆), 83.2 (C₂), 64.2 (C₁₈), 56.3 (C₁₄), 53.3 (C₂₂), 31.6 (C₁₆), 30.7 (C₁₉), 28.3 (C₁), 28.1 (C₁₃), 25.2 (C₁₅), 22.6 (C₁₂), 19.2 (C₂₀), 13.8 (C₂₁). ***m/z* HRMS** found [M + H]⁺ 583.3518, C₃₇H₄₇N₂O₄⁺ requires 583.3530.

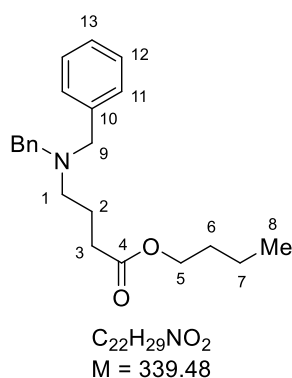
butyl 4-(dibenzylamino)-6-(5-methylfuran-2-yl)hexanoate (348x)



Prepared according to general procedure A using dibenzylamine (39 μL , 0.2 mmol), 3-(5-methyl-2-furyl)propionaldehyde (53 μL , 0.4 mmol), *n*-butyl acrylate (57 μL , 0.4 mmol), methoxyethyl- Hantzsch Ester (94 mg, 0.3 mmol), 4Å MS (100 mg), propanoic acid (3 μL , 40 μmol) and *fac*-Ir(ppy)₃ (1.4 mg, 2 μmol) in anhydrous degassed dichloromethane (2 mL). The crude reaction mixture was purified by flash column chromatography (0.5% Et₃N in

dichloromethane) to afford the product as a colorless oil (75 mg, 84%). **R_f** (10% EtOAc in P.E.): 0.46; **IR** $\nu_{\text{max}}/\text{cm}^{-1}$ (film): 3029, 2934, 1730, 1494, 1453, 1360, 1217, 1173, 1115, 950, 780, 745, 697. **¹H NMR** (400 MHz, CDCl₃) δ : 7.42 – 7.21 (10 H, m, H_{18,19,20}), 5.86 (1 H, s, H₃), 5.79 (1 H, d, $J = 2.8$ Hz, H₄), 4.10 – 4.00 (2 H, m, H₁₂), 3.68 (2 H, d, $J = 13.9$ Hz, H_{16a}), 3.56 (2 H, d, $J = 13.8$ Hz, H_{16b}), 2.74 – 2.64 (1 H, m, H_{6a}), 2.63 – 2.40 (3 H, m, H_{6b,8,10a}), 2.34 – 2.24 (4 H, m, H_{1,10b}), 2.12 – 2.00 (1 H, m, H_{7a}), 1.99 – 1.88 (1 H, m, H_{9a}), 1.77 – 1.66 (1 H, m, H_{9b}), 1.65 – 1.54 (3 H, m, H_{7b,13}), 1.40 (2 H, sext, $J = 7.7$ Hz, H₁₄), 0.98 (3 H, t, $J = 7.5$ Hz, H₁₅); **¹³C NMR** (101 MHz, CDCl₃) δ : 173.9 (C₁₁), 154.1 (C₅), 150.2 (C₂), 140.2 (C₁₇), 129.0 (C₁₈), 128.2 (C₁₉), 126.8 (C₂₀), 105.9 (C₃), 105.5 (C₄), 64.2 (C₁₂), 56.4 (C₈), 53.3 (C₁₆), 31.8 (C₁₀), 30.7 (C₁₃), 27.7 (C₇), 25.8 (C₆), 25.0 (C₉), 19.2 (C₁₄), 13.8 (C₁₅), 13.6 (C₁). **m/z HRMS** found $[M]^+$ 447.2784, C₂₉H₃₇NO₃⁺ requires 447.2779.

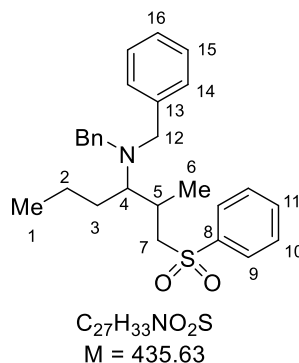
butyl 4-(dibenzylamino)butanoate (348ak)



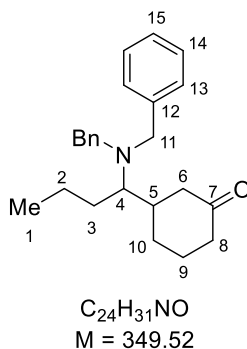
Prepared according to general procedure B using dibenzylamine (39 μL , 0.2 mmol), paraformaldehyde (18 mg, 0.60 mmol), *n*-butyl acrylate (32 μL , 0.22 mmol), ethyl- Hantzsch Ester (76 mg, 0.3 mmol), 4Å MS (100 mg), propanoic acid (3 μL , 40 μmol) and *fac*-Ir(ppy)₃ (1.4 mg, 2 μmol) in anhydrous degassed dichloromethane (2 mL). The crude reaction mixture was purified by flash column chromatography (0.5% Et₃N in dichloromethane) to afford the product as a colorless oil (28 mg, 41%). **R_f** (10% EtOAc in P.E.): 0.42; **IR** $\nu_{\text{max}}/\text{cm}^{-1}$ (film): 3063, 3029, 2958, 2872, 2799, 1731, 1494, 1452, 1364, 1245, 1171, 1117, 1071, 1027, 956, 732, 697. **¹H NMR** (500 MHz, CDCl₃) δ : 7.41 – 7.18 (10 H, m, H_{11,12,13}), 4.01 (2 H, t, $J = 6.8$ Hz, H₅), 3.55 (4 H, s, H₉), 2.45 (2 H, t, $J = 6.9$ Hz, H₁), 2.31 (2 H, t, $J = 7.5$ Hz, H₃), 1.83 (2 H, quint, $J = 6.9$ Hz, H₂), 1.57 (2 H, quint, $J = 6.9$ Hz, H₆), 1.36 (2 H, sext, $J = 7.5$ Hz, H₇), 0.93 (3 H, t, $J = 7.4$ Hz, H₈); **¹³C NMR** (126 MHz, CDCl₃) δ : 173.8 (C₄), 139.7 (C₁₀), 128.8

(C₁₁), 128.2 (C₁₂), 126.8 (C₁₃), 64.2 (C₅), 58.3 (C₉), 52.5 (C₁), 32.0 (C₃), 30.7 (C₆), 22.4 (C₂), 19.2 (C₇), 13.7 (C₈). **m/z** HRMS found [M + H]⁺ 340.2273, C₂₂H₃₀NO₂⁺ requires 340.2271.

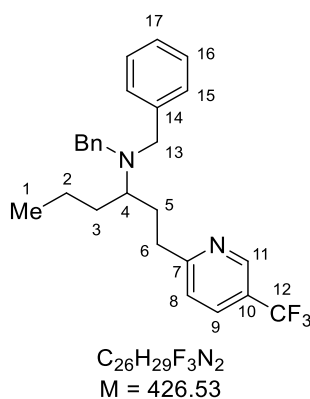
N,N-dibenzyl-2-methyl-1-(phenylsulfonyl)hexan-3-amine (359u)



Prepared according to general procedure A using dibenzylamine (39 μ L, 0.2 mmol), butyraldehyde (36 μ L, 0.4 mmol), 1-propenyl phenyl sulfone^[385] (73 mg, 0.4 mmol), ethyl-Hantzsch Ester (76 mg, 0.3 mmol), 4Å MS (100 mg), propanoic acid (3 μ L, 40 μ mol) and *fac*-Ir(ppy)₃ (1.4 mg, 2 μ mol) in anhydrous degassed dichloromethane (2 mL). The crude reaction mixture was purified twice by flash column chromatography (0.5% Et₃N in dichloromethane and subsequently 2% diethylether in toluene) to afford the product as a colorless oil (47.3 mg, 54%, 1:1 d.r.). **R_f** (20% ethyl acetate in petroleum ether): 0.26; **IR** ν_{max} /cm⁻¹ (film): 3027, 2958, 2925, 2871, 1494, 1447, 1303, 1147, 1086, 1027, 965; **¹H NMR** (400 MHz, CDCl₃) δ : [7.86 (d, *J* = 7.6 Hz), 7.71 (d, *J* = 7.6 Hz) total 2 H, H₉], 7.68 – 7.61 (1 H, m, H₁₁), 7.56 – 7.49 (2 H, m, H₁₀), 7.34 – 7.19 (10 H, m, H_{14,15,16}), [3.88 (d, *J* = 13.8 Hz), 2.98 – 2.90 (m) total 1 H, H_{7a}], [3.66 (d, *J* = 13.8 Hz), 3.64 (d, *J* = 13.8 Hz) total 2 H, H_{12a}], [3.44 (d, *J* = 13.8 Hz), 3.41 (d, *J* = 13.8 Hz) total 2 H, H_{12b}], [2.88 – 2.81 (m), 2.51 – 2.44 (m), total 1 H, H_{7b}], [2.50 – 2.43 (m), 2.22 – 2.16 (m) total 1 H, H₄], [2.42 – 2.32 (m), 2.30 – 2.22 (m) total 1 H, H₅], [1.77 – 1.65 (m), 1.65 – 1.58 (m) total 1 H, H_{3a}], 1.46 – 1.19 (3 H, m, H_{2,3b}), [1.16 (d, *J* = 7.0 Hz), 1.12 (d, *J* = 6.5 Hz) total 3 H, H₆], [0.94 (t, *J* = 7.2 Hz), 0.86 (t, *J* = 7.2 Hz) total 3 H, H₁]. **¹³C NMR** (126 MHz, CDCl₃) δ : [140.6, 140.0 (C₈)], [139.9, 139.6 (C₁₃)], [133.30, 133.28 (C₁₁)], 129.11 (C₁₀), [129.1, 129.00 (C₁₄)], [128.2, 128.3 (C₁₅)], [127.8, 127.7 (C₉)], [127.1, 126.9 (C₁₆)], [61.4, 61.0 (C₄)], [61.3, 60.5 (C₇)], [55.4, 53.7 (C₁₂)], [31.0, 29.9 (C₅)], [29.5, 27.7 (C₃)], [22.5, 20.9 (C₂)], [17.5, 16.4 (C₆)], [14.7, 14.2 (C₁)]. **m/z** HRMS found [M + H]⁺ 436.2301, C₂₇H₃₄NO₂S⁺ requires 436.2305.

3-(1-(dibenzylamino)butyl)cyclohexan-1-one (359v)

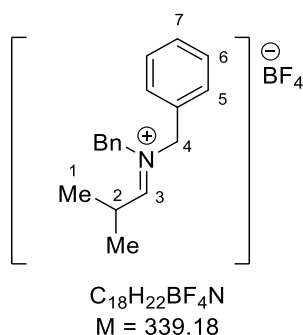
Prepared according to general procedure A using dibenzylamine (39 μL , 0.2 mmol), butyraldehyde (36 μL , 0.4 mmol), 2-cyclohexene-1-one (39 μL , 0.4 mmol), ethyl-Hantzsch Ester (76 mg, 0.3 mmol), 4Å MS (100 mg), propanoic acid (3 μL , 40 μmol) and *fac*-Ir(ppy)₃ (1.4 mg, 2 μmol) in anhydrous degassed dichloromethane (2 mL). The crude reaction mixture was purified by flash column chromatography (0.5% Et₃N in dichloromethane) to afford the product as a colorless oil (45 mg, 65%, 1:1 d.r.). **R_f** (20% ethyl acetate in petroleum ether): 0.45; **IR** $\nu_{\text{max}}/\text{cm}^{-1}$ (film): 3026, 2955, 2931, 2869, 1710, 1602, 1494, 1453, 1374, 1315, 1261, 1227, 1133, 1073, 1027; **¹H NMR** (400 MHz, CDCl₃) δ : 7.36 – 7.19 (10 H, m, H_{13,14,15}), [3.71 (d, $J = 14.0$ Hz), 3.67 (d, $J = 14.0$ Hz) total 2 H, H_{11a}], [3.50 (d, $J = 13.9$ Hz), 3.49 (d, $J = 13.9$ Hz) total 2 H, H_{11b}], [2.79 – 2.73 (m), 2.25 – 2.19 (m) total 1 H, H_{6a}], [2.45 – 2.38 (app q, $J = 7.0$ Hz), 2.37 – 2.32 (m) total 1 H, H₄], [2.37 – 2.30 (m), 2.24 – 2.15 (m) total 2 H, H₈], [2.18 – 2.11 (m), 1.92 – 1.84 (m) total 1 H, H_{6b}], [2.17 – 2.11 (m), 1.82 – 1.75 (m) total 1 H, H_{3/10}], 2.08 – 1.93 (2 H, m, H_{9a,5}), 1.74 – 1.58 (2 H, m, H_{3/10}), 1.58 – 1.47 (1 H, m, H_{9b}), 1.40 – 1.26 (3 H, m, H_{2,3/10}), 0.94 – 0.84 (3 H, m, H₁); **¹³C NMR** (101 MHz, CDCl₃) δ : [212.8, 212.4 (C₇)], [140.1, 140.0 (C₁₂)], [129.0, 128.9 (C₁₃)], 128.2 (C₁₄), [126.90, 126.86 (C₁₅)], [61.8, 61.1 (C₄)], [54.8, 54.3 (C₁₁)], [46.7, 46.5 (C₆)], [41.6, 41.2 (C₅)], 41.5 (C₈), [29.4, 29.2, 28.9, 28.8 (C_{3/10})], [25.64, 25.57 (C₉)], [22.3, 21.9 (C₂)], [14.6, 14.5 (C₁)]. ***m/z* HRMS** found [M + H]⁺ 350.2482, C₂₄H₃₂NO⁺ requires 350.2478.

***N,N*-dibenzyl-1-(5-(trifluoromethyl)pyridin-2-yl)hexan-3-amine (359ag)**

Prepared according to general procedure A using dibenzylamine (39 μL , 0.2 mmol), butyraldehyde (36 μL , 0.4 mmol), 5-(trifluoromethyl)-2-vinylpyridine (69 mg, 0.4 mmol), methoxyethyl-Hantzsch Ester (94 mg, 0.3 mmol), 4 Å MS (100 mg), propanoic acid (3 μL , 40 μmol) and *fac*-Ir(ppy)₃ (1.4 mg, 2 μmol) in anhydrous degassed dichloromethane (2 mL). The crude reaction mixture was purified by flash column chromatography (0.5% Et₃N in dichloromethane) to afford the product as a colorless oil (36 mg, 42%). **R_f** (15% EtOAc in P.E.): 0.40; **IR** $\nu_{\text{max}}/\text{cm}^{-1}$ (film): 3029, 2958, 1731, 1602, 1494, 1454, 1294, 1238, 1169, 1123, 1072, 1027, 900, 746, 699. **¹H NMR** (400 MHz, CDCl₃) δ : 8.74 (1 H, br s, H₁₁), 7.68 (1 H, dd, J = 2.3, 8.1 Hz, H₉), 7.38 – 7.17 (10 H, m, H_{15,16,17}), 6.96 (1 H, d, J = 8.1 Hz, H₈), 3.63 (2 H, d, J = 13.7 Hz, H_{13a}), 3.51 (2 H, d, J = 13.7 Hz, H_{13b}), 3.02 – 2.93 (1 H, m, H_{6a}), 2.81 – 2.72 (1 H, m, H_{6b}), 2.48 (1 H, quint, J = 6.8 Hz, H₄), 2.04 – 1.93 (1 H, m, H_{5a}), 1.79 – 1.63 (2 H, m, H_{3a,5b}), 1.36 – 1.21 (3 H, m, H_{2,3b}), 0.82 (3 H, t, J = 7.1 Hz, H₁); **¹³C NMR** (101 MHz, CDCl₃) δ : 166.6 (C₇), 146.1 (q, J = 4.1 Hz C₁₁), 140.5 (C₁₄), 133.1 (q, J = 3.4 Hz, C₉), 128.9 (C₁₅), 128.1 (C₁₆), 126.7 (C₁₇), 123.9 (q, J = 32.8 Hz, C₁₀), 123.8 (q, J = 272.2 Hz, C₁₂), 122.5 (C₈), 56.3 (C₄), 53.4 (C₁₃), 35.7 (C₆), 31.2 (C₃), 29.9 (C₅), 20.3 (C₂), 14.3 (C₁); **¹⁹F[¹H] NMR** (376 MHz, CDCl₃) δ : –63.2. ***m/z* HRMS** found [M + H]⁺ 427.2351, C₂₆H₃₀F₃N₂⁺ requires 427.2356.

***N*-benzyl-*N*-(2-methylpropylidene)-1-phenylmethanaminium tetrafluoroborate (364)**

Procedure modified from Melchiorre et al.^[231]

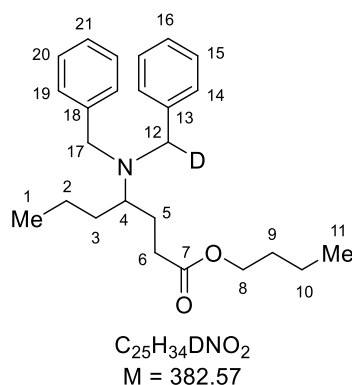


An oven dried Schlenk flask was cooled under a stream of nitrogen, charged with dibenzylammonium tetrafluoroborate (preparation see below, 500 mg, 1.75 mmol), isobutyraldehyde (1.6 mL, 17.5 mmol), powdered activated molecular sieves (4 Å, 250 mg) and anhydrous dichloromethane (6 mL). The flask was sealed under nitrogen and heated for 24 h at 40°C with vigorous stirring. The cooled reaction mixture was Schlenk-filtered and the

filtrate added via cannula into stirred anhydrous Et₂O (200 mL). The colorless precipitate was immediately collected by Schlenk-filtration, washed with anhydrous Et₂O (3 x 6 mL) and dried *in vacuo*. *N*-benzyl-*N*-(2-methylpropylidene)-1-phenylmethanaminium tetrafluoroborate (373 mg, 63%) was obtained as a moisture sensitive colorless powder. The product was stored in a nitrogen glovebox at ambient temperature with no decomposition observed after several months of storage. ¹H NMR (400 MHz, DMSO-*d*₆) δ: 8.96 (1 H, d, *J* = 9.5 Hz, H₃), 7.53 – 7.39 (8 H, m, H_{5/6/7}), 7.35 – 7.28 (2 H, m, H_{5/6/7}), 5.06 (4 H, d, *J* = 10.7 Hz, H₄), 3.35 – 3.20 (1 H, m, H₂), 1.21 (6 H, d, *J* = 6.5 Hz, H₁); ¹³C NMR (101 MHz, DMSO-*d*₆) δ: 189.1, 132.0, 131.8, 130.0, 129.7, 129.6, 129.4, 128.5, 64.1, 55.3, 31.4, 18.7. ¹⁹F[¹H] NMR (376 MHz, DMSO-*d*₆) δ: -149.2. *m/z* HRMS found [M – BF₄]⁺ 252.1735, C₁₈H₂₂N⁺ requires 252.1747.

Dibenzylammonium tetrafluoroborate was obtained by dissolving dibenzylamine (5 mmol) in dry Et₂O (15 mL) followed by dropwise addition of tetrafluoroboric acid diethyl ether complex (5.5 mmol) and collection of the precipitate. Dibenzylammonium tetrafluoroborate (4.3 mmol, 86%) was dried *in vacuo* and stored with the exclusion of moisture.

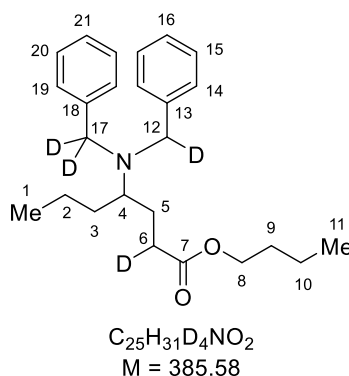
butyl 4-(benzyl(phenylmethyl-*d*)amino)heptanoate (*d*₁-348a)



Prepared according to general procedure A using dibenzylamine (39 μL, 0.2 mmol), butyraldehyde (20 μL, 0.22 mmol), *n*-butyl acrylate (32 μL, 0.22 mmol), diethyl 2,6-dimethyl-1,4-dihydropyridine-3,5-dicarboxylate-4,4-*d*₂ (77 mg, 0.3 mmol), 4Å MS (100 mg), propanoic acid (3 μL, 40 μmol) and *fac*-Ir(ppy)₃ (1.4 mg, 2 μmol) in anhydrous degassed dichloromethane (2 mL). The crude reaction mixture was purified by flash column chromatography (1% EtOAc in P.E.) to afford the product as a colorless oil (53 mg, 70%). *R*_f (10% EtOAc in P.E.): 0.47; **IR** ν_{max}/cm⁻¹ (film): 3058, 3027, 2957, 2929, 2871, 1732, 1602, 1494, 1453, 1245, 1172, 1071, 1027, 738, 697. ¹H NMR (400 MHz, CDCl₃) δ: 7.50 – 7.20

(10 H, m, H_{14,15,16,19,20,21}), 4.11 – 3.96 (2 H, m, H₈), 3.74 – 3.66 (1 H, m, H_{12/17}), 3.55 – 3.45 (2 H, m, H_{12/17}), 2.57 – 2.54 (2 H, m, H_{4,6a}), 2.35 – 2.24 (1 H, m, H_{6b}), 1.19 – 1.78 (1 H, m, H_{5a}), 1.77 – 1.65 (2 H, m, H_{3a,5b}), 1.61 (2 H, quint, $J = 7.0$ Hz, H₉), 1.45 – 1.32 (4 H, m, H_{2,10}), 1.29 – 1.18 (1 H, m, H_{3b}), 0.97 (3 H, t, $J = 7.4$ Hz, H₁₁), 0.91 (3 H, t, $J = 7.3$ Hz, H₁); ²H NMR (76.8 MHz, CHCl₃/CDCl₃) δ : 3.66 (br s, D_{12/17}), 3.47 (br s, D_{12/17}); ¹³C NMR (101 MHz, CDCl₃) δ : 174.1 (C₇), 140.4 (C_{13,18}), 128.9 (C_{14,19}), 128.1 (C_{15,20}), 126.7 (C_{16,21}), 64.1 (C₈), 56.5 (C₄), 53.3 (C_{12,17}), 31.8 (C₆), 31.0 (C₃), 30.7 (C₉), 25.5 (C₅), 20.4 (C₂), 19.2 (C₁₀), 14.3 (C₁), 13.8 (C₁₁). *m/z* HRMS found [M]⁺ 382.2728, C₂₅H₃₄DNO₂⁺ requires 382.2725.

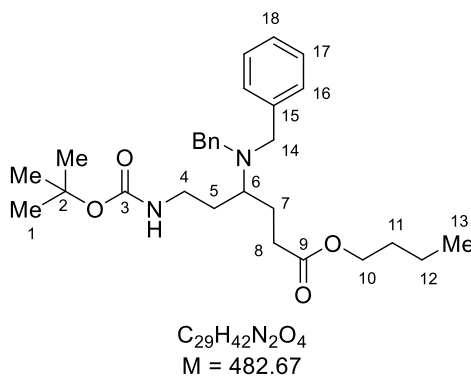
butyl 4-((phenylmethyl-*d*)(phenylmethyl-*d*₂)amino)heptanoate-2-*d* (d₄-348a)



Prepared according to general procedure A using bis(phenylmethyl-*d*₂)amine (39 μ L, 0.2 mmol), butyraldehyde (20 μ L, 0.22 mmol), *n*-butyl acrylate (32 μ L, 0.22 mmol), ethyl-Hantzsch Ester (76 mg, 0.3 mmol), 4Å MS (100 mg), propanoic acid (3 μ L, 40 μ mol) and *fac*-Ir(ppy)₃ (1.4 mg, 2 μ mol) in anhydrous degassed dichloromethane (2 mL). The crude reaction mixture was purified by flash column chromatography (1% EtOAc in P.E.) to afford the product as a colorless oil (52 mg, 67%). *R_f* (10% EtOAc in P.E.): 0.39; **IR** ν_{max} /cm⁻¹ (film): 3025, 2956, 2930, 2871, 1731, 1602, 1493, 1448, 1380, 1238, 1176, 1073, 1026, 836, 728, 696. ¹H NMR (400 MHz, CDCl₃) δ : 7.47 – 7.17 (10 H, m, H_{14,15,16,19,20,21}), 4.09 – 3.08 (2 H, m, H₈), [3.68 (s), 3.49 (s) total 1 H, H_{12,17}], 2.55 – 2.44 (1 H, m, H_{4,6a}), 2.28 (1 H, t, $J = 7.3$ Hz, H_{6b}), 1.90 – 1.79 (1 H, m, H_{5a}), 1.77 – 1.65 (2 H, m, H_{3a,5b}), 1.61 (2 H, quint, $J = 7.0$ Hz, H₉), 1.46 – 1.33 (4 H, m, H_{2,10}), 1.29 – 1.18 (1 H, m, H_{3b}), 0.97 (3 H, t, $J = 7.3$ Hz, H₁₁), 0.91 (3 H, t, $J = 7.1$ Hz, H₁); ²H NMR (76.8 MHz, CHCl₃/CDCl₃) δ : 3.67 (br s, D_{12/17}), 3.50 (br s, D_{12/17}), 2.50 (br s, D₆), 2.29 (br s, D₆); ¹³C NMR (101 MHz, CDCl₃) δ : 174.1 (C₇), 140.3 (C_{13,18}), 128.9 (C_{14,19}), 128.1 (C_{15,20}), 126.7 (C_{16,21}), 64.1 (C₈), 56.5 (C₄), 52.7 (C_{12,17}), 31.6

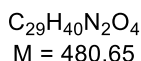
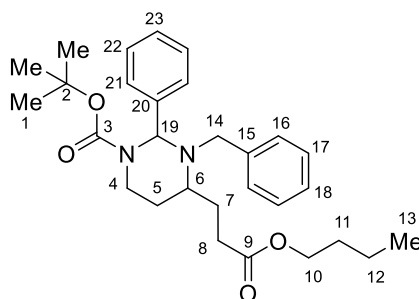
(C₆), 31.0 (C₃), 30.7 (C₉), 25.5 (C₅), 20.4 (C₂), 19.2 (C₁₀), 14.3 (C₁), 13.8 (C₁₁). *m/z* HRMS found [M + H]⁺ 386.2997, C₂₅H₃₂D₄NO₂⁺ requires 386.2996.

butyl 6-((*tert*-butoxycarbonyl)amino)-4-(dibenzylamino)hexanoate (369)



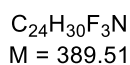
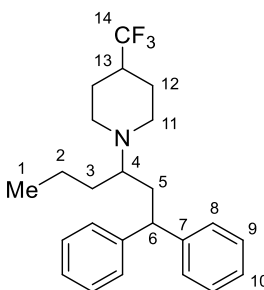
Prepared according to general procedure A using dibenzylamine (39 μ L, 0.2 mmol), *tert*-butyl 3-oxopropylcarbamate (38 mg, 0.22 mmol), *n*-butyl acrylate (32 μ L, 0.22 mmol), ethyl-Hantzsch Ester (76 mg, 0.3 mmol), 4Å MS (100 mg), propanoic acid (3 μ L, 40 μ mol) and *fac*-Ir(ppy)₃ (1.4 mg, 2 μ mol) in anhydrous degassed dichloromethane (2 mL). The crude reaction mixture was purified by flash column chromatography (1–8% EtOAc in dichloromethane) to afford the product as a colorless oil (28 mg, 29%). **R_f** (10% EtOAc in dichloromethane): 0.80; **IR** $\nu_{\text{max}}/\text{cm}^{-1}$ (film): 3363, 3030, 2959, 2930, 1711, 1494, 1453, 1364, 1245, 1166, 1071, 1027, 950, 746, 698. **¹H NMR** (500 MHz, CDCl₃) δ : 7.34 – 7.20 (10 H, m, H_{16,17,18}), 4.63 (1 H, br s, N–H), 4.04 – 3.95 (2 H, m, H₁₀), 3.55 (4 H, s, H₁₄), 3.27 – 3.18 (1 H, m, H_{4a}), 3.12 – 3.02 (1 H, m, H_{4b}), 2.50 (1 H, quint, *J* = 6.9 Hz, H₆), 2.32 (2 H, br t, *J* = 7.2 Hz, H₈), 2.00 – 1.91 (1 H, m, H_{7a}), 1.83 – 1.75 (1 H, m, H_{5a}), 1.63 – 1.52 (3 H, m, H_{7b,11}), 1.48 – 1.39 (10 H, m, H_{1,5b}), 1.36 (2 H, sext, *J* = 7.4 Hz, H₁₂), 0.94 (3 H, t, *J* = 7.5 Hz, H₁₃); **¹³C NMR** (126 MHz, CDCl₃) δ : 173.7 (C₉), 155.9 (C₃), 139.9 (C₁₅), 129.1 (C₁₆), 128.3 (C₁₇), 127.0 (C₁₈), 78.8 (C₂), 64.3 (C₁₀), 54.5 (C₆), 53.2 (C₁₄), 38.4 (C₄), 31.6 (C₈), 30.6 (C₁₁), 29.1 (C₅), 28.5 (C₁), 24.3 (C₇), 19.2 (C₁₂), 13.7 (C₁₃). *m/z* HRMS found [M + H]⁺ 483.3208, C₂₉H₄₃N₂O₄⁺ requires 483.3217. Cyclization product *tert*-butyl 3-benzyl-4-(3-butoxy-3-oxopropyl)-2-phenyltetra-hydropyrimidine-1(2*H*)-carboxylate (**370**) was also isolated from the reaction mixture as a colorless oil (21 mg, 22 %, mixture of diastereomers d. r. 5.5 : 1).

tert-butyl 3-benzyl-4-(3-butoxy-3-oxopropyl)-2-phenyltetrahydropyrimidine-1(2H)-carboxylate (370)



Major diastereomer: 1H NMR (500 MHz, $CDCl_3$) δ : 7.47 (2 H, d, J = 7.7 Hz, H_{16}), 7.39 – 7.16 (8 H, m, $H_{17,18,21,22,23}$), 5.83 (1 H, s, H_{19}), 4.28 (1 H, dd, J = 5.0, 13.4 Hz, H_{4a}), 4.06 (2 H, t, J = 6.7 Hz, H_{10}), 3.90 (1 H, d, J = 14.1 Hz, H_{14a}), 3.72 (1 H, d, J = 14.1 Hz, H_{14b}), 3.08 – 2.99 (1 H, m, H_6), 2.95 (1 H, dd, J = 3.9, 13.1 Hz, H_{4b}), 2.67 – 2.59 (1 H, m, H_{8a}), 2.51 – 2.43 (1 H, m, H_{8b}), 1.98 – 1.88 (1 H, m, H_{7a}), 1.88 – 1.78 (1 H, m, H_{5a}), 1.78 – 1.69 (1 H, m, H_{7b}), 1.63 – 1.55 (2 H, m, H_{11}), 1.37 (2 H, sext, J = 7.7 Hz, H_{12}), 1.30 (9 H, s, H_1), 1.18 (1 H, d, J = 13.2 Hz, H_{5b}), 0.93 (3 H, t, J = 7.6 Hz, H_{13}). ^{13}C NMR (126 MHz, $CDCl_3$) δ : 173.5 (C_9), 155.9 (C_3), 139.3 (C_{15}), 138.6 (C_{20}), 128.74 (C_{16}), 128.65 (C_{21}), 128.4 (C_{17}), 127.15 (C_{18}), 127.08 (C_{23}), 126.9 (C_{22}), 79.9 (C_2), 71.0 (C_{19}), 64.4 (C_{10}), 52.0 (C_6), 47.5 (C_{14}), 38.7 (C_4), 30.8 (C_8), 30.7 (C_{11}), 28.2 (C_1), 28.1 (C_7), 25.3 (C_5), 19.2 (C_{12}), 13.7 (C_{13}). ***m/z* HRMS** found $[M + H]^+$ 481.3057, $C_{29}H_{41}N_2O_4^+$ requires 481.3061.

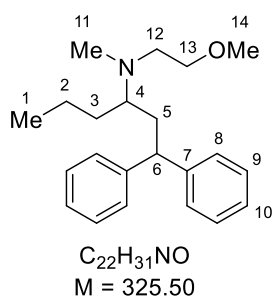
1-(1,1-diphenylhexan-3-yl)-4-(trifluoromethyl)piperidine (378b)



Prepared according to general procedure A using 4-(trifluoromethyl)piperidine hydrochloride (32 mg, 0.2 mmol), triethylamine (28 μ L, 0.2 mmol), butyraldehyde (36 μ L, 0.4 mmol), 1,1-

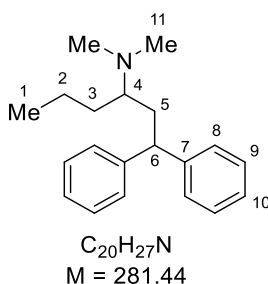
diphenylethene (71 μL , 0.4 mmol), ethyl-Hantzsch Ester (76 mg, 0.3 mmol), 4 \AA MS (100 mg), propanoic acid (3 μL , 40 μmol) and *fac*-Ir(ppy)₃ (1.4 mg, 2 μmol) in anhydrous degassed dichloromethane (2 mL). The crude reaction mixture was filtered, the solvent removed *in vacuo* and subsequently dissolved in a solution of lithium hydroxide monohydrate (84 mg, 20 mmol) in THF/H₂O (6 mL, 5:1). The mixture was heated to a vigorous reflux for 2 hours, cooled to room temperature and diluted with saturated aqueous NaHCO₃ (10 mL). The aqueous was extracted with EtOAc (3 x 10 mL) and the organics combined. The mixture was acidified using 10% HCl (aq.) (25 mL), the organics separated and the aqueous washed with Et₂O (2 x 20 mL). The aqueous was cooled in an ice bath and carefully basified using solid NaOH until pH = 10. The aqueous was extracted with dichloromethane (3 x 20 mL), the organics combined and washed with brine (25 mL), dried over Na₂SO₄, filtered and the solvent removed *in vacuo*. The subsequent residue was purified by flash column chromatography (gradient elution: 0.5% Et₃N in dichloromethane to 1% MeOH, 0.5% Et₃N in dichloromethane) to afford the product as a viscous colorless oil (42 mg, 54%). **R_f** (5% EtOAc in P.E.): 0.25; **IR** $\nu_{\text{max}}/\text{cm}^{-1}$ (film): 3027, 2954, 2929, 2864, 2804, 1735, 1599, 1494, 1451, 1382, 1338, 1281, 1253, 1136, 1080, 1030, 905, 747, 699. **¹H NMR** (500 MHz, CDCl₃) δ : 7.31 – 7.15 (10 H, m, H_{8,9,10}), 4.22 (1 H, dd, J = 6.0, 9.7 Hz), 2.76 (1 H, br d, J = 10.9 Hz, H_{11a}), 2.54 (1 H, 1 H, br d, J = 10.9 Hz, H_{11a'}), 2.36 (1 H, dt, J = 10.9, 2.0 Hz, H_{11b}), 2.24 – 2.13 (2 H, m, H₄, H_{11b'}), 2.10 – 1.99 (2 H, m, H₅), 1.97 – 1.88 (1 H, m, H₁₃), 1.84 – 1.77 (2 H, m, H_{12a}), 1.63 – 1.53 (2 H, m, H_{12b}), 1.48 – 1.41 (1 H, m, H_{3a}), 1.34 – 1.27 (1 H, m, H_{2a}), 1.21 – 1.14 (2 H, m, H_{2b,3b}), 0.82 (3 H, t, J = 7.1 Hz, H₁); **¹³C NMR** (126 MHz, CDCl₃) δ : 145.6 (C₇), 145.0 (C_{7'}), 128.3 (C_{8/8'/9/9'}), 128.3 (C_{8/8'/9/9'}), 128.1 (C_{8/8'/9/9'}), 127.8 (C_{8/8'/9/9'}), 127.6 (q, J = 277.9 Hz, C₁₄), 126.0 (C₁₀), 125.9 (C_{10'}), 61.0 (C₄), 49.4 (C₁₁), 47.6 (C₆), 45.1 (C_{11'}), 41.1 (q, J = 27.4 Hz, C₁₃), 36.6 (C₅), 31.1 (C₃), 25.5 (C₁₂), 25.3 (C_{12'}), 20.4 (C₂), 14.2 (C₁); **¹⁹F[¹H] NMR** (376 MHz, CDCl₃) δ : -74.70. ***m/z* HRMS** found [M + H]⁺ 390.2404, C₂₄H₃₁F₃N⁺ requires 390.2403.

***N*-(2-methoxyethyl)-*N*-methyl-1,1-diphenylhexan-3-amine (378k)**



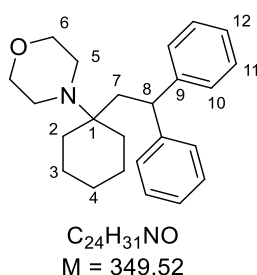
Prepared according to general procedure A using (2-methoxyethyl)methylamine (22 μ L, 0.2 mmol), butyraldehyde (36 μ L, 0.4 mmol), 1,1-diphenylethene (71 μ L, 0.4 mmol), ethyl-Hantzsch Ester (76 mg, 0.3 mmol), 4Å MS (100 mg), propanoic acid (3 μ L, 40 μ mol) and *fac*-Ir(ppy)₃ (1.4 mg, 2 μ mol) in anhydrous degassed dichloromethane (2 mL). The crude reaction mixture was filtered, the solvent removed *in vacuo* and subsequently dissolved in a solution of lithium hydroxide monohydrate (84 mg, 20 mmol) in THF/H₂O (6 mL, 5:1). The mixture was heated to a vigorous reflux for 2 hours, cooled to room temperature and diluted with saturated aqueous NaHCO₃ (10 mL). The aqueous was extracted with EtOAc (3 x 10 mL) and the organics combined. The mixture was acidified using 10% HCl (aq.) (25 mL), the organics separated and the aqueous washed with Et₂O (2 x 20 mL). The aqueous was cooled in an ice bath and carefully basified using solid NaOH until pH = 10. The aqueous was extracted with dichloromethane (3 x 20 mL), the organics combined and washed with brine (25 mL), dried over Na₂SO₄, filtered and the solvent removed *in vacuo*. The subsequent residue was purified by flash column chromatography (gradient elution: 0.5% MeOH in dichloromethane to 10% MeOH in dichloromethane) to afford the product as a colorless oil (56 mg, 86%). **R_f** (10% MeOH in dichloromethane): 0.44; **IR** ν_{max} /cm⁻¹ (film): 2955, 2929, 2868, 1599, 1493, 1450, 1119, 1068, 1030, 967, 746, 699. **¹H NMR** (400 MHz, CDCl₃) δ : 7.30 – 7.21 (8 H, m, H_{8/9}), 7.18 – 7.11 (2 H, m, H₁₀), 4.22 (1 H, dd, *J* = 6.7, 8.7 Hz, H₆), 3.33 – 3.25 (5 H, m, H_{13,14}), 2.62 – 2.53 (1 H, m, H_{12a}), 2.52 – 2.44 (1 H, m, H_{12b}), 2.29 – 2.22 (1 H, m, H₄), 2.20 (3 H, s, H₁₁), 2.08 – 1.96 (2 H, m, H₅), 1.49 – 1.37 (1 H, m, H_{3a}), 1.34 – 1.13 (3 H, m, H_{2a,2b,3b}), 0.81 (3 H, t, *J* = 7.0 Hz, H₁); **¹³C NMR** (101 MHz, CDCl₃) δ : 145.8 (C₇), 145.0 (C_{7'}), 128.3 (C_{8/9}), 128.3 (C_{8/9}), 128.2 (C_{8/9}), 127.9 (C_{8/9}), 126.0 (C₁₀), 125.9 (C_{10'}), 71.8 (C₁₃), 60.0 (C₄), 58.7 (C₁₄), 52.8 (C₁₂), 47.6 (C₆), 37.4 (C₁₁), 36.8 (C₅), 31.1 (C₃), 20.3 (C₂), 14.3 (C₁). **m/z HRMS** found [M + H]⁺ 326.2483, C₂₂H₃₂NO⁺ requires 326.2478.

N,N-dimethyl-1,1-diphenylhexan-3-amine (378I)



Prepared according to general procedure A using dimethylamine (40 wt.% in H₂O, 25 μ L, 0.2 mmol), butyraldehyde (36 μ L, 0.4 mmol), 1,1-diphenylethene (71 μ L, 0.4 mmol), ethyl-Hantzsch Ester (76 mg, 0.3 mmol), 4Å MS (100 mg), propanoic acid (3 μ L, 40 μ mol) and *fac*-Ir(ppy)₃ (1.4 mg, 2 μ mol) in anhydrous degassed dichloromethane (2 mL). The crude reaction mixture was filtered, the solvent removed *in vacuo* and subsequently dissolved in a solution of lithium hydroxide monohydrate (84 mg, 20 mmol) in THF/H₂O (6 mL, 5:1). The mixture was heated to a vigorous reflux for 2 hours, cooled to room temperature and diluted with saturated aqueous NaHCO₃ (10 mL). The aqueous was extracted with EtOAc (3 x 10 mL) and the organics combined. The mixture was acidified using 10% HCl (aq.) (25 mL), the organics separated and the aqueous washed with Et₂O (2 x 20 mL). The aqueous was cooled in an ice bath and carefully basified using solid NaOH until pH = 10. The aqueous was extracted with dichloromethane (3 x 20 mL), the organics combined and washed with brine (25 mL), dried over Na₂SO₄, filtered and the solvent removed *in vacuo*. The subsequent residue was purified by flash column chromatography (gradient elution: 0.5% MeOH in dichloromethane to 8% MeOH in dichloromethane) to afford the product as a colorless oil (50 mg, 88%). **R_f** (5% MeOH in dichloromethane): 0.10; **IR** ν_{max} /cm⁻¹ (film): 3026, 2956, 2929, 2856, 2771, 1599, 1493, 1450, 1378, 1263, 1154, 1030, 912, 774, 746, 697. **¹H NMR** (400 MHz, CDCl₃) δ : 7.33 – 7.26 (8 H, m, H_{8,9}), 7.22 – 7.15 (2 H, m, H₁₀), 4.20 (1 H, dd, *J* = 6.5, 8.5 Hz, H₆), 2.21 (7 H, br s, H_{4,11}), 2.17 – 2.08 (1 H, m, H_{5a}), 2.04 – 1.94 (1 H, m, H_{5b}), 1.52 – 1.41 (1 H, m, H_{3a}), 1.37 – 1.16 (3 H, m, H_{3b,2a,2b}), 0.85 (3 H, t, *J* = 7.2 Hz, H₁); **¹³C NMR** (126 MHz, CDCl₃) δ : 145.1 (br s, C₇), 128.4 (C_{8/9}), 128.3 (C_{8/9}), 128.1 (C_{8/9}), 127.9 (C_{8/9}), 126.0 (br s, C₁₀), 60.6 (br s, C₄), 47.7 (C₆), 40.1 (C₁₁), 36.1 (C₅), 30.6 (C₃), 20.2 (C₂), 14.2 (C₁). **m/z** **HRMS** found [M + H]⁺ 282.2223, C₂₀H₂₈N⁺ requires 282.2216.

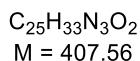
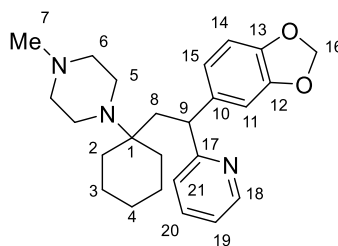
4-(1-(2,2-diphenylethyl)cyclohexyl)morpholine (380b)



Prepared according to general procedure A using 4-cyclohex-1-enylmorpholine (34 μ L, 0.2 mmol), 1,1-diphenylethene (71 μ L, 0.4 mmol), ethyl-Hantzsch Ester (76 mg, 0.3 mmol), 4Å

MS (100 mg), propanoic acid (3 μ L, 40 μ mol) and *fac*-Ir(ppy)₃ (1.4 mg, 2 μ mol) in anhydrous degassed dichloromethane (2 mL). The crude reaction mixture was filtered, the solvent removed *in vacuo* and subsequently dissolved in a solution of lithium hydroxide monohydrate (84 mg, 20 mmol) in THF/H₂O (6 mL, 5:1). The mixture was heated to a vigorous reflux for 2 hours, cooled to room temperature and diluted with saturated aqueous NaHCO₃ (10 mL). The aqueous was extracted with Et₂O (3 x 10 mL) and the organics combined, washed with brine (25 mL), dried over Na₂SO₄, filtered and the solvent removed *in vacuo*. The subsequent residue was purified by flash column chromatography (1% EtOAc and 0.5% Et₃N in P.E.) to afford the product as a colorless oil (41 mg, 59%). **R_f** (20% EtOAc in P.E.): 0.55; **IR** ν_{max} /cm⁻¹ (film): 3024, 2932, 2849, 1598, 1492, 1451, 1266, 1118, 1030, 979, 854, 743, 702. **¹H NMR** (400 MHz, CDCl₃) δ : 7.33 – 7.20 (8 H, m, H_{10/11/12}), 7.17 – 7.08 (2 H, m, H_{10/11/12}), 4.10 (1 H, t, *J* = 6.4 Hz, H₈), 3.65 – 3.60 (4 H, m, H₆), 2.59 – 2.48 (4 H, m, H₅), 2.24 (2 H, d, *J* = 6.3 Hz, H₇), 1.57 – 1.35 (5 H, m, H_{2/3/4}), 1.30 – 1.14 (5 H, m, H_{2/3/4}); **¹³C NMR** (101 MHz, CDCl₃) δ : 146.8 (C₉), 128.4 (C₁₀), 127.7 (C₁₁), 125.9 (C₁₂), 68.1 (C₆), 58.1 (C₁), 47.1 (C₈), 44.9 (C₅), 38.8 (C₇), 32.4 (C₂), 26.2 (C₄), 21.3 (C₃). ***m/z* HRMS** found [M + H]⁺ 350.2484, C₂₄H₃₂NO⁺ requires 350.2484.

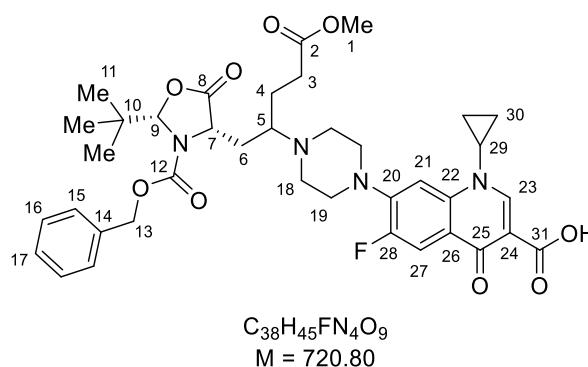
1-(1-(2-(benzo[*d*][1,3]dioxol-5-yl)-2-(pyridin-2-yl)ethyl)cyclohexyl)-4-methylpiperazine (380c)



Prepared according to general procedure A using 1-(cyclohex-1-en-1-yl)-4-methylpiperazine^[386] (36 mg, 0.2 mmol), 2-(1-(benzo[*d*][1,3]dioxol-5-yl)vinyl)pyridine (90 mg, 0.4 mmol), ethyl-Hantzsch Ester (76 mg, 0.3 mmol), 4Å MS (100 mg), propanoic acid (3 μ L, 40 μ mol) and *fac*-Ir(ppy)₃ (1.4 mg, 2 μ mol) in anhydrous degassed dichloromethane (2 mL). The crude reaction mixture was purified by flash column chromatography (1% aqueous ammonia, 9% MeOH in dichloromethane) to afford the product as a brown oil (26 mg, 32%).

R_f (EtOAc): 0.05; **IR** $\nu_{\text{max}}/\text{cm}^{-1}$ (film): 2919, 2849, 2790, 1588, 1485, 1432, 1243, 1094, 1037, 937, 799, 747. **¹H NMR** (400 MHz, C₆D₆) δ : 8.47 (1 H, br d, J = 4.6 Hz, H₁₈), 7.27 (1 H, d, J = 1.6 Hz, H₁₁), 6.99 (1 H, dt, J = 1.9, 7.6 Hz, H₂₀), 6.94 – 6.88 (2 H, m, H_{15,21}), 6.65 (1 H, d, J = 8.0 Hz, H₁₄), 6.53 (1 H, ddd, J = 1.2, 4.8, 7.4 Hz, H₁₉), 5.28 (1 H, d, J = 1.4 Hz, H_{16a}), 5.25 (1 H, d, J = 1.4 Hz, H_{16b}), 4.31 (1 H, br t, J = 5.9 Hz, H₉), 2.98 (1 H, dd, J = 7.3, 14.7 Hz, H_{8a}), 2.59 (4 H, br t, J = 4.8 Hz, H₅), 2.30 (4 H, br s, H₆), 2.16 (3 H, s, H₇), 2.15 (1 H, dd, J = 4.7, 14.5 Hz, H_{8b}), 1.62 – 1.17 (10 H, m, H_{2,3,4}); **¹³C NMR** (101 MHz, C₆D₆) δ : 165.4 (C₁₇), 149.4 (C₁₈), 148.3 (C₁₂), 146.4 (C₁₃), 140.9 (C₁₀), 135.9 (C₂₀), 123.0 (C₂₁), 121.2 (C₁₅), 120.9 (C₁₉), 109.0 (C₁₁), 108.3 (C₁₄), 100.7 (C₁₆), 58.2 (C₁), 56.7 (C₆), 49.3 (C₉), 46.2 (C₇), 44.4 (C₅), 39.0 (C₈), 32.9 (C_{2/2'/3/4}), 30.2 (C_{2/2'/3/4}), 26.7 (C_{2/2'/3/4}), 22.0 (C_{2/2'/3/4}). ***m/z*** **HRMS** found $[\text{M} + \text{H}]^+$ 408.2643, C₂₅H₃₄N₃O₂⁺ requires 408.2646.

7-(4-(1-(3-((benzyloxy)carbonyl)-2-(tert-butyl)-5-oxooxazolidin-4-yl)-5-methoxy-5-oxopentan-2-yl)piperazin-1-yl)-1-cyclopropyl-6-fluoro-4-oxo-1,4-dihydroquinoline-3-carboxylic acid (384)



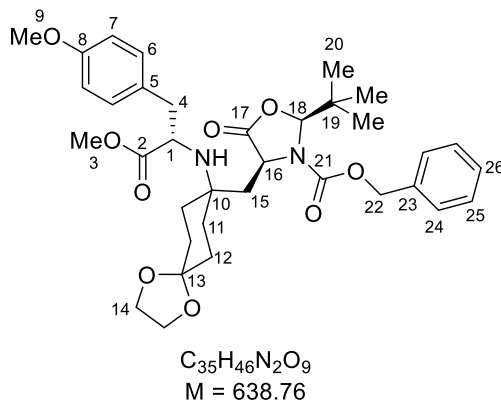
Prepared according to general procedure A using ciprofloxacin (66 mg, 0.2 mmol), methyl 4-oxobutanoate (42 μL , 0.4 mmol), (*S*)-2-(*tert*-butyl)-3-Cbz-4-methyleneoxazolidin-5-one **360** (87 mg, 0.3 mmol, 93% ee), ethyl-Hantzsch Ester (76 mg, 0.3 mmol), 4 \AA MS (100 mg), propanoic acid (3 μL , 40 μmol) and *fac*-Ir(ppy)₃ (1.4 mg, 2 μmol) in anhydrous degassed dichloromethane (2 mL). The crude reaction mixture was concentrated *in vacuo* and purified by flash column chromatography (gradient elution: 5% MeOH in dichloromethane to 1% aqueous ammonia, 9% MeOH in dichloromethane) to afford the product as a pale yellow gum (92 mg, 64%, d.r. 1:1). **R_f** (10% MeOH in dichloromethane): 0.43; **IR** $\nu_{\text{max}}/\text{cm}^{-1}$ (film): 2956, 1787, 1718, 1626, 1492, 1452, 1391, 1334, 1303, 1255, 1227, 1197, 1138, 1039, 1010, 968, 910, 888, 832, 807, 782, 726. **¹H NMR** (500 MHz, CDCl₃) δ : 15.03 (1 H, s, CO₂H), 8.73 (1

H, s, H₂₃), [7.98 (d, $J = 13.1$ Hz), 7.96 (d, $J = 13.1$ Hz) total 1 H, H₂₇], 7.41 – 7.27 (6 H, m, H_{15,16,17,21}), [5.57 (s), 5.55 (s) total 1 H, H₉], [5.19 (d, $J = 11.9$ Hz), 5.18 (d, $J = 11.9$ Hz) total 1 H, H_{13a}], [5.14 (d, $J = 11.9$ Hz), 5.13 (d, $J = 11.9$ Hz) total 1 H, H_{13b}], [4.78 (br d, $J = 5.9$ Hz), 4.60 (br s) total 1 H, H₇], 3.67 (3 H, s, H₁), 3.56 – 3.48 (1 H, m, H₂₉), 3.33 – 3.07 (4 H, m, H₁₉), [3.06 – 3.03 (m), 2.90 (br s) total 1 H, H₅], 2.80 – 2.54 (4 H, m, H₁₈), 2.38 – 2.25 (2 H, m, H₃), 2.16 – 1.93 (2 H, m, H_{6a,4a}), [1.86 – 1.77 (m), 1.72 – 1.64 (m) total 1 H, H_{6b}], 1.65 – 1.54 (1 H, m, H_{4b}), 1.41 – 1.35 (2 H, m, H_{30a}), 1.20 – 1.16 (2 H, m, H_{30b}), 0.97 (9 H, s, H₁₁); **¹³C NMR** (126 MHz, CDCl₃) δ : 177.1 (C₂₅), 173.7 (C₂), [173.5, 172.5 (C₈)], 167.0 (C₃₁), 155.7 (C₁₂), 153.6 (d, $J = 251.6$ Hz, C₂₈), 147.4 (C₂₃), 146.1 (d, $J = 10.2$ Hz, C₂₀), 139.1 (C₂₂), 135.1 (C₁₄), [128.8, 128.7, 128.7, 128.7 (C_{15/16/17})], 119.7 (C₂₆), 112.3 (d, $J = 23.6$ Hz, C₂₇), 108.1 (C₂₄), [104.8, 104.7 (C₂₁)], [96.2, 96.1 (C₉)], [68.6, 68.5 (C₁₃)], [60.5, 59.5 (C₅)], [54.7, 54.1 (C₇)], 51.6 (C₁), 50.3 (C₁₉), 47.4 (C₁₈), 37.1 (C₁₀), 35.3 (C₂₉), [34.2, 33.7 (C₆)], [31.8, 31.7 (C₃)], 24.9 (C₁₁), [24.4, 24.3 (C₄)], 8.2 (C₃₀); **¹⁹F[¹H] NMR** (376 MHz, CDCl₃) δ : –121.6, –121.7. **m/z HRMS** found $[M + H]^+$ 721.3245, C₃₈H₄₆FN₄O₉⁺ requires 721.3243.

5.2.2 Total synthesis of (–) FR901483 and (+)-TAN1251C

5.2.2.1 Development of the multicomponent reaction

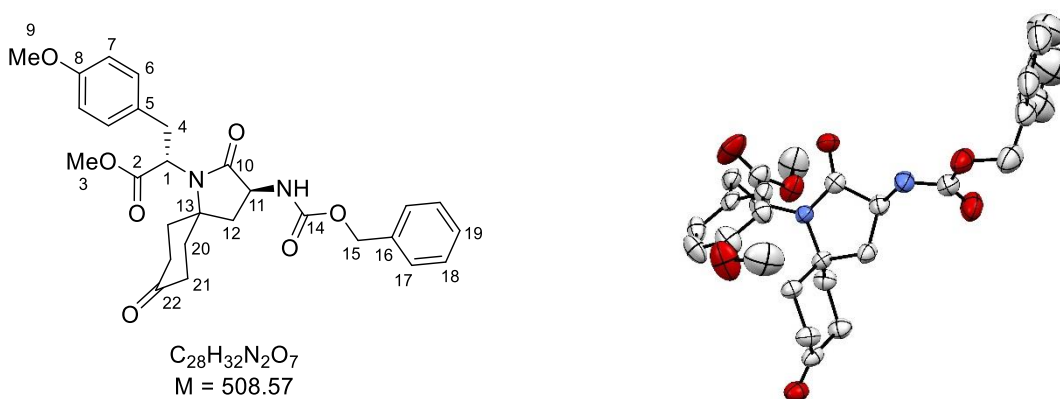
benzyl (2*S*,4*S*)-2-(tert-butyl)-4-((8-(((*S*)-1-methoxy-3-(4-methoxyphenyl)-1-oxopropan-2-yl)amino)-1,4-dioxaspiro[4.5]decan-8-yl)methyl)-5-oxooxazolidine-3-carboxylate (**605**)



A 4 mL PTFE/Silicone-lined septa screw cap (PP) clear glass vial equipped with magnetic stir bar was charged with methyl (*S*)-2-amino-3-(4-methoxyphenyl)propanoate **409** (21 mg, 0.10 mmol, 1.0 equiv), 1,4-cyclo-hexanedione monoethylene acetal (17 mg, 0.11 mmol, 1.1 equiv), benzyl (*S*)-2-(tert-butyl)-4-methylene-5-oxooxazolidine-3-carboxylate **360** (43 mg, 0.15 mmol, 1.5 equiv), Hantzsch Ester (38 mg, 0.15 mmol, 1.5 equiv), *fac*-Ir(ppy)₃ (0.7 mg, 1.5 μmol, 0.01 equiv) and activated 4 Å molecular sieves (50 mg). The vial was sealed and a needle inserted through the septa and the contents evacuated and backfilled with nitrogen (3 x). Anhydrous dichloromethane (1 mL) and trifluoroacetic acid (1.5 μL, 20 μmol) were added via syringe. The vial was positioned 5 cm from a 40 W Kessil A160WE LED light and irradiated for 2 h with vigorous stirring and fan-cooling, at which time the color of the reaction mixture had changed to a fluorescent canary yellow. Upon completion, the reaction mixture was filtered through a small plug of celite and the solvent removed *in vacuo*. The crude oil was purified by flash column chromatography (20 % EtOAc in petroleum ether) to afford the product (49 mg, 77 μmol, 77%) as a white amorphous solid. **R_f** (40% EtOAc in hexane): 0.35. **IR** ν_{max} /cm⁻¹ (solid): 2960, 1789, 1714, 1612, 1513, 1481, 1455, 1392, 1365, 1317, 1246, 1227, 1177, 1108, 1035, 994, 966. **¹H NMR** (500 MHz, CDCl₃) δ : 7.40 – 7.32 (5 H, m, H_{24,25,26}), 7.08 (2 H, d, *J* = 8.6 Hz, H₆), 6.78 (2 H, d, *J* = 8.6 Hz, H₇), 5.54 (1 H, s, H₁₈), 5.18 (1 H, d, *J* = 11.8 Hz, H_{22a}), 5.12 (1 H, d, *J* = 11.8 Hz, H_{22b}), 4.55 (1 H, d, *J* = 6.1 Hz, H₁₆), 3.92 – 3.82 (4 H, m, H₁₄), 3.77 (3 H, s, H₉), 3.56 – 3.54 (1 H, m, H₁), 3.53 (3 H, s, H₃), 2.85 – 2.71 (2 H, m, H₄), 2.04 (1 H, dd, *J* = 7.8, 14.6 Hz, H_{15a}), 1.79 (1 H, br s, N–H), 1.76 –

1.67 (2 H, m, H_{15b,11/12}), 1.64 – 1.28 (7 H, m, H_{11/12}), 0.92 (9 H, s, H₂₀); ¹³C NMR (126 MHz, CDCl₃) δ: 177.3 (C₂), 173.7 (C₁₇), 158.5 (C₈), 155.9 (C₂₁), 135.2 (C₂₃), 130.6 (2 C, C₆), 129.7 (C₅), 129.2 (C₂₆), 128.9 (2 C, C_{24/25}), 128.8 (2 C, C_{24/25}), 113.8 (2 C, C₇), 108.5 (C₁₃), 96.3 (C₁₈), 68.6 (C₂₂), 64.3 (C₁₄), 64.2 (C₁₄), 56.5 (C₁), 55.4 (C₉), 54.1 (C₁₀), 53.3 (C₁₆), 51.7 (C₃), 43.5 (br s, C₁₅), 41.1 (C₄), 37.1 (C₁₉), 33.3 (C_{11/12}), 31.5 (br s, C_{11/12}), 30.7 (C_{11/12}), 30.4 (C_{11/12}), 25.0 (3 C, C₂₀). [α]_D²⁵ = +8.6 (c = 1.0, CHCl₃) *m/z* HRMS found [M + H]⁺ 639.3262, C₃₅H₄₇N₂O₉⁺ requires 639.3276.

methyl (S)-2-((S)-3-(((benzyloxy)carbonyl)amino)-2,8-dioxo-1-azaspiro[4.5]decan-1-yl)-3-(4-methoxyphenyl)propanoate (609)



Method 1: Methylation of 611

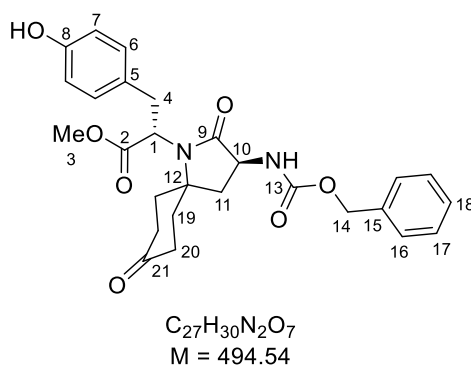
A Schlenk tube equipped with a magnetic stir bar was charged with methyl (S)-2-((S)-3-(((benzyloxy)carbonyl)amino)-2,8-dioxo-1-azaspiro [4.5] decan-1-yl)-3-(4-hydroxy-phenyl)-propanoate **611** (2.47 g, 5.0 mmol, 1.0 equiv) and cesium carbonate (2.44 g, 7.5 mmol, 1.5 equiv). Acetone (50 mL) was added, followed by methyl iodide (405 μ L, 6.5 mmol, 1.3 equiv) in one portion, and the vessel was sealed under a nitrogen atmosphere and heated to 50 °C for 5 h with vigorous stirring. The mixture was allowed to cool to ambient temperature and filtered through a short pad of celite. The filter cake was washed copiously with dichloromethane and the filtrate concentrated to dryness *in vacuo* to yield the product (2.51 g, 4.93 mmol, 99%) as a colorless solid, which can be recrystallized from methanol/Et₂O (5:1, 50 °C to –20 °C). **m.p.** 206 – 208 °C (diffusion. methanol, petroleum ether). **R_f** (70% EtOAc in dichloromethane): 0.21. **IR** ν_{max} /cm^{–1} (solid): 3302, 2949, 1740, 1692, 1584, 1543, 1510, 1444, 1418, 1368, 1344, 1326, 1301, 1262, 1243, 1174, 1146, 1109, 1085, 1058, 1032, 1007, 969. **¹H NMR** (400 MHz, CDCl₃) δ: 7.43 – 7.31 (5 H, m, H_{17,18,19}), 7.05 (2 H, d, *J* = 8.5 Hz,

H₆), 6.81 (2 H, d, $J = 8.5$ Hz, H₇), 5.44 (1 H, br s, N–H), 5.14 (2 H, s, H₁₅), 4.39 – 4.30 (1 H, m, H₁₁), 3.77 (3 H, s, H₉), 3.76 (3 H, s, H₃), 3.70 (1 H, dd, $J = 4.5, 11.0$ Hz, H₁), 3.54 (1 H, dd, $J = 11.0, 13.9$ Hz, H_{4a}), 3.38 (1 H, dd, $J = 4.5, 13.9$ Hz, H_{4b}), 3.10 (1 H, dd, $J = 9.1, 11.6$ Hz, H_{12a}), 2.54 – 2.32 (2 H, m, H_{21a,21b}), 2.20 (1 H, dt, $J = 5.3, 14.3$ Hz, H_{21c}), 2.11 – 1.97 (2 H, m, H_{20a,21d}), 1.75 (1 H, dt, $J = 5.6, 13.4$ Hz, H_{20b}), 1.52 (1 H, t, $J = 11.6$ Hz, H_{12b}), 1.34 (1 H, dt, $J = 4.7, 13.6$ Hz, H_{20c}), 0.37 (1 H, d, $J = 13.0$ Hz, H_{20d}); ¹³C NMR (101 MHz, CDCl₃) δ : 208.3 (C₂₂), 172.6 (C₁₀), 170.0 (C₂), 158.8 (C₈), 156.6 (C₁₄), 136.2 (C₁₆), 130.9 (2 C, C₆), 130.0 (C₅), 128.8 (2 C, C_{17/18}), 128.5 (C₁₉), 128.3 (2 C, C_{17/18}), 114.1 (2 C, C₇), 67.4 (C₁₅), 60.4 (C₁₃), 57.3 (C₁), 55.5 (C₉), 53.0 (C₃), 51.2 (C₁₁), 38.2 (C₂₁), 37.4 (C₂₁), 37.3 (br s, C₁₂), 35.5 (C₂₀), 34.3 (C₄), 32.2 (C₂₀). [α]_D²⁵ = –114.1 ($c = 0.32$, CHCl₃); m/z HRMS found $[M + H]^+$ 509.2276, C₂₈H₃₃N₂O₇⁺ requires 509.2282. X-ray structure deposited with the Cambridge Crystallographic Data Centre: CCDC 1934845.

Method 2: Cyclization of **605**

To a solution of benzyl (2*S*,4*S*)-2-(tert-butyl)-4-((8-(((*S*)-1-methoxy-3-(4-methoxyphenyl)-1-oxopropan-2-yl) amino)-1,4-dioxaspiro[4.5]decan-8-yl)methyl)-5-oxooxazolidine-3-carboxylate **605** (20 mg, 31 μ mol, 1.0 equiv) in THF (0.85 mL) was added aq. 1M HCl (0.15 mL), and the resulting solution stirred for 4 days. The mixture was then basified by addition of aq. sat. sodium bicarbonate solution and the aqueous phase extracted with Et₂O (3x). The combined organic phases were dried, filtered and concentrated *in vacuo*. The residue was purified by flash column chromatography (50 % EtOAc in dichloromethane) to yield the product (9.9 mg, 19.5 μ mol, 63%) as a colorless solid.

methyl (S)-2-((S)-3-(((benzyloxy)carbonyl)amino)-2,8-dioxo-1-azaspiro[4.5]decan-1-yl)-3-(4-hydroxyphenyl)propanoate (**611**)

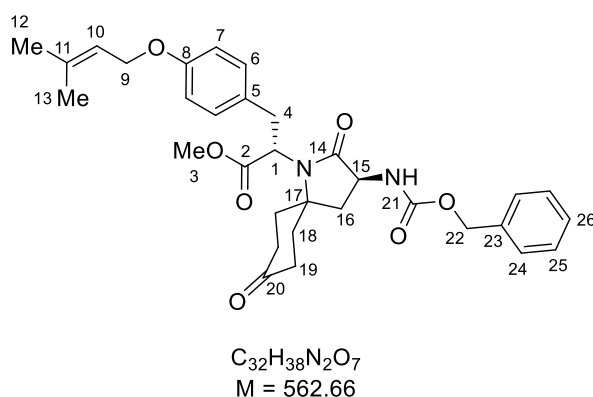


A 100 mL Schlenk tube (ϕ = ca. 35 mm) equipped with a magnetic stir bar was charged with L-tyrosine methyl ester (781 mg, 4.0 mmol, 1.0 equiv), 1,4-cyclohexanedione monoethylene acetal (687 mg, 4.4 mmol, 1.1 equiv), benzyl (*S*)-2-(tert-butyl)-4-methylene-5-oxooxazolidine-3-carboxylate **360** (1.50 g, 5.2 mmol, 1.3 equiv), Hantzsch Ester (1.52 g, 6.0 mmol, 1.5 equiv), *fac*-Ir(ppy)₃ (26 mg, 40 μ mol, 0.01 equiv) and activated 4 Å molecular sieves (2.0 g). The vessel was fitted with a rubber septum and the contents evacuated and backfilled with nitrogen (3 x). Dichloromethane (40 mL) and trifluoroacetic acid (61 μ L, 0.8 mmol, 0.2 equiv) were added successively via syringe, the septum replaced by a glass stopper, and the vessel sealed. The Schlenk tube was positioned between two 40 W Kessil A160WE LED lights (distance 5 cm each) and irradiated for 4 h with vigorous stirring and fan-cooling, at which time the color of the reaction mixture had changed to a fluorescent canary yellow. Upon completion the crude reaction mixture was filtered through Celite, the filter cake washed with copious amounts of dichloromethane and the resulting filtrate concentrated *in vacuo*. The viscous yellow oil was redissolved in tetrahydrofuran (40 mL) and aq. 3 M HCl (40 mL) was added. The mixture was placed under a nitrogen atmosphere and heated to 50 °C for 20 h with stirring. The solution was allowed to cool and quenched with aq. sat. sodium bicarbonate solution until pH 8, at which point a sticky precipitate formed. EtOAc was then added to the mixture and the aqueous phase extracted with EtOAc (3 x 500 mL). The combined organic phases were dried (MgSO₄), filtered, and the solvent removed *in vacuo*. The residue was resuspended in a 1:1 mixture of petroleum ether and Et₂O and sonicated. The voluminous precipitate was collected by vacuum filtration and washed with a 1:1 mixture of petroleum ether and Et₂O and a minimal amount of Et₂O. The obtained solid was dried under high vacuum to afford the product (1.44 g, 2.92 mmol, 73 %) as an off-white amorphous solid. **R_f** (60% EtOAc in dichloromethane): 0.33. **IR** ν_{max} /cm⁻¹ (solid): 3447, 3312, 2956, 1723, 1694, 1612, 1591, 1547, 1514, 1441, 1415, 1372, 1347, 1325, 1267, 1241, 1214, 1191, 1168, 1149, 1127, 1103, 1086, 1056, 1036, 1001, 982. **¹H NMR** (400 MHz, DMSO-d₆) δ : 9.15 (1 H, s, O–H), 7.82 (1 H, d, *J* = 8.8 Hz, N–H), 7.43 – 7.30 (5 H, m, H_{16,17,18}), 6.97 (2 H, d, *J* = 8.4 Hz, H₆), 6.64 (2 H, d, *J* = 8.4 Hz, H₇), 5.09 (2 H, s, H₁₄), 4.30 – 4.22 (1 H, m, H₁₀), 4.15 (1 H, t, *J* = 7.5 Hz, H₁), 3.60 (3 H, s, H₃), 3.14 (2 H, d, *J* = 7.5 Hz, H₄), 2.83 (1 H, dd, *J* = 8.5, 12.1 Hz, H_{11a}), 2.61 – 2.53 (1 H, m, H_{20a}), 2.25 (1 H, dt, *J* = 5.6, 14.7 Hz, H_{20'a}), 2.09 (1 H, d, *J* = 14.7 Hz, H_{20b}), 1.91 – 1.72 (3 H, m, H_{19,20b}), 1.51 – 1.38 (2 H, m, H_{11b,19'a}), 0.15 (1 H, br d, *J* = 10.8 Hz, H_{19'b}). **¹³C NMR** (101 MHz, DMSO-d₆) δ : 208.7 (C₂₁), 172.3 (C₉), 170.6 (C₂), 156.1 (C₁₃), 155.8 (C₈), 137.0 (C₁₅), 131.1 (2 C, C₆), 128.4 (2 C, C_{16/17}), 128.2 (C₅), 128.0 (2 C, C_{16/17}), 127.9 (C₁₈), 114.9 (2 C, C₇), 65.6 (C₁₄), 59.0 (C₁₂), 55.6 (C₁), 52.1 (C₃),

50.2 (C₁₀), 37.7 (C₂₀), 36.9 (C_{20'}), 34.9 (C₁₁), 33.7 (2 C, C_{4,19}), 30.8 (C_{19'}). $[\alpha]_D^{25} = -136.1$ (c = 0.23, MeOH). *m/z* HRMS found $[M + H]^+$ 495.2119, C₂₇H₃₁N₂O₇⁺ requires 495.2126.

5.2.2.2 Synthesis of TAN1251C

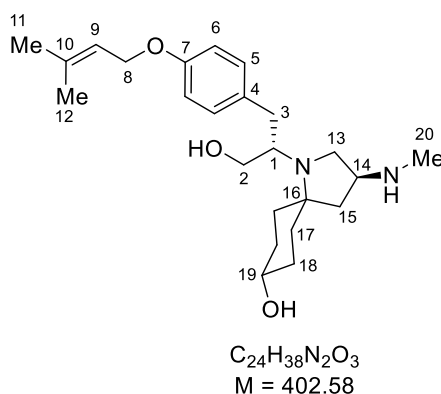
methyl (S)-2-((S)-3-(((benzyloxy)carbonyl)amino)-2,8-dioxo-1-azaspiro[4.5]decan-1-yl)-3-(4-((3-methylbut-2-en-1-yl)oxy)phenyl)propanoate (617)



A Schlenk tube equipped with a magnetic stir bar was charged with methyl (S)-2-((S)-3-(((benzyloxy)-carbonyl)amino)-2,8-dioxo-1-azaspiro [4.5] decan-1-yl)-3-(4-hydroxy-phenyl)-propanoate **611** (989 mg, 2.0 mmol, 1.0 equiv) and cesium carbonate (977 mg, 3.0 mmol, 1.5 equiv). Acetone (20 mL) was added, followed by prenyl bromide (462 μ L, 4.0 mmol, 2.0 equiv) in one portion, and the vessel was sealed under a nitrogen atmosphere and heated to 50 °C for 3 h with vigorous stirring. The mixture was allowed to cool to ambient temperature and filtered through a short pad of celite. The filter cake was washed copiously with dichloromethane and the filtrate concentrated to dryness and dried under high vacuum to yield the product (1.09 g, 1.94 mmol, 97%) as an off-white amorphous solid. *R_f* (60% EtOAc in dichloromethane): 0.46. **IR** $\nu_{\text{max}}/\text{cm}^{-1}$ (solid): 3297, 2946, 1741, 1716, 1690, 1610, 1557, 1538, 1508, 1445, 1408, 1375, 1328, 1264, 1237, 1221, 1195, 1176, 1146, 1111, 1061, 1051, 1038, 981. **¹H NMR** (400 MHz, CDCl₃) δ : 7.40 (5 H, m, H_{24,25,26}), 7.03 (2 H, d, *J* = 8.5 Hz, H₆), 6.81 (2 H, d, *J* = 8.5 Hz, H₇), 5.56 (1 H, s, N-H), 5.45 (1 H, tt, *J* = 1.4, 6.7 Hz, H₁₀), 5.13 (2 H, s, H₂₂), 4.46 (2 H, br d, *J* = 6.7 Hz, H₉), 4.39 – 4.30 (1 H, m, H₁₅), 3.74 (3 H, s, H₃), 3.69 (1 H, dd, *J* = 4.5, 11.0 Hz, H₁), 3.56 (1 H, dd, *J* = 11.0, 13.9 Hz, H_{4a}), 3.40 (1 H, dd, *J* = 4.5, 13.9 Hz, H_{4b}), 3.14 – 3.00 (1 H, m, H_{16a}), 2.53 – 2.30 (2 H, m, H_{19a,19b}), 2.18 (1 H, dt, *J* = 5.2, 14.5 Hz, H_{19'a}), 2.10 – 1.94 (2 H, m, H_{19'b,18a}), 1.78 (3 H, s, H_{12/13}), 1.76 – 1.73 (1 H, m, H_{18b}), 1.72 (3 H, s, H_{12/13}), 1.51 (1 H, t, *J* = 11.6 Hz, H_{16b}), 1.33 (1 H, dd, *J* = 4.7, 13.7 Hz, H_{18'a}),

0.37 – 0.27 (1 H, m, H_{18b}); ¹³C NMR (101 MHz, CDCl₃) δ: 208.3 (C₂₀), 172.5 (C₁₄), 170.0 (C₂), 158.0 (C₈), 156.6 (C₂₁), 138.3 (C₁₁), 136.2 (C₂₃), 130.8 (2 C, C₆), 129.9 (C₅), 128.7 (2 C, C_{24/25}), 128.4 (C₂₆), 128.3 (2 C, C_{24/25}), 119.6 (C₁₀), 114.8 (2 C, C₇), 67.3 (C₂₂), 64.9 (C₉), 60.4 (C₁₇), 57.2 (C₁), 52.9 (C₃), 51.2 (C₁₅), 38.2 (C₁₉), 37.3 (C_{19'}), 37.2 (br s, C₁₆), 35.4 (C₁₈), 34.3 (C₄), 32.1 (C_{18'}), 25.9 (C_{12/13}), 18.3 (C_{12/13}). [α]_D²⁵ = –104.8 (c = 1.0, CHCl₃). *m/z* HRMS found [M + H]⁺ 563.2745, C₃₂H₃₈N₂O₇⁺ requires 563.2752.

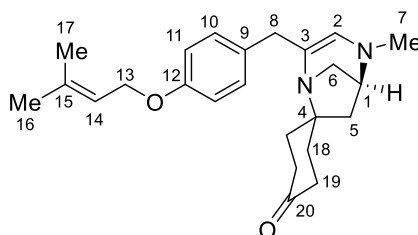
(3*S*,5*r*,8*S*)-1-((*S*)-1-hydroxy-3-(4-((3-methylbut-2-en-1-yl)oxy)phenyl)propan-2-yl)-3-(methylamino)-1-azaspiro[4.5]decan-8-ol (598)



A solution of methyl (*S*)-2-((*S*)-3-(((benzyloxy)carbonyl)amino)-2,8-dioxo-1-azaspiro[4.5]decan-1-yl)-3-(4-((3-methylbut-2-en-1-yl)oxy)phenyl)propanoate **617** (1.00 g, 1.78 mmol, 1.0 equiv) in anhydrous THF (60 mL) was cooled to 0 °C and LiAlH₄ (674 mg, 17.8 mmol, 10.0 equiv) was carefully added portion-wise with stirring. The cooling was removed and the stirred reaction mixture heated to a vigorous reflux for 16 h. The reaction mixture was allowed to cool to room temperature, then diluted with Et₂O, and solid NaSO₄·10H₂O was carefully added until no more gas evolution was observed. Methanol (10 mL) was added to the mixture and the suspension stirred for 1 hour. The formed off-white precipitate was removed by filtration through a pad of Celite, washed with ethyl acetate, and the filtrate concentrated *in vacuo*. The residue was purified by column chromatography (6% MeOH, 1% sat. aq. NH₃, 93% dichloromethane) to furnish the product (572 mg, 1.42 mmol, 80%) as a yellow amorphous solid. *R_f* (15% MeOH, 1% sat. aq. NH₃, 84% dichloromethane): 0.22. IR ν_{max}/cm^{–1} (solid): 3316 (br), 2928, 2854, 1675, 1610, 1581, 1508, 1444, 1365, 1327, 1297, 1231, 1175, 1139, 1112, 1065, 1041, 1002, 930. ¹H NMR (400 MHz, CDCl₃) δ: 7.02 (2 H, d, *J* = 8.5 Hz, H₅), 6.83 (2 H, d, *J* = 8.5 Hz, H₆), 5.48 (1 H, dt, *J* = 1.4, 6.8 Hz, H₉), 4.48 (2 H, d, *J* = 6.7 Hz, H₈), 3.63 – 3.54 (1 H, m, H₁₉), 3.32 (1 H, dd, *J* = 4.9, 10.1 Hz, H_{2a}), 3.22 –

3.10 (3 H, m, H_{2b,13a,14}), 3.06 – 2.96 (1 H, m, H₁), 2.90 (1 H, dd, $J = 3.1, 13.5$ Hz, H_{3a}), 2.64 (1 H, t, $J = 7.9$ Hz, H_{13b}), 2.46 (3 H, s, H₂₀), 2.44 (1 H, dd, $J = 10.6, 13.5$ Hz, H_{3b}), 2.19 (1 H, dd, $J = 8.2, 12.6$ Hz, H_{15a}), 2.09 – 1.90 (2 H, m, H_{17,18a}), 1.82 – 1.76 (4 H, m, H_{17,11/12}), 1.74 (3 H, s, H_{11/12}), 1.66 – 1.55 (2 H, m, H_{17,18'a}), 1.54 – 1.47 (1 H, m, H_{15b}), 1.46 – 1.34 (2 H, m, H_{17,18b}), 1.29 (1 H, dd, $J = 3.0, 12.9$ Hz, H_{18'b}). ¹³C NMR (101 MHz, CDCl₃) δ : 157.5 (C₇), 138.3 (C₁₀), 131.0 (C₄), 129.8 (2 C, C₅), 119.8 (C₉), 114.9 (2 C, C₆), 70.3 (C₁₉), 64.9 (C₈), 62.6 (C₁₆), 60.6 (C₂), 57.7 (C₁₄), 56.5 (C₁), 49.6 (C₁₃), 43.1 (C₁₅), 36.5 (C₁₈), 36.4 (C₃), 35.4 (C₂₀), 33.9 (C₁₈), 32.7 (2 C, C₁₇), 26.0 (C_{11/12}), 18.3 (C_{11/12}). $[\alpha]_D^{25} = -5.5$ ($c = 1.0$, CHCl₃). m/z HRMS found $[M + H]^+$ 403.2957, C₂₄H₃₉N₂O₃⁺ requires 403.2955. Configuration at C19 was tentatively assigned based on compound **622**. The data are in accordance with those previously reported in the literature.^[262]

(1S)-2-methyl-4-(4-((3-methylbut-2-en-1-yl)oxy)benzyl)-2,5-diazaspiro[bicyclo[3.2.1]octane-6,1'-cyclohexan]-3-en-4'-one, (+)-TAN1251C (2)



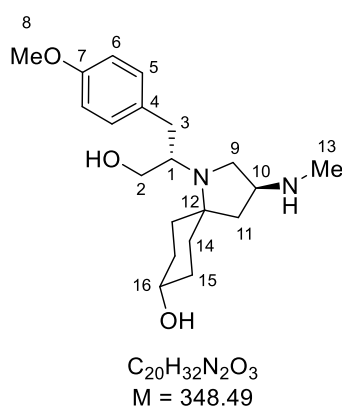
TAN1251C
C₂₄H₃₂N₂O₂
M = 380.53

A 10 mL microwave vial equipped with a magnetic stir bar was charged with (3S,5r,8S)-1-((S)-1-hydroxy-3-(4-((3-methylbut-2-en-1-yl)oxy)phenyl)propan-2-yl) -3- (methylamino)-1-azaspiro[4.5]decan-8-ol **598** (20 mg, 50 μ mol, 1.0 equiv), AZADO (0.8 mg, 5 μ mol, 0.1 equiv), CuCl (0.5 mg, 5 μ mol, 0.1 equiv), DMAP (1.2 mg, 10 μ mol, 0.2 equiv) and 2,2'-bipyridine (0.8 mg, 5 μ mol, 0.1 equiv). The vial was sealed with a septum cap under air, and a needle was inserted through the septum to allow exchange of atmosphere. Acetonitrile (0.7 mL) was then added and the reaction mixture stirred for 16 h at room temperature. The reaction was quenched by addition of sat. aq. sodium bicarbonate solution (5 mL) and stirred for 5 min. The aqueous layer was extracted with EtOAc (3 x) and the combined organic phases dried over anhydrous Na₂SO₄ and filtered and concentrated *in vacuo*. The residue was purified by flash column chromatography on neutral aluminium oxide (gradient elution: 100

% dichloromethane to 40 % EtOAc in dichloromethane) to yield the product (4.5 mg, 12 μ mol, 24%) as a yellow oil. **R_f** (50% EtOAc in dichloromethane): 0.21. **IR** $\nu_{\text{max}}/\text{cm}^{-1}$ (film): 2922 (br), 1715, 1672, 1640, 1609, 1582, 1507, 1445, 1373, 1324, 1297, 1231, 1172, 1121, 1054, 1003, 950. **¹H NMR** (500 MHz, CDCl₃) δ : 7.08 (2 H, d, J = 8.6 Hz, H₁₀), 6.82 (2 H, d, J = 8.6 Hz, H₁₁), 5.50 (1 H, tt, J = 1.4, 6.8 Hz, H₁₄), 5.24 (1 H, s, H₂), 4.48 (2 H, d, J = 6.7 Hz, H₁₃), 3.41 – 3.37 (1 H, m, H₁), 3.21 (2 H, s, H₈), 3.20 (1 H, dd, J = 2.8, 11.4 Hz, H_{6a}), 2.78 (1 H, dd, J = 1.8, 11.4 Hz, H_{6b}), 2.63 – 2.56 (1 H, m, C_{19a}), 2.51 (3 H, s, H₇), 2.49 – 2.43 (1 H, m, H_{19'a}), 2.43 – 2.30 (2 H, m, H_{18a,19b}), 2.29 – 2.17 (2 H, m, H_{18b,19'b}), 1.97 (1 H, ddd, J = 4.8, 10.7, 13.7 Hz, H_{18'a}), 1.90 – 1.82 (3 H, m, H_{18'b,5}), 1.79 (3 H, s, H_{16/17}), 1.74 (3 H, s, H_{16/17}). **¹³C NMR** (126 MHz, CDCl₃) δ : 211.8 (C₂₀), 157.3 (C₁₂), 138.1 (C₁₅), 132.1 (C₉), 130.0 (2 C, C₁₀), 128.4 (C₃), 127.9 (C₂), 120.0 (C₁₄), 114.5 (2 C, H₁₁), 71.6 (C₄), 64.9 (C₁₃), 59.2 (C₁), 52.3 (C₆), 43.1 (C₅), 41.6 (C₈), 40.5 (C₇), 39.7 (C₁₉), 38.0 (C_{19'}), 37.4 (C_{18'}), 34.8 (C₁₈), 26.0 (C_{16/17}), 18.3 (C_{16/17}); $[\alpha]_D^{25}$ = +24.2 (c = 0.45, MeOH) [lit. +24 (c = 0.44, MeOH)^[339]]; m/z **HRMS** found $[M + H]^+$ 381.2535, C₂₄H₃₃N₂O₂⁺ requires 381.2537. The obtained data are identical with those of the natural product.^[339]

5.2.2.3 Synthesis of FR901483

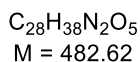
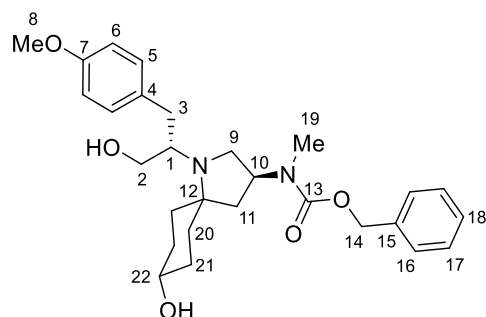
(3S,5r,8S)-1-((S)-1-hydroxy-3-(4-methoxyphenyl)propan-2-yl)-3-(methylamino)-1-azaspiro[4.5]decan-8-ol (588)



A solution of methyl (S)-2-(((S)-3-(((benzyloxy)carbonyl)amino)-2,8-dioxo-1-azaspiro[4.5]decan-1-yl)-3-(4-methoxyphenyl)propanoate **609** (192 mg, 0.377 mmol, 1.0 equiv) in anhydrous THF (15 mL) was cooled to 0 °C and LiAlH₄ (143 mg, 3.77 mmol, 10.0 equiv) was carefully added portion-wise with stirring. The cooling was removed and the

stirred reaction mixture heated to a vigorous reflux for 16 h. The reaction mixture was allowed to cool to room temperature, then diluted with Et₂O, and solid NaSO₄·10H₂O was carefully added until no more gas evolution was observed. Methanol (2 mL) was added to the mixture and the suspension stirred overnight. The formed off-white precipitate was removed by filtration through a pad of Celite, washed with ethyl acetate, and the filtrate concentrated under reduced pressure. The residue was purified by flash column chromatography (12% MeOH, 1% sat. aq. NH₃, 87% dichloromethane) to yield the product (117 mg, 336 μmol, 89%) as a pale red viscous oil. **R_f** (12% MeOH, 1% sat. aq. NH₃, 87% dichloromethane): 0.18. **IR** $\nu_{\text{max}}/\text{cm}^{-1}$ (solid): 3391 (br), 2933, 2856, 1645, 1611, 1583, 1510, 1442, 1366, 1325, 1299, 1243, 1176, 1139, 1064, 1029, 987. **¹H NMR** (500 MHz, CDCl₃) δ : 7.03 (2 H, d, J = 8.6 Hz, H₅), 6.82 (2 H, d, J = 8.5 Hz, H₆), 3.79 (3 H, s, H₈), 3.64 – 3.55 (1 H, m, H₁₆), 3.31 (1 H, dd, J = 5.0, 10.1 Hz, H_{2a}), 3.22 – 3.11 (3 H, m, H_{2b,9a,10}), 3.05 – 2.97 (1 H, m, H₁), 2.91 (1 H, dd, J = 3.2, 13.5 Hz, H_{3a}), 2.65 (1 H, t, J = 8.1 Hz, H_{9b}), 2.46 (3 H, s, H₁₃), 2.45 (1 H, dd, J = 10.7, 13.5 Hz, H_{3b}), 2.20 (1 H, dd, J = 8.1, 12.6 Hz, H_{11a}), 2.04 – 1.92 (2 H, m, H_{14,15a}), 1.80 (1 H, dq, J = 3.1, 12.5 Hz, H₁₄), 1.65 – 1.48 (3 H, m, H_{11b,14,15'a}), 1.44 – 1.35 (2 H, m, H_{14,15b}), 1.29 (1 H, dq, J = 3.2, 12.8 Hz, H_{15'b}); **¹³C NMR** (126 MHz, CDCl₃) δ : 158.3 (C₇), 131.1 (C₄), 129.8 (2 C, C₅), 114.1 (2 C, C₆), 70.3 (C₁₆), 62.6 (C₁₂), 60.6 (C₂), 57.7 (C₁₀), 56.5 (C₁), 55.4 (C₈), 49.6 (C₉), 43.1 (C₁₁), 36.5 (C_{15'}), 36.4 (C₃), 35.4 (C₁₃), 33.9 (C₁₅), 32.7 (2 C, C₁₄). **[α]_D²⁵** = −2.74 (c = 1.06, CHCl₃). **m/z HRMS** found $[\text{M} + \text{H}]^+$ 349.2490, C₂₀H₃₃N₂O₃⁺ requires 349.2486. Configuration at C16 was tentatively assigned based on compound **622**.

benzyl ((3*S*,5*r*,8*S*)-8-hydroxy-1-((*S*)-1-hydroxy-3-(4-methoxyphenyl)propan-2-yl)-1-azaspiro[4.5]decan-3-yl)(methyl)carbamate (622)



Method 1: Cbz-protection of 588

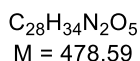
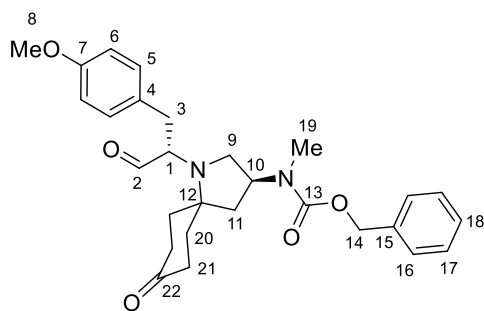
To a stirred solution of (3*S*,5*r*,8*S*)-1-((*S*)-1-hydroxy-3-(4-methoxyphenyl)propan-2-yl)-3-(methylamino)-1-azaspiro[4.5]decan-8-ol **588** (75 mg, 215 μ mol, 1.0 equiv) in anhydrous THF (1 mL) was added Na₂CO₃ (68 mg, 0.65 mmol, 3.0 equiv) and benzyl chloroformate (37 μ L, 0.26 mmol, 1.2 equiv) in one portion at room temperature. The reaction mixture was stirred at room temperature for 16 h, filtered through a pad of Celite, and the filter cake washed with dichloromethane. The filtrate was concentrated *in vacuo* and the residue purified by flash column chromatography (gradient elution: 1% MeOH in dichloromethane to 6% MeOH in dichloromethane) to yield the product (81 mg, 168 μ mol, 78%) as a pale yellow amorphous solid.

Method 2: Reduction and protection of 609 (2 steps)

Methyl (S)-2-((S)-3-(((benzyloxy)carbonyl)amino)-2,8-dioxo-1-azaspiro[4.5]decan-1-yl)-3-(4-methoxy-phenyl)propanoate **609** (2.51 g, 4.93 mmol, 1.0 equiv) was dissolved in anhydrous THF (60 mL) with gentle heating and then carefully added to a stirred solution of LiAlH₄ (1.87 g, 49.3 mmol, 10.0 equiv) in anhydrous THF (100 mL) at 0 °C. The cooling was removed and the reaction mixture heated to a vigorous reflux for 16 h. The mixture was allowed to cool to room temperature, then diluted with Et₂O and solid NaSO₄·10H₂O was carefully added until no more gas evolution was observed. Methanol (10 mL) and water (2 mL) was successively added to the mixture and the suspension stirred for 3 h at room temperature, at which point anhydrous Na₂SO₄ was added to the suspension. The off-white precipitate was then removed by filtration through a pad of Celite, the filter cake washed with ethyl acetate, and the filtrate concentrated *in vacuo*. The residue was dried under high vacuum and then redissolved in anhydrous THF (100 mL) and Na₂CO₃ (1.57 g, 14.8 mmol, 3.0 equiv) was added in one portion. Benzyl chloroformate (840 μ L, 5.92 mmol, 1.2 equiv) was added dropwise with stirring and the resulting suspension stirred at room temperature for 16 h. The mixture was filtered through a pad of Celite, and the filter cake washed with dichloromethane. The filtrate was concentrated *in vacuo* and the residue purified by flash column chromatography (gradient elution: 80% EtOAc in dichloromethane to 100% EtOAc) to yield the product (1.63 g, 3.38 mmol, 69%) as pale yellow amorphous solid. **R_f** (80% EtOAc in dichloromethane): 0.11. **IR** ν_{max} /cm⁻¹ (solid): 3390 (br), 2935, 2856, 1677, 1611, 1584, 1510, 1442, 1408, 1319, 1301, 1244, 1150, 1028, 986. **¹H NMR** (400 MHz, CDCl₃) δ : 7.40 – 7.29 (5 H, m, H_{16,17,18}), 7.03 (2 H, d, *J* = 8.6 Hz, H₅), 6.82 (2 H, d, *J* = 8.6 Hz, H₆), 5.17 (1 H, d, *J* = 12.5, H_{14a}), 5.14 (1 H, d, *J* = 12.5, H_{14b}), 4.63 (1 H, br s, H₁₀), 3.79 (3 H, s, H₈), 3.64 – 3.54

(1 H, m, H₂₂), 3.31 (1 H, dd, $J = 4.7, 10.3$ Hz, H_{2a}), 3.15 (1 H, t, $J = 10.1$ Hz, H_{2b}), 3.05 – 2.92 (3 H, m, H_{1,9}), 2.91 – 2.84 (4 H, m, H_{19,3a}), 2.78 (1 H, br s, OH), 2.43 (1 H, dd, $J = 10.9, 13.3$ Hz, H_{3b}), 2.08 (1 H, dd, $J = 9.6, 12.8$ Hz, H_{11a}), 2.05 – 1.91 (2 H, m, H_{20,21a}), 1.76 – 1.68 (2 H, m, H_{11b,20}), 1.63 – 1.58 (2 H, H_{20,21'a}), 1.42 – 1.30 (3 H, m, H_{20,21b,21'b}); ¹³C NMR (101 MHz, CDCl₃) δ : 158.3 (C₇), 156.6 (C₁₃), 136.8 (C₁₅), 130.9 (C₄), 129.8 (2 C, C₅), 128.7 (2 C, C_{16/17}), 128.2 (C₁₈), 128.1 (2 C, C_{16/17}), 114.1 (2 C, C₆), 70.2 (C₂₂), 67.4 (C₁₄), 62.3 (C₁₂), 60.8 (C₂), 56.7 (C₁), 55.4 (C₈), 53.6 (C₁₀), 44.4 (br s, C₉), 37.8 (br s, C₁₁), 36.4 (C₃), 36.1 (C_{21'}), 33.9 (C₂₁), 32.6 (2 C, C₂₀), 30.1 (C₁₉). $[\alpha]_D^{25} = -4.8$ ($c = 1.0$, CHCl₃). m/z HRMS found $[M + H]^+$ 483.2861, C₂₈H₃₉N₂O₅⁺ requires 483.2853. Configuration at C22 was tentatively assigned due to the following correlations observed in a ¹H-¹H-NOESY experiment: [H₂₂-H₅] (weak), [H₂₂-H_{2a}].

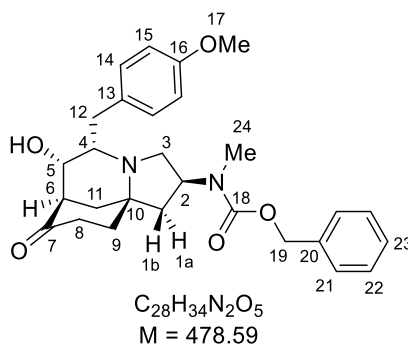
benzyl ((S)-1-((S)-1-(4-methoxyphenyl)-3-oxopropan-2-yl)-8-oxo-1-azaspiro[4.5]decan-3-yl)(methyl)carbamate (626)



Oxalyl chloride (910 μ L, 10.8 mmol, 8.0 equiv) was dissolved in anhydrous dichloromethane (30 mL) and cooled to -78 °C. Anhydrous dimethyl sulfoxide (1.53 mL, 21.5 mmol, 16.0 equiv) was added dropwise as a solution in dichloromethane (2.5 mL). The mixture was stirred for 15 min at -78 °C, then a solution of benzyl ((3*S*,5*r*,8*S*)-8-hydroxy-1-((*S*)-1-hydroxy-3-(4-methoxyphenyl)propan-2-yl)-1-azaspiro[4.5]decan-3-yl)(methyl)carbamate **622** (650 mg, 1.35 mmol, 1.0 equiv) in dichloromethane (18 mL) was added dropwise over the course of 30 min. The reaction mixture was stirred for a further 30 min at -78 °C, at which point the mixture was allowed to gradually warm to 0 °C. The mixture was stirred for 30 min at 0 °C, then H₂O (30 mL) and brine (10 mL) was added, and the aqueous layer extracted with dichloromethane (3 x). The combined organic phases were dried (MgSO₄), filtered and

concentrated *in vacuo*. The oily residue was purified by flash column chromatography (gradient elution: 30% EtOAc in petroleum ether to 50 % EtOAc in petroleum ether) to yield the product (395 mg, 0.824 mol, 61%) as a viscous yellow gum, which can be stored for several days at $-20\text{ }^{\circ}\text{C}$. **R_f** (50% EtOAc in petroleum ether): 0.22. **IR** $\nu_{\text{max}}/\text{cm}^{-1}$ (solid): 2935, 2836, 1691, 1611, 1584, 1511, 1441, 1410, 1383, 1314, 1301, 1245, 1145, 1031, 978, 958. **¹H NMR** (400 MHz, CDCl₃) δ : 9.65 (1 H, s, H₂), 7.40 – 7.28 (5 H, m, H_{16,17,18}), 7.07 (2 H, d, $J = 8.6\text{ Hz}$, H₅), 6.80 (2 H, d, $J = 8.6\text{ Hz}$, H₆), 5.15 (2 H, s, H₁₄), 4.88 (1 H, br s, H₁₀), 3.77 (3 H, s, H₈), 3.50 (1 H, t, $J = 7.2\text{ Hz}$, H₁), 3.19 (1 H, t, $J = 8.6\text{ Hz}$, H_{9a}), 3.12 – 3.06 (2 H, m, H_{9b,3a}), 2.83 (3 H, s, H₁₉), 2.64 (1 H, dd, $J = 7.8, 13.9\text{ Hz}$, H_{3b}), 2.46 – 2.26 (5 H, m, H_{21,11a}), 1.93 – 1.81 (1 H, m, H_{20a}), 1.80 – 1.60 (3 H, m, H_{11b,20'a,20b}), 1.36 – 1.29 (1 H, m, H_{20'b}). **¹³C NMR** (101 MHz, CDCl₃) δ : 210.1 (C₂₂), 201.1 (C₂), 158.4 (C₇), 156.5 (C₁₃), 136.8 (C₁₅), 130.4 (C₄), 130.2 (2 C, C₅), 128.7 (2 C, C_{16/17}), 128.2 (C₁₈), 128.1 (2 C, C_{16/17}), 114.0 (2 C, C₆), 67.4 (C₁₄), 63.9 (C₁), 62.0 (C₁₂), 55.4 (C₈), 52.9 (C₁₀), 46.8 (br s, C₉), 39.2 (C₂₁), 39.1 (C_{21'}), 37.4 (br s, C₁₁), 35.5 (C_{20'}), 34.7 (C₂₀), 32.7 (C₃), 29.4 (br s, C₁₉). **[α]_D²⁵** = -94.2 ($c = 1.0$, CHCl₃). **m/z HRMS** found $[\text{M} + \text{H}]^{+}$ 479.2538, C₂₈H₃₅N₂O₅⁺ requires 479.2540.

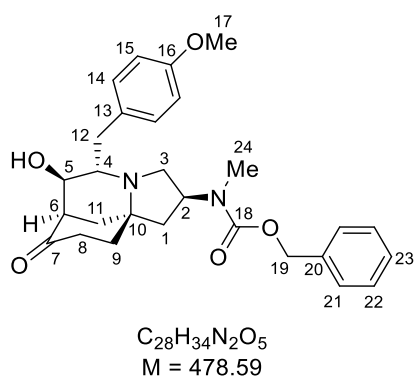
benzyl ((2S,5S,6S,7R,10aS)-6-hydroxy-5-(4-methoxybenzyl)-8-oxooctahydro-1H-7,10a-methanopyrrolo[1,2-a]azocin-2-yl)(methyl)carbamate (628)



To a stirred solution of benzyl ((*S*)-1-((*S*)-1-(4-methoxyphenyl)-3-oxopropan-2-yl)-8-oxo-1-azaspiro[4.5]decan-3-yl)(methyl)carbamate **626** (200 mg, 418 μmol , 1.0 equiv) in anhydrous MeOH (8 mL) was added sodium methoxide (45 mg, 836 μmol , 2.0 equiv) in one portion at room temperature. The mixture was stirred for 1 h at room temperature, then poured into half-saturated brine, and the mixture extracted with EtOAc (4 x). The combined organic phases were dried (MgSO₄), filtered and concentrated under reduced pressure. Separation of the mixture of diastereomers in the crude material by preparative TLC (60% EtOAc in dichloromethane) yielded the product (60 mg, 125 μmol , 30%) as a pale yellow foam. **R_f**

(40% EtOAc in dichloromethane): 0.10. **IR** $\nu_{\text{max}}/\text{cm}^{-1}$ (solid): 3435 (br), 2938, 1690, 1611, 1584, 1511, 1443, 1409, 1329, 1308, 1244, 1211, 1176, 1152, 1032, 984. **^1H NMR** (500 MHz, CDCl_3) δ : 7.41 – 7.29 (5 H, m, $\text{H}_{21,22,23}$), 7.10 (2 H, d, $J = 8.6$ Hz, H_{14}), 6.80 (2 H, d, $J = 8.6$ Hz, H_{15}), 5.12 (2 H, s, H_{19}), 4.85 (1 H, br s, H_2), 3.77 (3 H, s, H_{17}), 3.54 – 3.50 (1 H, m, H_5), 3.47 (1 H, br s, H_{3a}), 2.89 – 2.82 (1 H, m, H_4), 2.81 – 2.74 (3 H, m, $\text{H}_{3b,12}$), 2.77 (3 H, s, H_{24}), 2.68 (1 H, q, $J = 3.0$ Hz, H_6), 2.55 (1 H, ddd, $J = 8.2, 10.9, 18.0$ Hz, H_{8a}), 2.44 (1 H, ddd, $J = 3.8, 8.2, 18.0$ Hz, H_{8b}), 2.25 – 2.08 (3 H, m, $\text{H}_{1a,9a,11a}$), 2.20 (1 H, d, $J = 7.2$ Hz, OH), 1.97 (1 H, t, $J = 11.8$ Hz, H_{9b}), 1.79 (1 H, dd, $J = 3.0, 13.4$ Hz, H_{11b}), 1.67 (1 H, dd, $J = 6.1, 13.7$ Hz, H_{1b}); **^{13}C NMR** (126 MHz, CDCl_3) δ : 213.0 (C_7), 158.3 (C_{16}), 156.5 (C_{18}), 136.9 (C_{20}), 130.1 (3 C, $\text{C}_{13,14}$), 128.6 (2 C, $\text{C}_{21/22}$), 128.2 (C_{23}), 128.1 (2 C, $\text{C}_{21/22}$), 114.1 (2 C, C_{15}), 69.0 (C_5), 67.4 (C_{19}), 58.7 (C_{10}), 57.8 (C_4), 55.4 (C_{17}), 52.1 (2 C, $\text{C}_{2,6}$), 49.2 (C_3), 43.7 (br s, C_1), 37.9 (C_8), 35.8 (C_{12}), 29.9 (br s, C_9), 29.3 (C_{24}), 27.5 (br s, C_{11}). $[\alpha]_D^{25} = -27.2$ ($c = 1.0$, CHCl_3). **m/z HRMS** found $[\text{M} + \text{H}]^+$ 479.2545, $\text{C}_{28}\text{H}_{35}\text{N}_2\text{O}_5^+$ requires 479.2540. The following correlations were observed in a ^1H - ^1H -NOESY experiment: $[\text{H}_4\text{--}\text{H}_{8b}]$, $[\text{H}_4\text{--}\text{H}_5]$; $[\text{H}_5\text{--}\text{H}_8]$ (weak), $[\text{H}_5\text{--}\text{H}_6]$, $[\text{H}_2\text{--}\text{H}_{1a}]$, $[\text{H}_{1b}\text{--}\text{H}_{9b}]$, $[\text{H}_{9a}\text{--}\text{H}_4]$.

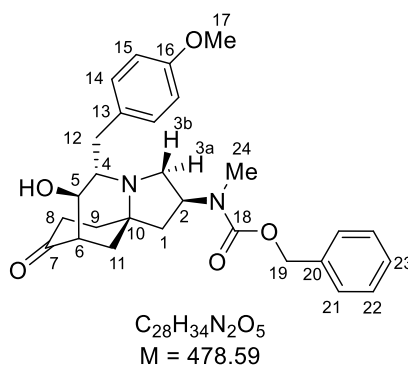
benzyl ((2*S*,5*S*,6*R*,7*R*,10*aS*)-6-hydroxy-5-(4-methoxybenzyl)-8-oxooctahydro-1*H*-7,10a-methanopyrrolo[1,2-*a*]azocin-2-yl)(methyl)carbamate (627)



R_f (40% EtOAc in dichloromethane): 0.21. **IR** $\nu_{\text{max}}/\text{cm}^{-1}$ (solid): 3416 (br), 2936, 2835, 1690, 1611, 1584, 1511, 1442, 1410, 1329, 1307, 1244, 1210, 1177, 1153, 1114, 1061, 1031, 995. **^1H NMR** (500 MHz, CDCl_3) δ : 7.39 – 7.29 (5 H, m, $\text{H}_{21,22,23}$), 7.16 (2 H, d, $J = 8.5$ Hz, H_{14}), 6.80 (2 H, d, $J = 8.5$ Hz, H_{15}), 5.08 (2 H, s, H_{19}), 4.85 (1 H, br s, H_2), 3.82 – 3.77 (1 H, m, H_5), 3.77 (3 H, s, H_{17}), 3.29 (1 H, dd, $J = 3.7, 15.3$ Hz, H_{12a}), 3.27 – 3.18 (1 H, m, H_{3a}), 3.04 (1 H, dt, $J = 3.8, 10.5$ Hz, H_4), 2.80 (1 H, d, $J = 8.0$ Hz, OH), 2.77 (1 H, dd, $J = 3.6, 10.5$ Hz, H_{3b}), 2.72 (1 H, br s, H_6), 2.67 – 2.54 (2 H, m, H_8), 2.51 (1 H, dd, $J = 10.2, 15.1$ Hz, H_{12b}), 2.46 (3

H, s, H₂₄), 2.17 – 1.93 (4 H, m, H_{1a,9,11a}), 1.88 (1 H, dd, $J = 3.8, 13.7$ Hz, H_{11b}), 1.56 (1 H, dd, $J = 6.7, 13.4$, H_{1b}). **¹³C NMR** (126 MHz, CDCl₃) δ : 216.8 (C₇), 158.0 (C₁₆), 156.4 (C₁₈), 136.9 (C₂₀), 131.3 (C₁₃), 129.6 (2 C, C₁₄), 128.6 (2 C, C_{21/22}), 128.1 (C₂₃), 128.0 (2 C, C_{21/22}), 113.8 (2 C, C₁₅), 69.0 (br s, C₅), 67.2 (C₁₉), 59.2 (C₄), 58.3 (C₁₀), 55.4 (C₁₇), 51.7 (C₂), 50.0 (C₆), 47.8 (br s, C₃), 43.1 (br s, C₁), 38.7 (C₈), 35.1 (C₁₂), 31.1 (C₉), 30.6 (br s, C₁₁), 28.4 (br s, C₂₄). ***m/z* HRMS** found $[M + H]^+$ 479.2544, C₂₈H₃₅N₂O₅⁺ requires 479.2540. The following correlations were observed in a ¹H-¹H-NOESY experiment: [H₄-H₅], [H₄-H_{12a}], [H₄-H₈], [H₄-H_{12b}], [H₄-H₉]; [H₅-H_{3a}], [H₅-H₆], [H₅-H_{12b}], [H₅-H₁₁], [H_{3a}-H₂].

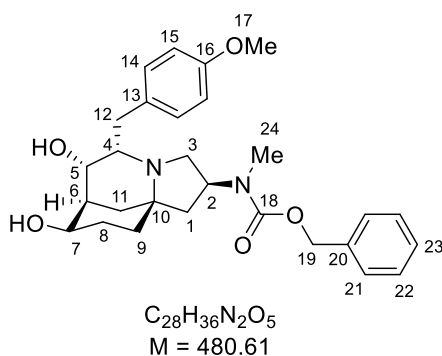
benzyl ((2*S*,5*S*,6*R*,7*S*,10*aR*)-6-hydroxy-5-(4-methoxybenzyl)-8-oxooctahydro-1*H*-7,10a-methanopyrrolo[1,2-*a*]azocin-2-yl)(methyl)carbamate (629)



R_f (40% EtOAc in dichloromethane): 0.36. **IR** ν_{max} /cm⁻¹ (solid): 3416 (br), 1692, 1610, 1584, 1510, 1441, 1412, 1386, 1343, 1314, 1299, 1246, 1209, 1176, 1149, 1105, 1069, 1028, 987. **¹H NMR** (500 MHz, CDCl₃) δ : 7.40 – 7.30 (5 H, m, H_{21,22,23}), 7.17 (2 H, d, $J = 8.5$ Hz, H₁₄), 6.82 (2 H, d, $J = 8.5$ Hz, H₁₅), 5.17 (2 H, s, H₁₉), 4.93 (1 H, br s, H₂), 3.79 (3 H, s, H₁₇), 3.54 (1 H, t, $J = 7.4$ Hz, H_{3a}), 3.49 (1 H, dd, $J = 2.8, 8.2$ Hz, H₅), 2.99 (1 H, dd, $J = 3.8, 14.1$ Hz, H_{12a}), 2.87 (3 H, s, H₂₄), 2.86 – 2.83 (1 H, m, H₄), 2.77 (1 H, dd, $J = 5.6, 14.1$ Hz, H_{12b}), 2.57 (1 H, dd, $J = 9.0, 10.6$ Hz, H_{3b}), 2.47 (1 H, br s, H₆), 2.46 – 2.39 (1 H, m, H_{8a}), 2.23 (1 H, dt, $J = 3.3, 13.5$ Hz, H_{11a}), 2.07 (1 H, br d, $J = 15.0$ Hz, H_{8b}), 1.91 – 1.82 (3 H, m, H_{11b,9a,1a}), 1.79 (1 H, dd, $J = 6.3, 11.6$ Hz, H_{1b}), 1.56 (1 H, br s, OH), 1.48 (1 H, dt, $J = 5.1, 12.8$ Hz, H_{9b}). **¹³C NMR** (126 MHz, CDCl₃) δ : 212.5 (C₇), 158.5 (C₁₆), 156.7 (C₁₈), 136.8 (C₂₀), 131.0 (2 C, C₁₄), 129.5 (C₁₃), 128.7 (2 C, C_{21/22}), 128.2 (C₂₃), 128.1 (2 C, C_{21/22}), 114.1 (2 C, C₁₅), 70.9 (C₅), 67.5 (C₁₉), 65.5 (C₄), 58.1 (C₁₀), 56.4 (br s, C₃), 55.4 (C₁₇), 54.4 (C₆), 52.6 (C₂), 40.4 (br s, C₁), 39.4 (C₉), 37.7 (br s, C₁₂), 35.8 (C₈), 32.9 (C₁₁), 28.8 (C₂₄). ***m/z* HRMS** found $[M + H]^+$ 479.2546, C₂₈H₃₅N₂O₅⁺ requires 479.2540. The following correlations were observed in a ¹H-

^1H -ROESY experiment: $[\text{H}_4\text{--H}_{12\text{b}}]$, $[\text{H}_4\text{--H}_{3\text{b}}]$, $[\text{H}_4\text{--H}_{11\text{a}}]$, $[\text{H}_4\text{--H}_5]$, $[\text{H}_4\text{--H}_{12\text{a}}]$; $[\text{H}_5\text{--H}_{12\text{a}}]$, $[\text{H}_5\text{--H}_{12\text{b}}]$, $[\text{H}_5\text{--H}_{8\text{a}}]$, $[\text{H}_2\text{--H}_{3\text{a}}]$.

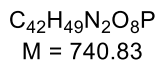
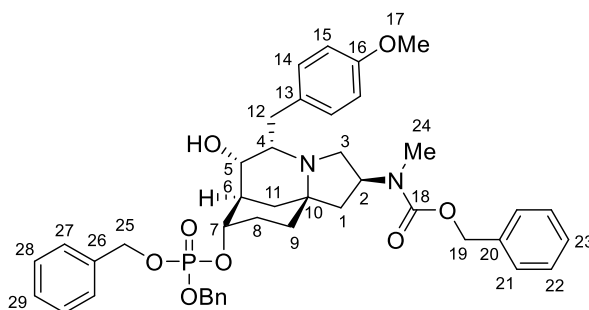
benzyl ((2*S*,5*S*,6*S*,7*S*,8*R*,10*aS*)-6,8-dihydroxy-5-(4-methoxybenzyl)octahydro-1*H*-7,10*a*-methanopyrrolo[1,2-*a*]azocin-2-yl)(methyl)carbamate (404)



A solution of benzyl ((2*S*,5*S*,6*S*,7*R*,10*aS*)-6-hydroxy-5-(4-methoxybenzyl)-8-oxooctahydro-1*H*-7,10*a*-methanopyrrolo[1,2-*a*]azocin-2-yl)(methyl)carbamate **628** (70 mg, 0.146 mmol, 1.0 equiv) in THF (2.2 mL) was cooled to -78°C and L-selectride (364 μL , 1 M in THF, 0.364 mmol, 2.5 equiv) was added dropwise with stirring. The reaction was stirred for 4 h at -78°C , at which point residual hydride was quenched by the careful dropwise addition of H_2O at -78°C , followed by warming to room temperature with stirring. The mixture was poured into aq. 10% NaOH solution (8 mL) and stirred vigorously for 1 h at room temperature (monitored by TLC). Upon completion, the biphasic mixture was diluted with brine and the aqueous phase extracted with EtOAc (3 x). The combined organic phases were dried over MgSO_4 , filtered and concentrated *in vacuo*. Purification of the residue by flash column chromatography (gradient elution: 2% MeOH in dichloromethane to 9% MeOH, 1% sat. aq. NH_3 , 90% dichloromethane) yielded the product (54 mg, 0.112 mmol, 77%) as a colorless foam. R_f (7.5% MeOH in dichloromethane): 0.05. **IR** $\nu_{\text{max}}/\text{cm}^{-1}$ (solid): 3376 (br), 2938, 1674, 1611, 1584, 1511, 1442, 1410, 1329, 1302, 1245, 1210, 1150, 1030, 978. **^1H NMR** (400 MHz, CD_3CN) δ : 7.42 – 7.48 (5 H, m, $\text{H}_{21,22,23}$), 7.25 (2 H, d, $J = 8.3$ Hz, H_{14}), 6.84 (2 H, d, $J = 8.3$ Hz, H_{15}), 5.05 (2 H, s, H_{19}), 4.67 (1 H, br s, H_2), 3.88 (1 H, br s, H_7), 3.75 (3 H, s, H_{17}), 3.68 – 3.45 (3 H, m, $\text{H}_{5,4,3\text{a}}$), 2.83 (5 H, br s, $\text{H}_{3\text{b},12}$), 2.65 (3 H, br s, H_{24}), 2.15 (2 H, br s, $\text{H}_{6,11\text{a}}$), 1.91 – 1.70 (4 H, m, $\text{H}_{8,9}$), 1.65 (1 H, br s), 1.40 (1 H, br s), 0.99 (1 H, br s, $\text{H}_{11\text{b}}$). **^{13}C NMR** (101 MHz, CD_3CN) δ : 159.0 (C_{16}), 156.9 (C_{18}), 138.5 (C_{20}), 132.8 (C_{13}), 131.2 (2 C, C_{14}), 129.4 (2 C, $\text{C}_{21/22}$), 128.8 (C_{23}), 128.6 (2 C, $\text{C}_{21/22}$), 114.5 (2 C, C_{15}), 70.3 (br s, C_7), 67.4

(C₁₉), 66.3 (br s, C₄), 60.5 (br s, C₅), 59.4 (br s, C₁₀), 55.8 (C₁₇), 52.8 (C₂), 51.6 (C₃), 44.9 (br s, C₆), 43.1 (br s, C₁), 36.1 (br s, C₁₂), 34.7, 31.5 (C₉), 29.6 (C₂₄), 28.3 (C₁₁). [α]_D²² = -2.3 (c = 0.6, CHCl₃). *m/z* HRMS found [M + H]⁺ 481.2702, C₂₈H₃₇N₂O₅⁺ requires 481.2697. The following correlations were observed in a ¹H-¹H-NOESY experiment: [H₇-H₁₁], [H₇-H₉], [H₇-H₆]. The data are in accordance with those previously reported in the literature.^[269]

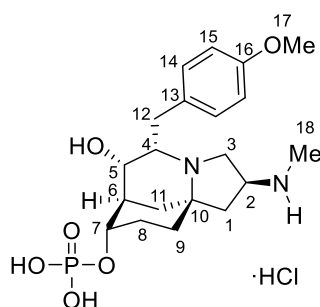
benzyl ((2S,5S,6S,7R,8S,10aS)-8-((bis(benzyloxy)phosphoryl)oxy)-6-hydroxy-5-(4-methoxybenzyl)octahydro-1H-7,10a-methanopyrrolo[1,2-a]azocin-2-yl)(methyl)carbamate (423)



To a stirred solution of benzyl ((2S,5S,6S,7S,8R,10aS)-6,8-dihydroxy-5-(4-methoxybenzyl)octahydro-1H-7,10a-methanopyrrolo [1,2-a] azocin-2-yl)(methyl)carbamate **404** (54 mg, 0.112 mmol, 1.0 equiv) in anhydrous THF (2.3 mL) was added, successively at room temperature, dibenzyl phosphate (187 mg, 0.673 mmol, 6.0 equiv) in anhydrous THF (1.6 mL), tris(4-chlorophenyl)phosphine (122 mg, 0.336 mmol, 3.0 equiv) in anhydrous THF (1.6 mL), DIAD (66 μ L, 0.336 mmol, 3.0 equiv) and anhydrous triethylamine (156 μ L, 1.12 mmol, 10.0 equiv). The mixture was stirred for 1 h at room temperature, poured into half-saturated brine and the resulting mixture extracted with EtOAc (3 x). The combined organic phases were dried (MgSO₄), filtered and concentrated *in vacuo*. The residue was purified by preparative TLC (3% MeOH, 97% EtOAc) to yield the product (28 mg, 38 μ mol, 34%) as a colorless foam. **R_f** (3% MeOH in EtOAc): 0.44. **IR** ν_{max} /cm⁻¹ (film): 3424 (br), 3030, 2936, 1691, 1610, 1584, 1511, 1497, 1455, 1410, 1379, 1327, 1301, 1245, 1214, 1152, 1107, 990. **¹H NMR** (500 MHz, CDCl₃) δ : 7.40 – 7.28 (15 H, m, H_{27,28,29}), 7.15 (2 H, d, *J* = 8.6 Hz, H₁₄), 6.82 (2 H, d, *J* = 8.6 Hz, H₁₅), 5.11 (2 H, s, H₁₉), 5.05 – 4.94 (4 H, m, H₂₅), 4.79 (1 H, br s, C₂), 4.33 (1 H, br s, H₇), 3.79 (3 H, s, H₁₇), 3.44 (1 H, br s, H_{3a}), 3.30 (1 H, t, *J* = 7.0 Hz, H₄),

3.17 – 3.14 (1 H, m, H₅), 2.81 – 2.79 (2 H, m, H₁₂), 2.78 (3 H, s, H₂₄), 2.74 (1 H, dd, $J = 5.4$, 9.8 Hz, H_{3b}), 2.13 (1 H, br s, H₆), 2.09 – 1.99 (1 H, m, H_{8a}), 1.94 – 1.73 (4 H, m, H_{1a,8b,9a,11a}), 1.71 (1 H, d, $J = 5.6$ Hz, OH), 1.65 – 1.56 (1 H, m, H_{9b}), 1.49 (1 H, d, $J = 12.9$ Hz, H_{11b}), 1.42 (1 H, dd, $J = 6.5$, 13.4 Hz, H_{1b}). ¹³C NMR (126 MHz, CDCl₃) δ : 158.2 (C₁₆), 156.5 (C₁₈), 137.0 (C₂₀), 136.0 (2 C, d, $J_{C-P} = 6.3$ Hz, C₂₆), 130.9 (br s, C₁₃), 130.2 (2 C, C₁₄), 128.69 (4 C), 128.65, 128.64, 128.60 (2 C), 128.07 (3 C), 128.04 (2 C), 128.00 (2 C), 113.9 (2 C, C₁₅), 75.1 (d, $J_{C-P} = 6.0$ Hz, C₇), 69.4 (d, $J_{C-P} = 5.7$ Hz, C₂₅), 69.3 (d, $J_{C-P} = 5.7$ Hz, C₂₅), 67.2 (C₁₉), 67.1 (C₅), 58.6 (C₄), 58.4 (C₁₀), 55.4 (C₁₇), 52.0 (C₂), 50.3 (C₃), 43.6 (d, $J_{C-P} = 4.2$ Hz, C₆), 43.1 (C₁), 35.8 (C₁₂), 30.0 (br s, C₉), 29.1 (br s, C₂₄), 28.8 (d, $J_{C-P} = 4.2$ Hz, C₈), 24.0 (br s, C₁₁). ³¹P NMR (202 MHz, CDCl₃) δ : -1.33 (s). $[\alpha]_D^{22} = +7.7$ ($c = 1.0$, CHCl₃). m/z HRMS found $[M + H]^+$ 741.3291, C₄₂H₅₀N₂O₈P⁺ requires 741.3299. The data are in accordance with those previously reported in the literature.^[252]

(2*S*,5*S*,6*S*,7*R*,8*S*,10*aS*)-6-hydroxy-5-(4-methoxybenzyl)-2-(methylamino)octahydro-1*H*-7,10*a*-methanopyrrolo[1,2-*a*]azocin-8-yl dihydrogen phosphate, (-)-FR901483 (1)



(-)-FR901483 · HCl

C₂₀H₃₁N₂O₆P
M = 426.45

To a solution of benzyl ((2*S*,5*S*,6*S*,7*R*,8*S*,10*aS*)-8-((bis(benzyloxy)phosphoryl)oxy)-6-hydroxy-5-(4-methoxybenzyl)octahydro-1*H*-7,10*a*-methanopyrrolo[1,2-*a*]azocin-2-yl)-(methyl)carbamate **423** (19 mg, 26 μ mol, 1.0 equiv) in MeOH (3 mL) was added aq. 3 M HCl (9.6 μ L, 28.8 μ mol, 1.1 equiv), and the resulting solution was concentrated *in vacuo*. The residue was dried for 1 h under high vacuum and redissolved in methanol (1.5 mL) under a nitrogen atmosphere. Pd/C (8.4 mg, 10%, 7.9 μ mol, 0.3 equiv) was then added in one portion, the atmosphere exchanged to 1 atm of H₂, and the solution stirred at r.t. for 4 h. The mixture was filtered through a pad of celite, the filter cake washed with MeOH, and the filtrate

concentrated under reduced pressure to yield (–)-FR901483·HCl (10 mg, 22 μ mol, 85%) as a colorless solid. **m.p.** = 220 – 225 $^{\circ}$ C, decomp. (MeOH/Et₂O) (lit. 210 – 213 $^{\circ}$ C).^[250] **IR** $\nu_{\text{max}}/\text{cm}^{-1}$ (solid): 3329 (br), 3276 (br), 2937, 2706, 2450, 1611, 1513, 1443, 1301, 1246, 1178, 999. **¹H NMR** (500 MHz, methanol-d₄) δ : 7.32 (2 H, d, J = 8.4 Hz, H₁₄), 6.88 (2 H, d, J = 8.4 Hz, H₁₅), 4.47 (1 H, dd, J = 9.8, 12.9 Hz, H_{3a}), 4.25 (1 H, br s, H₇), 4.23 – 4.16 (1 H, m, H₂), 3.88 – 3.80 (2 H, m, H_{3b,4}), 3.78 (3 H, s, H₁₇), 3.60 (1 H, br s, H₅), 3.30 – 3.25 (1 H, m, H_{12a}), 3.05 (1 H, d, J = 10.6 Hz, H_{12b}), 2.72 (3 H, s, H₁₈), 2.65 – 2.56 (1 H, m, H_{1a}), 2.45 (1 H, br s, H₆), 2.31 – 2.20 (2 H, m, H_{11a,8a}), 2.19 – 2.03 (4 H, m, H_{8b,9,1b}), 1.90 (1 H, d, J = 13.7 Hz, H_{11b}). **¹³C NMR** (126 MHz, methanol-d₄) δ : 160.4 (C₁₆), 131.7 (2 C, C₁₄), 128.6 (C₁₃), 115.3 (2 C, C₁₅), 71.1 (d, $J_{\text{C-P}}$ = 5.3 Hz, C₇), 68.3 (C₁₀), 64.0 (C₅), 61.7 (C₄), 55.7 (C₁₇), 54.9 (C₂), 51.8 (C₃), 42.9 (d, $J_{\text{C-P}}$ = 3.7 Hz, C₆), 41.8 (C₁), 34.0 (C₁₂), 32.3 (C₁₈), 28.3 (C₈), 27.9 (C₉), 22.4 (C₁₁). **³¹P NMR** (162 MHz, methanol-d₄) δ : –0.09 (s). $[\alpha]_{\text{D}}^{22}$ = –10.7 (c = 0.28, MeOH) [lit. $[\alpha]_{\text{D}}^{25}$ = –11 (c = 0.74, MeOH)^[250]] ***m/z* HRMS** found $[\text{M} + \text{H}]^{+}$ 427.1997, C₂₀H₃₂N₂O₆P⁺ requires 427.1992. The obtained data are identical with those of the natural product.^[250]

6. References

- [1] H. D. Roth, *Angew. Chem. Int. Ed.* **1989**, 28, 1193–1207.
- [2] R. E. Schofield, in *Oxford Dictionary of National Biography*, Oxford University Press, Oxford, **2013**.
- [3] R. E. Schofield, *The enlightened Joseph Priestley : a study of his life and work from 1773 to 1804*, Pennsylvania State University Press, University Park, Pa., **2004**.
- [4] J. Priestley, *Experiments and observations on different kinds of air*, W. Bowyer and J. Nichols, London, **1790**.
- [5] J. W. Döbereiner, *Pharmazeutisches Centralblatt* **1831**, 383–385.
- [6] D. H. R. Barton, P. de Mayo, M. Shafiq, *J. Chem. Soc.* **1957**, 929–935.
- [7] D. H. R. Barton, P. de Mayo, M. Shafiq, *J. Chem. Soc.* **1958**, 140–145.
- [8] Kahler, *Arch. Pharm.* **1830**, 34, 318–319.
- [9] A. Alms, *Arch. Pharm.* **1830**, 34, 319–320.
- [10] H. Trommsdorff, *Annalen der Pharmacie* **1834**, 11, 190–207.
- [11] F. S. S. Cannizzaro, *Gazz. Chim. Ital.* **1873**, 3, 241–251.
- [12] O. L. Chapman, L. F. Englert, *J. Am. Chem. Soc.* **1963**, 85, 3028–3029.
- [13] M. H. Fisch, J. H. Richards, *J. Am. Chem. Soc.* **1963**, 85, 3029–3030.
- [14] E. Zimmerman Howard, in *Pure Appl. Chem.*, Vol. 78, **2006**, p. 2193.
- [15] C. J. Fritzsche, *J. Prakt. Chem.* **1867**, 101, 333–343.
- [16] M. Ehrenberg, *Acta Crystallographica* **1966**, 20, 177–182.
- [17] W. H. Perkin, *J. Chem. Soc., Trans.* **1881**, 39, 409–452.
- [18] C. Liebermann, *Ber. Dtsch. Chem. Ges.* **1895**, 28, 1443–1448.
- [19] J. Schramm, *Ber. Dtsch. Chem. Ges.* **1884**, 17, 2922–2925.
- [20] H. Klinger, *Ber. Dtsch. Chem. Ges.* **1886**, 19, 1862–1870.
- [21] G. Ciamician, P. Silber, *Ber. Dtsch. Chem. Ges.* **1886**, 19, 2899–2900.
- [22] Authorized reprint, Courtesy of Prof. Vincenzo Balzani, Alma Mater Studiorum University of Bologna - Sistema Museale di Ateneo - Collection Giacomo Ciamician.
- [23] N. D. Heindel, M. A. Pfau, *J. Chem. Educ.* **1965**, 42, 383.
- [24] G. Ciamician, *Science* **1912**, 36, 385.
- [25] H. Okabe, *Photochemistry of small molecules*, Wiley, New York, **1978**.
- [26] E. V. Anslyn, D. A. Dougherty, *Modern physical organic chemistry*, University Science, Sausalito, CA, **2006**.
- [27] A. Gilbert, J. E. Baggott, *Essentials of molecular photochemistry*, Blackwell Scientific Publications, Oxford ; Boston, **1991**.

- [28] S. W. Benson, *J. Chem. Educ.* **1965**, *42*, 502.
- [29] A. Albin, M. Fagnoni, *Photochemically-generated intermediates in synthesis*, Wiley, Hoboken, New Jersey, **2013**.
- [30] Reprinted as licensed under the Creative Commons Attribution 3.0 Unported license, "Compact fluorescent light bulb", 12 November 2009, created by PiccoloNamek.
- [31] Reprinted as licensed under the Creative Commons Attribution-Share Alike 3.0 Unported license. "Blue light emitting diodes over a proto-board", 11 March 2010, created by Gussisaurio.
- [32] N. A. Romero, D. A. Nicewicz, *Chem. Rev.* **2016**, *116*, 10075–10166.
- [33] C. K. Prier, D. A. Rankic, D. W. C. MacMillan, *Chem. Rev.* **2013**, *113*, 5322–5363.
- [34] K. Kalyanasundaram, *Coord. Chem. Rev.* **1982**, *46*, 159–244.
- [35] A. Juris, V. Balzani, F. Barigelletti, S. Campagna, P. Belser, A. von Zelewsky, *Coord. Chem. Rev.* **1988**, *84*, 85–277.
- [36] A. Juris, V. Balzani, P. Belser, A. von Zelewsky, *Helv. Chim. Acta* **1981**, *64*, 2175–2182.
- [37] L. Flamigni, A. Barbieri, C. Sabatini, B. Ventura, F. Barigelletti, in *Photochemistry and Photophysics of Coordination Compounds II* (Eds.: V. Balzani, S. Campagna), Springer, Berlin, Heidelberg, **2007**, pp. 143–203.
- [38] S. Campagna, F. Puntoriero, F. Nastasi, G. Bergamini, V. Balzani, in *Photochemistry and Photophysics of Coordination Compounds I* (Eds.: V. Balzani, S. Campagna), Springer Berlin Heidelberg, Berlin, Heidelberg, **2007**, pp. 117–214.
- [39] J. K. McCusker, *Acc. Chem. Res.* **2003**, *36*, 876–887.
- [40] C. R. Bock, J. A. Connor, A. R. Gutierrez, T. J. Meyer, D. G. Whitten, B. P. Sullivan, J. K. Nagle, *J. Am. Chem. Soc.* **1979**, *101*, 4815–4824.
- [41] T. J. Meyer, *Acc. Chem. Res.* **1989**, *22*, 163–170.
- [42] D. M. Hedstrand, W. H. Kruizinga, R. M. Kellogg, *Tetrahedron Lett.* **1978**, *19*, 1255–1258.
- [43] T. J. Van Bergen, D. M. Hedstrand, W. H. Kruizinga, R. M. Kellogg, *J. Org. Chem.* **1979**, *44*, 4953–4962.
- [44] H. Cano-Yelo, A. Deronzier, *Tetrahedron Lett.* **1984**, *25*, 5517–5520.
- [45] H. Cano-Yelo, A. Deronzier, *J. Chem. Soc., Perkin Trans. 2* **1984**, 1093–1098.
- [46] H. Cano-Yelo, A. Deronzier, *J. Photochem.* **1987**, *37*, 315–321.
- [47] K. Okada, K. Okamoto, N. Morita, K. Okubo, M. Oda, *J. Am. Chem. Soc.* **1991**, *113*, 9401–9402.

- [48] K. Okada, K. Okubo, N. Morita, M. Oda, *Tetrahedron Lett.* **1992**, 33, 7377–7380.
- [49] K. Okada, K. Okubo, N. Morita, M. Oda, *Chem. Lett.* **1993**, 22, 2021–2024.
- [50] M. H. Shaw, J. Twilton, D. W. C. MacMillan, *J. Org. Chem.* **2016**, 81, 6898–6926.
- [51] K. Hironaka, S. Fukuzumi, T. Tanaka, *J. Chem. Soc., Perkin Trans. 2* **1984**, 1705–1709.
- [52] S. Fukuzumi, S. Koumitsu, K. Hironaka, T. Tanaka, *J. Am. Chem. Soc.* **1987**, 109, 305–316.
- [53] S. Fukuzumi, S. Mochizuki, T. Tanaka, *J. Phys. Chem.* **1990**, 94, 722–726.
- [54] C. Pac, M. Ihama, M. Yasuda, Y. Miyauchi, H. Sakurai, *J. Am. Chem. Soc.* **1981**, 103, 6495–6497.
- [55] O. Ishitani, C. Pac, H. Sakurai, *J. Org. Chem.* **1983**, 48, 2941–2942.
- [56] C. Pac, Y. Miyauchi, O. Ishitani, M. Ihama, M. Yasuda, H. Sakurai, *J. Org. Chem.* **1984**, 49, 26–34.
- [57] O. Ishitani, M. Ihama, Y. Miyauchi, C. Pac, *J. Chem. Soc., Perkin Trans. 1* **1985**, 1527–1531.
- [58] O. Ishitani, S. Yanagida, S. Takamuku, C. Pac, *J. Org. Chem.* **1987**, 52, 2790–2796.
- [59] R. Pschorr, *Ber. Dtsch. Chem. Ges.* **1896**, 29, 496–501.
- [60] K. Okada, K. Okamoto, M. Oda, *J. Chem. Soc., Chem. Commun.* **1989**, 1636–1637.
- [61] M. A. Ischay, M. E. Anzovino, J. Du, T. P. Yoon, *J. Am. Chem. Soc.* **2008**, 130, 12886–12887.
- [62] T.-G. Baik, A. L. Luis, L.-C. Wang, M. J. Krische, *J. Am. Chem. Soc.* **2001**, 123, 6716–6717.
- [63] L.-C. Wang, H.-Y. Jang, Y. Roh, V. Lynch, A. J. Schultz, X. Wang, M. J. Krische, *J. Am. Chem. Soc.* **2002**, 124, 9448–9453.
- [64] Y. Roh, H.-Y. Jang, V. Lynch, N. L. Bauld, M. J. Krische, *Org. Lett.* **2002**, 4, 611–613.
- [65] J. Yang, D. F. Cauble, A. J. Berro, N. L. Bauld, M. J. Krische, *J. Org. Chem.* **2004**, 69, 7979–7984.
- [66] J. Yang, G. A. N. Felton, N. L. Bauld, M. J. Krische, *J. Am. Chem. Soc.* **2004**, 126, 1634–1635.
- [67] M. A. Cismesia, T. P. Yoon, *Chem. Sci.* **2015**, 6, 5426–5434.
- [68] D. A. Nicewicz, D. W. C. MacMillan, *Science* **2008**, 322, 77–80.
- [69] M. P. Sibi, M. Hasegawa, *J. Am. Chem. Soc.* **2007**, 129, 4124–4125.
- [70] T. D. Beeson, A. Mastracchio, J.-B. Hong, K. Ashton, D. W. C. MacMillan, *Science* **2007**, 316, 582–585.

- [71] H.-Y. Jang, J.-B. Hong, D. W. C. MacMillan, *J. Am. Chem. Soc.* **2007**, *129*, 7004–7005.
- [72] H. Kim, D. W. C. MacMillan, *J. Am. Chem. Soc.* **2008**, *130*, 398–399.
- [73] J. M. R. Narayanam, J. W. Tucker, C. R. J. Stephenson, *J. Am. Chem. Soc.* **2009**, *131*, 8756–8757.
- [74] R. C. McAtee, E. J. McClain, C. R. J. Stephenson, *Trends Chem.* **2019**, *1*, 111–125.
- [75] D. M. Arias-Rotondo, J. K. McCusker, *Chem. Soc. Rev.* **2016**, *45*, 5803–5820.
- [76] X. Lang, J. Zhao, X. Chen, *Chem. Soc. Rev.* **2016**, *45*, 3026–3038.
- [77] M. D. Levin, S. Kim, F. D. Toste, *ACS Cent. Sci.* **2016**, *2*, 293–301.
- [78] J. Twilton, C. Le, P. Zhang, M. H. Shaw, R. W. Evans, D. W. C. MacMillan, *Nat. Rev. Chem.* **2017**, *1*, 0052.
- [79] D. Cambié, C. Bottecchia, N. J. W. Straathof, V. Hessel, T. Noël, *Chem. Rev.* **2016**, *116*, 10276–10341.
- [80] D. A. DiRocco, K. Dykstra, S. Krska, P. Vachal, D. V. Conway, M. Tudge, *Angew. Chem. Int. Ed.* **2014**, *53*, 4802–4806.
- [81] H. G. Yayla, F. Peng, I. K. Mangion, M. McLaughlin, L.-C. Campeau, I. W. Davies, D. A. DiRocco, R. R. Knowles, *Chem. Sci.* **2016**, *7*, 2066–2073.
- [82] Y. Y. Loh, K. Nagao, A. J. Hoover, D. Hesk, N. R. Rivera, S. L. Colletti, I. W. Davies, D. W. C. MacMillan, *Science* **2017**, *358*, 1182–1187.
- [83] G. S. Timmins, *Expert Opin. Ther. Pat.* **2014**, *24*, 1067–1075.
- [84] J. Luo, J. Zhang, *ACS Catal.* **2016**, *6*, 873–877.
- [85] T. P. Nicholls, D. Leonori, A. C. Bissember, *Nat. Prod. Rep.* **2016**, *33*, 1248–1254.
- [86] L. Furst, J. M. R. Narayanam, C. R. J. Stephenson, *Angew. Chem. Int. Ed.* **2011**, *50*, 9655–9659.
- [87] S. Lin, M. A. Ischay, C. G. Fry, T. P. Yoon, *J. Am. Chem. Soc.* **2011**, *133*, 19350–19353.
- [88] R. J. Crutchley, A. B. P. Lever, *J. Am. Chem. Soc.* **1980**, *102*, 7128–7129.
- [89] M. J. Schnermann, L. E. Overman, *Angew. Chem. Int. Ed.* **2012**, *51*, 9576–9580.
- [90] M. J. Schnermann, L. E. Overman, *J. Am. Chem. Soc.* **2011**, *133*, 16425–16427.
- [91] M. J. Schnermann, N. L. Untiedt, G. Jiménez-Osés, K. N. Houk, L. E. Overman, *Angew. Chem. Int. Ed.* **2012**, *51*, 9581–9586.
- [92] J. Hu, J. Wang, T. H. Nguyen, N. Zheng, *Beilstein J. Org. Chem.* **2013**, *9*, 1977–2001.
- [93] J. W. Beatty, C. R. J. Stephenson, *Acc. Chem. Res.* **2015**, *48*, 1474–1484.
- [94] H. G. Roth, N. A. Romero, D. A. Nicewicz, *Synlett* **2016**, *27*, 714–723.

- [95] D. D. M. Wayner, J. J. Dannenberg, D. Griller, *Chem. Phys. Lett.* **1986**, *131*, 189–191.
- [96] P. J. DeLaive, J. T. Lee, H. W. Sprintschnik, H. Abruna, T. J. Meyer, D. G. Whitten, *J. Am. Chem. Soc.* **1977**, *99*, 7094–7097.
- [97] P. J. DeLaive, T. K. Foreman, C. Giannotti, D. G. Whitten, *J. Am. Chem. Soc.* **1980**, *102*, 5627–5631.
- [98] S. Maity, M. Zhu, R. S. Shinabery, N. Zheng, *Angew. Chem. Int. Ed.* **2012**, *51*, 222–226.
- [99] S. Cai, X. Zhao, X. Wang, Q. Liu, Z. Li, D. Z. Wang, *Angew. Chem. Int. Ed.* **2012**, *51*, 8050–8053.
- [100] A. G. Condie, J. C. González-Gómez, C. R. J. Stephenson, *J. Am. Chem. Soc.* **2010**, *132*, 1464–1465.
- [101] D. P. Hari, B. König, *Org. Lett.* **2011**, *13*, 3852–3855.
- [102] Y. Pan, C. W. Kee, L. Chen, C.-H. Tan, *Green Chem.* **2011**, *13*, 2682–2685.
- [103] D. B. Freeman, L. Furst, A. G. Condie, C. R. J. Stephenson, *Org. Lett.* **2012**, *14*, 94–97.
- [104] M. Rueping, C. Vila, R. M. Koenigs, K. Poscharny, D. C. Fabry, *Chem. Commun.* **2011**, *47*, 2360–2362.
- [105] M. Rueping, S. Zhu, R. M. Koenigs, *Chem. Commun.* **2011**, *47*, 8679–8681.
- [106] G. Zhao, C. Yang, L. Guo, H. Sun, C. Chen, W. Xia, *Chem. Commun.* **2012**, *48*, 2337–2339.
- [107] W. Fu, W. Guo, G. Zou, C. Xu, *J. Fluorine Chem.* **2012**, *140*, 88–94.
- [108] J. Xuan, Z.-J. Feng, S.-W. Duan, W.-J. Xiao, *RSC Adv.* **2012**, *2*, 4065–4068.
- [109] D. A. DiRocco, T. Rovis, *J. Am. Chem. Soc.* **2012**, *134*, 8094–8097.
- [110] G. Bergonzini, C. S. Schindler, C.-J. Wallentin, E. N. Jacobsen, C. R. J. Stephenson, *Chem. Sci.* **2014**, *5*, 112–116.
- [111] Y.-Q. Zou, L.-Q. Lu, L. Fu, N.-J. Chang, J. Rong, J.-R. Chen, W.-J. Xiao, *Angew. Chem. Int. Ed.* **2011**, *50*, 7171–7175.
- [112] M. Rueping, D. Leonori, T. Poisson, *Chem. Commun.* **2011**, *47*, 9615–9617.
- [113] Z.-Q. Wang, M. Hu, X.-C. Huang, L.-B. Gong, Y.-X. Xie, J.-H. Li, *J. Org. Chem.* **2012**, *77*, 8705–8711.
- [114] S. Zhu, M. Rueping, *Chem. Commun.* **2012**, *48*, 11960–11962.
- [115] P. Renaud, L. Giraud, *Synthesis* **1996**, *1996*, 913–926.
- [116] M. Fagnoni, D. Dondi, D. Ravelli, A. Albini, *Chem. Rev.* **2007**, *107*, 2725–2756.
- [117] N. Hoffmann, *Chem. Rev.* **2008**, *108*, 1052–1103.

- [118] U. C. Yoon, P. S. Mariano, *Acc. Chem. Res.* **1992**, 25, 233–240.
- [119] K. Nakajima, Y. Miyake, Y. Nishibayashi, *Acc. Chem. Res.* **2016**, 49, 1946–1956.
- [120] A. McNally, C. K. Prier, D. W. C. MacMillan, *Science* **2011**, 334, 1114–1117.
- [121] P. Kohls, D. Jadhav, G. Pandey, O. Reiser, *Org. Lett.* **2012**, 14, 672–675.
- [122] Y. Miyake, K. Nakajima, Y. Nishibayashi, *J. Am. Chem. Soc.* **2012**, 134, 3338–3341.
- [123] S. Zhu, A. Das, L. Bui, H. Zhou, D. P. Curran, M. Rueping, *J. Am. Chem. Soc.* **2013**, 135, 1823–1829.
- [124] L. Ruiz Espelt, E. M. Wiensch, T. P. Yoon, *J. Org. Chem.* **2013**, 78, 4107–4114.
- [125] X. Dai, D. Cheng, B. Guan, W. Mao, X. Xu, X. Li, *J. Org. Chem.* **2014**, 79, 7212–7219.
- [126] X. Dai, R. Mao, B. Guan, X. Xu, X. Li, *RSC Adv.* **2015**, 5, 55290–55294.
- [127] H. B. Hepburn, P. Melchiorre, *Chem. Commun.* **2016**, 52, 3520–3523.
- [128] J. J. Murphy, D. Bastida, S. Paria, M. Fagnoni, P. Melchiorre, *Nature* **2016**, 532, 218.
- [129] Y. Miyake, Y. Ashida, K. Nakajima, Y. Nishibayashi, *Chem. Commun.* **2012**, 48, 6966–6968.
- [130] D. W. Cho, U. C. Yoon, P. S. Mariano, *Acc. Chem. Res.* **2011**, 44, 204–215.
- [131] K. Nakajima, M. Kitagawa, Y. Ashida, Y. Miyake, Y. Nishibayashi, *Chem. Commun.* **2014**, 50, 8900–8903.
- [132] L. Ruiz Espelt, I. S. McPherson, E. M. Wiensch, T. P. Yoon, *J. Am. Chem. Soc.* **2015**, 137, 2452–2455.
- [133] D. Lenhart, A. Bauer, A. Pöthig, T. Bach, *Chem. Eur. J.* **2016**, 22, 6519–6523.
- [134] L. Chu, C. Ohta, Z. Zuo, D. W. C. MacMillan, *J. Am. Chem. Soc.* **2014**, 136, 10886–10889.
- [135] Z. Zuo, D. W. C. MacMillan, *J. Am. Chem. Soc.* **2014**, 136, 5257–5260.
- [136] A. Noble, D. W. C. MacMillan, *J. Am. Chem. Soc.* **2014**, 136, 11602–11605.
- [137] Y. Yasu, T. Koike, M. Akita, *Adv. Synth. Catal.* **2012**, 354, 3414–3420.
- [138] K. Miyazawa, T. Koike, M. Akita, *Adv. Synth. Catal.* **2014**, 356, 2749–2755.
- [139] Y. Miyake, K. Nakajima, Y. Nishibayashi, *Chem. Eur. J.* **2012**, 18, 16473–16477.
- [140] H. Zhou, P. Lu, X. Gu, P. Li, *Org. Lett.* **2013**, 15, 5646–5649.
- [141] D. Uraguchi, N. Kinoshita, T. Kizu, T. Ooi, *J. Am. Chem. Soc.* **2015**, 137, 13768–13771.
- [142] C. J. Cowden, *Org. Lett.* **2003**, 5, 4497–4499.
- [143] J. J. Douglas, K. P. Cole, C. R. J. Stephenson, *J. Org. Chem.* **2014**, 79, 11631–11643.
- [144] W.-M. Cheng, R. Shang, Y. Fu, *ACS Catal.* **2017**, 7, 907–911.

- [145] R. S. J. Proctor, H. J. Davis, R. J. Phipps, *Science* **2018**, *360*, 419–422.
- [146] J. Ye, I. Kalvet, F. Schoenebeck, T. Rovis, *Nat. Chem.* **2018**, *10*, 1037–1041.
- [147] M. A. Ashley, C. Yamauchi, J. C. K. Chu, S. Otsuka, H. Yorimitsu, T. Rovis, *Angew. Chem. Int. Ed.* **2019**, *58*, 4002–4006.
- [148] K. L. Skubi, T. R. Blum, T. P. Yoon, *Chem. Rev.* **2016**, *116*, 10035–10074.
- [149] M. N. Hopkinson, B. Sahoo, J.-L. Li, F. Glorius, *Chem. Eur. J.* **2014**, *20*, 3874–3886.
- [150] Z. Zuo, D. T. Ahneman, L. Chu, J. A. Terrett, A. G. Doyle, D. W. C. MacMillan, *Science* **2014**, *345*, 437–440.
- [151] S. Biswas, D. J. Weix, *J. Am. Chem. Soc.* **2013**, *135*, 16192–16197.
- [152] S. L. Zultanski, G. C. Fu, *J. Am. Chem. Soc.* **2013**, *135*, 624–627.
- [153] Z. Zuo, H. Cong, W. Li, J. Choi, G. C. Fu, D. W. C. MacMillan, *J. Am. Chem. Soc.* **2016**, *138*, 1832–1835.
- [154] J. C. Tellis, D. N. Primer, G. A. Molander, *Science* **2014**, *345*, 433–436.
- [155] M. El Khatib, R. A. M. Serafim, G. A. Molander, *Angew. Chem. Int. Ed.* **2016**, *55*, 254–258.
- [156] A. Noble, S. J. McCarver, D. W. C. MacMillan, *J. Am. Chem. Soc.* **2015**, *137*, 624–627.
- [157] C. L. Joe, A. G. Doyle, *Angew. Chem. Int. Ed.* **2016**, *55*, 4040–4043.
- [158] J. Xuan, T.-T. Zeng, Z.-J. Feng, Q.-H. Deng, J.-R. Chen, L.-Q. Lu, W.-J. Xiao, H. Alper, *Angew. Chem. Int. Ed.* **2015**, *54*, 1625–1628.
- [159] M. H. Shaw, V. W. Shurtleff, J. A. Terrett, J. D. Cuthbertson, D. W. C. MacMillan, *Science* **2016**, *352*, 1304–1308.
- [160] C. Le, Y. Liang, R. W. Evans, X. Li, D. W. C. MacMillan, *Nature* **2017**, *547*, 79.
- [161] H. Bönemann, C. Grard, W. Kopp, W. Pump, K. Tanaka, G. Wilke, *Angew. Chem. Int. Ed.* **1973**, *12*, 964–975.
- [162] M. Graetzel, *Acc. Chem. Res.* **1981**, *14*, 376–384.
- [163] K. Kalyanasundaram, M. Grätzel, *Coord. Chem. Rev.* **1998**, *177*, 347–414.
- [164] T. C. Nugent, *Chiral amine synthesis: methods, developments and applications*, John Wiley & Sons, **2010**.
- [165] T. P. T. Cushnie, B. Cushnie, A. J. Lamb, *Int. J. Antimicrob. Agents* **2014**, *44*, 377–386.
- [166] S. F. Nelsen, J. T. Ippoliti, *J. Am. Chem. Soc.* **1986**, *108*, 4879–4881.
- [167] S. M. Thullen, T. Rovis, *J. Am. Chem. Soc.* **2017**, *139*, 15504–15508.
- [168] K. N. Lee, M.-Y. Ngai, *Chem. Commun.* **2017**, *53*, 13093–13112.

- [169] K. Atsutaka, H. Junji, N. Masayasu, Y. Yasuo, S. Kazuo, *Bull. Chem. Soc. Jpn.* **1983**, *56*, 2442–2446.
- [170] S. Suga, S. Suzuki, J.-i. Yoshida, *J. Am. Chem. Soc.* **2002**, *124*, 30–31.
- [171] M. Szostak, N. J. Fazakerley, D. Parmar, D. J. Procter, *Chem. Rev.* **2014**, *114*, 5959–6039.
- [172] X. Zheng, J. He, H.-H. Li, A. Wang, X.-J. Dai, A.-E. Wang, P.-Q. Huang, *Angew. Chem. Int. Ed.* **2015**, *54*, 13739–13742.
- [173] P. S. Mariano, *Tetrahedron* **1983**, *39*, 3845–3879.
- [174] P. S. Mariano, *Acc. Chem. Res.* **1983**, *16*, 130–137.
- [175] G. Opitz, H. Hellmann, H. W. Schubert, *Liebigs Ann.* **1959**, *623*, 117–124.
- [176] H. Böhme, G. Auterhoff, *Chem. Ber.* **1971**, *104*, 2013–2017.
- [177] J. R. Hargreaves, P. W. Hickmott, B. J. Hopkins, *J. Chem. Soc. C* **1968**, 2599–2603.
- [178] P. Kollman, J. McKelvey, P. Gund, *J. Am. Chem. Soc.* **1975**, *97*, 1640–1645.
- [179] P. A. Kollman, W. F. Trager, S. Rothenberg, J. E. Williams, *J. Am. Chem. Soc.* **1973**, *95*, 458–463.
- [180] D. Griller, F. P. Lossing, *J. Am. Chem. Soc.* **1981**, *103*, 1586–1587.
- [181] A. Holý, J. Krupička, Z. Arnold, *Collect. Czech. Chem. Commun.* **1965**, *30*, 4127–4142.
- [182] C. P. Andrieux, J. M. Savéant, *J. Electroanal. Chem.* **1970**, *26*, 223–235.
- [183] C. Andrieux, J. Savéant, *Bull. Soc. Chim. Fr.* **1968**, 4671.
- [184] C. P. Andrieux, J. M. Savéant, *J. Electroanal. Chem.* **1970**, *28*, 446–450.
- [185] C. P. Andrieux, J. M. Savéant, *J. Electroanal. Chem.* **1970**, *28*, 339–348.
- [186] P. S. Mariano, J. L. Stavinoha, R. Swanson, *J. Am. Chem. Soc.* **1977**, *99*, 6781–6782.
- [187] P. S. Mariano, J. L. Stavinoha, G. Pepe, E. F. Meyer, *J. Am. Chem. Soc.* **1978**, *100*, 7114–7116.
- [188] P. S. Mariano, A. Leone-Bay, *Tetrahedron Lett.* **1980**, *21*, 4581–4584.
- [189] J. L. Stavinoha, P. S. Mariano, *J. Am. Chem. Soc.* **1981**, *103*, 3136–3148.
- [190] J. L. Stavinoha, P. S. Mariano, A. Leone-Bay, R. Swanson, C. Bracken, *J. Am. Chem. Soc.* **1981**, *103*, 3148–3160.
- [191] D. Hager, D. W. C. MacMillan, *J. Am. Chem. Soc.* **2014**, *136*, 16986–16989.
- [192] M. H. V. Huynh, T. J. Meyer, *Chem. Rev.* **2007**, *107*, 5004–5064.
- [193] A. D. Trowbridge, Doctoral thesis, *New strategies for the synthesis and functionalization of aliphatic amines*, University of Cambridge (Cambridge, United Kingdom), **2019**.

- [194] J. L. Jeffrey, F. R. Petronijević, D. W. C. MacMillan, *J. Am. Chem. Soc.* **2015**, *137*, 8404–8407.
- [195] M. Nakajima, E. Fava, S. Loescher, Z. Jiang, M. Rueping, *Angew. Chem. Int. Ed.* **2015**, *54*, 8828–8832.
- [196] S. Humbel, I. Côte, N. Hoffmann, J. Bouquant, *J. Am. Chem. Soc.* **1999**, *121*, 5507–5512.
- [197] S. Humbel, N. Hoffmann, I. Côte, J. Bouquant, *Chem. Eur. J.* **2000**, *6*, 1592–1600.
- [198] C. Dragonetti, L. Falciola, P. Mussini, S. Righetto, D. Roberto, R. Ugo, A. Valore, F. De Angelis, S. Fantacci, A. Sgamellotti, M. Ramon, M. Muccini, *Inorg. Chem.* **2007**, *46*, 8533–8547.
- [199] E. Fava, A. Millet, M. Nakajima, S. Loescher, M. Rueping, *Angew. Chem. Int. Ed.* **2016**, *55*, 6776–6779.
- [200] L. Qi, Y. Chen, *Angew. Chem. Int. Ed.* **2016**, *55*, 13312–13315.
- [201] T. Schuster, M. Kurz, M. W. Göbel, *J. Org. Chem.* **2000**, *65*, 1697–1701.
- [202] J. Kadota, D. Pavlović, J.-P. Desvergne, B. Bibal, F. Peruch, A. Deffieux, *Macromolecules* **2010**, *43*, 8874–8879.
- [203] A. L. Fuentes de Arriba, F. Urbitsch, D. J. Dixon, *Chem. Commun.* **2016**, *52*, 14434–14437.
- [204] K. N. Lee, Z. Lei, M.-Y. Ngai, *J. Am. Chem. Soc.* **2017**, *139*, 5003–5006.
- [205] X. Guo, O. S. Wenger, *Angew. Chem. Int. Ed.* **2018**, *57*, 2469–2473.
- [206] V. V. Pavlishchuk, A. W. Addison, *Inorg. Chim. Acta* **2000**, *298*, 97–102.
- [207] A. G. Capacci, J. T. Malinowski, N. J. McAlpine, J. Kuhne, D. W. C. MacMillan, *Nat. Chem.* **2017**, *9*, 1073.
- [208] J. M. Aurrecoechea, A. Fernández-Acebes, *Synlett* **1996**, *1996*, 39–42.
- [209] A. L. J. Beckwith, *Chem. Soc. Rev.* **1993**, *22*, 143–151.
- [210] N. J. Flodén, A. Trowbridge, D. Willcox, S. M. Walton, Y. Kim, M. J. Gaunt, *J. Am. Chem. Soc.* **2019**, *141*, 8426–8430.
- [211] J. W. Tucker, Y. Zhang, T. F. Jamison, C. R. J. Stephenson, *Angew. Chem. Int. Ed.* **2012**, *51*, 4144–4147.
- [212] C. C. Le, M. K. Wismer, Z.-C. Shi, R. Zhang, D. V. Conway, G. Li, P. Vachal, I. W. Davies, D. W. C. MacMillan, *ACS Cent. Sci.* **2017**, *3*, 647–653.
- [213] E. H. Cordes, W. P. Jencks, *J. Am. Chem. Soc.* **1962**, *84*, 832–837.
- [214] E. P. Serjeant, B. Dempsey, *Ionisation constants of organic acids in aqueous solution* Pergamon, Oxford, **1979**.

- [215] J. B. Milne, T. J. Parker, *J. Solution Chem.* **1981**, *10*, 479–487.
- [216] F. Cardellini, R. Germani, G. Cardinali, L. Corte, L. Roscini, N. Spreti, M. Tiecco, *RSC Adv.* **2015**, *5*, 31772–31786.
- [217] D. R. Lide, *CRC handbook of chemistry and physics*, Vol. 85, CRC press, **2004**.
- [218] G. Wuitschik, M. Rogers-Evans, K. Müller, H. Fischer, B. Wagner, F. Schuler, L. Polonchuk, E. M. Carreira, *Angew. Chem. Int. Ed.* **2006**, *45*, 7736–7739.
- [219] E. M. Carreira, T. C. Fessard, *Chem. Rev.* **2014**, *114*, 8257–8322.
- [220] R. D. Taylor, M. MacCoss, A. D. G. Lawson, *J. Med. Chem.* **2014**, *57*, 5845–5859.
- [221] B. Giese, *Angew. Chem. Int. Ed.* **1983**, *22*, 753–764.
- [222] P. Zhang, T. Xiao, S. Xiong, X. Dong, L. Zhou, *Org. Lett.* **2014**, *16*, 3264–3267.
- [223] C. Nájera, J. M. Sansano, *Chem. Rev.* **2007**, *107*, 4584–4671.
- [224] J. R. Axon, A. L. J. Beckwith, *J. Chem. Soc., Chem. Commun.* **1995**, 549–550.
- [225] A. L. J. Beckwith, C. L. L. Chai, *J. Chem. Soc., Chem. Commun.* **1990**, 1087–1088.
- [226] S. Karady, J. S. Amto, L. M. Weinstock, *Tetrahedron Lett.* **1984**, *25*, 4337–4340.
- [227] D. Seebach, A. Fadel, *Helv. Chim. Acta* **1985**, *68*, 1243–1250.
- [228] R. A. Aycock, D. B. Vogt, N. T. Jui, *Chem. Sci.* **2017**, *8*, 7998–8003.
- [229] T. Kanzian, T. A. Nigst, A. Maier, S. Pichl, H. Mayr, *Eur. J. Org. Chem.* **2009**, 2009, 6379–6385.
- [230] H.-W. Shih, M. N. Vander Wal, R. L. Grange, D. W. C. MacMillan, *J. Am. Chem. Soc.* **2010**, *132*, 13600–13603.
- [231] M. Silvi, C. Verrier, Y. P. Rey, L. Buzzetti, P. Melchiorre, *Nat. Chem.* **2017**, *9*, 868.
- [232] P.-Z. Wang, J.-R. Chen, W.-J. Xiao, *Org. Biomol. Chem.* **2019**, *17*, 6936–6951.
- [233] P. Yu, J.-S. Lin, L. Li, S.-C. Zheng, Y.-P. Xiong, L.-J. Zhao, B. Tan, X.-Y. Liu, *Angew. Chem. Int. Ed.* **2014**, *53*, 11890–11894.
- [234] L. Huang, S.-C. Zheng, B. Tan, X.-Y. Liu, *Org. Lett.* **2015**, *17*, 1589–1592.
- [235] G. H. Lonca, D. Y. Ong, T. M. H. Tran, C. Tejo, S. Chiba, F. Gagosz, *Angew. Chem. Int. Ed.* **2017**, *56*, 11440–11444.
- [236] J. Jung, J. Kim, G. Park, Y. You, E. J. Cho, *Adv. Synth. Catal.* **2016**, *358*, 74–80.
- [237] M. J. Gaunt, J. Yu, J. B. Spencer, *J. Org. Chem.* **1998**, *63*, 4172–4173.
- [238] F. E. R. Simons, *N. Engl. J. Med.* **2004**, *351*, 2203–2217.
- [239] M. Ahmed, C. Buch, L. Routaboul, R. Jackstell, H. Klein, A. Spannenberg, M. Beller, *Chem. Eur. J.* **2007**, *13*, 1594–1601.
- [240] S. Li, K. Huang, J. Zhang, W. Wu, X. Zhang, *Org. Lett.* **2013**, *15*, 1036–1039.

- [241] A. Hager, N. Vrielink, D. Hager, J. Lefranc, D. Trauner, *Nat. Prod. Rep.* **2016**, *33*, 491–522.
- [242] A. F. Abdel-Magid, S. J. Mehrman, *Org. Process Res. Dev.* **2006**, *10*, 971–1031.
- [243] G. Stork, A. Brizzolara, H. Landesman, J. Szmuszkowicz, R. Terrell, *J. Am. Chem. Soc.* **1963**, *85*, 207–222.
- [244] A. G. Cook, *Enamines : synthesis, structure, and reactions*, 2nd ed., M. Dekker, New York, **1988**.
- [245] G. W. Kabalka, R. M. Pagni, P. Bridwell, E. Walsh, H. M. Hassaneen, *J. Org. Chem.* **1981**, *46*, 1513–1514.
- [246] D. D. M. Wayner, D. J. McPhee, D. Griller, *J. Am. Chem. Soc.* **1988**, *110*, 132–137.
- [247] U. K. Pandit, J. B. Steevens, F. R. M. Cabré, *Bioorg. Chem.* **1973**, *2*, 293–300.
- [248] M. Fushimi, N. Baba, J. Oda, Y. Inouye, *Bull. Inst. Chem. Res.* **1980**, *58*, 357–365.
- [249] A. Trowbridge, D. Reich, M. J. Gaunt, *Nature* **2018**, *561*, 522–527.
- [250] K. Sakamoto, E. Tsujii, F. Abe, T. Nakanishi, M. Yamashita, N. Shigematsu, S. Izumi, M. Okuhara, *J. Antibiot.* **1996**, *49*, 37–44.
- [251] E. Tsujii, T. Nakanishi, S. Takase, M. Yamashita, S. Izumi, M. Okuhara, WO9312125, **1992**,
- [252] B. B. Snider, H. Lin, *J. Am. Chem. Soc.* **1999**, *121*, 7778–7786.
- [253] J. Bonjoch, F. Diaba, in *Stud. Nat. Prod. Chem., Vol. 32* (Ed.: Atta-ur-Rahman), Elsevier, **2005**, pp. 3–60.
- [254] T. Kino, H. Hatanaka, M. Hashimoto, M. Nishiyama, T. Goto, M. Okuhara, M. Kohsaka, H. Aoki, H. Imanaka, *J. Antibiot.* **1987**, *40*, 1249–1255.
- [255] T. Kino, H. Hatanaka, S. Miyata, N. Inamura, M. Nishiyama, T. Yajima, T. Goto, M. Okuhara, M. Kohsaka, H. Aoki, T. Ochiai, *J. Antibiot.* **1987**, *40*, 1256–1265.
- [256] H. Hatanaka, M. Iwami, T. Kino, T. Goto, M. Okuhara, *J. Antibiot.* **1988**, *41*, 1586–1591.
- [257] H. Hatanaka, T. Kino, S. Miyata, N. Inamura, A. Kuroda, T. Goto, H. Tanaka, M. Okuhara, *J. Antibiot.* **1988**, *41*, 1592–1601.
- [258] M. A. Ciufolini, *Il Farmaco* **2005**, *60*, 627–641.
- [259] M. A. Ciufolini, S. Canesi, M. Ousmer, N. A. Braun, *Tetrahedron* **2006**, *62*, 5318–5337.
- [260] H. Liang, M. A. Ciufolini, in *Biomimetic Organic Synthesis*, John Wiley & Sons, Inc, New York, **2011**, pp. 61–89.
- [261] G. Scheffler, H. Seike, E. J. Sorensen, *Angew. Chem. Int. Ed.* **2000**, *39*, 4593–4596.

- [262] M. Ousmer, N. A. Braun, C. Bavoux, M. Perrin, M. A. Ciufolini, *J. Am. Chem. Soc.* **2001**, *123*, 7534–7538.
- [263] M. Ousmer, N. A. Braun, M. A. Ciufolini, *Org. Lett.* **2001**, *3*, 765–767.
- [264] N. A. Braun, M. A. Ciufolini, K. Peters, E.-M. Peter, *Tetrahedron Lett.* **1998**, *39*, 4667–4670.
- [265] Z. Ruan, C. Li, D. Shen, S.-H. Huang, R. Hong, *Synthesis* **2019**, *51*, 2237–2251.
- [266] S. Ieda, A. Masuda, M. Kariyama, T. Wakimoto, T. Asakawa, T. Fukuyama, T. Kan, *Heterocycles* **2012**, *86*, 1071–1092.
- [267] A.-J. Ma, Y.-Q. Tu, J.-B. Peng, Q.-Y. Dou, S.-H. Hou, F.-M. Zhang, S.-H. Wang, *Org. Lett.* **2012**, *14*, 3604–3607.
- [268] H.-H. Huo, H.-K. Zhang, X.-E. Xia, P.-Q. Huang, *Org. Lett.* **2012**, *14*, 4834–4837.
- [269] H.-H. Huo, X.-E. Xia, H.-K. Zhang, P.-Q. Huang, *J. Org. Chem.* **2013**, *78*, 455–465.
- [270] J.-H. Maeng, R. L. Funk, *Org. Lett.* **2001**, *3*, 1125–1128.
- [271] T. Kan, T. Fujimoto, S. Ieda, Y. Asoh, H. Kitaoka, T. Fukuyama, *Org. Lett.* **2004**, *6*, 2729–2731.
- [272] S. Ieda, Y. Asoh, T. Fujimoto, H. Kitaoka, T. Kan, T. Fukuyama, *Heterocycles* **2009**, *79*, 721–738.
- [273] K. M. Brummond, S.-p. Hong, *J. Org. Chem.* **2005**, *70*, 907–916.
- [274] C. A. Carson, M. A. Kerr, *Org. Lett.* **2009**, *11*, 777–779.
- [275] B. B. Snider, H. Lin, B. M. Foxman, *J. Org. Chem.* **1998**, *63*, 6442–6443.
- [276] R. L. Funk, J. U. Daggett, *Heterocycles* **1987**, *26*, 2175–2182.
- [277] K. V. Gothelf, K. A. Jørgensen, *Chem. Rev.* **1998**, *98*, 863–910.
- [278] K. C. K. Swamy, N. N. B. Kumar, E. Balaraman, K. V. P. P. Kumar, *Chem. Rev.* **2009**, *109*, 2551–2651.
- [279] H. Vorbrüggen, K. Krolikiewicz, *Tetrahedron* **1993**, *49*, 9353–9372.
- [280] N. A. Braun, M. Ousmer, J. D. Bray, D. Bouchu, K. Peters, E.-M. Peters, M. A. Ciufolini, *J. Org. Chem.* **2000**, *65*, 4397–4408.
- [281] D. A. Evans, K. T. Chapman, E. M. Carreira, *J. Am. Chem. Soc.* **1988**, *110*, 3560–3578.
- [282] A. K. Saksena, P. Mangiaracina, *Tetrahedron Lett.* **1983**, *24*, 273–276.
- [283] S. Ieda, T. Kan, T. Fukuyama, *Tetrahedron Lett.* **2010**, *51*, 4027–4029.
- [284] K. Rikimaru, A. Yanagisawa, T. Kan, T. Fukuyama, *Synlett* **2004**, *2004*, 41–44.
- [285] H. Seike, E. J. Sorensen, *Synlett* **2008**, *2008*, 695–701.

- [286] A. Nishiyama, T. Sugawa, H. Manabe, K. Inoue, N. Yoshida, Kaneka Corp., **1996**, US5929284A.
- [287] P. Wieland, K. Miescher, *Helv. Chim. Acta* **1950**, 33, 2215–2228.
- [288] T. A. Spencer, K. K. Schmiegell, K. L. Williamson, *J. Am. Chem. Soc.* **1963**, 85, 3785–3793.
- [289] K. M. Brummond, J. Lu, *Org. Lett.* **2001**, 3, 1347–1349.
- [290] J. Jurczak, A. Golebiowski, *Chem. Rev.* **1989**, 89, 149–164.
- [291] C. M. Cain, R. P. C. Cousins, G. Coumbarides, N. S. Simpkins, *Tetrahedron* **1990**, 46, 523–544.
- [292] N. S. Simpkins, M. D. Weller, *Org. React.* **2013**, 79, 317–636.
- [293] H. K. Grover, M. R. Emmett, M. A. Kerr, *Org. Biomol. Chem.* **2015**, 13, 655–671.
- [294] M. A. Kerr, *Isr. J. Chem.* **2016**, 56, 476–487.
- [295] C. A. Carson, M. A. Kerr, *Chem. Soc. Rev.* **2009**, 38, 3051–3060.
- [296] A. P. Krapcho, G. A. Glynn, B. J. Grenon, *Tetrahedron Lett.* **1967**, 8, 215–217.
- [297] A. Paul Krapcho, E. Ciganek, *Org. React.* **2013**, 81, 1–536.
- [298] S. Grecian, J. Aubé, in *Organic Azides*, John Wiley & Sons, Inc., New York, **2009**, pp. 191–237.
- [299] J. Aube, G. L. Milligan, *J. Am. Chem. Soc.* **1991**, 113, 8965–8966.
- [300] E. D. Goddard-Borger, R. V. Stick, *Org. Lett.* **2007**, 9, 3797–3800.
- [301] B. M. Trost, P. H. Scudder, *J. Am. Chem. Soc.* **1977**, 99, 7601–7610.
- [302] J. M. Villalgordo, A. Linden, H. Heimgartner, *Helv. Chim. Acta* **1996**, 79, 213–219.
- [303] E. L. Bentz, R. Goswami, M. G. Moloney, S. M. Westaway, *Org. Biomol. Chem.* **2005**, 3, 2872–2882.
- [304] M. Puppala, A. Murali, S. Baskaran, *Chem. Commun.* **2012**, 48, 5778–5780.
- [305] X.-G. Wang, A.-E. Wang, P.-Q. Huang, *Chin. Chem. Lett.* **2014**, 25, 193–196.
- [306] S.-C. Tuo, J.-L. Ye, A.-E. Wang, S.-Y. Huang, P.-Q. Huang, *Org. Lett.* **2011**, 13, 5270–5273.
- [307] R.-F. Yang, P.-Q. Huang, *Chem. Eur. J.* **2010**, 16, 10319–10322.
- [308] H. Zhang, X. Li, H. Huang, P. Huang, *Sci. China Chem.* **2011**, 54, 737.
- [309] R. Fu, Y. Du, Z.-Y. Li, W.-X. Xu, P.-Q. Huang, *Tetrahedron* **2009**, 65, 9765–9771.
- [310] K.-J. Xiao, J.-M. Luo, K.-Y. Ye, Y. Wang, P.-Q. Huang, *Angew. Chem. Int. Ed.* **2010**, 49, 3037–3040.
- [311] P.-Q. Huang, *Acta Chimica. Sinica* **2018**, 76, 357–365.
- [312] F. Garro-Helion, A. Merzouk, F. Guibe, *J. Org. Chem.* **1993**, 58, 6109–6113.

- [313] S. G. Davies, D. R. Fenwick, *Chem. Commun.* **1997**, 565–566.
- [314] N. Yamazaki, H. Suzuki, C. Kibayashi, *J. Org. Chem.* **1997**, 62, 8280–8281.
- [315] G. Köbrich, *Angew. Chem. Int. Ed.* **1973**, 12, 464–473.
- [316] J. Y. W. Mak, R. H. Pouwer, C. M. Williams, *Angew. Chem. Int. Ed.* **2014**, 53, 13664–13688.
- [317] H. Suzuki, N. Yamazaki, C. Kibayashi, *Tetrahedron Lett.* **2001**, 42, 3013–3015.
- [318] D. J. Wardrop, W. Zhang, *Org. Lett.* **2001**, 3, 2353–2356.
- [319] J. Bonjoch, F. Diaba, G. Puigbó, D. Solé, V. Segarra, L. Santamaría, J. Beleta, H. Ryder, J. M. Palacios, *Biorg. Med. Chem.* **1999**, 7, 2891–2897.
- [320] J. Bonjoch, F. z. Diaba, G. Puigbó, E. Peidró, D. Solé, *Tetrahedron Lett.* **2003**, 44, 8387–8390.
- [321] E. Piers, P. C. Marais, *J. Org. Chem.* **1990**, 55, 3454–3455.
- [322] E. Piers, J. Renaud, *J. Org. Chem.* **1993**, 58, 11–13.
- [323] T. Wang, J. M. Cook, *Org. Lett.* **2000**, 2, 2057–2059.
- [324] H. Cao, J. Yu, X. Z. Wearing, C. Zhang, X. Liu, J. Deschamps, J. M. Cook, *Tetrahedron Lett.* **2003**, 44, 8013–8017.
- [325] D. Solé, E. Peidró, J. Bonjoch, *Org. Lett.* **2000**, 2, 2225–2228.
- [326] D. Solé, F. Diaba, J. Bonjoch, *J. Org. Chem.* **2003**, 68, 5746–5749.
- [327] A. Asari, P. Angelov, J. M. Auty, C. J. Hayes, *Tetrahedron Lett.* **2007**, 48, 2631–2634.
- [328] M. S. Kharasch, E. V. Jensen, W. H. Urry, *Science* **1945**, 102, 128.
- [329] F. Diaba, A. Martínez-Laporta, J. Bonjoch, *J. Org. Chem.* **2014**, 79, 9365–9372.
- [330] J. E. Kropf, I. C. Meigh, M. W. P. Bebbington, S. M. Weinreb, *J. Org. Chem.* **2006**, 71, 2046–2055.
- [331] J. E. Kropf, S. M. Weinreb, *Chem. Commun.* **1998**, 2357–2358.
- [332] S. T. M. Simila, A. Reichelt, S. F. Martin, *Tetrahedron Lett.* **2006**, 47, 2933–2936.
- [333] S. T. M. Simila, S. F. Martin, *J. Org. Chem.* **2007**, 72, 5342–5349.
- [334] S. Kaden, H.-U. Reissig, *Org. Lett.* **2006**, 8, 4763–4766.
- [335] S. Perreault, T. Rovis, *Synthesis* **2013**, 45, 719–728.
- [336] S. Perreault, T. Rovis, *Chem. Soc. Rev.* **2009**, 38, 3149–3159.
- [337] R. K. Friedman, K. M. Oberg, D. M. Dalton, T. Rovis, *Pure Appl. Chem.* **2010**, 82, 1353–1364.
- [338] B.-L. Li, W.-Y. Gao, H. Li, S.-Q. Zhang, X.-Q. Han, J. Lu, R.-X. Liang, X. Hong, Y.-X. Jia, *Chin. J. Chem.* **2019**, 37, 63–70.

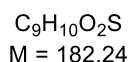
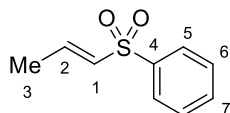
- [339] H. Shirafuji, S. Tsubotani, T. Ishimaru, S. Harada, Takeda Chemical Industries Ltd., **1991**, WO9113887.
- [340] B. B. Snider, H. Lin, *Org. Lett.* **2000**, 2, 643–646.
- [341] D. Widzowski, E. S. C. Wu, H. F. Helander, *Drug Discovery Today* **1997**, 2, 341–350.
- [342] H. Zhang, Z. Lin, H. Huang, H. Huo, Y. Huang, J. Ye, P. Huang, *Chin. J. Chem.* **2010**, 28, 1717–1724.
- [343] S. Nagumo, A. Nishida, C. Yamazaki, K. Murashige, N. Kawahara, *Tetrahedron Lett.* **1998**, 39, 4493–4496.
- [344] S. Nagumo, A. Nishida, C. Yamazaki, A. Matoba, K. Murashige, N. Kawahara, *Tetrahedron* **2002**, 58, 4917–4924.
- [345] D. J. Wardrop, A. Basak, *Org. Lett.* **2001**, 3, 1053–1056.
- [346] H. Mizutani, J. Takayama, Y. Soeda, T. Honda, *Tetrahedron Lett.* **2002**, 43, 2411–2414.
- [347] H. Mizutani, J. Takayama, Y. Soeda, T. Honda, *Heterocycles* **2004**, 62, 343–355.
- [348] S. Nagumo, A. Matoba, Y. Ishii, S. Yamaguchi, N. Akutsu, H. Nishijima, A. Nishida, N. Kawahara, *Tetrahedron* **2002**, 58, 9871–9877.
- [349] J. M. A. Auty, I. Churcher, C. J. Hayes, *Synlett* **2004**, 2004, 1443–1445.
- [350] H. Mizutani, J. Takayama, T. Honda, *Synlett* **2005**, 2005, 328–330.
- [351] Y. Nagasaka, S. Shintaku, K. Matsumura, A. Masuda, T. Asakawa, M. Inai, M. Egi, Y. Hamashima, Y. Ishikawa, T. Kan, *Org. Lett.* **2017**, 19, 3839–3842.
- [352] G. Grundke, W. Keese, M. Rimpler, *Synthesis* **1987**, 1987, 1115–1116.
- [353] T. Oshima, S.-y. Ueno, T. Nagai, *Heterocycles* **1995**, 2, 607–617.
- [354] K. Omura, A. K. Sharma, D. Swern, *J. Org. Chem.* **1976**, 41, 957–962.
- [355] F. A. Davis, M. S. Haque, *J. Org. Chem.* **1986**, 51, 4083–4085.
- [356] F. A. Davis, B. C. Chen, *Chem. Rev.* **1992**, 92, 919–934.
- [357] C. Schotten, *Ber. Dtsch. Chem. Ges.* **1884**, 17, 2544–2547.
- [358] E. Baumann, *Ber. Dtsch. Chem. Ges.* **1886**, 19, 3218–3222.
- [359] R. Gabaitsekgosi, C. J. Hayes, *Tetrahedron Lett.* **1999**, 40, 7713–7716.
- [360] S. Ohira, K. Okai, T. Moritani, *J. Chem. Soc., Chem. Commun.* **1992**, 721–722.
- [361] R. Pappo, J. D. S. Allen, R. U. Lemieux, W. S. Johnson, *J. Org. Chem.* **1956**, 21, 478–479.
- [362] T. Honda, *Pure Appl. Chem.* **2010**, 82, 1773–1783.
- [363] F. Gosselin, W. D. Lubell, *J. Org. Chem.* **1998**, 63, 7463–7471.
- [364] J. P. Adams, G. Robertson, *Contemp. Org. Synth.* **1997**, 4, 183–195.

- [365] J. P. Adams, *Contemp. Org. Synth.* **1997**, 4, 517–543.
- [366] L.-W. Xu, J. Luo, Y. Lu, *Chem. Commun.* **2009**, 1807–1821.
- [367] C. Lamazzi, P. Calinaud, *Heterocycles* **2003**, 60, 1447–1456.
- [368] R. Sterzycki, *Synthesis* **1979**, 1979, 724–725.
- [369] P. A. Grieco, Y. Yokoyama, G. P. Withers, F. J. Okuniewicz, C. L. J. Wang, *J. Org. Chem.* **1978**, 43, 4178–4182.
- [370] R. C. F. Jones, D. J. C. Berthelot, J. N. Iley, *Tetrahedron* **2001**, 57, 6539–6555.
- [371] J. D. Hargrave, G. Bish, G. K. Köhn, C. G. Frost, *Org. Biomol. Chem.* **2010**, 8, 5120–5125.
- [372] R. A. Aycock, C. J. Pratt, N. T. Jui, *ACS Catal.* **2018**, 8, 9115–9119.
- [373] Y. Sasano, S. Nagasawa, M. Yamazaki, M. Shibuya, J. Park, Y. Iwabuchi, *Angew. Chem. Int. Ed.* **2014**, 53, 3236–3240.
- [374] J. E. Steves, S. S. Stahl, *J. Am. Chem. Soc.* **2013**, 135, 15742–15745.
- [375] C. Xie, M. T. C. Runnegar, B. B. Snider, *J. Am. Chem. Soc.* **2000**, 122, 5017–5024.
- [376] S. V. Ley, J. Norman, W. P. Griffith, S. P. Marsden, *Synthesis* **1994**, 1994, 639–666.
- [377] A. J. Bailey, W. P. Griffith, S. I. Mostafa, P. A. Sherwood, *Inorg. Chem.* **1993**, 32, 268–271.
- [378] K. Omura, D. Swern, *Tetrahedron* **1978**, 34, 1651–1660.
- [379] P. Garner, *Tetrahedron Lett.* **1984**, 25, 5855–5858.
- [380] A. Moyano, R. Rios, *Chem. Rev.* **2011**, 111, 4703–4832.
- [381] D. Seebach, J. Goliński, *Helv. Chim. Acta* **1981**, 64, 1413–1423.
- [382] D. Neuhaus, M. P. Williamson, *The nuclear Overhauser effect in structural and conformational analysis*, 2nd ed., Wiley, New York, **2000**.
- [383] H. P. Kokatla, P. F. Thomson, S. Bae, V. R. Doddi, M. K. Lakshman, *J. Org. Chem.* **2011**, 76, 7842–7848.
- [384] S. Rendler, D. W. C. MacMillan, *J. Am. Chem. Soc.* **2010**, 132, 5027–5029.
- [385] T. Berranger, Y. Langlois, *J. Org. Chem.* **1995**, 60, 1720–1726.
- [386] W. W. Schoeller, J. Niemann, P. Rademacher, *J. Chem. Soc., Perkin Trans. 2* **1988**, 369–373.
- [387] P. J. Voorstad, J. M. Chapman, G. H. Cocolas, S. D. Wyrick, I. H. Hall, *J. Med. Chem.* **1985**, 28, 9–12.
- [388] Y.-H. Zhu, M. Zhang, Q.-Y. Li, Q. Liu, J. Zhang, Y.-Y. Yuan, F.-J. Nan, M.-W. Wang, *Chin. Chem. Lett.* **2014**, 25, 693–698.

- [389] J. Jurczak, D. Gryko, E. Kobrzycka, H. Gruza, P. Prokopowicz, *Tetrahedron* **1998**, *54*, 6051–6064.
- [390] M. K. Gurjar, S. Pal, A. V. Rama Rao, R. J. Pariza, M. S. Chorghade, *Tetrahedron* **1997**, *53*, 4769–4778.

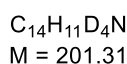
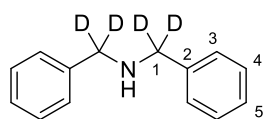
Appendix I: Miscellaneous experimental procedures

(*E*)-1-propenyl phenyl sulfone (**657**)^[385]



Allyl phenyl sulfone (1.82 g, 10 mmol) was dissolved in dichloromethane (10 mL), and 1 M aq. NaOH (5 mL) and Bu₄NOH (0.26 g, 1 mmol) was added. The reaction mixture was stirred for 4 h at room temperature, diluted with dichloromethane (40 mL), washed with water (20 mL) and brine (20 mL). The organic phase was dried (MgSO₄), filtered, and concentrated under reduced pressure. The obtained mixture of isomers was purified by recrystallization from triethylamine to afford the product (207 mg, 1.13 mmol, 11%) as a crystalline solid. **R_f** (20% EA in petroleum ether): 0.17. **¹H NMR** (400 MHz, CDCl₃) δ: 7.93 – 7.85 (2 H, m, H₅), 7.64 – 7.57 (1 H, m, H₇), 7.57 – 7.49 (2 H, m, H₆), 6.99 (1 H, dq, *J* = 6.9, 15.0 Hz, H₂), 6.34 (1 H, dq, *J* = 1.6, 15.0 Hz, H₁), 1.93 (3 H, dd, *J* = 1.6, 6.9 Hz, H₃). **¹³C NMR** (101 MHz, CDCl₃) δ: 142.7 (C₂), 140.8 (C₄), 133.4 (C₇), 132.0 (C₁), 129.4 (2 C, C₆), 127.7 (2 C, C₅), 17.5 (C₃). The data are in accordance with those previously reported in the literature.^[385]

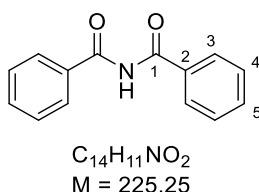
bis(phenylmethyl-*d*₂)amine (**d₄-346**)



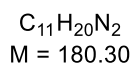
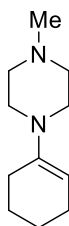
N-benzoylbenzamide (225 mg, 1.0 mmol) was dissolved in THF (10 mL). After careful addition of lithium aluminium deuteride (126 mg, 3.0 mmol) the reaction mixture was heated to reflux with stirring for 18 h. The purple solution was allowed to cool to ambient temperature and then quenched by slow addition of solid sodium sulphate hexahydrate under vigorous stirring. The resulting slurry was diluted with Et₂O and filtered. The colorless filtrate was concentrated *in vacuo*. The resulting oil was purified using flash column chromatography

(50% EtOAc in P.E.) to afford bis(phenylmethyl- d_2)amine (141 mg, 70%) as a colorless oil. **R_f** (50% EtOAc in P.E.): 0.35; **IR** $\nu_{\text{max}}/\text{cm}^{-1}$ (film): 3059, 3024, 2160, 2061, 1947, 1493, 1447, 1420, 1234, 1131, 1071, 1025, 912, 842, 787, 695. **¹H NMR** (400 MHz, CDCl₃) δ : 7.43 – 7.26 (10 H, m, H_{3,4,5}), 1.68 (1 H, br s, N–H); **¹³C NMR** (101 MHz, CDCl₃) δ : 140.3 (C₂), 128.4 (C_{3/4}), 128.2 (C_{3/4}), 127.0 (C₅), 52.4 (quint, J = 20.5 Hz, C₁). ***m/z* HRMS** found [M + H]⁺ 202.1528, C₁₄H₁₂D₄N requires 202.1528.

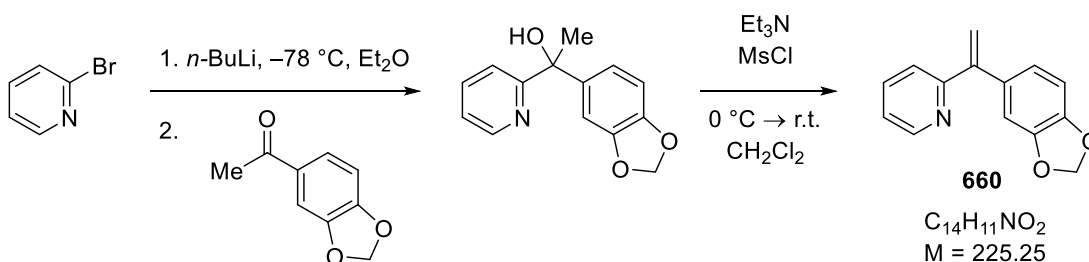
***N*-benzoylbenzamide (658)**^[387]



Benzamide (15 g, 124 mmol) was dissolved in pyridine (75 mL) and cooled to 0°C. After the dropwise addition of benzoyl chloride (17.5 mL, 125 mmol) the reaction mixture was stirred at 0 °C for 8 h, then H₂O (300 mL) was added in one portion to the reaction. The reaction mixture was extracted with Et₂O (2 x 100 mL). The combined organic phases were washed with 10% aqueous H₂SO₄ (2 x) leading to the formation of a colorless crystalline precipitate, which was collected by filtration. A second crop of crystals can be obtained from the organic layer upon standing. The combined precipitate was recrystallized from EtOAc to afford *N*-benzoylbenzamide (3.26 g, 12%) as colorless needles. **m.p.** 139 – 140 °C; **IR** $\nu_{\text{max}}/\text{cm}^{-1}$ (neat): 3246, 3061, 1703, 1674, 1600, 1582, 1498, 1464, 1443, 1218, 1175, 1114, 1070, 1024, 1000, 972, 851, 806, 706. **¹H NMR** (400 MHz, CDCl₃) δ : 8.97 (1 H, br s, N–H), 7.90 (4 H, d, J = 7.3 Hz, H₃), 7.64 (2 H, t, J = 7.3 Hz, H₅), 7.53 (4 H, t, J = 7.4 Hz, H₄); **¹³C NMR** (101 MHz, CDCl₃) δ : 166.3 (C₁), 133.4 (C₂), 133.1 (C₅), 128.9 (C_{3/4}), 127.9 (C_{3/4}). ***m/z* HRMS** found [M + H]⁺ 226.0863, C₁₄H₁₂NO₂ requires 226.0863. The data are in accordance with those previously reported in the literature.^[387]

4-(cyclohex-1-en-1-yl)-1-methylpiperidine (659)^[386]

A solution of 1-methyl piperazine (5.54 mL, 50 mmol, 1.0 equiv), cyclohexanone (6.22 mL, 60 mmol, 1.2 equiv) and PTSA (50 mg) in toluene (30 mL) was heated to reflux using a Dean-Stark trap for 24 h. After removal of the solvent by distillation. Purification of the residue by vacuum distillation afforded the product (6.80 g, 37.7 mmol, 75%) as a colorless liquid. **b.p.** 64 °C (0.09 mbar). **¹H NMR** (400 MHz, CDCl₃) δ: 4.52 (1 H, br s), 2.67 (4 H, br s), 2.30 (4 H, br s), 2.15 (3 H, s), 1.91 (4 H, br s), 1.52 (2 H, br s), 1.40 (2 H, br s); **¹³C NMR** (101 MHz, CDCl₃) δ: 145.2, 100.2, 55.2, 47.7, 46.0, 27.1, 24.4, 23.2, 22.7. Product obtained via this procedure is in agreement with literature preparations.^[386, 388]

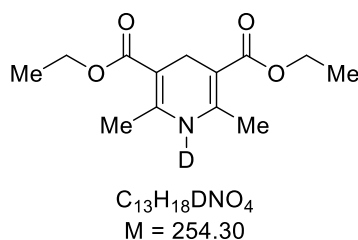
2-(1-(benzo[d][1,3]dioxol-5-yl)vinyl)pyridine (660)**Step 1**

2-Bromopyridine (3.95 g, 2.38 mL, 25.0 mmol) was dissolved in anhydrous Et₂O (100 mL) and cooled to −78 °C under N₂. *n*-Butyllithium (2.5 M in hexanes, 10.0 mL, 25.0 mmol) was added dropwise and the resulting solution stirred at −78 °C for 45 min. A solution of 3',4'-(methylenedioxy)acetophenone in warm THF (20 mL) was added dropwise at −78 °C and the resulting mixture stirred for 18 h while gradually being allowed to warm to ambient temperature. After the addition of aqueous saturated NH₄Cl solution (75 mL) the biphasic mixture was diluted with Et₂O, the organic phase separated, and the aqueous phase extracted

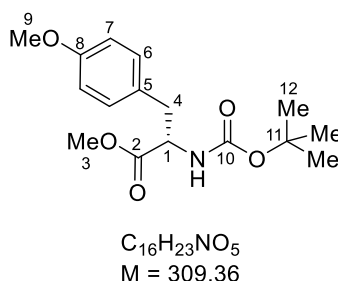
once with Et₂O. The organics were combined and aqueous HCl (3 M, 100 mL) was added. The layers were separated and the aqueous layer extracted twice with Et₂O. The aqueous layer was basified by addition of aqueous NaOH (2.5 M) to pH = 10 and extracted three times with Et₂O. The organic phases were combined, dried (MgSO₄), and removed *in vacuo* to give crude 1-(benzo[d][1,3]dioxol-5-yl)-1-(pyridin-2-yl)ethan-1-ol as a brown oil which was used without further purification. ¹H NMR (400 MHz, CDCl₃) δ: 4.63 (1 H, d, *J* = 5.2 Hz), 7.67 (1 H, t, *J* = 7.5 Hz), 7.29 (1 H, d, *J* = 7.5 Hz), 7.20 (1 H, dd, *J* = 5.3, 7.1 Hz), 7.00 – 6.93 (2 H, m), 6.76 (1 H, d, *J* = 8.8 Hz), 5.93 (2 H, s), 5.82 (1 H, s), 1.90 (3 H, s).

Step 2 (prepared according to modified procedure)^[204]

The crude benzo[d][1,3]dioxol-5-yl)-1-(pyridin-2-yl)ethan-1-ol from step 1 was dissolved in dichloromethane (125 mL) and cooled to 0 °C. After the addition of triethylamine (14 mL, 100 mmol), methanesulfonyl chloride (5.80 mL, 75 mmol) was added dropwise to the reaction mixture. The cooling was then removed and the reaction mixture stirred at ambient temperature for 24 h. After addition of aqueous saturated NH₄Cl solution the biphasic mixture was extracted three times with dichloromethane and the combined organic phases dried (MgSO₄), filtered and concentrated *in vacuo*. The residue was purified by flash column chromatography (gradient elution: 20% EtOAc in P.E. to 30 % EtOAc in P.E.) to afford the product 2-(1-(benzo[d][1,3]dioxol-5-yl)vinyl)pyridine as a pale brown oil that turned dark brown on standing (3.64 g, 64% over 2 steps). *R_f* (20% EtOAc in P.E.): 0.20; *IR* ν_{max}/cm⁻¹ (film): 3048, 3005, 2891, 2777, 1582, 1562, 1500, 1486, 1429, 1354, 1324, 1230, 1104, 1035, 935, 916, 863, 800, 747, 733. ¹H NMR (400 MHz, CDCl₃) δ: 8.62 (1 H, d, *J* = 4.5 Hz), 7.63 (1 H, dt, *J* = 7.7, 1.8 Hz), 7.30 (1 H, d, *J* = 7.7 Hz), 7.19 (1 H, dd, *J* = 7.5, 5.2 Hz), 6.85 – 6.76 (3 H, m), 5.96 (2 H, s), 5.84 (1 H, d, *J* = 1.2 Hz), 5.54 (1 H, d, *J* = 1.2 Hz); ¹³C NMR (101 MHz, CDCl₃) δ: 158.8, 149.3, 148.8, 147.5, 147.4, 136.3, 134.5, 122.9, 122.4, 122.1, 116.8, 108.9, 108.1, 101.1. *m/z* HRMS found [M + H]⁺ 226.0863, C₁₄H₁₂NO₂ requires 226.0863.

diethyl 2,6-dimethyl-1,4-dihydropyridine-3,5-dicarboxylate-1-*d* (*N-d-316*)

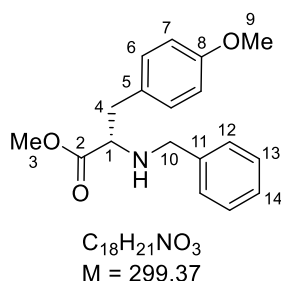
N-d-316 was prepared according to Inouye *et al.*^[248] Commercial ethyl-Hantzsch Ester (2.03 g, 8.00 mmol) was dissolved in a 2:1 mixture of THF (10 mL) and D₂O (5 mL), brought to reflux until all solids were dissolved. The heating was removed and the mixture slowly allowed to cool to −5 °C. The mother liquor was decanted and the described recrystallization repeated. The obtained crystals were collected via vacuum filtration, and dried in vacuum, yielding *N-d-316* (1.31 g, 5.14 mmol, 64%, 97% N-d₁ via ¹H-NMR). ¹H NMR (400 MHz, DMSO-*d*₆) δ: 4.05 (4 H, q, *J* = 7.0 Hz), 3.11 (2 H, br s), 2.11 (6 H, s), 1.18 (6 H, t, *J* = 7.0 Hz); ¹³C NMR (101 MHz, DMSO-*d*₆) δ: 167.1, 146.4, 97.0, 58.9, 24.7, 17.8, 14.4.

methyl (*S*)-2-((tert-butoxycarbonyl)amino)-3-(4-methoxyphenyl)propanoate (448)

Boc-L-tyrosine methyl ester (25.0 g, 84.6 mmol, 1.0 equiv) was dissolved in anhydrous DMF (85 mL). After the addition of solid K₂CO₃ (23.4 g, 169 mmol, 2.0 equiv) and methyl iodide (5.79 mL, 93.1 mmol, 1.1 equiv) the mixture was stirred for 16 h at ambient temperature (monitored by TLC). The reaction mixture was diluted with water (1.5 L) and extracted with dichloromethane (3 x 500 mL). The combined organic phases were successively washed with water and brine, dried (MgSO₄), and concentrated under reduced pressure. The crude oil was purified by flash column chromatography (gradient elution: 10% EtOAc in petroleum ether to 20% EtOAc in petroleum ether) to furnish the product (25.5 g, 82.3 mmol, 97%) as an amorphous colorless solid. *R_f* (20% EtOAc in petroleum ether): 0.27. **IR** *v*_{max}/cm^{−1} (solid): 3394, 2970, 2840, 1736, 1698, 1612, 1585, 1515, 1501, 1440, 1392, 1370, 1295, 1244, 1221,

1162, 1138, 1118, 1063, 1032, 1017, 983. **¹H NMR** (400 MHz, CDCl₃) δ: 7.03 (2 H, d, *J* = 8.6 Hz, H₆), 6.82 (2 H, d, *J* = 8.6 Hz, H₇), 4.97 (1 H, d, *J* = 7.4 Hz, N–H), 4.58 – 4.48 (1 H, m, H₁), 3.77 (3 H, s, H₉), 3.70 (3 H, s, H₃), 3.09 – 2.95 (2 H, m, H₄), 1.41 (9 H, s, H₁₂); **¹³C NMR** (101 MHz, CDCl₃) δ: 172.5 (C₂), 158.8 (C₈), 155.2 (C₁₀), 130.4 (2 C, C₆), 128.0 (C₅), 114.1 (2 C, C₇), 80.0 (C₁₁), 55.3 (C₉), 54.6 (C₁), 52.3 (C₃), 37.6 (C₄), 28.4 (3 C, C₁₂); [**α**]_D²⁵ = + 50.3 (*c* = 1.0, CHCl₃); *m/z* **HRMS** found [M + H]⁺ 310.1653, C₁₆H₂₄NO₅⁺ requires 310.1649. The data are in accordance with those previously reported in the literature.^[389]

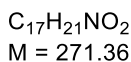
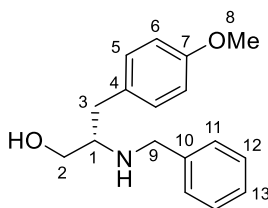
methyl (S)-2-(benzylamino)-3-(4-methoxyphenyl)propanoate (661)



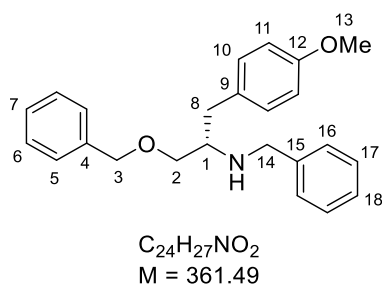
Methyl (S)-2-((tert-butoxycarbonyl)amino)-3-(4-methoxyphenyl)propanoate **448** (3.09 g, 10 mmol, 1.0 equiv) was dissolved in a mixture of dichloromethane (30 mL) and trifluoroacetic acid (10 mL). The solution was stirred for 2 h at room temperature, and all volatiles removed under reduced pressure. The residue was redissolved in dichloromethane (40 mL), cooled to 0 °C, and triethylamine (1.39 mL, 10 mmol, 1.0 equiv) was added, and the resulting solution stirred for 5 min. Benzaldehyde (1.12 mL, 11 mmol, 1.1 equiv) and NaBH(OAc)₃ (3.18 g, 15 mmol, 1.5 equiv) were added successively in one portion. Cooling was removed and the resulting solution was allowed to stir for 16 h at ambient temperature. The mixture was quenched by addition of saturated aq. NaHCO₃ solution, stirred for 30 min, and the aqueous phase extracted with dichloromethane (3 x). The combined organic phases were washed with water, dried (MgSO₄) and concentrated *in vacuo*. The crude residue was purified by flash column chromatography (20% EtOAc in petroleum ether) to yield the product (2.31 g, 7.72 mmol, 77%) as a colorless oil. **R_f** (20% EtOAc in petroleum ether): 0.12. **IR** ν_{max}/cm⁻¹ (film): 3028, 2997, 2950, 2836, 1731, 1611, 1584, 1511, 1453, 1440, 1300, 1245, 1197, 1174, 1128, 1111, 1032, 990. **¹H NMR** (400 MHz, CDCl₃) δ: 7.31 – 7.20 (5 H, m, H_{12,13,14}), 7.07 (2 H, d, *J* = 8.5 Hz, H₆), 6.81 (2 H, d, *J* = 8.5 Hz, H₇), 3.83 – 3.77 (4 H, m, H_{4a,9}), 3.66 – 3.60 (4 H, m, H_{3,4b}), 3.50 (1 H, t, *J* = 6.8 Hz, H₁), 2.91 (2 H, d, *J* = 6.8 Hz, H₄), 1.79 (1 H, br s, N–H); **¹³C**

NMR (101 MHz, CDCl₃) δ : 175.2 (C₂), 158.5 (C₈), 139.7 (C₁₁), 130.3 (2 C, C₆), 129.4 (C₅), 128.5 (2 C), 128.3 (2 C), 127.1 (C₁₄), 113.9 (2 C, C₇), 62.3 (C₁), 55.4 (C₉), 52.1 (C₁₀), 51.8 (C₃), 39.0 (C₄). $[\alpha]_D^{25} = +2.6$ ($c = 1.0$, CHCl₃); **m/z** **HRMS** found $[M + H]^+$ 300.1597, C₁₈H₂₂NO₃⁺ requires 300.1594. The data are in accordance with those previously reported in the literature.^[390]

(S)-2-(benzylamino)-3-(4-methoxyphenyl)propan-1-ol (662)

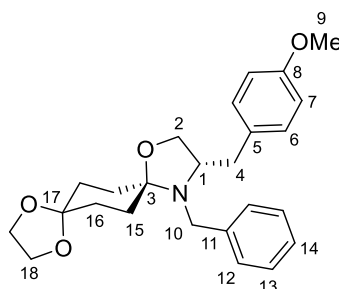


LiAlH₄ (150 mg, 3.96 mmol, 1.2 equiv) was suspended in anhydrous THF (30 mL) at 0 °C, and a solution of methyl (S)-2-(benzylamino)-3-(4-methoxyphenyl)propanoate **661** (1.0 g, 3.3 mmol, 1.0 equiv) in anhydrous THF (10 mL) is added dropwise. The cooling was removed and the reaction mixture was allowed to stir at ambient temperature for 16 h. The suspension was then diluted with Et₂O, and solid NaSO₄·10H₂O was carefully added until no more gas evolution was observed. Methanol (5 mL) was added to the mixture and the suspension stirred for 1 hour. The formed off-white precipitate was removed by filtration through a plug of Celite, washed with dichloromethane, and the filtrate concentrated under reduced pressure. The residue was dried under high vacuum to yield the product (775 mg, 2.85 mmol, 87%) as an colorless solid. **m.p.** 87 – 89 °C (MeOH). **IR** $\nu_{\max}/\text{cm}^{-1}$ (solid): 3294, 3058, 3030 (br), 2998, 2915, 2832, 1611, 1583, 1511, 1463, 1454, 1441, 1376, 1344, 1300, 1247, 1202, 1183, 1177, 1156, 1113, 1073, 1053, 1035, 959. **¹H NMR** (400 MHz, CDCl₃) δ : 7.33 – 7.15 (5 H, m, H_{11,12,13}), 7.05 (2 H, d, $J = 8.5$ Hz, H₅), 6.82 (2 H, d, $J = 8.5$ Hz, H₆), 3.78 (3 H, s, H₈), 3.75 (2 H, s, H₉), 3.63 (1 H, dd, $J = 3.8, 10.7$ Hz, H_{2a}), 3.32 (1 H, dd, $J = 5.2, 10.7$ Hz, H_{2b}), 2.93 – 2.86 (1 H, m, H₁), 2.78 – 2.65 (2 H, m, H₃); **¹³C NMR** (101 MHz, CDCl₃) δ : 158.4 (C₇), 140.2 (C₁₀), 130.5 (C₄), 130.3 (2 C, C₅), 128.6 (2 C), 128.1 (2 C), 127.2 (C₁₃), 114.1 (2 C, C₆), 62.5 (C₂), 59.5 (C₁), 55.4 (C₈), 51.2 (C₉), 37.3 (C₃). $[\alpha]_D^{25} = -6.1$ ($c = 1.0$, CHCl₃); **m/z** **HRMS** found $[M + H]^+$ 272.1647, C₁₇H₂₂NO₂⁺ requires 272.1645.

(S)-N-benzyl-1-(benzyloxy)-3-(4-methoxyphenyl)propan-2-amine (663)

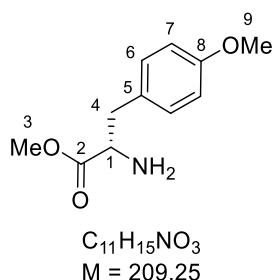
To a solution of (S)-2-(benzylamino)-3-(4-methoxyphenyl)propan-1-ol **662** (1.09 g, 4.00 mmol, 1.0 equiv) in anhydrous THF (40 mL) was carefully added sodium hydride (176 mg, 60% in mineral oil, 4.40 mmol, 1.1 equiv) and the resulting mixture was heated to reflux for 30 min. The reaction mixture was allowed to cool and benzyl bromide (571 μL , 4.8 mmol, 1.2 equiv) was added dropwise at room temperature with stirring. The reaction mixture was heated to reflux for 14 h, quenched by careful addition of methanol, and concentrated under reduced pressure. The residue was taken up in dichloromethane (40 mL) and sat. aq. sodium bicarbonate solution (40 mL). The phases were separated and the aqueous phase was extracted three times with dichloromethane. The combined organic phases were dried (MgSO_4), filtered and concentrated *in vacuo*. The crude material was purified by flash column chromatography (20% EtOAc in petroleum ether) to yield the product (984 mg, 2.72 mmol, 68%) as a colorless oil. **R_f** (40% EtOAc in petroleum ether): 0.20. **IR** $\nu_{\text{max}}/\text{cm}^{-1}$ (film): 3061, 3028, 2906 (br), 2855, 2835, 1611, 1583, 1510, 1495, 1453, 1362, 1300, 1244, 1205, 1176, 1090, 1071, 1028, 909. **¹H NMR** (400 MHz, CDCl_3) δ : 7.36 – 7.19 (10 H, m, $\text{H}_{5,4,7,16,17,18}$), 7.06 (2 H, d, $J = 8.5$ Hz, H_{10}), 6.81 (2 H, d, $J = 8.5$ Hz, H_{11}), 4.48 (2 H, s, H_3), 3.81 (2 H, br s, H_{14}), 3.79 (3 H, s, H_{13}), 3.47 – 3.37 (2 H, m, H_2), 3.00 (1 H, quint, $J = 6.0$ Hz, H_1), 2.81 – 2.70 (2 H, m, H_8), 1.76 (1 H, br s, N–H); **¹³C NMR** (101 MHz, CDCl_3) δ : 158.1 (C_{12}), 140.7 (C_{15}), 138.5 (C_4), 131.1 (C_9), 130.4 (2 C, C_{10}), 128.49 (2 C), 128.47 (2 C), 128.2 (2 C), 127.8 (2 C), 127.7, 126.9, 113.9 (2 C, C_{11}), 73.3 (C_3), 71.8 (C_2), 58.2 (C_1), 55.4 (C_{13}), 51.6 (C_{14}), 37.4 (C_8). $[\alpha]_{\text{D}}^{25} = -0.6$ ($c = 1.0$, CHCl_3). ***m/z* HRMS** found $[\text{M} + \text{H}]^+$ 362.2116, $\text{C}_{16}\text{H}_{20}\text{NO}_4^+$ requires 362.2115.

(S)-12-benzyl-11-(4-methoxybenzyl)-1,4,9-trioxa-12-azadispiro[4.2.48.25]tetradecane
(664)

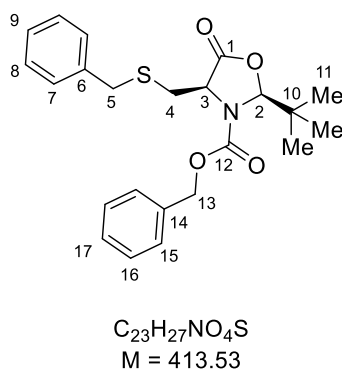


$C_{25}H_{31}NO_4$
 $M = 409.53$

(S)-2-(benzylamino)-3-(4-methoxyphenyl)propan-1-ol **662** (1.0 g, 3.69 mmol, 1.0 equiv) and 1,4-cyclo-hexanedione monoethylene acetal (2.30 g, 14.7 mmol, 4.0 equiv) were suspended in xylene (10 mL). After addition of activated molecular sieves (3 Å, 800 mg) and PTSA (70 mg) the mixture was set to reflux for 48 h with vigorous stirring. The reaction mixture was allowed to cool, taken up in dichloromethane, filtered and concentrated *in vacuo*. The residue was subjected to flash column chromatography (gradient elution: 10% EtOAc in petroleum ether to 20% EtOAc in petroleum ether) to yield the product (795 mg, 1.94 mmol, 53%) as a yellow oil. R_f (50% EtOAc in petroleum ether): 0.54. **IR** $\nu_{\max}/\text{cm}^{-1}$ (film): 3026, 2931, 2878, 2835, 1716, 1611, 1583, 1511, 1494, 1441, 1373, 1337, 1300, 1245, 1208, 1177, 1138, 1102, 1032, 967. **^1H NMR** (400 MHz, CDCl_3) δ : 7.42 (2 H, d, $J = 7.3$ Hz, H_{12}), 7.32 (2 H, t, $J = 7.3$ Hz, H_{13}), 7.24 (1 H, t, $J = 7.3$ Hz, H_{14}), 6.87 (2 H, d, $J = 8.6$ Hz, H_6), 6.73 (2 H, d, $J = 8.6$ Hz, H_7), 4.02 (1 H, d, $J = 14.1$ Hz, H_{10a}), 3.96 – 3.89 (4 H, m, H_{18}), 3.79 – 3.75 (1 H, m, H_{2a}), 3.75 (3 H, s, H_9), 3.69 – 3.69 (2 H, m, $\text{H}_{2a,10b}$), 3.26 – 3.17 (1 H, m, H_1), 2.53 (1 H, d, $J = 3.6, 13.5$ Hz, H_{4a}), 2.24 (1 H, d, $J = 10.3, 13.5$ Hz, H_{4b}), 2.00 – 1.76 (4 H, m, $\text{H}_{15/16}$), 1.75 – 1.64 (4 H, m, $\text{H}_{15/16}$); **^{13}C NMR** (101 MHz, CDCl_3) δ : 158.1 (C_8), 141.1 (C_{11}), 131.4 (C_5), 129.9 (2 C, C_6), 128.5 (2 C, C_{12}), 128.3 (2 C, C_{13}), 127.0 (C_{14}), 113.9 (2 C, C_7), 108.6 (C_{17}), 95.7 (C_3), 68.7 (C_2), 64.5 (C_{18}), 64.5 (C_{18}), 64.3 (C_1), 55.3 (C_9), 52.5 (C_{10}), 40.1 (C_4), 34.2 ($\text{C}_{15/16}$), 32.2 ($\text{C}_{15/16}$), 31.7 ($\text{C}_{15/16}$), 27.2 ($\text{C}_{15/16}$). $[\alpha]_D^{25} = -15.9$ ($c = 1.0$, CHCl_3); m/z **HRMS** found $[\text{M} + \text{H}]^+$ 410.2321, $\text{C}_{25}\text{H}_{32}\text{NO}_4^+$ requires 410.2326.

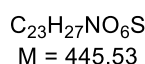
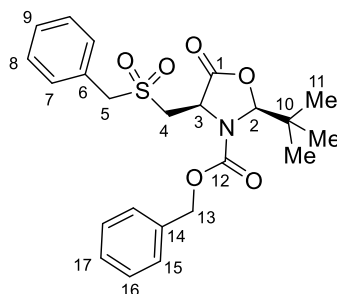
methyl (S)-2-amino-3-(4-methoxyphenyl)propanoate (409)

Methyl (S)-2-((tert-butoxycarbonyl)amino)-3-(4-methoxyphenyl)propanoate **448** (6.18 g, 20 mmol, 1.0 equiv) was dissolved in dichloromethane (20 mL) and trifluoroacetic acid (20 mL). The resulting solution was stirred for 3 h. The solvent was removed under reduced pressure and the oily residue was taken up in aq. sat. sodium bicarbonate solution. The resulting aqueous phase extracted with dichloromethane (3 x). The combined organic phases were dried (MgSO_4), filtered and concentrated *in vacuo* to yield the product (3.64 g, 13.8 mmol, 69%) as a pale orange oil. The product slowly forms insoluble decomposition products at ambient temperature. Storage at $-20\text{ }^\circ\text{C}$ allowed the product to remain sufficiently pure for several weeks. **IR** $\nu_{\text{max}}/\text{cm}^{-1}$ (film): 2998, 2951, 2837, 1733, 1611, 1583, 1511, 1440, 1300, 1244, 1195, 1175, 1111, 1032, 817. **^1H NMR** (400 MHz, CDCl_3) δ : 7.09 (2 H, d, $J = 8.6$ Hz, H_6), 6.83 (2 H, d, $J = 8.6$ Hz, H_7), 3.77 (3 H, s, H_9), 3.70 (3 H, s, H_3), 3.68 (1 H, dd, $J = 5.3, 7.8$ Hz, H_1), 3.01 (1 H, dd, $J = 5.3, 13.6$ Hz, H_{4a}), 2.80 (1 H, dd, $J = 7.7, 13.6$ Hz, H_{4b}), 1.43 (2 H, s, NH_2); **^{13}C NMR** (101 MHz, CDCl_3) δ : 175.6 (C_2), 158.6 (C_8), 130.3 (2 C, C_6), 129.2 (C_5), 114.1 (2 C, C_7), 56.0 (C_1), 55.3 (C_9), 52.0 (C_3), 40.3 (C_4). m/z **HRMS** found $[\text{M} + \text{H}]^+$ 210.1132, $\text{C}_{11}\text{H}_{16}\text{NO}_3^+$ requires 210.1125.

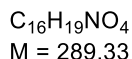
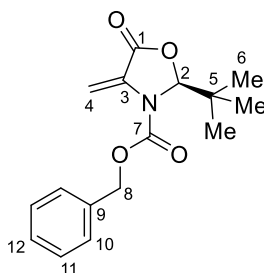
benzyl (2S,4R)-4-((benzylthio)methyl)-2-(tert-butyl)-5-oxooxazolidine-3-carboxylate (615)^[228]

In a three-neck round-bottom flask, *S*-benzyl-L-cysteine (63.3 g, 0.3 mol, 1.0 equiv) was suspended in anhydrous methanol (2.0 L) and freshly powdered NaOH (12 g, 0.3 mol, 1.0 equiv) was added in one portion under N₂. The resulting mixture was stirred at room temperature for 10 minutes until clear and pivaldehyde (33 mL, 0.3 mol, 1.0 equiv) and activated molecular sieves (200 g) were added. The reaction mixture was stirred under a nitrogen atmosphere for 16 h at room temperature, rapidly filtered through a plug of celite, washed with methanol and the solvent removed *in vacuo*. The residue was dried at 60°C under high vacuum for 6 hours. The resulting white solid was dissolved in dichloromethane (2.0 L) and the solution cooled to –5 °C. The flask was fitted with an addition funnel and benzyl chloroformate (63.4 mL, 0.45 mol, 1.5 equiv) was added dropwise over 2 h at –5 °C to the stirred solution. The mixture was stirred at –5 °C for a further 18 h, then warmed to room temperature and stirred for an additional 16 h. Aqueous ammonia (10M, 100 mL) was added and the biphasic mixture stirred for 2 h. The mixture was washed with aqueous sodium hydroxide solution (3%, 750 mL) and brine, and the organic phase dried (MgSO₄), filtered and concentrated. Purification of the resulting yellow residue by sequential flash column chromatography (silica, 0% to 10% EtOAc in petroleum ether) furnished the product (26.1 g, 63.1 mmol, 21%) as a colorless oil. **R_f** (7.5% EtOAc in toluene): 0.47. **IR** ν_{max} /cm^{–1} (film): 3064, 3031, 2961, 1790, 1716, 1481, 1454, 1390, 1324, 1281, 1221, 1195, 1168, 1117, 1035, 1016, 968; **¹H NMR** (400 MHz, CDCl₃) δ : 7.37 – 7.32 (5 H, m, H_{15,16,17}), 7.28 – 7.20 (5 H, m, H_{7,8,9}), 5.51 (1 H, s, H₂), 5.20 (1 H, d, *J* = 12.0 Hz, H_{13a}), 5.15 (1 H, d, *J* = 12.0 Hz, H_{13b}), 4.51 (1 H, t, *J* = 6.9 Hz, H₃), 3.78 (1 H, d, *J* = 13.4 Hz, H_{5a}), 3.71 (1 H, d, *J* = 13.4 Hz, H_{5b}), 2.90 (1 H, dd, *J* = 7.9, 14.0 Hz, H_{4a}), 2.75 (1 H, dd, *J* = 6.2, 14.0 Hz, H_{4b}), 0.89 (9 H, s, H₁₁); **¹³C NMR** (101 MHz, CDCl₃) δ : 171.4 (C₁), 156.0 (C₁₂), 137.9 (C₆), 135.2 (C₁₄), 192.2 (2 C), 128.9 (3 C), 128.71 (2 C), 128.66 (2 C), 127.3 (C₉), 96.5 (C₂), 68.7 (C₁₃), 57.7 (C₃), 37.1 (C₁₀), 36.7 (C₅), 33.5 (C₄), 25.0 (3 C, C₁₁); *m/z* **HRMS** found [M + H]⁺ 414.1736, C₂₃H₂₈NO₄S⁺ requires 414.1734. The data are in accordance with those previously reported in the literature.^[228]

benzyl (2*S*,4*R*)-4-((benzylsulfonyl)methyl)-2-(tert-butyl)-5-oxooxazolidine-3-carboxylate^[228] (616)



To a stirred solution of benzyl (2*S*,4*R*)-4-((benzylthio)methyl)-2-(tert-butyl)-5-oxooxazolidine-3-carboxylate **718** (26.1 g, 63.2 mmol, 1.0 equiv) in dichloromethane (1.0 L) was added *m*-chloroperoxybenzoic acid (70 %, 38.9 g, 158 mmol, 2.5 equiv) portionwise. The solution was stirred at room temperature for 16 h and then washed with aq. sodium hydroxide (1 M, 3 x 500mL). The organic phase was dried (MgSO_4), filtered and evaporated *in vacuo*. The residue was dried under high vacuum overnight to obtain the pure product as a white amorphous solid (26.9 g, 60.3 mmol, 95%). **IR** $\nu_{\text{max}}/\text{cm}^{-1}$ (solid): 2969, 1790, 1719, 1496, 1482, 1456, 1393, 1310, 1285, 1225, 1198, 1178, 1118, 1038, 1015, 966. **¹H NMR** (400 MHz, CDCl_3) δ : 7.44 – 7.33 (10 H, m, $\text{H}_{7,8,9,15,16,17}$), 5.62 (1 H, s, H_2), 5.28 (1 H, d, $J = 12.1$ Hz, H_{13a}), 5.21 (1 H, d, $J = 12.1$ Hz, H_{13b}), 5.08 (1 H, dd, $J = 4.1, 8.0$ Hz, H_3), 4.67 (1 H, d, $J = 14.0$ Hz, H_{5a}), 4.42 (1 H, d, $J = 14.0$ Hz, H_{5b}), 3.44 (1 H, dd, $J = 8.0$ Hz, 15.3 Hz, H_{4a}), 3.15 (1 H, dd, $J = 4.1, 15.3$ Hz, H_{4b}), 0.89 (9 H, s, H_{11}). **¹³C NMR** (101 MHz, CDCl_3) δ : 170.8 (C_1), 155.4 (C_{12}), 135.0, 131.1 (2 C), 129.3, 129.2 (2 C), 129.0, 128.92 (2 C), 128.89 (2 C), 128.0, 97.0 (C_2), 69.1 (C_{13}), 60.5 (C_5), 53.8 (C_3), 52.8 (C_4), 37.3 (C_{10}), 24.7 (3 C, C_{11}). ***m/z* HRMS** found $[\text{M} + \text{H}]^+$ 446.1634, $\text{C}_{23}\text{H}_{28}\text{NO}_6\text{S}^+$ requires 446.1632. The data are in accordance with those previously reported in the literature.^[228]

benzyl (S)-2-(tert-butyl)-4-methylene-5-oxooxazolidine-3-carboxylate (360)

A stirred solution of benzyl (2*S*,4*R*)-4-((benzylsulfonyl)methyl)-2-(tert-butyl)-5-oxooxazolidine-3-carboxylate **719** (26.9 g, 60.3 mmol, 1.0 equiv) in dichloromethane (600 mL) was cooled to 0 °C, then DBU (9.9 mL, 66.3 mol, 1.1 equiv) was added dropwise with stirring over the course of 10 min. The reaction was stirred for a further 5 minutes or until complete by TLC. The mixture was then quenched by addition of saturated aq. ammonium chloride solution (250 mL) at 0 °C, and the aqueous phase extracted with dichloromethane (3 x 150 mL). The combined organic phases were dried (MgSO₄), filtered and evaporated under reduced pressure. The residue was purified by flash column chromatography (10% EtOAc in petroleum ether) to yield the product as a colorless oil that solidifies on standing (15.8 g, 54.6 mmol, 91%). *R_f* (20% EtOAc in petroleum ether): 0.45; *IR* $\nu_{\text{max}}/\text{cm}^{-1}$ (solid): 2959, 2904, 2871, 1777, 1718, 1661, 1481, 1467, 1456, 1388, 1367, 1327, 1268, 1255, 1205, 1160, 1132, 1093, 1033, 1009, 962; *¹H NMR* (400 MHz, CDCl₃) δ : 7.43 – 7.35 (5 H, m, H_{10,11,12}), 5.72 (2 H, s, H₄), 5.69 (1 H, br s, H₂), 5.26 (2 H, s, H₈), 0.93 (9 H, s, H₆); *¹³C NMR* (101 MHz, CDCl₃) δ : 164.7 (C₁), 152.5 (br s, C₇), 134.8 (C₉), 130.3 (C₃), 129.0, 128.9 (2 C), 128.8 (br s, 2 C), 104.5 (C₄), 94.1 (C₂), 68.9 (C₈), 38.8 (C₅), 24.5 (3 C, C₆). [α]_D²⁵ = –36.6 (c = 1.0, CHCl₃). *m/z* *HRMS* found [M + H]⁺ 290.1391, C₁₆H₂₀NO₄⁺ requires 290.1387. **Chiral HPLC** *t_R*(major) = 14.5 min, *t_R*(minor) = 18.9 min (98%ee, Daicel CHIRALPAK®-IC, 4.6 mm x 250 mm, eluted with 2% *i*-propanol in hexane, flow 1.0 mLmin^{–1}; see Appendix II). The data are in accordance with those previously reported in the literature.^[371]

Appendix II: Supplementary data

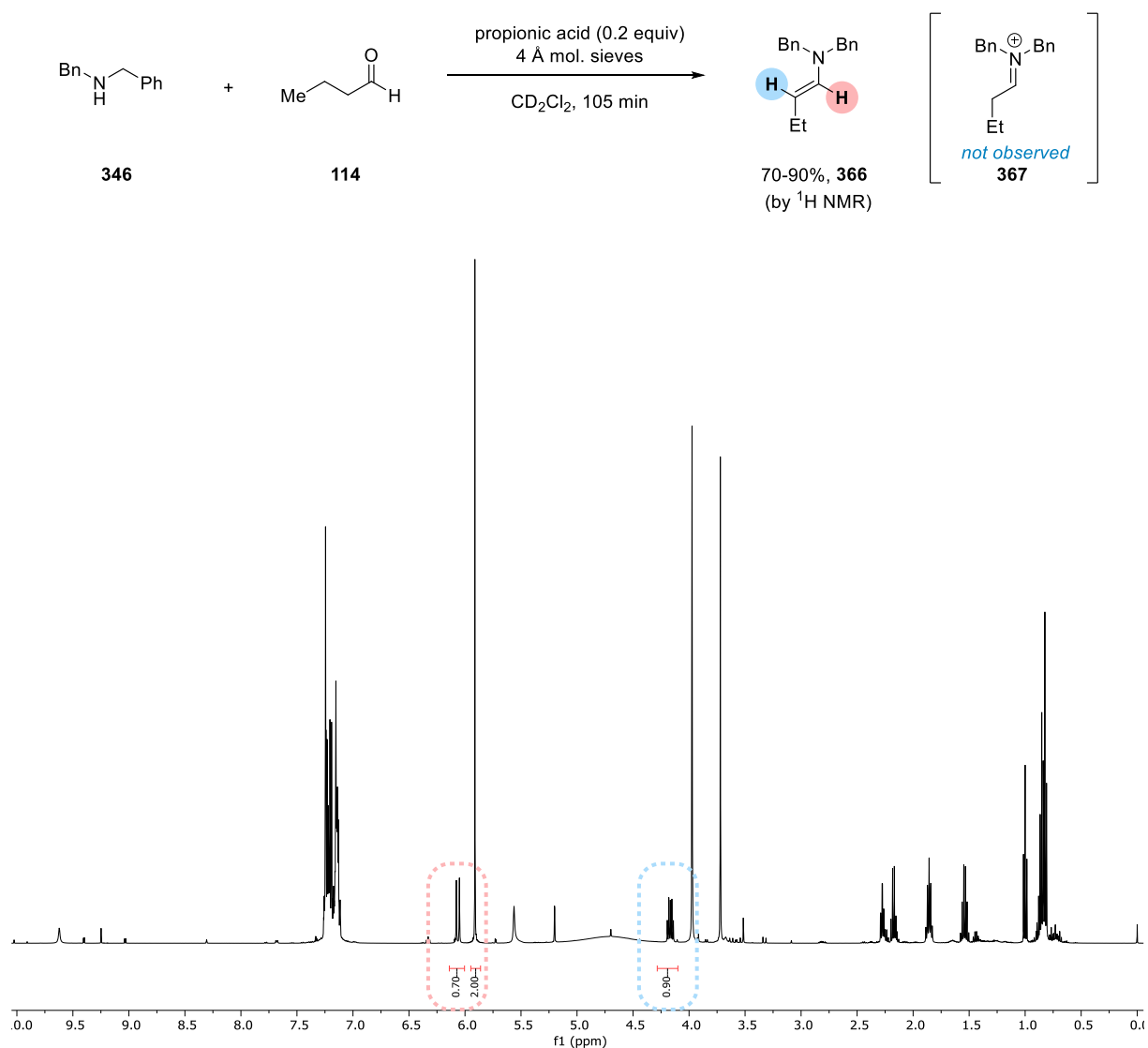
i) ^1H NMR study of the reaction mixture

Figure 24. NMR study to determine the predominant species in the crude reaction mixture. Crude mixture of dibenzylamine, butyraldehyde, propionic acid (0.2 equiv) in CD_2Cl_2 . Data recorded after 105 min. Internal standard 1,1,2,2-tetrachloroethane (1.0 equiv).

ii) Stern Volmer quenching studies

Emission intensities were recorded using a Shimadzu RF-6000 spectrofluorometer. Experiments were recorded using a quartz cell equipped with septa-lined screw cap under Ar. All *fac*-Ir(ppy)₃ solutions were excited at 320 nm and the emission intensity recorded at 518 nm. The iminium ion was weighed in a glove box and a stock solution formed in anhydrous degassed dichloromethane and stored in a Schlenk tube. The appropriate amount of *fac*-Ir(ppy)₃, as a solution in anhydrous degassed dichloromethane, and iminium tetrafluoroborate **364** was added to the dry quartz cell equipped with septa-lined screw cap under Ar and the emission spectra collected. The emission of each concentration was recorded 5 times and an average was taken.

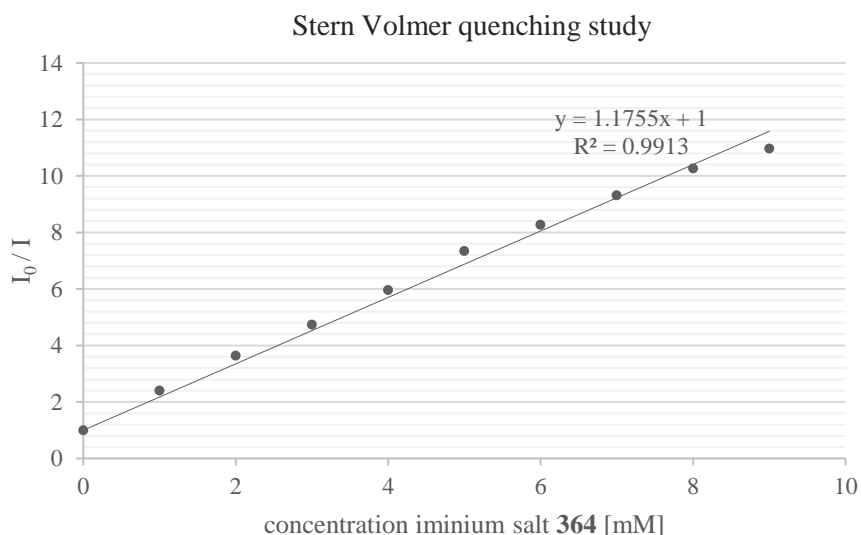


Figure 25. Stern Volmer quenching study recording emission intensities of *fac*-Ir(ppy)₃ ($c = 10 \mu\text{M}$ in dichloromethane) with varying concentration of iminium salt **364**.

$$\text{Stern Volmer equation: } F_0/F = 1 + k_q \tau_0 [Q]$$

$$k_q \tau_0 = 1.176 \text{ L} \cdot \text{mol}^{-1}$$

$$\tau_0 = 1.9 \mu\text{s}$$

$$k_q = 6.2 \times 10^5 \text{ L} \cdot \text{mol}^{-1} \text{s}^{-1}$$

iii) UV-Vis studies

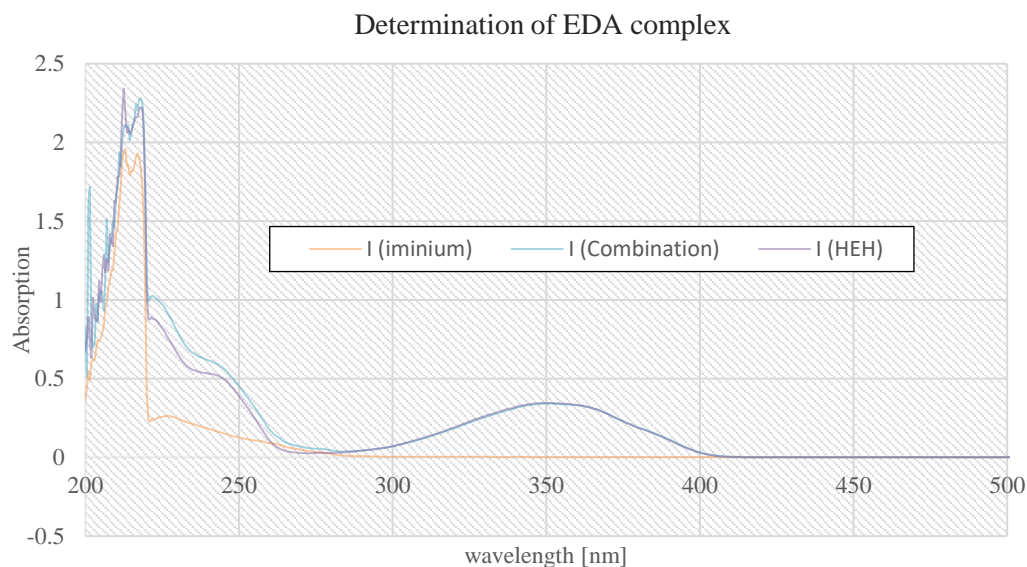
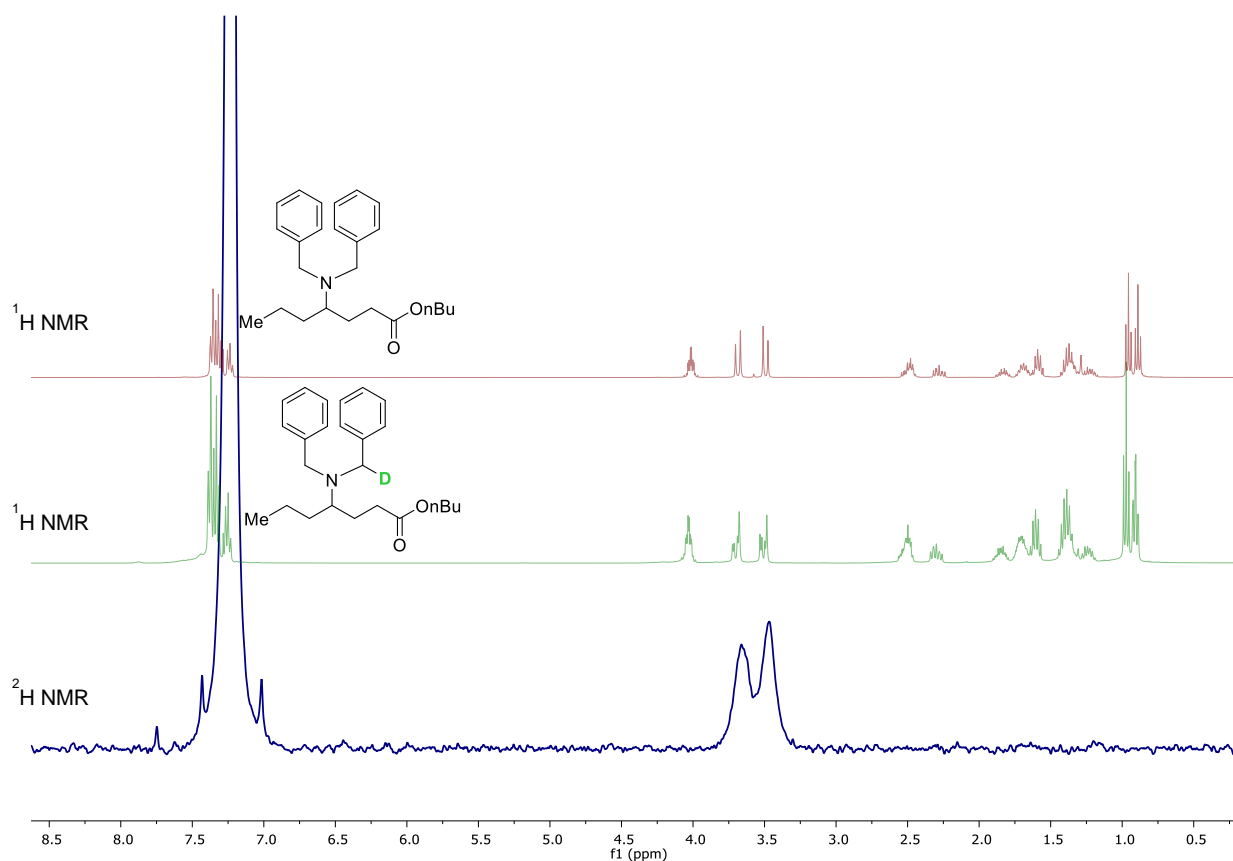
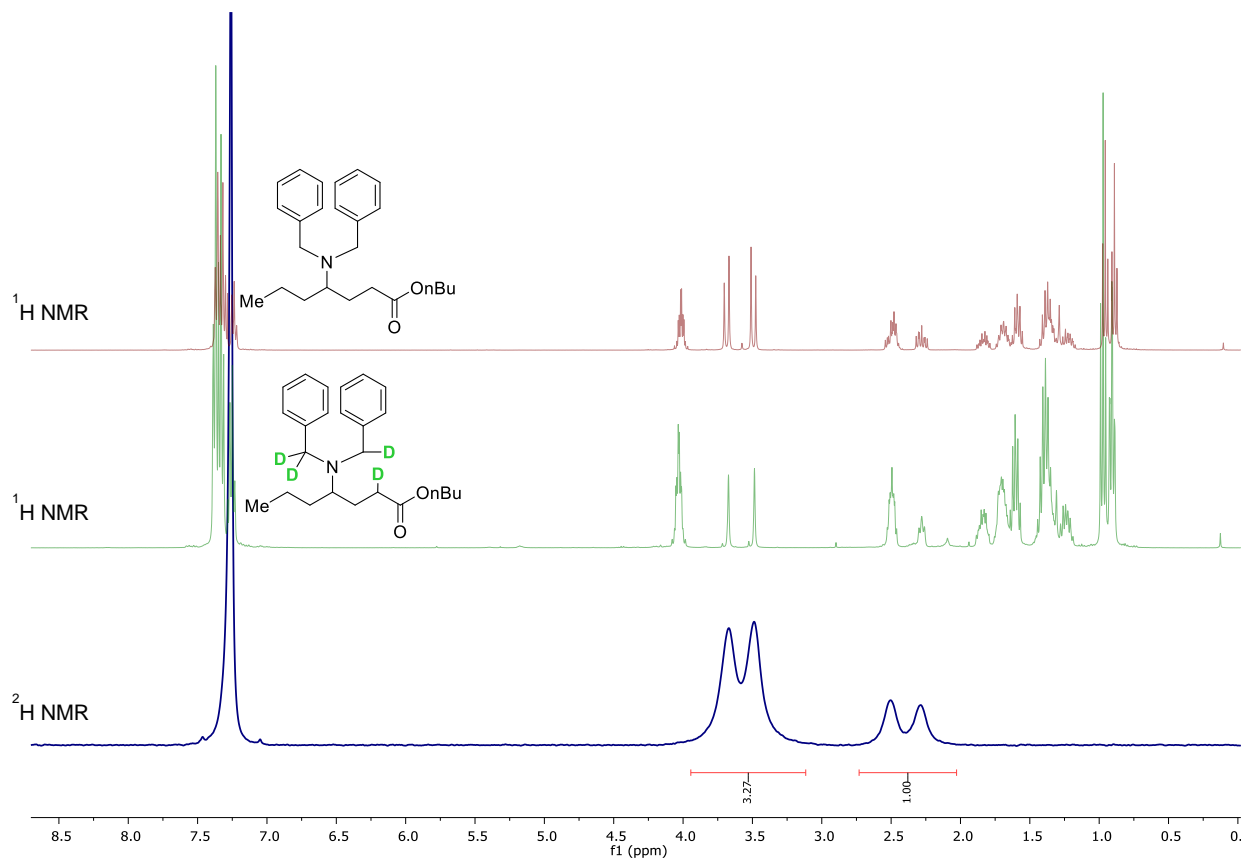


Figure 26 UV-Vis studies on iminium salt **364** and Hantzsch ester **316**. Study performed by A. Trowbridge.

UV-Vis analysis was performed on a Shimadzu UV-1800 spectrophotometer. Experiments were recorded using a quartz cell equipped with septa-lined screw cap under Ar. In a typical experiment, the iminium salt **364** was weighed in a glove box and a stock solution formed in anhydrous degassed dichloromethane and stored in a Schlenk tube (2 mM). The appropriate amount of Hantzsch ester, as a solution in anhydrous degassed dichloromethane (2 mM), and iminium ion was added to the dry quartz cell equipped with septa-lined screw cap under Ar and made up to a total volume of 3.5 mL with anhydrous degassed dichloromethane (0.057 mM). The presence of an electron donor-acceptor (EDA) complex was not observed.

iv) Deuterium labelling study 1

**Figure 27.** ^1H - and ^2H -NMR data for deuterium labelling study 1 using deuterated Hantzsch Ester d_2 -316.**Figure 28.** ^1H - and ^2H -NMR data for deuterium labelling study 1 using d_4 -dibenzylamine d_4 -346.

v) Deuterium labelling study with enamines and 1,1- diphenylethylene acceptor

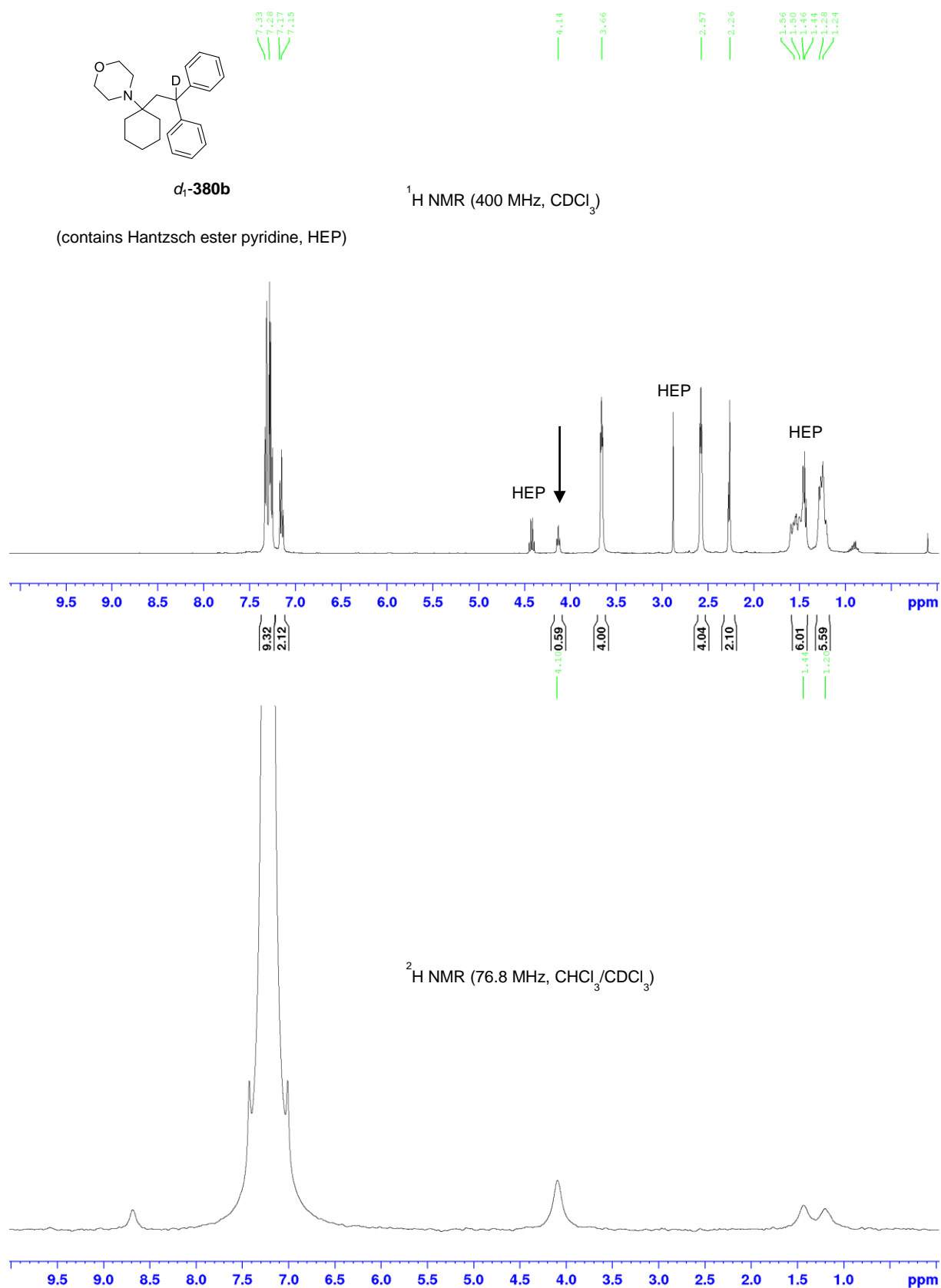


Figure 29. ¹H and ²H NMR of deuterium labelling study with enamines and 1,1- diphenylethylene acceptor. HEP. Hantzsch Ester pyridine.

vi) Deuterium labelling study with enamines and deuterium labelled Brønsted acid

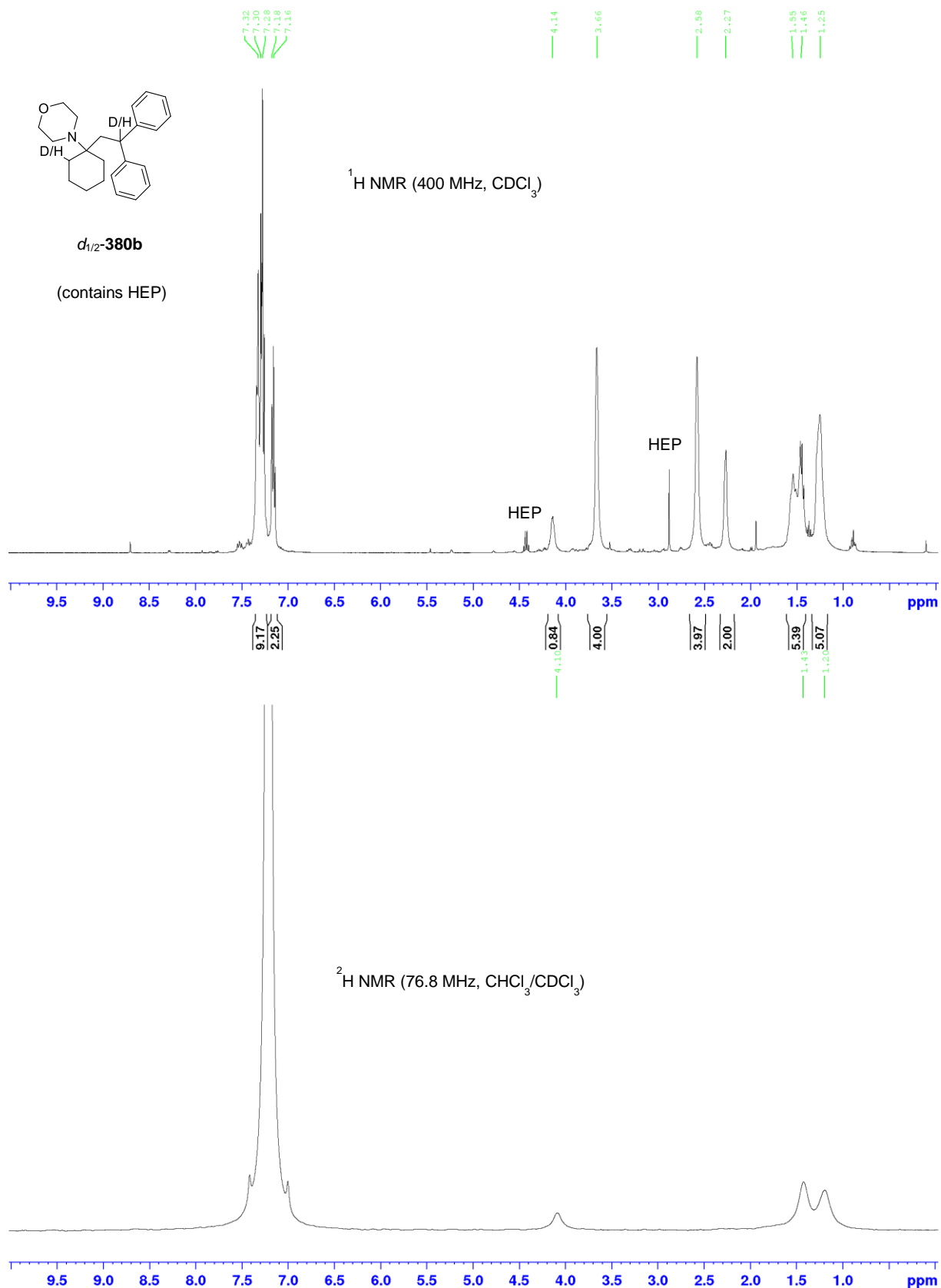
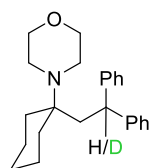


Figure 30. ^1H and ^2H NMR of deuterium labelling study with enamines and 1,1- diphenylethylene acceptor and deuterium labelled Brønsted acid. HEP. Hantzsch Ester pyridine.

***d*₁-4-(1-(2,2-diphenylethyl)cyclohexyl)morpholine (*d*₁-**380b**)**

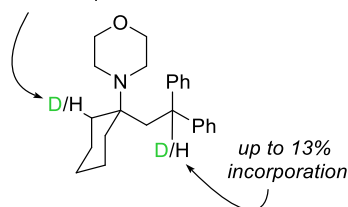
(41% deuterium-incorporation)

d*₁-**380b*

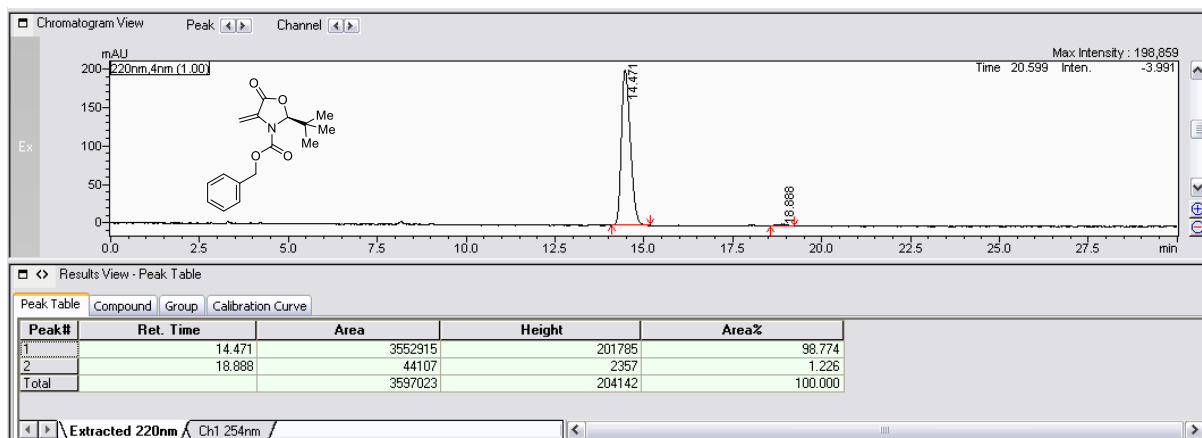
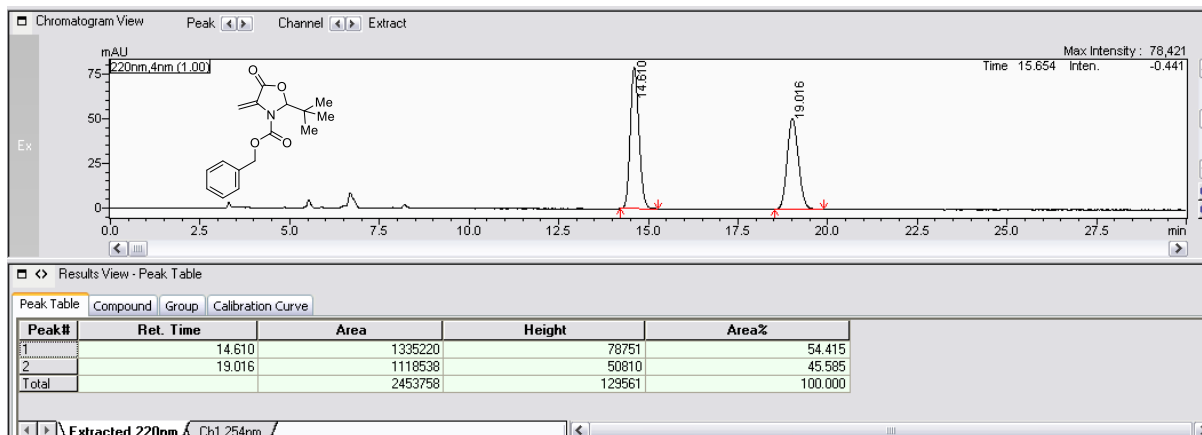
Deuterated compound *d*₁-**380b** was prepared according to general procedure A using 4-cyclohex-1-enylmorpholine (34 μ L, 0.2 mmol), 1,1-diphenylethene (71 μ L, 0.4 mmol), *d*₂-**316** (77 mg, 0.3 mmol), propanoic acid (3 μ L, 40 μ mol) and *fac*-Ir(ppy)₃ (1.4 mg, 2 μ mol) in anhydrous degassed dichloromethane (2 mL). The solvent removed *in vacuo* and the residue purified by flash column chromatography (gradient elution: 1% EtOAc to 3% EtOAc in P.E.) to afford the product as a colorless oil (12 mg, 17%). *R*_f (20% EtOAc in P.E.): 0.54. ²H NMR (76.8 MHz, CHCl₃/CDCl₃) δ : 4.10 (br s, Ph₂CDR, major), 1.43 (br s), 1.20 (br s). *m/z* HRMS found [M + H]⁺ 351.2540 (major), C₂₄H₃₁DNO requires 351.2541.

***d*_{1/2}-4-(1-(2,2-diphenylethyl)cyclohexyl)morpholine (*d*_{1/2}-**380b**)**

up to 80% incorporation

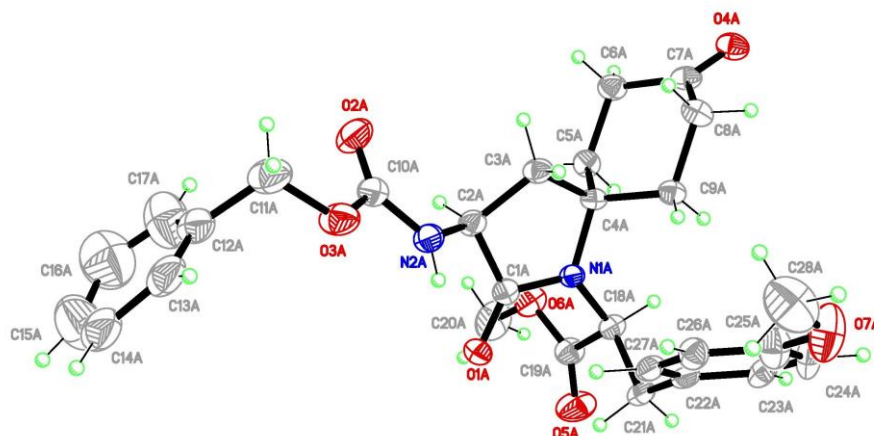
***d*_{1/2}-**380b****

Deuterated compound *d*_{1/2}-**380b** was prepared according to general procedure A using 4-cyclohex-1-enylmorpholine (34 μ L, 0.2 mmol), 1,1-diphenylethene (71 μ L, 0.4 mmol), *N*-*d*-**316** (76 mg, 0.3 mmol), *d*₄-acetic acid (2.3 μ L, 40 μ mol) and *fac*-Ir(ppy)₃ (1.4 mg, 2 μ mol) in anhydrous degassed dichloromethane (2 mL). The crude reaction mixture was purified by flash column chromatography (0.5% Et₃N in dichloromethane) to afford the product as a colorless oil (33 mg, 47%). *R*_f (20% EtOAc in P.E.): 0.54. ²H NMR (76.8 MHz, CHCl₃/CDCl₃) δ : 4.10 (br s, minor), 1.43 (br s, major), 1.17 (br s, major). *m/z* HRMS found [M + H]⁺ 351.2541 (major), C₂₄H₃₁DNO requires 351.2541, found [M + H]⁺ 352.2597 (minor), C₂₄H₃₀D₂NO requires 352.2604.

vii) Chiral HPLC analysis of Karady-Beckwith alkene (**360**)

Daicel CHIRALPAK®-IC, 4.6 mm x 250 mm, 2% *i*-propanol in hexane, flow 1.0 mLmin⁻¹

viii) X-ray crystallography, 609



Identification code	MG_B1_0047	
Empirical formula	C ₂₈ H ₃₂ N ₂ O ₇	
Formula weight	508.55	
Temperature	180(2) K	
Wavelength	1.54178 Å	
Crystal system	Monoclinic	
Space group	P2 ₁	
Unit cell dimensions	a = 23.1440(7) Å	a = 90°.
	b = 9.0587(3) Å	b = 91.403(2)°.
	c = 25.1442(8) Å	g = 90°.
Volume	5270.0(3) Å ³	
Z	8	
Density (calculated)	1.282 Mg/m ³	
Absorption coefficient	0.761 mm ⁻¹	
F(000)	2160	
Crystal size	0.300 x 0.080 x 0.040 mm ³	
Theta range for data collection	2.564 to 66.699°.	
Index ranges	-27<=h<=27, -10<=k<=10, -29<=l<=29	
Reflections collected	69895	
Independent reflections	18016 [R(int) = 0.0891]	
Completeness to theta = 66.699°	99.9 %	
Absorption correction	Semi-empirical from equivalents	
Max. and min. transmission	0.7528 and 0.6561	
Refinement method	Full-matrix least-squares on F ²	
Data / restraints / parameters	18016 / 673 / 1333	
Goodness-of-fit on F ²	1.021	
Final R indices [I>2sigma(I)]	R1 = 0.0776, wR2 = 0.1979	
R indices (all data)	R1 = 0.1128, wR2 = 0.2233	
Absolute structure parameter	-0.24(14)	
Extinction coefficient	n/a	
Largest diff. peak and hole	0.662 and -0.370 e.Å ⁻³	

Appendix III: Published work

LETTER

<https://doi.org/10.1038/s41586-018-0537-9>

Multicomponent synthesis of tertiary alkylamines by photocatalytic olefin–hydroaminoalkylation

Aaron Trowbridge¹, Dominik Reich¹ & Matthew J. Gaunt^{1*}

There is evidence to suggest that increasing the level of saturation (that is, the number of sp^3 -hybridized carbon atoms) of small molecules can increase their likelihood of success in the drug discovery pipeline¹. Owing to their favourable physical properties, alkylamines have become ubiquitous among pharmaceutical agents, small-molecule biological probes and pre-clinical candidates². Despite their importance, the synthesis of amines is still dominated by two methods: *N*-alkylation and carbonyl reductive amination³. Therefore, the increasing demand for saturated polar molecules in drug discovery has continued to drive the development of practical catalytic methods for the synthesis of complex alkylamines^{4–7}. In particular, processes that transform accessible feedstocks into sp^3 -rich architectures provide a strategic advantage in the synthesis of complex alkylamines. Here we report a multicomponent, reductive photocatalytic technology that combines readily available dialkylamines, carbonyls and alkenes to build architecturally complex and functionally diverse tertiary alkylamines in a single step. This olefin–hydroaminoalkylation process involves a visible-light-mediated reduction of in-situ-generated iminium ions to selectively furnish previously inaccessible alkyl-substituted α -amino radicals, which subsequently react with alkenes to form $C(sp^3)–C(sp^3)$ bonds. The operationally straightforward reaction exhibits broad functional-group tolerance, facilitates the synthesis of drug-like amines that are not readily accessible by other methods and is amenable to late-stage functionalization applications, making it of interest in areas such as pharmaceutical and agrochemical research.

The physiological properties of tertiary aliphatic amines and their ability to interfere with natural neurotransmission pathways have rendered them highly effective pharmaceutical agents⁸, in areas that range from the treatment of neurodegenerative disorders (such as Alzheimer's disease)⁹ to metabolic syndromes (such as obesity)¹⁰ (Fig. 1a). Traditionally, synthetic routes towards these molecules have required multiple steps and tedious purifications, which severely hamper drug discovery efforts. Therefore, the development of straightforward methods that enable the construction of complex tertiary amines from simple starting materials would have far-reaching implications for both the synthetic and the medicinal chemistry communities. Whereas the abundance, diversity and predictable reactivity of sp^2 -hybridized feedstocks has led to the emergence of new transition-metal-catalysed methods of amine synthesis—namely the Buchwald–Hartwig amination¹¹ and olefin–hydroamination^{12–14}—strategies for the synthesis of more complex alkylamines are more limited^{13–15}. We reasoned that an operationally simple and mechanistically distinct catalytic process involving available dialkylamines, olefins and aliphatic carbonyl feedstocks would expand the capacity of olefin–hydroaminoalkylation-based strategies to the synthesis of tertiary alkylamines.

We proposed that an electrophilic iminium ion, formed through the well established reaction between secondary alkylamines and alkyl-substituted carbonyls, could be susceptible to a catalytic single-electron reduction process (Fig. 1b). The resulting α -amino radical could then engage a third reaction component, such as an alkene, in a subsequent

cross-coupling reaction to form a $C(sp^3)–C(sp^3)$ bond. However, there are few methods that report the generation of 'all-alkyl' α -amino radicals from pre-formed iminium ions, and all have issues relating to their practical application. Subsequently, addition of such α -amino radicals to alkenes has been limited to specific intramolecular examples^{16,17}. To overcome these problems we proposed that, first, a visible-light-activated photocatalyst could mediate single-electron transfer (SET) to an in-situ-generated alkyl-substituted iminium ion, generating the desired α -amino radical under mild reaction conditions (Fig. 1b). Second, we considered that a polarity-matched hydrogen-atom transfer (HAT) from a suitable reagent could facilitate cross-coupling to the alkene by intercepting the resulting alkyl-substituted radical. An important feature of this proposed catalytic activation pathway is the regiospecific positioning of the newly formed α -amino radical, made possible by the SET to the iminium ion, regardless of the groups surrounding the reactive centre. Selective formation of an 'all-alkyl' α -amino radical would not be possible via related photocatalytic approaches without the use of pre-functionalized starting materials or inherently selective substrates^{18–20} (Fig. 1c).

We were mindful of several factors that could impede the development of the photocatalytic olefin–hydroaminoalkylation process. Whereas protonated imines and iminium ions that are conjugated with multiple aromatic substituents (half-wave reduction potential, $E_{1/2}^{\text{red}} = -0.8$ to -1.2 V versus saturated calomel electrode (SCE) in acetonitrile)²¹ have been found to partake in a limited range of reductive coupling reactions^{22,23}, the reduction potential of an 'all-alkyl'-iminium ion could be up to $E_{1/2}^{\text{red}} = -1.95$ V (versus SCE in acetonitrile)²¹ and would require a highly reducing photocatalyst that may be incompatible with existing functional groups. Moreover, alkyliminium ions are known to exist in (often unfavourable) equilibrium with the corresponding enamines, which can also undergo SET reactions to form radical species, presenting competing pathways²⁴. Finally, the addition of α -amino radicals to simple alkenes is known to be low-yielding owing to oligomerization of the resulting radical²⁵. We hereby report a comprehensive strategy for the modular and efficient construction of complex tertiary alkylamines via photocatalytic olefin–hydroaminoalkylation.

The initial evaluation of the proposed amine synthesis focused on a reaction between butyraldehyde **1a**, dibenzylamine **2a**, butyl acrylate **3a** and Hantzsch ester **4a** catalysed by $\text{Ir}(\text{ppy})_3$ (ppy, 2-phenylpyridinato), under irradiation by visible light (Fig. 2a). Optimized reaction conditions were readily established (for a detailed account of the optimization study, see Supplementary Materials), using 1 mol% $\text{Ir}(\text{ppy})_3$ and a 40 W blue light-emitting diode (LED) for 2 hours at room temperature. Under these conditions, near-equimolar quantities of aldehyde, amine and alkene, with 1.5 equivalents of Hantzsch ester in a 0.1 M solution of dichloromethane containing molecular sieves and 20 mol% of propionic acid, formed the desired amine **5a**, which was isolated in 84% yield after chromatography (Fig. 2b). The reaction displayed remarkable selectivity; we observed only trace quantities of the reductive-amination side product, which presumably resulted from HAT to the α -amino radical from **4a**²⁶.

¹Department of Chemistry, University of Cambridge, Cambridge, UK. *e-mail: m.jg32@cam.ac.uk

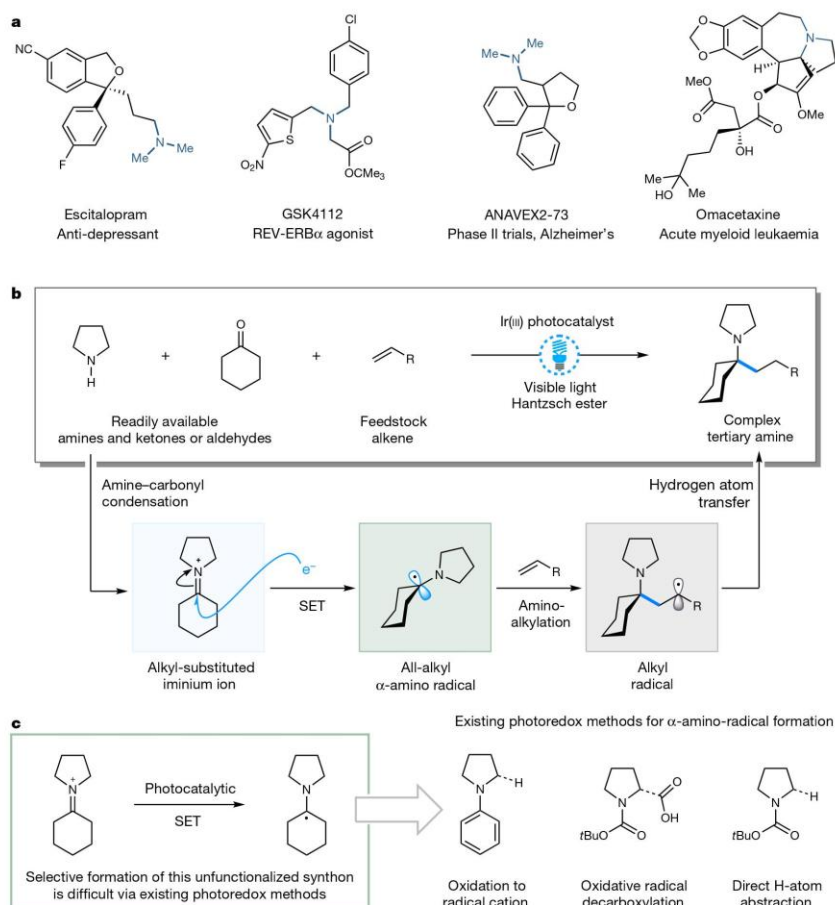


Fig. 1 | Evolution of a strategy for the multicomponent photocatalytic synthesis of tertiary alkylamines. a, Examples highlighting the importance of tertiary amines in the pharmaceutical industry. **b,** Multicomponent photocatalytic olefin-hydroaminoalkylation to yield

tertiary alkylamines via the selective formation of alkyl-substituted α -amino radicals. **c,** Catalytic photoredox methods for the generation of α -amino radicals.

Under the optimized conditions we found that various linear aldehydes, including those bearing electron-rich heteroarenes, reacted efficiently to give amines **5a–5f** in good yields (Fig. 2b). Aldehydes displaying α -branching produced the expected amines **5g–5l** in good yield; notable examples included saturated heterocycles and strained ring features often found in pharmaceutical agents. The α -amino radical formed from formaldehyde and dibenzylamine was effective in the reaction, producing the γ -aminobutyric-acid derivative **5m**; however, benzaldehyde-derived iminium ions failed to deliver the desired cross-coupling products. Next, we found that benzylamine derivatives containing many different functionalized aryl and heteroaryl groups were amenable to the reaction and gave good yields of the corresponding amines **5n–5u**. Amines displaying linear and branched alkyl substituents, as well as ester, hydroxyl and nitrile functionality, reacted well to give amines **5v–5aa**. The photocatalytic process was effective with a range of electron-deficient alkenes. A reaction with benzyl acrylate **3c** could be adapted to a gram-scale process, yielding 1.4 g of product **5ac** in 84% yield. Notably, acrylonitrile (giving **5ae**) proved a suitable coupling partner, despite being prone to oligomerization in radical

reactions. Substituents at either the α - or the β -positions on the alkene (**5ag–5ak**) could be accommodated despite the lower electrophilicity and greater steric demand of these acceptors, with a diastereoselectivity of 2.3:1 observed in the reaction of methacrylate to form **5al**. Vinyl pyridine derivatives also proved to be viable acceptors (giving **5am–5ap**), enabling facile access to chlorphenamine derivative **5am**. The addition of the α -amino radical to a chiral dehydroalanine derivative led to enantioenriched non-proteogenic amino acid derivative **5aq** in good yield. We also found that perfluorinated alkenes, dienes and electron-deficient alkynes functioned well as acceptors (giving **5ar–5at**); the reaction with methyl propiolate delivered (*E*)-allylic amine **5at** in 66% yield as a single geometric isomer.

Our mechanistic proposal for the photocatalytic olefin-hydroaminoalkylation is shown in Fig. 3a. The reaction begins with visible-light excitation of Ir(ppy)₃ to the long-lived photoexcited ^{*}Ir(III) species, with a lifetime²⁷, τ , of 1.9 μ s. Although this species may be sufficiently reducing (Ir(IV)/^{*}Ir(III), $E_{1/2}^{\text{red}} = -1.73$ V versus SCE in acetonitrile)²⁷ to undergo SET to alkyliminium ion **Int-I**, we recognized that ^{*}Ir(III)/ppy₃ is efficiently quenched by Hantzsch ester **4a** (^{*}Ir(III)/Ir(II),

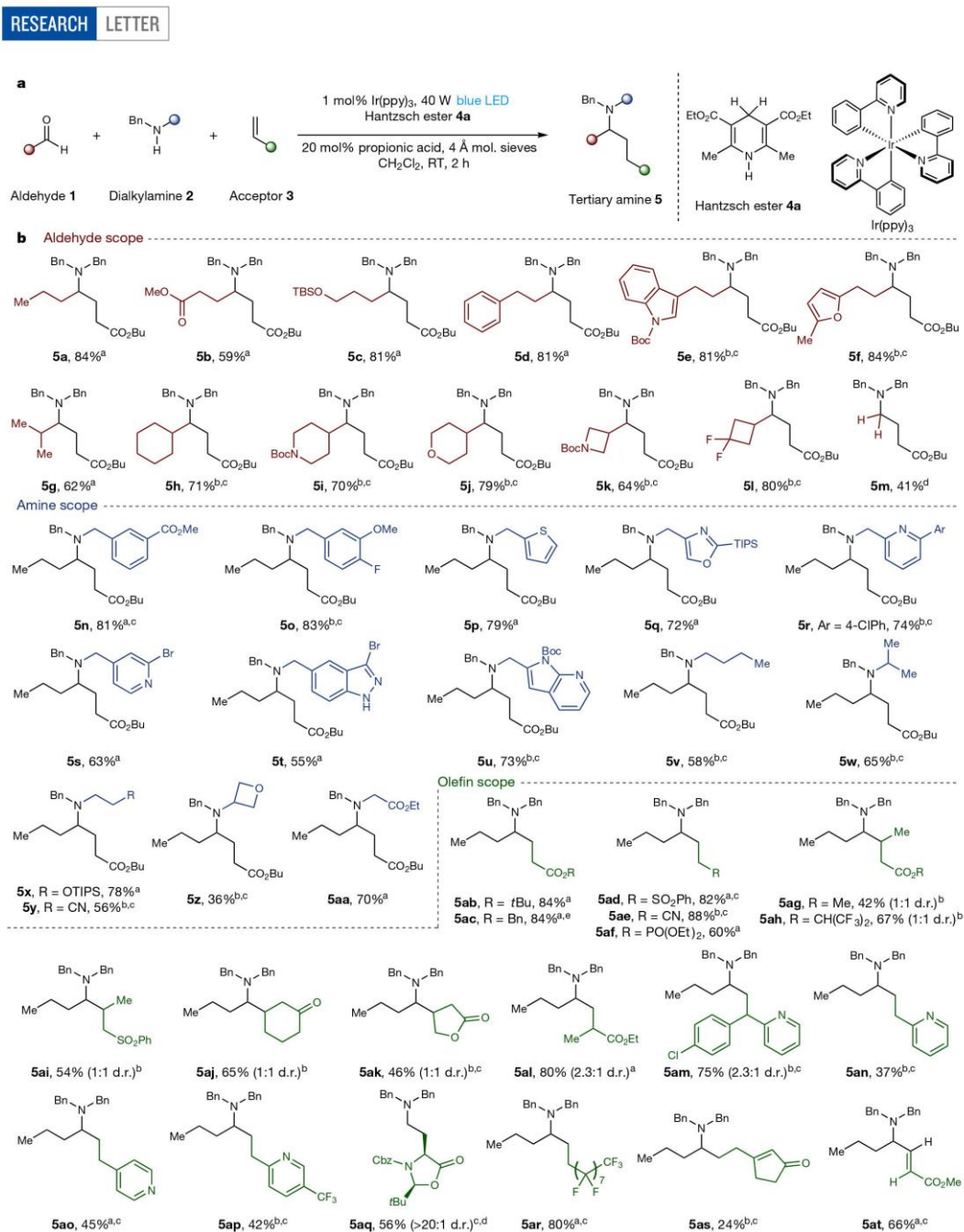


Fig. 2 | Scope of the multicomponent photocatalytic synthesis of tertiary alkylamines. a, Optimized conditions for photocatalytic olefin-hydroaminoalkylation. **b**, Scope of photocatalytic olefin-hydroaminoalkylation. ^aamine:aldehyde:acceptor (1:1.1:1.1), **4a** (1.5 equiv.); ^bamine:aldehyde:acceptor (1:2:2), **4a** (1.5 equiv.); ^cmethoxyethyl-

Hantzsch ester (1.5 equiv.); ^dparaformaldehyde (5 equiv.), preheated for 1 h; ^e4 mmol scale. Boc, *tert*-butoxycarbonyl; Cbz, benzyloxycarbonyl; d.r. diastereomeric ratio; ppy, 2-phenylpyridinato; RT, room temperature; TBS, *tert*-butyldimethylsilyl; TIPS, triisopropylsilyl.

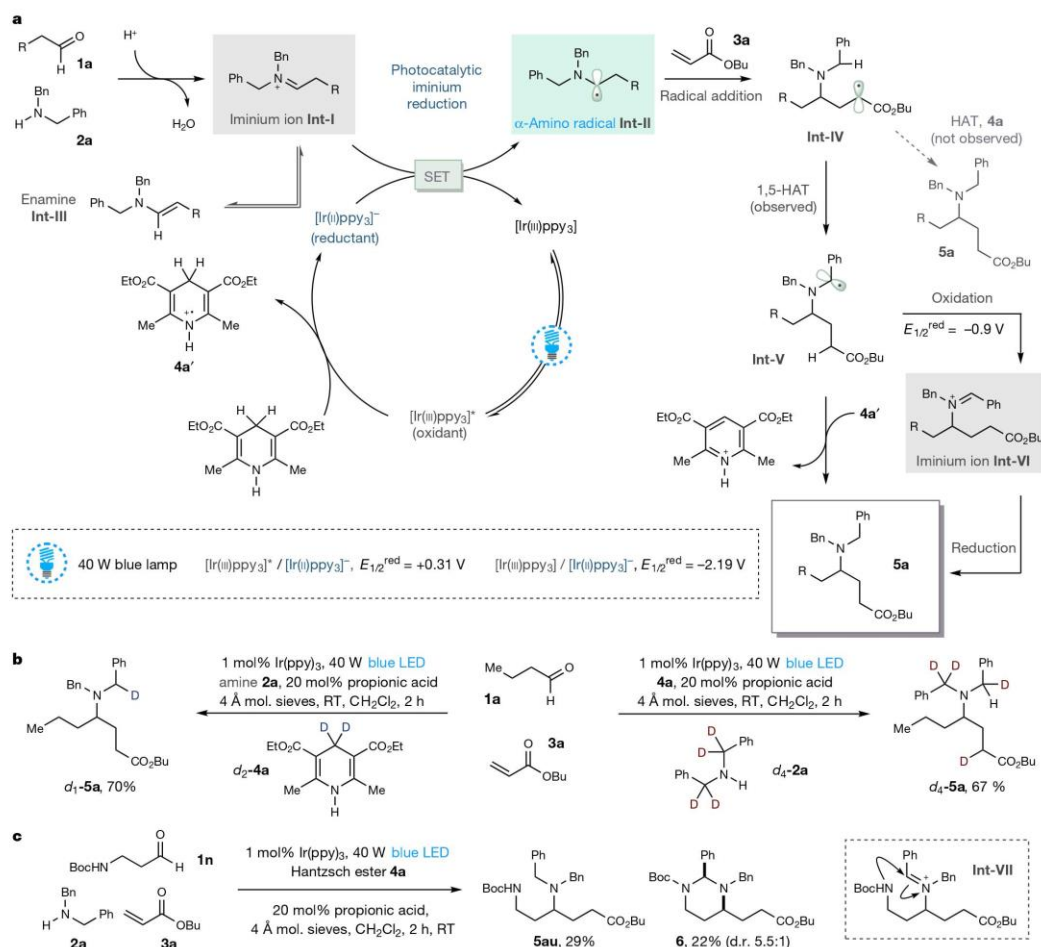


Fig. 3 | Studies towards understanding the mechanism of the multicomponent photocatalytic synthesis of tertiary alkylamines. **a**, Proposed mechanism for the photocatalytic olefin-

hydroaminoalkylation. **R** = Et. **b**, Deuterium-labelling studies. **c**, Evidence for the iminium-ion redox-relay mechanism.

$E_{1/2}^{\text{red}} = +0.31$ V versus SCE in acetonitrile)²⁷ leading to $[\text{Ir(II)ppy}_3]^-$ and the corresponding Hantzsch ester-radical cation **4a'**. Importantly, $[\text{Ir(II)ppy}_3]^-$ is sufficiently reducing (Ir(III)/Ir(II) , $E_{1/2}^{\text{red}} = -2.19$ V versus SCE in acetonitrile)²⁷ to undergo SET with the full range of alkyliminium ions²¹, leading to α -amino radical **Int-II**. We identified enamine **Int-III** as the predominant species in the ¹H NMR spectrum of the reaction mixture; we believe this is an off-cycle precursor to the iminium ion **Int-I**, with the acid maintaining a low concentration of iminium **Int-I** by protonation of enamine **Int-III**. The α -amino radical **Int-II** now engages the polarity-matched acrylate **3a**, creating a carbon-carbon bond and α -ester radical **Int-IV**. Given the propensity for monosubstituted α -ester radical **Int-IV** to undergo oligomerization²⁵, we anticipated that an intramolecular 1,5-HAT to the benzylic position may act as a kinetic trap to form stabilized radical **Int-V**²⁸. Finally, we expected that the Hantzsch ester **4a** or its radical cation **4a'** would participate in a HAT reaction with **Int-V** to form amine **5a**. A reaction using deuterium-labelled Hantzsch ester **d₂-4a** (Fig. 3b) confirmed our hypothesis; deuterium was incorporated exclusively at

the benzylic position of amine **d₁-5a**, showing that 1,5-HAT occurred before interception with **4a** or **4a'**. This theory was further corroborated using labelled dibenzylamine **d₄-2a**, wherein a deuterium atom was transferred to the position adjacent to the ester in amine **d₄-5a**. We also found that an aldehyde bearing a β -nucleophilic group (**1n**) underwent cyclization onto the benzylic position to form **6**, as a side reaction in the formation of **5au** (Fig. 3c). This result suggests that the α -aminobenzyl radical (**Int-V**) can undergo oxidation ($E_{1/2}^{\text{red}} = -0.9$ V versus SCE in acetonitrile)²⁹ to iminium **Int-VI**, which is accessible to a range of oxidants including $^*\text{Ir(III)}$ ²⁷. The selective reduction of benzaldiminium ion **Int-VI** over the initially formed iminium **Int-I** can be rationalized by the inability of **Int-VI** to form a stable enamine intermediate, compared to the interconversion between **Int-I** and **Int-III**. The reduction of **Int-VI** can proceed either by a two-electron process with **4a** or by photocatalytic SET and HAT. Notably, a pathway whereby iminium **Int-I** is translated into a new iminium species **Int-VI** represents an overall mechanism that can be described as a redox relay of iminium ions, which, to the best of our knowledge, has not been reported previously.

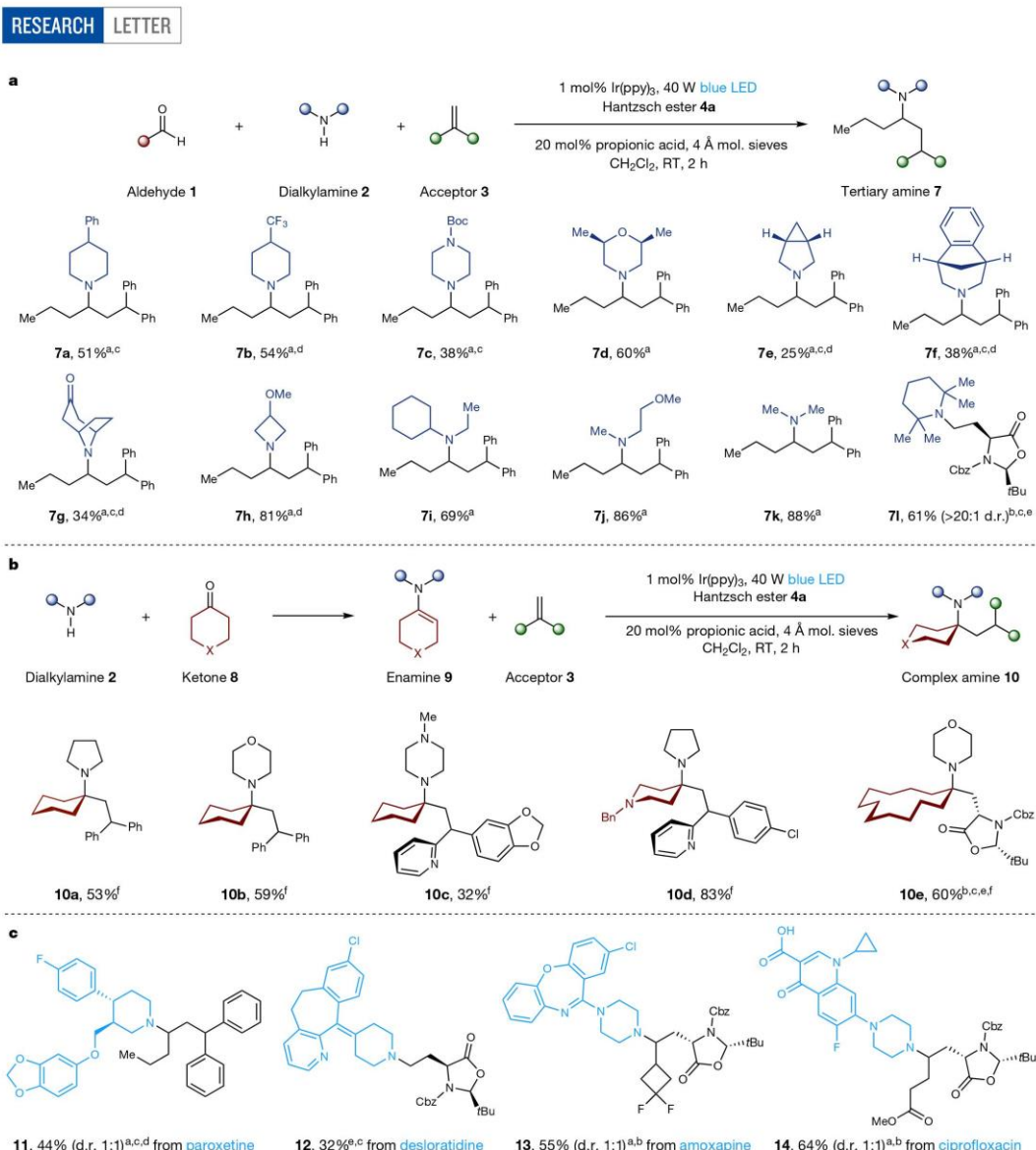


Fig. 4 | Expanding the scope of the multicomponent photocatalytic synthesis of tertiary alkylamines. a, Scope of non-benzylic amines in the photocatalytic olefin-hydroaminoalkylation. **b**, The synthesis of alkyl-substituted α -tertiary amines from dialkylketones. **c**, Late-stage photocatalytic olefin-hydroaminoalkylation with pharmaceutical agents.

^aamine:aldehyde:acceptor (1:2:2), 4a (1.5 equiv.); ^bacceptor (1.5 equiv.); ^cmethoxyethyl-Hantzsch ester (1.5 equiv.); ^damine hydrochloride and Et₃N (1 equiv.); ^eparaformaldehyde (5 equiv.), preheated for 1 h; ^fenamine (1 equiv.), acceptor (2 equiv.).

In this context, benzylamines not only overcome the inherent challenges posed by the addition of α -amino radicals to electron-deficient alkenes, but also act as a protecting group for primary and secondary alkylamines. Nonetheless, we reasoned that the use of an alkene that would produce a less-electrophilic radical should favour direct reaction with the Hantzsch ester-radical cation 4a', obviating the need for the 1,5-HAT process, and hence permitting the use of various dialkylamines. To test this, 1,1-diphenylethylene was combined with aldehyde 1a and 4-phenylpiperidine under the standard conditions, upon which

the desired tertiary amine 7a was formed in 51% yield (Fig. 4a). Other amine heterocycles were also compatible with this alkene acceptor, giving the amine products 7b–7k in good yield; notably, 1,1-diaryl-propylamines are key motifs commonly found in H₁-antihistamines³⁰. Among these examples, a number of amines found in pharmaceuticals formed the corresponding complex tertiary amines (7c–7h), demonstrating the potential to construct 'drug-like' molecules in a single step from readily available materials. The use of non-benzylic amines was not restricted to reactions with 1,1-diarylethenes; the reaction of

tetramethylpiperidine, formaldehyde and a dehydroalanine acceptor proceeded smoothly to form amine **71** as a single diastereomer.

We anticipated that the use of dialkylketones would be an important extension to the photocatalytic process, because these reactions would give rise to α -tertiary amine products³¹. Aware that the formation of ketiminium ions often requires more forcing conditions, we reasoned that protonation of a pre-formed enamine **9** would provide a more accessible source of alkylketiminium ions, as alkyl enamines can be readily prepared on a gram scale in one step (Fig. 4b). Under the standard conditions, a range of alkyl enamines underwent smooth cross-coupling with alkene acceptors to form α -tertiary amines **10a–10e**. The olefin-hydroaminoalkylation method was able to generate complex α -tertiary alkylamine scaffolds in a single step; such scaffolds would be difficult to assemble using classical methods.

Given that dialkylamine motifs are present in a range of small-molecule drugs and pre-clinical candidates, the late-stage functionalization of such molecules would be a powerful demonstration of the utility of this process. To confirm this strategy, we selected four pharmaceutical agents and subjected them to the photocatalytic reaction (Fig. 4c). Each of these architecturally complex amines underwent smooth olefin-hydroaminoalkylation with a variety of aldehydes to furnish the tertiary amine products **11–14**. In particular, the combination of desloratidine with formaldehyde and a chiral dehydroalanine acceptor forms a single diastereomer of the tertiary amine derivative **12**, constituting a potentially useful linker strategy through which further functionalization of drug scaffolds could be realized.

We expect that the operational simplicity, efficacy and broad scope of this highly selective, multicomponent photocatalytic amine synthesis will find widespread use among organic chemistry end-users both in academia and in industry. Moreover, we believe that the convenience with which this method generates underexplored alkyl-substituted α -amino radicals will inspire further advances in the synthesis of complex tertiary amine scaffolds.

Complex tertiary amine scaffolds

Data availability
The data that support the findings of this study are available within the paper and its supplementary information files. Raw data are available from the corresponding author on reasonable request. Materials and methods, experimental procedures, useful information, mechanistic studies, optimization studies, ¹H NMR spectra, ¹³C NMR spectra and mass spectrometry data are available in the Supplementary Materials. Crystallographic data are available free of charge from the Cambridge Crystallographic Data Centre (<https://www.ccdc.cam.ac.uk/>) under reference number CCDC 1819790.

Online content

Any methods, additional references, Nature Research reporting summaries, source data, statements of data availability and associated accession codes are available at <https://doi.org/10.1038/s41586-018-0537-9>.

Received: 9 April 2018; Accepted: 10 August 2018;

Published online 26 September 2018.

- Lovering, F., Bikker, J. & Humblet, C. Escape from flatland: Increasing saturation as an approach to improving clinical success. *J. Med. Chem.* **52**, 6752–6756 (2009).
- Blakemore, D. C. et al. Organic synthesis provides opportunities to transform drug discovery. *Nat. Chem.* **10**, 383–394 (2018).
- Roughley, S. D. & Jordan, A. M. The medicinal chemist's toolbox: An analysis of reactions used in the pursuit of drug candidates. *J. Med. Chem.* **54**, 3451–3479 (2011).
- Yang, Y., Shi, S.-L., Niu, D., Liu, P. & Buchwald, S. L. Catalytic asymmetric hydroamination of unactivated internal olefins to aliphatic amines. *Science* **349**, 62–66 (2015).
- Musacchio, A. J. et al. Catalytic intermolecular hydroaminations of unactivated olefins with secondary alkyl amines. *Science* **355**, 727–730 (2017).
- Johnston, C. P., Smith, R. T., Allmendinger, S. & MacMillan, D. W. C. Metallophotoredox-catalysed sp^3 – sp^3 cross-coupling of carboxylic acids with alkyl halides. *Nature* **536**, 322–325 (2016).
- Matier, C. D., Schwaben, J., Peters, J. C. & Fu, G. C. Copper-catalyzed alkylation of aliphatic amines induced by visible light. *J. Am. Chem. Soc.* **139**, 17707–17710 (2017).

- Mayol-Llinàs, J., Nelson, A., Farnaby, W. & Ayscough, A. Assessing molecular scaffolds for CNS drug discovery. *Drug Discov. Today* **22**, 965–969 (2017).
- Lahmy, V., Long, R., Morin, D., Villard, V. & Maurice, T. Mitochondrial protection by the mixed muscarinic/ σ_1 ligand ANAVEX2–73, a tetrahydrofuran derivative, in A β _{25–35} peptide-injected mice, a nontransgenic Alzheimer's disease model. *Front. Cell. Neurosci.* **8**, 463 (2015).
- Marciano, D. P. et al. The therapeutic potential of nuclear receptor modulators for treatment of metabolic disorders: PPAR γ , ROR α , Rev-erbs. *Cell Metab.* **19**, 193–208 (2014).
- Ruiz-Castillo, P. & Buchwald, S. L. Application of palladium-catalyzed C–N cross-coupling reactions. *Chem. Rev.* **116**, 12564–12649 (2016).
- Huang, L., Arndt, M., Gooßen, K., Heydt, H. & Gooßen, L. J. Late transition metal-catalyzed hydroamination and hydroamidation. *Chem. Rev.* **115**, 2596–2697 (2015).
- Kalck, P. & Urrutigoity, M. Tandem hydroaminomethylation reaction to synthesize amines from alkenes. *Chem. Rev.* **118**, 3833–3861 (2018).
- Herzon, S. B. & Hartwig, J. F. Hydroaminoalkylation of unactivated olefins with dialkylamines. *J. Am. Chem. Soc.* **130**, 14940–14941 (2008).
- Perez, F., Oda, S., Geary, L. M. & Krische, M. J. Ruthenium catalyzed transfer hydrogenation for C–C bond formation: hydrohydroxyalkylation and hydroaminoalkylation via reactant redox pairs. *Top. Curr. Chem.* **374**, 35 (2016).
- Renaud, P. & Giraud, L. 1-Amino- and 1-amidoalkyl radicals: generation and stereoselective reactions. *Synthesis* **1996**, 913–926 (1996).
- Mariano, P. S. Electron-transfer mechanisms in photochemical transformations of iminium salts. *Acc. Chem. Res.* **16**, 130–137 (1983).
- Chu, L., Ohta, C., Zuo, Z. & MacMillan, D. W. C. Carboxylic acids as a traceless activation group for conjugate additions: a three-step synthesis of (\pm)-pregabalin. *J. Am. Chem. Soc.* **136**, 10886–10889 (2014).
- Nakajima, K., Miyake, Y. & Nishibayashi, Y. Synthetic utilization of α -amino radicals and related species in visible light photoredox catalysis. *Acc. Chem. Res.* **49**, 1946–1956 (2016).
- Thullen, S. M. & Rovis, T. A mild hydroaminoalkylation of conjugated dienes using a unified cobalt and photoredox catalytic system. *J. Am. Chem. Soc.* **139**, 15504–15508 (2017).
- Andrieux, C. P. & Savéant, J. M. Electrodimerization: II. Reduction mechanism of iminium cations. *J. Electroanal. Chem.* **26**, 223–235 (1970).
- Lee, K. N. & Ngai, M.-Y. Recent developments in transition-metal photoredox-catalysed reactions of carbonyl derivatives. *Chem. Commun.* **53**, 13093–13112 (2017).
- Heinz, C. et al. Ni-catalyzed carbon–carbon bond-forming reductive amination. *J. Am. Chem. Soc.* **140**, 2292–2300 (2018).
- Capacci, A. G., Malinowski, J. T., McAlpine, M. J., Kuhne, J. & MacMillan, D. W. C. Direct, enantioselective α -alkylation of aldehydes using simple olefins. *Nat. Chem.* **9**, 1073–1077 (2017).
- Dai, X. et al. The coupling of tertiary amines and acrylate derivatives via visible-light photoredox catalysis. *J. Org. Chem.* **79**, 7212–7219 (2014).
- Guo, X. & Wenger, O. S. Reductive amination by photoredox catalysis and polarity-matched hydrogen atom transfer. *Angew. Chem. Int. Ed.* **57**, 2469–2473 (2018).
- Flamigni, L., Barbieri, A., Sabatini, C., Ventura, B. & Barigelli, F. Photochemistry and photophysics of coordination compounds: iridium. *Top. Curr. Chem.* **281**, 143–203 (2007).
- Yu, P. et al. Enantioselective C–H bond functionalization triggered by radical trifluoromethylation of unactivated alkene. *Angew. Chem. Int. Ed.* **53**, 11890–11894 (2014).
- Wayner, D. D. M., Dannenberg, J. J. & Griller, D. Oxidation potentials of α -aminoalkyl radicals: bond dissociation energies for related radical cations. *Chem. Phys. Lett.* **131**, 189–191 (1986).
- Simons, F. E. R. Advances in H₁-antihistamines. *N. Engl. J. Med.* **351**, 2203–2217 (2004).
- Hager, A., Vrielink, N., Hager, D., Lefranc, J. & Trauner, D. Synthetic approaches towards alkaloids bearing α -tertiary amines. *Nat. Prod. Rep.* **33**, 491–522 (2016).

Acknowledgements We thank A. Bond for X-ray crystallographic analysis, the EPSRC UK National Mass Spectrometry Facility at Swansea University for HRMS analysis, and M. Nappi, J. C. K. Chu and T. Hunt (AstraZeneca) for useful discussion. We acknowledge the Herschel Smith Scholarship Scheme and AstraZeneca for studentships (to A.T. and D.R., respectively) and the Royal Society for a Wolfson Merit Award (M.J.G.).

Author contributions M.J.G., A.T. and D.R. designed the experiments. A.T. and D.R. performed and analysed the experiments. M.J.G., A.T. and D.R. prepared the manuscript.

Competing interests The authors declare no competing interests.

Additional information

Supplementary information is available for this paper at <https://doi.org/10.1038/s41586-018-0537-9>.

Reprints and permissions information is available at <http://www.nature.com/reprints>.

Correspondence and requests for materials should be addressed to M.J.G.
Publisher's note: Springer Nature remains neutral with regard to jurisdictional claims in published maps and institutional affiliations.

COMMUNICATION

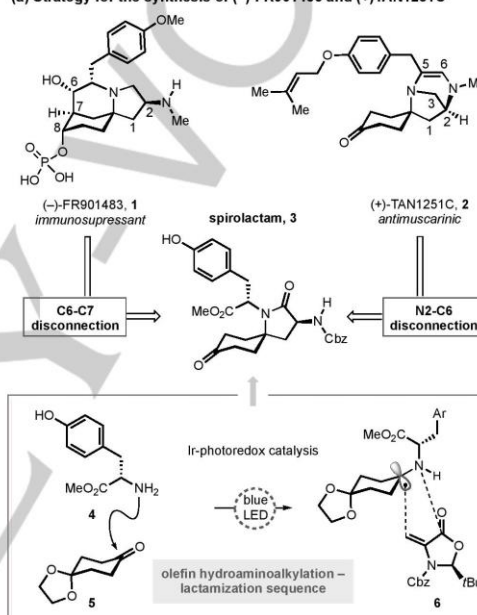
Rapid syntheses of (–)-FR901483 and (+)-TAN1251C enabled by complexity-generating photocatalytic olefin hydroaminoalkylation

Dominik Reich,^[a] Aaron Trowbridge^[a] and Matthew J. Gaunt^{*,[a]}

Abstract: We report a common strategy to facilitate the syntheses of the polycyclic alkaloids (–)-FR901483 (**1**) and (+)-TAN1251C (**2**). A divergent synthetic strategy provides access both natural products through a pivotal spiroactam intermediate (**3**), which can be accessed on a gram-scale. A photocatalytic olefin hydroaminoalkylation brings together three readily available building blocks and forges the majority of the carbon framework present in **1** and **2** in a single operation, leading to concise total syntheses. The complexity-generating photocatalytic process also provides direct access to novel non-racemic spiroactam scaffolds that are likely to be of interest to early-stage drug discovery programs.

Nitrogen-containing spirocyclic scaffolds are common structural features in many pharmaceutical candidates and biologically-active alkaloid natural products.^[1] The rigidity of these spirocyclic frameworks helps to project polar functionality in well-defined orientations, which can facilitate interactions made with a protein receptor site and often accounts for their potent bioactive properties. Displaying a distinct type of amino-substituted aza-spirocyclic framework, (–)-FR901483^[2] (**1**) and (+)-TAN1251C^[3] (**2**) are biosynthetically related di-tyrosine-derived alkaloids,^[4] which have attracted significant attention from the synthetic community by virtue of their biological activity and the challenges posed by their relatively small but architecturally complex structures (Figure 1a). FR901483 was first isolated from the fermentation broth of *Cladobotryum* sp. No. 11231 by Fujisawa Pharmaceutical Co. in 1996^[2] and exhibited exceedingly potent immunosuppressant activity (>100 times more active than cyclosporine).^[5] As a result, much effort has been invested into the development of step-economic and scalable syntheses of FR901483 as a potential therapeutic lead for the treatment of arthritis, Crohn's disease and organ transplant rejection. The TAN1251 family of natural products, first isolated by Takeda in 1991,^[3] show potent bioactivity as muscarinic antagonists with potential applications as antispasmodic and antiulcer agents. Despite a number of elegant and inventive syntheses of FR901483^[6–15] and the TAN1251 alkaloids,^[8,16–23] the concise and efficient construction of the amino-substituted aza-spirocyclic scaffold of these natural products remains a formidable synthetic challenge.^[24–25]

(a) Strategy for the synthesis of (–)-FR901483 and (+)-TAN1251C



(b) Readily assembled bioactive scaffolds

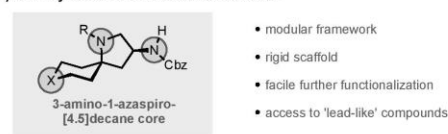


Figure 1. Strategy for the synthesis of (–)-FR901483, (+)-TAN1251C and related aza-spirocyclic scaffolds.

Many syntheses of (–)-FR901483 and (+)-TAN1251C stem from strategies founded on biomimetic oxidative dearomatization of di-tyrosine derivatives. In contrast, we focused on disconnections between the C6–C7^[6,11] in (–)-FR901483, and between amino group at the C2 position (N2) and C6 in (+)-TAN1251C^[11,17] to reveal novel spiroactam **3**. In turn, we questioned whether a tyrosine amino ester, a cyclohexanone derivative and a non-racemic dehydroalanine derivative could be combined through a variation of the visible light-mediated

[a] D. Reich, Dr. A. Trowbridge and Prof. Dr. M. J. Gaunt
Department of Chemistry
University of Cambridge
Lensfield Road, Cambridge, CB2 1EW, United Kingdom.
E-mail: mjg32@cam.ac.uk

Supporting information for this article is given via a link at the end of the document.

COMMUNICATION

photocatalytic olefin hydroaminoalkylation process that was recently developed in our laboratory.^[26] This methodology exploits

the reaction of α -amino radicals, generated by single electron reduction of all-

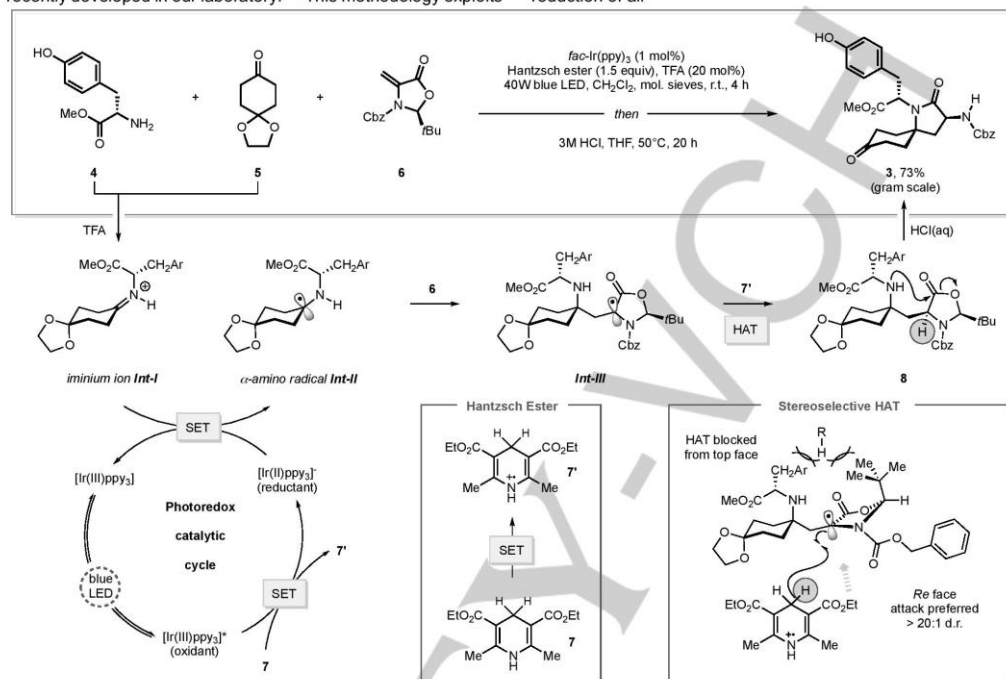


Figure 2. Synthesis of key precursor spiroactam **3** and proposed mechanism.

alkyl iminium ions, with activated alkene acceptors. Not only could this technology provide a valuable precursor for the synthesis of **1** and **2**, but we envisaged that this modular process could be utilized for the rapid assembly of a vast number of pharmaceutically privileged, chiral 3-amino-1-azaspiro[4.5]decane core fragments (Figure 1b), which are likely to be of interest for drug discovery programs.

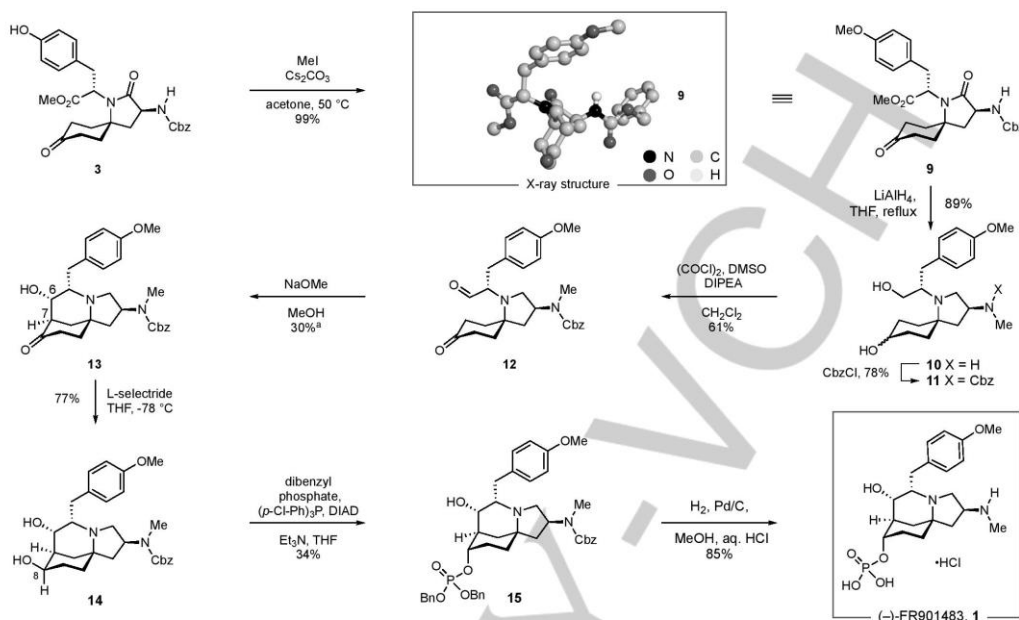
While our previous work demonstrated an effective coupling for the reductive union of aldehyde, secondary amine and alkene acceptors, the corresponding reaction between ketones and secondary amines required a stepwise approach. The requisite tetra-alkyl iminium ion required generation *in situ* by protonation of a preformed enamine, which, itself, required prior condensation of a secondary amine and ketone under Dean-Stark conditions. As part of a streamlined strategy, our synthesis plan not only required successful deployment of a previously unexplored primary amine in the photocatalytic olefin hydroaminoalkylation, but ideally, would enable direct *in situ* iminium ion formation and also affect a post-coupling cyclization of the incipient secondary amine product to form the desired spiroactam intermediate (**3**).

Herein, we report the successful realization of this idea through the development of a modular strategy for the total syntheses of (–)-FR901483 and (+)-TAN1251C. The construction of an amino-substituted azaspirocyclic, common to both natural

products, can be achieved in a single 'one-pot' process via a photocatalytic olefin hydroaminoalkylation using readily available and commercial building blocks. Beyond completion of the syntheses of **1** and **2**, we also demonstrate how this photocatalytic olefin hydroaminoalkylation can provide the basis for a general platform to access functionally diverse non-racemic spirocyclic lactams on gram-scale from primary amines and cyclic ketone feedstocks.

In contrast to our previous studies, wherein single electron reduction of an activated iminium ion facilitated the formation of the putative N-tertiary α -amino radicals, the use of a primary amine would generate a neutral imine that may not be sufficiently reactive for the reductive coupling process. Accordingly, employing our reaction original conditions with the primary amine coupling partner led to very low conversions to the desired product. However, we were delighted to find that, in the presence of a catalytic amount of trifluoroacetic acid (TFA), the union of L-tyrosine methyl ester (**4**), 1,4-cyclohexanedione monoethylene acetal **5** and dehydroalanine derivative **6**^[27] was readily achieved by visible light irradiation (40 W blue LED light for 2 h) of a dichloromethane solution containing these coupling partners in the presence of activated molecular sieves, 1 mol% *fac*-Ir(ppy)₃ (ppy, 2-phenylpyridinato) and Hantzsch ester (**7**). Subsequent treatment of the reaction mixture with aqueous acid yielded the

COMMUNICATION

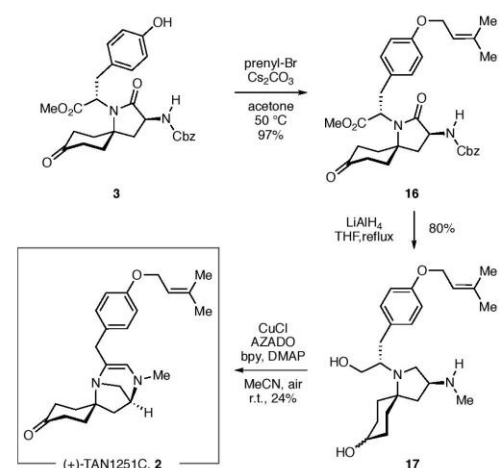


Scheme 1. Total synthesis of (-)-FR901483. (a) total yield of aldol products 79% (2 steps from **11**), for characterization of all aldol products, see SI. (DIPEA: *N,N*-Diisopropylethylamine; DIAD: diisopropyl azodicarboxylate).

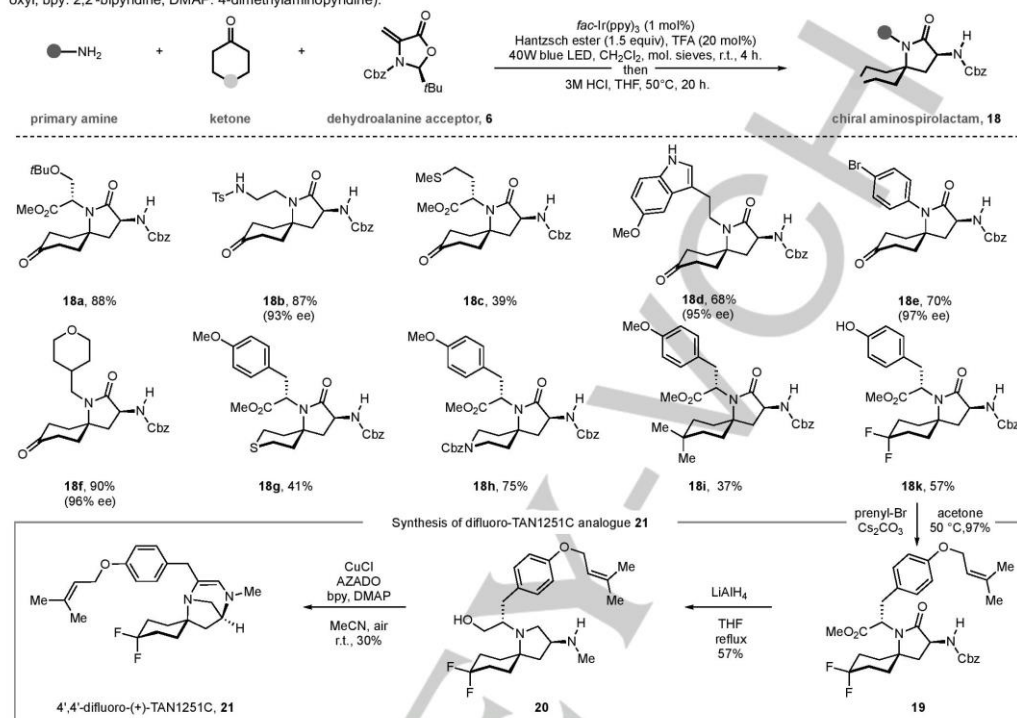
desired spiroactam precursor **3** in 73% yield on gram-scale, following a simple filtration as the only purification step (Figure 2). It seems most likely that TFA protonates the incipient imine and the resulting iminium ion undergoes single electron reduction to form the N-secondary α -amino radical **Int-II**. A plausible pathway for the photocatalysis begins with visible-light excitation of the photocatalyst to the excited triplet state $^3\text{Ir(III)}$ species; reductive quenching with Hantzsch ester (**7**) furnishes the corresponding radical cation **7'** and the highly reducing $[\text{Ir(II)}(\text{ppy})_3]^+$ species (Ir(III)/Ir(II) , $E_{1/2}^{\text{red}} = -2.19$ V versus SCE in acetonitrile),^[28] which engages the iminium ion **Int-I** through a single electron reduction. The resulting N-secondary α -amino radical **Int-II** undergoes addition to the alkene **6** resulting in the stabilized α -carbonyl radical species **Int-III**. Diastereoselective hydrogen atom transfer from Hantzsch ester radical cation **7'** occurs from the least-hindered face to afford the lactone product **8** (see supporting information for details).^[29,30] Finally, acid-mediated cyclization forms the desired spiroactam **3** without erosion of stereochemical integrity at the C2 position.

With a concise method to produce gram quantities of spiroactam **3** in hand, we next turned our attention to the synthesis of (-)-FR901483 (**1**) (Scheme 1). The synthesis commenced with the O-methylation of the phenol group in **3**, furnishing ether **9**, followed by exhaustive reduction of the ester, ketone, lactam, and benzyl carbamate motifs with excess LiAlH₄, furnishing amino-diol **10** in good overall yield. Protection of the secondary amine function in **10** as its benzyl carbamate (to **11**) was followed by a modified Swern oxidation^[7] to achieve the

simultaneous oxidation of the 1° and 2° alcohols in **11**, which gave keto-aldehyde **12** and was amenable to operation on a gram-scale. Completion of the tricyclic framework, via intramolecular aldol reaction, was investigated initially using previously reported condition for similar C6–C7 bond constructions in other syntheses.^[6–8, 31]



COMMUNICATION

Scheme 2. Total synthesis of (+)-TAN1251C (AZADO: 2-azaadamantane-*N*-oxyl; bpy: 2,2'-bipyridine; DMAP: 4-dimethylaminopyridine).**Figure 3.** Scope of chiral amino-spirolactam products and synthesis of natural product analogue 21.

Ultimately, we found the use of sodium methoxide in methanol, similar to Snider's protocol,^[6] were the most suitable, affording 30% yield of the desired aldol product **13** alongside other diastereomers (see supporting information for full details of this study). While the selectivity of the aldol process could not be increased over ratios previously reported in the literature for similar scaffolds (a 7.3:1 diastereoselectivity has been previously reported),^[6–8] we were able to isolate and characterize two of the remaining diastereomers of hydroxy ketone **13**, which could offer future opportunities for the synthesis of epimers of the natural product (see supporting information). Access to the desired C8 axial alcohol was achieved hydroxyl-assisted delivery of the hydride from the convex face of the tricyclic hydroxyl-ketone **13**, using L-selectride, to afford a single (equatorial) epimer of alcohol **14** in 77% yield.

Inversion of the C8 carbinol with concomitant installation of the phosphate ester was achieved via Mitsunobu reaction with dibenzyl phosphate **14**, according to the procedure of Sorensen.^[7] Finally, palladium catalyzed hydrogenolysis of the dibenzyl phosphate ester and benzyl carbamate in **15**, coupled with the addition of hydrochloric acid, completed a concise synthesis of (–)-FR901483 (**1**), as its HCl salt, in 85% yield.

With a synthesis of (–)-**1** in hand, we turned our attention to exploring the divergence of the synthetic strategy, which would

convert key spirolactam **3** into the diazatricyclic (+)-TAN1251C. The synthesis began with O-prenylation of phenol **3**, followed by global reduction of the ester, ketone, lactam and benzyl carbamate functions in **16** with excess LiAlH₄, to give **17** in 80% yield (Scheme 2), similar to the related step in the (–)-FR901483 synthesis.

We envisaged that the synthesis of (+)-TAN1251C could be directly achieved from amino diol **17**. Simultaneous oxidation of both the 1' and 2' alcohols to the corresponding keto-aldehyde should facilitate an intramolecular condensation, which after tautomerization would furnish (+)-TAN1251C (**2**). We anticipated two challenges that may preclude the successful realization of this tactic: firstly, the oxidation step may not be compatible with the presence of the free(NH)-methylamine motif required for the condensation; and secondly, that the intermediate keto-aldehyde may undergo competitive intramolecular aldol reaction, as exploited in the synthesis of (–)-FR901483. Initial attempts employing Omura-Sharma-Swern^[32] oxidation followed by basic hydrolysis of the (in situ generated) trifluoroacetamide, as reported by Snider and co-workers,^[6] failed to give satisfactory results, likely due to an aldol cyclization occurring during the basic work-up.^[6] Oxidation with Dess-Martin-Periodinane or catalytic tetrapropylammonium perruthenate (TPAP) led to significant decomposition of the starting materials. Ultimately, we found that

COMMUNICATION

direct oxidation-condensation could be achieved using an AZADO/copper-mediated aerobic oxidation developed by Iwabuchi,^[33] completing the total synthesis of (+)-TAN1251C (**2**) in a single step from **17**. Underlining the utility of this divergent approach, the photocatalytic olefin hydroaminoalkylation allowed for the rapid assembly of a unique spirolactam (**3**), which enabled the concise and stereocontrolled synthesis of both (–)-FR901483 (**1**) and (+)-TAN1251C (**2**) in a common fashion, with the longest linear sequences encompassing 12 steps for **1**, and 7 steps for **2** (total number of steps to **1** and **2** is 12 and 7 respectively). Both routes are significantly shorter than previous enantioselective syntheses of (–)-FR901483 (**1**) and (+)-TAN1251C (**2**).²⁵

Beyond its use in total synthesis, we recognized that the multicomponent nature of this complexity-generating tandem photocatalytic hydroaminoalkylation–cyclization methodology could be useful for the rapid stereocontrolled synthesis of a variety of chiral spirolactams by exploiting combinations of readily available ketones and primary amines. Indeed, a selection of primary amines (Figure 3, **18a–18f**) proved effective coupling partners, with the reaction accommodating the presence of range of useful functional groups. A less-nucleophilic substituted aniline was also compatible with the reaction, giving access to *N*-aryl spirolactams (**18e**) in good yield, significantly broadening the scope of potentially available products. Pleasingly, a number of ketones also proved amenable to coupling reaction, further demonstrating the capacity of this strategy by incorporating thianes (**18g**), protected piperidines (**18h**), and alkyl- & fluoro-substituted cyclohexane motifs (**18i** and **18k**) into the spirolactam products.

The modular nature of the multicomponent photocatalytic coupling potentially facilitates rapid synthetic access to analogues of TAN1251C. Towards this, we found that geminal difluoro-analogue of TAN1251C **21** could be readily assembled following the same synthetic route starting from the commercial ketone, 4,4-difluorocyclohexane. The photocatalytic olefin hydroaminoalkylation smoothly afforded spirolactam **18k**, which could be advanced to the TAN125C analogue in three further steps and good overall yield, thereby demonstrating the suitability of this methodology for the preparation of enantioenriched complex small molecule scaffolds.

In conclusion, we report a highly modular multicomponent photocatalytic hydroaminoalkylation approach for the synthesis of the complex amino-substituted azaspirocyclic-containing natural products, (–)-FR901483 (**1**) and (+)-TAN1251C (**2**). The protocol allowed access to a key spirolactam precursor, which can be advanced rapidly, through a divergent synthetic strategy, to the natural products. Due to its ease of operation and availability of starting materials, we envision this new technology will provide access to molecules that will be attractive as "lead-like" structures based on the versatile 3-amino-1-azaspiro[4.5]decane scaffold.

Acknowledgements

We thank the EPSRC UK National Mass Spectrometry Facility at Swansea University for HRMS analysis, Duncan Howe and Andrew Mason for assistance with NMR spectroscopic analysis, and Dr. Thomas Hunt (Astra-Zeneca) for useful discussion. We gratefully acknowledge funding from AstraZeneca (D.R.) and the

Herchel Smith Scholarship Scheme (A.T.) for studentships, the EPSRC (EP/S020292/1), and the Royal Society for a Wolfson Merit Award (M.J.G.).

Keywords: natural product synthesis • photoredox chemistry • radical chemistry • amine synthesis • medicinal chemistry

- [1] (a) Y.-J. Zheng, C. M. Tice, S. B. Singh, *Bioorg. Med. Chem. Lett.* **2014**, *24*, 3673–3682. (b) Y.-J. Zheng, C. M. Tice, *Expert Opin. Drug Discov.* **2016**, *11*, 831–834. (c) E. M. Carreira, T. C. Fessard, *Chem. Rev.* **2014**, *114*, 8257–8322. For recent examples of the synthesis of *N*-spiropcycles, see (e) W.-Y. Siau, J. W. Bode, *J. Am. Chem. Soc.* **2014**, *136*, 17726–17729. (f) N. J. Flodén, A. Trowbridge, D. Willcox, S. M. Walton, Y. Kim, M. J. Gaunt, *J. Am. Chem. Soc.* **2019**, *141*, 8426–8430 and references therein. For examples of *N*-spiropcycles in natural products, see (g) A. Hager, N. Vrielink, D. Hager, J. Lefranc, D. Trauner, *Nat. Prod. Rep.* **2016**, *33*, 491–522.
- [2] K. Sakamoto, E. Tsujii, F. Abe, T. Nakanishi, M. Yamashita, N. Shigematsu, S. Izumi, M. Okuhara, *J. Antibiot.* **1996**, *49*, 37–44.
- [3] H. Shirafuji, S. Tsubotani, T. Ishimaru, S. Harada (Takeda Chemical Industries Ltd.), WO9113887, **1991**.
- [4] H. Liang, M. A. Ciufolini in *Biomimetic Organic Synthesis*, (Eds.: E. Poupon, B. Nay), John Wiley & Sons, New York, **2011**, pp. 61–89.
- [5] M. A. Ciufolini, *Il Farmaco* **2005**, *60*, 627–641.
- [6] B. B. Snider, H. Lin, *J. Am. Chem. Soc.* **1999**, *121*, 7778–7786.
- [7] G. Scheffler, H. Seike, E. J. Sorensen, *Angew. Chem. Int. Ed.* **2000**, *39*, 4593–4596; *Angew. Chem.* **2000**, *112*, 4783–4785.
- [8] M. Ousmer, N. A. Braun, C. Bavoux, M. Perrin, M. A. Ciufolini, *J. Am. Chem. Soc.* **2001**, *123*, 7534–7538.
- [9] J.-H. Maeng, R. L. Funk, *Org. Lett.* **2001**, *3*, 1125–1128.
- [10] T. Kan, T. Fujimoto, S. Ieda, Y. Asoh, H. Kitaoka, T. Fukuyama, *Org. Lett.* **2004**, *6*, 2729–2731.
- [11] K. M. Brummond, S. Hong, *J. Org. Chem.* **2005**, *70*, 907–916.
- [12] C. A. Carson, M. A. Kerr, *Org. Lett.* **2009**, *11*, 777–779.
- [13] A.-J. Ma, Y.-Q. Tu, J.-B. Peng, Q.-Y. Dou, S.-H. Hou, F.-M. Zhang, S.-H. Wang, *Org. Lett.* **2012**, *14*, 3604–3607.
- [14] S. Ieda, A. Masuda, M. Kariyama, T. Wakimoto, T. Asakawa, T. Fukuyama, T. Kan, *Heterocycles* **2012**, *86*, 1071–1092.
- [15] H.-H. Huo, X.-E. Xia, H.-K. Zhang, P.-Q. Huang, *J. Org. Chem.* **2013**, *78*, 455–465.
- [16] S. Nagumo, A. Nishida, C. Yamazaki, K. Murashige, N. Kawahara, *Tetrahedron Lett.* **1998**, *39*, 4493–4496.
- [17] B. B. Snider, H. Lin, *Org. Lett.* **2000**, *2*, 643–646.
- [18] D. J. Wardrop, A. Basak, *Org. Lett.* **2001**, *3*, 1053–1056.
- [19] S. Nagumo, A. Matoba, Y. Ishii, S. Yamaguchi, N. Akutsu, H. Nishijima, A. Nishida, N. Kawahara, *Tetrahedron* **2002**, *58*, 9871–9877.
- [20] H. Mizutani, J. Takayama, Y. Soeda, T. Honda, *Tetrahedron Lett.* **2002**, *43*, 2411–2414.
- [21] J. M. A. Auty, I. Churcher, C. J. Hayes, *Synlett* **2004**, *2004*, 1443–1445.
- [22] H. Mizutani, J. Takayama, T. Honda, *Synlett* **2005**, *2005*, 328–330.
- [23] Y. Nagasaka, S. Shintaku, K. Matsumura, A. Masuda, T. Asakawa, M. Inai, M. Egi, Y. Hamashima, Y. Ishikawa, T. Kan, *Org. Lett.* **2017**, *19*, 3839–3842.
- [24] J. Bonjoch, F. Diaba in *Stud. Nat. Prod. Chem.*, Vol. 32 (Ed.: Atta-ur-Rahman), Elsevier, **2005**, pp. 3–60.
- [25] Z. Ruan, C. Li, D. Shen, S.-H. Huang, R. Hong, *Synthesis* **2019**, *51*, 2237–2251.
- [26] A. Trowbridge, D. Reich, M. J. Gaunt, *Nature* **2018**, *561*, 522–527.
- [27] J. R. Axon, A. L. J. Beckwith, *J. Chem. Soc., Chem. Commun.* **1995**, 549–550.
- [28] L. Flamigni, A. Barbieri, C. Sabatini, B. Ventura, F. Barigelli in *Photochemistry and Photophysics of Coordination Compounds II* (Eds.: V. Balzani, S. Campagna), Springer, Berlin, Heidelberg, **2007**, pp. 143–203.

COMMUNICATION

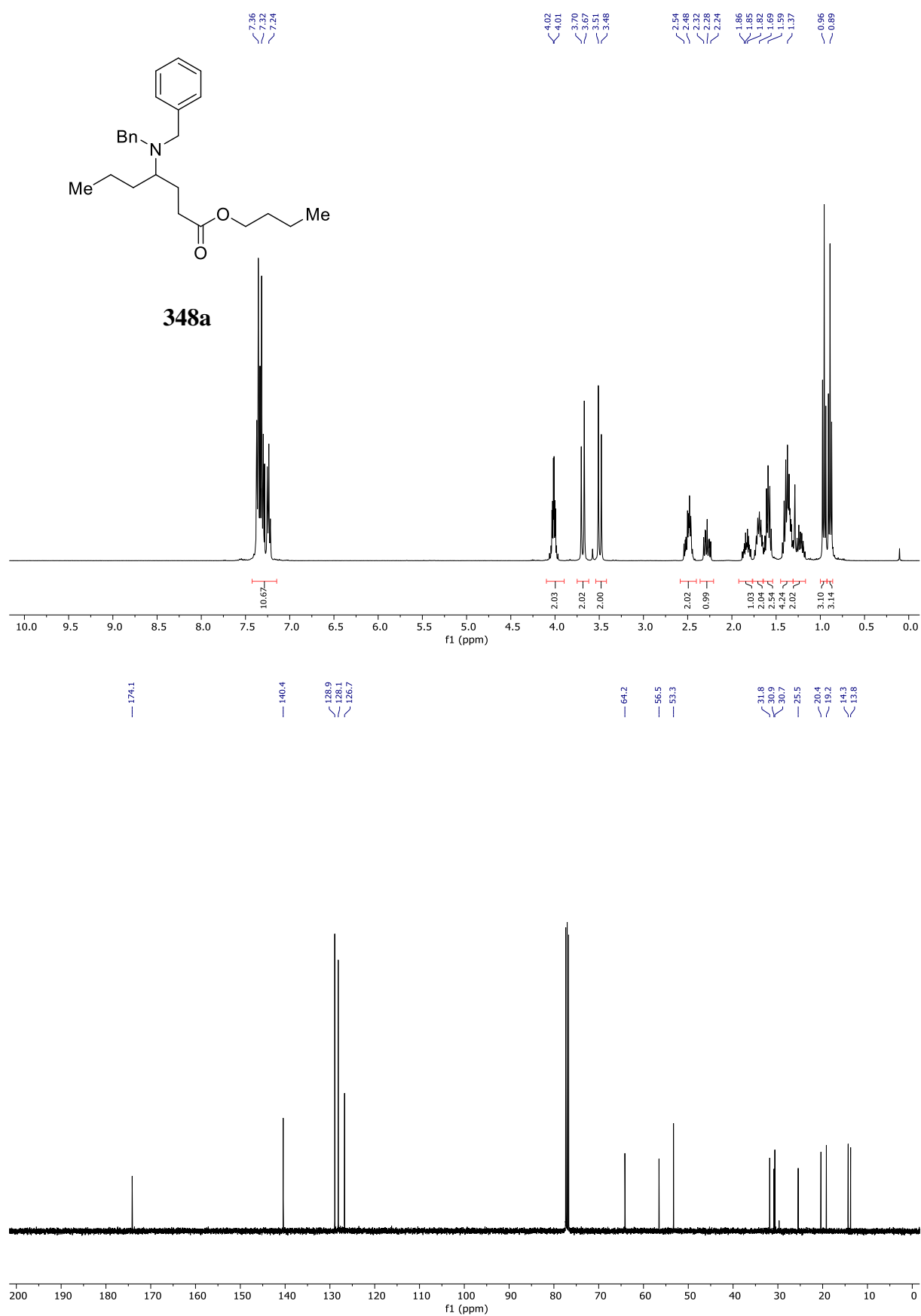
- [29] (a) A. L. J. Beckwith, C. L. L. Chai, *J. Chem. Soc., Chem. Commun.* **1990**, 1087–1088. (b) S. Karady, J. S. Amato, L. M. Weinstock, *Tetrahedron Lett.* **1984**, 25, 4337–4340. (c) R. A. Aycock, D. B. Vogt, N. T. Jui, *Chem. Sci.* **2017**, 8, 7998–8003.
- [30] T. Rossolini, J. A. Leitch, R. Grainger, D. J. Dixon, *Org. Lett.* **2018**, 20, 6794–6798.
- [31] B. B. Snider, H. Lin, B. M. Foxman, *J. Org. Chem.* **1998**, 63, 6442–6443.
- [32] K. Omura, A. K. Sharma, D. Swern, *J. Org. Chem.* **1976**, 41, 957–962.
- [33] Y. Sasano, S. Nagasawa, M. Yamazaki, M. Shibuya, J. Park, Y. Iwabuchi, *Angew. Chem. Int. Ed.* **2014**, 53, 3236–3240; *Angew. Chem.* **2014**, 126, 3300–3304.

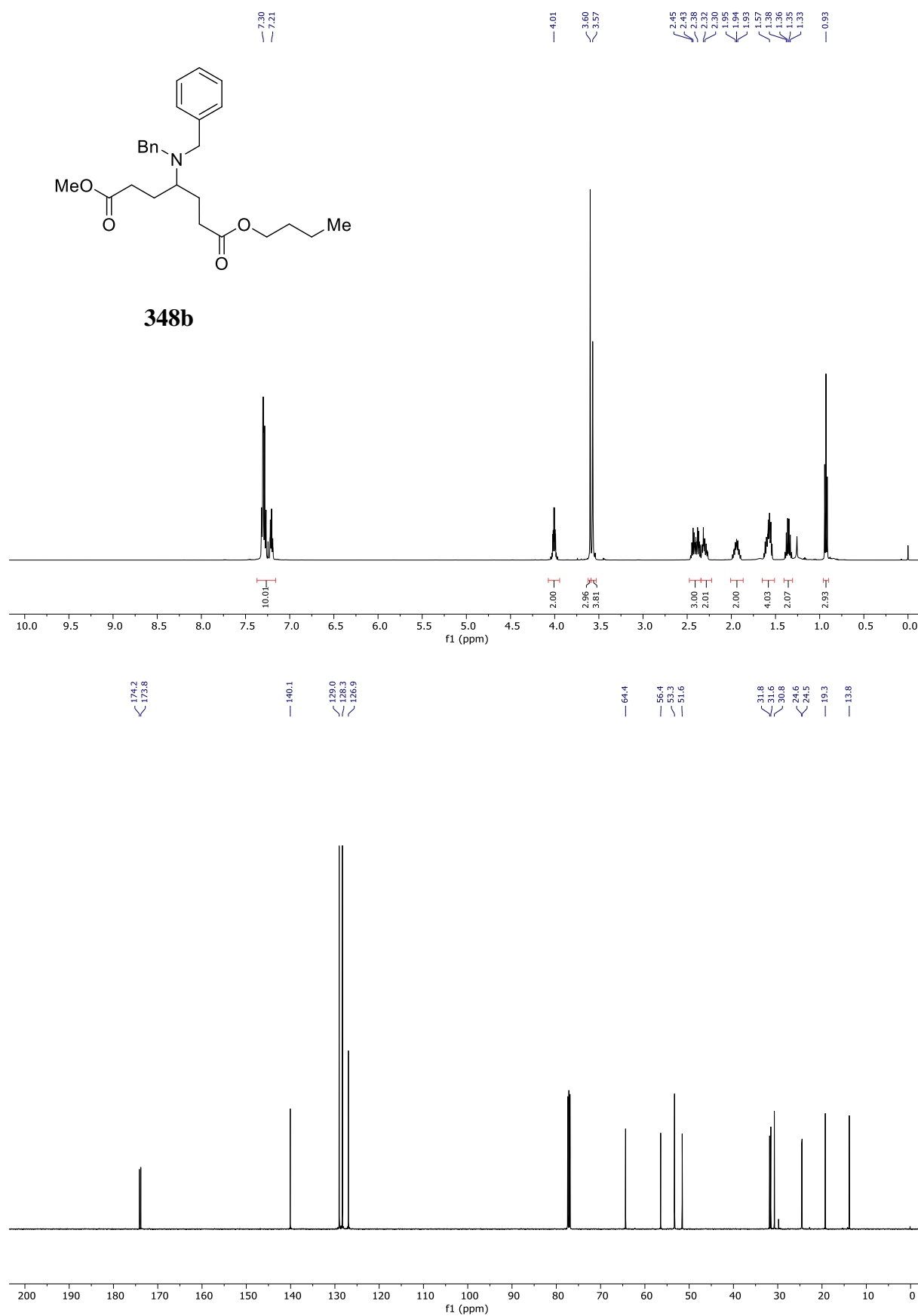
WILEY-VCH

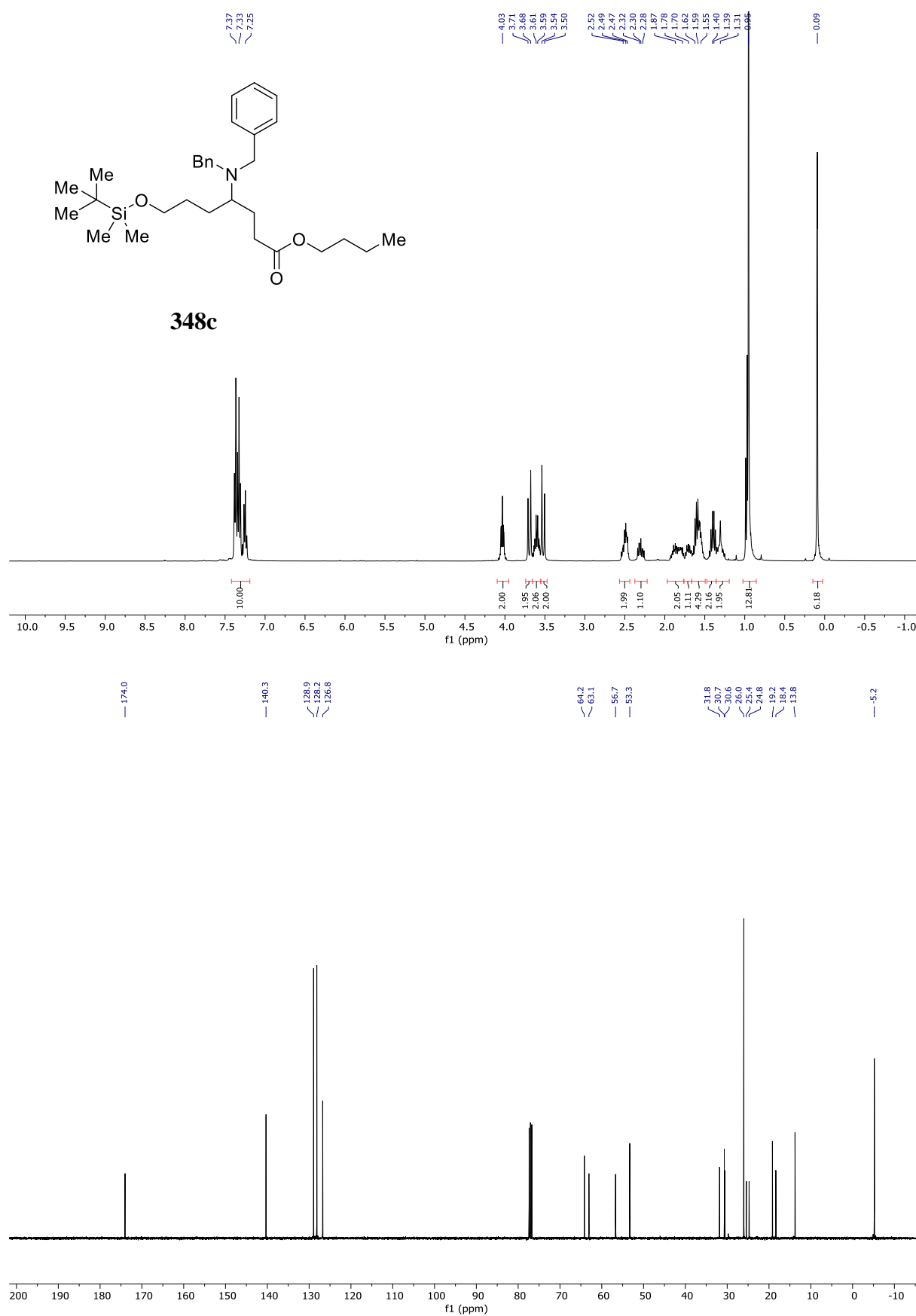
Accepted Manuscript

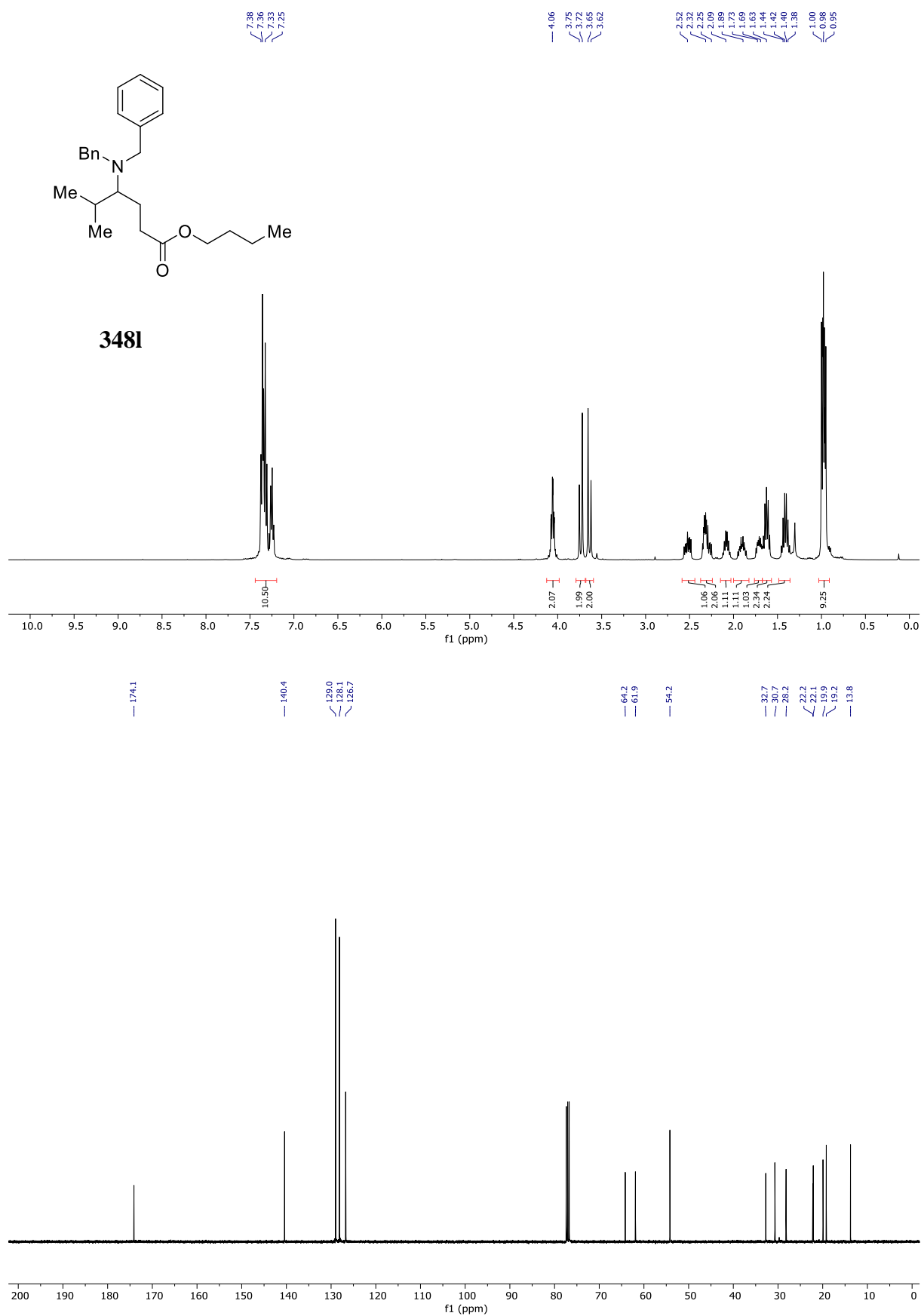
Appendix IV: ^1H and ^{13}C NMR spectral data

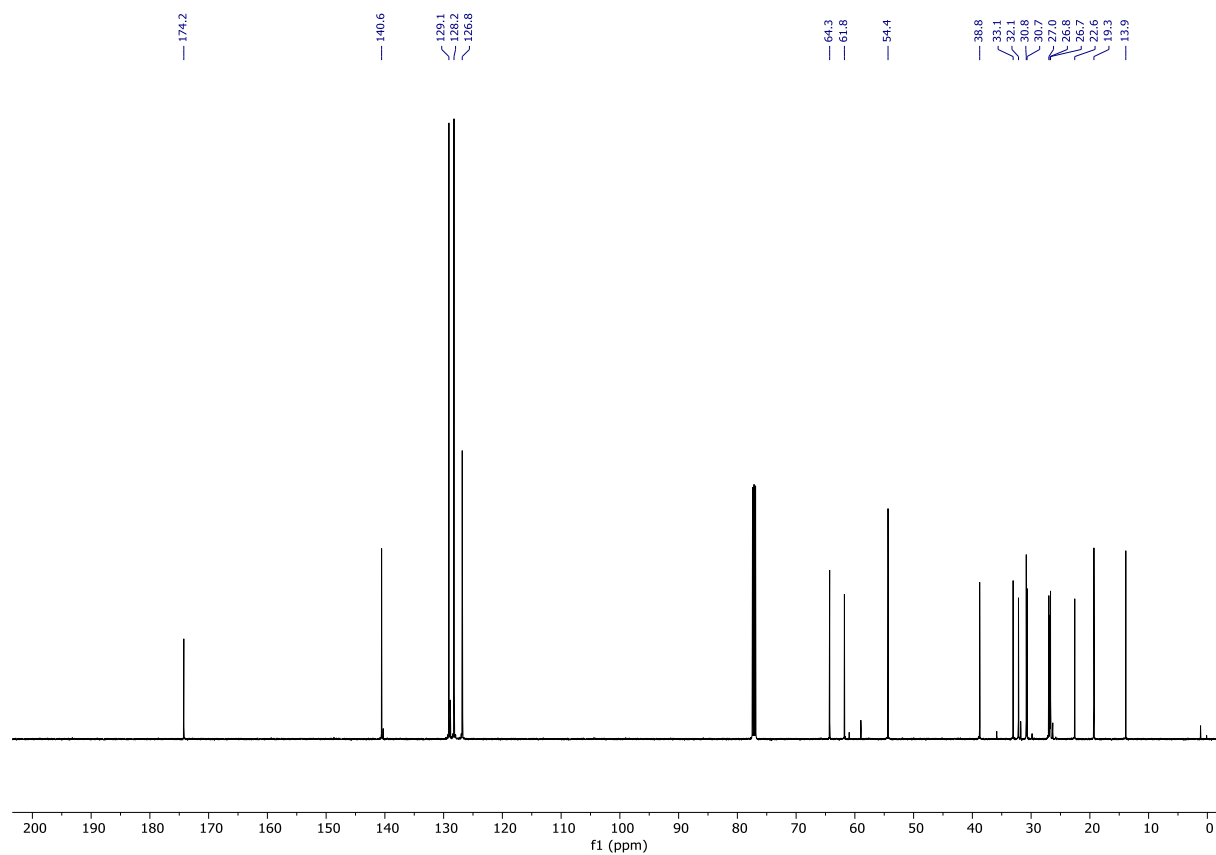
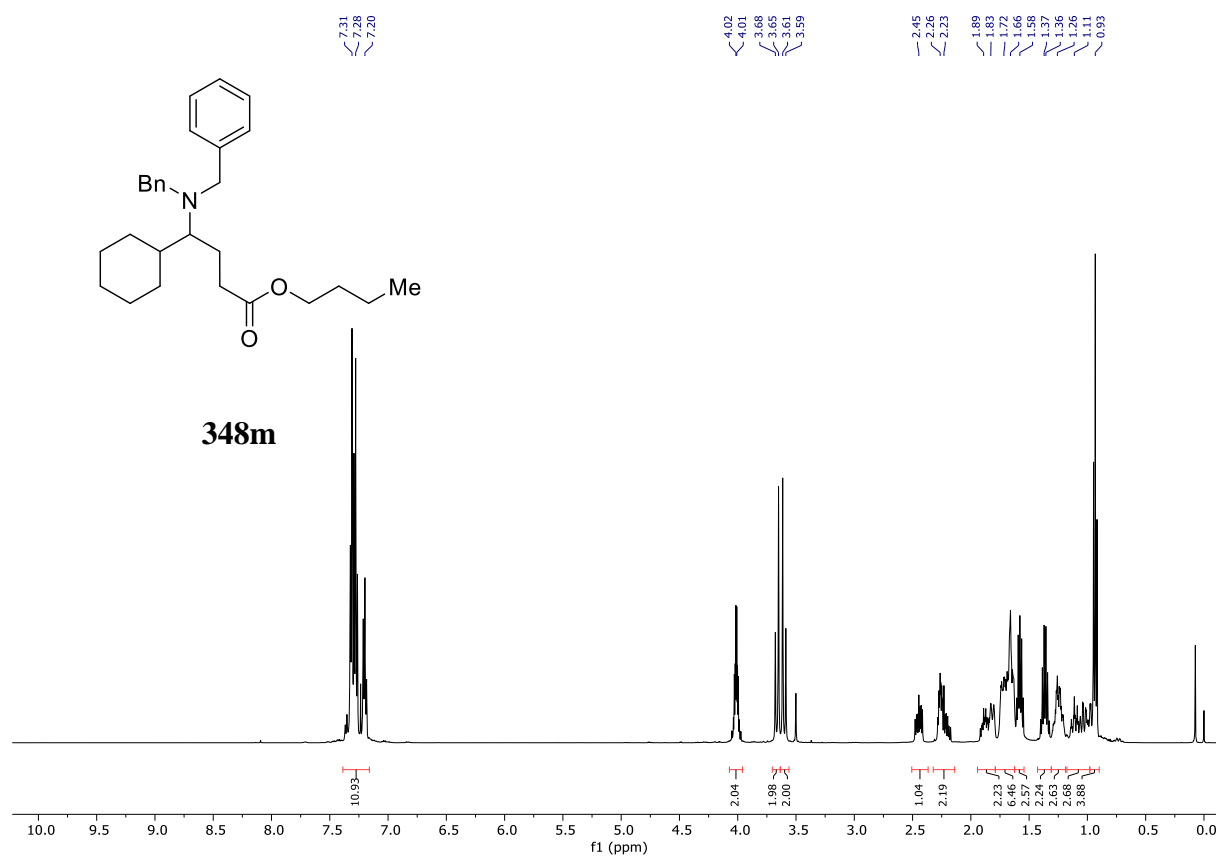
^1H and ^{13}C NMR Spectra (Key Compounds)

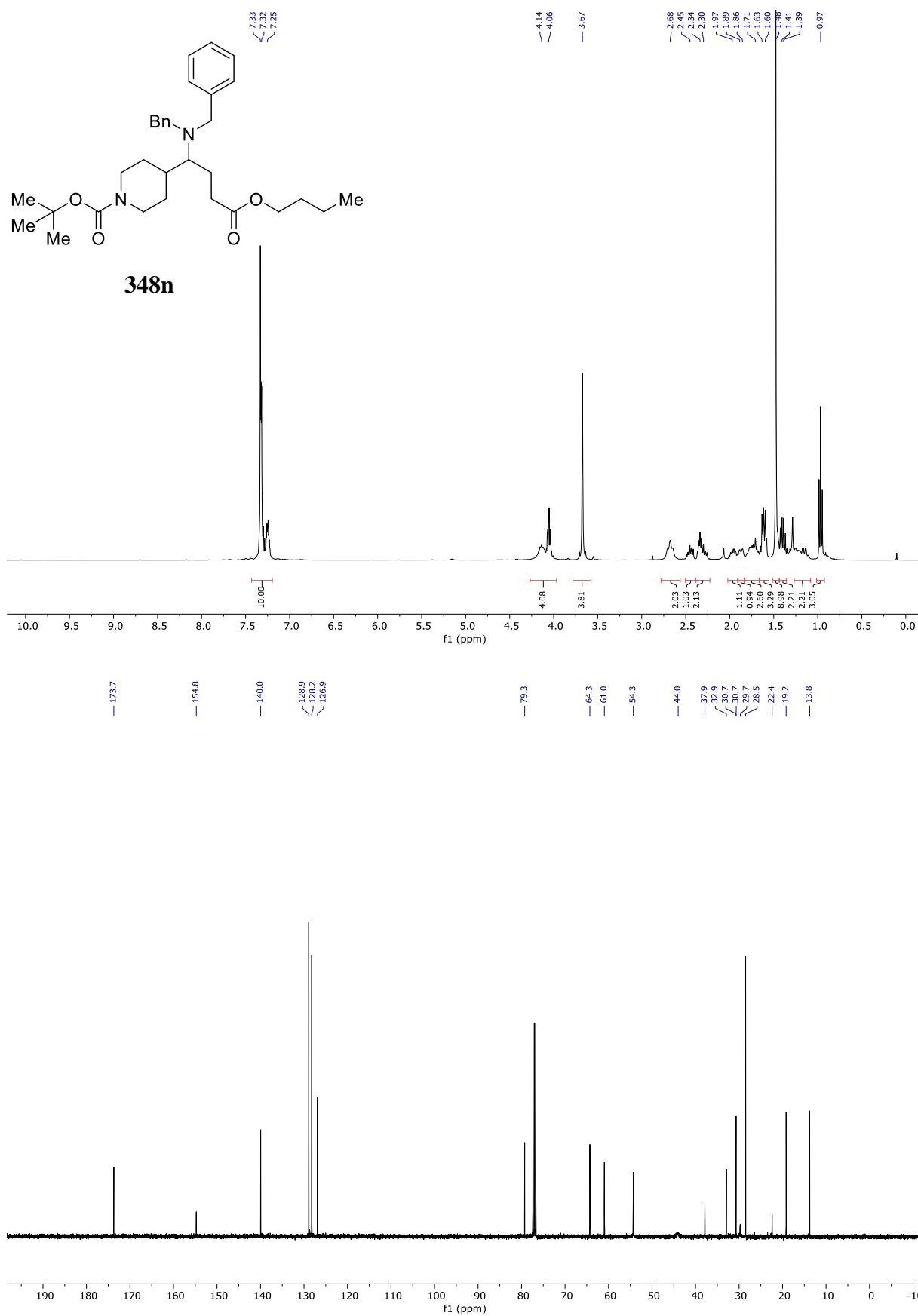


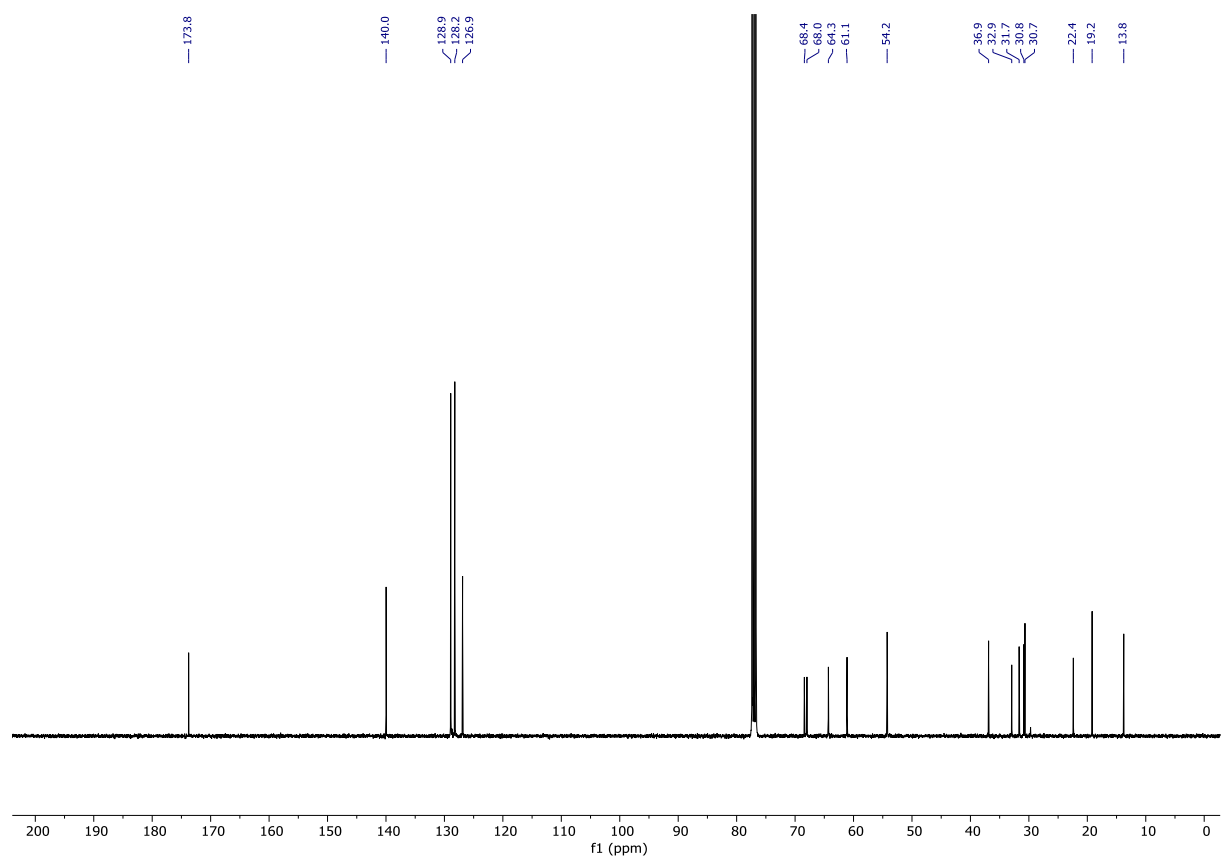
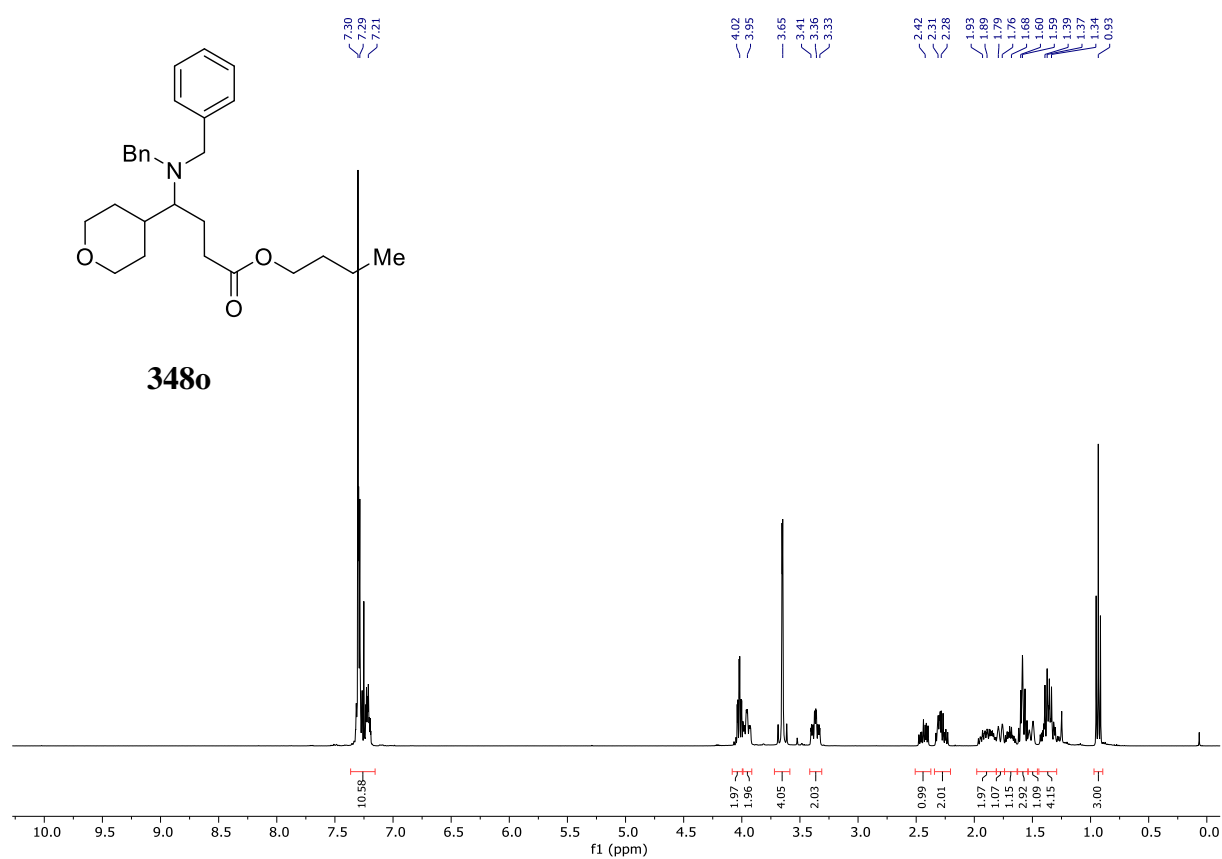


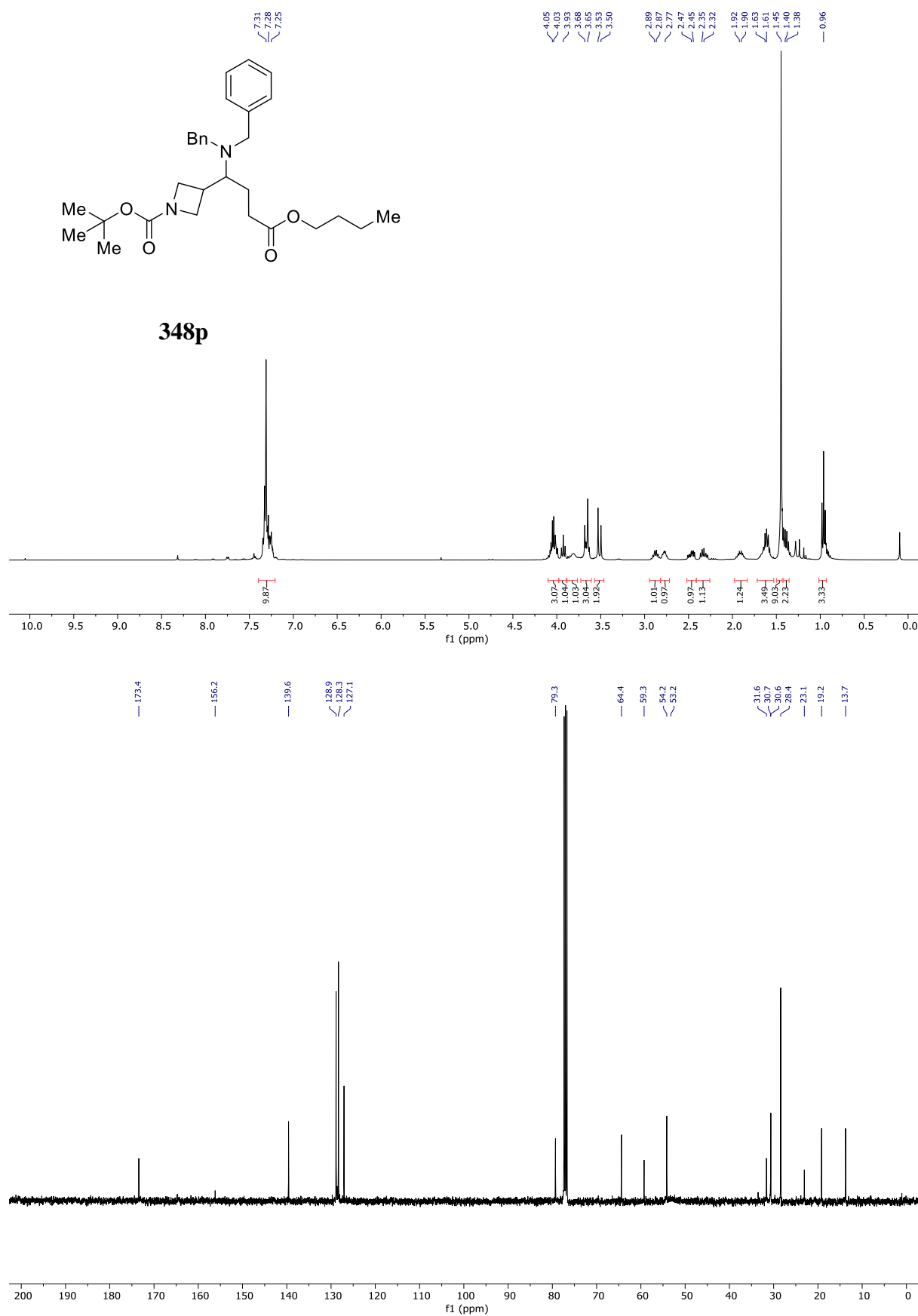


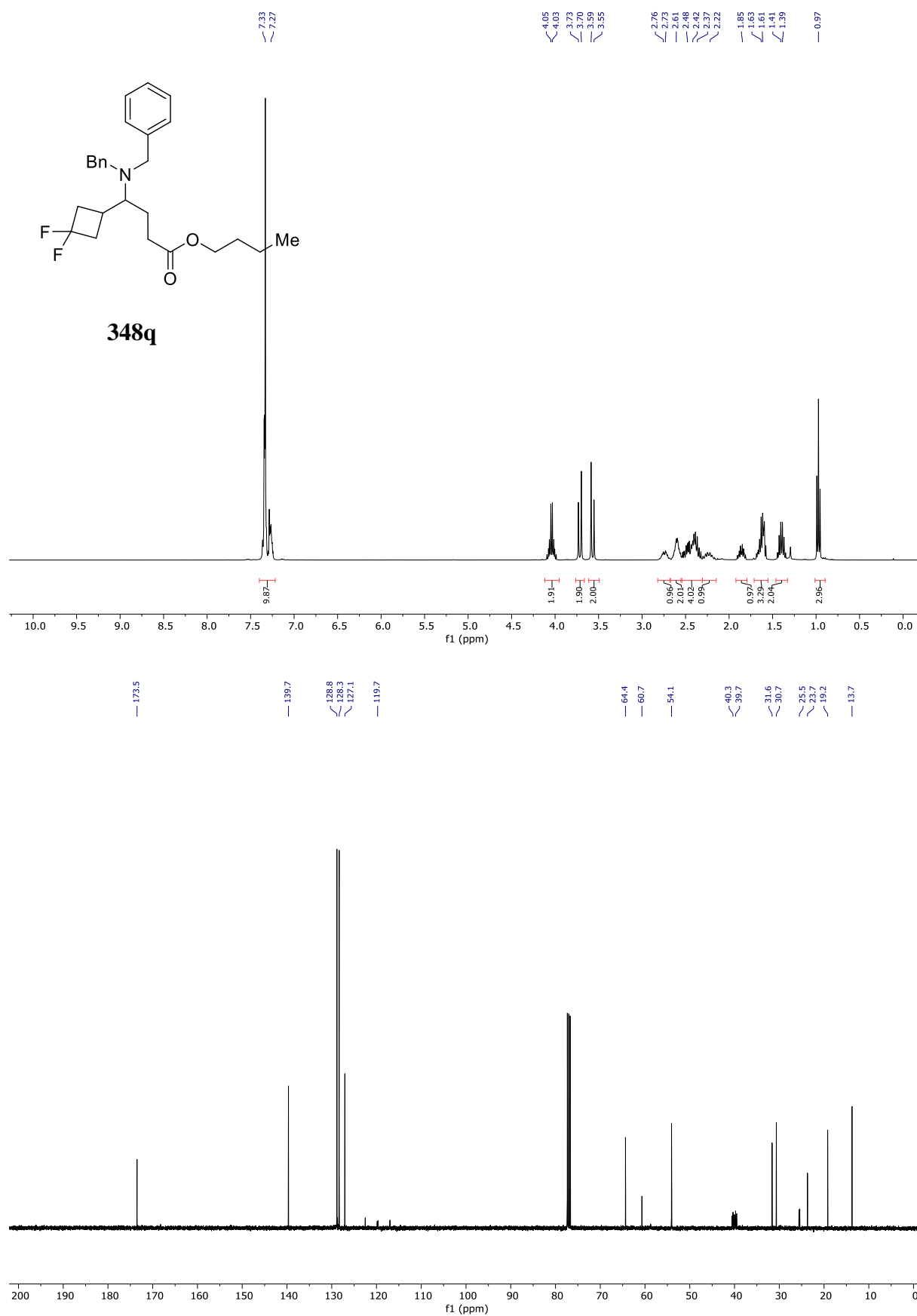


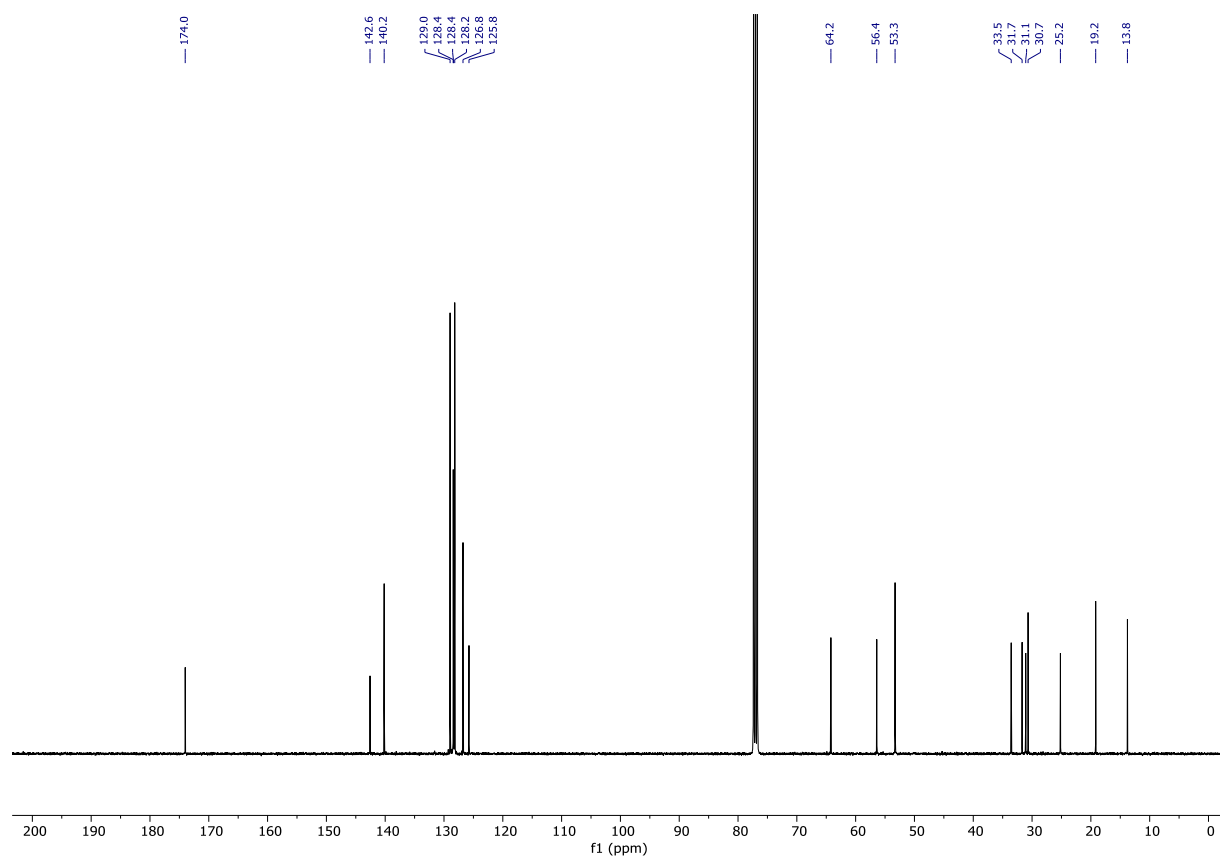
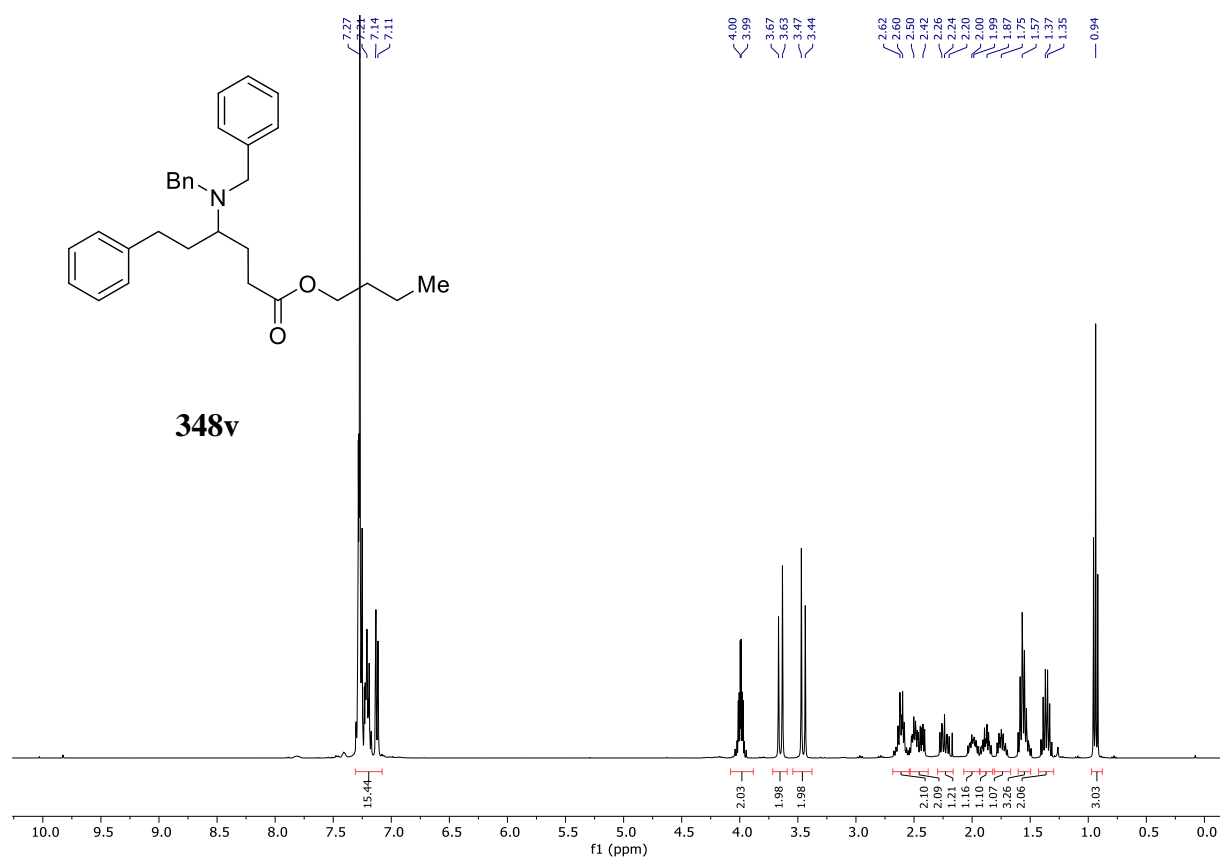


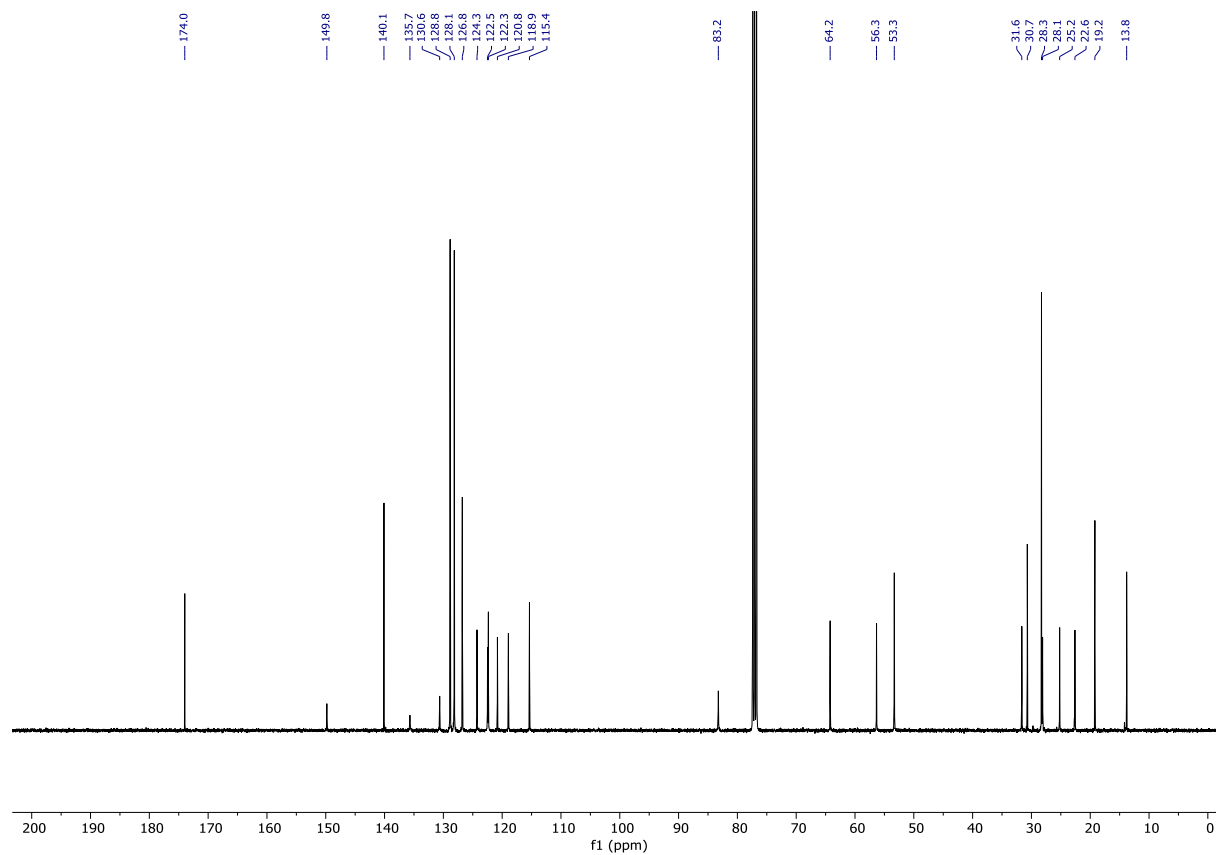
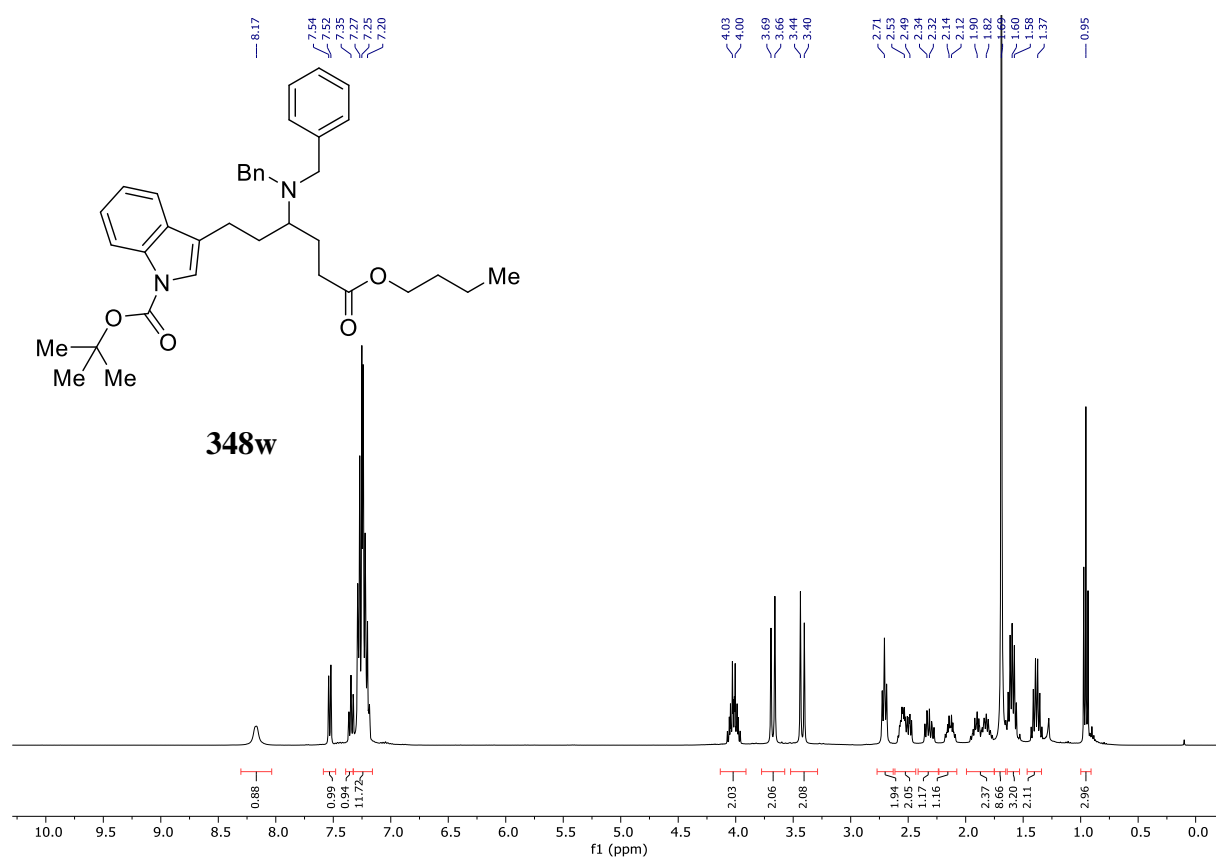


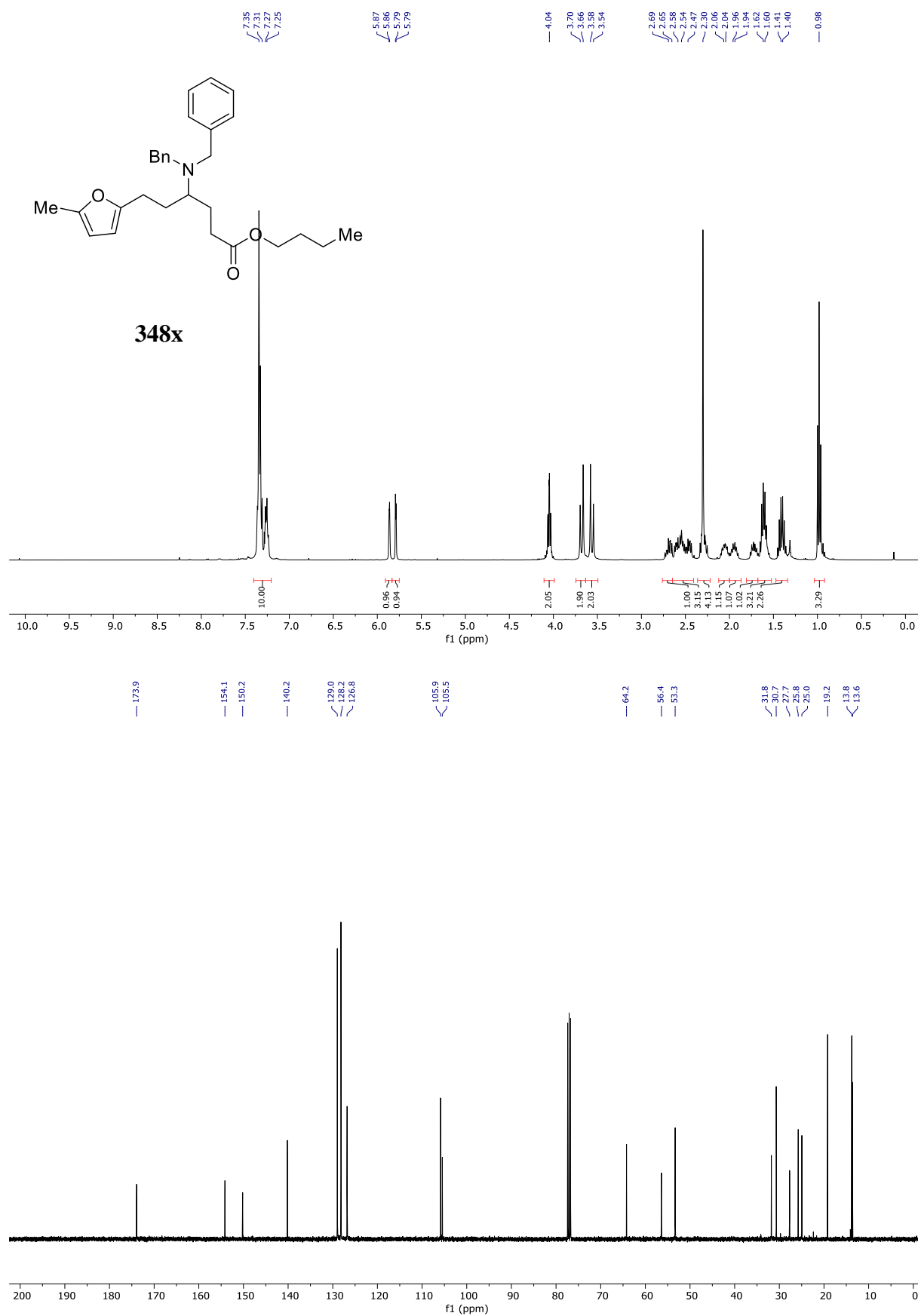


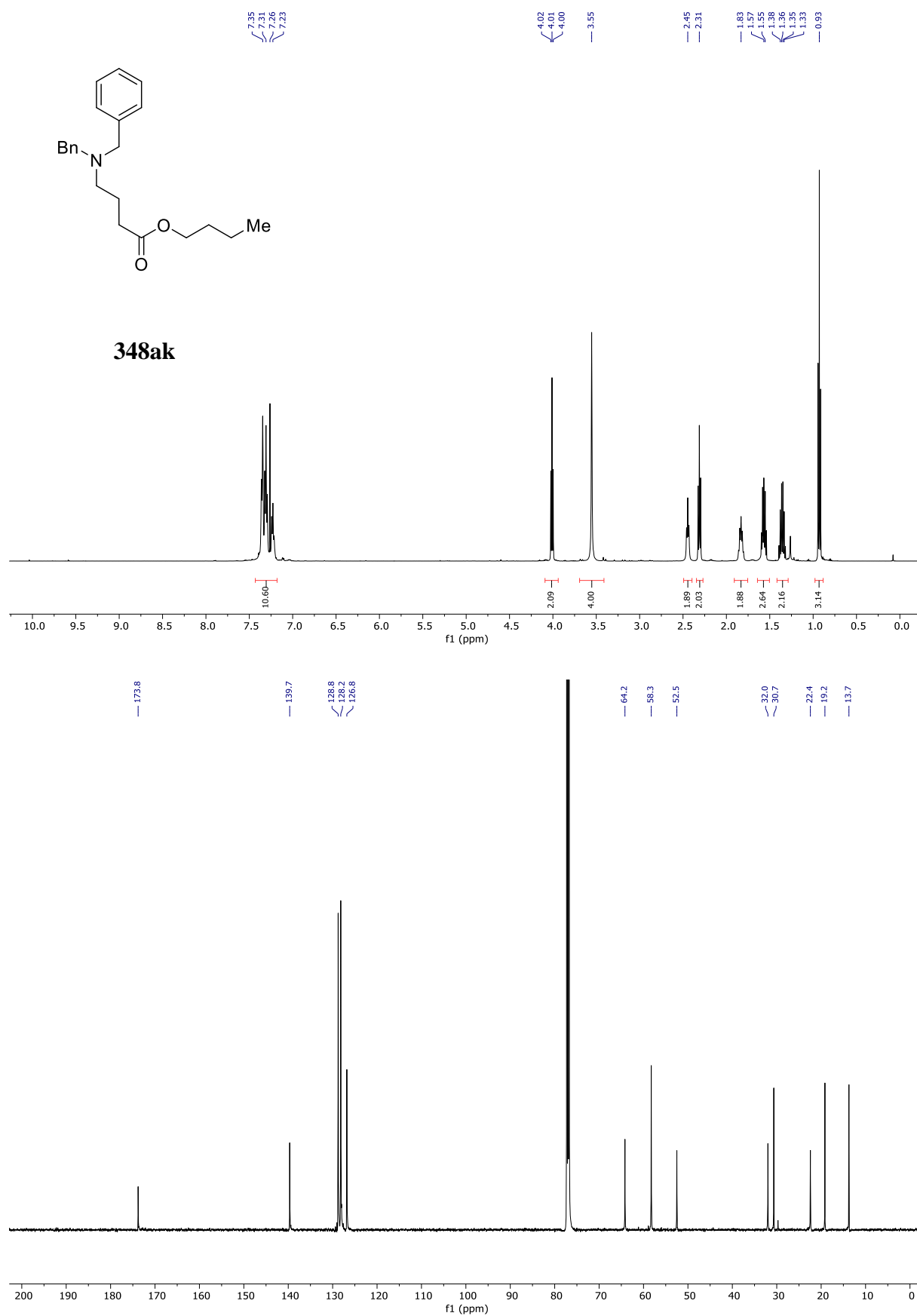


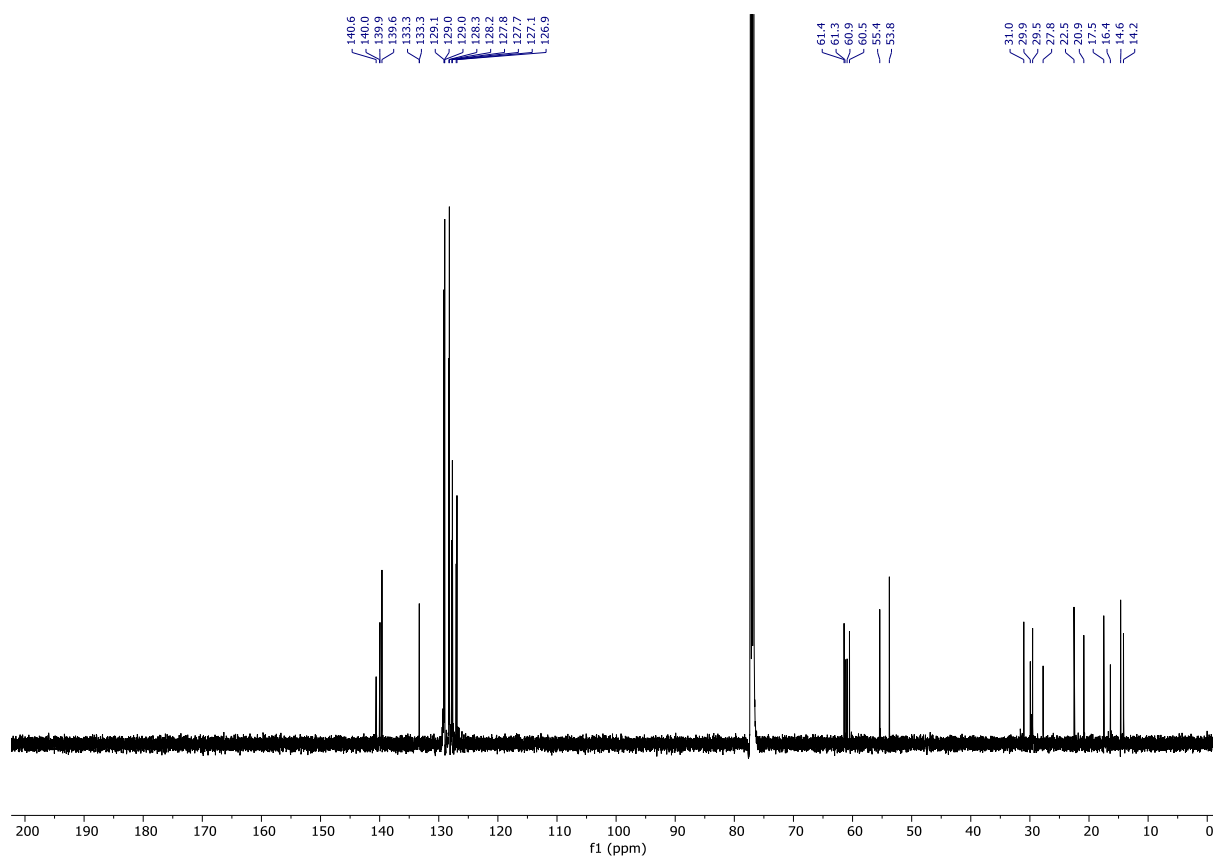
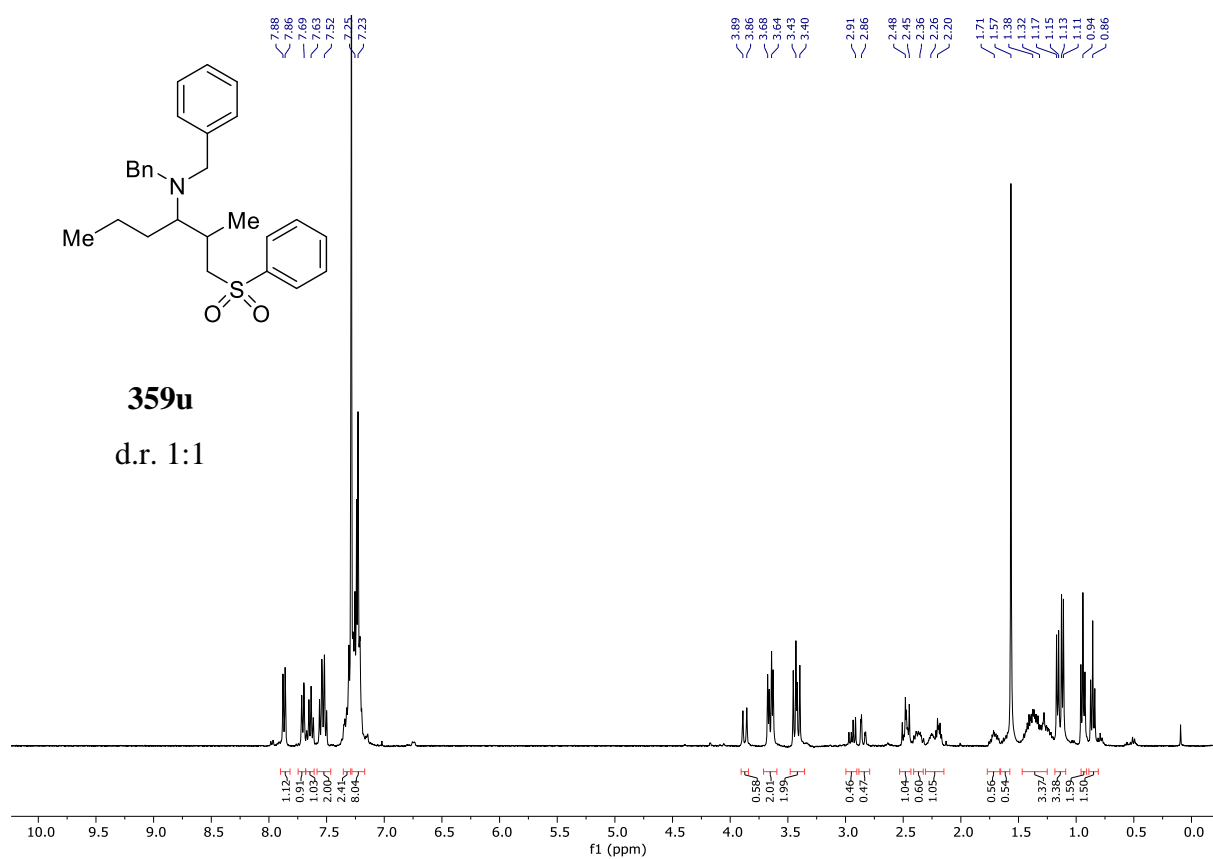


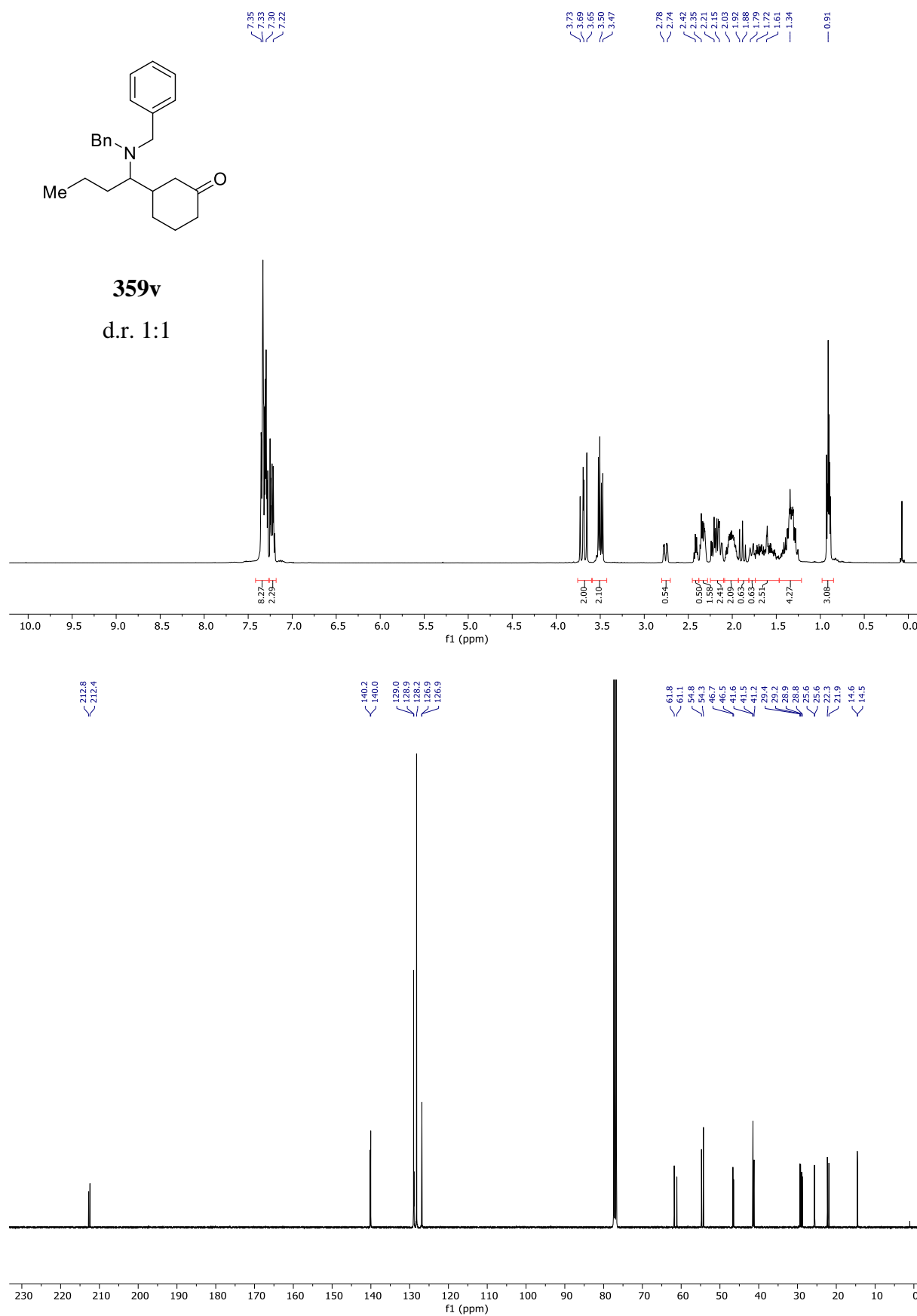


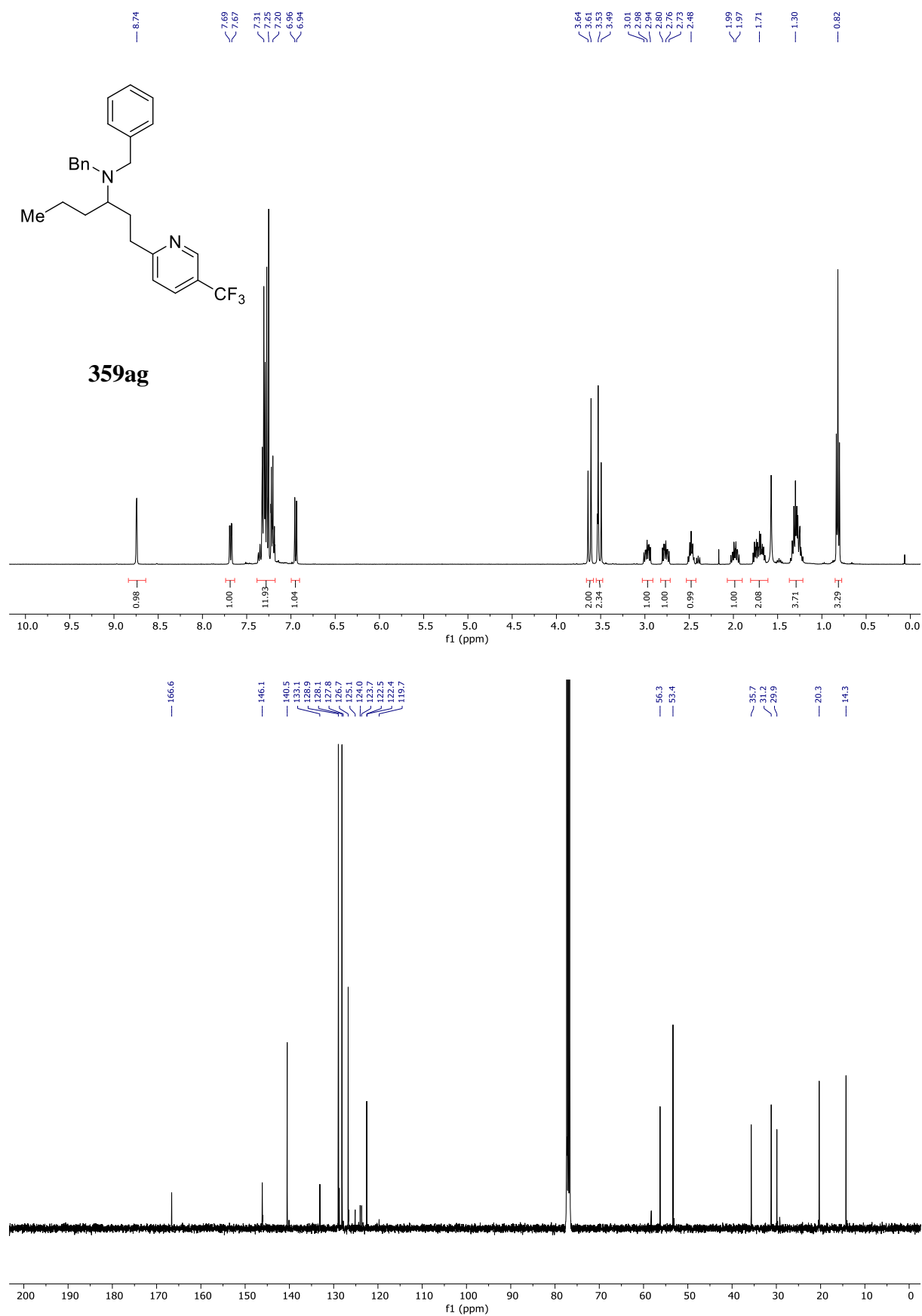


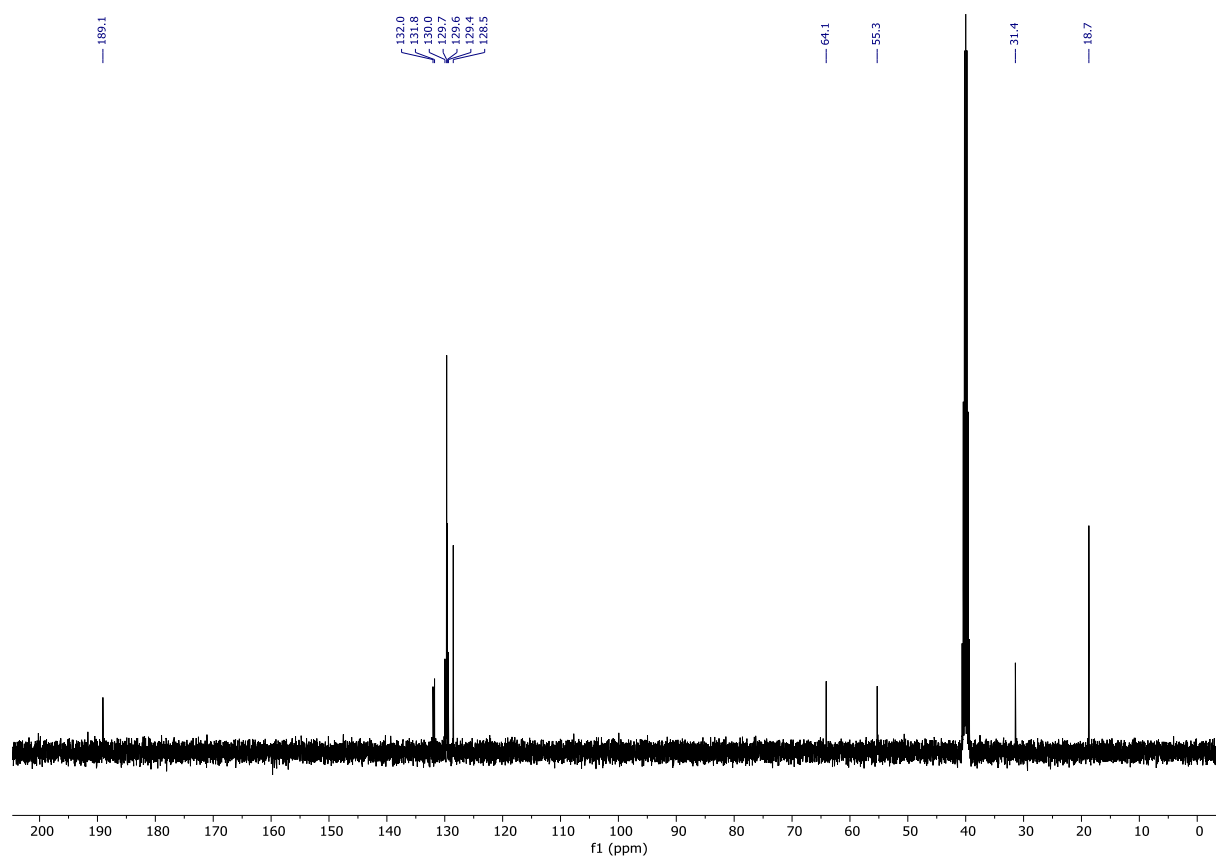
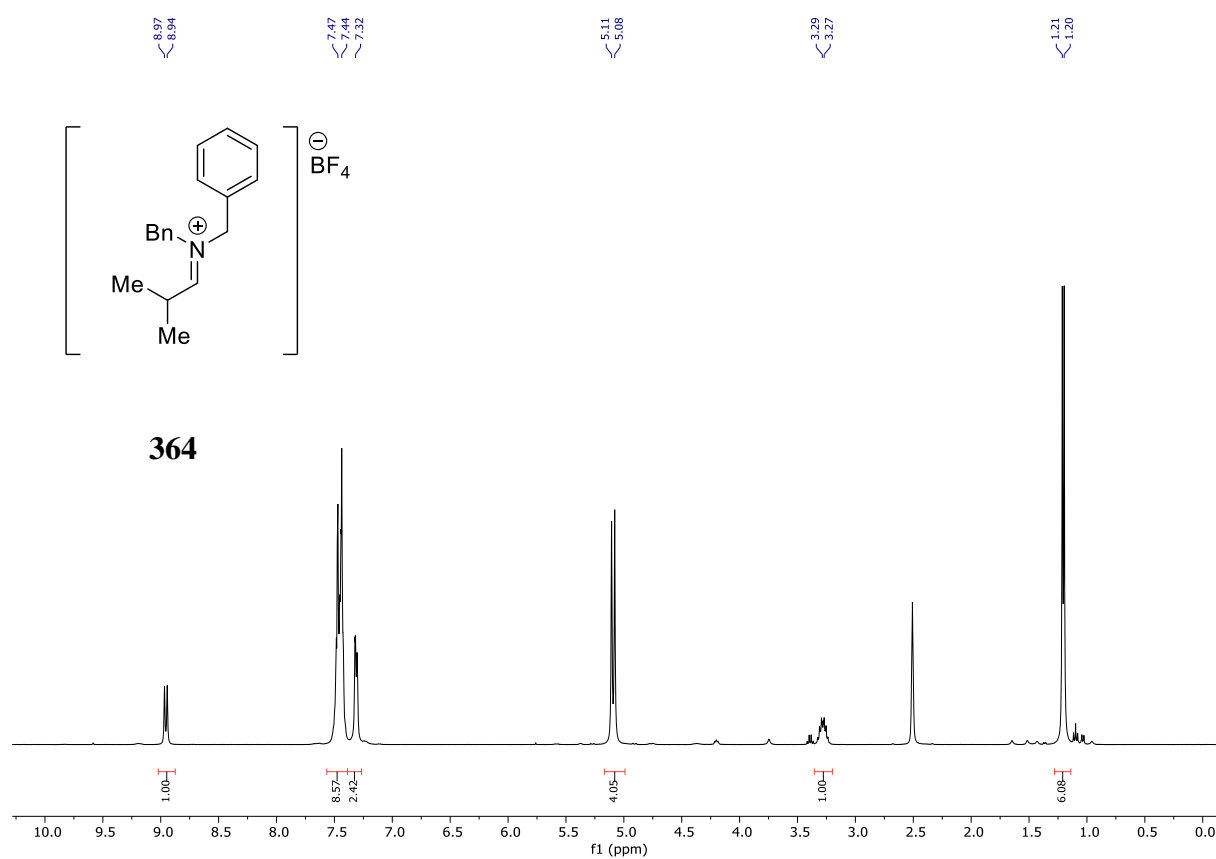


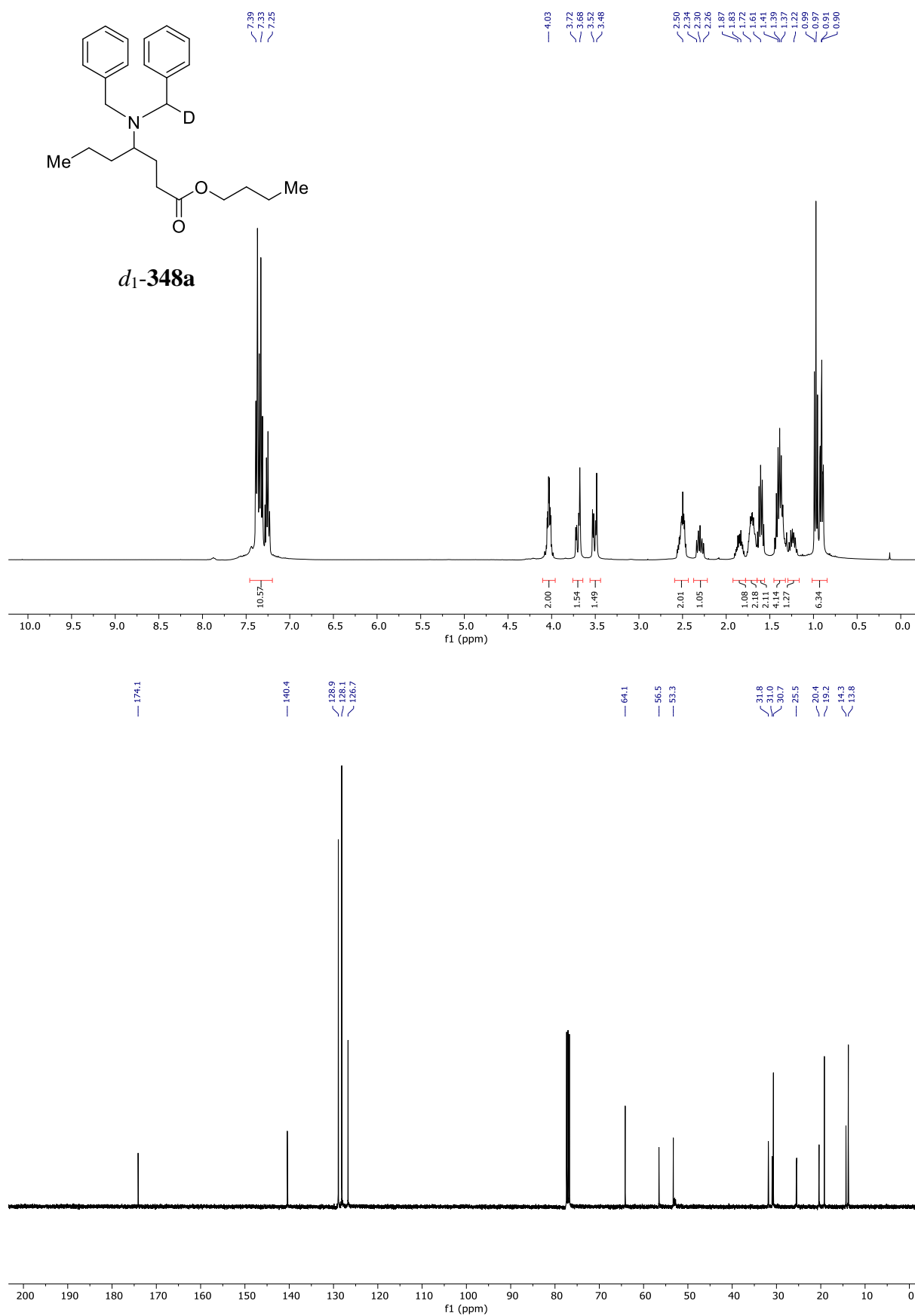


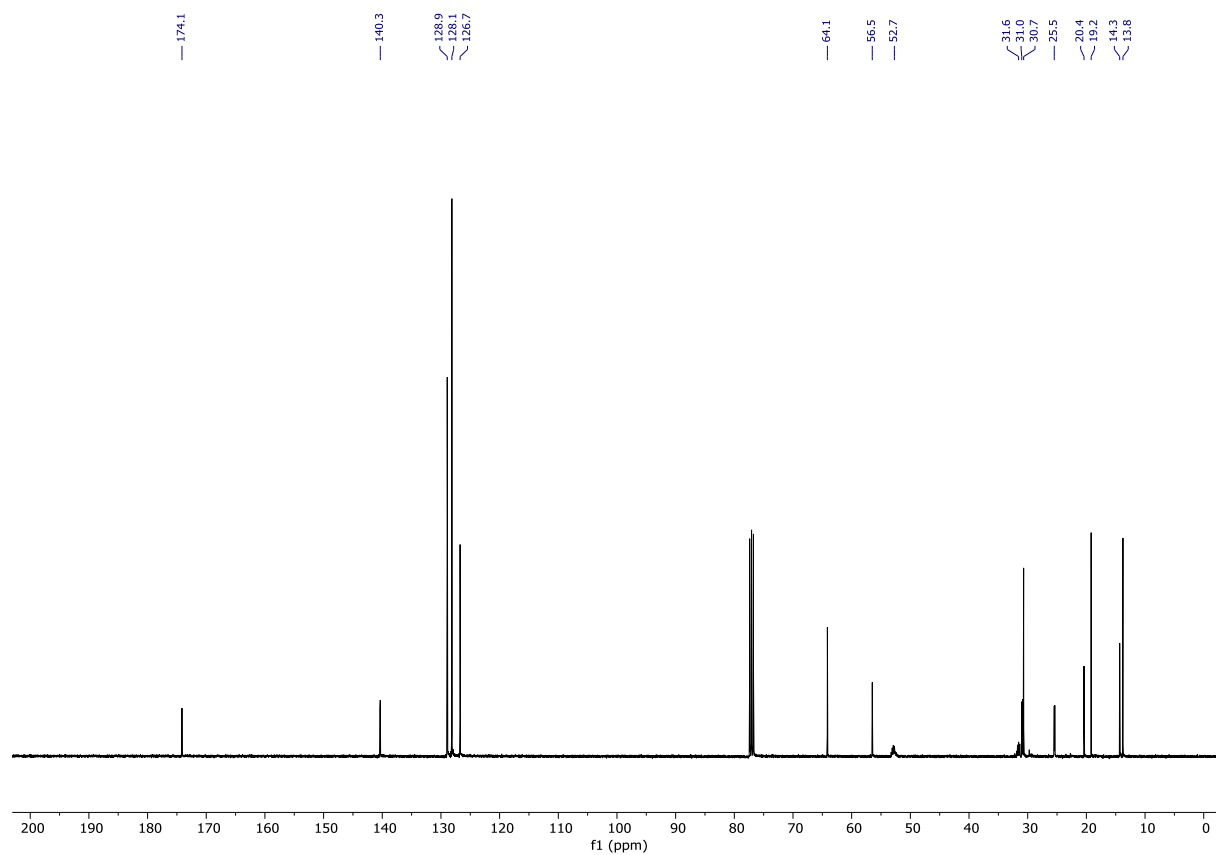
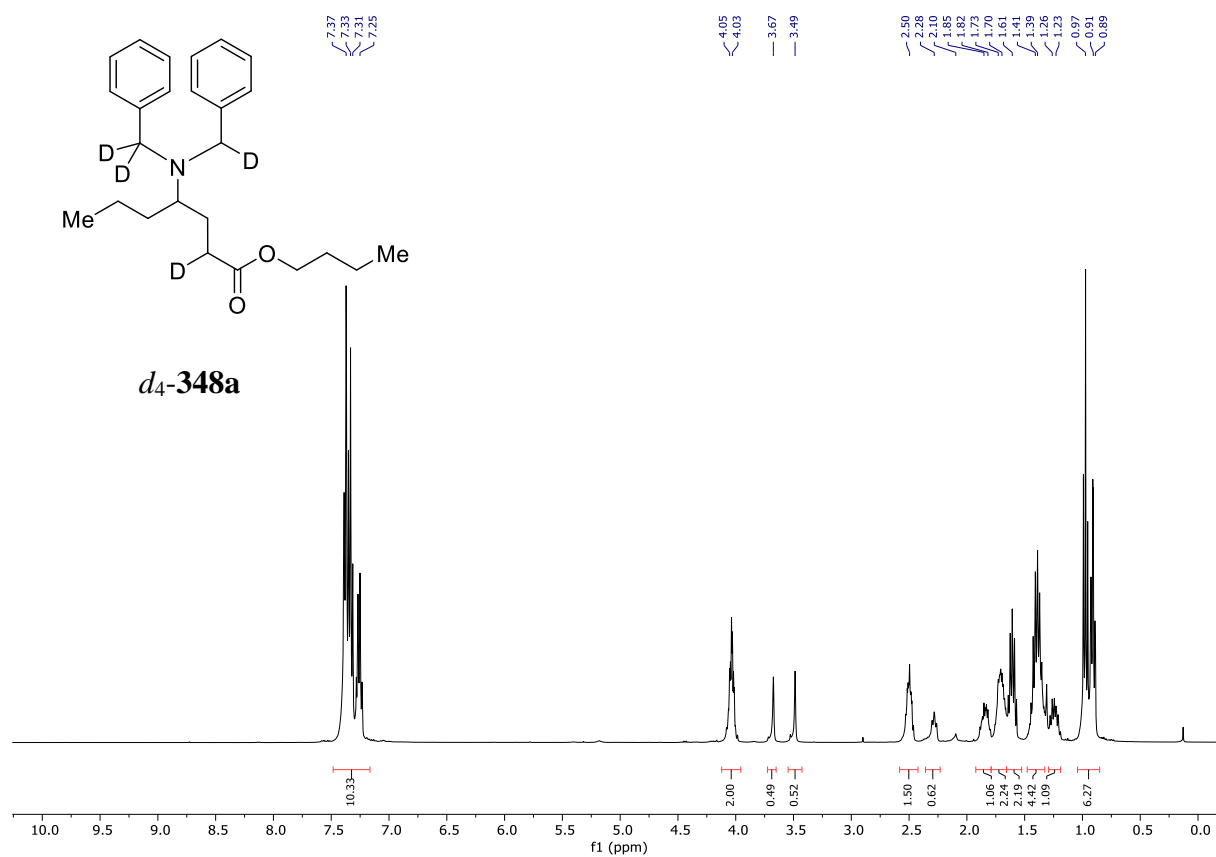


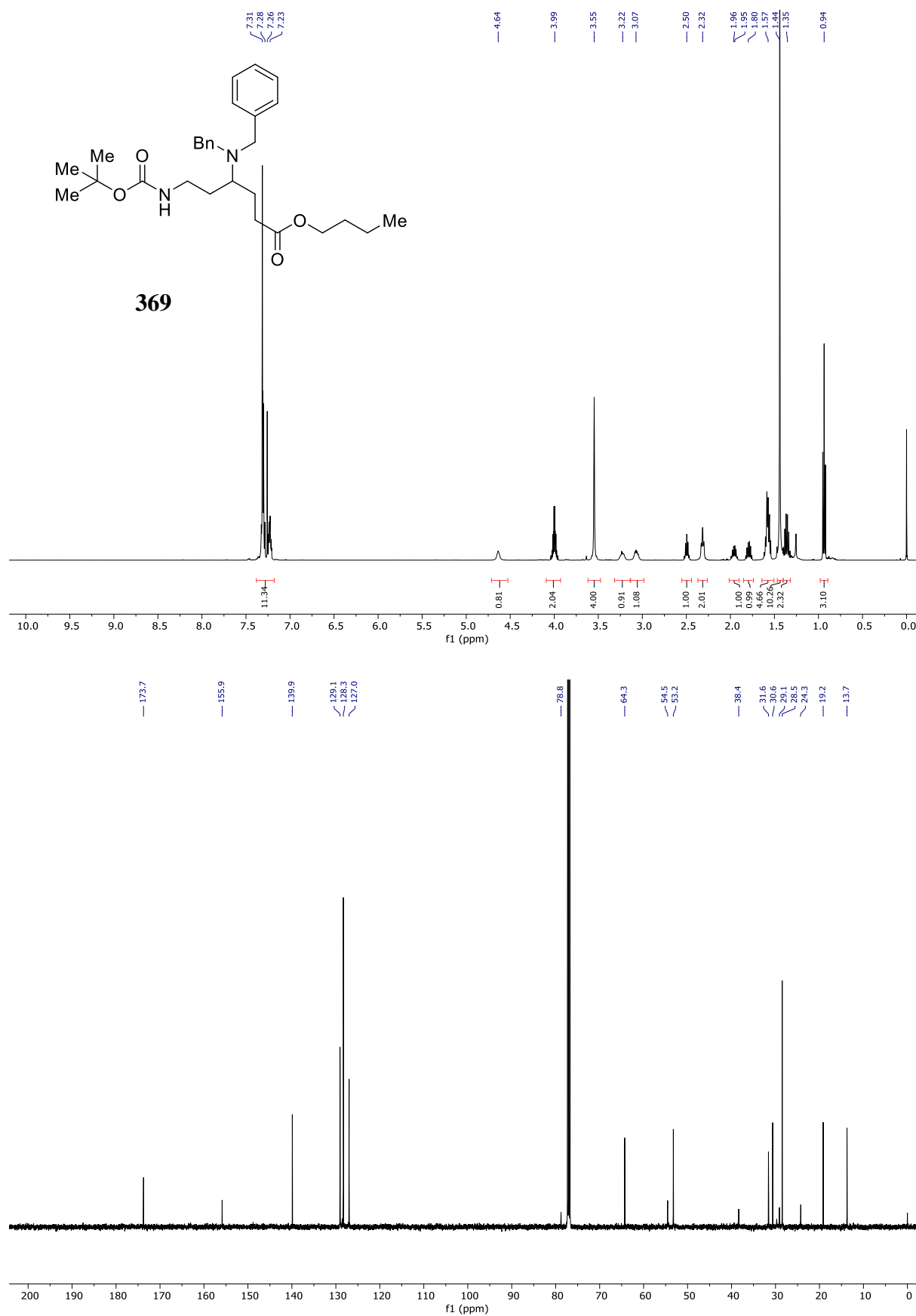


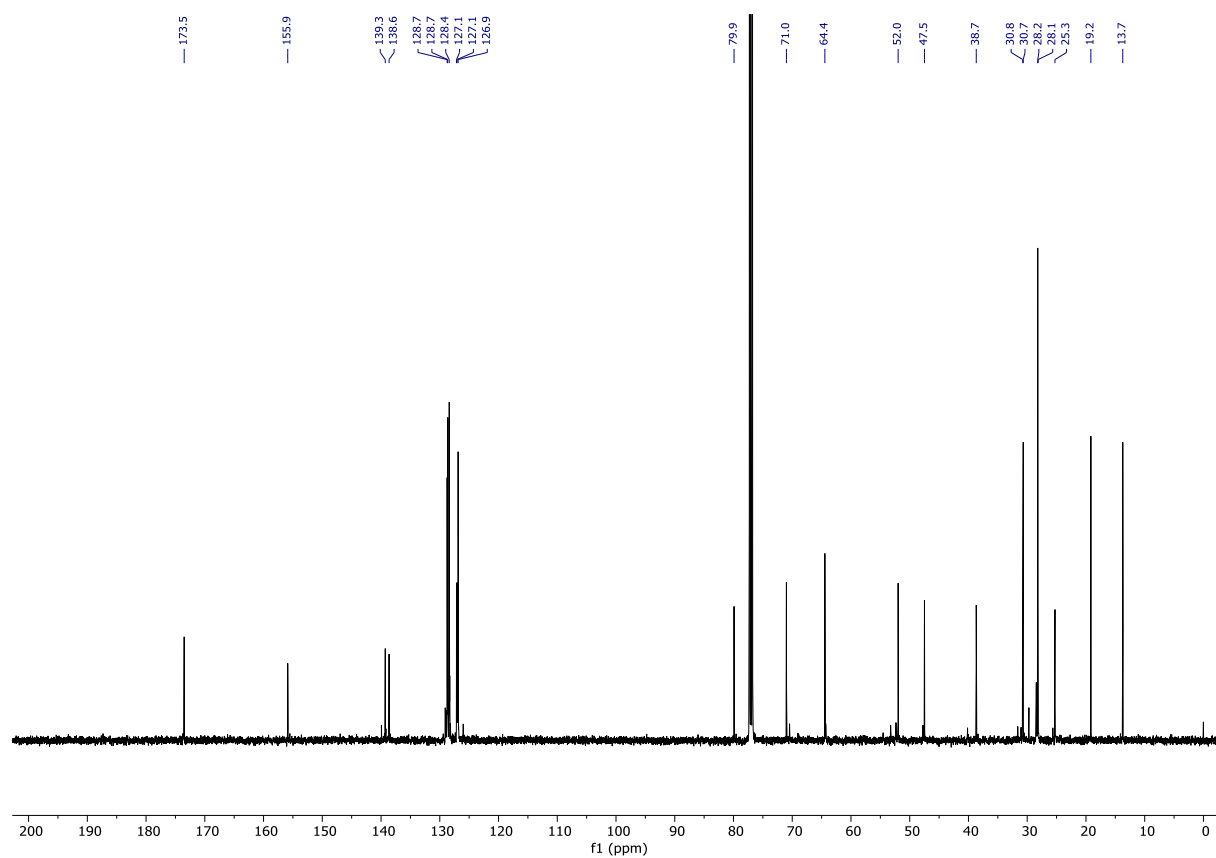
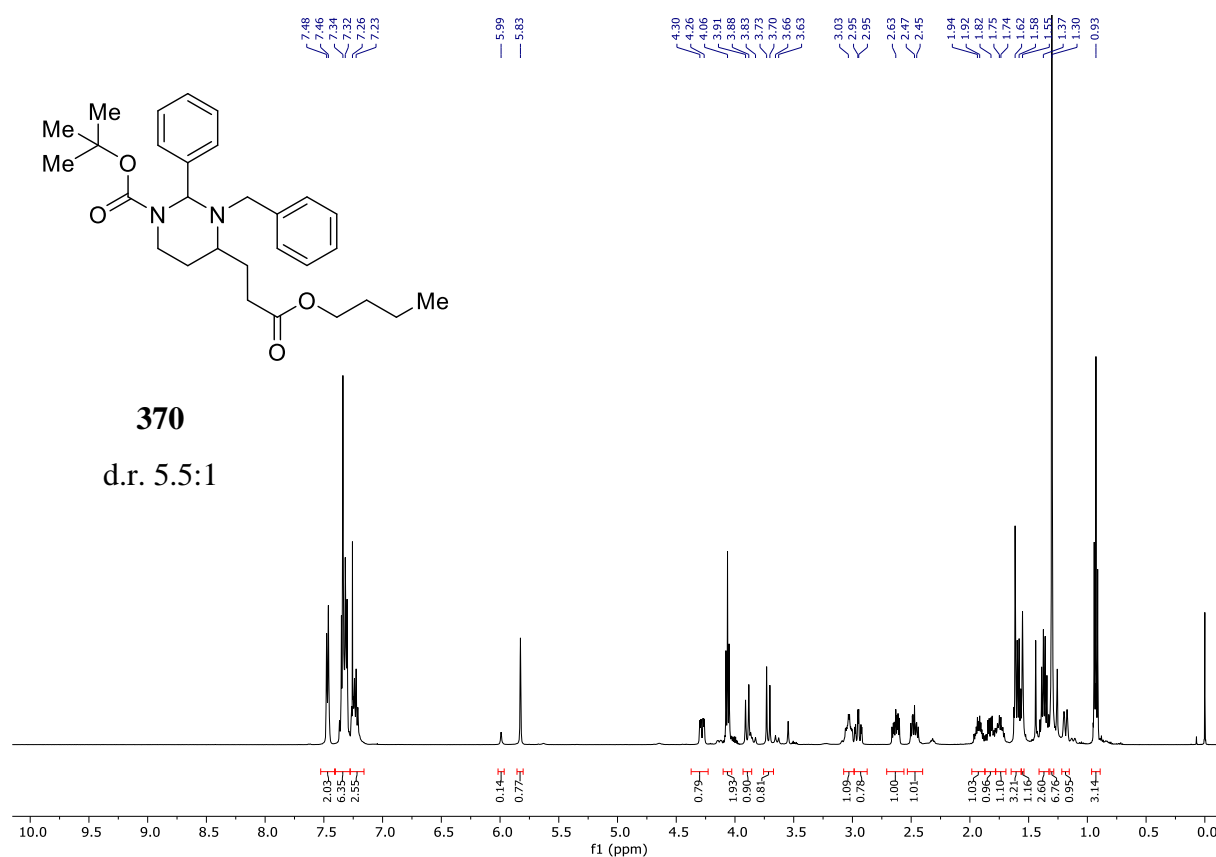


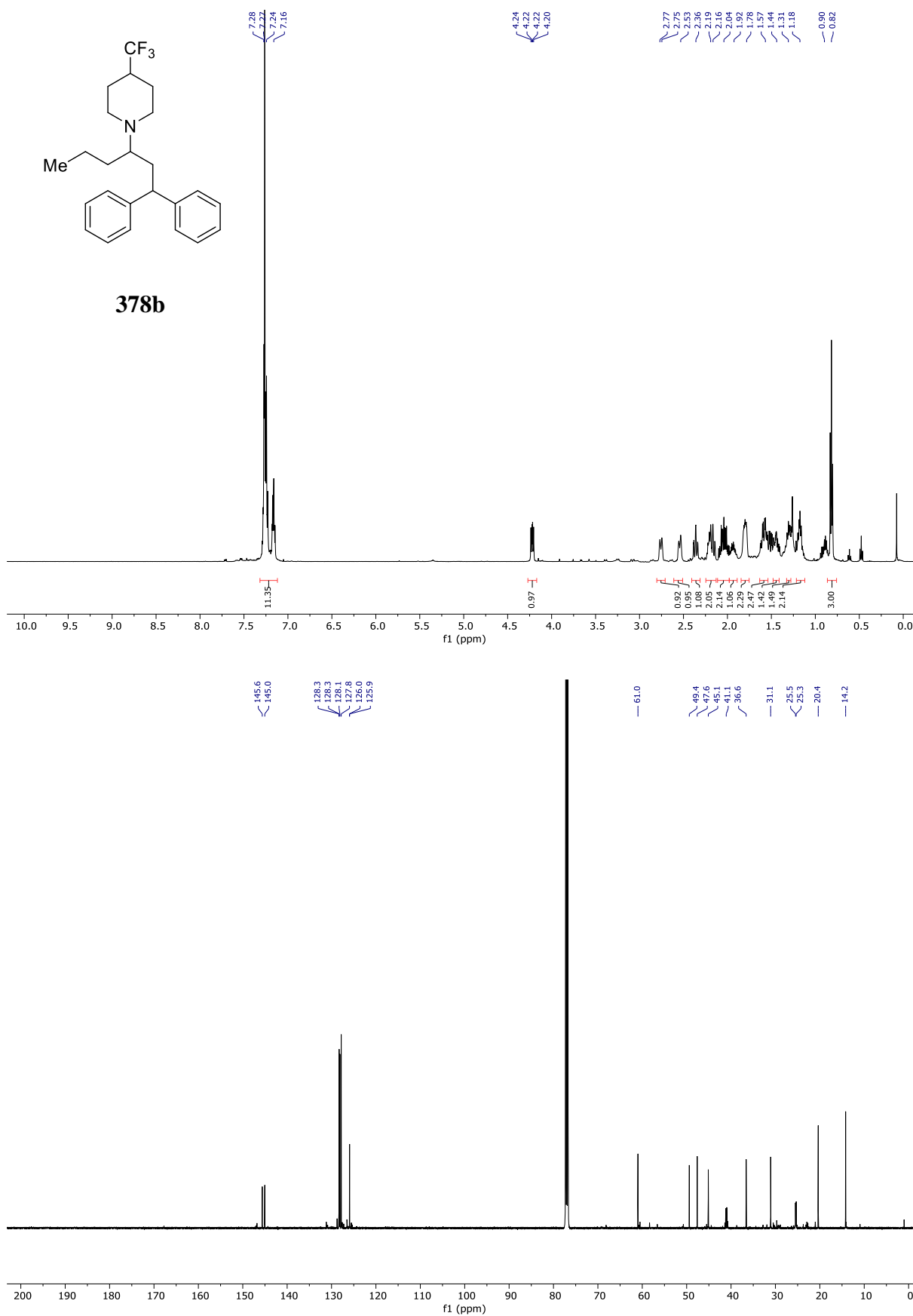


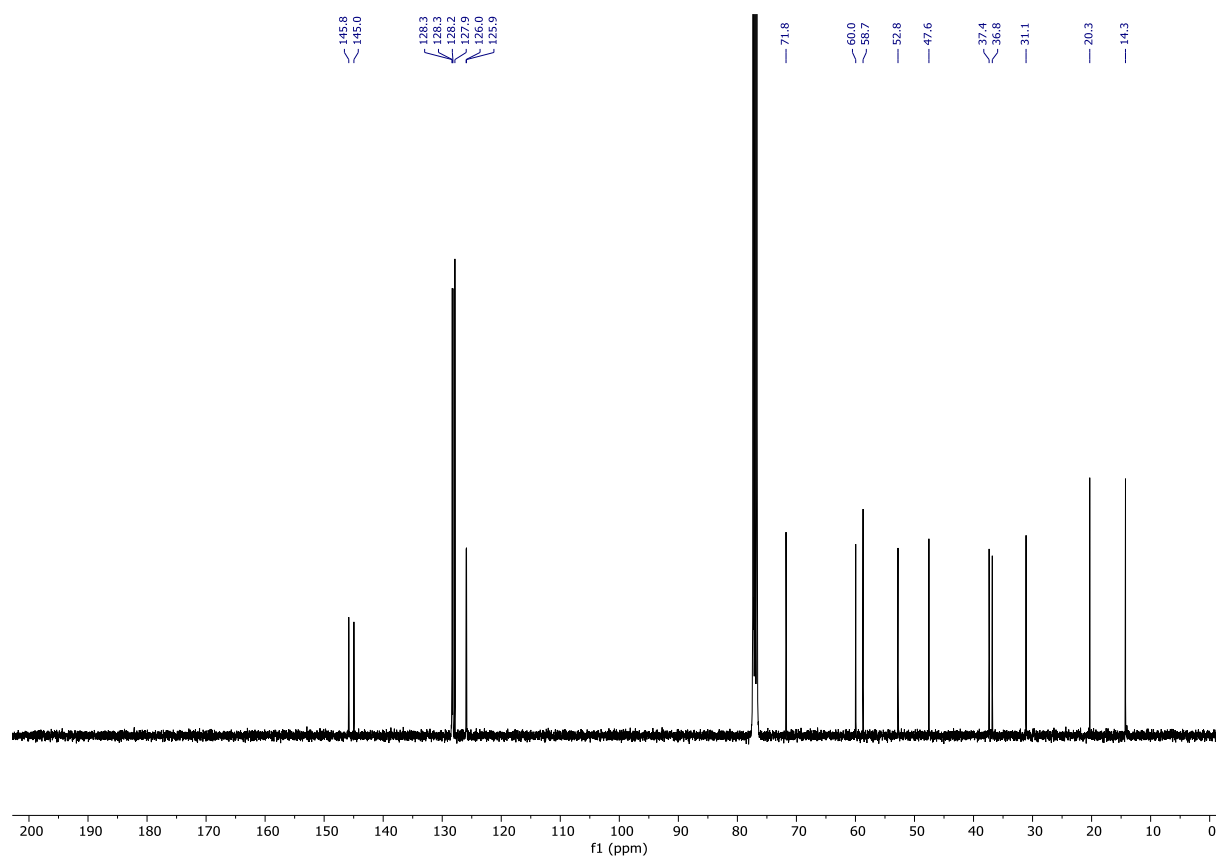
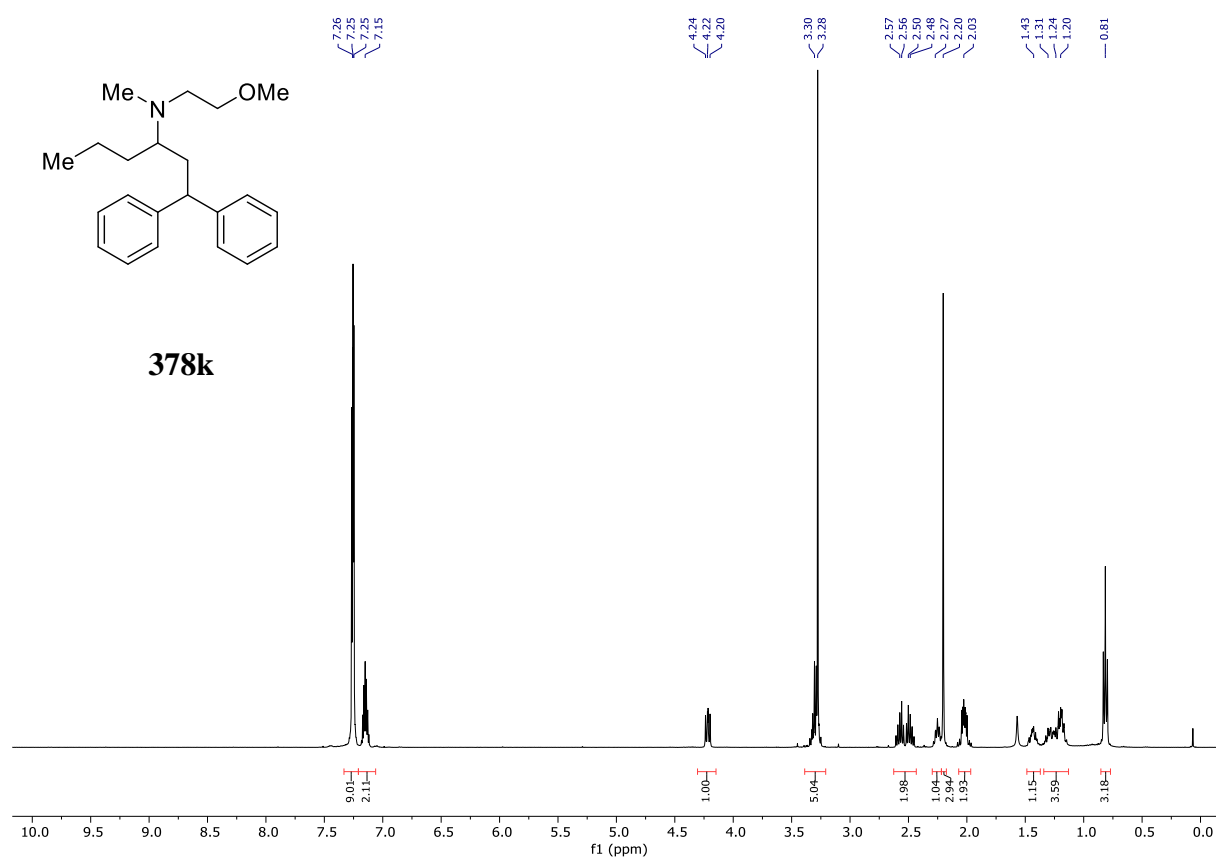


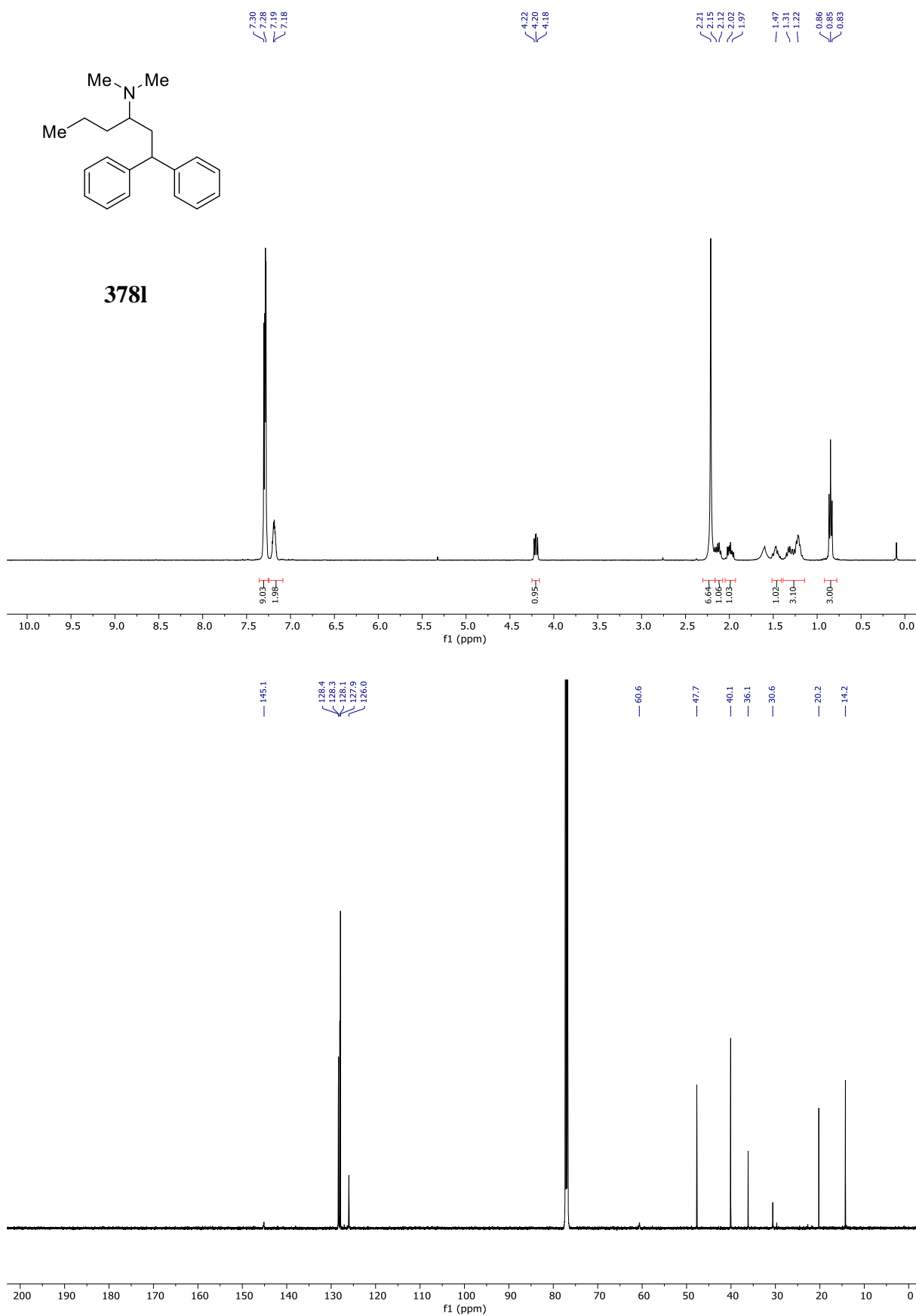


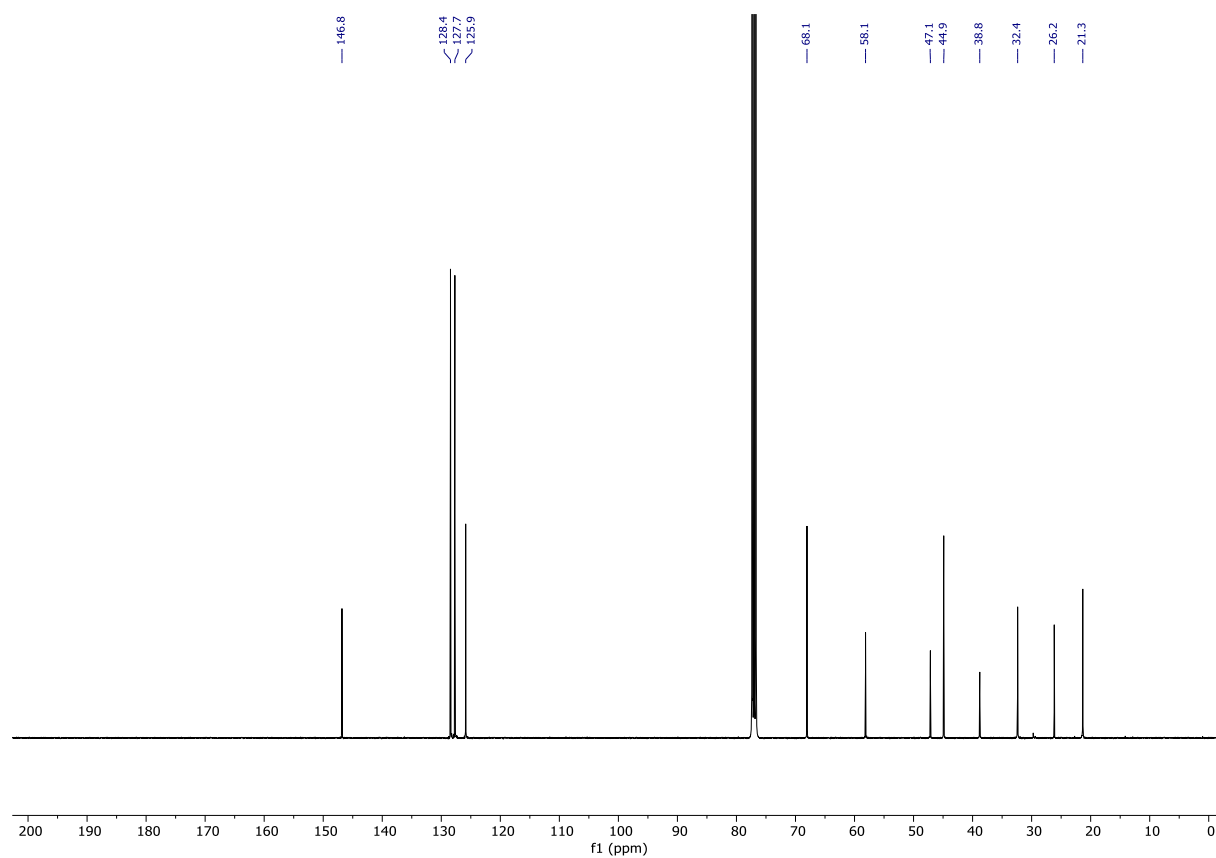
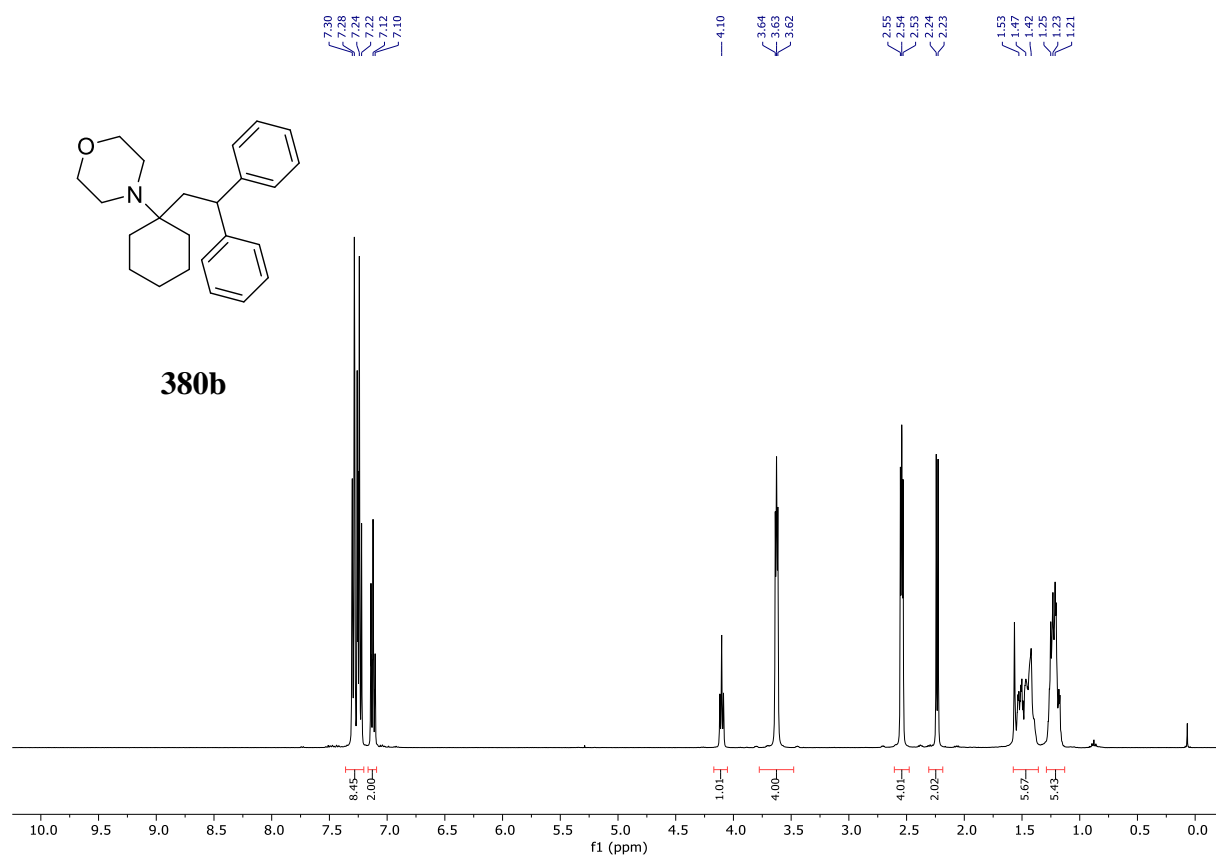


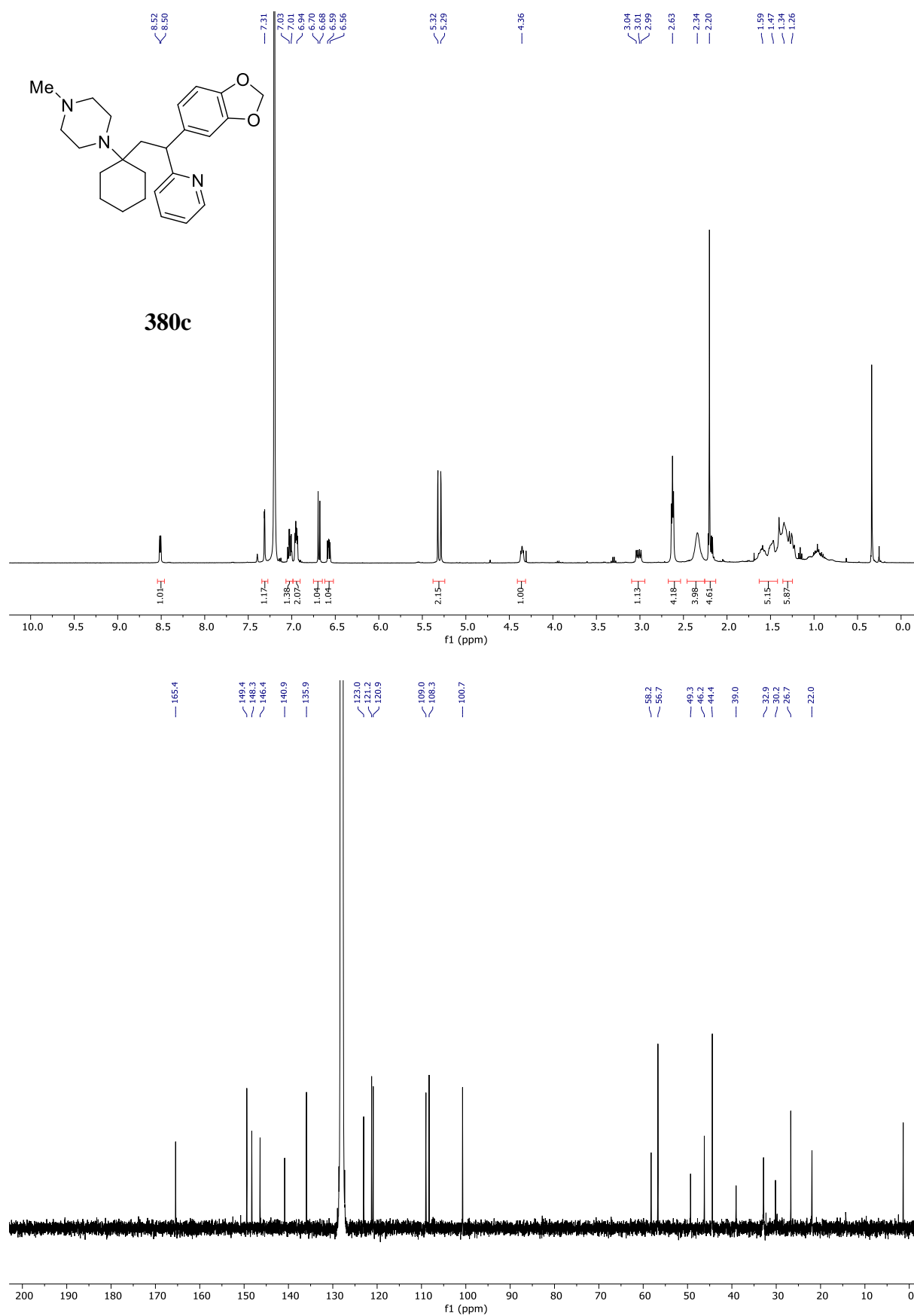


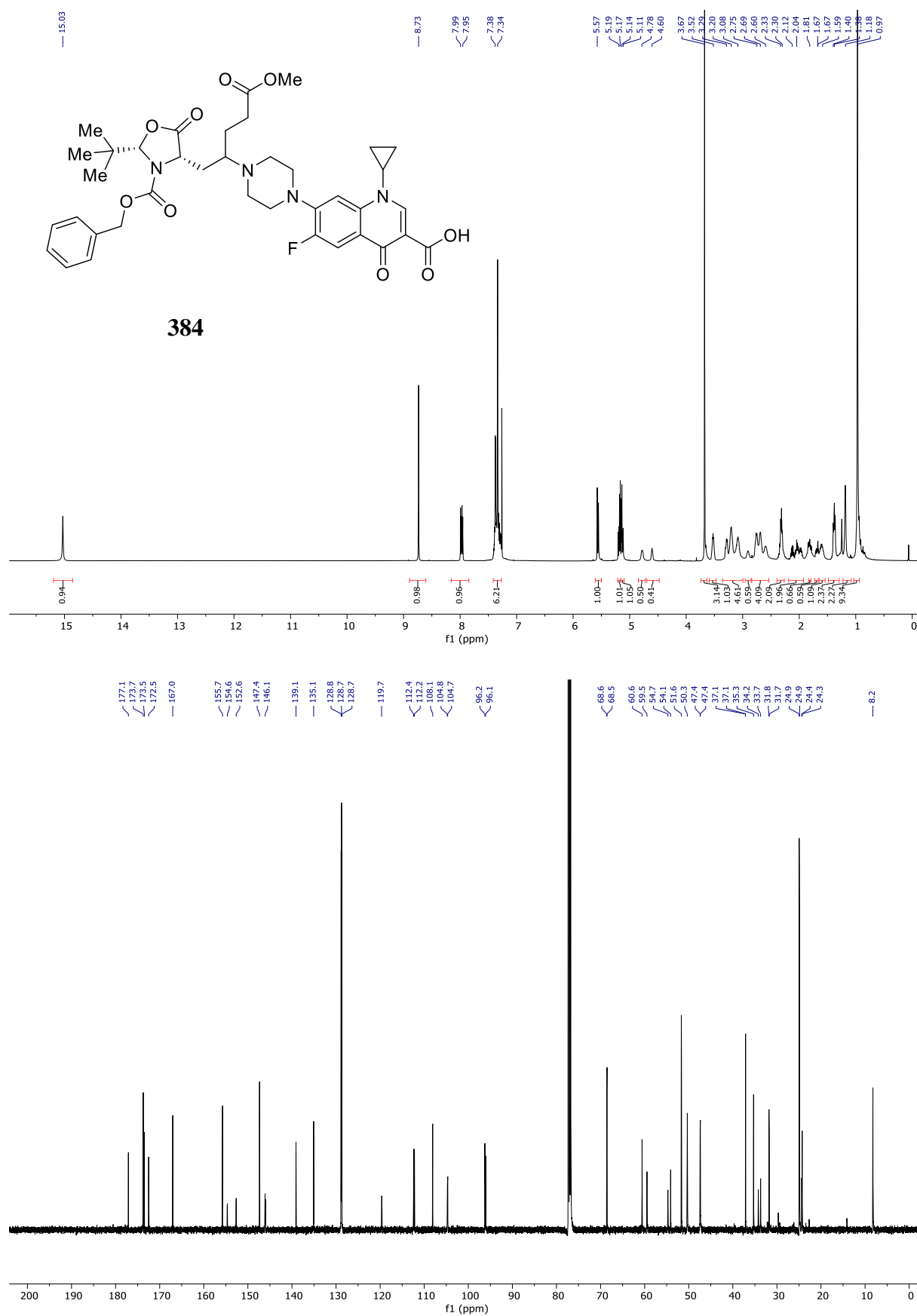


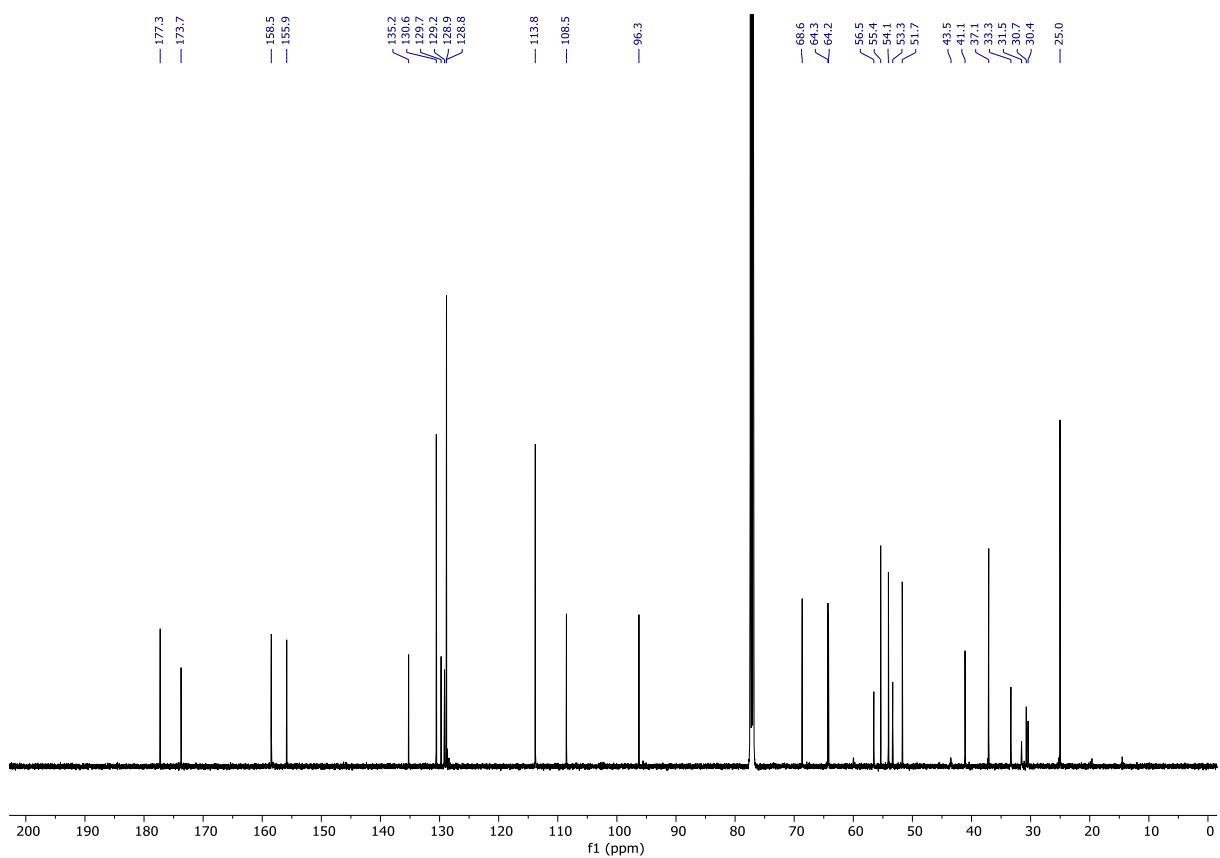
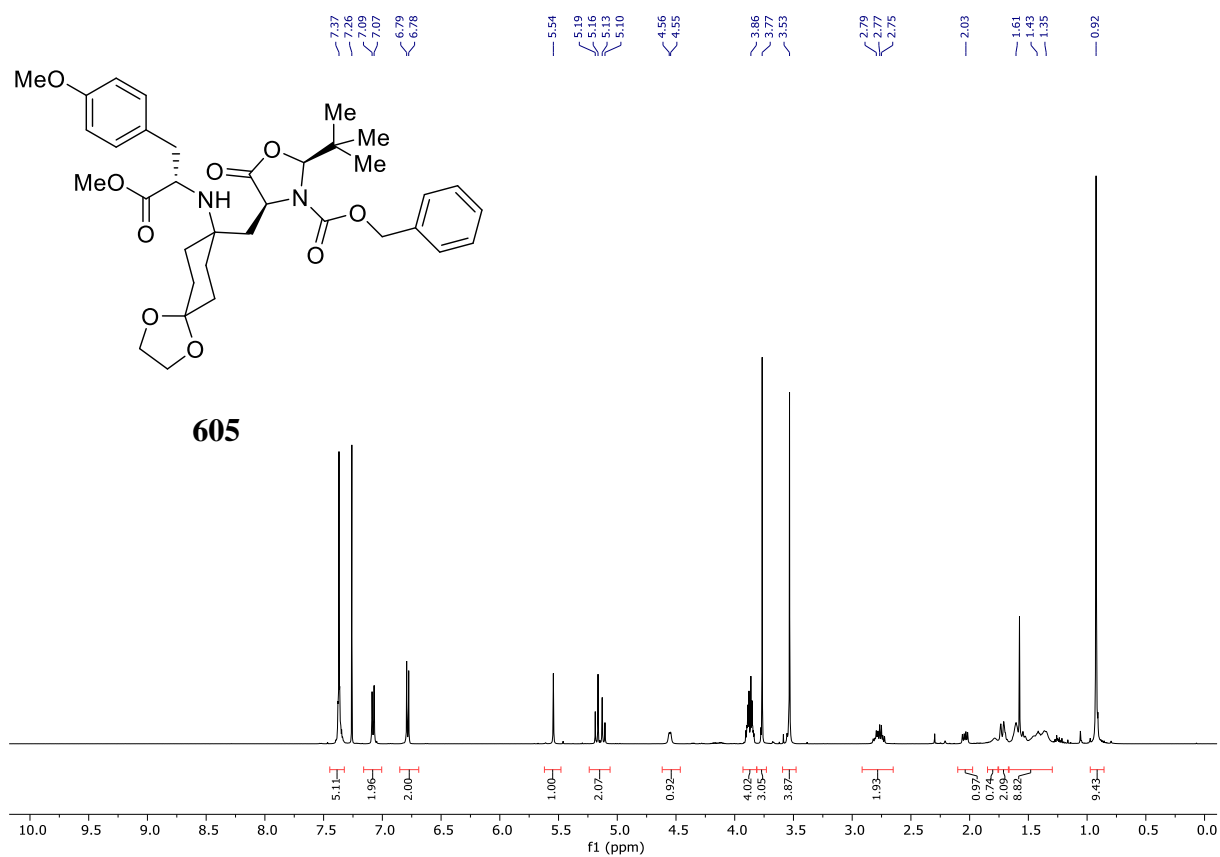


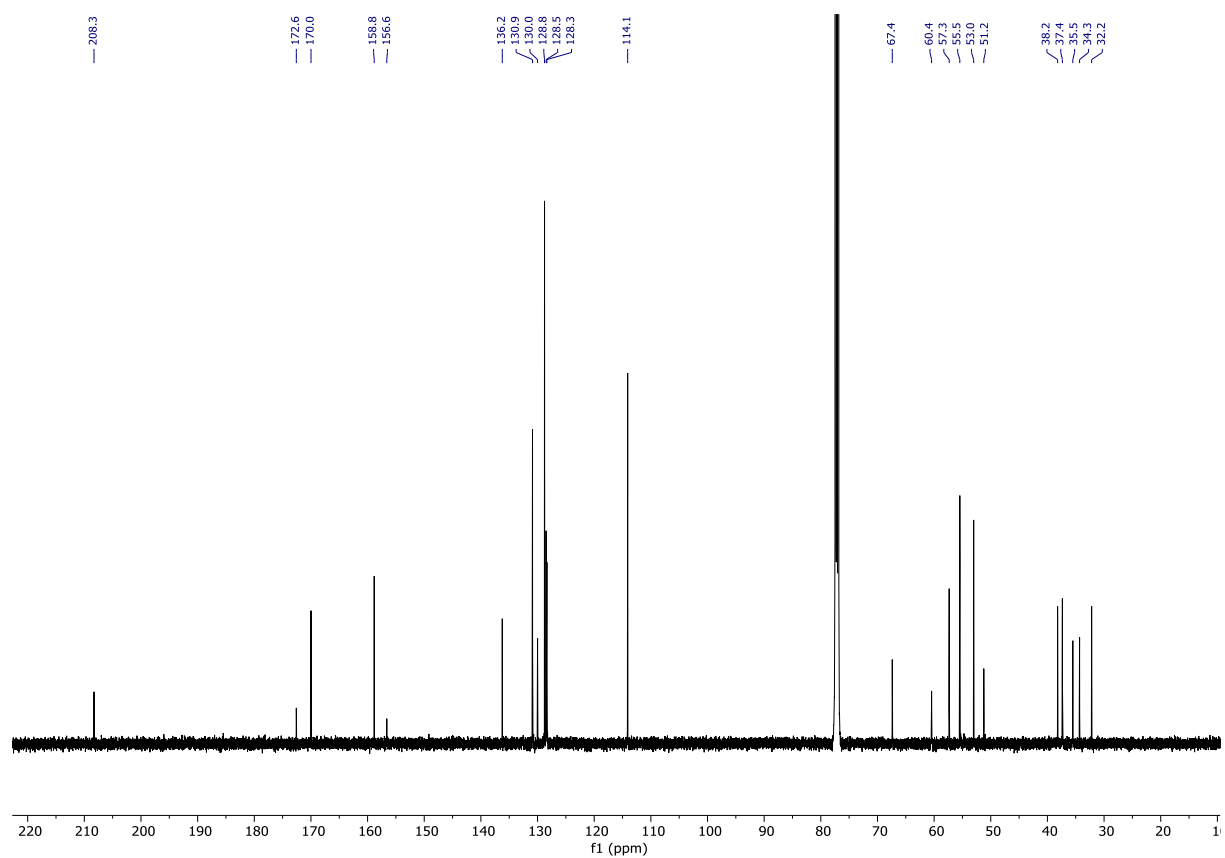
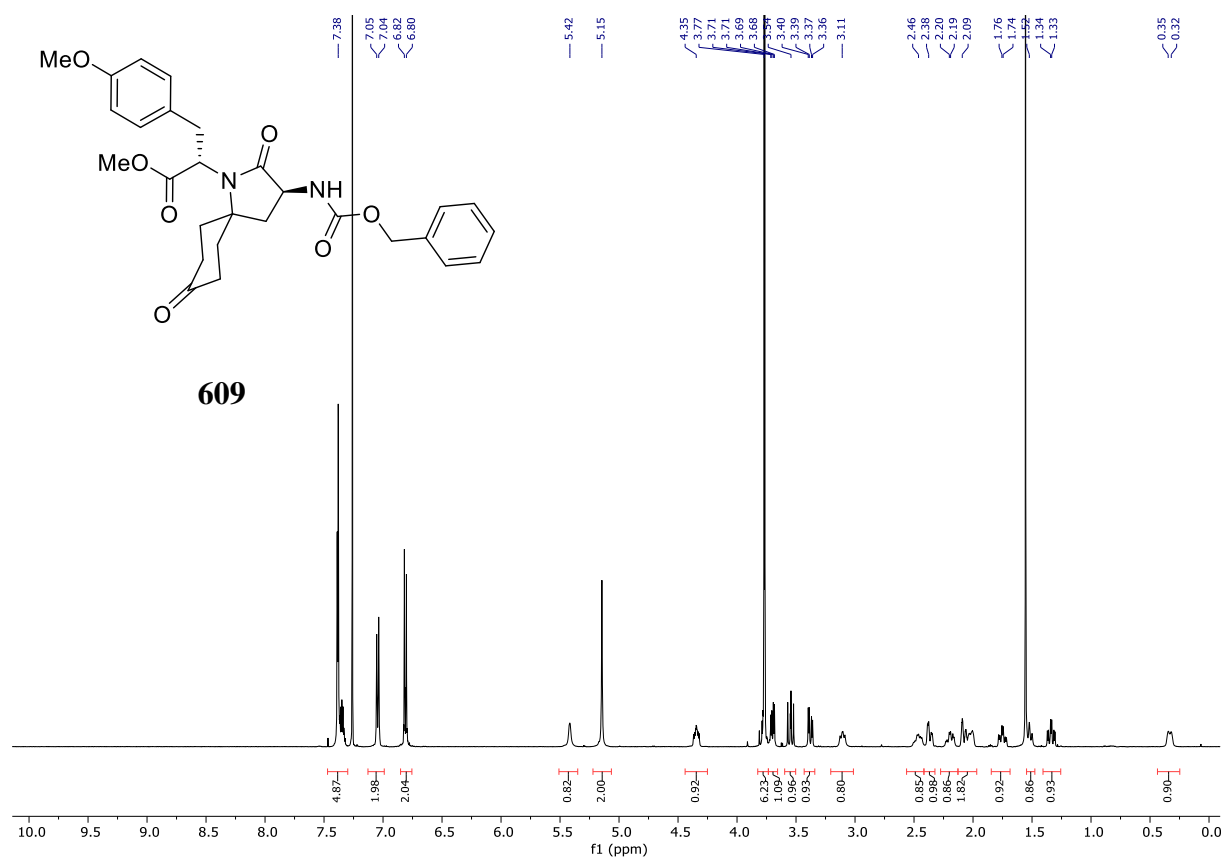


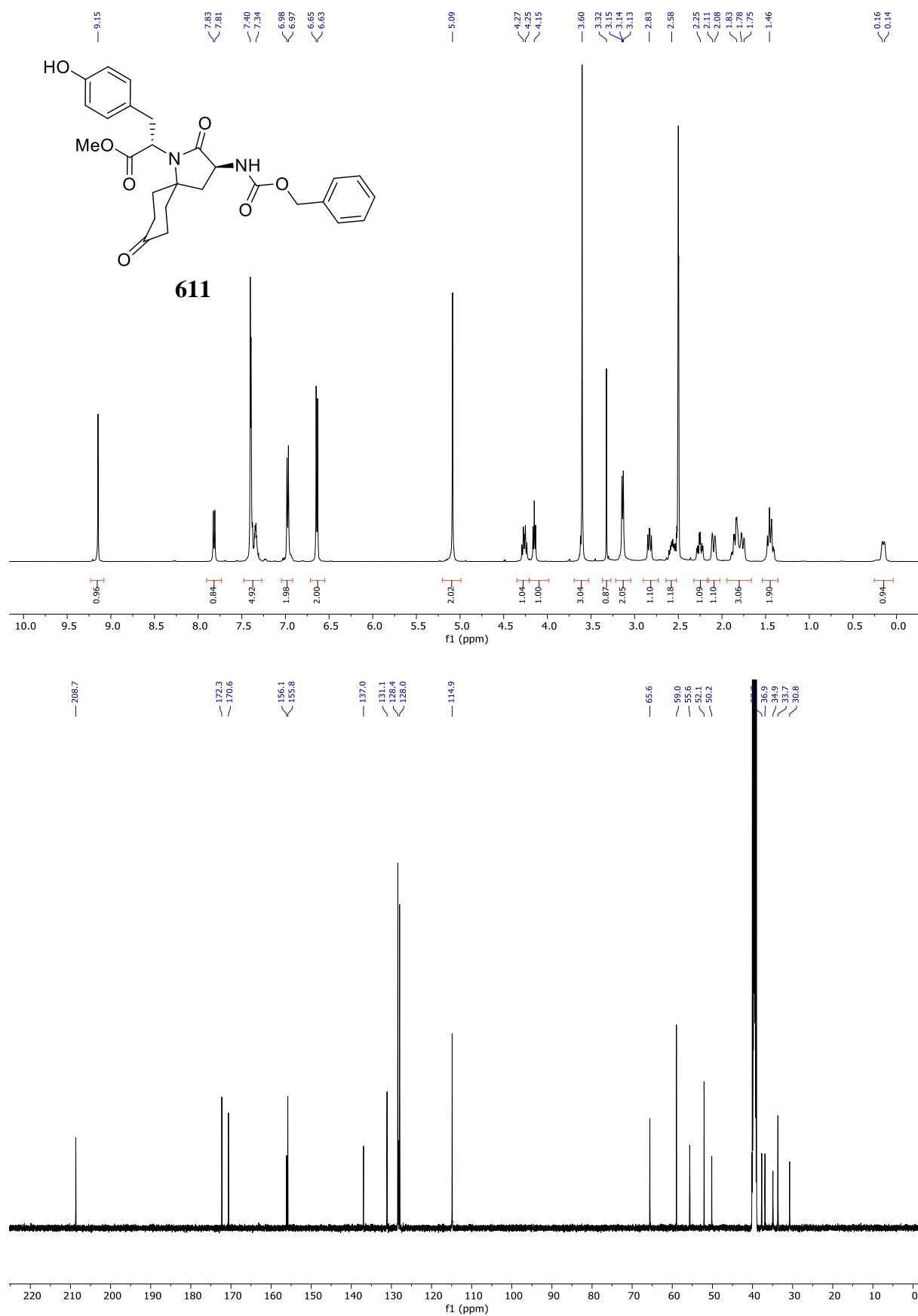


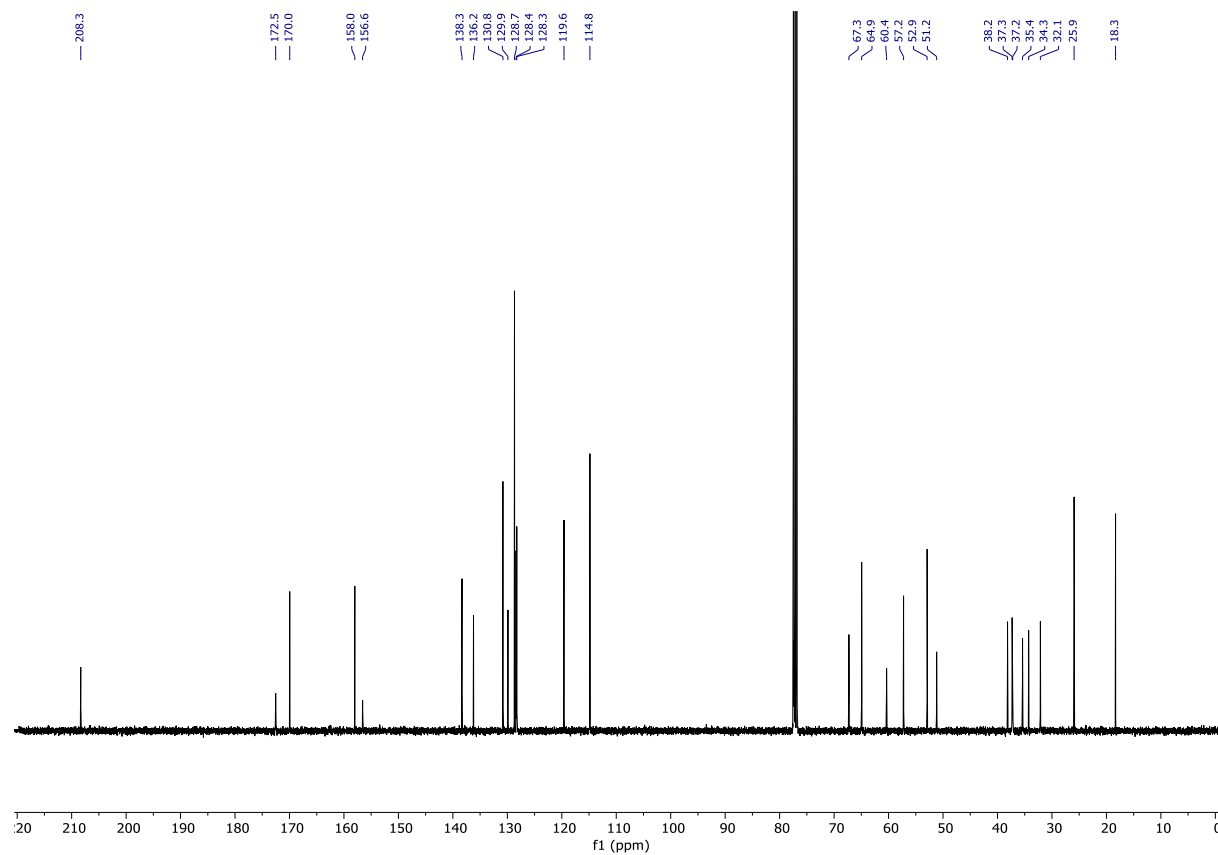
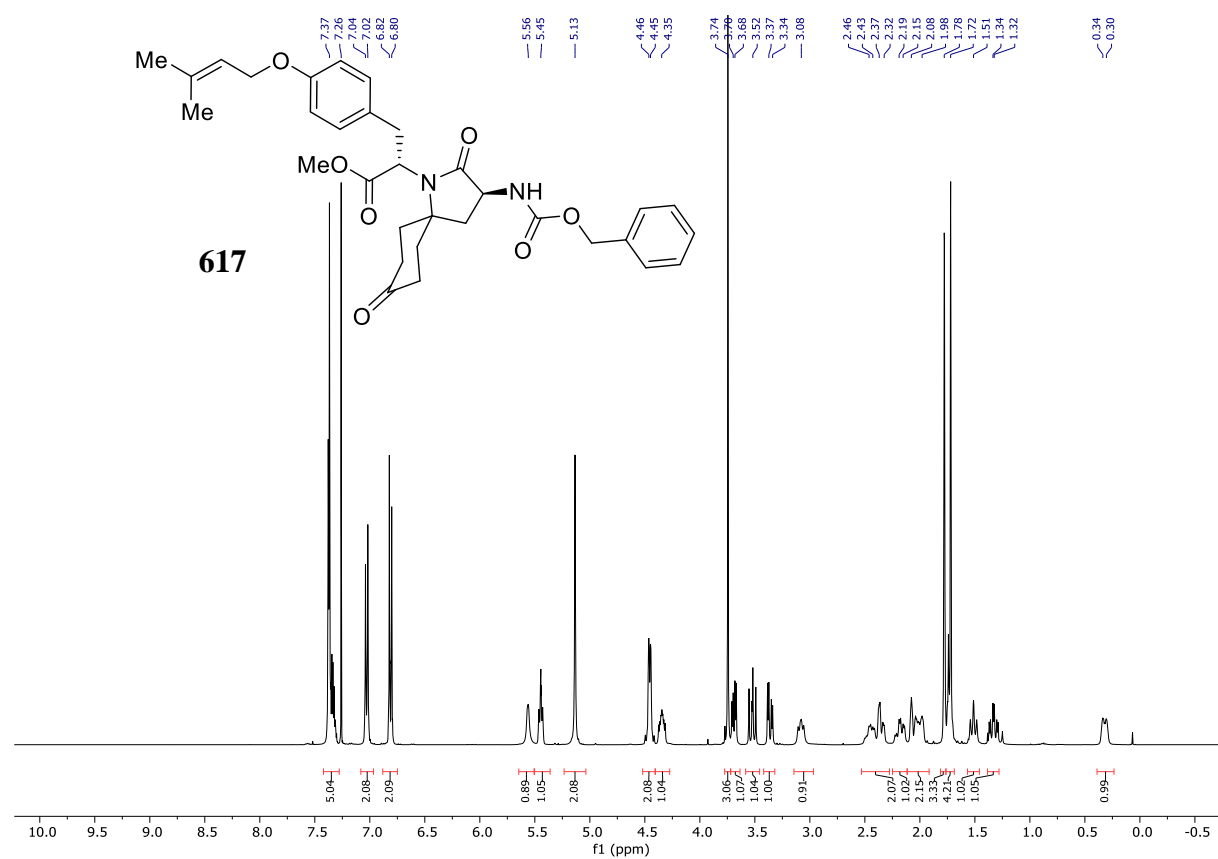


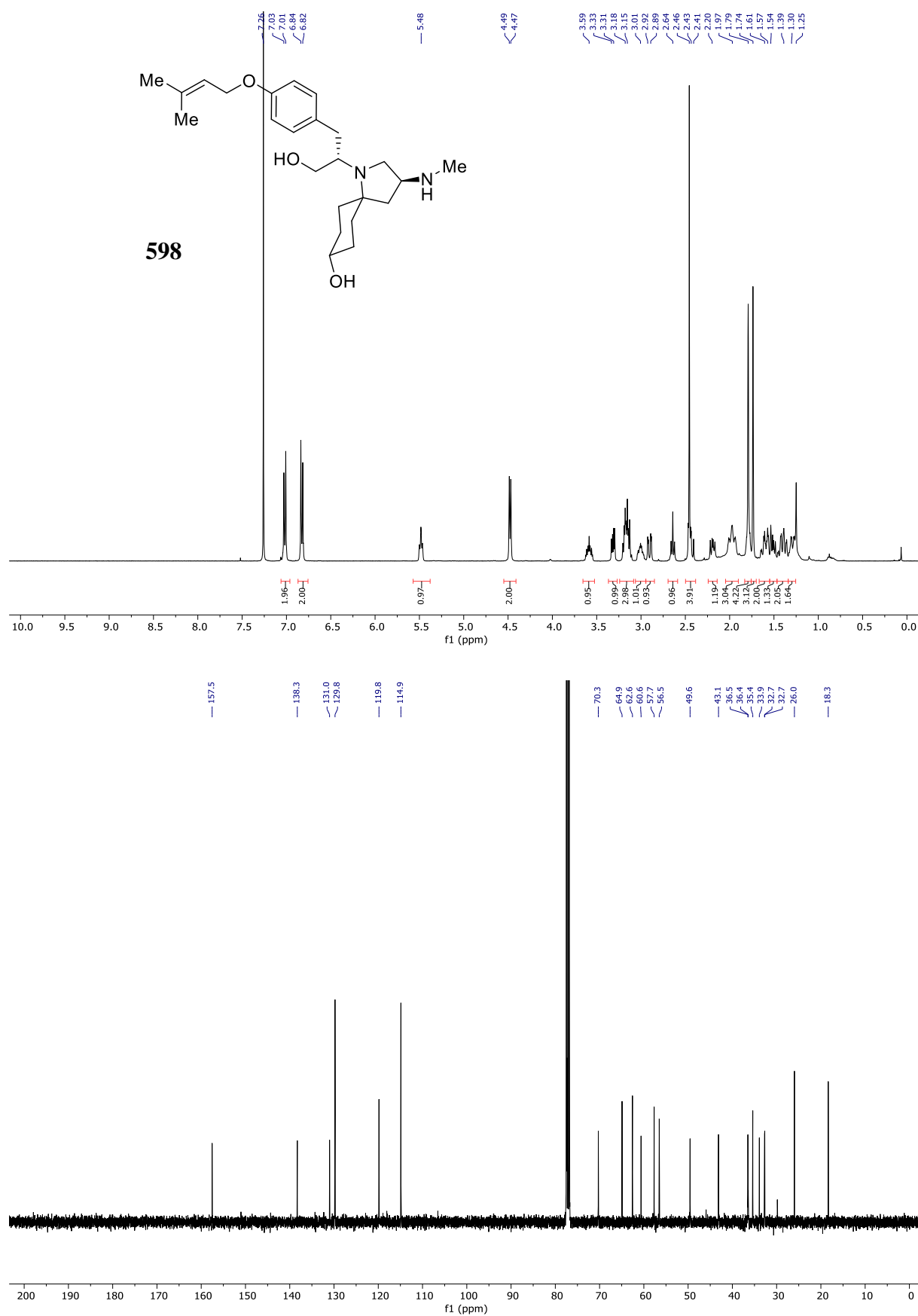


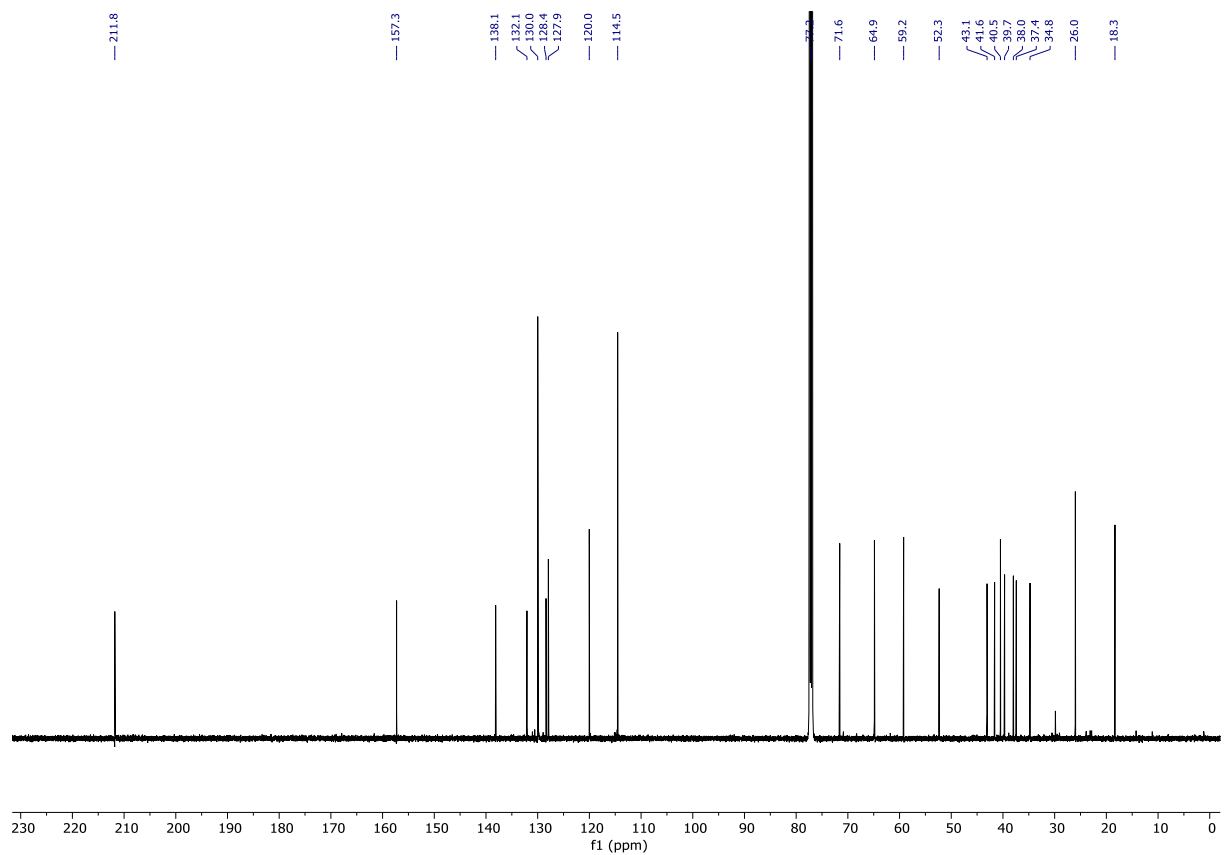
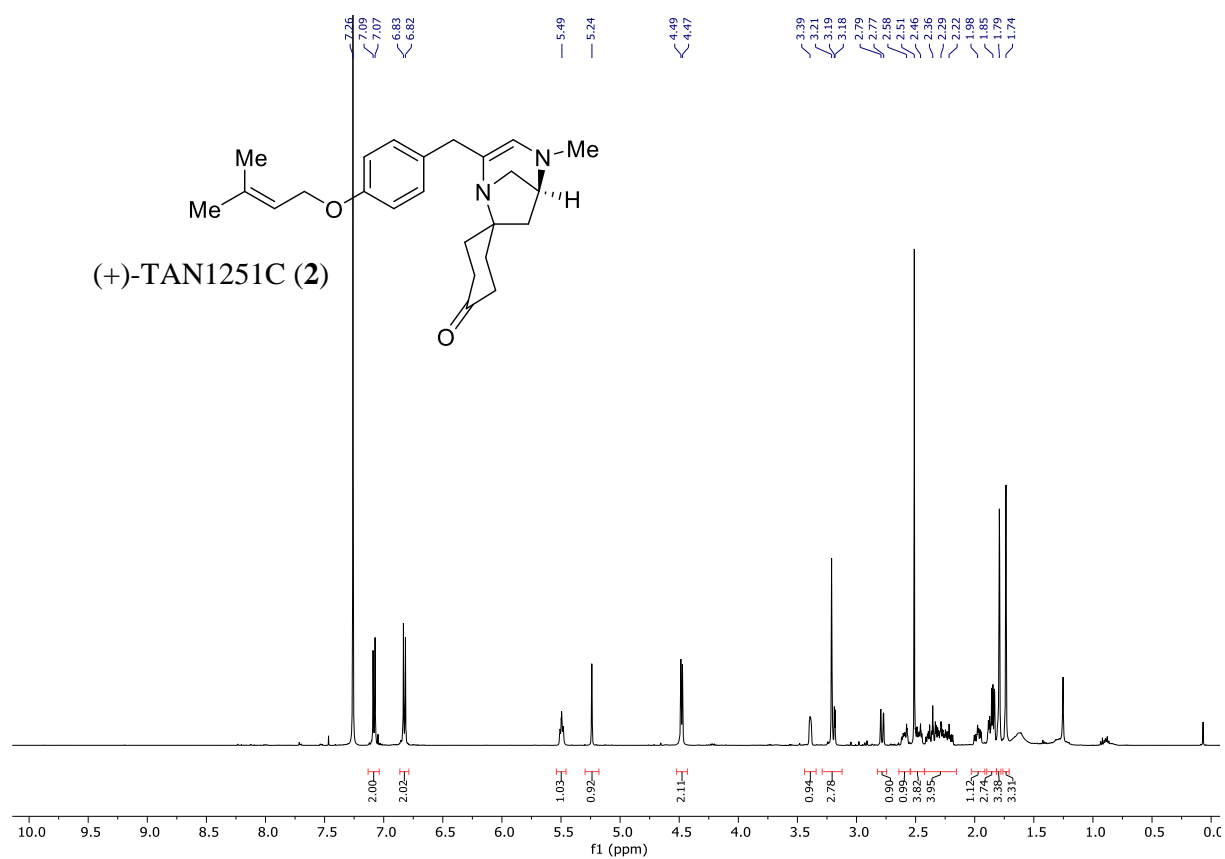


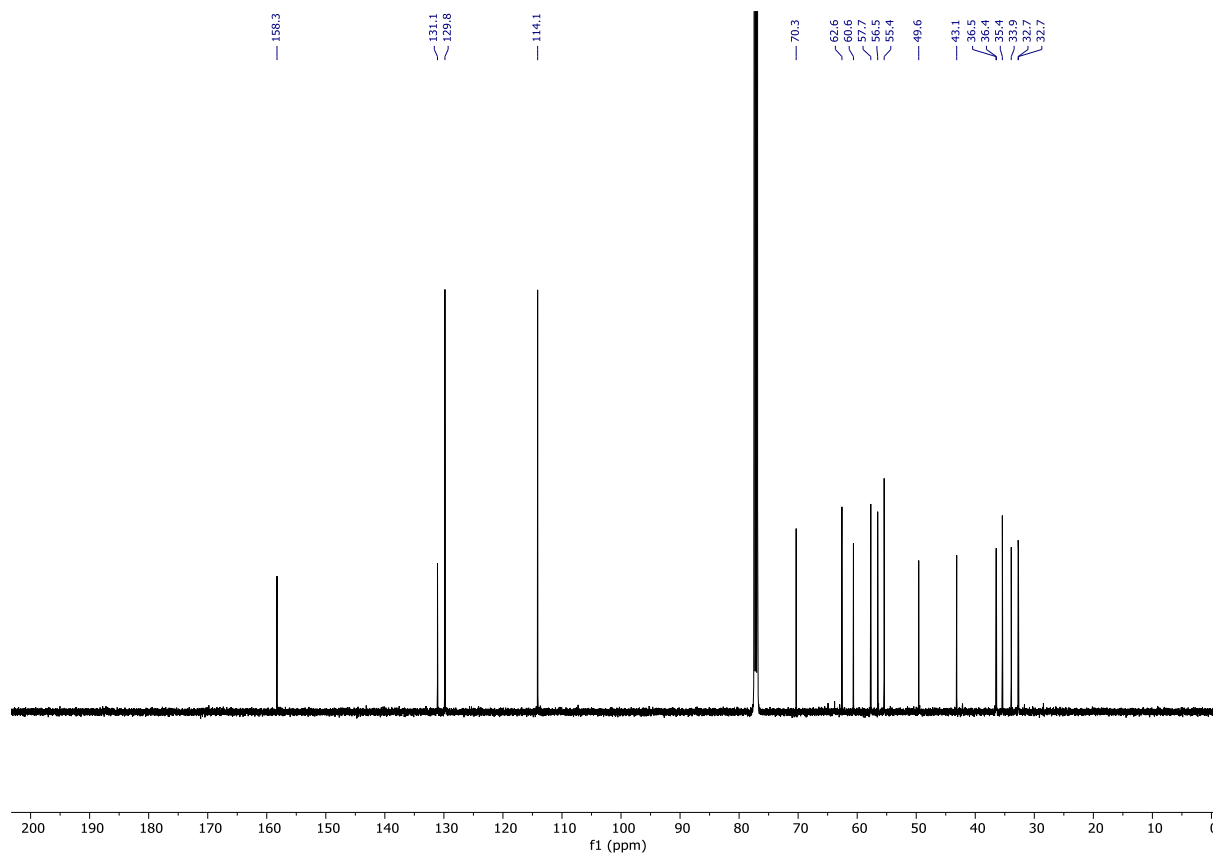
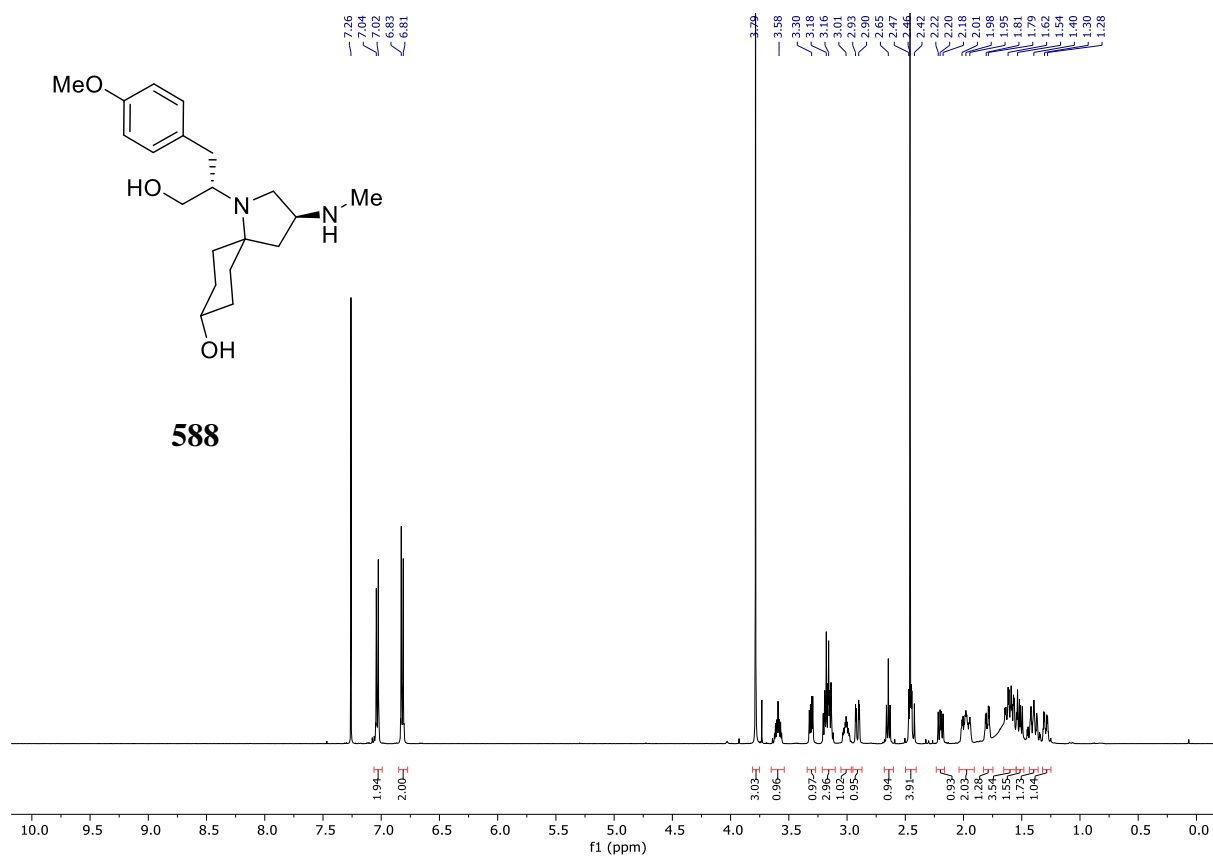


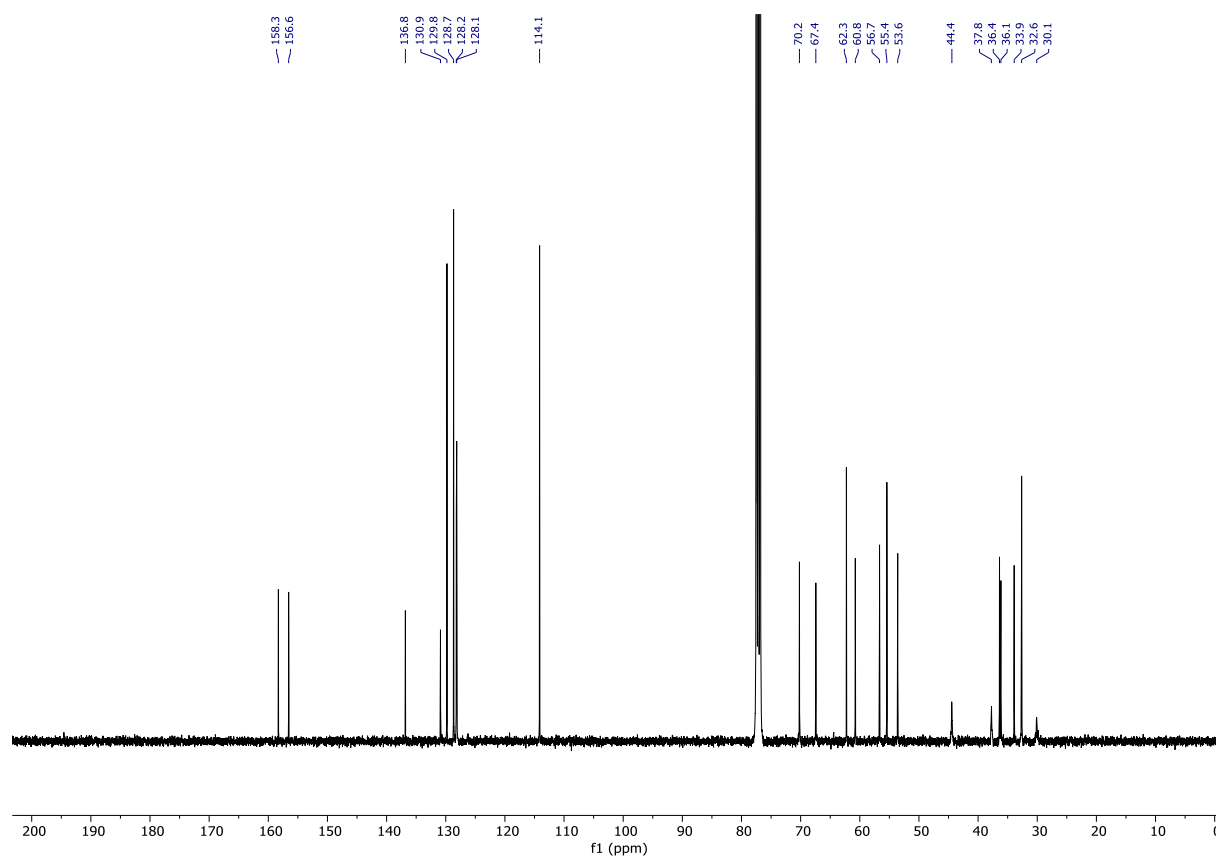
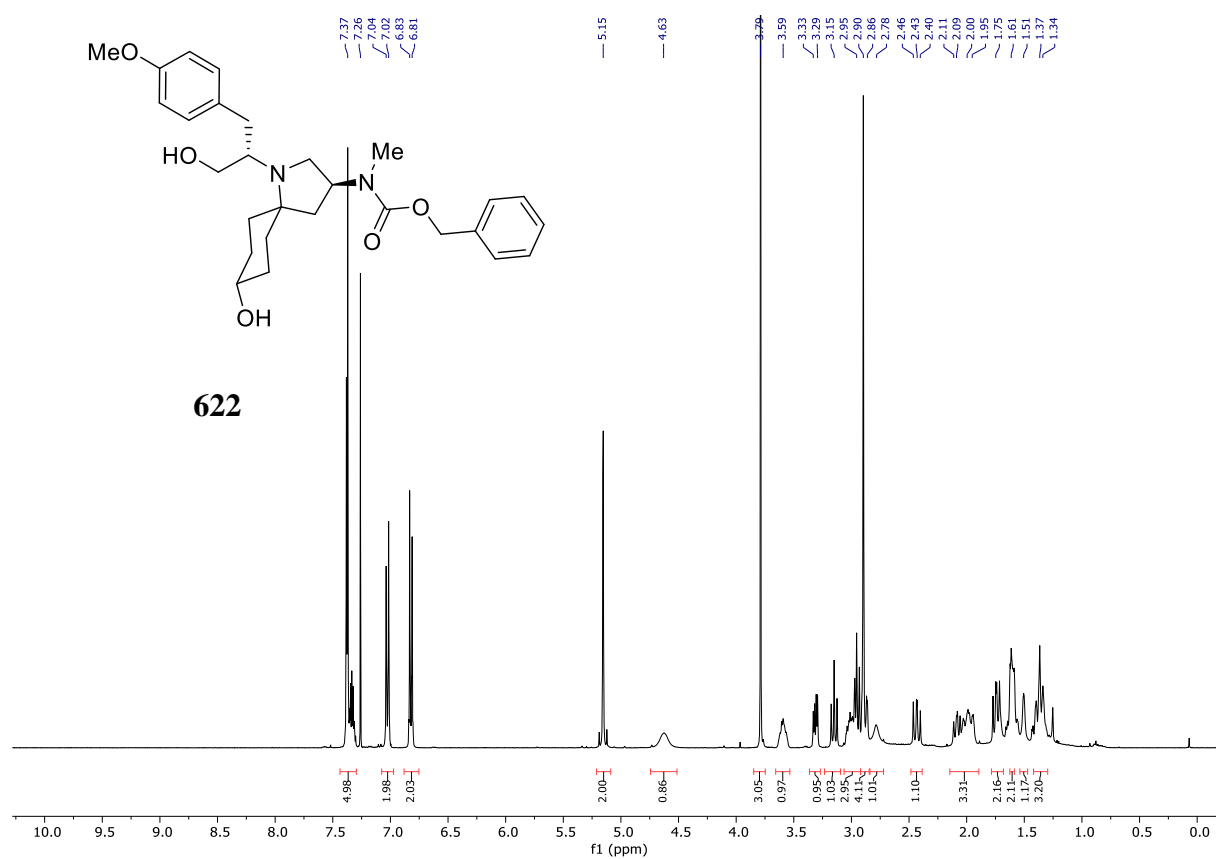


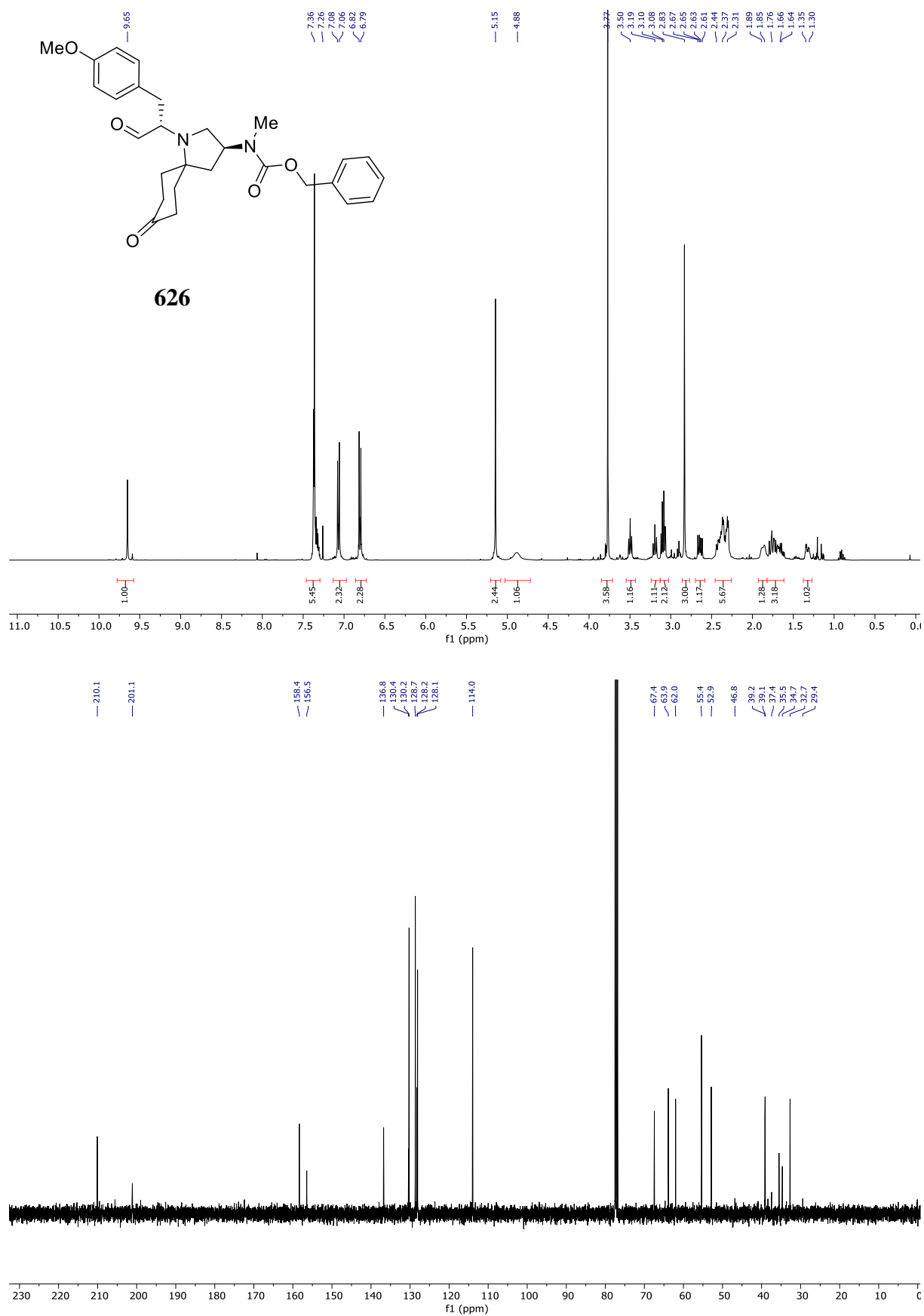


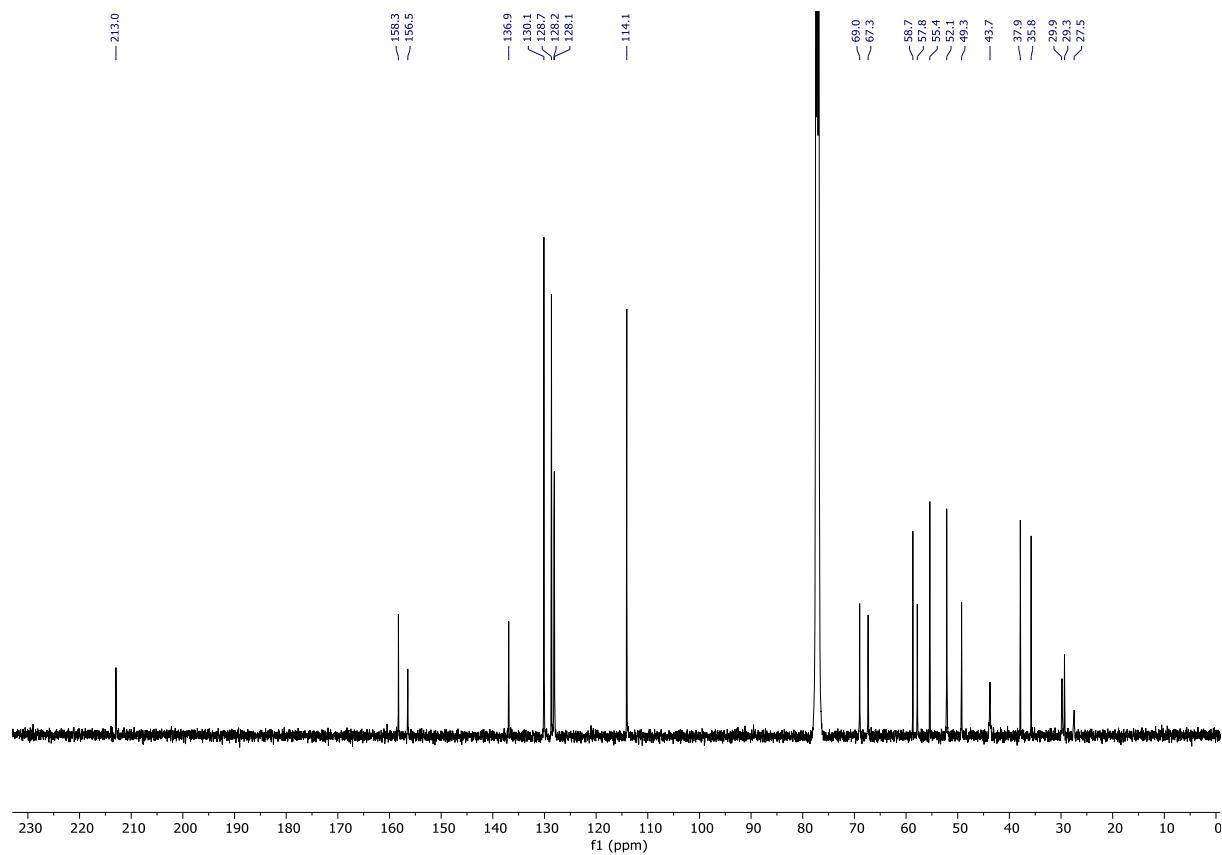
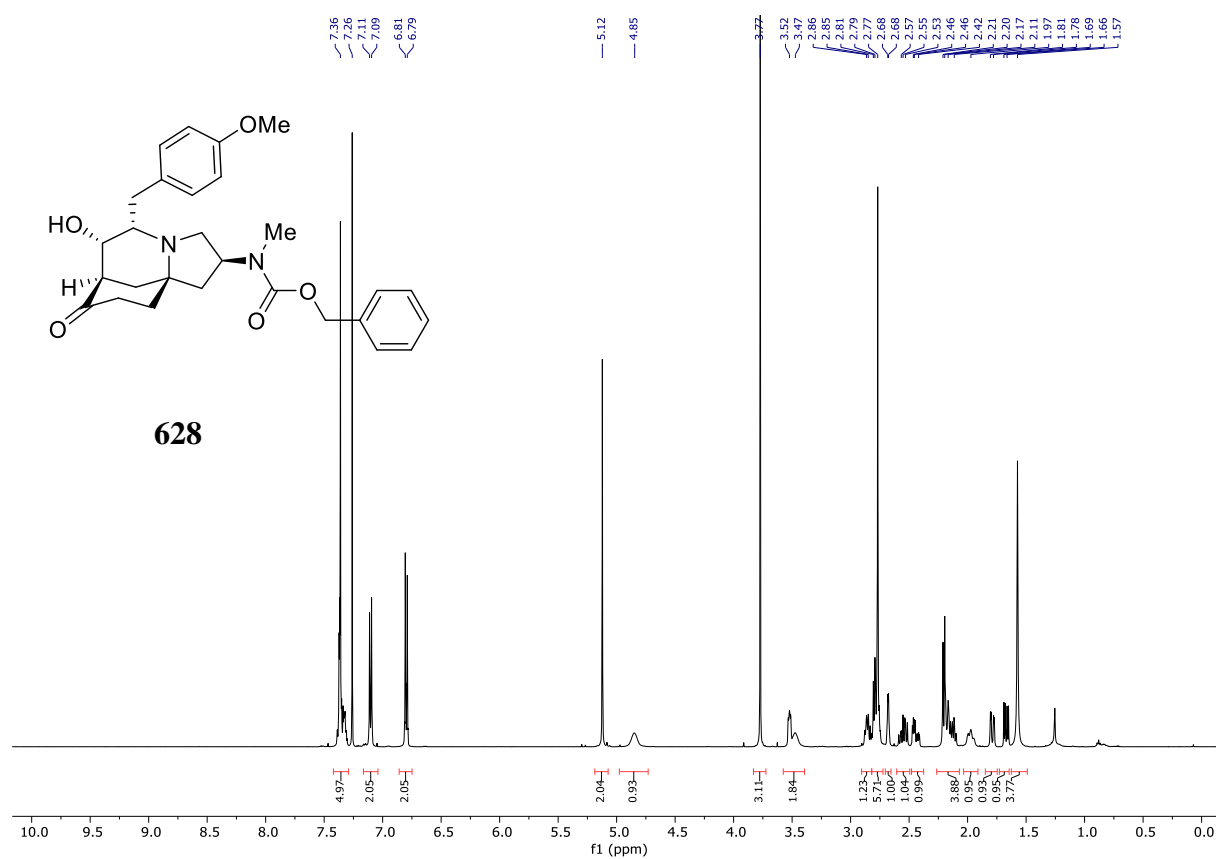


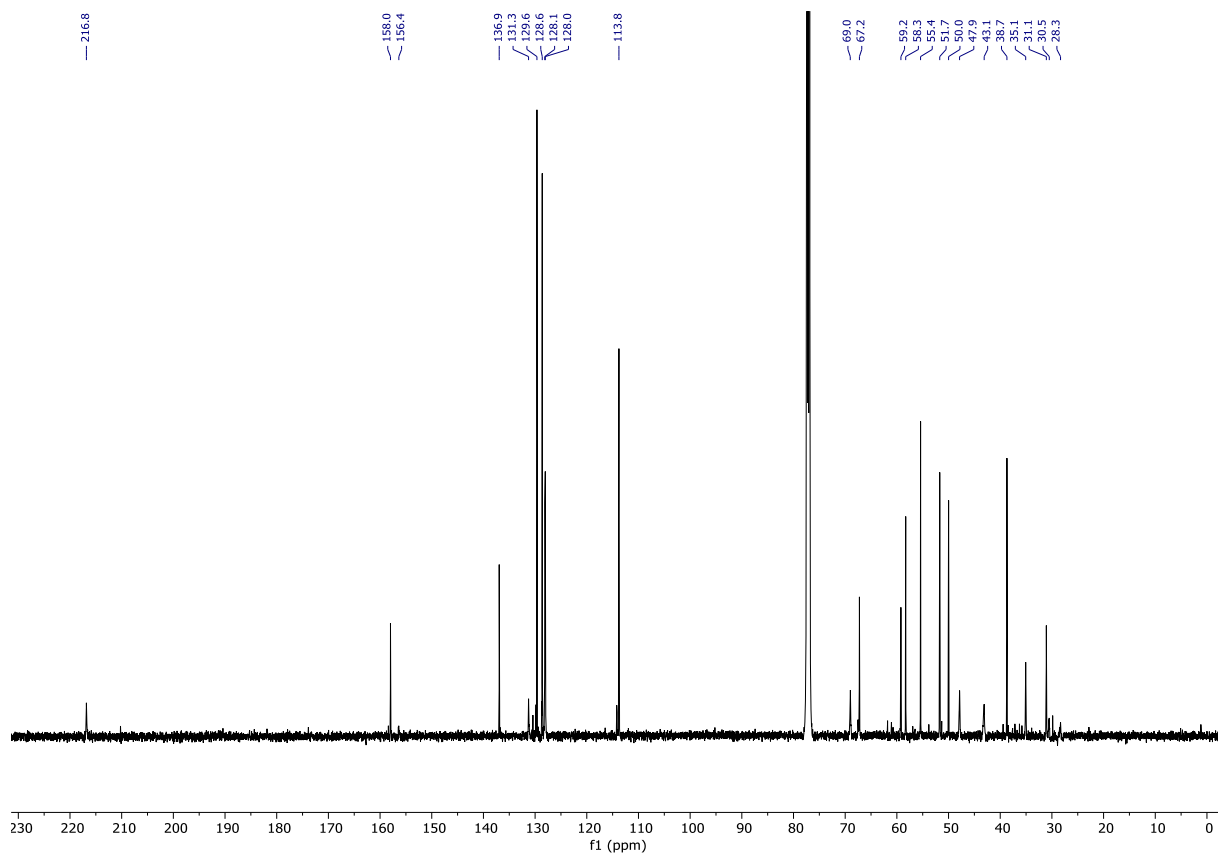
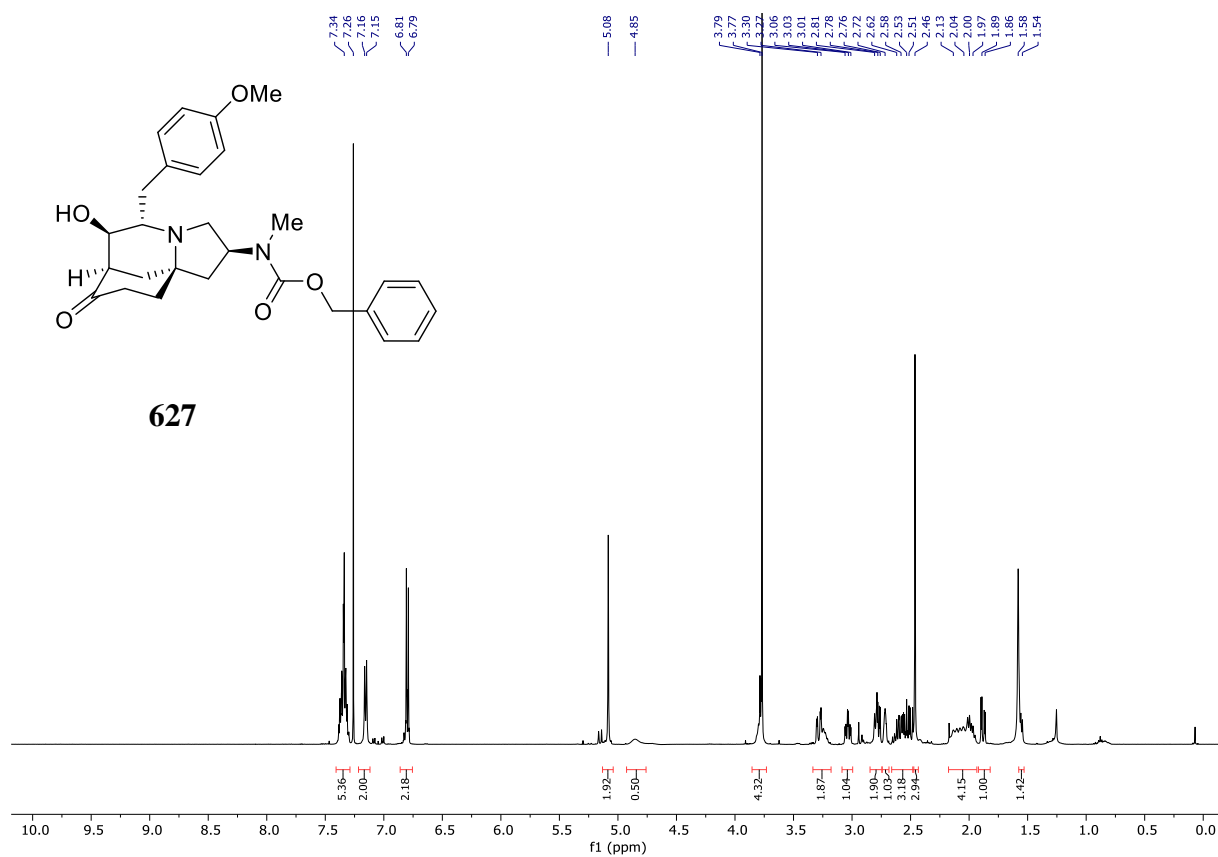


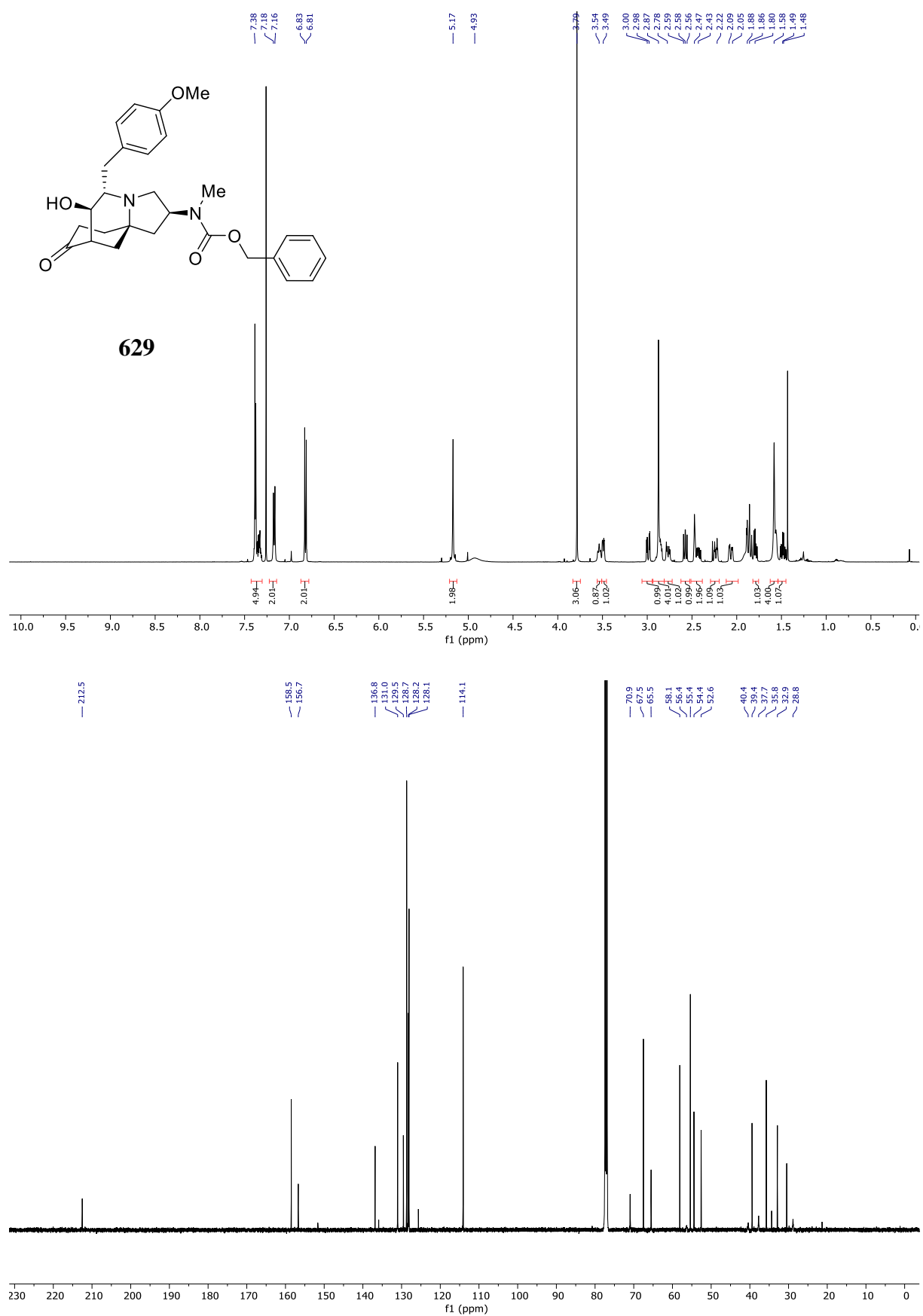


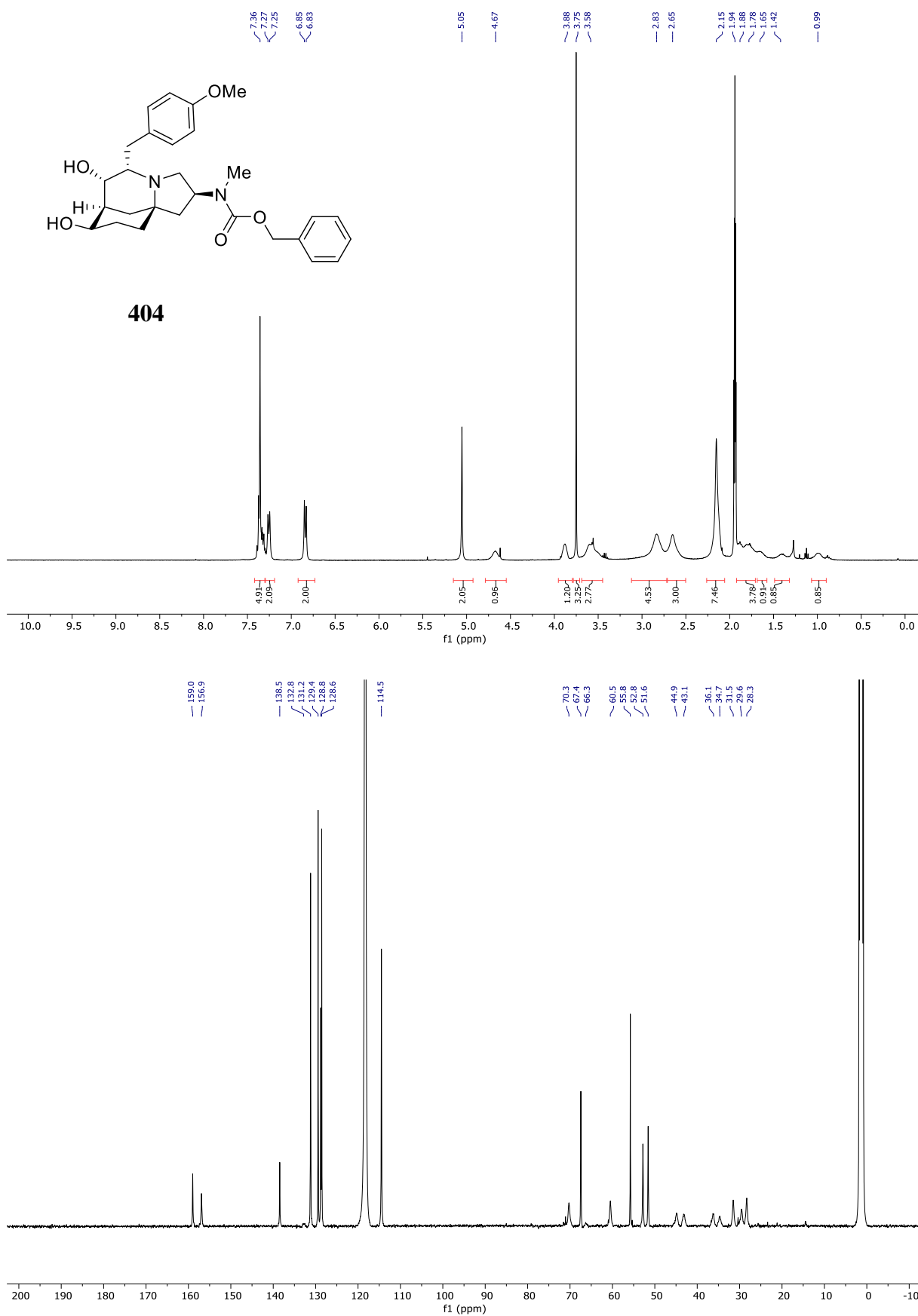


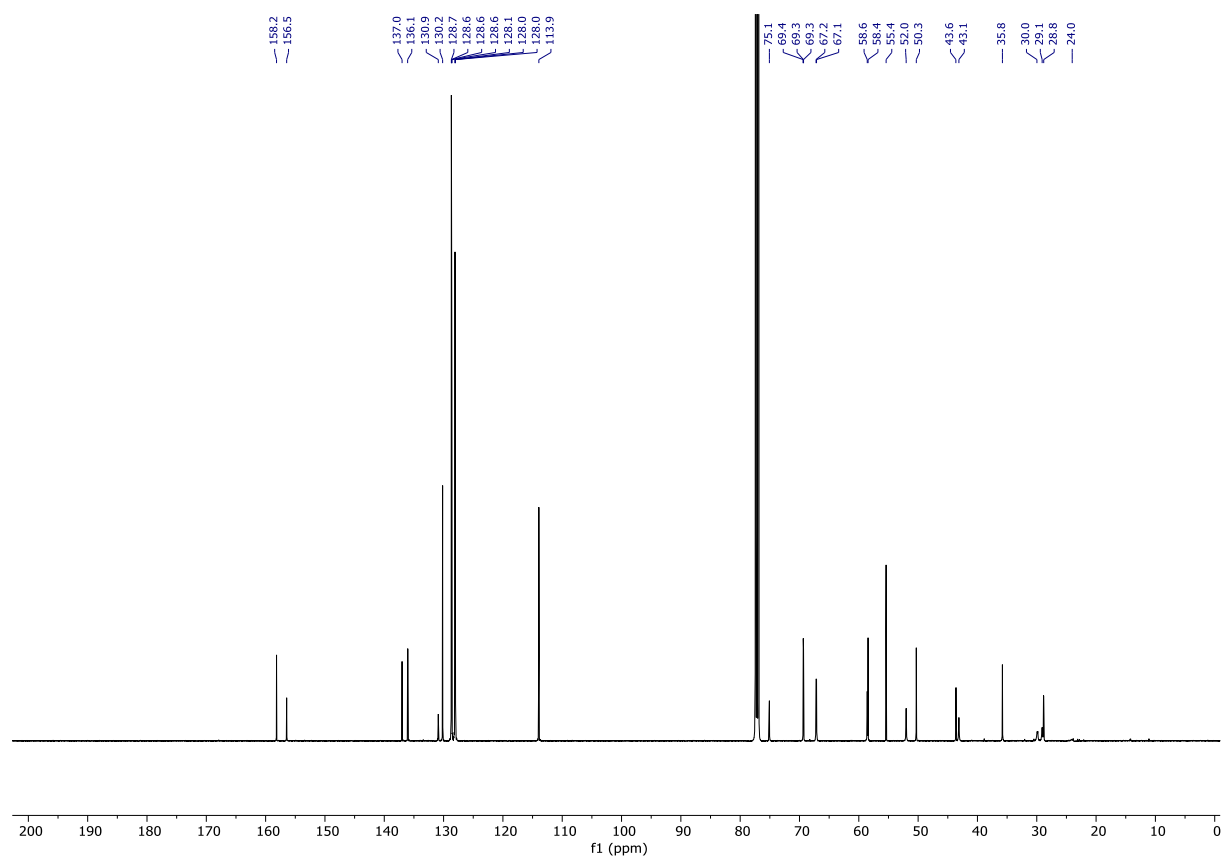
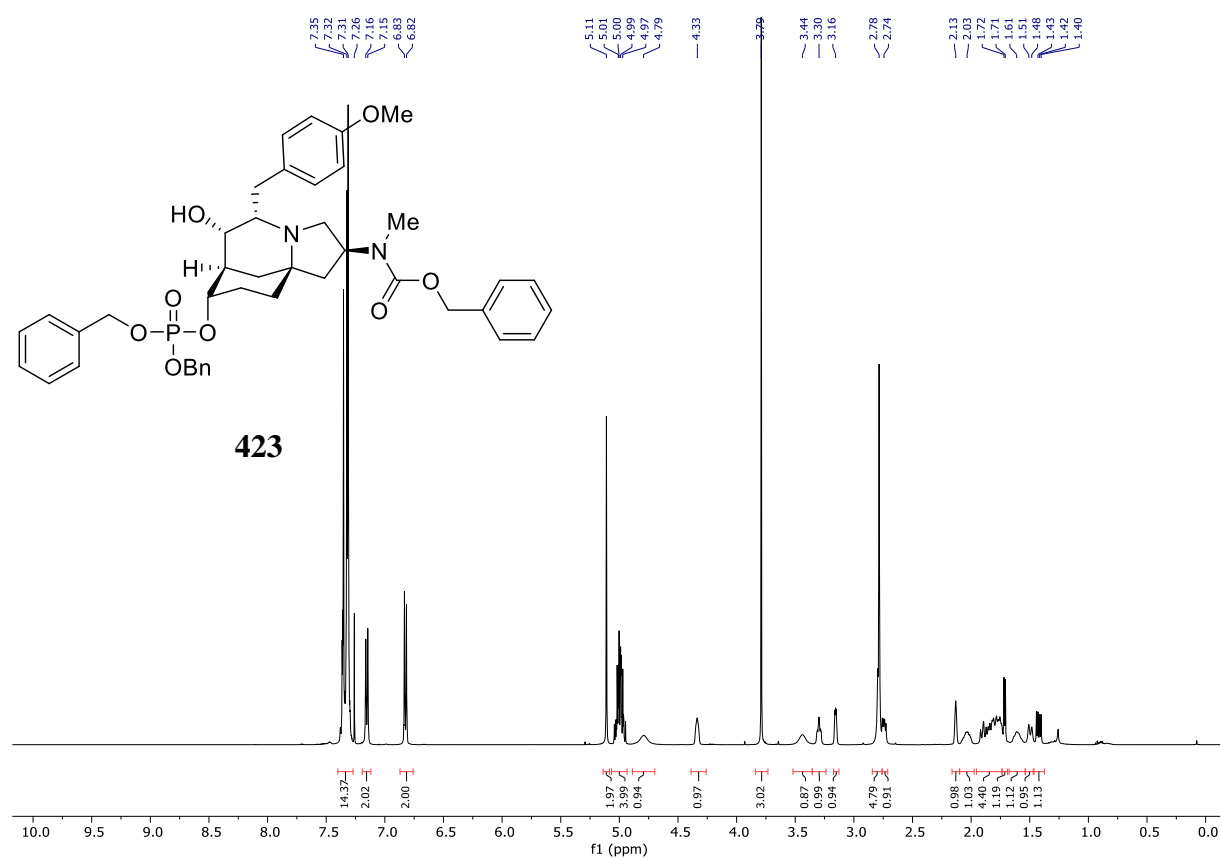


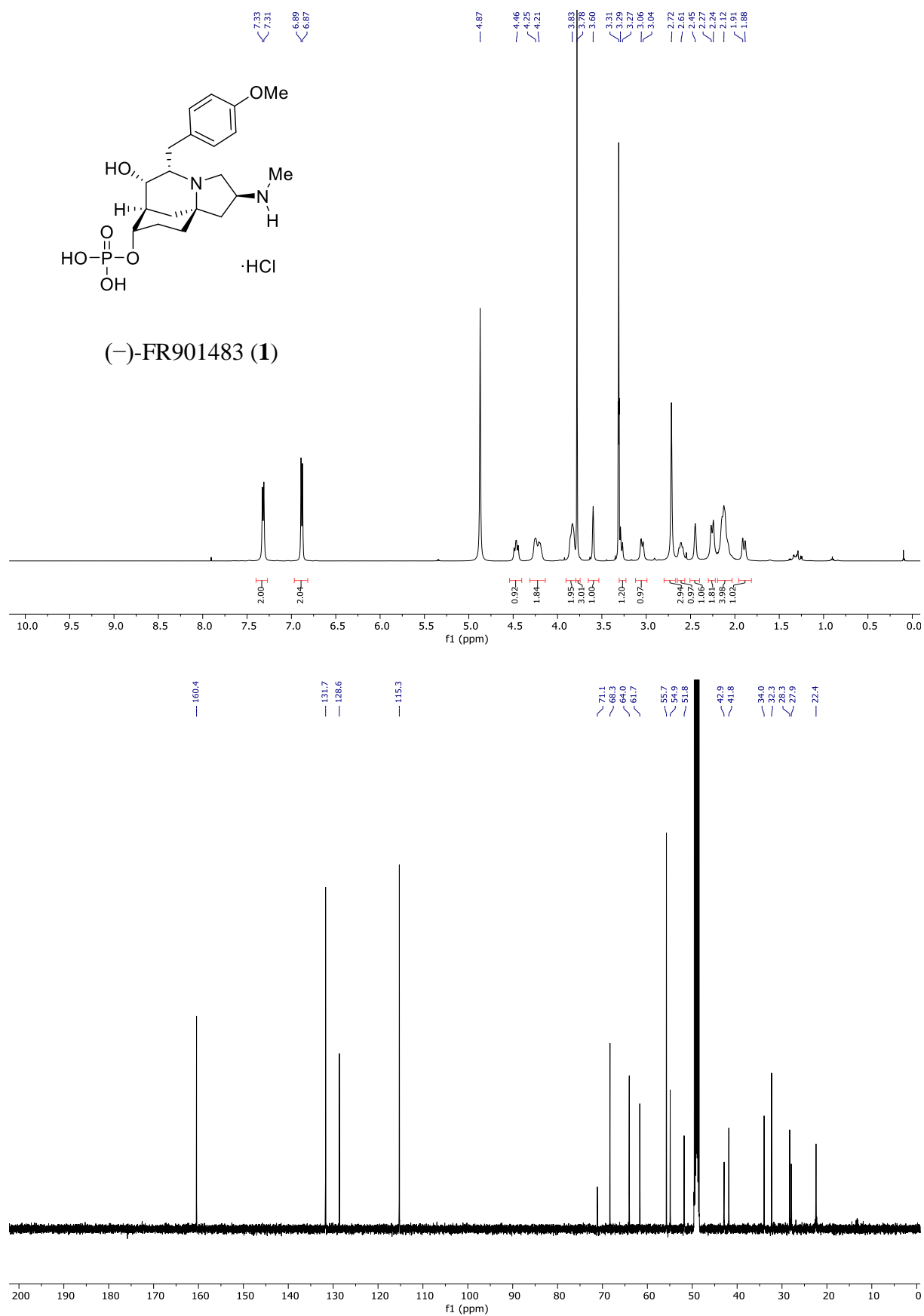












^1H and ^{13}C NMR Spectra (Miscellaneous)

